Terms and Conditions of Use of Digitised Theses from Trinity College Library Dublin

Copyright statement

All material supplied by Trinity College Library is protected by copyright (under the Copyright and Related Rights Act, 2000 as amended) and other relevant Intellectual Property Rights. By accessing and using a Digitised Thesis from Trinity College Library you acknowledge that all Intellectual Property Rights in any Works supplied are the sole and exclusive property of the copyright and/or other IPR holder. Specific copyright holders may not be explicitly identified. Use of materials from other sources within a thesis should not be construed as a claim over them.

A non-exclusive, non-transferable licence is hereby granted to those using or reproducing, in whole or in part, the material for valid purposes, providing the copyright owners are acknowledged using the normal conventions. Where specific permission to use material is required, this is identified and such permission must be sought from the copyright holder or agency cited.

Liability statement

By using a Digitised Thesis, I accept that Trinity College Dublin bears no legal responsibility for the accuracy, legality or comprehensiveness of materials contained within the thesis, and that Trinity College Dublin accepts no liability for indirect, consequential, or incidental, damages or losses arising from use of the thesis for whatever reason. Information located in a thesis may be subject to specific use constraints, details of which may not be explicitly described. It is the responsibility of potential and actual users to be aware of such constraints and to abide by them. By making use of material from a digitised thesis, you accept these copyright and disclaimer provisions. Where it is brought to the attention of Trinity College Library that there may be a breach of copyright or other restraint, it is the policy to withdraw or take down access to a thesis while the issue is being resolved.

Access Agreement

By using a Digitised Thesis from Trinity College Library you are bound by the following Terms & Conditions. Please read them carefully.

I have read and I understand the following statement: All material supplied via a Digitised Thesis from Trinity College Library is protected by copyright and other intellectual property rights, and duplication or sale of all or part of any of a thesis is not permitted, except that material may be duplicated by you for your research use or for educational purposes in electronic or print form providing the copyright owners are acknowledged using the normal conventions. You must obtain permission for any other use. Electronic or print copies may not be offered, whether for sale or otherwise to anyone. This copy has been supplied on the understanding that it is copyright material and that no quotation from the thesis may be published without proper acknowledgement.

Therapeutic Stratagems for Dominant Genetic Disorders

A Thesis submitted to the University of Dublin for the Degree of Doctor of Philosophy

by

Fiona Kernan
Department of Genetics
University of Dublin
Trinity College
Dublin

November 2005

Declaration

This thesis has not been previously submitted to this or any other university for the examination of a higher degree. The work presented here is entirely my own except where noted. This thesis may be made available for consultation within the university library. It may be photocopied or lent to other libraries for the purpose of consultation.

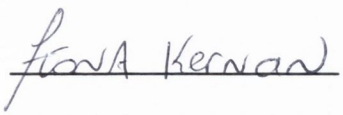

Fiona Kernan

November, 2005

Abstract

Autosomal dominant genetic diseases exhibit a phenotype when one gene allele is mutated whereas recessive diseases require both alleles to be mutated for disease pathology to arise. Disease alleles inherited in a dominant manner may give rise to disease pathology via a combination of one or more of the following mechanisms: 1) a reduction in the level of wild-type (wt) protein (haplo-insufficiency), 2) interference with the activity of the wt protein or 3) the gaining of new functions. For diseases where pathology arises from haploinsufficiency, delivery of the wt gene may be sufficient to provide therapeutic benefit. However, for mutations that have a dominant effect, delivery of the wt gene alone may not be sufficient and hence, suppression of the mutant gene may be necessary. Examples of diseases that arise as a result of dominant mutations include autosomal dominant retinitis pigmentosa (adRP) and osteogenesis imperfecta (OI) (Millington-Ward *et al.,* 1997). In addition, mutations that act in a dominant manner may contribute to the pathology of multi-factorial diseases such as p53-related cancer and Alzheimer's disease (Farrar *et al.,* 2002).

Developing gene-based therapeutic strategies for disorders caused either entirely or in part by dominantly acting mutations, can involve targeting the primary genetic mutation or a secondary effect associated with disease pathology, while possibly maintaining expression of the wt allele. This thesis describes the evaluation of such therapeutic strategies for an autosomal dominant Mendelian disorder, adRP and a multi-factorial disease, p53-related cancer. adRP is a degenerative retinopathy that primarily effects the rod and cone photoreceptors, which have been shown to die by a final common pathway of cell death, apoptosis (Chang *et al.,* 1993; Portera-Cailliau *et al.,* 1994). Given the genetic and mutational heterogeneity of adRP, tailoring individual therapies to each mutation may not be feasible, thus targeting a common secondary effect such as apoptosis offers a means of overcoming this mutational heterogeneity. Chapter 3 describes a study evaluating the potential protective effect of expressing a number of anti-apoptotic proteins, X-linked inhibitor of apoptosis protein (XIAP), c-IAP-1 and c-IAP-2, in a line of cone photoreceptor cells, 661W, exposed to a variety of apoptotic insults. Results show that stable expression of XIAP was found to be moderately protective against apoptosis (approximately 13% cell rescue) induced by etoposide, a chemotherapeutic agent, while c-IAP-1 and c-IAP-2 expression provides no observable protection.

Given the results from a previous study completed in the laboratory in Trinity College Dublin, demonstrating that another anti-apoptotic protein, p35, provides a significant level of cell rescue in 661W cells exposed to apoptosis-inducing chemicals (Tuohy *et al.,* 2002), further evaluation of p35 was undertaken and is described in Chapter 5. The anti-apoptotic activity of p35 expression was assessed in cultured retinal explants from wt C57BL/6J mice exposed to an apoptotic insult, and the results demonstrate a significant cell rescue of approximately 50%. In addition for this study, a transgenic mouse model with conditional expression of p35 was obtained (Hisahara *et al.,* 2000). p35 expression in this model is silent due to the presence of a neomycin resistance gene flanked by *lox*P sites between the transgene promoter and the p35 gene, which can be removed by expression of the enzyme Cre

recombinase (Cre). As this model potentially represents a model in which the effect of p35 expression in photoreceptors could be evaluated, experiments were undertaken as part of the study in Chapter 5 to establish if p35 expression could be activated in retinal explants from *lox*P-p35 mice. However, no p35 expression was detected suggesting that the level of Cre expression obtained from plasmid electroporation was possibly inadequate. Hence, the exploration of using adeno-associated viral (AAV) vectors to deliver Cre is described as the final aspect of Chapter 5.

Another possible approach for activating p35 in *lox*P-p35 mice is to inter-cross these mice with transgenic mouse models with photoreceptor-specific expression of Cre. Chapter 4 describes the generation and *in cellulo* evaluation of such constructs with rod and cone photoreceptor promoter-driven expression of Cre, for the generation of two lines of transgenic mice. The results show the functionality of Cre *in cellulo* and in cultured retinal explants. Furthermore, transgenic mouse models with photoreceptor-specific expression of Cre, could be used to investigate the anti-apoptotic effects of other genes, in addition to p35, and explore the role of genes involved in the pathogenesis of adRP and other retinal degenerations.

As stated above, another therapeutic approach for genetic disorders caused either entirely or in part by dominantly acting mutations is to target the primary genetic mutation. The mutational heterogeneity of many disorders presents a challenge for such an approach, and the mutation-independent strategies developed in this laboratory offer a means of overcoming this (Millington-Ward *et al.,* 1997; O'Neill *et al.,* 2000). p53 is a tumour suppressor protein, mutated in approximately 50% of human tumours (Hollstein *et al.,* 1991). Results from studies have demonstrated that many p53 mutations act in a dominant-negative manner with possible gain-of-function activities (Harvey *et al.,* 1995; Sigal *et al.,* 2000; de Vries *et al.,* 2002). Chapter 6 describes a study involving the *in vitro* evaluation of six hammerhead ribozymes targeting the p53 transcript, using a mutation-independent strategy. One particularly efficient ribozyme, Rz 1561 was identified, and although results from an initial *in cellulo* evaluation were disappointing, further evaluation, possibly using AAV technology described in Chapter 5, may be worthwhile.

In summary this thesis describes the evaluation of a number of gene therapy based strategies for disorders where disease pathology arises as a result of dominantly acting mutations, either by targeting a secondary effect associated with disease pathology or targeting the primary genetic mutation in a mutation-independent manner. More specifically, the work involves the exploration of strategies for modulating apoptosis in degenerating photoreceptors and targeting the primary genetic mutations of the p53 gene, frequently mutated in human tumours. The work here represents the initial steps toward the development of therapeutic strategies for dominantly acting mutations for disorders such as adRP and p53-related cancers.

Acknowledgements

I would like to firstly thank my supervisor Dr. Jane Farrar for her guidance and encouragement during the course of this thesis and Professor Peter Humphries for his support. To all the many members of the Ocular Genetics Unit, who made the lab an enjoyable place to come to and provided so much advice and support. I would also like to acknowledge the technical staff of the Department of Genetics for their help. The support of my many great friends has been invaluable. I would finally like to thank my parents, Mary and Gerard, for all their love, support and encouragement, my brother Brian for his advice and my grandmother, Elizabeth Daly.

"Tender-handed stroke a nettle.
And it stings you for the pain;
Grasp it like a man of mettle.
And it soft as silk remains."

Aaron Hill
Verses Written on a Window in Scotland

List of Figures

Chapter 1

Chapter 3

Chapter 4

Chapter 5

Chapter 6

Abbreviations

4',6'-Diamidine-2-phenylindole dihydrochloride: DAPI

5-bromo-4-chloro-3-indolyl-β-D-galactoside: X-gal

Adenovirus: Ad

Adeno-associated virus: AAV

Ammonium persulphate: APS

Autosomal dominant RP: adRP

Autosomal recessive RP: arRP

Base pair: bp

Bovine serum albumen: BSA

Chimeric intron: Chi intron

Counts per minute: cpm

Cytomegalovirus: CMV

Diethylpyrocarbonate: DEPC

Double distilled H_20: ddH_20

Dulbecco's modified Eagle medium: D-MEM

Electroretinogram: ERG

Enhanced green fluorescent protein: EGFP

Escherichia coli: *E.coli*

Ethidium bromide: EtBr

Ethylenediaminetetra-acetic acid disodium salt: EDTA

Foetal calf serum: FCS

Ganglion cell layer: GCL

Glyceraldehyde-3-phosphate dehydrogenase: GAPDH

Gram: g

Hanks' buffered saline solution: HBSS

High performance liquid chromatography: HPLC

Horseradish peroxidase: HRP

Human growth hormone intron: hGH intron

Improved Cre recombinase: iCre

Infectious particles: ip

Inhibitor of apoptosis protein: IAP

Inner nuclear layer: INL

Inner plexiform layer: IPL

Interphotoreceptor retinol binding protein: IRBP

Kilobase: kb

Leber congenital amaurosis: LCA

Lentivirus: LV

Litre: L

Luria-Bertani medium: LB medium

Microcurie: mCi

Microlitre: µl

Milliamp: mA

Millijoules: mJ

Millilitre: ml

Millisecond: ms

Molecular weight: MW

Multiplicity of infection: MOI

N,N,N,'N'- tetramethylethylenediamine: TEMED

Optical density: OD

Osteogenesis imperfecta: OI

Outer nuclear layer: ONL

Outer plexiform layer: OPL

Phosphate buffered saline: PBS

Picomoles: pmol

Postnatal: P

Pounds per square inch: p.s.i.

Retinitis pigmentosa: RP

Reverse transcription PCR: RT-PCR

Short hairpin RNA: shRNA

Shrimp alkaline phosphatase: SAP

Small interfering RNA: siRNA

Sodium dodecyl sulphate:SDS

Standard error: S.E.

Tris-acetate buffer: TAE buffer

Tris-borate buffer: TBE buffer

Tris-HCl-EDTA buffer: TE buffer

Unit: U

Untranslated region: UTR

Viral particles: vp

Wild-type: wt

β-galactosidase: β-gal

Table of Contents

CHAPTER 1

General Introduction

1.1 Introduction

This introductory chapter describes the basic anatomy of the human retina and photoreceptors, the genetics of autosomal dominant retinitis pigmentosa (adRP) and the most recent developments in gene therapy strategies for adRP including a review of transgenic animal models. The following section introduces the p53 protein, explaining its role in cancer development and how it is an important therapeutic target for cancer treatment. The origin, mechanism of function and uses of ribozymes as suppression tools for gene therapy are described. The final section focuses on methods for delivering gene therapies that overcome the mutational heterogeneity associated with dominant disorders such as adRP and p53-related cancers.

1.2 Retinitis pigmentosa

1.2.1 The retina

The retina forms the innermost layer of the eye and is composed of a sensory region and a layer of retinal pigment epithelium (RPE) (Newell 1996). The RPE acts as a protective barrier between the neural retina and choroidal circulation supplying the outer retina. It has several other important functions, including outer photoreceptor segment phagocytosis and visual pigment regeneration (Kalloniatis *et al.,* 2004). The neural retina comprises six main layers (Figure 1.1): 1) rod and cone photoreceptors, the nuclear bodies of which are located within 2) an outer nuclear layer (ONL). These photoreceptors synapse with horizontal cells at 3) the outer plexiform layer (OPL) and bipolar cells, the nuclei of which are located in 4) an inner nuclear layer (INL). Further processing of the visual signal continues via amacrine cells in 5) the inner plexiform layer (IPL) to 6) the ganglion cell layer (GCL), from where sensory impulses are relayed via the optic nerve to the occipital lobe of the cortex.

1.2.2 Photoreceptor cells

There are two types of light-sensitive photoreceptors in the retina known as rods and cones (Newell 1996). Rods operate under conditions of dim light (scotopic vision) and comprise about 95-97% of photoreceptor cells (Curcio *et al.,* 1990; Applebury *et al.,*

2000). The remaining 3-5% are cone cells, which function in bright light (photopic vision) and are responsible for visual acuity and pattern detection. Cone cells are concentrated in a central region of the retina known as the fovea centralis, where rods are absent, and are also scattered in the peripheral retina.

Both cell types have the same basic structure (Figure 1.2): (1) an outer segment, composed of flattened discs; (2) a cilium, a tubular structure that connects the outer and inner segments; (3) an inner segment containing the mitochondria and other organelles; (4) the outer rod (or cone) fiber connecting the inner segment to the cell body; (5) the cell body that contains the nucleus; and (6) the inner rod (or cone) fiber that terminates in a specialised synaptic ending. The light sensitive pigments are located in the outer segment of each cell. Rhodopsin is the visual pigment of rods and has a maximum absorption at about 507nm. There are three types of cone cells containing different visual pigments that absorb light at approximately 440nm (blue), 535nm (green) and 570nm (red).

1.2.3 Visual transduction cascade

As rods comprise the majority of photoreceptors, the visual transduction cascade within these cells will be described here (Figure 1.2) (Newell 1996; Molday 1998). The rod visual pigment rhodopsin is composed of an opsin (a seven transmembrane G-protein-coupled receptor), and a small chromophore 11-*cis* retinal. Following light absorption, 11-*cis* retinal is converted to its all-*trans* isomer, dissociating from the now activated rhodopsin (Rho*). Rho* binds transducin, a member of the G-family of proteins, catalysing the conversion of GDP to GTP, activating transducin. This activated transducin in turn activates the enzyme cGMP phosphodiesterase (PDE), which then hydrolyses cGMP to 5'-GMP. The fall in cGMP levels leads to the closure of cGMP-gated cation channels on the plasma membrane of the rod outer segment (ROS), preventing the influx of sodium and calcium ions. The resulting hyperpolarisation of the entire rod-cell plasma membrane inhibits the release of the rod's neurotransmitter, glutamate, at its synaptic terminal, producing an electrical signal, which is relayed via the optic nerve to the brain. The deactivation of Rho* begins with phosphorylation by

rhodopsin kinase, followed by arrestin binding, preventing further activation of transducin. Transducin hydrolyses GTP to GDP, and so is unavailable for further activation of PDE. The drop in intracellular calcium, results in the synthesis of cGMP by the enzyme guanylate cyclase, reopening the cGMP-gated channels and returning the photoreceptor to its depolarized state. The all-*trans* isomer of the chromophore, which dissociated from opsin on light activation, is reduced to all-*trans* retinol and transported to the RPE where it is converted to 11-*cis* retinal and returned to the photoreceptor.

1.2.4 Retinal dystrophies

Hereditary retinal disorders encompass a large group of genetically and clinically heterogeneous diseases, which are classified by clinical features including: age of onset, rod vs cone involvement, pattern of vision loss, retina appearance, and the genes involved (Rattner *et al.,* 1999). Retinal dystrophies can be broadly placed in three categories, the first of which is retinitis pigmentosa (RP). RP is clinically characterised by night blindness (nyctalopia) as a result of the initial death of rod photoreceptors, followed by a progressive loss of vision owing to secondary degeneration of cone cells (Phelan *et al.,* 2000; Kalloniatis *et al.,* 2004). The second category is referred to as the cone or macular dystrophies, in which visual loss results from cone photoreceptor death in the central, cone-rich part of the central retina. Rod-cone diseases comprise the third category, which show an early loss of cone-mediated central vision, with deterioration in night and peripheral vision, as a result of simultaneous degeneration of rod and cone photoreceptors (Phelan *et al.,* 2000). For a comprehensive review of retinal dystrophies and the genes involved refer to the RetNet database: http://www.sph.uth.tmc.edu/Retnet/.

1.2.5 Clinical features of RP

RP is the leading cause of visual handicap among working populations in developed countries with an estimated 1.5 million patients worldwide (Weleber 2001). Clinical features vary between patients and even among family members carrying the same mutation (Kalloniatis *et al.,* 2004). In typical cases the first symptom is night blindness, as a result of rod photoreceptor degeneration with the age of onset varying from infancy

to late middle age. This is usually followed by a loss of mid-peripheral visual fields, and without the support of the rods, cone photoreceptors begin to gradually degenerate resulting in a loss of central vision, which can lead to complete blindness. It is this progressive loss of cone photoreceptors that has the greatest impact on the patient's vision. A characteristic symptom of RP, from which the name derives, is abnormal pigmentation (Figure 1.3). As rod photoreceptors die, pigment is released into the retinal pigment epithelium (RPE) and accumulates within the retina as "bone-spicule formations" (Phelan *et al.,* 2000). In later stages of the disease, the optic nerve appears waxy and pale, the retinal blood vessels are narrowed and the peripheral and central retina are atrophied.

1.2.6 Genetics of RP

RP is a genetically heterogeneous disease, which can be inherited in an autosomal dominant, recessive, X-linked recessive, digenic or mitochondrial mode, with around 40 known or predicted genes implicated in disease pathology (http://www.sph.uth.tmc.edu/Retnet/). In addition, RP can also present as part of a multi-system disorder, including Usher syndrome, which involves sensorineural deafness and in some cases, vestibular dysfunction. Of the RP genes with known functions, some encode proteins involved in phototransduction, including rhodopsin, the first gene to be implicated in RP (McWilliam *et al.,* 1989; Farrar *et al.,* 1990), phosphodiesterase (PDE) (Huang *et al.,* 1995) and a cGMP gated channel (Dryja *et al.,* 1995). Rhodopsin mutations are estimated to account for approximately 25% of adRP cases and to date, up to 100 mutations have been identified within the rhodopsin gene (Briscoe *et al.,* 2004). Another gene frequently mutated in RP encodes for *rds*-peripherin, a structural protein that localizes to the outer disc rims in both rod and cone photoreceptors (Farrar *et al.,* 1991; Kajiwara *et al.,* 1991). In addition to RP, mutations in *rds*-peripherin can cause other retinal dystrophies such as cone-rod and pattern dystrophies (Molday 1998). Genes that encode proteins of the visual cycle, such as RPE65 (Marlhens *et al.,* 1997), ABCR (Martinez-Mir *et al.,* 1998) and CRALBP (Maw *et al.,* 1997), are mutated in many cases of autosomal recessive RP (arRP). Interestingly a number of adRP genes are widely expressed but only cause disease pathology in the

retina. Included in this latter category are the genes *PRPF3* (Chakarova *et al.,* 2002), *PRPF8* (McKie *et al.,* 2001) and *PRPF31* (Vithana *et al.,* 2001) encoding pre-mRNA splicing factors and the gene which encodes inosine monophosphate dehydrogenase type I (IMPDH1) (Bowne *et al.,* 2002; Kennan *et al.,* 2002), the rate limiting enzyme of the *de novo* pathway of guanine nucleotide biosynthesis. While great progress has been made in characterising RP genes, a number of genes that are implicated in adRP, arRP, X-linked RP and allied diseases remain to be identified. The genetic heterogeneity highlighted in this section presents a challenge for therapeutic development. Thus exploring alternative approaches to targeting the primary mutation, such as slowing photoreceptor cell death (see 1.2.10.1), as described in the studies in Chapters 3 and 5, represent a valid therapeutic strategy for adRP.

1.2.7 Photoreceptor cell death

Although RP is genetically heterogeneous, photoreceptors in retinal degenerations have been shown to die by a final common pathway of cell death, apoptosis (Chang *et al.,* 1993; Portera-Cailliau *et al.,* 1994). Apoptosis is a regulated mode of cell death that is essential for normal development and tissue homeostasis (Jacobson *et al.,* 1997; Danial *et al.,* 2004). However, abnormal regulation of apoptosis can result in either excessive or impaired activation of apoptotic pathways, contributing to many disease pathologies including cancer (Hanahan *et al.,* 2000; Ghobrial *et al.,* 2005), autoimmune disorders (Vaux *et al.,* 2000) and retinal degenerations (Chang *et al.,* 1993). Numerous studies in cell culture (Tuohy *et al.,* 2002) and in various animal models of retinal degeneration, including inherited and light-induced models of retinal damage (Reme *et al.,* 1998; Liu *et al.,* 1999; Bode *et al.,* 2003) support the initial observation by Chang *et al.* that photoreceptors die by apoptosis.

1.2.8 Apoptosis

Apoptosis can be mediated by caspases, a group of cysteine aspartyl-specific proteases (Thornberry *et al.,* 1998; Earnshaw *et al.,* 1999; Nicholson 1999). To date, 14 mammalian caspases have been identified, a subset of which are involved in apoptosis, while the remainder are involved in processing pro-inflammatory cytokines (Shi 2002). Apoptotic caspases fall broadly into two categories, initiators and effectors. Initiator

caspases, such as caspase-8, -10, and -12 are the first to be activated in response to a death stimulus, which in turn activate the effector caspases, namely caspase-3, -6 and -7. Once activated these caspases mediate cell destruction by degrading a broad range of structural and regulatory proteins. Apoptosis can be initiated from both outside and within the cell, depending on the pro-apoptotic stimulus (Yan *et al.,* 2005). The extrinsic pathway is triggered via the activation of cell surface death receptors, e.g., Fas (or CD95) receptor and the tumour necrosis factor receptor 1 (TNFR1), which in turn activates caspase-8 within the cell. The intrinsic pathway can be activated by a variety of stimuli, including UV light, chemotherapeutic agents or growth factor deprivation, which triggers mitochondrial outer membrane permeabilisation (MOMP), releasing cytochrome-*c* and pro-apoptotic factors such as Smac/DIABLO. MOMP is a central event in cell death, and is tightly regulated by the Bcl-2 family of proteins, comprising both pro- and anti-apoptotic members. An intrinsic pathway that centres on the endoplasmic reticulum (ER) has also been identified, where insults that induce ER stress including misfolded proteins and oxidative stress, lead to caspase-12 activation (Rao *et al.,* 2001).

Additionally, programmed cell death (PCD) can occur independent of caspase activation, so called caspase-independent cell death, where dying cells contain several of the morphological characteristics of apoptosis (Leist *et al.,* 2001; Kroemer *et al.,* 2005). Alternative proteases, including cathepsin B, calpains and serine proteases such as granzyme B, have been shown to mediate caspase-independent cell death via several pathways (Leist *et al.,* 2001). Calpains are a family of ubiquitously expressed calcium-dependent cysteine proteases, comprising at least 15 members, the best characterised of which are μ– and m-calpain (Goll *et al.,* 2003). These proteases have been implicated in the pathogenesis of cell death in cerebral ischaemia (Rami 2003), cataract formation (Takeuchi *et al.,* 2001), neurodegenerative disorders including Huntington's disease (Gafni *et al.,* 2002) and retinal degenerations (Donovan *et al.,* 2002; Sharma *et al.,* 2004). Calpains are activated in response to elevated levels of intracellular calcium, which is associated with neurodegenerative disorders (Sattler *et al.,* 2000; Arundine *et al.,* 2003). Although the role of calpains remains to be fully understood, like the

caspases, calpains degrade intracellular proteins, including cytoskeleton proteins, such as actin and spectrin, transcription factors and growth factor receptors (Saido *et al.*, 1994). Elucidating the role of calpains is further complicated by studies demonstrating cross-talk between the two proteolytic systems of caspases and calpains, including the activation of caspase-3 and -12 by calpain (Nakagawa *et al.*, 2000; Blomgren *et al.*, 2001). Programmed cell death is clearly a complex process, involving at least one type of protease, the activation of which is likely to be dependent on critical factors such as cell type and cell death stimulus. Understanding the molecular pathways that lead to cell death may facilitate the design of effective therapeutic strategies for diseases such as RP, where programmed cell death is associated with pathogenesis.

1.2.9 Pathways to photoreceptor degeneration

Although the genetics of RP are well characterised, much remains to be learned about the pathways between the primary mutation and final photoreceptor degeneration. It is unlikely that each RP mutation initiates an equivalent number of separate cell death pathways, so what is more probable is that such events converge and progress via one, or a limited number of cell death cascades. As rhodopsin is one of the most commonly mutated genes in adRP, understanding how cell death is initiated by these mutations has been a major focus of research (Briscoe *et al.*, 2004). Various models have been proposed to explain the underlying mechanisms of degeneration, which involve dominant-negative and/or gain-of-function activities, as none of the adRP disease alleles appear to be null mutations. In addition, heterozygous rhodopsin-knockout mice do not show significant photoreceptor degeneration (Humphries *et al.*, 1997).

One group of rhodopsin mutants, referred to as Class II, have been shown to misfold and accumulate in the ER when expressed in cell culture (Sung *et al.*, 1991; Kaushal *et al.*, 1994; Illing *et al.*, 2002). *In vivo* this may result in chronic ER stress and the induction of the unfolded protein response (UPR) (Rutkowski *et al.*, 2004). In a recent study, Galy *et al.* demonstrated that in a *Drosophila* model of retinal degeneration, mutant rhodopsin accumulated in the ER resulting in the activation of UPR associated MAPK kinases, p38 and JNK (Galy *et al.*, 2005). Further evidence supporting this

model is provided by a study investigating the mechanism another adRP gene, *CA4*, which encodes for carbonic anhydrase IV, which showed that expression of the mutant protein in COS-7 cells, led to the up-regulation of a number of proteins associated with ER stress including an ER stress chaperone, BiP, a proapoptotic transcription factor, CHOP and an ER stress-inducible kinase, PERK (Rebello *et al.,* 2004). While the pathways from these signalling molecules to cell death remain to be elucidated, ER stress is likely to be involved in some cases of photoreceptor degeneration in adRP.

Another mechanism that has been suggested is defective trafficking of rhodopsin (Sung *et al.,* 1994; Chuang *et al.,* 2004). Arg135Leu rhodopsin mutations are associated with a severe form of adRP (Ponjavic *et al.,* 1997). Arg135Leu mutants expressed *in cellulo* were shown to bind with high affinity to arrestin, a protein of the visual transduction cascade (Chuang *et al.,* 2004). Furthermore, these rhodopsin-arrestin complexes were internalised by intracellular vesicles, in a process known as endocytosis, which has an essential role in normal cell homeostasis. *In vivo*, a disruption to endocytotic processes such as nutrient uptake and iron transport may result in photoreceptor degeneration. In the case of impaired nutrient uptake for example, given that the retina is one of the most metabolically active tissues in the body (Yu *et al.,* 2001), a reduction in the supply of ATP may result in critical cell damage, initiating photoreceptor degeneration.

While studying the biochemical effects of rhodopsin mutations *in cellulo* or using *Drosophila* models is informative, the relevance to photoreceptor degeneration in the mammalian retina must be considered. Animal models of rhodopsin-associated RP have been used to investigate the mechanisms of cell death. For example, in the retina of transgenic pigs carrying the Pro347Leu rhodopsin mutation, abnormal rhodopsin localisation was observed together with aggresomes of misfolded rhodopsin (Petters *et al.,* 1997; Li *et al.,* 1998). However, much of the present knowledge of *in vivo* pathways of degeneration has been generated from light-induced models of photoreceptor cell death (Reme *et al.,* 1998; Wenzel *et al.,* 2001; Donovan *et al.,* 2002). One of the significant advantages of this model is that cell death is synchronised and rapid, so key molecules may be more readily identified compared to the slower

photoreceptor degeneration in many inherited genetic models. An example of a signalling molecule that was studied using light-induced degeneration is c-Fos, a component of the proapoptotic transcription factor AP-1 (Smeyne *et al.,* 1993). After abnormal expression of the *c-fos* gene was observed in the *rd* model of retinal degeneration, the role of *c-fos* was further investigated. *c-fos* -/- mice, exposed to light were shown to be completely protected from photoreceptor degeneration (Hafezi *et al.,* 1997), suggesting the possible involvement of AP-1 in light-induced cell death. However, knocking out *c-fos* in two models of inherited degeneration, the *rd* and *Rho-/-* models, was not found to be protective (Hafezi *et al.,* 1998; Hobson *et al.,* 2000), indicating that *c-fos* is not significantly involved in photoreceptor degeneration for at least these inherited models.

Although this result does question the relevance of light-induced apoptosis to genetic models of retinal degeneration, using light-induced models does help in studying of mechanisms of retinal cell death. For example, a study by Hao *et al.* demonstrated that two different pathways of apoptosis were induced by light in knockout mice with defects in the phototransduction pathway (Hao *et al.,* 2002). Exposure to low levels of light resulted in apoptosis that was dependent on transducin, an essential protein in phototransduction, indicating that light-activated rhodopsin was a necessary component of this cell death pathway. This result supports the so-called "equivalent light hypothesis" (Lisman *et al.,* 1995), which proposes that mutations that result in defective rhodopsin deactivation leads to retinal degeneration (Yamamoto *et al.,* 1997; Khani *et al.,* 1998). In contrast, bright-light induced apoptosis independent of transducin accompanied by induction of AP-1. This study clearly highlights the complexity of photoreceptor degeneration and using both light and inherited models of degeneration, should continue to aid in the elucidation of the mechanisms of these pathways.

1.2.10 Therapeutic strategies for RP

1.2.10.1 Targeting apoptosis

Photoreceptors have been demonstrated to die by a common pathway of apoptosis, hence inhibiting cell death represents a potential therapeutic strategy for treating RP, including adRP. As such an approach is independent of the primary genetic mutation, inhibiting apoptosis offers the potential of overcoming the considerable genetic heterogeneity inherent in RP. As results from studies have demonstrated that caspases are activated in photoreceptor degenerations, caspase inhibition has been explored as a potential therapeutic strategy. For example, there is substantial evidence to support the activation of caspase-3 in various animal models of retinal degeneration, including the *rd* mouse (Kim *et al.,* 2002; Sharma *et al.,* 2004), the rhodopsin mutant rat (Liu *et al.,* 1999) and the *tubby* mouse (Bode *et al.,* 2003). Although there is significant evidence to support caspase-3 activation, the impact of caspase-3 ablation in knockout mice has been shown to provide only minimal protection against photoreceptor degeneration in the *rd* mouse model (Zeiss *et al.,* 2004). Caspase-3 is an effector caspase, thus it is activated downstream of mitochondrial outer membrane permeabilisation (MOMP), a critical event in apoptosis, which is suggested to be irreversible (Green *et al.,* 2004). Targeting caspases upstream of MOMP, using the pan-caspase inhibitor p35 has been demonstrated to be more effective at inhibiting apoptosis in models of retinal degeneration.

p35 is a pan-caspase inhibitor that targets both initiator (caspase -2, -8, -10) and effector (caspase-3, -6, -7) caspases (Bump *et al.,* 1995; Xue *et al.,* 1995; Zhou *et al.,* 1998) and was originally identified in the *Autographica californica* nucleopolyhedrovirus (AcNPV) (Clem *et al.,* 1991; Clem *et al.,* 1994). The expression of p35 in mammalian cells was shown to effectively block apoptosis induced by a variety of signals, such as nerve growth factor withdrawal, ionising radiation and Fas ligation (Beidler *et al.,* 1995; Martinou *et al.,* 1995; Datta *et al.,* 1997). Hence, p35 has been evaluated as a therapeutic agent for inhibiting apoptosis, which contributes to many disease pathologies: examples include diabetes (Hollander *et al.,* 2005), cerebral ischaemia (Shibata *et al.,* 2000) and spinal cord injury (Tamura *et al.,* 2005). With

regard to retinal degeneration, p35 expression has been shown to rescue photoreceptor degeneration in *Drosophila* models of retinal degeneration (Davidson *et al.,* 1998; Alloway *et al.,* 2000; Galy *et al.,* 2005). Furthermore, p35 has also been shown to protect against chemical-induced apoptosis in the cone photoreceptor cell line, 661W, in this laboratory (Tuohy *et al.,* 2002). Hence, there was a clear rationale to continue exploring the anti-apoptotic potential of this effective inhibitor of photoreceptor cell death using primary retinal systems and animal models. Chapter 5 describes the evaluation of the potential protective effect of p35 expression against chemical-induced apoptosis in cultured retinal explants from wild-type (wt) C57BL/6J animals. To further assess the therapeutic potential of p35 *in vivo*, a conditional Cre/*lox*P transgenic model of p35 was obtained from Professor Masayuki Miura (Department of Genetics, University of Tokyo, Japan) and is discussed in Chapter 5 (also see 1.2.11.2).

Another group of caspase inhibitors, first identified in baculoviruses (Crook *et al.,* 1993), are the inhibitor of apoptosis proteins (IAPs), of which eight mammalian members are known to date (Yan *et al.,* 2005). IAPs contain one to three cysteine-based motifs of approximately 65 amino acids known as baculoviral IAP repeats (BIRs), and many also have a RING zinc-finger protein motif. The best characterised member of the IAPs is X-chromosome-linked IAP, XIAP, which has been demonstrated to inhibit caspase-3, -7 and -9 *in vitro* (Deveraux *et al.,* 1997) and *in cellulo* (Duckett *et al.,* 1996; Deveraux *et al.,* 1998). Hence, XIAP has been evaluated as a therapeutic anti-apoptotic agent for a number of disorders including forebrain ischaemia (Xu *et al.,* 1999), diabetes (Emamaullee *et al.,* 2005) and glaucoma (McKinnon *et al.,* 2002). Two other IAPs with similar caspase specificity to XIAP are c-IAP-1 and c-IAP-2 (Roy *et al.,* 1997; Deveraux *et al.,* 1998). Following the successful evaluation of p35 using 661W cone photoreceptor cells by Tuohy *et al.*, all three IAPs were assessed as potential protective agents against apoptosis: results from the study are described in Chapter 3. Although XIAP was found to only modestly protect against apoptosis in 661W cells in the current study described in Chapter 3, results from a recent study demonstrated structural and functional photoreceptor protection against chemical-induced retinal

degeneration in Sprague-Dawley rats using adeno-associated viral (AAV) vector delivery of XIAP (Petrin *et al.,* 2003).

1.2.10.2 Alternative targets in programmed cell death

While caspase activation has been demonstrated in models of retinal degeneration, a number of other studies support the case for caspase-independent mechanisms of photoreceptor cell death (Donovan *et al.,* 2002; Doonan *et al.,* 2003; Zeiss *et al.,* 2004; Sharma *et al.,* 2004). This may be explained by the use of different retinal degeneration models, which may have subtle differences in programmed cell death pathways and by possible cross-talk between the different protease systems. As outlined above in 1.2.8, calpains, an alternative group of proteases, have been shown to interact with caspases. One study demonstrated that caspase-3 and calpain were activated in the *rd* mouse model of retinal degeneration (Sharma *et al.,* 2004; Paquet-Durand *et al.,* 2006). The *rd* mouse carries a recessive mutation in the β subunit of cGMP phosphodiesterase, involved in the phototransduction cascade (Bowes *et al.,* 1990). The resulting decrease in cytoplasmic cGMP concentration leads to the opening of cGMP-gated channels and intracellular levels of ions, particularly calcium, increase significantly (Fox *et al.,* 1999). To further investigate the mechanisms of photoreceptor degeneration, in the same study by Sharma *et al.,* cell death was induced by calcium in 661W cone photoreceptor cells, to mimic the *in vivo* scenario in the *rd* retina, and shown to be caspase-3 and calpain dependent. Analysis of other possible key molecules involved in this pathway, revealed that there was an increase in the cleavage of Bid, a pro-apoptotic protein and a collapse of mitochondrial membrane potential, followed by a release of cytochrome-*c*. Furthermore, a calpain inhibitor was shown to block these events and protect the 661W cells from calcium-induced cell death, suggesting a possible therapeutic strategy for retinal degenerations.

In another study, activation of calpain was again observed in the *rd* mouse model, accompanied by the cleavage of calpastatin, an endogenous inhibitor of μ– and m-calpain (Doonan *et al.,* 2005). Interestingly, the activation of cathepsin D, an aspartyl protease was also demonstrated. However, treatment of *rd* retinal explants with a

calpain inhibitor did not protect against photoreceptor degeneration, suggesting that multiple components of the cell death pathways may need to be targeted to successfully inhibit photoreceptor degeneration. What is apparent is that elucidation of the mechanisms underlying photoreceptor degeneration, are revealing the complexity of the cell death pathways. Increasing our understanding of these mechanisms will likely aid in designing effective therapeutic strategies and it was with this aim in mind, that the conditional gene targeting strategy described in Chapter 4 was undertaken, discussed further in 1.2.11.2. In principle, the transgenic mouse with a *lox*P-flanked p35 gene described in Chapter 4 provides an opportunity to explore the anti-apoptotic effects of p35 expression in rod or cone photoreceptor cells.

In addition to modulating photoreceptor cell death, other therapeutic strategies for RP include promoting photoreceptor survival using neurotrophic factors (Tao *et al.,* 2002; Lawrence *et al.,* 2004; Leveillard *et al.,* 2004), or replacing lost photoreceptor cells by retinal transplantation (Lund *et al.,* 2003) or stem cell therapy (Ahmad 2001). As a review of these areas is beyond the scope of this thesis, refer to the recent papers indicated.

1.2.10.3 Targeting primary genetic mutations

Therapies targeting the primary mutations implicated in RP, will likely involve either delivery of the wild-type gene for autosomal recessive RP (arRP) or alternatively some form of suppression of the mutant gene for autosomal dominant RP (adRP). There have been notable successes in the treatment of arRP and other recessive retinal degenerations, including Leber congenital amaurosis (LCA). Results from these studies have demonstrated that delivery of wt genes including the *rds*-peripherin gene to the *rds* mouse (Ali *et al.,* 2000; Schlichtenbrede *et al.,* 2004) and the *Mertk* gene to the Royal College of Surgeon rat model of retinal degeneration (Smith *et al.,* 2003; Tschernutter *et al.,* 2005) resulted in photoreceptor cell rescue and a preservation of photoreceptor structure. LCA is an early onset retinal degeneration, effecting both rod and cone photoreceptors, and mutations in RPE65, a retinal isomerohydrolase expressed in the RPE (Moiseyev *et al.,* 2005), are responsible for approximately 10-

15% of LCA cases. Photoreceptor cell rescue has been shown in a $RPE65^{-/-}$ canine model of LCA, by viral delivery of the *RPE65* gene (Acland *et al.,* 2001; Narfstrom *et al.,* 2003). Most recently, Pawlyk *et al.* rescued photoreceptors in a mouse model of LCA by delivery of the *RPGRIP* gene, another gene associated with LCA, which codes for a photoreceptor structural protein.

With respect to adRP, targeting primary mutations presents a formidable challenge, as it involves suppression of the mutant gene by tools such as ribozymes or RNA interference (RNAi), in addition to maintaining expression of wild-type gene. Multiple mutations have been encountered in adRP disease-causing genes, such as *rhodopsin* or *rds*-peripherin, thus targeting each individual mutation will likely not be feasible. Mutation-independent based therapeutic strategies, previously developed in the laboratory, represent a possible approach to overcoming the challenge of mutational heterogeneity in adRP (Millington-Ward *et al.,* 1999; O'Neill *et al.,* 2000; Kiang *et al.,* 2005; Palfi *et al.,* 2006).

One strategy involves targeting untranslated regions of the transcript (UTRs), so both the mutant and wt alleles are suppressed. This approach is mutation-independent and so in principle, could suppress transcripts from many mutated genes. Notably, in conjunction with suppression, a wt replacement gene is provided whose sequence has been altered in the UTRs, thereby protecting the transcripts from suppression. A second approach utilises suppression agents targeting the coding sequence and exploits the degeneracy of the genetic code, i.e. a single amino acid may be encoded by more than one codon. Again the suppression agent suppresses both mutant and wt alleles, and the replacement gene is protected from suppression by altering the sequence around the target site. As sequence changes are made at third base wobble positions, the replacement gene still encodes a wild-type protein. Finally a third strategy exploits intragenic polymorphisms that occur frequently in the genome. By targeting such polymorphisms, instead of individual mutations, a potential gene therapy may be applicable to a larger number of patients (Millington-Ward *et al.,* 1999; Millington-Ward *et al.,* 2002). Millington-Ward *et al.* and O'Neill *et al.* demonstrated the

successful suppression of a number of photoreceptor-specific transcripts *in vitro*, using these mutation-independent based therapeutic approaches. Most recently, Kiang *et al.* showed the downregulation of rhodopsin *in cellulo* and *in vivo*, using an RNA interference (RNAi)-based mutation-independent approach, establishing the validity of this strategy for treating adRP.

1.2.11 Transgenic animal models

1.2.11.1 Introduction

Animal models for human disease are important for understanding the pathways from genetic mutations to the resulting disease pathology, which in addition can lead to the identification of novel therapeutic targets. These same models can be used to evaluate the efficacy of new therapies, before possibly progressing toward clinical trials in humans. While there are several naturally occurring models for recessive RP, including the well-characterised retinal degeneration slow (*rds*), retinal degeneration (*rd*) mouse models, there are no comparable models for adRP (Chader 2002). Rapid developments in genetic engineering over the last 20 years have made it possible to generate animal models of many human diseases, including adRP. Transgenic models can be generated either by direct pronuclear injection of DNA into fertilized zygotes (Wagner *et al.*, 1981) or injection of genetically modified embryonic stem (ES) cells into blastocysts (Thomas *et al.*, 1987). The first technique is limited in its application as it depends on the over-expression of the randomly inserted DNA to produce a disease phenotype. However, application of this method has enabled the generation of many transgenic mouse models of adRP expressing genes, such as rhodopsin with dominant mutations of Pro23His (Olsson *et al.*, 1992), Thr17Met (Li *et al.*, 1998b) and Pro347Ser (Li *et al.*, 1996).

The second technique, known as gene targeting, employs homologous recombination, where designed targeting constructs recombine with the endogenous gene in ES cells, and was first reported in 1987 (Doetschman *et al.*, 1987; Thomas *et al.*, 1987). With advances in genetic engineering technology, it is now possible to engineer site-specific modification of the genome, ranging from single base-pair changes to deletion of entire

genes. Gene targeting has been used to generate transgenic mouse models of adRP including for example a model carrying a single base pair deletion at codon 307 of the *rds* gene (*rds*-307) (McNally *et al.,* 2002). Transgenic adRP models generated by random integration or gene targeting such as the Pro23His and *rds*-307 models are valuable tools for elucidating mechanisms of disease pathology and evaluating therapeutic strategies. The transgenic models described so far, carry mutations in photoreceptor specific genes such as rhodopsin and peripherin, but to explore the role of some non-photoreceptor specific genes in photoreceptors, conditional gene expression is required.

1.2.11.2 Conditional gene expression

Advances in genetic engineering techniques have made it possible to modify genes in a tissue or temporal specific manner, known as conditional gene expression (Muller 1999). This approach is useful as deleting a gene or expressing a transgene in all tissues of the animal may result in embryonic lethality. There are two main techniques, transcriptional transactivation, and site-specific recombination (van der Weyden *et al.,* 2002). Several transcriptional transactivation systems have been described, but the most widely used is the tetracycline-dependent regulatory system (Figure 1.4). It is composed of two elements: 1) the target gene under the control of a tetracycline responsive element (TRE), which is activated by a tetracycline-dependent transactivator (tTA), and 2) a plasmid expressing tissue-specific tTA. In the presence of tetracycline, tTA does not bind to TRE inactivating expression of the target gene (tet-off). A complementary approach was developed using a mutated tTA known as reverse tTA (rtTA), which binds TRE in the presence of tetracycline (tet-on), activating expression of the target gene. Transgenic mouse models with rod photoreceptor-specific expression of tTA and rtTA have been generated allowing activation and inactivation of target genes in a tissue-specific and temporal manner (Chang *et al.,* 2000; Angeletti *et al.,* 2003). The tetracycline-inducible system has been used in the development of transgenic models for numerous diseases, including Huntington's disease (Tanaka *et al.,* 2005), chronic myeloid leukemia (Huettner *et al.,* 2003) and proliferative retinopathy (Nambu *et al.,* 2005).

The second main technique for conditional gene expression is site-specific recombination. Essentially this system comprises a recombinase enzyme and its target sequence. Examples of two such systems are Cre recombinase-*lox*P and Flp recombinase-*FRT*. Cre recombinase, derived from the bacteriophage P1, is the most widely used recombination system. Cre binds and cleaves DNA at conserved 34 bp recognition sequences, known as *lox*P sites (Figure 1.5: A). The number and position of *loxP* sites in the transgene determine the type of genetic modification: excision, inversion or translocation. For example, if two *lox*P sites in the same orientation flank the target gene, Cre recombinase activity excises the region between the *lox*P sites, resulting in deletion of the target gene (Figure 1.5: B1).

To generate transgenic models with tissue-specific activation or deletion of genes using the Cre-*lox*P system, two lines of animals are required: one with Cre recombinase expression driven by a tissue-specific promoter and a second carrying the transgene flanked by *lox*P sites. Crossing of these two lines should result in an F1 transgenic model with tissue-specific target gene deletion or activation, catalysed by Cre activity at the *lox*P sites. Alternatively Cre recombinase can be delivered directly to the transgenic model carrying the *lox*P-flanked transgene using viral vectors such as adeno-associated viral (AAV) vectors, allowing temporal control of gene activation or deletion.

The Cre-*lox*P system is widely used in generating transgenic models for investigating the function of genes, the underlying pathologies of human disease and the evaluation of potential therapeutic strategies for these diseases. Tissue-specific gene modification has allowed the generation of more accurate animal models of disease and the targeting of genes that would not have been previously possible using conventional gene targeting techniques due to embryonic lethality. Examples of transgenic disease mouse models generated by conditional gene targeting include models for prostrate cancer (Maddison *et al.*, 2004), acute myeloid leukemia (Higuchi *et al.*, 2002) and Parkinson's disease (Drago *et al.*, 1998).

To further explore the mechanisms of photoreceptor degeneration in RP, including adRP and investigate novel therapeutic approaches, transgenic models allowing photoreceptor specific gene targeting would be valuable tools. One of the goals of this PhD project was to generate constructs enabling the generation of transgenic mouse models with rod and cone photoreceptor-specific expression of Cre recombinase. This work is described in Chapter 4 together with a review of transgenic models with retinal specific expression of Cre recombinase, which have become available since the initiation of this project.

1.3 p53-Related Cancer

1.3.1 Introduction

There are two gene therapy approaches for treating genetic diseases: targeting the primary genetic mutation, or modulating a secondary effect associated with disease pathology. Targeting a common pathway such as apoptosis in RP, including adRP, potentially provides a means of overcoming the mutational heterogeneity associated with adRP and other Mendelian disorders (Farrar *et al.,* 2002). Chapters 3, 4 and 5 of this thesis describe the evaluation of therapeutic strategies to inhibit photoreceptor apoptosis in adRP, which may indeed be applicable to other retinal degenerations. Given this mutational heterogeneity, strategies targeting the primary genetic mutation in a mutation-independent manner have been developed in our laboratory (also see 1.2.10.3 above) (Millington-Ward *et al.,* 1997; O'Neill *et al.,* 2000). Furthermore, in recent years, it has become evident that dominant mutations contribute to the pathology of multi-factorial diseases, including p53-related cancer, Alzheimer's disease (AD) and neurofibromatosis (Farrar *et al.,* 2002). Thus, it was considered that the mutation-independent suppression/replacement gene therapy approaches described in 1.2.10.3 above, for treating adRP, could potentially be applied to treat such disorders.

p53 is a tumour suppressor protein mutated in approximately 50% of human cancers (Hollstein *et al.,* 1991) and as such is an important therapeutic target for anti-cancer strategies (Hupp *et al.,* 2000; Lane *et al.,* 2002). As results from a number of studies have demonstrated that many p53 mutations act in a dominant-negative manner

(Dittmer *et al.,* 1993; Liu *et al.,* 2000; de Vries *et al.,* 2002), targeting p53 using gene suppression/replacement strategies represents a novel therapeutic approach to treating p53-related cancer. Chapter 6 describes a study evaluating a mutation-independent approach to cleaving the p53 transcript using ribozymes as a suppression tool.

1.3.2 p53 tumour suppressor protein

The p53 tumour suppressor protein, often referred to as the "guardian of the genome", (Lane 1992) is a 53kDa transcription factor that induces senescence, cell-cycle arrest or apoptosis, in response to cellular stresses such as UV light, chemotherapeutic agents, hypoxia or DNA damage (Levine 1997; Volgelstein *et al.,* 2000; Vousden *et al.,* 2002; Oren 2003). Through these activities, p53 prevents the proliferation of damaged or mutated cells, which otherwise may lead to tumour development. Cellular response pathways to stress are complex, with several factors influencing whether p53 mediates cell-growth arrest or apoptosis, including cell type, the type of stress-signal, and p53 expression levels (Sionov *et al.,* 1999; Balint *et al.,* 2001). Under normal conditions, p53 protein is maintained at a low level by E3 ubiquitin ligases, including MDM2, that bind p53, targeting it for degradation (Oren *et al.,* 2003; Lu *et al.,* 2005). In response to stress, p53 levels are mainly increased at the protein level through the inhibition of MDM2 by proteins such as $p14^{ARF}$ and post-translational modifications that stabilise p53 (Vousden *et al.,* 2002; Lu *et al.,* 2005). To date approximately 100 target genes of p53 have been identified, and expression analyses have revealed many more potential p53-binding sites in the genome, thus highlighting the complexity of the signaling pathways mediated by the p53 protein (Zhao *et al.,* 2000; Lu *et al.,* 2005). Examples of target genes include *p21Waf1/Cip1* (el-Deiry *et al.,* 1993; Harper *et al.,* 1993) encoding an enzyme that is involved in controlling cell division, and pro-apoptotic genes, *Bax* and *Noxa* (Thornborrow *et al.,* 2002; Oda *et al.,* 2000). Considering the critical functions of p53, it is conceivable that mutated p53 may result in uncontrolled cell proliferation or the survival of damaged cells with oncogenic potential.

1.3.3 p53 Mutations

The genetic heterogeneity of p53-related cancer is considerable, with approximately 1,300 different mutations identified to date (Soussi *et al.,* 2001; Soussi *et al.,* 2005).

p53 mutations are catalogued in a number of databases including the International Association of Cancer Registries database (http://www.iarc.fr/p53), and the p53 web site (http://www.p53.curie.fr). The majority of these mutations (71%) are missense, resulting in single amino acid changes to the DNA binding core of the p53 protein (Brachman 2004) (Figure 1.6). These alterations result in a misfolded protein and/or alter sites that directly contact DNA which are essential for the transcriptional activation function of p53. A number of sites in the DNA binding domain of the protein are frequently mutated and so are referred to as "hotspot" mutation sites. Examples include arginine to histidine mutations at codons 175 and 273, and glycine to serine at codon 245 of the p53 protein (Hollstein *et al.*, 1991).

As a result of partial or complete impairment of DNA binding by the mutated p53 protein, there is a loss of cell cycle control, and an increased resistance to apoptosis (Lu *et al.*, 2003). Furthermore, p53 functions as a tetrameric protein, so the activity of the remaining wild-type p53 can be adversely affected by oligomerisation with mutant p53 protein, as illustrated in Figure 1.7. This dominant-negative effect of mutant p53 has been demonstrated *in cellulo* (Kern *et al.*, 1992; de Vries *et al.*, 2002) and in experimental animal models (Harvey *et al.*, 1995; Liu *et al.*, 2000). Harvey *et al.* demonstrated that transgenic expression of a mutant p53 gene (Ala135Val) in p53-deficient mice ($p53^{+/-}$) resulted in enhanced tumour progression. Several studies have also shown that p53 mutants may have a "gain of function" effect, independent of wild-type p53, which may contribute to tumour progression (van Oijen *et al.*, 2000; Tsang *et al.*, 2005). Mutant p53 can induce overexpression of the multiple drug resistance oncogene (*MDR1*), and bind the pro-apoptotic protein Daax, inhibiting a pathway of apoptosis (Dittmer *et al.*, 1993; Ohiro *et al.*, 2003). Another p53 family member, p73, that also plays an essential role in cellular response to stress (Flores *et al.*, 2002), has been shown to be inhibited by mutant p53 (di Como *et al.*, 1999). While these studies demonstrate the dominant-negative function of some p53 mutants in cancerous cells, the function and regulation of mutant p53 still remains to be fully understood.

1.3.4 Therapeutic strategies

There is a clear rationale for targeting and suppressing the mutant p53 gene to inhibit tumour growth, in parallel with wt gene replacement. Furthermore, individuals with p53 mutations often show a poor clinical response to chemotherapeutic agents and γ-radiation treatment (Soussi *et al.,* 2001; Iacopetta 2003; Tweddle *et al.,* 2001), so a restoration of wt p53 activity could potentially result in an improved response to standard cancer treatment: Currently, the principle gene therapy strategy for restoring p53 function is delivery of wt p53 to cancerous cells. Studies have demonstrated that expression of wt p53 in cancer cell lines and animals models reduces tumour growth, through a restoration of normal p53 activity (Fujiwara *et al.,* 1994a; Hsiao *et al.,* 1997; Logunov *et al.,* 2004; Irie *et al.,* 2005). Logunov *et al.* showed that adenoviral (Ad) vector delivery of wt p53 to a nude mouse model with an epithelial carcinoma, resulted in tumour regression and a restoration of p53 activity. Furthermore, there are a number of ongoing current clinical trials evaluating Ad delivery of wt p53 as a treatment for non-small cell lung cancer and carcinoma of the head and neck (listed at: http://www.wiley.co.uk/genmed/clinical/). One adenoviral vector delivered p53 gene, known as INGN-101, has been evaluated in several published clinical trials, which have reported a good response in patients with non-small cell lung cancer (Swisher *et al.,* 1999; Nemunaitis *et al.,* 2000; Swisher *et al.,* 2003): see 1.5.3.5 for more details.

Although introducing a wt p53 gene is a reasonably effective therapeutic strategy, it does not address the dominant-negative effect of many p53 mutant genes. The genetic heterogeneity of p53 mutations makes targeting the mutant p53 gene a challenge. A number of papers have evaluated RNAi as a strategy to downregulate mutant p53 expression (Martinez *et al.,* 2002; Shen *et al.,* 2003) using small interfering RNA (siRNA) or short hairpin RNA (shRNA) expressing constructs (see 1.4.4). Martinez *et al.* demonstrated that siRNA targeting a known dominant-negative mutant, Arg248Trp, *in cellulo*, suppressed mutant p53 expression and restored wt p53 activity. Significantly the siRNA targeted the mutant p53 specifically and did not suppress the endogenous wt p53.

An additional approach is the use of another RNA based tool, namely *trans*-splicing ribozymes. Like the hammerhead ribozymes described in 1.4, *trans*-splicing ribozymes cleave RNA in a sequence specific manner. In addition *trans*-splicing ribozymes replace the sequence downstream of the cleavage site with a new exon sequence. Essentially the ribozyme mediates the repair of the transcript, by replacing the mutated sequence of the gene with the wt sequence. A number of studies have shown repair of the p53 transcript using a *trans*-splicing ribozyme attached to wt p53 sequence (Watanabe *et al.*, 2000; Shin *et al.*, 2004). Shin *et al.* demonstrated that expression of a *trans*-splicing ribozyme in ovarian cancer cell lines, restored wt p53 activity and also observed a significant increase in the expression of the p53 responsive genes, *p21* and *Bax*. In addition expression of the ribozyme also resulted in an increased level of apoptosis, indicating a restoration of p53-responsive pathways. This approach represents a promising therapeutic strategy and could potentially be applied to a large number of p53 mutants, overcoming the obstacle of mutational heterogeneity. Another possible approach to overcoming mutational heterogeneity is described in Chapter 6, which involves the *in vitro* evaluation of hammerhead ribozymes targeting the p53 transcript, using mutation-independent strategies.

1.4 Suppression Tools

1.4.1 Introduction

Targeting the primary genetic mutation by suppressing the expression of the messenger RNA (mRNA) is a possible therapeutic approach for diseases caused either entirely or in part by dominant-negative mutations. Over the last thirty years a number of suppression tools have been developed, including antisense oligonucleotides (Scanlon 2004), DNAzymes (Schubert *et al.*, 2004), peptide-nucleic acids (Phylactou 2000), hairpin ribozymes (Puerta-Fernandez *et al.*, 2003) and RNAi (Leung *et al.*, 2005). A number of these technologies are reviewed in the following section, with a particular focus on hammerhead ribozymes.

1.4.2 Antisense oliognucleotides (ASO)

1.4.2.1 Introduction

Antisense molecules are composed of single-stranded oligodeoxynucleotides, usually 12-28 bases, which act by binding complementary target mRNA, resulting in the inhibition of mRNA processing or translation (Jansen *et al.,* 2002; Patil *et al.,* 2005). In addition the antisense molecule forms a heteroduplex with the mRNA, which can be degraded by RNase H. ASOs were the earliest suppression tool to be developed and Zamecnik and Stephenson first demonstrated this approach almost thirty years ago by showing that targeting the Rous sarcoma virus using an ASO, blocked viral replication in chicken fibroblasts (Zamecnik *et al.,* 1978). Following this discovery, the technology rapidly developed, dominating the suppression field for a number of years but on failing to fulfil expectations in clinical trials, the focus gradually moved to other suppression tools, including ribozymes and more recently, RNAi. However, a number of companies continued developing ASOs and recent improvements in delivery combined with the generation of more biologically stable ASOs indicate that this technology may yet prove to be more successful than originally predicted.

1.4.2.2 Therapeutic applications

Antisense therapy is being developed for a range of diseases, including cancer (Badros *et al.,* 2005), ulcerative colitis (Myers *et al.,* 2003) and cardiovascular disease (Crooke *et al.,* 2005). Currently there is one antisense drug available on the market, which was approved by the Food and Drug Administration in 1998. The drug, known as Vitravene, is produced by Isis Pharmaceuticals and used for treating cytomegalovirus retinitis associated with HIV infection (Crooke 1998). Isis is evaluating a number of other antisense molecules, including ISIS 2302, that targets intracellular adhesion molecule 1 (ICAM-1), involved in inflammation. Although the results from a Phase III clinical trial to treat patients with Crohn's disease were disappointing, ISIS 2302 will being assessed as a potential therapeutic for ulcerative colitis in Phase III clinical trials (www.isispharm.com).

Antisense molecules targeting genes involved in cancer are also being developed. One target is the anti-apoptotic *bcl-2* gene, a member of the Bcl-2 family of proteins, which is overexpressed in many types of cancer (Selzer *et al.,* 1998). Genasense, produced by Aventis and Genta, is an oligonucleotide of 18 modified DNA bases which has been evaluated in Phase III trials for patients with chronic lymphocytic leukaemia and malignant melanoma with a modest response reported (Chanan-Khan *et al.,* 2004). A multi-centre clinical Phase I/II study began in May 2005 with another ASO targeting Bcl-2, SPC2996, produced by Santaris (www.santaris.com). SPC2996 is based on nucleic acid analogs known as locked nucleic acids (LNA), which have a higher binding affinity for their targets and longer half-lives than unmodified nucleotides, so it may be potentially more effective than Genasense (Kumar *et al.,* 1998). Bcl-xL is another member of the Bcl-2 family of proteins, which is often coexpressed with Bcl-2 in many tumours (Jansen *et al.,* 2002). In preclinical studies, a novel bispecific ASO targeting Bcl-2 and Bcl-xL was demonstrated to induce apoptosis and enhance chemosensitivity in a number of cancer cell lines (Zangemeister-Wittke *et al.,* 2000; Yamanaka *et al.,* 2005).

The future for ASO technology appears considerably brighter than a decade ago and this was most recently reflected in the first meeting of the Oligonucleotide Therapeutics Society in September of 2005, which focused both on ASOs and siRNAs (http://www.nyas.org/ebriefreps/splash.asp?intEbriefID=441). However, for the project described in Chapter 6 of this thesis, using ASO technology is not a suitable approach as ASOs are less specific compared to ribozymes or siRNA, which can discriminate between transcripts with a single base change. Thus, this approach is not suitable for diseases such as adRP and p53-related cancer, where the aim is to suppress the expression of the mutant transcript, and introduce a modified wild-type transcript that is protected from suppression.

1.4.3 Ribozymes

1.4.3.1 Introduction

Ribozymes are RNA molecules with enzymatic activity capable of site-specific cleavage of target mRNAs. Thomas Cech and his colleagues first coined the term in 1982 to describe the activity of a self-splicing sequence in pre-ribosomal RNA (rRNA) of the ciliate *Tetrahymena* (Kruger *et al.,* 1982). Known as a Group I intron, this natural ribozyme catalyses its own excision from the rRNA, which is followed by ligation of the two flanking exons. This represented a highly significant discovery, as previously it had been believed that proteins were the sole catalytic agents of the cell. Since then many other natural ribozymes have been identified in a diverse range of organisms, involved in essential biological processes such as: 1) replication of RNA plant viruses (Symons 1992), 2) RNA splicing in bacteria, fungi and yeast (Pyle 1996) and 3) peptide bond formation during translation (Nissen *et al.,* 2000). Furthermore, the ability of ribozymes to catalyse site-specific cleavage of RNA, has been exploited to develop ribozymes as suppression tools used to elucidate gene function and treat genetic diseases. Most ribozymes used as therapeutic agents are based on two types from the small catalytic RNA family: hairpin and hammerhead ribozymes, the latter of which is the focus of this introduction. Hairpin ribozymes have been used less widely as there are more limitations on selecting potential target sites (Earnshaw *et al.,* 1997). For a review of other naturally occurring catalytic ribozymes, refer to the following papers: Doherty *et al.,* 2000, Puerta-Fernandez *et al.,* 2003 and Schubert *et al.,* 2004.

1.4.3.2 Hammerhead ribozymes

The hammerhead ribozyme is one of the best-characterised ribozymes and is found mainly in the plant virus satellite RNAs and plant viroids (Symons 1992). This ribozyme is the smallest of the natural ribozymes, composed of approximately 40 nucleotides, arranged as three base-paired helices with a conserved core (Doudna *et al.,* 2002) (Figure 1.8). As the catalytic domain is located in stem II and the substrate domain in stem III, this is a *cis*-cleavage reaction involving site-specific cleavage by a 2'-hydroxyl group in stem II, generally 3' of a GUC triplet. The discovery that the catalytic and substrate domains were separated in the Avocado sunblotch viroid

(ASBV), led to the development of synthesised *trans*-acting ribozymes, which could be designed to target and cleave specific RNA sequences (Uhlenbeck 1987; Haseloff *et al.,* 1988). Most *trans*-acting ribozymes are composed of a single-stranded, conserved catalytic core (stem II) flanked by two arms complementary to the target sequence, which form stems I and III based on the original design by Haseloff *et al.* (Figure 1.9). Cleavage of the target RNA proceeds by the same mechanism as for naturally occurring hammerhead ribozymes, with a 2'-hydroxyl group in the catalytic core attacking a phosphate group in the target, generating two fragments, one with a 5'-hydroxyl group and the other a 2', 3'-cyclic phosphate group (Fedor *et al.,* 2005). Hammerhead ribozymes require divalent metal ions, such as magnesium (Mg^{2+}) to catalyse the reaction and to stabilise the conformation of the ribozyme-substrate complex (Bassi *et al.,* 1997).

Trans-acting hammerhead ribozymes, like their natural counterparts, cleave target RNA in a site-specific manner. However, mutation studies revealed that *trans*-acting ribozymes cleave at additional sites to GUC, which led to the widely accepted NUX rule that states: a site where N is any nucleotide, U is uracil and X is any nucleotide except guanine, can be cleaved by a hammerhead ribozyme (Ruffner *et al.,* 1990; Shimayama *et al.,* 1995). There is some evidence for a hierarchy of preferred cleavage sites with the most efficient cleavage occurring at GUC and AUC codons (Zoumadakis *et al.,* 1995).

1.4.3.3 Hammerhead ribozyme as gene therapy tools

1.4.3.3.1 Introduction

Site-specific cleavage of RNA by *trans*-acting hammerhead ribozymes (referred to as hammerhead ribozymes hereafter) has been harnessed for therapeutic application and for functional gene studies. The focus of this section is the use of hammerhead ribozymes as suppression tools for disease. For a review of other applications refer to Kato *et al.,* 2004 and Kruger *et al.,* 2001. There are several stages to applying hammerhead ribozymes as therapeutic tools: the first is identifying suitable cleavage sites in target mRNA, whether that is for example a mutated gene contributing to a

carcinoma, a viral gene, for example in hepatitis C (Lee *et al.,* 2000) or a mutated photoreceptor gene resulting in retinitis pigmentosa (Fritz *et al.,* 2004). Following selection of cleavage sites, hammerhead ribozymes targeting these sites are designed, generated and evaluated *in vitro*. Efficient ribozymes are then further evaluated in relevant cell culture and animal models, prior to possible testing in clinical studies.

1.4.3.3.2 Selection of hammerhead ribozyme cleavage sites

Cleavage efficiency at NUX sites depends on the critical factor of accessibility, so sequence flanking the site should be single-stranded to be available for base-pairing with the two antisense arms of the hammerhead ribozyme (Fritz *et al.,* 2004; Citti *et al.,* 2005). However, due to base-pairing within mRNA sequences, the resulting secondary structures are complex and chosen cleavage sites may not be accessible to ribozymes. Indeed, up to 90% of potential cleavage sites have been shown to be inaccessible to suppression tools such as ribozymes (Fritz *et al.,* 2004). There are however a number of different methods for predicting accessibility of these sites. One method involves using computer-modeling programmes to predict mRNA secondary structure, using algorithms based on free energy minimisation parameters derived from experimental cleavage of known simple structures. Examples of programs include Mfold/PlotFold (Zuker *et al.,* 1989; Zuker 2003) and RNAdraw (Matzura *et al.,* 1996), which were used to predict the mRNA secondary structure of the tumour suppressor protein p53 in Chapter 6. The other available methods are experimental and include screening random ribozyme libraries (Lieber *et al.,* 1995) and mapping the accessibility of target mRNA using RNase H (Birikh *et al.,* 1997).

1.4.3.3.3 Hammerhead ribozyme design

Once cleavage sites have been selected, hammerhead ribozymes are then designed to target these sites. Most therapeutic hammerhead ribozymes are based on Haseloff and Gerlach's (Haseloff *et al.,* 1998) original design, which has a conserved catalytic core of 13 nucleotides. The sequences of the flanking arms of the ribozyme change as they determine target specificity and flanking arm length can also vary. Optimal arm length is approximately 6-8 nucleotides: shorter arms result in a loss of specificity and longer

arms in a slower catalytic turnover, as the ribozyme is more strongly hybridised to the target mRNA (Hertel *et al.,* 1994; Hertel *et al.,* 1996). It is also been suggested that ribozymes with asymmetric arms have a higher catalytic turnover than those with symmetric arms (Hendry *et al.,* 1996).

1.4.3.3.4 Hammerhead ribozyme delivery

Following ribozyme design, the next stage in development is to evaluate ribozyme catalytic efficiency for cleaving target mRNA. Ribozymes are usually tested using *in vitro* methods, to select the most efficient ribozymes for further *in cellulo* and *in vivo* evaluation. A widely used method involves expressing radioactively labeled ribozyme and target mRNA from plasmid vectors, undertaking cleavage reactions and resolving the target mRNA cleavage products on a polyacrylamide gel (Millington-Ward *et al.,* 2000; O'Neill *et al.,* 2000; Shaw *et al.,* 2001; Fritz *et al.,* 2004). Although nonradioactive methods are also available including resolution of target cleavage products on high-resolution agarose gels or silver-stained polyacrylamide gels (Liu *et al.,* 2002; Palfner *et al.,* 1995), these methods are not commonly used, as radioactive labelling has been proven to be a sensitive and effective technique for *in vitro* ribozyme evaluation. In Chapter 6, rUTP [α-P^{32}] labeling was used for evaluating ribozymes targeting p53 tumour suppressor mRNA.

The success of ribozymes as therapeutic tools *in cellulo* and *in vivo* depends on several factors including: 1) the amount of active ribozyme present in cells 2) localisation of ribozyme within the cell, 3) catalytic efficiency of the ribozyme and 4) accessibility of the target mRNA cleavage sites (Shiota *et al.,* 2004). Ribozyme concentrations are determined in part by the efficiency of the delivery method used, reviewed in 1.5.2, and the stability of the ribozymes. Ribozymes are rapidly degraded by 3' exonucleases and pyrimidine specific nucleases present in serum (Sproat *et al.,* 1986; Schubert *et al.,* 2004), however they may be protected at least in part by chemical modifications of the 2'-hydroxyl group of ribose or the phosphodiester linkage for example. Substituting 2'-hydroxyl with groups including, 2'-O-methyl, 2'-O-fluoro or 2'-amino groups protects

the ribozyme from degradation, thus prolonging its half-life (Pieken *et al.,* 1991; Beigelman *et al.,* 1995; Usman *et al.,* 2000).

Localisation of the ribozyme to target cells can be controlled using several techniques, including coupling ribozymes to antibodies or ligands that bind cell receptors (Hudson *et al.,* 1999), generating ribozymes that function in an allosteric fashion and designing ribozyme expression constructs with tissue-specific promoters. Allosteric ribozymes have a binding site for target mRNA, which upon binding the mRNA, induces a catalytically favourable conformational change in the ribozyme, thus increasing target cleavage specificity (Porta *et al.,* 1995; Tanabe *et al.,* 2000).

For ribozymes expressed endogenously from plasmid and viral vectors, the choice of promoter can determine their expression levels and subcellular localisation. Polymerase (pol) II and III promoters have been used to drive ribozyme expression (Bertrand *et al.,* 1997; Good *et al.,* 1997). Pol II promoters have the advantage of directing cell-specific expression and resulting RNA transcripts have a 5'-cap and poly (A) tail, enhancing ribozyme stability (Shiota *et al.,* 2004). While pol II promoters are useful for evaluating ribozymes *in vitro* and *in cellulo*, pol III promoters including tRNA and U6 snRNA, which transcribe short RNAs may be more suitable for ribozyme expression *in vivo.* The therapeutic potential of pol III promoters compared to pol II promoters was demonstrated in a recent study which evaluated lentiviral vector delivery of a triple RNA-based gene therapy (shRNA, ribozyme, decoy RNA) targeting three genes involved in HIV-1 infection (Li *et al.,* 2005a). Seven weeks after the infection of a human T cell line with the lentiviral vector, transcripts of a hammerhead ribozyme driven by a pol III promoter were still present, in comparison there was a reduction in pol II promoter-driven EGFP expression, attributed to silencing of the pol II promoter. Although, pol III promoters are not tissue specific, they can be used to direct subcellular localisation of expressed ribozymes, with tRNA and U6 snRNA directing cytoplasmic and nuclear localisation respectively (Kato *et al.,* 2001). It should be noted that pol III promoters have been widely used for expression of another RNA suppression agent, small interfering RNA (siRNA), reviewed in 1.4.4 below.

1.4.3.3.6 Hammerhead ribozyme therapeutic applications

Ribozymes have been used as tools to suppress gene expression for a range of diseases including cancer (Irie *et al.,* 2005), cardiovascular disease (Gu *et al.,* 2001) viral infections (Sun *et al.,* 1995) and autosomal dominant diseases (Millington-Ward *et al.,* 2002). The pathology associated with an autosomal dominant disease results from the expression of a mutant gene, hence one therapeutic approach may be to target the primary genetic defect by ribozyme-mediated gene suppression, while still maintaining expression of the wt gene. In several studies ribozymes have been evaluated as a potential therapy for adRP, and successful *in vitro* and *in vivo* cleavage of mutant photoreceptor gene transcripts has been demonstrated (Lewin *et al.,* 1998; La Vail *et al.,* 2000; O'Neill *et al.,* 2000; Shaw *et al.,* 2001). Viral delivery of a ribozyme targeting mutant rhodopsin to a transgenic rat model of a retinal degeneration, resulted in a slowing of photoreceptor cell loss for up to three months post administration of the ribozyme (Lewin *et al.,* 1998; La Vail *et al.,* 2000). O'Neill *et al.* demonstrated *in vitro* cleavage of ribozymes targeting rhodopsin and peripherin, other genes frequently mutated in adRP, using mutation-independent strategies (see 1.2.10.3). The genetic and mutational heterogeneity extant in adRP presents a considerable challenge to the development of therapeutic strategies, as it is likely to be commercially unviable to tailor therapies to individual mutations. Hence, mutation-independent therapeutic approaches would be preferable and these have been previously used in the exploration of therapies for another autosomal dominant disease, osteogenesis imperfecta (OI). Furthermore, dominantly acting mutations may underlie multi-factorial diseases such as p53-related cancers (Dittmer *et al.,* 1993; Liu *et al.,* 2000; de Vries *et al.,* 2002). As reviewed in section 1.3, p53 is a tumour suppressor protein, mutated in approximately 50% of tumours, and is highly genetically heterogeneous, thus presenting the same challenge as RP to achieve therapeutic gene suppression. Mutation-independent strategies could potentially be used to develop therapies for p53-related cancers. Chapter 6 describes a study undertaken to design and explore potential suppression and replacement gene-based therapies targeting the p53 gene, using hammerhead ribozymes as the suppression tool.

Ribozymes have been widely evaluated as therapeutic tools for cancer, targeting a range of mutant genes that contribute to the development, growth and invasiveness of tumours. Oncogenes are involved in normal cell growth and differentiation but are frequently mutated and/or over expressed in tumours. Examples include *ras*, a GTPase enzyme and *myc*, a transcriptional activator. Downregulation of ras and myc transcripts using ribozymes has been demonstrated in cancer cell lines and nude mouse models (Zhang *et al.,* 2000; Wang *et al.,* 2002; Cheng *et al.,* 2000). Genes involved in controlling apoptotic cell death also represent attractive targets for anti-cancer therapies. Apoptosis is a normal process that is essential for removing cells with critical DNA damage and over-proliferating cells. Defects in the apoptotic pathway can contribute to tumour development. Anti-apoptotic genes that have been targeted by ribozymes include *survivin* and *bcl-2*. Survivin inhibits caspases, enzymes that mediate apoptosis and Bcl-2 inhibits the release of cytochrome-*c* from the mitochondria, a critical step in one of the main pathways of apoptosis. Ribozymes targeting survivin transcript have been demonstrated to increase the susceptibility of cancer cells to apoptosis induced by chemotherapeutic agents, and reduce tumour formation in nude mice models (Choi *et al.,* 2003; Pennati *et al.,* 2004).

Although there are no approved ribozymes for use in cancer therapy, a number are currently being assessed in human clinical trials. Angiozyme or RPI.4610 is an example of a ribozyme being developed for a clinical application, with phase I studies for advanced solid tumours (Kobayashi *et al.,* 2005) and phase III studies for metastatic colorectal cancer have recently been completed (Hurwitz *et al.,* 2004). Vascular endothelial growth factor (VEGF) promotes the growth of tumour blood vessels, known as angiogenesis, via binding to endothelial cell surface receptors. Angiozyme cleaves and targets the transcript for one of these receptors, VEGFR-1. Preclinical studies have demonstrated that Angiozyme inhibited tumour growth in renal, ovarian and prostate cancer cell lines and in mouse models of lung and colorectal cancer (Pavco *et al.,* 2000; Weng *et al.,* 2001; Kobayashi *et al.,* 2005). There are numerous other examples of ribozymes targeting genes for cancer therapy, which are beyond the scope of this thesis.

For further reviews of this area, refer to Schubert *et al.,* 2004, Citti *et al.,* 2005, and Zaffaroni *et al.,* 2005.

1.4.4 RNA Interference (RNAi)

1.4.4.1 Introduction

RNAi is the most recent suppression technology to emerge and has been shown to have great potential as a therapeutic tool. Indeed, although it is less then five years since RNAi was first demonstrated to specifically suppress mammalian genes (Elbashir *et al.,* 2001; Caplen *et al.,* 2001), there are currently several ongoing phase I clinical trials evaluating RNAi-based therapeutics for treating asthma, HIV-1 and a retinal degenerative disorder, Age-related Macular degeneration (AMD) (Leung *et al.,* 2005). As p53-related tumours could potentially be treated using an RNAi-based mutation-independent approach, in addition to the potential use of the ribozymes described in Chapter 6, the application of RNAi in the development of genetic therapies is briefly reviewed here.

1.4.4.2 Mechanism of RNA interference (RNAi)

RNAi refers to post-transcriptional gene silencing by small interfering RNAs (siRNAs) approximately 21-28 nucleotides in length, processed from double stranded RNA (dsRNA) (Elbashir *et al.,* 2001). RNAi in vertebrates was first described in a pivotal paper by Fire *et al.,* 1998 demonstrating that delivery of dsRNA targeting genes in the *C. elegans* worm, resulted in specific gene suppression. From this initial discovery, it was subsequently reported that the mechanism of RNAi is a conserved biological response in eukaryotes (Hammond *et al.,* 2001; Elbashir *et al.,* 2001), related to post-transcriptional gene silencing in plants (Jorgensen *et al.,* 1996). Briefly, RNAi involves the cleavage of dsRNA by an RNase III-like enzyme known as Dicer into siRNA, and recruited to a protein RNA-induced silencing complex (RISC) (Berstein *et al.,* 2001; Nykanen *et al.,* 2001). Following RISC activation, siRNA binds to the complementary mRNA target sequence, which is then catalytically cleaved by RISC. For a recent review of the mechanism of RNAi refer to Leung *et al.,* 2005.

1.4.4.3 Therapeutic applications of RNAi

RNAi interference can be mediated by directly introducing siRNAs targeting the gene of interest or delivering expression vectors to endogenously transcribe short hairpin RNAs (shRNAs) (Paddison *et al.,* 2002; Dykxhoorn *et al.,* 2003). shRNAs are subsequently processed by Dicer, as described above in 1.4.4.2, into siRNAs. Both approaches have been demonstrated to successfully downregulate gene expression as a therapeutic strategy for cancer (Li *et al.,* 2004), viral infections (Dave *et al.,* 2004; Wilson *et al.,* 2003), respiratory disease (Shao *et al.,* 2004) and dominant disease (Xia *et al.,* 2004; Kiang *et al.,* 2005; Palfi *et al.,* 2006). Several papers have been published showing successful downregulation of p53 *in cellulo* using siRNA and viral vector delivery of shRNA (Martinez *et al.,* 2002; Zhao *et al.,* 2003a; Liu *et al.,* 2004). Martinez *et al.* demonstrated that siRNA delivered to cells stably expressing mutant p53, suppressed the expression of mutant but not wt p53, highlighting the specificity of siRNA cleavage. Furthermore, the suppressed mutant p53 is a dominant-negative mutation, so reducing the levels of the p53 mutant gene, resulted in a restoration of wt p53 function. This paper highlights the potential therapeutic benefit of suppressing p53 dominant-negative mutations as a therapeutic strategy for p53-related cancers, and supports the therapeutic approach described in Chapter 6. A future study exploring an RNAi-based mutation-independent suppression/replacement approach for p53-related cancer would be of great interest.

Although in recent years, there has been a diminished interest in ribozymes, due in part to the emergence of RNAi based technology, they have great potential as therapeutic agents, which is indicated by the ongoing successful clinical trials of the anti-HIV-1 ribozyme and the pre-clinical studies described above in 1.4.3.3.6. In addition, ribozymes may be used in conjunction with other suppression agents, such as RNAi to develop more effective therapeutic agents. A recent paper demonstrated that lentiviral vector delivery of a triple combination of an shRNA, ribozyme and decoy peptide targeting different HIV-1 genes was more effective at suppressing HIV-1 infection *in cellulo* than single or double combination therapy (Li *et al.,* 2005a). Although the developments in RNAi technology have been quite remarkable, there are concerns

regarding off-target effects of siRNA (Jackson *et al.,* 2003; Scacheri *et al.,* 2004) and induction of the interferon response (Bridge *et al.,* 2003; Sledz *et al.,* 2003), a primitive anti-viral mechanism that can induce the non-specific degradation of mRNAs (Hall 2004). Further research is required to understand the mechanisms underlying these effects, to develop more effective and safe RNAi based therapeutics, for use in a clinical setting. For detailed reviews of the therapeutic application of RNAi, refer to the recent excellent reviews of Mittal 2004, Hall 2004, Leung *et al.*, 2005 and Dykxhoorn, *et al.*, 2005.

1.5 Delivery of Genetic Therapies

1.5.1 Introduction

The success of suppression tools, anti-apoptotic agents or indeed any gene therapy for disease depends on efficient, safe delivery to the target tissue *in vivo*. This section reviews current delivery systems and examines how these systems are being employed for RP and p53-related cancer gene therapy. There are two basic delivery strategies: exogenous and endogenous delivery, the former involving delivery of chemically synthesised nucleic acids, the latter, expression of genes from plasmid or viral vectors (Schubert *et al.,* 2004). Cellular uptake of synthesised nucleic acids such as ribozymes, antisense oligonucleotides and siRNA is inefficient so they are usually complexed with liposomes, polymeric dendrimers or polypeptides to enhance uptake, and chemically modified to protect them from degradation by endogenous nucleases (Shiota *et al.,* 2004; Scanlon 2004; Dykxhoorn *et al.,* 2005). These non-viral delivery methods may also be employed to deliver plasmid vectors carrying ribozyme or other therapeutic genes, which are then expressed endogenously. Therapeutic genes can also be expressed from viral vectors, which unlike plasmid vectors do not require complexing with liposomes or polypeptides, as they are capable of self-delivery to target tissues (Verma *et al.,* 2005).

1.5.2 Non-viral delivery

Non-viral delivery systems are an essential tool in the research laboratory for safely and efficiently delivering plasmid DNA, antisense oligonucleotides (ASOs) or siRNA. A

frequently used lipid-based system employs positively charged (cationic) lipids, usually in the form of liposomes, vesicle-like structures composed of a bilayer of cationic lipids (Selsek 2004; El-Aneed 2004). Liposomes interact with negatively charged DNA, and the complex is absorbed across the cell membrane by endocytosis. While this system is widely used *in vitro*, liposomes often have a toxic effect when delivered systemically *in vivo* and are rapidly removed from the blood stream. So to prolong the circulation period of liposomes, polyethylene glycol (PEG)-lipid derivatives can be used as stabilising agents. In addition, PEG-liposomes can be targeted using conjugated antibodies to generate PEG-immunoliposomes (PILs) (Shi *et al.,* 2001; Zhang *et al.,* 2003). In the study by Zhang *et al.*, expression of reporter genes β–galactosidase and luciferase was shown in the retina of rhesus monkeys following intravenous delivery of plasmid constructs using PILs.

Another group of gene delivery agents, which also act by endocytosis across the cell membrane are cationic polymers (Selsek 2004; El-Aneed 2004). Polyethylenimine (PEI) is an example of a widely studied polymer, with efficient cellular uptake due to its strong buffering capacity at essentially any pH value. *In vivo* toxicity does limit the use of PEI, but the development of low molecular weight and linear PEI with lower toxicity may allow PEI to be used safely *in vivo*. Studies have demonstrated the delivery of ribozymes and siRNA using PEI to successfully downregulate gene expression (Aigner *et al.,* 2002; Ge *et al.,* 2004). Polyamidoamine (PAMAM) is another example of a cationic polymer that is used as a delivery agent (Selsek 2004). This highly ordered polymer forms spherical dendrimers, which are used for mainly *in vitro* gene delivery: commercial agents include Superfect and Polyfect (Qiagen). Further tools include nanospheres, peptide carriers, antibodies, receptor ligands and biodegradable polymers (Selsek 2004).

In addition, suppression agents such as ribozymes and siRNA can also be delivered directly, without any of the non-viral systems described above (Scanlon *et al.,* 2004; Citti *et al.,* 2005). Naked nucleic acids have a very short half-life due to endogenous nucleases, however they may be chemically modified to protect them from degradation.

Modifications include blocking the 3' end of the molecule or substituting the 2'-hydroxyl groups of the ribose moiety with other chemical groups, such as 2'-O-methyl of 2'-fluoro groups (Goodchild 1992; Heidenreich *et al.,* 1994; Chiu *et al.,* 2003). Recent studies have demonstrated the therapeutic efficacy of siRNA (Song *et al.,* 2003), ribozyme (Macejak *et al.,* 2001; Sandberg *et al.,* 2000): and antisense-ODN (Kim *et al.,* 2004; Gautschi *et al.,* 2001) suppression agents delivered in this way. One study showed the anti-tumour activity of an antisense ODN (OL(1)p53) targeting the p53 tumour suppressor gene in a lymphoma cell line (Sharp *et al.,* 2001). Phase I clinical trials were begun to evaluate OL(1)p53 as a therapy for patients with acute myelogenous leukemia (AML) but discontinued due to poor efficacy, possibly as a result of both suppression of mutant and wt p53 without concomitant replacement of wt p53, which may have reduced p53-dependent apoptosis (Jansen *et al.,* 2002). However, an OLG that targets MDM2, a negative regulator of p53, frequently overexpressed in various tumours (Zhang *et al.,* 2004b), has been demonstrated to have anti-tumour activity in various *in vitro* and *in vivo* models of breast, colon and prostate cancer, and so may be of potential benefit in treating human cancer patients (Wang *et al.,* 2001; Wang *et al.,* 2002; Zhang *et al.,* 2004b).

Direct delivery of plasmid vectors expressing therapeutic genes or suppression tools such as ribozymes, has also been undertaken. Plasmid expression of the therapeutic agent has several advantages to delivery of the pre-synthesised form: 1) expression is more sustained, 2) chemical modification, which may be toxic to cells, is not required and 3) cost-effectiveness. siRNA in particular, can be expensive to synthesise, which is a limiting factor for siRNA use. Plasmid vectors on the other hand are readily prepared in bulk. In one study a reduction in the metastatic potential of a murine melanoma *in vivo* using a systemically delivered plasmid ribozyme targeting telomerase was demonstrated (Nosrati *et al.,* 2004). Constructs expressing siRNA or shRNA have also been shown to successfully downregulate expression of target genes in murine disease models of hepatitis B (McCaffrey *et al.,* 2002), hepatitis C (Giladi *et al.,* 2003) and renal-perfusion injury (Hamar *et al.,* 2004) following tail-vein injection.

As stated earlier, one approach to treating adRP is suppression of the mutant gene in conjunction with wt gene replacement. In a recent study the downregulation of rhodopsin in cultured retinal explants using plasmids expressing shRNA targeting rhodopsin (siMR3) was demonstrated (Kiang *et al.,* 2005). In addition a replacement rhodopsin target was generated with altered binding sites for siMR3, but as these changes were made to degenerate bases within the rhodopsin coding sequence, there were no amino acid changes. No suppression of co-delivered altered rhodopsin by siMR3 was found in liver tissue *in vivo*, following tail vein injections of mice, compared to a 90% suppression of wild-type rhodopsin. As well as demonstrating the effective delivery of siRNA directly, this study highlights the potential of mutation-independent strategies for adRP, (described in 1.2.10.3) to overcome the challenge that genetic heterogeneity presents to the development of adRP therapies.

Non-viral methods of gene delivery are essential tools for therapeutic evaluation *in vitro* and more efficient systems continue to be developed. *In vivo*, the application of these tools is more limited compared to viral vectors, but advantages include less adverse immune responses and cost-effective production in bulk. Results from numerous studies have demonstrated the efficacy of these methods for gene delivery *in vivo*, which due to their transient nature, are particularly suitable for acute diseases such as cancer and viral infections (Putney *et al.,* 1999; Jansen *et al.,* 2000; Zhang *et al.,* 2004a; Urban-Klein *et al.,* 2005). A number of ongoing clinical trials using non-viral methods for delivering gene therapy agents are listed in Table 1.1.

Table 1.1*: Current clinical trials employing non-viral methods of gene delivery

Company	Disease	Status	Technology
Alnylam Pharm[1].	RS Virus[2]	Phase I Clinical	Direct siRNA
Benitec Pharm.	HIV	Phase I Clinical	Multiple siRNA
Genta Pharm.	Melanoma	Phase II Clinical	Antisense-siRNA
Intradigm Corporation	Solid Tumour	Preclinical	Nanoparticle- siRNA
Isis Pharm.	CMV-retinitis	Approved	Antisense-ODN
Sirna Therapeutics	Solid Tumour	Phase II Clinical	Modified ribozyme
Sirna Therapeutics	Hepatitis C	Preclinical	Modified siRNA
Sirna Therapeutics	Asthma	Phase I Clinical	Aerosol siRNA

*Modifed from Leung *et al.*, 2005, [1]Pharmaceuticals, [2]Respiratory Syncytial Virus

Ribozymes targeting p53, as described in Chapter 6, or other suppression tools could potentially be delivered as a therapeutic for p53-related cancer using the methods described here. With regard to therapeutic gene delivery for RP, non-viral methods are useful for initially evaluating therapeutic strategies in cell lines and *in vivo*, as described above with the siRNA targeting rhodopsin. However, the use of non-viral vectors is limited as the effect of the delivered agent is transient. More significantly, delivery using these methods is inefficient, since agents delivered systemically must, in order to target the retina, cross the blood-retina barrier. Also as photoreceptors are not easily transduced by non-viral methods, subretinal injections may not deliver sufficient levels of the therapeutic agent to be of clinical benefit. Gene delivery using viral vectors such as adeno-associated viral (AAV) vectors is a more efficient method for further evaluating therapeutic strategies in transgenic disease models and in a clinical setting as AAV can potentially provide stable long-term expression of therapeutic genes.

1.5.3 Viral Delivery

1.5.3.1 Introduction

Viral vectors can be subdivided into two categories, integrating and non-integrating vectors (Robbins *et al.*, 1998; Lundstrom 2003; Verma *et al.*, 2005). Integrating vectors

include retroviral, lentiviral and AAV vectors, which are capable of integrating into the genome, potentially providing sustained expression of the therapeutic gene. Adenoviral vectors are the most commonly used non-integrating vectors and are maintained in the cell nucleus as episomes. The underlying principle is essentially the same for each type of viral-vector, involving the removal of vital viral genes necessary for replication and subsequent replacement with the therapeutic gene. The pros and cons of each type are discussed in the following sections, with a review of current viral vector based gene therapy for adRP and p53-related cancers.

1.5.3.2 Retroviral vectors

Retroviral vectors are based on RNA viruses with either a single-stranded or double-stranded RNA genome. Vectors based on one family of retroviruses, the *Retroviridae*, were the first to be designed, with the majority based on the moloney murine leukemia virus (MoLV). Retroviral vectors have been used to deliver therapeutic agents like ribozymes (Millington-Ward *et al.,* 2002), RNA decoys (Michienzi *et al.,* 2002) and siRNA (Brummelkamp *et al.,* 2002; Liu *et al.,* 2004) as well as a wide variety of genes for primarily treating cancer (Barzon *et al.,* 2003; Finger *et al.,* 2005). One recently completed clinical trial using retroviral delivery evaluated the safety of an anti-HIV-1 ribozyme (RRz2), targeting the *tat* gene, which is essential for HIV-1 viral replication (Macpherson *et al.,* 2005). CD4+ T cells, which differentiate into T helper cells targeted and destroyed by HIV-1, were transduced *ex vivo* with a retroviral vector expressing RRz2 and infused into patients. Preclinical studies evaluated the efficiency of RRz2, *in vitro* and *in cellulo*, therefore, the aim of this phase I trial was to demonstrate safety and feasibility (Sun *et al.,* 1994; Wang *et al.,* 1998). No serious adverse effects were observed and expression of the transduced T lymphocytes was detectable for up to 44 months following treatment. Given these results, phase II trials will be designed and undertaken.

Retroviral vectors do have a number of disadvantages. While they are effective at transducing dividing cells like precursor T cells, they cannot transduce non-dividing tissues, such as photoreceptor cells making them ineffective for treating RP. In recent

years retroviral vectors have also been associated with serious side effects. Several patients being treated for X-linked severe combined immunodeficiency (X-SCID), with retroviral vectors, developed a form of leukaemia as a result of retroviral insertional mutagenesis (Hacein-Bey-Abina *et al.,* 2003). Subsequent studies have found that integration by MoMLV is not random, preferentially targeting regions around gene promoters (Wu *et al.,* 2003; Mitchell *et al.,* 2004), a discovery which strongly supports a cautious approach towards the use of retroviral vectors in gene delivery. However, to date there have been no similar cases observed in clinical trials using retroviral vectors to transduce mature precursor T cells (Muul *et al.,* 2003), and with the continuing development of self-inactivating vector (SIN) technology, together with the emergence of other retroviral vectors based on lentiviruses, the role of retroviral vectors as gene delivery agents is promising (Anson 2004). Indeed, retroviral vector delivery accounts for approximately 25% of current gene therapy clinical trials (http://www.wiley.co.uk/genmed/clinical/).

1.5.3.3 Lentiviral vectors

Lentiviruses are another type of retrovirus with the important property of stably transducing non-dividing and dividing cells, and a well-known example is human immunodeficiency virus (HIV) (Delenda 2004; Verma *et al.,* 2005). Most lentiviral (LV) vectors are based on HIV serotype 1 and efficient gene delivery to various cell types has been successfully demonstrated *in vivo*, including to hippocampal cells (Ahmed *et al.,* 2004), hepatocytes (Kafri *et al.,* 1997) and chronic myelogenous leukaemia cells (Soda *et al.,* 2004). With regard to delivery to the eye, a study by Miyoshi *et al.* demonstrated the efficient transduction of RPE and photoreceptor cells in postnatal day 0-2 (P0-P2) infant rats using a LV vector carrying GFP. Further work showed photoreceptor rescue in a mouse model of retinal degeneration with LV vector delivery of a therapeutic gene (Takahashi *et al.,* 1999). However, results from a subsequent study showed that LV transduction of photoreceptors in adult mice was inefficient (Bainbridge *et al.,* 2001). Thus, LV-mediated delivery is clearly unsuitable for adRP and other retinal degenerations where the associated pathogenic gene is expressed in photoreceptor cells. However, in recent years, another viral vector, based

on the adeno-associated virus (AAV) has emerged as a potentially powerful gene delivery tool for retinal degenerations.

1.5.3.4 Adeno-associated viral vectors

Adeno-associated viruses are non-pathogenic single stranded DNA viruses that belong to the Parvoviridae family (Carter *et al.,* 2000; Buning *et al.,* 2003; Verma *et al.,* 2005). AAV are replication defective, so a helper virus (adeno-or herpesvirus) is necessary for infection of target cells and numerous different serotypes have been identified in humans and primates (Verma *et al.,* 2005). Vectors based on AAV have several advantages compared to the other viral vectors: 1) ability to infect a broad range of dividing and non-dividing cells, 2) derivation from a non-pathogenic virus, 3) minimal immunogenicity and 4) stable integration into host genome. Vectors based on the well-characterised AAV2 serotype, are the most widely used for gene delivery. AAV2 has a 4.7 kb genome encoding four replication and three structural capsid proteins. Currently a new generation of AAV2 vectors are being developed, with AAV2 genomes and other serotype capsid proteins. As the range of cells infected by AAV depends on the serotype, this is being exploited to generate more efficient, tissue specific expression of therapeutic genes. For example, AAV2/1 and 2/7 vectors have been demonstrated to infect muscle efficiently *in vivo* (Gao *et al.,* 2002; Rabinowitz *et al.,* 2002), AAV2/8, liver tissue (Gao *et al.,* 2002) and AAV2/5, photoreceptor cells of the retina (Auricchio *et al.,* 2001; Yang *et al.,* 2002). These exciting advances in AAV technology mark another important step in the development of AAV vectors for clinical use.

AAV vectors have been used to deliver therapeutic genes for a range of diseases including haemophilia (Arruda *et al.,* 2005), Duchenne muscular dystrophy (Athanasopoulos *et al.,* 2004) and cystic fibrosis (Flotte *et al.,* 2001). Clinical trials evaluating AAV delivered therapies for these disorders are currently on going (http://www.wiley.co.uk/genmed/clinical/). For the purpose of this thesis, a review of AAV vector mediated gene therapy for RP is discussed. AAV vectors are ideally suited for use in the retina for the reasons outlined above and in addition, results from a phase II clinical trial treating cystic fibrosis patients have shown AAV to be safe (Moss *et al.,*

2004). AAV-mediated delivery of RP genetic therapies have been evaluated in animal models of retinal degeneration. Several studies have showed that AAV2 delivery of ribozymes targeting mutant rhodopsin with a proline to histidine mutation at codon 23 in a rat model of adRP, resulted in a significant slowing of photoreceptor degeneration (Lewin *et al.*, 1998; La Vail *et al.*, 2000). As RP is genetically heterogeneous, with Pro23His representing 1 of approximately 100 rhodopsin mutations, such an approach is limited in its application. A recently published paper evaluated ribozyme (Rz397) suppression of wild-type rhodopsin in heterozygous rhodopsin knockout mice ($Rho^{+/-}$) using AAV vector delivery (Gorbatyuk *et al.*, 2005). An 80% reduction in rhodopsin protein, as assessed by Western blotting, was demonstrated 2 months after injection of $Rho^{+/-}$ mice with AAV-Rz397. Suppression of both wild-type and mutant rhodopsin could be used to treat adRP, where the ribozyme would be co-delivered with a replacement rhodopsin construct modified to protect it from ribozyme suppression. This is similar to the mutation-independent approaches described in 1.2.10.3.

Delivery of replacement genes has been undertaken in studies of gene therapeutic strategies for arRP, which unlike adRP does not involve additional gene suppression. AAV2 delivery of *rds*-peripherin has been evaluated in the *rds* mouse model, homozygous for a mutation in the *rds*-peripherin (Ali *et al.*, 2000; Sarra *et al.*, 2001; Schlichtenbrede *et al.*, 2003, 2004). The study by Ali *et al.*, showed that there was an improvement in photoreceptor morphology for up to 10 weeks following injection together with a significant electroretinogram (ERG) response compared to *rds* control animals. Although subsequent papers found that this effect was transient, a study published last year, demonstrated that treated *rds* mice had improved visual function (Schlichtenbrede *et al.*, 2004).

Another retinal degeneration that has been successfully treated using AAV delivered gene therapy is Leber congenital amaurosis (LCA), a severe, early-onset retinopathy that involves both rod and cone photoreceptors (Allikmets 2004; Koenekoop *et al.*, 2004). Mutations in the *RPE65* gene, expressed in the retinal pigment epithelium, can result in LCA. AAV delivery of *RPE65* to murine and canine models of LCA, restored

vision significantly, and as a result human clinical trials are being initiated (Acland *et al.,* 2001; Narfstrom *et al.,* 2003; Acland *et al.,* 2005). AAV delivery of another gene associated with LCA, *RPGRIP*, to a murine model of LCA resulted in significant preservation of photoreceptor morphology and function, as assessed by ERG (Pawlyk *et al.,* 2005). For further information on AAV delivery to the retina, refer to two excellent recent reviews, Rolling 2004 and Dinculescu *et al.,* 2005.

Another therapeutic approach for retinal degenerations such as RP, is to promote photoreceptor survival using neurotrophic factors including glial cell line-derived neurotrophic factor (GDNF) (Frasson *et al.,* 1999; McGee Sanfter *et al.,* 2001), rod-derived cone viability factor (Leveillard *et al.,* 2004) and ciliary neurotrophic factor (CNTF) (Liang *et al.,* 2001; Bok *et al.,* 2002). Although AAV2 delivered CNTF was shown to preserve photoreceptor morphology in murine models of retinal degeneration, photoreceptor abnormalities and suppressed ERGs were noted, possibly due to high expression levels (Liang *et al.,* 2001; Bok *et al.,* 2002). Notably, the development of a novel delivery system for CNTF, namely an encapsulated cell therapy device (ECT), may potentially overcome the problems with excessive levels of CNTF (Tao *et al.,* 2002).

AAV2 vectors have great potential as gene delivery vectors for retinal degenerations and the development of second-generation vectors with enhanced cell targeting specificity represents a significant step toward realising this potential. By exchanging the AAV2 capsid protein with capsids from other AAV serotypes, several studies demonstrated that the AAV2 transduction efficiency in the retina is modified (Auricchio *et al.,* 2001; Yang *et al.,* 2002). For example while AAV2/2 infects the RPE and photoreceptors, using the capsid from serotype 1 results in expression predominantly in the RPE (AAV2/1) and using AAV2/5 is more effective for transducing photoreceptors. Additionally, the capsid serotype determines the onset and level of gene expression in the photoreceptors, varying from 24-48 hours following administration with AAV2/1 to 14-28 days with AAV2/2 (Auricchio *et al.,* 2001).

With regard to gene delivery for cancer therapy, AAV vectors are not widely used, and the majority of clinical trials employ adenoviral viral vectors, discussed below. However, results exploiting the recent discoveries regarding varying tissue tropism among different AAV serotypes, indicate that AAV vectors may be promising delivery agents for cancer gene therapy (Hacker *et al.,* 2005). By comparing the transduction efficiency among a range of cancer cell lines with different AAV serotypes, AAV2 was found to be the most efficient compared to AAV1-AAV4. In addition, a number of papers have shown that AAV sensitises cancer cells to chemotherapeutic agents (Hillgenberg *et al.,* 1999) and radiation (Walz *et al.,* 1992), suggesting that further evaluation of AAV vectors for gene based cancer therapy is worthwhile.

1.5.3.5 Adenoviral vectors

Adenoviruses are a family of double-stranded DNA viruses, which have been isolated from avian and mammalian species (Volpers *et al.,* 2004; Verma *et al.,* 2005). Within the human adenoviruses, there are approximately 50 serotypes, but the majority of adenoviral vectors are based on serotype 2 or 5 (Ad2, Ad5). Ad vectors are important gene delivery vectors as they have a low pathogenicity, can be generated at a high titre and have a transgene capacity of approximately 30 kb, which is considerably more than AAV which is limited to less than 5 kb. In addition, unlike the other viral vectors so far described, Ad vectors are non-integrating (Voplers *et al.,* 2004). Ad vectors have been widely applied as delivery agents for human gene therapy and notably, were one of the first viral vectors to be used in clinical trials (Crystal *et al.,* 1994). At present there are approximately 200 ongoing clinical trials evaluating Ad vector delivered genes for vascular diseases (angina), Mendelian disorders (cystic fibrosis) and cancer (melanoma, prostate cancer) (http://www.wiley.co.uk/genmed/clinical/).

As Ad vectors provide high levels of short-term expression, they may be optimal for treating acute diseases such as cancer. Indeed, almost 80% of Ad clinical trials are evaluating various therapeutic strategies for cancer. Examples of cancer therapeutic genes delivered using Ad vectors in preclinical studies include expression constructs for ribozymes targeting genes involved in oncogenesis, such as *K-ras* (Kijima *et al.,* 2004)

and *Her-2/neu* (Irie *et al.,* 2005), pro-apoptotic genes including *TRAIL* (El-Zawahry *et al.,* 2005) and *Smac* (Hasenjager *et al.,* 2004) and cytokines (Slos *et al.,* 2001; Dummer *et al.,* 2004).

As the p53 gene is mutated in approximately 50% of human cancers (Hollstein *et al.,* 1991), it is an important focus for the development of therapeutic strategies for cancer (see 1.3). One approach is to deliver the p53 gene using Ad vectors to cancer cells, restoring the p53 apoptotic pathway, thereby inducing cell death and sensitising the cells to cytotoxic agents and radiation therapy (Nielsen *et al.,* 1998; Horowitz 1999). Results from studies *in cellulo* (Fujiwara *et al.,* 1994a; Sandig *et al.,* 1997) and *in vivo* (Turturro *et al.,* 2000; Logunov *et al.,* 2004) have demonstrated that the delivery of wt p53 using Ad vectors, results in reduced cell proliferation and tumourogenicity. Currently there are approximately 30 clinical trials worldwide, evaluating Ad vector delivered p53 gene for cancers including non-small cell lung cancer (NSCLC), ovarian cancer and head and neck squamous cell carcinoma (HNSCC) (http://www.wiley.co.uk/genmed/clinical/). Many of these trials are evaluating a p53 Ad vector, produced by Introgen Therapeutics (Austin, TX, USA), known as INGN-201. Several phase I and II trials have been undertaken, to evaluate INGN 201 in patients with lung (Swisher *et al.,* 2003), ovarian (Wolf *et al.,* 2004) and bladder cancer (Pagliaro *et al.,* 2003). Results from phase I clinical trials demonstrated that INGN-201 delivery was safe with minimal toxicity (Pagliaro *et al.,* 2003; Wolf *et al.,* 2004), while results from the phase II trial were encouraging with a full (5%) or partial (58%) tumour regression in a total of 19 patients with non-small cell lung cancer (Swisher *et al.,* 2003). Phase III trials are currently ongoing to evaluate the efficacy of INGN-201 with co-administration of chemotherapeutic agents, for treating head and neck squamous cell carcinoma (http://www.wiley.co.uk/genmed/clinical/). Examples of other clinical trials using p53 delivered using Ad vectors are shown in Table 1.2. Furthermore, while clinical trials are ongoing in the United States, the State Food and Drug Administration of China recently granted a drug license to Shenzhen SiBono Gene Technologies to produce Adp53 for treating head and neck squamous cell carcinoma, the world's first commercially approved gene therapy (Pearson *et al.,* 2004).

Ad vectors, unlike retroviral vectors transduce non-dividing cells, and so have been used to deliver therapeutic genes for retinal degenerations. Ad vectors efficiently transduce retinal pigment epithelium (RPE) and Müller cells (Bennett *et al.,* 1994; Li *et al.,* 1994), so retinal degenerations resulting from mutations in RPE specific genes can be potentially treated using Ad-mediated gene transfer. Mertk is a receptor tyrosine kinase, mainly expressed in the RPE and mutations in this gene can result in arRP. A study undertaken in 2001, demonstrated photoreceptor cell rescue in the Royal College of Surgeons (RCS) rat model of arRP, using Ad delivered *Mertk* (Vollrath *et al.,* 2001). In addition, Ad vectors have been used to deliver neurotrophic factors to mouse models of retinal degeneration, including ciliary neurotrophic factor (CNTF) and brain-derived neuorotrophic factor, thus retarding photoreceptor cell loss. However, as Ad vectors do not efficiently transduce photoreceptor cells (Bennett *et al.,* 1994; Cashman *et al.,* 2002), this observed protective effect is possibly from the direct preservation of the supporting Muller cells.

Like other viral vectors there are safety concerns with Ad vectors, particularly since the death of a patient enrolled in a phase I clinical trial due to a severe immune response (Raper *et al.,* 2002). Immune responses to Ad vectors are a significant challenge to using them safely and efficiently, but a better understanding of these responses has enabled researchers to develop new techniques and develop safer Ad vectors. For a review of this area refer to St George 2003. With continued improvements in safety, Ad vectors have great potential as gene delivery agents for certain diseases. Indeed, adenoviral vector gene delivery accounts for 25% of current clinical gene therapy trials (http://www.wiley.co.uk/genmed/clinical/).

Table 1.2: Examples of some proposed and current clinical trials employing viral methods of delivery

Researcher	Disease	Status	Technology
Professor MacGregor University of Pennsylvania Medical Center, PA, USA	HIV-1	Phase I Clinical	Lentiviral HIV-1 *Env*
Professor David Stein Albert Einstein College of Medicine, NY, USA	HIV-1	Phase I/II Clinical	Lentiviral HIV-1 *Env*
Aventis Pharmaceuticals	Head and Neck Carcinoma	Phase III Clinical	Adenoviral-*p53*
Introgen Therapeutics, Austin, TX, USA	NSC[1] Cancer	Phase II/III Clinical	Adenoviral-*p53*
GenVec, Gaithersburg, MD, USA	Pancreatic Cancer	Phase II Clinical	Adenoviral-TNF-α[3]
Professor Robin Ali Institute of Opthalmology, University of London, UK	LCA[2]	Enrolling for Phase I Clinical	AAV-*RPE65*
Professor Jean Bennett, Department of Opthalmology, University of Pennsylvania, USA	LCA[2]	Enrolling for Phase I Clinical	AAV-*RPE65*

[1]Non-small cell, [2]Leber congenital amaurosis, [3] Tumour necrosis factor-alpha

Following this introduction are five chapters, the first of which is a review of the materials and methods used for the experimental studies undertaken as part of this Ph.D. Chapter 3 describes the evaluation of three inhibitory of apoptosis proteins (IAPs) as anti-apoptotic agents for adRP in a line of cone photoreceptor cells, 661W. The next chapter gives details on the design, generation and *in cellulo* evaluation of constructs with photoreceptor-specific promoter-driven expression of Cre recombinase, for the future generation of transgenic mouse models. Following on from a previous study in the laboratory in TCD, Chapter 5 describes the further evaluation of another anti-apoptotic protein, p35, using cultured retinal explants and a transgenic mouse

model with conditional expression of p35. The final chapter describes the *in vitro* evaluation of a ribozyme-based mutation-independent approach to p53-related cancer.

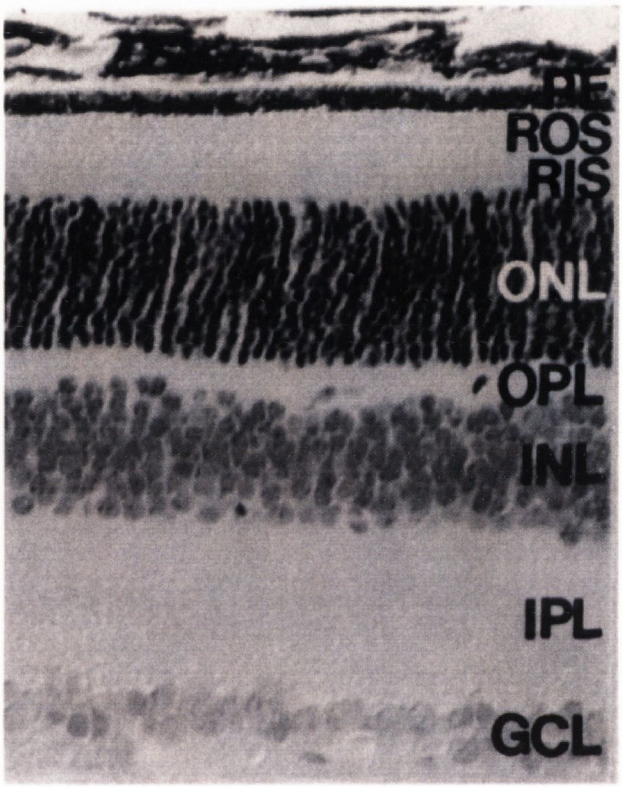

Figure 1.1: Retinal histology from a wild-type retina. The various layers of the retina are identified: retinal pigment epithelium (RPE), rod outer segments (ROS), inner segments (RIS), outer nuclear layer (ONL), outer plexifom layer (OPL), inner nuclear layer (INL), inner plexiform layer (IPL) and ganglion cell layer (GCL).

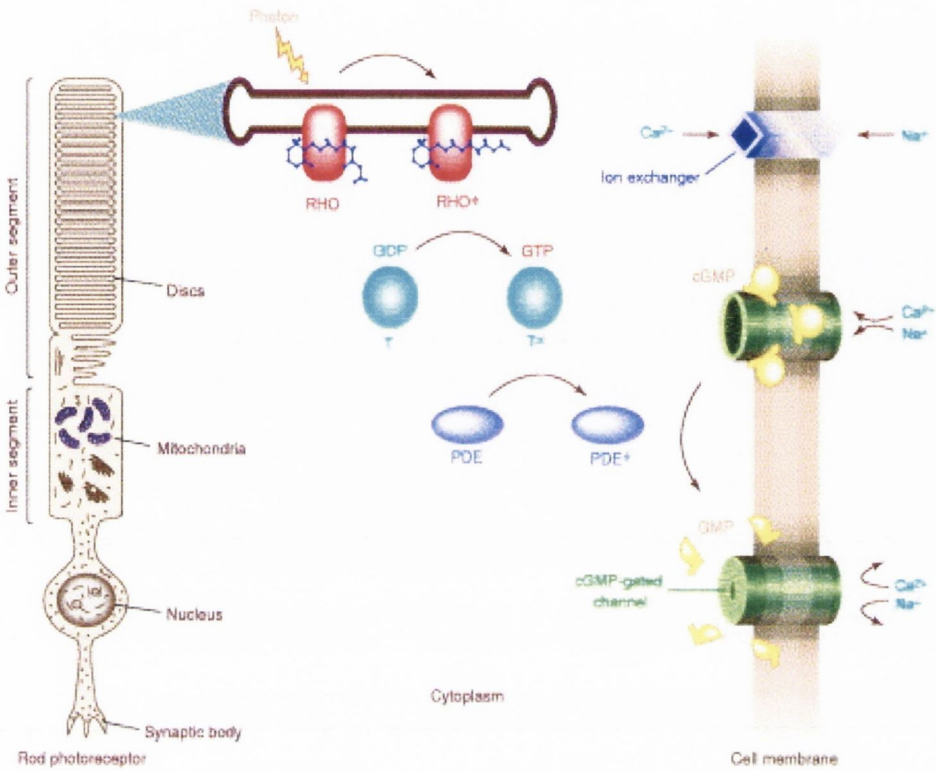

Figure 1.2: Diagram of a photoreceptor and the visual transduction cascade*. The cascade is initiated by the absorption of a photon of light by rhodopsin (Rho), converting 11-*cis* retinal to all-*trans* retinal and activating Rho to Rho*. Rho*, activates transducin (T) by catalysing the exchange of GDP for GTP, which in turn activates cGMP-phosphodiesterase (PDE). PDE hydrolyses cGMP to 5'-GMP, and the resulting decrease in cGMP levels causes the c-GMP gated-channels to close. The photoreceptor becomes hyperpolarised inhibiting the release of the neurotransmitter, glutamate, at its synaptic terminal, which is relayed as an electrical signal via the optic nerve to the brain. The Na^{+}/Ca^{2+} ion exchanger continues to transport Ca^{2+}, decreasing levels within the outer segments and triggering a feedback mechanism to facilitate photoreceptor recovery. *Image from Kennan *et al.*, 2005.

A

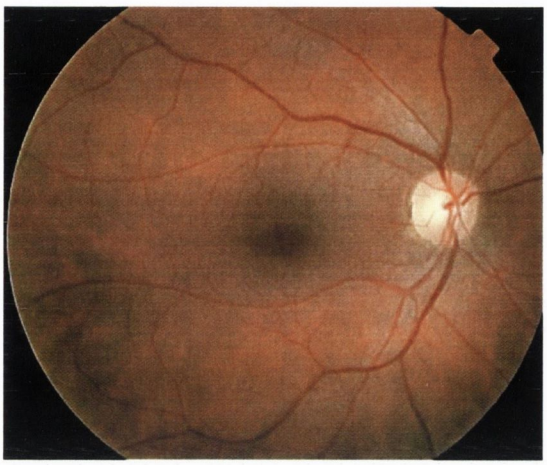

B

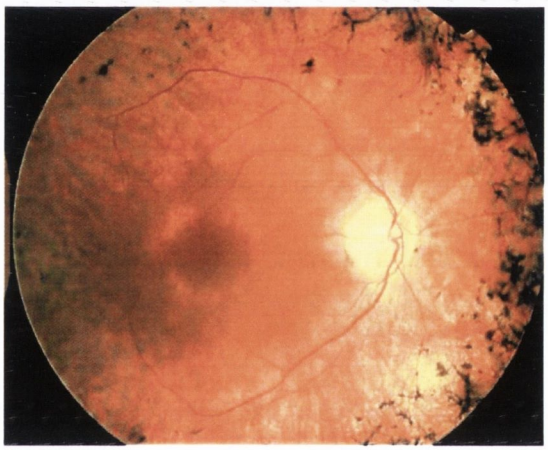

Figure 1.3*: Photographs of a normal (A) and RP retina (B). Features typical of RP, such as marked pigment epithelial thinning, optic disc pallor, retinal vascular attenuation and the classical 'bone spicule' intraretinal pigmentary deposits, are clearly evident in the RP retina.*Image kindly provided by Dr. Paul Kenna, Ocular Genetics Unit, Trinity College Dublin.

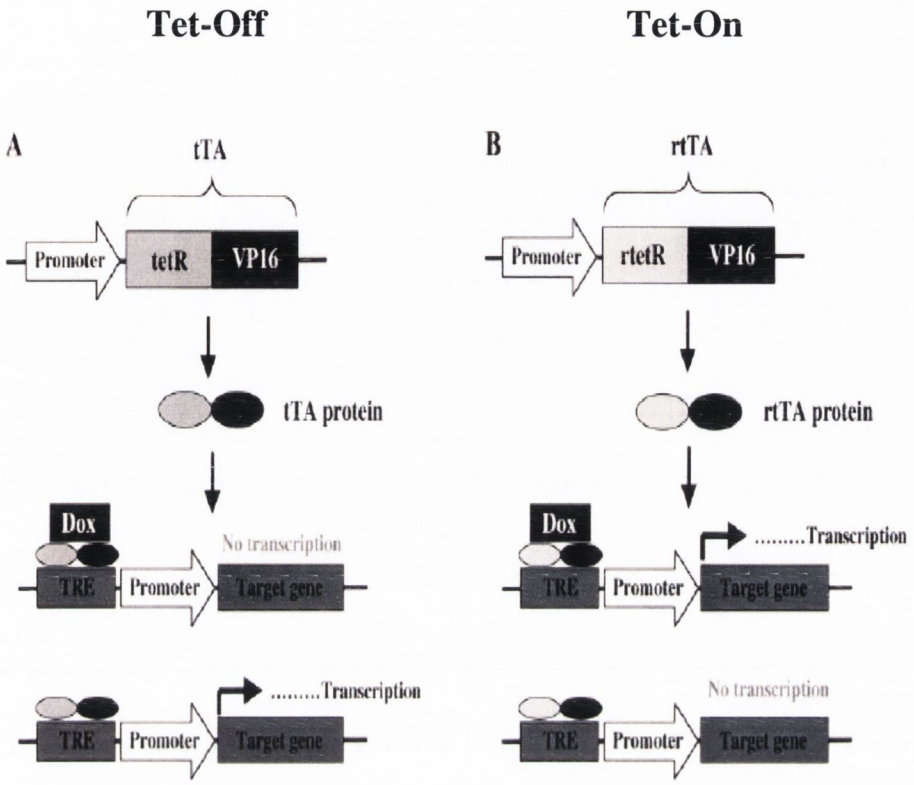

Figure 1.4*: Diagram of the tetracycline-inducible system for gene expression. **(A)** The tetracycline-dependent transactivator (tTA) is a fusion of the tetracycline repressor (tetR) and viral transcriptional regulator (VP16). The second element of the system is a plasmid with a tetracycline responsive element (TRE) controlling expression of the target gene. A tissue-specific promoter drives the expression of tTA, which binds to TRE in the presence of doxycyclin, a tetracycline analog, preventing expression of the target gene. **(B)** The Tet-On system operates in the reverse fashion, with a reverse tTA which binds to the TRE in the presence of doxycyclin, activating expression of the target gene.*Image from van der Weyden *et al.*, 2002.

A: *lox*P Sequence

5'-ATAACTTCGTATAATGTATGCTATCAGAAGTTAT-3'

3'-TATTGAAGCATATTACATACGATATGCTTCAATA-5'

B

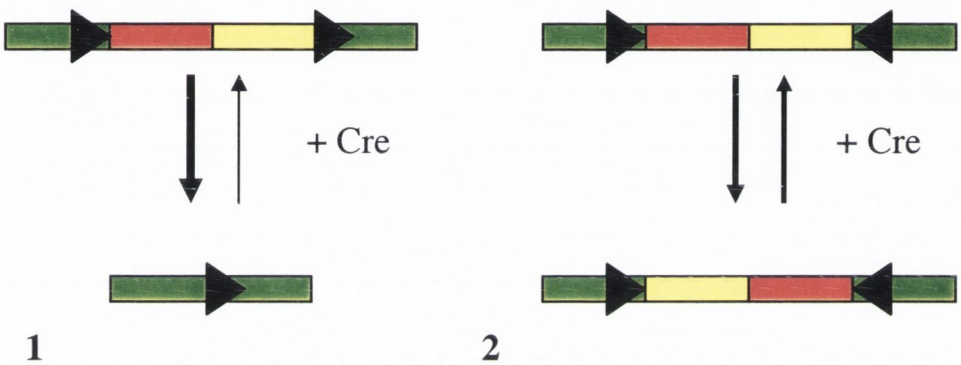

Figure 1.5*: Diagram of a *lox*P sequence and recombinations catalysed by Cre recombinase. Diagram **(A)** shows the 34 bp *lox*P sequence with the 13 bp symmetric elements underlined with red arrows and the 8 bp AT-rich core in blue font. Diagram **(B1)** shows a target gene (red and yellow rectangles) flanked by *lox*P sites (triangles) in the same orientation. Cre activity excises the target gene. **(B2)** shows the target gene flanked by *lox*P sites orientated in opposite directions so Cre activity inverts the target gene. The arrows indicate the reversibility of the reactions.*Images modified from van der Weyden *et al.*, 2002.

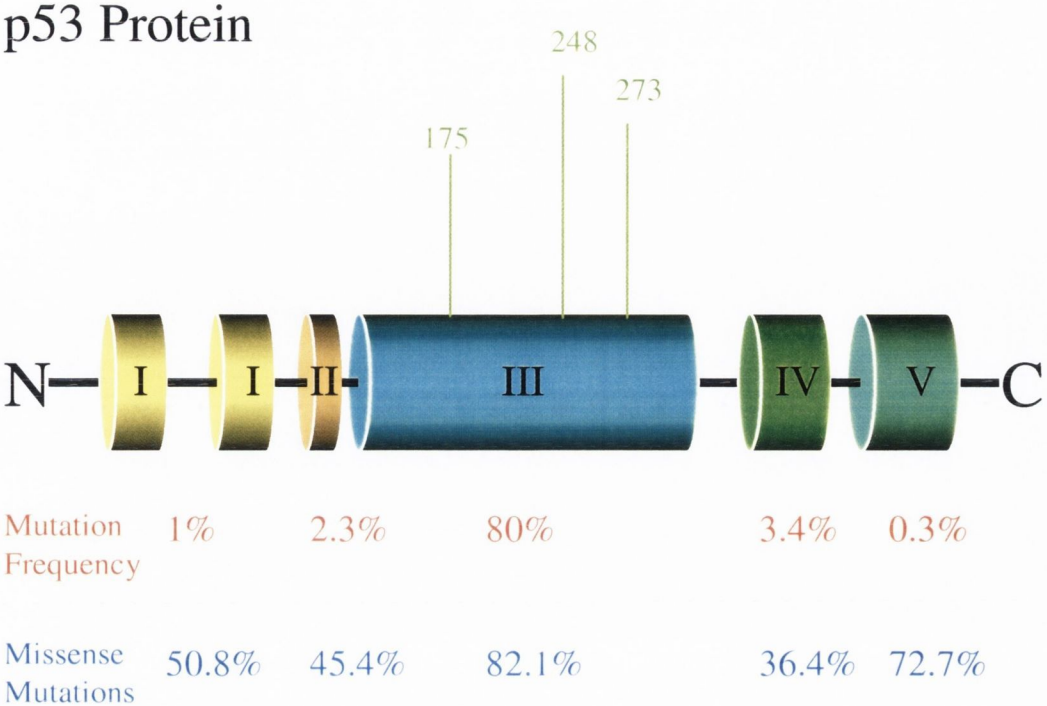

I: Transactivation domains: aa 1-42, 43-62

II: Proline-rich region: aa 65-97

III: DNA binding domain: aa 102-292

IV: Oligomerisation domain: aa 323-356

V: Regulatory domain: aa 363-393

Figure 1.6*: Diagram of the p53 protein. The 53 kDa p53 protein can be divided into 5 domains: 1) a transactivation domain that also contains the site for MDM2 protein binding (negative regulator of p53), 2) a conserved proline-rich region, 3) a DNA binding domain where approximately 80% of mutations are located, 4) an oligomerisation domain for dimerisation with another p53 protein (p53 functions as two dimers: tetramer) and 5) a regulatory domain which contains nuclear localisation signals and is involved in downregulation of DNA binding of the central domain. Codons that are frequently mutated are indicated in green, with the relative frequency of each represented by the length of the line. The relative proportion of p53 mutations that occur in each domain and that are missense are indicated in red and blue respectively.*Diagram modified from http://www-iarc.p53.fr/.

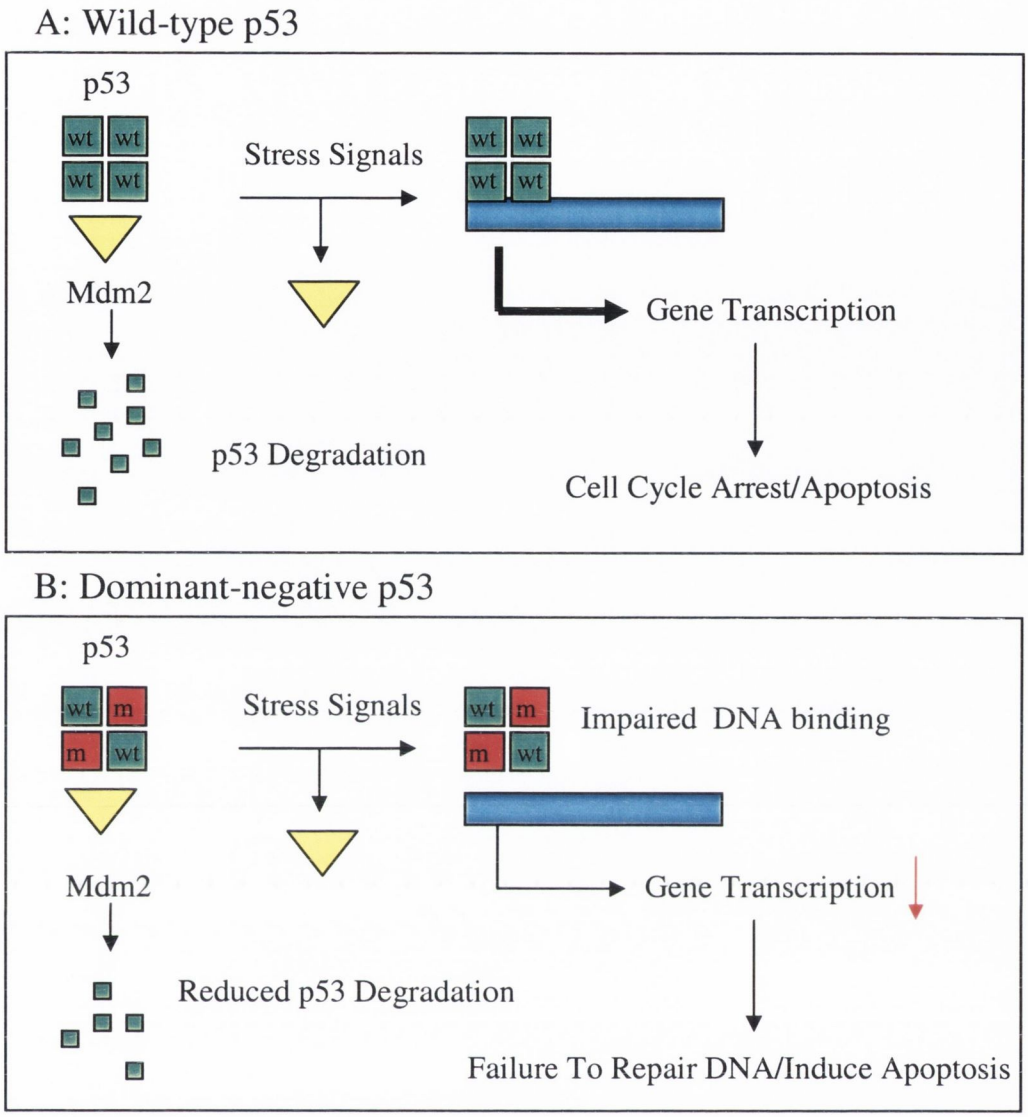

Figure 1.7: Diagram of p53 activity. A) Wild-type (wt) p53 functions as a tetramer and is maintained at low levels in unstressed cells by a number of mechanisms, including binding by MDM2, which targets p53 for proteosomal degradation. In response to stress (i.e. DNA damage, hypoxia), p53 levels increase and by activating the transcription of target genes, p53 induces cell cycle arrest or apoptosis. B) Mutant p53 may have a dominant-negative effect on the activity of wt p53 by oligomerising to form wt/mutant tetramers. p53 levels may increase as degradation by MDM2 is inhibited and in response to stress, the wt/mutant tetramer may not efficiently activate gene transcription for DNA repair or apoptosis, possibly leading to tumour development.

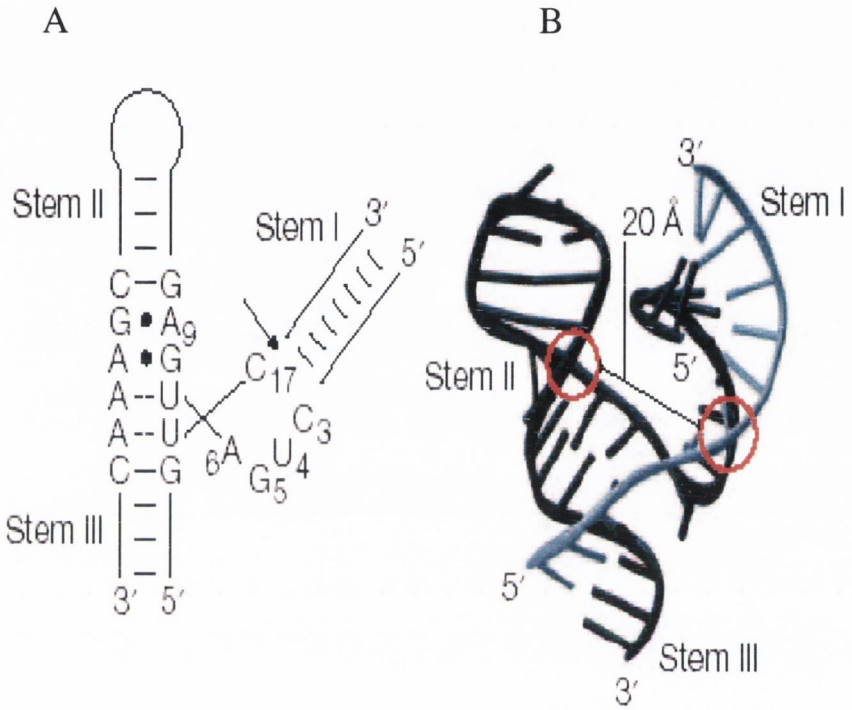

Figure 1.8*: Structure of a self-cleaving hammerhead ribozyme. (A) shows the secondary structure with stems I, II, and III. An arrow marks the cleavage site. **(B)** shows the crystal structure with red circles marking the cleavage site to the right and an important catalytic adenosine (A_9) to the left.*Image from Fedor *et al.*, 2005.

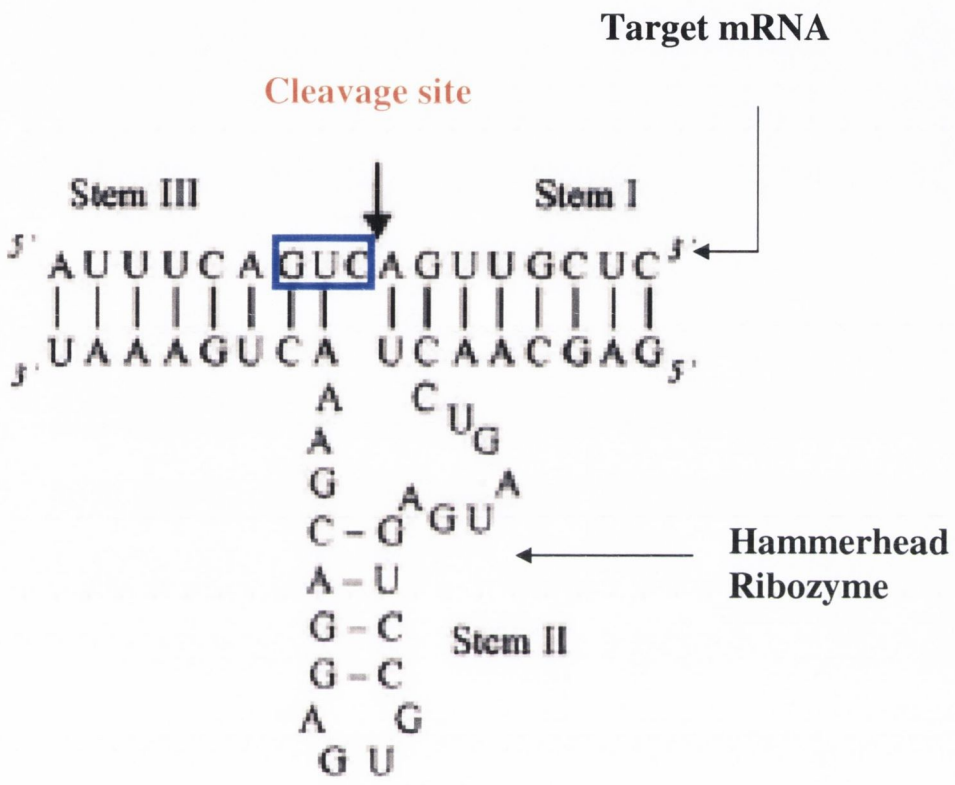

Figure 1.9*: Diagram of the structure of a *trans*-cleaving hammerhead ribozyme. The structure consists of a catalytic core (stem II), flanked by two arms that bind the target mRNA forming stems I and III. The cleavage site after a GUC triplet, outlined in blue, is marked by a red arrow.*Diagram is modified from Schubert *et al.*, 2004.

CHAPTER 2

Materials and Methods

2.1 Materials

2.1.1 Reagents

(i) Chemicals and antibiotics: All chemical reagents, growth media and antibiotics, unless stated, were obtained from: 1) BDH Laboratory Supplies, Poole, England, 2) Calbiochem, Nottingham, UK, 3) Gibco, Paisley, UK or 4) Sigma-Aldrich, Stenheim, Germany.

(ii) Enzyme and buffers: Restriction enzymes and buffers were obtained from New England Biolabs, Frankfurt, Germany. Taq DNA polymerase, PfuTurbo DNA polymerase, T4 DNA ligase and RNaceIT were obtained from Stratagene, La Jolla, CA, USA. Lysozyme was obtained from Sigma-Aldrich. Klenow enzyme and T4 DNA polymerase were obtained from Roche Diagnostics, Penzberg, Germany. Shrimp alkaline phosphatase (SAP) was obtained from USB Corporation, Cleveland, OH, USA.

(iii) Molecular weight standards: 100 bp and 1 kb DNA ladders were obtained from New England Biolabs. Kaleidoscope prestained protein ladder was obtained from Bio-Rad Laboratories, Munich, Germany.

(iv) Molecular biology kits: Ribomax Large Scale RNA Production System-T7 and Access RT-PCR kits were obtained from Promega, Madison, WI, USA. EndoFree Plasmid Maxi Kit, HiSpeed Plasmid Maxi Kit, Qiaquick Gel Extraction Kit, Omniscript RT Kit and RNeasyMini Kit were obtained from Qiagen, Hilden, Germany. QuikChange Site Directed Mutagenesis Kit was obtained from Stratagene. ViraKit was obtained from Virapure, San Diego, CA, USA.

(v) Tissue culture: Dulbecco's modified Eagle medium (D-MEM), RPMI 1640 medium, foetal calf serum (FCS), L-glutamine, taurine, B-27 supplement, trypsin-EDTA, phosphate buffered saline (PBS, pH 7.2), Hanks' balanced salt solution (HBSS) and Opti-MEM I were obtained from Gibco-Invitrogen, Paisley, UK.

2.1.2 Solutions

(i) Luria-Bertani medium (LB medium): 1% (w/v) tryptone, 0.5% (w/v) yeast extract, 1% (w/v) NaCl. To prepare agar plates 1.5% (w/v) Agar grade A was added to the medium. LB agar and broth were autoclaved at 15 p.s.i. for 20 minutes. *E. coli* (XL-1B) cultures were selected using 50μg/ml ampicillin and 25μg/ml tetracycline.

(ii) 1X-Tris-acetate (TAE) buffer (pH 8.0): 0.04M Tris-acetate, 0.01M ethylenediaminetetra-acetic acid disodium salt (EDTA, pH 8.0).

(iii) Gel loading dye: 0.25% (w/v) bromophenol blue, 0.25% (w/v) xylene cyanol and 30% (w/v) glycerol in double-distilled water (ddH_20).

(iv) 10X-PCR buffer: 500mM KCl, 100mM Tris-HCl (pH 9.0), 0.1% gelatin, 1% Triton X-100 and either 10, 15, 20 or 25mM $MgCl_2$.

(v) Miniprep solutions: *Lysis solution 1*: 50mM Tris-HCl (pH 8.0), 0.25% sucrose and 2mM EDTA (pH 8.0). *M-STET solution*: 5% Triton X-100, 50mM EDTA (pH 8.0), 50mM Tris-HCl (pH 8.0) and 5% sucrose.

(vi) Caesium chloride maxiprep solutions: *Lysis solution 1*: 50mM glucose, 25mM Tris-HCl (pH 8.0) and 10mM EDTA (pH 8.0). *Lysis solution 2*: 0.2M NaOH and 1% sodium dodecyl sulphate (SDS). *Lysis solution 3*: 3M sodium acetate (pH 5.2). *Top-up solution*: 0.95g CsCl per 1ml Tris-HCl, pH 8.0.

(vii) RNA solutions: *RNA loading dye*: 1mM EDTA, 0.25% bromophenol blue, 0.25% xylene cynanol and 50% glycerol. *DEPC H_20*: 500ml ddH_20 treated with 1ml diethylpyrocarbonate (DEPC) overnight at 37°C, followed by autoclaving at 15 p.s.i. for twenty minutes. *10X-Tris-borate (TBE) buffer*: 55g boric acid, 108g Trizma base and 40ml 0.5M EDTA (pH 8.0) in a final volume of 1L. *20% acrylamide*: 96.5g acrylamide, 3.35g bis-acrylamide, 233.5g urea and 50ml 10X-TBE in a final volume of 500ml. *7.75M urea*: 233.5g urea, 50ml 10X-TBE and ddH_20 to 500ml. *Polyacrylamide gel (4%)*: 45ml 7.75M urea, 30ml 20% acrylamide, 600μl ammonium persulphate (APS) and 75μl N,N,N,'N'- tetramethylethylenediamine (TEMED).

(viii) Western blot analysis: *RIPA buffer*: 50mM Tris-HCl, pH 7.5, 150mM NaCl, 1% NP-40, 0.5% sodium deoxycholate, 0.1% SDS. *Polyacrylamide gel (10%)*: 10% polyacrylamide mix, 0.375M Tris-HCl (pH 6.8), 1% SDS, 1% APS, 0.04% TEMED. *5X SDS Loading Buffer*: 50mM Tris-HCl (pH 6.8), 100mM dithiothreitol (dTT), 2% SDS, 0.1% bromophenol blue and 10% glycerol. *Tris-glycine electrophoresis buffer*: 25mM Tris base, 250mM glycine (pH 8.3), 0.1% SDS. *Transfer buffer*: 39mM glycine, 48mM Tris base, 0.037% SDS, 20% methanol. *Blocking solution (5% Milk TBS-Tween)*: 10mM Tris-HCl (pH 8.0), 150mM NaCl, 0.05% Tween-20, 5% non-fat dried milk, 0.05% sodium azide. *Wash solution (TBS-Tween)*: 10mM Tris-HCl (pH 8.0), 150mM NaCl, 0.05% Tween-20.

(ix) Tissue culture medium: *Complete D-MEM*: D-MEM, 10% (v/v) FCS, 2mM sodium pyruvate, 2mM L-glutamine. *Complete RPMI 1640*: RPMI 1640, 15% (v/v) FCS, 2mM sodium pyruvate. *Complete D-MEM/F12*: 10% (v/v) FCS, 2mM taurine, 2% (v/v) B-27 supplement.

(x) 2X-HBS buffer: 280mM NaCl, 10mM KCl, 1.5mM Na_2HP0_4, 12mM dextrose and 50mM Hepes (pH 7.1).

(xi) β-galactosidase (β-gal) staining solutions: *Fixative solution*: 0.2% glutaraldehyde and 2% paraformaldehyde in PBS (pH 7.2). *Staining solution*: 5mM potassium ferricyanide, 5mM potassium ferrocyanide, 2mM $MgCl_2$, 0.02% NP-40, 0.01% SDS in PBS. 5-bromo-4-chloro-3-indolyl-β-D-galactoside (X-gal) at a stock concentration of 20mg/ml (in dimethyl formamide) was added fresh before use at a final concentration of 1mg/ml.

(xii) 10% Neutral formalin: 100ml formalin, 6.5g sodium phosphate dibasic and 4.0g sodium phosphate monobasic in a final volume of 1L ddH_20.

(xiii) TUNEL assay mix: 50μl 5X buffer, 2.5μl Terminal deoxynucleotidyl Transferase (Promega), 1.5μl tetramethylrhodamine-5-dUTP (Roche Diagnostics) in a final volume of 500μl ddH_20.

2.1.3 Oligonucleotide synthesis

Oligonucleotides were supplied by Sigma-Genosys, Pampisford, Cambridgeshire, UK. They were resuspended in ddH_20 at a final concentration of 100μM and diluted appropriately for use.

2.1.4 Cell lines

Human embryonic kidney (HEK) 293 cells were obtained from Stratagene. Professor Seamus Martin of Trinity College Dublin provided HEK 293T (adenovirus-transformed) cells and HeLa human epitheloid carcinoma cells. The mouse photoreceptor cell line 661W was supplied by Professor Muayyad Al-Ubaidi of the Department of Cell Biology, University of Oklahoma Health Sciences Center, Oklahoma City, OK, USA. Dr. Michael Cheetham of the Institute of Opthalmology, London, UK, provided the Y79 human retinoblastoma cells.

2.1.5 Animals

All experiments using animals were conducted in compliance with the Association for Research in Vision and Opthalmology (ARVO) statement regarding the use of animals in ophthalmic and vision research. Two strains of mice were used: 1) wild-type (wt) C57BL/6J mice from Harlan Laboratories, Oxfordshire, UK and 2) *lox*P-p35 transgenic mice kindly provided by Professor Masayuki Miura from the Department of Genetics, University of Tokyo, Japan.

2.2 General Methods

2.2.1 Phenol/chloroform extraction of DNA and RNA

Samples were mixed with equal volumes of buffer saturated phenol (pH 7.5), vortexed for 30 seconds and centrifuged at 13,200rpm on a Micromax centrifuge (International Equipment Company: Thermo-Electron, Waltham, MA, USA) for 5 minutes to separate the phases. The upper aqueous phase was transferred to a fresh eppendorf. An equal volume of phenol/chloroform was added and the sample was vortexed and centrifuged as before. The upper phase was removed, an equal volume of chloroform was added and the sample was treated as before. The aqueous phase was removed and the nucleic acid was ethanol precipitated.

2.2.2 Ethanol precipitation of DNA and RNA

Nucleic acids were precipitated by adding 0.1x volume of 3M sodium acetate (pH 7.0) and 2.5x volume of ethanol. Samples were mixed and left for thirty minutes at room temperature. They were then centrifuged for twenty minutes at 13,200rpm (Micromax) and the supernatant was removed. The pellet was washed with 70% ethanol and resuspended in ddH_20.

2.2.3 Restriction enzyme digestion

Restriction enzyme digestions of DNA were carried out in final volumes of 20-50µl. Restriction enzymes were used at a concentration of 1U per 1µg DNA with the appropriate buffer. The reactions were incubated for a minimum of 2 hours at 37°C or other specified temperature according to the manufacturer's instructions.

2.2.4 Visualisation of DNA by agarose gel electrophoresis

Agarose gels were prepared by boiling 0.8-3.0% (w/v) of agarose in 1X-TAE buffer. The higher percentage gels were used for visualising DNA bands smaller than 500 bp. Agarose solutions were allowed to cool for several minutes and ethidium bromide (EtBr) was added at a final concentration of 0.5µg/ml. Combs were inserted and gels were allowed set for 30 minutes. Combs were removed and 1X-TAE was added to the gel rig (Bio-Rad Laboratories). The DNA samples (mixed with 0.1x volume of DNA

loading dye) were loaded into the wells alongside a DNA size marker. Samples were electrophoresed at 80mA. DNA was visualised on the Gene Genius Gel Documentation System with GeneSnap software (Syngene, Cambridge, UK).

2.2.5 Purification of DNA fragments from agarose gels

Restriction enzyme digested or PCR amplified DNA samples were mixed with 0.1x volume of loading dye, loaded on 1-1.5% agarose gels as described above in 2.2.4. Gels were visualised with a TFX20M UV transilluminator and required fragments cut out with sterile razor blades. Gel isolated fragments were cleaned using the Qiaquick Gel Extraction Kit (Qiagen) in accordance with the manufacturer's instructions. An aliquot of the purified DNA was run on an agarose gel to ensure accuracy of isolation. Gel-purified fragments were then sequenced or used for cloning.

2.2.6 Ligations

In a 15µl reaction volume, varying concentrations of insert DNA were added to 100ng vector. 1.5µl of 10X buffer and 1.5µl rATP was subsequently added with 1µl ligase enzyme. The final volume was adjusted to 15µl with ddH_20 and the mix was incubated at 18°C overnight.

2.2.7 Competent cell preparation for XL-1B cells

Overnight cultures of *E. coli* (XL-1B) in 1ml LB selective (with tetracycline) media were used to inoculate 50ml LB selective media to an OD_{600} of 0.4 to 0.6. The cells were centrifuged for 10 minutes at 3,200rpm on a GS-6 centrifuge (Beckman Coulter, Fullerton, CA, USA). The supernatant was discarded and the cells were washed in an equal volume of 100mM $MgCl_2$ (4°C). The cells were centrifuged again for 10 minutes. The $MgCl_2$ was discarded and the cells were resuspended in 0.5x volume of 100mM $CaCl_2$. The cells were then left on ice for 20 minutes. The cells were then centrifuged as before and resuspended in 0.05x volume of 100mM $CaCl_2$ (4°C).

2.2.8 Transformation

5µl of each ligation mix was made up to a final volume of 100µl with 100mM $CaCl_2$, and added to 150µl competent cells, incubated on ice for 30 minutes and heat shocked for 2 minutes at 42°C. 2ml of LB medium was added to the cells, which were then incubated at 37°C for 90 minutes and inoculated to selective (ampicillin or kanomycin) agar media plates at 37°C overnight.

2.2.9 Selection of positive XL-1B transformants using PCR analysis

Single XL-1B colonies were re-inoculated to fresh selective agar media plates for a further night, and screened using PCR analysis (see 2.2.15). A sterile toothpick was used to transfer each single colony to 5µl Tris-HCl-EDTA (TE) buffer in an eppendorf. To this, a solution containing 10pmol forward and reverse primer, 0.2mM dNTPs, 1.5U Taq polymerase and 2µl 10X-PCR buffer (2.1.2 {iv}, with a final concentration of 10-25mM $MgCl_2$) made to a final volume of 15µl with ddH_20, was added. The reactions were cycled as described in 2.2.15. Amplified DNA products were run on an agarose gel with a DNA sizing ladder, to identify the colonies carrying the plasmid construct. Positive single colonies were re-inoculated in 10ml selective LB medium with shaking in an orbital incubator at 37°C overnight for plasmid mini-prep analysis.

2.2.10 Boiling miniprep procedure

Cultures were centrifuged at 3,200rpm (GS-6) for 10 minutes. The pelleted cells were resuspended in 60µl resuspension buffer (2.1.2 {v}) and transferred to a 1.5ml eppendorf on ice. 20µl lysozyme solution (40mg/ml in 250mM Tris-HCl pH 8.0) was added and the samples were left for 10 minutes on ice. 550µl M-STET (2.1.2 {v}) was added and the samples were left to stand at room temperature for 10 minutes. The lids of the eppendorfs were opened and the samples were boiled for 1 minute. They were then centrifuged for 30 minutes at 13,200rpm (Micromax). The pellet was pulled out with a sterile toothpick and 1µl RNaceIT (Stratagene) was added to each sample. They were incubated at 37°C for 15 minutes before one phenol extraction. 0.6x volume isopropanol was added to the samples, which were left for 15 minutes at room

temperature. The samples were centrifuged for 10 minutes and washed with 80% ethanol. The pellets were resuspended in 50µl ddH_20.

2.2.11 Qiagen plasmid maxipreps

To prepare large quantities of clean DNA for techniques including transfection to mammalian cell lines and electroporation of retinal explants, HiSpeed and EndoFree Plasmid Maxi Kits were used (Qiagen) in accordance with the manufacturer's instructions.

2.2.12 Caesium chloride DNA maxipreps

Overnight cultures of transformed *E. coli* (XL-1B) in 5ml selective LB media were used to inoculate 1L selective LB media and grown for 7 hours. 0.1g of chloramphenicol was then added and the culture was grown overnight. Following centrifugation at 7,000rpm on a Sorvall RC-5B centrifuge (Thermo-Electron, Waltham, MA, USA) for 10 minutes, the pellets were pooled in 50ml lysis solution I (2.1.2 {vi}), and left on ice for 30 minutes. 50ml lysis solution II was added slowly and the suspension was left on ice for 15 minutes after mixing well. The suspension was then centrifuged at 8,000rpm for 5 minutes, 0°C. The supernatant was filtered through gauze into a new bottle and 0.6x volume of cold isopropanol was added. It was then centrifuged immediately for 10 minutes at 8,000rpm, 0°C. The supernatant was discarded and the pellet was briefly dried upside down. The pellet was resuspended in 8.3ml of 10mM Tris-HCl (pH 8.0). 8.8g of caesium chloride was weighed into a 50ml tube and 8.7ml of the plasmid mix was added. 0.35g of 10mg/ml EtBr was then added. The caesium chloride was dissolved fully and the solution was transferred into a centrifuge tube. It was then filled with top-up solution, and centrifuged overnight at 45,000rpm in a Beckman L8-M ultracentrifuge. The bottom band of plasmid DNA was removed by side puncture (approximately 3ml). This solution was washed with saturated butanol to remove the ethidium bromide. Following pressure concentration, the DNA solution was dialysed against 10mM Tris-HCl (pH 8.0) for 8 hours, which was changed 4 times every 15 minutes and then 1 time per hour for 5 hours. DNA was

then quantified (2.2.13) and sequenced (2.2.14) to confirm its integrity before use in experiments.

2.2.13 Quantification of DNA and RNA

DNA and RNA were quantified at 260nm and 280nm respectively on a CE 3021 spectrophotometer (Cecil Instruments, Cambridge, UK). The amount of nucleic acid present was calculated on the basis that an optical density (OD) of 1 corresponds to 50μg/ml for double-stranded DNA and 40μg/ml for single-stranded DNA and RNA. The ratio between the readings at 260nm and 280nm also indicate the purity of the nucleic acid. Pure preparations of DNA and RNA should have $OD_{260/280}$ values of 1.8 and 2.0 respectively.

2.2.14 DNA sequencing

Sequencing was performed using the ABI 310 Genetic Analyser (Applied Biosystems, Santa Clara, CA, USA) using BigDye Terminator chemistry (PerkinElmer, Boston, MA, USA). 250ng of DNA, 2 pmol primer, 2μl BigDye Terminator mix and 2μl 5X-buffer were made up to a final volume of 10μl. The reaction was cycled 25 times at 96°C for 30 seconds, 50°C for 15 seconds, 60°C for 4 minutes. The samples were then ethanol precipitated and resuspended in 25μl template suppression reagent (PerkinElmer). The resuspended samples were heated at 94°C for 2 minutes, and then chilled on ice. Samples were loaded onto an ABI 310 Genetic Analyser. Sequence data was collected and analysed using the ABI Prism 310 collection and Sequencing Analysis 3.4.1 programs.

2.2.15 Polymerase chain reaction (PCR)

A typical 25μl PCR reaction had the following components: 0.2mM dNTPs, 10 pmol of forward and reverse primer, 1.5U Taq polymerase, 20ng DNA template and 2.5μl 10X-PCR buffer (2.1.2 {iv}, with a final concentration of 10-25mM $MgCl_2$) brought to a final volume of 25μl with ddH_20. Following denaturation at 94°C for 5 minutes the reactions were typically cycled 35 times at 94°C for 1 minute to denature, 55°C for 1 minute to amplify, and 72°C for 1 minute to elongate. These times did vary according

to the particular fragment being amplified. A 10 minute step at 72°C was added at the end to increase product yield. PCR amplifications were carried out on a DNA engine PTC-200 (MJ Research: Thermo-Electron, Waltham, MA, USA) using a heated lid to prevent evaporation.

2.2.16 End-filling of DNA fragments using Klenow enzyme and T4 DNA polymerase

Klenow enzyme was used to end-fill 5' overhangs of DNA fragments. A 50µl reaction contained 1µl enzyme, 2mM dNTPs, 5µl Roche A buffer and 1µg DNA. The reaction was incubated at 37°C for 30 minutes. The Klenow enzyme was then removed by phenol/chloroform extraction (see 2.2.1). T4 DNA polymerase was used to end-fill 3' overhangs of DNA fragments. A 50µl reaction contained 1µl enzyme, 2mM dNTPs, 10µl incubation buffer and 1µg DNA. The reaction was incubated at 12°C for 10 minutes and then immediately cleaned using phenol/chloroform extraction.

2.2.17 Dephosphorylation of 5'-phosphorylated ends of DNA

Shrimp alkaline phosphatase (SAP) is used to dephosphorylate 5'-phosphorylated ends of linearised plasmid DNA, to prevent re-ligation of the plasmid. Each reaction contained 5µl 10X supplied buffer, 2µl SAP enzyme, 1µg DNA made up to a final volume of 50µl with ddH_20. The reaction was incubated for 1 hour at 37°C and SAP was inactivated by heating at 65°C for 15 minutes. 1µl of the reaction was then run on a 1% agarose gel to estimate the quantity of vector to use for the ligation.

2.3 RNA Methods

2.3.1. Working with RNA

RNA is more susceptible to degradation than DNA and so several precautions were taken to reduce the risk of sample degradation. These included using nuclease-free eppendorfs, nuclease-free water, filtered tips and treating all solutions with DEPC as described in 2.1.2 (vii).

2.3.2. Computer-aided RNA-folding

RNA forms a complex secondary structure *in vivo*, formed by hydrogen-bonded pairings of complimentary bases (Uhlenbeck *et al.*, 1997). A number of computer modelling programs have been developed that predict RNA secondary structure based on the primary sequence by using different algorithms or mathematical formulas (Matzura *et al.*, 1996; Zuker 1989). The widely used Mfold program, uses a recursive algorithm that determine the optimal structures based on the lowest equilibrium free energy as according to basic thermodynamic principles, this structure should be the most stable (http://www.bioinfo.rpi.edu/application/mfold; Zuker 1989; Zuker *et al.*, 2003). As the Mfold algorithm generates the structure base by base, the free energy contributions of base-pairs, hairpin loops and other secondary structural interactions are calculated. These free energy values are based on thermodynamic parameters derived from *in vitro* experimental data generated by analysing the thermodynamics of melting short RNA oligonucleotides (Frier *et al.*, 1986; Walter *et al.*, 1994; Matthews *et al.*, 1999). A detailed description of the Mfold algorithm can be found in Zuker 1989 and Zuker *et al.*, 1994.

Folding constraints can be placed on the generated secondary structures to include a specific helix or hairpin loop for example, or prevent specified regions from base-pairing. In addition, the temperature is set at 37°C and ionic conditions at 1M Na^+ and 0M Mg^{2+}, to reflect physiological conditions. To display the optimal and suboptimal RNA secondary structures generated by Mfold, a companion program PlotFold is used. A range of representations can be used including an energy dotplot, which takes the

form of a two-dimensional graph, or a squiggles plot, which shows the base-pairing of stems, loops and other secondary structures. To identify NUX ribozyme cleavage sites located in open accessible loops, as described in Chapter 6, a squiggles plot output was selected (Figure 6.1).

A second folding program, RNAdraw, was used to compare the prediction of open loop structures to those generated by Mfold/Plotfold to select the most likely regions to form open accessible loops (http://www.rnadraw.com; Matzura *et al.*, 1996). RNAdraw can be used on an Intel compatible computer with any recent Windows program, in contrast to Mfold/Plotfold, which relies on an Intel/Linux mainframe computer located at Renssalaer Polytechnic Institute, New York, USA. RNAdraw also uses a recursive algorithm from Hofacker *et al.*, to generate an optimal secondary structure (Hofacker *et al.*, 1994). This can be viewed as a two-dimensional graph, showing the base-pairing probability or as a base-paired structure similar to a squiggle plot (Figure 6.2).

2.3.3 Isolation of RNA from cultured cells

TRI Reagent (Molecular Research Center, Cincinnati, OH, USA) was used to isolate total RNA from cultured cells. 1ml TRI Reagent was pipetted onto a 3.5cm dish. This was left for 5 minutes at room temperature and then transferred to an eppendorf. 200µl of chloroform was then added and the solution was vortexed for 15 seconds. This was left for 2-3 minutes again at room temperature. The solution was centrifuged for 15 minutes at 12,000rpm (Micromax) at 4°C. Approximately 600µl of the upper phase was transferred to a new eppendorf. The RNA was precipitated with 500µl isopropanol and left for 10 minutes. It was then centrifuged for 10 minutes at 12,000rpm 4°C. The isopropanol was poured off and the RNA was washed with 1ml of 75% ethanol and resuspended in 20µl DEPC dd$H_2$0. Isolated RNA was treated with RNase-free DNase (Promega), cleaned using phenol/chloroform extraction and resuspended in 20µl dd$H_2$0.

2.3.4 Isolation of RNA from mouse retina

Wild-type C57BL/6J animals were culled, and RNA was extracted from the retinas using TRI Reagent as described in 2.3.3 above. Following treatment with RNase-free DNase, RNA was resuspended in 20µl ddH_20.

2.3.5 Analysis of RNA by reverse-transcription PCR (RT-PCR)

50ng-2µg of DNase treated total RNA was reverse transcribed to cDNA using the Omniscript RT kit (Qiagen) as follows: A reverse transcription mix was made consisting of 2µl of 10X RT buffer, 2µl dNTP mix, 1µl Omniscript RT, 1µl random primers (Promega, 500µg/ml), Yµl of RNA and Xµl of H_20, such that X + Y was 14µl. The reaction was then incubated for 1 hour at 37°C and terminated by heating to 65°C for 10 minutes. PCR reactions were set up using 2µl cDNA, 0.1U Taq polymerase, 2µl 10X-PCR buffer with 15mM $MgCl_2$, 200µM dNTPs, 10pmol forward and reverse primers and ddH_20 to 20µl. The reaction was cycled as follows: 94°C for 1 minute followed by 30 cycles of 94°C for 1 minute, 55°C for 1 minute, 72°C for 1 minute and a final 10 minute extension time at 72°C.

2.3.6 Analysis of RNA by quantitative real-time RT-PCR

RNA was analysed by real-time RT-PCR using a Quantitect Sybr Green Kit (Qiagen-Xeragon, Crawley, UK) on a LightCycler (Roche Diagnostics) or an Applied Biosystems 7300 Real Time PCR System. Reactions were carried out in a final volume of 20µl with 10µl supplied mix, 0.2µl enzyme, 0.5µl of each primer, 4.3µl ddH_20 and 4.5µl RNA sample. The following cycling conditions were used: 50°C for 20 minutes; 95°C for 15 minutes; 35 cycles of 94°C for 15 seconds, 57°C for 20 seconds and 72°C for 10 seconds. Primers used were purified by high performance liquid chromatography (HPLC) and the RNA levels of transcript of interest were standardised to house keeping genes: β-actin, glyceraldehyde-3-phosphate dehydrogenase (GAPDH) or 18s rRNA.

2.3.7. Expression and radioactive labeling of RNA

Ribomax Large Scale RNA Transcription Kits (Promega) were used to express RNA from plasmid constructs in accordance with the manufacturer's guidelines. 1.6µg of

clean digested DNA was transcribed with 4µl 5X-T7 buffer, 2µl T7 enzyme mix, 25mM ATP, CTP, GTP, 2.5mM UTP, 25mM rUTP [α-^{32} P] (Amersham Biosciences) and made up to 20µl with nuclease-free water. Samples were incubated at 37°C for 3 hours and incubated with 1µl RNase-free DNase (Promega) for 15 minutes. Following incubation at 65°C for 10 minutes to inactivate the DNase, RNA samples were stored at -80°C.

2.3.8 Polyacrylamide gel electrophoresis

5µl of RNA loading dye (2.1.2 {vii}) was added to the RNA transcription reaction (21µl), heated to 94°C for 3 minutes and then chilled on ice prior to loading on a 4% polyacrylamide gel (2.1.2 {vii}). Samples were electrophoresed at 43mA for approximately 3 hours dependent on transcript length. Gels were blotted to chromatography paper (Albet, Barcelona, Spain), and viewed by autoradiography on Hyperfilm MP (Amersham Biosciences) before desired fragments were excised from gels with sterile scalpels.

2.3.9 RNA gel extraction and purification

Excised bands were incubated overnight in an orbital shaker at 37°C in 700µl 0.3M sodium acetate (pH 5.2) and 0.2% SDS. RNA transcripts were cleaned with 4-5 phenol/chloroform washes, ethanol precipitated and resuspended in 20µl nuclease-free dd$H_2$0. 1µl of transcript was quantified by scintillation counting of incorporated radio-nucleotide in 5ml Ecoscint (National Diagnostics, Atlanta, Georgia) on a Beckman LS-6500 Scintillation Counter.

2.3.10 Ribozyme: substrate cleavage reactions

Ribozymes were incubated with RNA targets with 1µl 100mM $MgCl_2$ and 10mM Tris-HCl in a final volume of 10µl for 3 hours at 37°C. For time point cleavage reactions, 2µl were removed from reactions at appropriate times and added to 2µl RNA loading dye. Time point samples were heated to 94°C for 3 minutes and then chilled on ice prior to loading on a 4% polyacrylamide gel for 3 hours. Gels were transferred to chromatography paper, dried down under vacuum for 1 hour and exposed to autorad

film overnight at –70°C. Dried blots of cleavage reactions were visualised and quantified using phosphor screens, a Typhoon Imaging System (Amersham Biosciences) and ImageQuant software (Molecular Dynamics, Sunnyvale, CA, USA).

2.3.11 Molecular weight markers for RNA

A radioactive DNA ladder was made by end-filling 1µg of *Msp*I digested pBR322 (New England Biolabs) with Klenow in a reaction containing 3µl 10X-buffer, 1.5µl dCTP [α^{32} P] (10mCi/ml), 0.5U Klenow in a final volume of 30µl. 2µl of end-labeled digest was mixed with 60µl dd$H_2$0 and 60µl formamide dye. 2µl of labeled ladder mix was loaded per gel.

2.4 Cell Culture and Protein Methods

2.4.1 Routine mammalian cell culture conditions

Cells were maintained in a sterile humidified environment at 37°C and 5% CO_2 and passaged every 2-3 days. They were grown in either complete D-MEM or RPMI-1640 (2.1.2 {ix}). Adherent cells were passaged by removing old media and then by washing the monolayers with PBS, to remove any residual media. The cells were dissociated from culture plates by trypsinisation in approximately 1-2ml of trypsin-EDTA. Cells were returned to the incubator for a period of 5-10 minutes and dissocation of monolayers was monitored by visual inspection under light microscopy. The trypsin was then neutralised by the addition of approximately 5ml of complete medium and cells were resuspended in 10ml fresh pre-warmed medium following centrifugation at 1,100rpm (Centra-3C centrifuge, International Equipment Company) for 5 minutes. An aliquot of 10µl was resuspended on a haemocytometer slide and a cell count was undertaken as described below. For passaging, cells were plated at a concentration of 1 x 10^6 on 10cm plates.

2.4.2 Cell cryopreservation and thawing

Individual cell-lines in routine culture were maintained in continuous passage for no longer than 2-3 months in order to avoid *in vitro* accumulation of further mutations that might alter the defined characteristics of the line. Upon receipt of a new cell line, cells of low passage number were harvested in exponential growth, as described in 2.4.1 and pellets resuspended in 2ml of freezing medium (10% dimethyl sulfoxide {DMSO}, 40% complete D-MEM, or RPMI-1640 medium and 50% FCS). Aliquots of 500µl of cells were placed in cryogenic storage vials and allowed to freeze slowly in a –70°C freezer. Following freezing, cells were maintained in liquid nitrogen tanks for long-term storage. To revive frozen stocks, cells were rapidly defrosted by placing storage vials in a 37°C incubator. Complete thawing or warming of aliquots was avoided. The cryopreservation medium was removed by diluting 500µl of defrosted cells in 20ml medium without FCS. The cells were then centrifuged at 1,100rpm (IECCentra-3C

centrifuge) for 5 minutes. The supernatant was aspirated off and the cell pellet was resuspended in 10ml complete medium.

2.4.3 Haemocytometer cell counting

Before use the haemocytometer was washed with 70% ethanol and dried. A coverslip was placed over the counting area of the haemocytometer chamber. Following trypsinisation the cell sample was resuspended in 10ml medium and 10µl was placed on the edge of the coverslip, which then filled the chamber. The haemocytometer was transferred to a microscope and viewed under the 10X objective. The number of cells present in 16 squares was noted. This was repeated for the 3 other 16 squared areas and the average number of cells calculated. The number of cells in the sample counted = average cell count X dilution 10^4/ml.

2.4.4 Transfection using the calcium phosphate precipitation method

200ng of plasmid DNA was diluted in a final volume of 100µl ddH_20 (per transfection). 25µl of 2.5M $CaCl_2$ was then added and mixed well. The DNA/$CaCl_2$ solution was added drop-wise to 125µl of 2X-HBS buffer, pH 7.1 (2.1.2 {x}). Following a 20-30 minute incubation period the DNA precipitate was added slowly to cells plated in 6-well plates the night before and re-incubated at 37°C for 4-5 hours prior to changing the cell medium. Cells were then incubated for at least a further 24 hours prior to analysis.

2.4.5 β-galactosidase staining of transfected cells

Transfected adherent cells were washed with cold PBS, fixed with 1ml fixative solution (2.1.2 {xi}) per well in a 6-well plate and incubated for 5 minutes at room temperature. The fixative was removed and the cell monolayer was again washed with ice-cold PBS for 5 minutes. 0.8ml β–gal staining buffer (2.1.2 {xi}) with 1mg/ml X-gal was added to each well in a 6-well plate and incubated at 37°C for 1-2 hours. Cells were scored for β–gal expression using a CK30 light microscope (Olympus, Munich, Germany).

2.4.6 Immunocytochemistry of transfected cells

For immunocytochemistry, 1.3 x 10^5 HeLa cells were plated on 15mm sterilised glass coverslips (Scientific Laboratory Supplies, Nottingham, UK) in each well of a 24-well

plate. 48 hours following transfection, cells were washed twice with PBS for 5 minutes and fixed with 500µl of 4% paraformaldehyde for 1 hour. After 2 further washes with PBS, cells were incubated in a blocking buffer (1-3% serum, 0.1% Triton X-100) for 1 hour. During this time, a 10cm plate was filled with blotting paper soaked in water and covered with parafilm to create a humidified chamber. Cells on coverslips were then carefully transferred to the parafilm and 80µl of diluted primary antibody per coverslip area was gently pipetted on top of the cells. A lid was placed on the chamber, and the cells were incubated with primary antibody overnight at 4°C. The following day, the coverslips were placed back in 24-well plates and washed twice with PBS for 10 minutes. Cells were incubated with appropriate secondary antibody in the humidified chamber for 1-2 hours and washed twice more with PBS. Cells were then mounted on polylysine glass slides (Menzel-Glaser, Braunschweig, Germany) using Aqua-Poly/Mount (Polysciences, Warrington, PA, USA) covered with a 24 x 60mm coverslip (Scientific Laboratory Supplies) and examined using a Zeiss Axioplan-2 Optical Fluorescent Microscope (Carl Zeiss, Oberkoclen, Germany) with the appropriate Zeiss filter and analysis^B Imaging Software (Olympus).

2.4.7 Protein extraction, quantification and Western blot analysis

The cells were harvested 24-48 hours following transfection. The medium was removed, 800µl of RIPA Buffer (2.1.2 {viii}) was added to the cells and they were incubated on ice for 5 minutes. The lysates were then centrifuged at 11,800rpm for 15 minutes on a Microfuge 22R centrifuge (Beckman Coulter) at 4°C and the supernatant was stored at –20°C. To quantify the protein, dilutions of 1/10 and 1/20 of each sample were prepared and 20µl of each was assayed in 980µl of Bio-Rad protein assay (Bio-Rad Laboratories) and read in triplicate on a spectrophotometer (Bio-Rad SmartSpec 3000) at 595nm. Approximately 100µg of each sample (final volume of 30µl with 5X-SDS loading dye) was heated to 90°C for 6 minutes, chilled on ice and then electrophoresed at 80V for 3-4 hours through a 10% polyacrylamide gel (2.1.2 {viii}). A prestained protein ladder was loaded to monitor protein separation and act as a molecular weight marker. The protein gel was then transferred to a nitrocellulose membrane (Schleicher and Schuell, Dassel, Germany) and transferred for 2 hours at

120mA. Membranes were blocked for 1 hour in 5% Milk TBST-Tween (2.1.2 {viii}) and then probed overnight at 4°C with an appropriate dilution (1/750-1/2000) of a primary antibody diluted in the same buffer. Membranes were then washed for 1 hour in 4 changes of TBS-Tween (2.1.2 {viii}) and incubated for 2 hours with a horseradish peroxidase-coupled secondary antibody (Abcam, Cambridge, UK). Bound antibody was detected by enhanced chemi-luminescence, using the SuperSignal West Pico Kit (Pierce, Rockford, IL, USA).

2.6 Recombinant AAV-2 Methods

2.6.1 Production of high-titre recombinant AAV-2 (rAAV-2) in the absence of helper adenovirus

The method followed here is based on the published method of Xiao *et al.,* 1998. For rAAV-2 (referred to as AAV hereafter) production, the expression construct was first cloned into the plasmid vector pAAV-MCS (Stratagene), prepared in bulk using EndoFree Plasmid Maxi Kit (Qiagen) and resuspended in TE buffer, pH 8.0 at a final concentration of 1μg/ml. The pHelper (Stratagene) and control plasmid, pAAV-RC (Stratagene) were prepared in a similar way. 24 hours prior to transfection, 293 cells were plated at a concentration of 2×10^6 cells per 10cm tissue culture plate in 5ml of complete DMEM. For each 10cm plate, 10μl of each of the three plasmid solutions (10μg of each) was pipetted into a 15ml conical tube. 1ml of 0.3M $CaCl_2$ was added and mixed gently. 1ml of 2X-HBS buffer, pH 7.1 (2.1.2 {x}) was pipetted into a second 15ml conical tube and the 1.03ml DNA/$CaCl_2$ was added slowly to the buffer. Following 30 minutes incubation at room temperature, the DNA/$CaCl_2$/HBS suspension was added to the 10cm plate of 293 cells dropwise, while swirling gently to evenly distribute the suspension. The 293 cells were incubated at 37°C for 12 hours, and then the old medium replaced with 5ml fresh complete DMEM. 293 cells were incubated for a further 48 hours.

293 cells were dislodged from 10cm plates by gently pipetting up and down, thus resuspending cells in 5ml DMEM. Two methods were routinely used employed to harvest AAV, caesium chloride (CsCl) density gradient centrifugation, and membrane based purification (Virakit, from Virapure). The method using CsCl, was followed according to the protocol of Zolotukhin *et al.*, 1999. Vector-containing cells were centrifuged at 3,000rpm (Centra-3C centrifuge) for 30 minutes. Cell pellets were resuspended in 10ml PBS and subjected to three rounds of freeze/thaw (-80°C, 37°C), followed by 30 minutes incubation at 37°C with 25U/ml Benzonase (recombinant DNase/RNase from Novagen: Merck, Darnstadt, Germany). Following a 15 minute centrifugation at 3,000rpm, the supernatant was transferred to a new tube and incubated

with 0.5% (final concentration) deoxycholate for 30 minutes at 37°C to further lyse any remaining cells. Following the collection of AAV in 50ml tubes, 0.454g CsCl/ml was added to each sample and incubated on ice for 5 min. A density gradient was prepared in polyallomer centrifuge tubes (Beckman-Coulter), with 9ml of 8.16g/ml CsCl and 9ml of 5.48g/ml CsCl. The AAV samples were then applied to the top of the gradient and spun at 25,000rpm (Beckman L8-M ultracentrifuge) for 18 hours at 4°C. 1ml fractions from the gradient were collected and analysed using a refractometer (Thermo-Electron, Waltham, MA, USA). Fractions within the range of 1.373-1.368 were collected, pooled in polyallomer tubes and equilibrated with 5.48g/ml CsCl. Samples were spun at 59,000rpm (Beckman L8-M ultracentrifuge) for 18 hours at 4°C. 0.5ml fractions were collected and those within the refractive index of 1.373-1.368 were pooled into a polyallomer Beckman tube and centrifuged as above. Following collection, 0.5ml fractions from within the refractive range 1.373-1.368 were dialysed against 10L of PBS, pH 7.0 over 40 hours (1L/4hrs) using 0.5ml Slide-A-Lysers (Pierce). Purifed AAV was then stored at -80°C, and the genomic titre was determined.

The second method of AAV purification involved using the membrane based ViraKit from Virapure, according to the manufacturer's instructions. After dislodging 293 cells from 10cm plates, cell lysate and media were collected in 50ml tubes, and subjected to three rounds of freeze/thaw (-80°C, 37°C), followed by a 30 minute incubation at 37°C with 25U/ml Benzonase (recombinant DNase/RNase). Samples were centrifuged at 3,000rpm (Centra-3C centrifuge) for 30 minutes and the supernatant collected in fresh 50ml tubes. Briefly, the supernatant was purified using a 0.45µ filter, and following the addition of supplied buffers, further purified using two additional filters. Purifed AAV was then stored at -80°C and the genomic titre was determined.

2.6.2 Titration of genomic AAV particles using quantitative real-time PCR

The genomic titre of AAV was determined following the method of Rohr *et al.*, 2002. 5µl of AAV was made up to 30µl ddH_20. 15µl of this was added to 29µl ddH_20, 1µl RNase-Free DNase enzyme (Qiagen), 5µl of supplied buffer and then incubated for 30 minutes at 37°C and for 10 minutes at 70°C. 1µl Proteinase K was added to the DNase

treated virus, which was further incubated for 1 hour at 50°C, and 20 minutes at 95°C. The remaining untreated 15µl of diluted virus was made up to 50µl ddH_20. Quantitation was carried out on an Applied Biosystems 7300 Real Time PCR System with the LightCycler-FastStart DNA Master SYBR Green system (Qiagen). Each reaction contained 10µl enzyme mix, 1µl primer mix (10pmol forward and reverse), 4.5µl ddH_20 and 4.5µl sample. Primer sequences were designed to amplify 100-150 bp products. Following denaturation at 95°C for 15 minutes, the reactions were cycled 35 times at 95°C for 15 seconds and 60°C for 1 minute. A standard curve was generated using a serially diluted plasmid vector. By relating the quantitative PCR curves of AAV to the standard curves of the plasmid vector, the concentration of AAV was calculated.

Genomic particles/ml = (copy number in qPCR) x **a** x **b**

a= dilution factor (20)

b= factor to yield genomic particles per ml (222.22, as 4.5µl of AAV was used)

2.6.3 Titration of infectious AAV particles using quantitative real-time PCR

The infectious titre of AAV was determined following the method of Rohr *et al.,* 2005. 5 x 10^3 293 cells were plated per well of a 96-well plate. 1 hour later, 2µl of AAV to be titred was added. Following 24 hrs, 293 cells were trypsinised (see 2.4.1), pellets washed twice with PBS, pH 7.2 and resuspended in 50µl PBS (without Ca^{2+} or Mg^{2+}). 1µl of Proteinase K was added to each sample, incubated at 50°C for 60 minutes and then inactivated at 95°C for 15 minutes. Samples were then centrifuged at 14,000rpm (Micromax) for 10 minutes and the supernatant transferred to a fresh tube. 10µl of the supernatant was digested with 10U S1 nuclease (Promega) for 30 minutes at 37°C, and then inactivated at 95°C for 5 minutes. To prevent PCR inhibition by S1 nuclease, the mixture was diluted 1/100.

Quantitative real-time PCR was performed as described in 2.6.2 using 2µl of prepared sample. A standard curve was generated using a serially diluted plasmid vector. By relating the quantitative PCR curves of AAV to the standard curves of the plasmid

vector, the number of infectious viral particles per ml can be calculated. The calculation is shown below:

$$\text{Infectious particles/ml} = \frac{(\text{copy number in qPCR}) \times \mathbf{a} \times \mathbf{b} \times \mathbf{c}}{\mathbf{d}}$$

a=dilution of whole cell lysate (100)

b=final volume of whole cell lysate (55)

c= factor to yield infectious particles per ml (500, as 2µl of AAV was used)

d=template volume in qPCR (2µl)

2.6.4 Infection of cells with AAV

661W cells and 293 cells were plated at concentrations of 1.5×10^4 and 2.5×10^4 cells respectively, per well of a 24-well plate. The following day cells were washed with serum free D-MEM and twice with PBS, pH 7.2. Typically between $10^{9\text{-}12}$ viral particles/ml (vp/ml) were diluted in 200µl PBS and applied to cells for 90 minutes. Following addition of 250µl of D-MEM with serum, the cells were incubated for three days, fixed in 4% paraformaldehyde and either examined directly for EGFP fluorescence using a Zeiss Axioplan-2 Optical Fluorescent Microscope using Zeiss filter set 38 (excitation maximum: 470nm) with analysis^B Imaging Software, or immunostained prior to examination as described in 2.4.6.

2.7 Animal Methods

2.7.1 Isolation and purification of DNA from mouse-tails

1cm of tail tip was cut with a sterile blade and placed in an eppendorf. 400µl of tail lysis buffer (50mM Tris-HCl, pH 8, 100mM EDTA, pH 8, 100mM NaCl, 1% SDS) was then added with 15µl of Proteinase K (20mg/ml) and incubated overnight in a 55°C water bath. 400µl of phenol/chloroform was added to the tail solution, which was vortexed for 3 minutes. Following centrifugation at 12,000rpm (Micromax) for 8 minutes, the upper layer was transferred to a fresh eppendorf with 400µl chloroform and the solution was vortexed and centrifuged as before. The upper layer was transferred to a fresh eppendorf and 2x volume of ice-cold ethanol was added. The precipitated DNA was spooled out using a plastic tip, transferred into a clean eppendorf and air-dryed for 10 minutes. The DNA was resuspended in 200µl ddH_20, incubated at 37°C for 20 minutes and vortexed briefly before quantifying using a spectrophotometer (see 2.2.13).

2.7.2 Preparation, electroporation and culturing of retinal explants

Newborn mouse pups (postnatal day 0-2 {P0-P2}) were culled, and dissected retinas were transferred to a micro electroporation chamber (Nepa Gene, Chiba, Japan) filled with a DNA solution of plasmid of interest (1µg/µl in Hanks' balanced salt solution), and five square pulses (30V) of 50 ms duration with 950 ms intervals were applied by using pulse generator ECM 830 (BTX). 1ml complete D-MEM/F12 (2.1.2{ix}) was pipetted into the lower compartment of a Costar transwell polycarbonate membrane chamber (Corning Life Sciences, Acton, MA, USA) and 2ml into the upper compartment. Electroporated retinas were placed in the upper compartment, the medium was removed and the retinal explants gently flattened onto the membrane. Retinal explants were cultured at 37°C, 5% CO_2. The medium was changed the next day and then every 2-3 days.

2.7.3 Isolation of RNA from retinal explants

Media was aspirated from the retinal explants and 350µl (+ 10µl/ml β-mercaptoethanol) of RLT buffer from the RNeasy Mini Kit (Qiagen) was added directly to each pair of retinal explants. The buffer was pipetted up and down several times to homogenise explants before transferring them to an 800µl column provided by the kit. The remaining steps were carried out according to the manufacturer's instructions.

2.7.4 Preparation of retinal explants for cryosectioning and vibratome sectioning

Retinal explants were harvested 8-14 days following electroporation and sectioned using either a cryostat or a vibratome.

To prepare for cryosectioning:

Media was removed from retinal explants and they were washed twice with PBS. 1ml of 10% neutral formalin (2.1.2 {xii}) was pipetted underneath the explants, which were then incubated at 4°C for 4-5 hours. Explants were cryoprotected in 30% sucrose in PBS overnight at 4°C, followed by embedding in OCT compound (Sakura, Tokyo, Japan). Sections of 7-20µm were cut on a Leica CMI900 cryostat (Leica Biosciences, PA, USA) at -16°C and collected on polylysine slides (Menzel-Glaser).

To prepare for vibratome sectioning:

Media was removed from retinal explants and they were washed twice with PBS. 1ml of 4% paraformaldehyde was pipetted underneath the explants, which were then incubated at room temperature for 1 hour. Explants were washed twice in PBS, carefully cut from the insert and set in 6% select agar (prepared by boiling 6g select agar in 100ml PBS). Sections of 20-50µm were cut using a Leica VT1000S Vibratome and stored in PBS at 4°C prior to immunohistochemistry.

2.7.5 Immunohistochemistry of retinal explant sections

Retinal sections prepared by cryosectioning:

A PAP pen (Sigma-Aldrich) was used to create an impermeable barrier around 2-3 retinal sections. Sections were first blocked with 50µl 1-3% BSA or serum solution with 0.1-3% Triton X-100 in PBS (pH 7.0), for 1 hour. The sections were then incubated with a primary antibody diluted to the appropriate concentration overnight at 4°C, in a humidified chamber to prevent the retinal explant sections drying out. The next day, the sections were washed with PBS three times for 10 minutes and incubated with a secondary antibody for 2 hours at room temperature. Following three 10 minute washes with PBS, the sections were fixed using Aqua Poly/Mount and examined using a Zeiss Axioplan-2 Optical Fluorescent Microscope with the appropriate Zeiss filter and analysis^B Imaging Software.

Retinal sections prepared using the vibratome:
Unlike the cryosections, these retinal sections float freely in PBS so immunostaining was undertaken in 24-well tissue culture plates. To move the sections easily between wells, chambers were created using cut segments of 5ml syringes with gauze melted onto the bases. The retinal sections were carefully placed in the fabricated chamber within a well of the 24-well plate, and immunostained as described for the cryosections, using solution volumes of approximately 500µl.

2.7.6 TUNEL staining of retinal sections

Frozen retinal explant sections, cut as described in 2.7.4 above, were thawed at room temperature for 10 minutes. Slides were placed in PBS for 5 minutes, excess PBS was removed and a PAP pen (Sigma-Aldrich) was used to create an impermeable barrier around 2-3 retinal sections. 50µl of 0.1% Triton X-100 in PBS was pipetted onto sections and left for 2 minutes at room temperature. Slides were washed in PBS for 5 minutes twice and 50µl of TUNEL Mix (2.1.2 {xiii}) was placed onto sections, which were then incubated for 1 hour at 37°C. Slides were then placed in 1µg/ml DAPI solution for 2 minutes and washed in PBS three times for 10 minutes. Slides were dried, mounted in Aqua-Poly/Mount and examined using a Zeiss Axioplan-2 Optical Fluorescent Microscope with the appropriate Zeiss filter and analysis^B Imaging Software.

CHAPTER 3

Evaluation of three Inhibitor of Apoptosis (IAP) Proteins in 661W Cone Photoreceptor Cells

3.1 Introduction

Autosomal dominant retinitis pigmentosa (adRP) is an hereditary degenerative disease of the retina, for which there is currently no effective treatment available (Weleber 2001; Kalloniatis *et al.,* 2004). Although adRP is a genetically heterogeneous disease, photoreceptors degenerate by a common form of cell death, apoptosis (Chang *et al.,* 1993; Portera-Cailliau *et al.,* 1994). Inhibition of apoptosis is an alternative or possibly complementary therapeutic strategy to targeting the underlying primary mutation. While the apoptotic pathways leading from the primary mutations to photoreceptor cell death are not fully understood, a number of possible targets have emerged through research *in vitro* and with animal models of retinal degeneration.

One of these is the caspase group of cysteine aspartyl-specific proteases that can mediate apoptosis (Thornberry *et al.,* 1998; Earnshaw *et al.,* 1999; Nicholson 1999). Using animal models of retinal degeneration, caspases have been shown to be involved in the death of photoreceptors (Liu *et al.,* 1999; Jomary *et al.,* 2001; Kim *et al.,* 2002; Sharma *et al.,* 2004) and so are potential therapeutic targets for adRP. In several of these papers inhibition of caspase-3 using specific inhibitors including Z-DEVD-FMK, was found to slow retinal degeneration (Liu *et al.,* 1999; Yoshizawa *et al.,* 2000; Bode *et al.,* 2003). However, the protection afforded by caspase-3 inhibition has been shown to be transient (Yoshizawa *et al.,* 2002). There has been more success with pan-caspase inhibitors, most notably the p35 protein. p35 was originally identified in the baculovirus, *Autographica californica* nucleopolyhedrosis virus (AcMNPV), (Clem *et al.,* 1991; Clem *et al.,* 1994) and has been shown to rescue photoreceptor degeneration in *Drosophila* models of retinal degeneration (Davidson *et al.,* 1998; Alloway *et al.,* 2000; Galy *et al.,* 2005). Furthermore, p35 has been shown to protect against chemical-induced apoptosis in the cone photoreceptor cell line, 661W (Tuohy *et al.,* 2002).

Encouraged by these results, the therapeutic potential of another group of caspase inhibitors, the inhibitor of apoptosis (IAP) proteins, was evaluated. Like p35, the IAPs were originally identified in baculoviruses (Crook *et al.,* 1993; Birnbaum *et al.,* 1994) and to date eight IAP mammalian homologues are known (Salvesen *et al.,* 2002). The

best characterised of the IAPs are the X-linked inhibitor of apoptosis protein (XIAP), c-IAP-1 and c-IAP-2, which each inhibit caspase-3, -7 and -9 (Deveraux *et al.,* 1997; Roy *et al.,* 1997; Deveraux *et al.,* 1998). Cell culture provides an efficient, reproducible means of evaluating the therapeutic potential of the IAPs, prior to moving to *in vivo* models. There are several photoreceptor cell models available, including primary retinal cultures, retinoblastoma cultures and genetically engineered cultures (Seigel 1999). For the purpose of this research, primary retinal cultures were unsuitable as they are heterogeneous, with a very limited passage number and are labour intensive. Transformed cell lines on the other hand, have the advantages of being homogeneous. reducing the number of animals used in research and can be easily cultured to a higher passage number. 661W cells, a line of transformed mouse cone photoreceptor cells, which had been used previously to evaluate the potential of p35 as a protective agent for photoreceptors, were selected as the model for this research. 661W cells are one of the most recently developed retinal cell lines and were originally cloned from a retinal tumour of a transgenic mouse line expressing the simian virus (SV)-40 T antigen under the control of the interphotoreceptor retinol binding protein (IRBP) (Agarwal 1998). 661W cells have been shown to express cone-specific proteins including blue and green cone pigments, arrestin and cone transducin, thus making them a useful tool for studying photoreceptor cell biology and function (Tan *et al.,* 2004). Notably, 661W cells have been previously used in a number of studies of photoreceptor apoptosis (Tuohy *et al.,* 2002; Sanvicens *et al.,* 2004; Gomez-Vicente *et al.,* 2005; Miller *et al.,* 2005).

For evaluating the IAPs, apoptosis was induced using UV light and two chemotherapeutic agents, daunorubicin and etoposide. UV light induces apoptosis through cytochrome-c release and activation of caspase-3 (Kluck *et al.,* 1997). Daunorubicin and etoposide are chemotherapeutic agents, routinely used in cancer therapy (Slevin 1991; Monneret 2001). Daunorubicin is an anthracycline antibiotic, derived from Streptomyces peucetius, which intercalates into DNA, interfering with DNA transcription resulting in cell death (Frederick *et al.,* 1990; Gewirtz 1999). Etoposide, a semi-synthetic derivative of podophyllotoxin, interferes with

topoisomerase II, a nuclear enzyme involved in DNA replication and transcription resulting in DNA strand breaks, and eventual cell death by apoptosis (Robertson *et al.*, 2000). Etoposide-induced apoptosis proceeds through the mitochondrial apoptotic pathway, resulting in mitochondrial outer membrane permeabilisation (MOMP) and the release of cytochrome-*c*. In summary, the aim of this chapter was to evaluate the potential protective effect of three IAPs, XIAP, c-IAP-1 and c-IAP-2, against apoptosis induced by UV light and chemotherapeutic agents in the mouse 661W photoreceptor-derived cell line.

3.2 Materials and Methods

3.2.1 Culturing and passaging

Cell cultures were maintained and passaged as described in Chapter 2: 2.4.1. Cultures were routinely seeded in a 6-well plate at a density of 2 x 10^5 cells for the 661W cells and 5 x 10^5 for the 293T cells. The cultures were expanded to approximately 75-80% confluency in a volume of 3ml complete D-MEM (2.1.2 {ix}) prior to transfection.

3.2.2 Culture cryopreservation and thawing

661W and 293T cells were maintained for a limited number of passages to minimise genetic changes: up to passage 30 for 661W cells and passage 20 for 293T cells. Early passages of both cells lines were cryopreserved as described in Chapter 2: 2.4.2 to maintain adequate stocks. To thaw frozen 661W and 293T cells, one 500µl vial of frozen stock at a concentration of 1 x10^7 cells was thawed at 37°C as described in 2.4.2.

3.2.3 Inhibitor of apoptosis protein (IAP) constructs

The three IAP plasmids, pcDNA-myc.XIAP (pcXIAP), pcDNA-myc.cIAP1 (pcIAP-1) and pcDNA-myc.cIAP2 (pcIAP-2) (Figure 3.1), were kindly provided by Professor Seamus Martin of Trinity College Dublin. These plasmids were originally constructed by Professor John Reed (Burnham Institute, La Jolla, CA, USA) (Deveraux *et al.*, 1997; Roy *et al.*, 1997). All three constructs were sequenced to confirm their sequence integrity (Chapter 2: 2.2.14).

3.2.4 Transfection of 661W cone photoreceptor and 293T cells with pCMVβ-galactosidase, pcXIAP, pcIAP-1 and pcIAP-2:

A number of commercially available transfection agents were evaluated in 661W cells as per manufacturer's instructions including Superfect (Qiagen), NeuroPorter (Gene Therapy Systems, San Diego, CA, USA), Effectene (Qiagen) and Lipofectamine 2000 (Gibco-Invitrogen). 293T cells were transfected according to the calcium phosphate-based transfection method, as described in Chapter 2: 2.4.4. 661W and 293T cells were transfected with: (a) pcXIAP, (b) pcIAP-1, (c) pc-IAP-2 and (d) pCMVβ-galactosidase

(Figure 3.2). After 48 hours, 661W cells transfected with pCMVβ-galactosidase were assayed for β-gal expression (2.4.5).

3.2.5 Cell death assays

To assess the potential protection of the IAPs, the following agents were used to induce cell death:

(i) UV radiation was conducted on a TFX20M transilluminator for 75 seconds (Tuohy 2001).

(ii) Daunorubicin was used at a final concentration of 2.5μM (Tuohy 2001). The exposure time was 20 hours.

(iii) Etoposide was used at a final concentration of 30μM (Roy *et al.*, 1997). The exposure time was 48 hours.

Cells were scored as either apoptotic or viable according to morphology. Apoptotic cells are characterised by membrane blebbing and the formation of numerous apoptotic bodies (Kerr *et al.*, 1972). At least 300 cells were evaluated per cell sample from 3 fields of view, and subsequent mean values and standard errors calculated. Significance was assessed using an unpaired *t*-test ($P < 0.05$). Apoptosis was also assessed using 4',6-Diamidine-2'-phenylindole dihydrochloride (DAPI, Roche Diagnostics), a fluorescent dye that binds DNA to form a complex. To assess cell death, 661W and 293T cells were trypsinised and resuspended in 4% paraformaldehyde containing 5μg/ml DAPI. 10μl of this suspension was placed on a glass slide and covered with a cover slip. Cell morphology was observed using a Zeiss Axioplan-2 Optical Fluorescent Microscope with Zeiss filter set 01 (excitation maximum, 365nm) and analysis^B Imaging Software. Apoptotic nuclei were identified by bright condensed chromatin compared to the less fluorescent viable cells. Again approximately 300 cells per sample were evaluated as described above.

3.2.6 Detection of XIAP transcript using RT-PCR

661W cells transfected with 2μg of pcXIAP, were harvested after 48 hours. RNA was isolated using TRI Reagent (Molecular Research Center) as described in Chapter 2: 2.3.3. 1μg of total RNA was used for RT-PCR reactions and these were carried out as

described in 2.3.5. A comparison of the mouse and human XIAP sequences showed that the sequences were similar. To avoid potentially amplifying mouse XIAP in the 661W cells, a forward primer was designed to bind in the N-terminal myc tag of the human pcXIAP construct. The sequences of both primers used in the RT-PCR reaction are shown below:

Forward Myc: 5' AGAAACTCATCTCTGAAGAG 3'
Reverse XIAP: 5' CCTTATTGATGTCTGCAGG 3'

In addition, part of the housekeeping gene glyceraldehyde-3-phosphate dehydrogenase (GAPDH), was amplified by PCR to assess the quality of the cDNA. The sequences of the primers used are shown below:

Forward GAPDH: 5' CCATGGAGAAGGCCGGGG 3'
Reverse GAPDH: 5' GTGGTTCACACCCATCACAA 3'

3.2.7 Western blot analysis of XIAP expression in 661W cone photoreceptor cells

661W cells were plated at a concentration of 1.6 x 10^6 on 10cm dishes and transfected with 4μg of pcXIAP. The cells were harvested after 48 hours as described in Chapter 2: 2.4.8 and the extracted protein analysed by Western blot (2.4.7) using the following antibodies:

Primary Antibodies:

(i) Rabbit anti-human/mouse XIAP polyclonal antibody targeting amino acids 244-263 of human XIAP (R and D Systems, Minneapolis, MN, USA).

(ii) Rabbit anti-human/mouse β-actin polyclonal antibody targeting amino acids 1-100 of human β-actin epitope (Abcam, Cambridge, UK).

Secondary Antibodies:

(iii) Horseradish peroxidase-coupled rabbit anti-mouse IgG (Abcam).

3.2.8 Establishment of a stable 661W cone photoreceptor cell line expressing XIAP

Stable lines of 661W cells expressing XIAP were generated using antibiotic selection with G418 (Gibco-Invitrogen). Initially it was important to determine the concentration of G418 to be used for selection as sensitivity to G418 varies between cell types. The optimal concentration results in complete cell death within 14 days and this was established to be 400μg/ml. 661W cells were plated in 6-well tissue culture plates and transfected with 4μg of pcXIAP. Controls of cells transfected with vector alone (pcDNA3.1+) and untransfected cells were also set up. At 48 hours post-transfection, cells were placed under selection with 400μg/ml G418 following reseeding in 6-well plates. Medium with G418 was replaced every 2-3 days. Approximately 10 days following transfection, 661W cells on negative control plates had died, so isolation of stable clones, which were G418 resistant, was proceeded with. Cells were trypsinised, resuspended at a concentration of 5-10 cells/50μl and plated in 200μl medium with G418 on a 48 well plate. Cells were grown for 2 weeks and colonies that had grown well were transferred to a 6-well plate. Expression was assessed in two established lines 661W-XIAP/A and 661W-XIAP/B by quantitative RT-PCR using the LightCycler (Roche Diagnostics), as described in Chapter 2: 2.3.6 using the same primers for XIAP and the housekeeping gene, glyceraldehyde-3-phosphate dehydrogenase (GADPH) as in 3.2.6. Protein was isolated from 661W-XIAP/A and probed for XIAP by Western blot analysis as described in 3.2.7.

3.2.9 Cell death assay for stable 661W cone photoreceptor cells expressing XIAP

661W-XIAP/A cells were plated at a concentration of 2 x 10^5 cells per well of a 6-well plate and exposed to etoposide at final concentrations of 15μM, 30μM, 60μM and 90μM. 48 hours following exposure, cells were trypsinised and resuspended in 4% paraformaldehyde containing 5μg/ml DAPI. Cell death was assessed as described in 3.2.5 above.

3.2.10 Generation of adeno-associated viral vector with CMV promoter-driven EGFP (AAV-EGFP)

To generate the plasmid construct for AAV-EGFP, pEGFP-1 (Clontech, Mountain View, CA, USA) (Figure 3.3) was digested with *Bam*HI and *Xba*I to isolate a 749 bp fragment carrying the EGFP gene. pAAV-MCS (Stratagene, La Jolla, CA, USA) (Figure 3.4) is a plasmid construct used to generate AAV, containing inverted terminal repeats to direct viral replication and packaging. The EGFP gene was ligated into pAAV-MCS digested with *Bam*HI and *Xba*I to generate pAAV-EGFP (cloning undertaken by Dr. Naomi Chadderton). With this construct, AAV virus was produced by triple-plasmid calcium phosphate transient transfection of 293 cells, as described in Chapter 2: 2.6.1. The genomic titre of AAV-EGFP was determined according to the method of Rohr *et al.*, 2002, (see 2.6.2) using the primers for the EGFP gene below:

Forward EGFP: 5' TTCAAGGAGGACGGCAACATCC 3'
Reverse EGFP: 5' CACCTTGATGCCGTTCTTCTGC 3'

3.2.11 Infection of 661W and 293 cells with AAV-EGFP

661W cells and 293 cells were plated at a concentration of 1.5 x 10^4 and 2.5 x 10^4 cells respectively, per well of a 24-well plate. The following day cells were washed with serum free D-MEM and twice with PBS. 1µl of AAV-EGFP (1.7 x 10^7 viral particles{vp}) was diluted in 200µl PBS and applied to cells for 90 minutes. Following addition of 250µl of D-MEM with serum, the cells were incubated for three days, fixed in 4% paraformaldehyde and examined for EGFP fluorescence as described in 3.2.5 using Zeiss filter set 38 (excitation maximum: 470nm).

3.2.12 Genomic titration of AAV-XIAP

AAV-XIAP, kindly provided by Professor William Hauswirth (University of Florida, Gainesville, FL, USA) was titrated according to the method of Rohr *et al.*, 2002, using quantitative real-time PCR (Chapter 2: 2.6.2). Primer sequences (shown below) were designed to amplify a 100 bp product of the XIAP gene. The copy number of AAV-EGFP, was calculated using a standard curve generated from amplifying the 100 bp

XIAP product from the plasmid construct, pcXIAP, allowing the genomic titre of AAV-XIAP to be estimated.

Forward XIAP RT: 5' TGGCCAGACTATGCTCACCT 3'

Reverse XIAP RT: 5' TTTCCACCACAACAAAAGCA 3'

3.3 Results

3.3.1 Optimisation of the transfection of 661W cone photoreceptor cells using a CMV promoter-driven β–galactosidase reporter gene

To assess whether the IAPs may protect against apoptosis in 661W cells, it was important to determine the efficiency with which the plasmids carrying the IAPs could be transfected into 661W cells. Previous work had shown a transfection efficiency of approximately 20% with Lipofectamine Plus (Tuohy *et al.,* 2002). Several transfection agents were evaluated to determine if this could be improved upon to ensure that the protective effect was not limited by transfection efficiency. In all cases transfection efficiency was quantified using a reporter construct, CMV promoter-driven β-galactosidase (Figure 3.5), and agents producing transfection levels of less than 20% were not considered further. The calcium phosphate-based transfection method was evaluated but this method was found to be very poor with a transfection efficiency of approximately 5% (data not shown), so a number of commercial transfection agents were then assessed. Of the four commercial agents evaluated, Lipofectamine 2000, was the most efficient with a transfection efficiency of 21.85 ± 1.20% with 1.25 x 10^5 cells per well of a 12-well plate, and a ratio of DNA (μg) to Lipofectamine 2000 (μl) of 1:2. The results are shown in Table 3.1 below and Figure 3.6.

Table 3.1: Percentage transfection efficiency with CMV promoter-driven β-galactosidase reporter gene using Lipofectamine 2000 in 661W photoreceptor cells

Cell Number	Ratio DNA (μg): Lipofectamine (μl)	% Transfection Efficiency*
0.625×10^5	1:1	11.76 ± 0.53
0.625×10^5	1:2	14.07 ± 1.52
0.625×10^5	1:3	14.13 ± 1.33
1.25×10^5	1:1	13.66 ± 0.99
1.25×10^5	1:2	21.85 ± 1.20
1.25×10^5	1:3	19.12 ± 0.95

*Mean of two independent experiments with duplicate samples ± standard error (S.E.)

3.3.2 Evaluation of protection of 661W cone photoreceptor cells transfected with pcXIAP, using UV light and daunorubicin to induce apoptosis

661W cells were exposed to UV light for 75 seconds on a TFX20M transilluminator ($10mJ/cm^2$) and the optimal time point for scoring cells (as described in 3.2.5) i.e. when cell death was maximal, was found to be 22 hours following exposure. Figures 3.7: A, B, show 661W cells before and after exposure to UV light. The characteristic features of apoptosis, including membrane blebbing and the formation of apoptotic cell bodies are evident in the cells exposed to UV light (Kerr *et al.*, 1972). 661W cells were plated as described in 3.2.1, transfected with varying concentrations of pcXIAP and then exposed to UV light for 75 seconds. The cells were then scored for apoptosis 22 hours later (Table 3.2, Figure 3.8). Although there was no significant protection ($P > 0.05$) against UV light-induced apoptosis in 661W cells transfected with pcXIAP, compared to vector alone, marginally higher levels of cell survival were observed. This indicates a marginal trend toward protection, which cannot however be considered significant.

Table 3.2: Percentage survival of 661W cells transfected with pcXIAP, 22 hours following exposure to UV light

Sample	pcDNA3.1+ (ng)	pcXIAP (ng)	% Cell Survival*
1	400	0	21.64 ± 1.79
2	0	400	23.97 ± 2.00
3	800	0	12.78 ± 2.92
4	0	800	14.91 ± 2.03
5	1600	0	14.95 ± 2.44
6	0	1600	16.10 ± 2.64
7	0	0	23.37 ± 2.61

*Mean of two independent experiments with triplicate samples ± standard error (S.E.)

The chemotherapeutic agent, daunorubicin, was used to induce apoptosis in order to further evaluate the potential protective effect of XIAP. 661W cells had previously been shown to undergo apoptosis when exposed to daunorubicin (Tuohy 2001). An advantage of using a chemical agent was that the dose could be adjusted with greater accuracy than exposure to UV light. 661W cells were transfected with increasing amounts of pcXIAP, exposed to 2.5μM daunorubicin and cells were scored as described in 3.2.5. The results, as shown in Table 3.3 and Figure 3.9, indicated that across three concentrations of pcXIAP, XIAP expression provided no significant protection ($P > 0.05$) against daunorubicin-induced apoptosis in 661W cells, compared to the transfection of vector alone.

Table 3.3: Percentage survival of 661W cells transfected with pcXIAP, 22 hours following exposure to 2.5μM daunorubicin

Sample	pcDNA3.1+ (ng)	pcXIAP (ng)	% Cell Survival*
1	400	0	23.94 ± 3.03
2	0	400	22.15 ± 2.91
3	800	0	17.48 ± 1.79
4	0	800	19.82 ± 2.86
5	1600	0	15.67 ± 2.43
6	0	1600	11.32 ± 3.23
7	0	0	20.45 ± 1.93

*Mean of two independent experiments with triplicate samples ± standard error (S.E.)

3.3.3 Detection of XIAP expression using reverse transcription (RT)-PCR

As no protection was observed with transient transfection of pcXIAP in 661W cells exposed to UV light and daunorubicin, RNA from transfected 661W cells was analysed by RT-PCR to assess XIAP gene transcription. Using XIAP gene specific primers, a 100 bp fragment was amplified by RT-PCR confirming that the XIAP gene was being transcribed (Figure 3.10: Lane 2).

3.3.4 Western blot analysis of XIAP protein in 661W cells

To confirm that XIAP protein was being expressed, total protein was isolated from transfected 661W cells and analysed by Western blotting (3.2.7). The 56 kDa XIAP protein was detected in transiently transfected cells (Figure 3.11: B1). The XIAP antibody also detected endogenous XIAP protein but the level of XIAP expression was greater in the transiently transfected cells compared to the untransfected cells (Figure 3.11: A1). Equal loading of the protein samples was assessed by probing for β-actin, and Figure 3.11: A2, B2, show bands of equal intensity. This indicates that the more intense band for XIAP protein in Figure 3.11: B1, is not as a result of loading a greater quantity of protein lysate from 661W cells transfected with pcXIAP, compared to protein lysate from cells transfected with vector alone.

3.3.5 Evaluation of protection of 293T and 661W cells transfected with pcXIAP, using etoposide to induce apoptosis

RT-PCR and Western blotting confirmed that XIAP was expressed in 661W cells at the RNA and protein level respectively. The lack of significant protection against apoptosis induced by UV light or daunorubicin contrasted with other papers showing protection with XIAP, although in different cell lines. One study showed that transient expression of XIAP in a breast carcinoma cell line, provided a percentage cell survival of 61 ± ~5% compared to 6 ± ~5% of cells transfected with vector alone, when exposed to UV light (Duckett *et al.*, 1998). Another study demonstrated that XIAP was protective against UV-induced apoptosis in NT2 carcinoma cells, with a percentage cell survival of 89 ± ~5% compared to 21 ± ~10% of cells transfected with vector alone (Silke *et al.*, 2002). It was decided to use a control cell line of 293T cells, in which c-IAP-1 and c-IAP-2 had been shown to be protective against apoptosis, in parallel with 661W cells. This was to demonstrate that the lack of protection in 661W cells was not a function of some other parameter and that functional XIAP protein was being expressed from the pcXIAP plasmid. To minimise variation, the method of Roy *et al.*, 1997, was followed, in which 30μM of etoposide was used to induce apoptosis in both cell lines. 293T cells were transfected with increasing amounts of pcXIAP, exposed to 30μM of etoposide and scored as described in 3.2.5. Figure 3.12 shows 293T cells following exposure to 30μM of etoposide for 48 hours. The results in Table 3.4 show that XIAP expression resulted in a significant percentage cell rescue ($P < 0.01$) of approximately 16% across the three concentrations of XIAP, with no significant titration of its protective effect. Even accounting for an approximate transfection efficiency of ~70% in 293T cells (as assayed by transfection of a β-gal reporter construct, data not shown), this is a somewhat lower than expected level of protection considering the original paper by Roy *et al.*, 1997, in which c-IAP-1 and c-IAP-2 provided a percentage cell rescue of 34 ± ~8% and 22 ± ~9% respectively. Furthermore, XIAP has been demonstrated to be a more efficient caspase inhibitor than c-IAP-1 or c-IAP-2 (Deveraux *et al.*, 1997; Deveraux *et al.*, 1998).

Table 3.4: Percentage survival of 293T cells transfected with pcXIAP, 48 hours following exposure to 30μM etoposide

Sample	pcDNA3.1+ (ng)	pcXIAP (ng)	% Cell Survival*
1	400	0	26.44 ± 1.80
2	0	400	39.98 ± 2.67
3	800	0	34.43 ± 2.35
4	0	800	51.33 ± 1.61
5	1600	0	27.99 ± 2.58
6	0	1600	44.47 ± 1.88
7	0	0	32.64 ± 3.14

*Mean of three independent experiments with duplicate samples ± standard error (S.E.)

To complete this work and demonstrate that absence of protection by XIAP against induced apoptosis in 661W cells was a valid result, the above experiment was repeated in parallel with 661W cells.

Table 3.5: Percentage survival of 293T and 661W cells transfected with pcXIAP, 48 hours following exposure to 30μM etoposide

Sample	Cell Type	pcDNA3.1+(ng)	pcXIAP (ng)	% Cell Survival*
1	293T	400	0	29.33 ± 3.39
2	293T	0	400	44.09 ± 2.19
3	293T	800	0	25.65 ± 3.36
4	293T	0	800	40.94 ± 0.87
5	293T	1600	0	26.36 ± 2.64
6	293T	0	1600	41.72 ± 3.03
7	293T	0	0	28.37 ± 3.65
8	661W	400	0	34.01 ± 3.44
9	661W	0	400	36.22 ± 0.74
10	661W	800	0	30.30 ± 0.67
11	661W	0	800	35.42 ± 0.31
12	661W	1600	0	30.80 ± 1.16
13	661W	0	1600	35.68 ± 0.48
14	661W	0	0	29.12 ± 2.66

*Mean of three independent experiments with duplicate samples ± standard error (S.E.)

Again, on average (calculated across the three concentrations of pcXIAP transfected), XIAP expression in 293T cells resulted in a significant percentage cell rescue ($P < 0.01$), of approximately 15% shown above in Table 3.5 and in Figure 3.13. On average (calculated across two higher concentrations of pcXIAP) there was a small but significant rescue ($P < 0.01$) of approximately 5% in 661W cells transfected with pcXIAP. c-IAP-1 and c-IAP-2 are two other members of the IAP family, which have also been shown to be effective inhibitors of apoptosis in mammalian cells (Roy *et al.*, 1997; Deveraux *et al.*, 1998). The above experiment was repeated for both of these IAPs. As the pcIAP-1 and pcIAP-2 constructs were routinely used by Professor Seamus

Martin's group (personal communication) and the constructs were not modified, no analysis of IAP-1 or IAP-2 expression was undertaken for the current study.

Table 3.6: Percentage survival of 293T and 661W cells transfected with pcIAP-1, 48 hours following exposure to 30μM etoposide

Sample	Cell Line	pcDNA3.1+	pcIAP-1	% Cell Survival*
1	293T	400	0	35.19 ± 3.26
2	293T	0	400	47.80 ± 1.98
3	293T	800	0	31.45 ± 2.80
4	293T	0	800	41.67 ± 1.87
5	293T	1600	0	34.96 ± 1.19
6	293T	0	1600	44.20 ± 3.77
7	293T	0	0	38.10 ± 2.09
8	661W	400	0	36.17 ± 2.48
9	661W	0	400	32.92 ± 0.76
10	661W	800	0	40.47 ± 0.77
11	661W	0	800	42.83 ± 1.28
12	661W	1600	0	41.71 ± 0.97
13	661W	0	1600	41.03 ± 1.19
14	661W	0	0	36.40± 0.70

*Mean of three independent experiments with duplicate samples ± standard error (S.E.)

On average (calculated across the three concentrations of pcIAP-1 transfected), c-IAP-1 expression in 293T cells resulted in a significant percentage cell rescue ($P < 0.01$) of approximately 11% as shown in Table 3.6 above and in Figure 3.14. There was no significant protection ($P > 0.05$) against etoposide-induced apoptosis in 661W cells transfected with pcIAP-1, compared to vector alone. The experiment was repeated for c-IAP-2.

Table 3.7: Percentage survival of 293T and 661W cells transfected with pcIAP-2, 48 hours following exposure to 30μM etoposide

Sample	Cell Line	pcDNA3.1+	pcIAP-2	% Cell Survival*
1	293T	400	0	31.47 ± 3.01
2	293T	0	400	31.42 ± 0.72
3	293T	800	0	28.77 ± 1.83
4	293T	0	800	38.18 ± 0.75
5	293T	1600	0	23.73 ± 2.72
6	293T	0	1600	33.39 ± 1.64
7	293T	0	0	38.57 ± 1.56
8	661W	400	0	28.63 ± 3.71
9	661W	0	400	31.36 ± 1.53
10	661W	800	0	37.14 ± 1.49
11	661W	0	800	33.52 ± 1.17
12	661W	1600	0	31.66 ± 0.86
13	661W	0	1600	32.70 ± 1.13
14	661W	0	0	36.41 ± 2.10

*Mean of three independent experiments with duplicate samples ± standard error (S.E.)

On average (calculated across the two higher concentrations of pcIAP-2 transfected), c-IAP-2 expression in 293T cells resulted in a significant percentage cell rescue ($P < 0.01$) of approximately 9% as shown in Table 3.7 above and in Figure 3.15. There was no significant protection ($P > 0.05$) against etoposide-induced apoptosis in 661W cells transfected with pcIAP-2, compared to vector alone. The level of protection afforded by IAPs in 293T cells was less than had been reported in the literature, so to confirm these results, DAPI staining was used to evaluate cell death in 293T cells exposed to etoposide. When cells undergo apoptosis, the chromatin condenses within the nucleus, and this can be observed using a fluorescent DNA-specific stain like DAPI (Figure

3.16: D). 293T cells were transiently transfected with plasmid DNA expressing each of the IAPs, exposed to etoposide and cell death assessed (Table 3.8 and Figure 3.17).

Table 3.8: Percentage survival of 293T cells transfected with pcXIAP, pcIAP-1 and pcIAP-2, 48 hours following exposure to 30μM etoposide by evaluation of DAPI-stained nuclei

Sample	pcDNA3.1+	pcXIAP	pcIAP-1	pcIAP-2	% Cell Survival*
1	1600	0	0	0	44.09 ± 2.71
2	0	1600	0	0	67.42 ± 0.97
3	0	0	1600	0	57.79 ± 0.18
4	0	0	0	1600	55.27 ± 2.35
5	0	0	0	0	48.46 ± 2.33

*Mean of three independent experiments with duplicate samples ± standard error (S.E.)

Using DAPI staining to evaluate cell death, each of the IAPs rescued 293T cells from apoptosis, ranging from an average of 23% for XIAP, 14% for c-IAP-1 and 11% for c-IAP-2 ($P < 0.01$). This is a similar trend to what had been observed in the current study when cell death was quantified by assessing apoptotic morphology with a percentage rescue of approximately 15% for XIAP, 11% for IAP-1 and 9% for IAP-2 (Tables 3.5-7). The percentage cell survival was moderately greater when quantified by DAPI staining, compared to assessment of apoptotic cell morphology by eye. For the DAPI staining protocol, the cells are prepared in a single cell suspension, so the fluorescence of individual cells is easily noted. Characterising the morphology of cells in a 6-well dish is more difficult as individual cells are not as readily distinguished. Given the results for this experiment, it may be that DAPI staining is a more reliable method for assessing apoptosis in a cell population.

3.3.6 Evaluation of protection of pcXIAP in a stable line of 661W cells

Given the lower than expected protection afforded by IAPs against etoposide-induced apoptosis in 293T cells, the lack of protection observed in 661W cells (~5%, Figure 3.13) may possibly be the result of the low transfection efficiency in 661W cells. Hence, to establish the level of protection that XIAP may possibly afford in 661W cells exposed to an apoptotic insult, a stable line of 661W cells expressing XIAP was generated using selection with G418 over a time-frame of six weeks (see 3.2.8). XIAP expression was assessed in two of the resulting clones, using RT-PCR to compare relative XIAP levels and thereby select the line with highest expression. Note that using a forward primer for the myc tag incorporated into the pcXIAP construct, excluded the possibility of PCR amplification of endogenous XIAP. Figure 3.18 shows a melting curve analysis of XIAP and GAPDH PCR products from isolated RNA of 661W cells with stable expression of XIAP, indicating expression of the XIAP transcript from pcXIAP.

Table 3.9: Comparison of RNA levels of myc.XIAP in stable lines of 661W-XIAP cells using quantitative RT-PCR

Cell Line	Myc.XIAP Levels Standardised with GAPDH (%)
661W-XIAP/A	100 ± 3.59
661W-XIAP/B	97.27 ± 4.32

*Mean of three independent experiments with duplicate samples ± Standard Error (S.E.). Level of XIAP in 661W-XIAP/B is expressed as a percentage of the level in 661W-XIAP/A.

As can be seen from Table 3.9 there was no significant difference in expression between the two stable cell lines, so 661W-XIAP/A was used in further experiments, following confirmation of XIAP protein expression by Western blot analysis (see 3.2.7). Figure 3.19 of the Western blot shows that there is a higher level of XIAP expressed in isolated protein from 661W-XIAP/A cells (C1), compared to protein from 661W cells transiently transfected with empty vector pcDNA3.1+ (A1) or pcXIAP

(B1). Equal loading of the protein samples was assessed by probing for β-actin, and Figure 3.19: A2, B2, C2 show bands of equal intensity. This indicates that the more intense bands for XIAP protein in Figure 3.19: A2, and A3, corresponding to protein from 661W cells with transient and stable expression of XIAP respectively, compared to the band in Figure 3.19: A1, are not as a result of loading greater quantities of protein.

Having established XIAP expression by RT-PCR and Western blotting in this line of 661W cells stably expressing XIAP, the possible protective effect of XIAP was evaluated by exposing the stable 661W cell line to the chemotherapeutic agent, etoposide (3.2.9). As results from the current study has suggested that DAPI staining was possibly a more reliable method for assessing cell death (3.3.8: Table 3.8), this method was used to quantify cell death in 661W cells stably expressing XIAP, following exposure to etoposide (Table 3.11 and Figure 3.20).

Table 3.11: Percentage survival of 661W cells stably expressing XIAP, 48 hours following exposure to 15-90μM etoposide by evaluation of DAPI-stained nuclei

Sample	Etoposide (μM)	% Cell Survival
1-661W	15	25.14 ± 1.52
2-661W-XIAP/A	15	37.82 ± 0.97
3-661W	30	22.86 ± 2.58
4-661W-XIAP/A	30	32.90 ± 2.65
5-661W	60	22.46 ± 2.05
6-661W-XIAP/A	60	29.22 ± 2.41
7-661W	90	26.04 ± 1.64
8-661W-XIAP/A	90	31.00 ± 2.24

*Mean of three independent experiments with duplicate samples ± S.E.

Stable expression of XIAP provided an average rescue of approximately 9% across the four concentrations of etoposide, ranging from approximately 13% for 15μM etoposide to 5.00% for 90μM etoposide ($P < 0.01$). The observed protection was consistent with earlier results from 661W cells treated with etoposide following transient transfection with pcXIAP, indicating that XIAP expression provides a low level of protection against etoposide-induced apoptosis in the 661W cone photoreceptor cell line. As other caspase inhibitors such as the baculoviral protein p35 have been shown to protect against apoptosis in 661W cells (Tuohy *et al.,* 2002), it may be appropriate to continue further evaluation of p35 as a potential therapeutic agent rather than focus on XIAP. However, as the research described here on XIAP was being undertaken, a paper was published demonstrating that adeno-associated virus (AAV) vector delivery of XIAP subretinally, provided significant protection in a chemical-induced model of retinal degeneration in Sprague-Dawley rats (Petrin *et al.,* 2003). This finding contrasts somewhat with the low level of protection observed in the current study. Furthermore, while 661W cells are derived from mouse photoreceptors (Agarwal 1998), the results using IAPs in this cell line, may not mirror the potential of IAPs to protect retinal tissues against apoptosis *in vivo*. In addition, as the 661W cell line stably expressing XIAP was not monoclonal, there may have been varying expression of XIAP within the cell population. AAV efficiently infects many cell types (Bueler 1999; Buning *et al.,* 2003), including photoreceptors (Rolling 2004; Dinculescu *et al.,* 2005), so it could potentially be used to deliver XIAP to the majority of 661W cells, thereby circumventing the potential problems associated with transient transfection and the generation of stable cell lines. The research group that generated the AAV-XIAP, headed by Professor William Hauswirth, kindly provided an aliquot of AAV-XIAP to evaluate in 661W cells.

To establish the optimal multiplicity of infection (MOI: ratio of infectious particles to number of cells infected) for 661W cells, the cells were infected with AAV-EGFP, however, unfortunately 661W cells proved to be difficult to infect compared to the control cell line of 293 cells. Figure 3.21: B shows a small number of 661W cells expressing EGFP (approximately 2-3 per field of view). However, this contrasts with

the high level of expression in 293 cells in Figure 3.21: D. Both cell lines were infected with approximately 10^7 vp, providing an MOI of approximately 1000 for 661W cells and 600 for 293 cells (differences due to original number of cells plated). Increasing the viral particles on 661W cells, should in principle result in higher numbers of infected cells. Note that although a high titre AAV-EGFP was not available at the time, the aliquot of AAV-XIAP we received had, on personal communication, a high titre of 3 x 10^{13} vp/ml. To confirm this viral titre, the viral genome copy number was quantified using real-time PCR, and calculated to be approximately 6.45 x 10^8 vp/ml. Notably, the viral titre obtained from this experiment was 10^5 fold lower than expected, compared to expected titre of 3 x 10^{13} vp/ml. The reduction in viral titre may possibly have been due to delays during transit from the United States. Unfortunately, given this scenario, it was decided that this titre was too low to use for the proposed experiments in 661W cells. Nevertheless, in principle, AAV-mediated delivery may provide an alternative means of exploring the anti-apoptotic potential of XIAP in 661W cells.

3.4 Discussion

Photoreceptors in retinal degenerations such as adRP, have been shown to die by apoptosis, a so-called "final common pathway of cell death". Inhibiting photoreceptor degeneration may provide therapeutic benefit and one approach is to target caspases, an important group of enzymes that can mediate apoptosis. The aim of this chapter was to evaluate the anti-apoptotic potential of three members of the IAP family, a group of caspase inhibitors, in 661W cone photoreceptor cells.

One of the limitations of 661W cells and other neuronal cell lines is low transfection efficiency. Considerable time was spent evaluating several of the main commercial transfections agents, including a specialised agent for neuronal cells, NeuroPorter. Although 661W cells are a transformed cell line, they were originally derived from neuronal precursor cells, so it was thought that this agent could be useful. However, NeuroPorter was found to be an inefficient agent for transfecting these cells. The maximum transfection efficiency that could be achieved using three different commercial agents was ~20%. Lipofectamine 2000 was selected as the transfection agent, as it was marginally more effective that Superfect (data not shown). An alternative method for delivering exogenous DNA that was not assessed is electroporation, and newly developed systems are now available to optimise transfection such as the Nucleofector Device from Amaxa (Cologne, Germany). This approach may be worth exploring for future experiments using 661W cells.

XIAP is the best characterised of the IAPs to date, hence XIAP was evaluated first in 661W cells exposed to UV light, which induces apoptosis. Transient expression of XIAP was not found to be protective (Figure 3.8). This was in contrast to several other papers that had shown XIAP to be significantly protective against apoptosis induced by UV light, with a percentage cell rescue ranging from 55% in MCF7 cells to 37% in NT2 cells (Duckett *et al.*, 1998; Silke *et al.*, 2001). This lack of protection could be a function of the cell line used, as apoptotic pathways vary between cell lines, both in threshold of activation and pathway followed. For example, two retinoblastoma cell

lines, Y79 and Weri Rb-1 were found to respond differently to apoptosis-inducing cytokines (Cullinan *et al.,* 2004).

Daunorubicin, a chemotherapeutic agent, was also used to induce cell death in 661W cells. It had been used in previous studies of apoptosis in 661W cells (Tuohy *et al.,* 2002). Daunorubicin induces cell death though a number of mechanisms of action, including activation of caspase-3, -6, -7 and -8 (Wesselborg *et al.,* 1999). In 661W cells, daunorubicin is a potent apoptosis-inducing agent, resulting in approximately 80% cell death after an exposure time of 20 hours. However, no protection was observed in 661W cells transiently expressing XIAP (Figure 3.9). Although the sequence integrity of pcXIAP had been confirmed (data not shown), to exclude the possibility that XIAP protein was not being expressed, RT-PCR and Western blot analysis confirmed that XIAP was being transcribed and translated (Figures 3.10-11).

A control cell line (293T cells), in which IAPs had been previously shown to protect against apoptosis, was treated in parallel with 661W cells to exclude errors associated with experimental technique or other parameter as the reason for the lack of protection afforded by XIAP (Figures 3.8-9). In a previous study by Roy *et al.*, c-IAP-1 and c-IAP-2 had been found to result in a percentage survival of approximately 34% and 22% respectively in 293T cells exposed to 30μM etoposide (Roy *et al.,* 1997). In the current study, transient expression of XIAP afforded a significant ($P < 0.01$) percentage cell rescue of approximately 16% in 293T cells (Table 3.4), confirming that functional XIAP was being expressed. Although the protective effect of XIAP was not evaluated by Roy *et al.*, whose method of etoposide-induced apoptosis was being followed for the current study, XIAP has been demonstrated to be more potent than c-IAP-1 and c-IAP-2 in a number of studies (Deveraux *et al.,* 1997; Deveraux *et al.,* 1998). Considering this, the protection obtained in the current study is lower than would have been expected. In addition, XIAP had been previously shown to be protective in NT2 and 293 cells exposed to etoposide, with an average cell rescue of approximately 45% (Sauerwald *et al.,* 2002; Silke *et al.,* 2002). In the current study, expression of c-IAP-1

and c-IAP-2 provided significant ($P < 0.01$) cell rescue of approximately 11% and 9% respectively, which is also less than that obtained previously by Roy *et al.*, 1997.

To confirm the results obtained here, cell death was assessed using another method, DAPI staining (Figure 3.16). Notably, a similar trend in protection was observed, with a significant ($P < 0.01$) percentage rescue of 293T cells ranging from an average of 23% for XIAP, 14% for c-IAP-1 and 11% for c-IAP-2 (Figure 3.17). For the DAPI staining assay, cells are trypsinised, generating a single cell suspension, hence assessing the morphology of individual cells is more straightforward compared to assessing the morphology of cells *in situ*, where cells are frequently clumped together. Thus, on consideration, DAPI staining was more likely the more reliable method for assessing cell death. The transfection efficiency in 293T cells in the current study was in the order of 70% (data not shown), so this may at least in part account for the difference in XIAP-based protection observed between this study and previous ones. With regard to the other studies that demonstrated that XIAP significantly protects against apoptosis induced by UV light, etoposide and other chemotherapeutic agents, variations in the protocol, including the length of exposure to UV light (Duckett *et al.*, 1998), concentration of etoposide (Sauerwald *et al.*, 2002), or cell type (Silke *et al.*, 2002), may explain the difference in protection observed compared to the current study.

Transient expression of XIAP afforded a slight but significant ($P < 0.01$) rescue of 5% in 661W cells exposed to the same concentration of etoposide as 293T cells (Table 3.5, Figure 3.13). Consistent with the trend observed in 293T cells where c-IAP-1 and c-IAP-2 protected significantly less than XIAP against etoposide-induced apoptosis, a similar trend emerged for 661W cells, with no significant protection afforded by c-IAP-1 or c-IAP-2. Clearly the low transfection efficiency of 661W cells was a limiting factor in assessing the potential protective effect of IAPs. However, recent publications have continued to show that XIAP protects against apoptosis in a number of cell death models. For example, transgenic mice overexpressing XIAP were found to be more resistant to brain injury following transient forebrain ischaemia (Trapp *et al.*, 2003) and adenoviral delivery of XIAP was demonstrated to protect retinal ganglion cells (Kugler

et al., 2000; Straten *et al.*, 2002), motor neurons (Perrelet *et al.*, 2002) and hippocampal neurons after axotomy (Xu *et al.*, 1999). Hence in an attempt to circumvent low transfection efficiency in 661W cells and to satisfactorily establish to what extent XIAP may protect from apoptosis in 661W cells, a stable cell line was generated. Further research was not continued with the other two IAPs as this work suggested that they may be less effective at inhibiting apoptosis compared to XIAP, a finding consistent with other studies (Deveraux *et al.*, 1997; Deveraux *et al.*, 1998).

Stable expression of XIAP provided a low level of rescue of 661W cells ranging from approximately 13% for 15μM etoposide to 5% for 90μM etoposide, comparable to the level of rescue observed in the transient studies (Table 3.11, Figure 3.20). As using the same assays as those used for XIAP, other caspase inhibitors have been shown to be effective in 661W cells such as the p35 baculoviral protein, the low level of protection afforded by XIAP, did not encourage further research. However, in this regard, it is worth noting that a further paper has emerged recently however, in which AAV was used to deliver XIAP to rats with a chemical-induced retinal degeneration (MNU: *N*-methyl-*N*-nitrosourea) (Petrin *et al.*, 2003; Leonard *et al.*, 2005). In the study undertaken by Petrin *et al.*, significant protection of the outer nuclear layer (ONL) of the retina was observed in four out of six animals treated with AAV-XIAP one week after MNU-induced degeneration, compared to control-injected or uninjected eyes at the same time-point, where the ONL was essentially destroyed. Two of the animals with structural protection of the ONL, also had a weak but recordable electroretinogram (ERG) response at 1 week, with b-wave amplitudes of approximately 5-15% compared to pre-treatment with MNU. Considering that only 20% of the retina was transduced with AAV, as suggested by the authors, this result suggests that XIAP may be significantly protective, further validating apoptosis inhibition as a potential therapeutic approach for adRP and other retinal degenerations. More recently at the 2005 meeting of The Association for Research in Vision and Opthalmology (ARVO), Leonard *et al.*, 2005, presented results on AAV delivery of XIAP to the Pro23His and Ser344Ter rat models of retinal degeneration, both of which carry autosomal dominant RP mutations of rhodopsin. In the study, significant protection of the ONL was observed in both

models of RP, following subretinal injection of AAV-XIAP at postnatal day 16 (P16), up to 32 weeks. Although the slight improvement in ERG function of the Ser344Ter model, declined after 18 weeks following injection, the results with the Pro23His model were encouraging, with an ERG improvement maintained to 20 weeks post-injection of AAV-XIAP. Clearly recent data published subsequent to this study in 661W cells undertaken as part of this Ph.D. would suggest that XIAP may have a role in protecting photoreceptors from apoptosis *in vivo*.

As the level of expression of stably transfected plasmids can vary within a stable cell line that is not monoclonal, the level of protection afforded by XIAP in the stable line of 661W cells generated in the current study, may not reflect the full inhibitory potential of XIAP. Given the encouraging results from the study by Petrin *et al.*, 2003, demonstrating significant protection in a chemical-induced animal model of retinal degeneration, following XIAP expression, it was considered valuable to firmly establish the protective effect of XIAP in 661W cells. As AAV-XIAP, generated in the former study was available, and AAV gene delivery has been shown to be highly efficient compared to transient transfection, a study was undertaken to evaluate the potential protective effect of AAV-delivered XIAP in 661W cells exposed to etoposide. Professor William Hauswirth kindly provided an aliquot of AAV-XIAP, with a titre of 3×10^{13} vp/ml. As the multiplicity of infection (MOI) varies between cell lines, 661W cells were transduced with AAV-EGFP, generated on site, to determine the MOI. Using 10^7 viral particles, only a small percentage (1-5%) of 661W cells expressed EGFP (Figure 3.21: B), indicating that 661W cells have a high MOI: that is a high ratio of viral particles to number of cells being infected is required. As the AAV-XIAP had a high-titre of 10^{13}, it should, in principle, have been possible to achieve a sufficiently high MOI (suggested MOI for 661W cells of 1000-10,000: via personal communication, Dr. Adam Baker, Eastern Ontario Research Institute, Ottawa, Ontario, Canada). Unfortunately however, the genomic viral titre was determined by real-time PCR to be 6.45×10^8, approximately 5 fold lower than expected. This may have been due to delays in transit from the United States. Given this titre, the study was not undertaken with the AAV-XIAP provided by Professor Hauswirth. However, results

from Petrin *et al.,* 2003, and Leonard *et al.,* 2005, highlight the validity of the approach that was being followed in the current study, and suggest that further work to explore the full anti-apoptotic potential of XIAP for photoreceptors should be undertaken. In this regard, given that the team in Trinity College Dublin can now produce high-titre AAV, one possibility for future work may involve the generation of AAV serotype 2/5, which transduces photoreceptors efficiently, (Chapter 1: 1.5.3.4) for the further exploration of the anti-apoptotic effect of XIAP *in vivo*.

In summary, suppressing photoreceptor apoptosis represents a potential therapeutic strategy for adRP and other retinal degenerations. An essential element of this research involves identifying and evaluating anti-apoptotic agents in relevant *in cellulo* and *in vivo* systems. The aim of the study described here was to evaluate three members of the inhibitor of apoptosis protein (IAP) family, in 293T cells and 661W cone photoreceptors. Previous studies have shown that IAPs are effective caspase inhibitors, conferring protection against numerous apoptotic agents. In this current study, XIAP, c-IAP-1 and c-IAP-2 were shown to be less effective than previous studies at inhibiting chemical-induced apoptosis in 293T cells. Percentage cell rescue ranged from approximately 23% for XIAP, 14% for c-IAP-1 and 11% for c-IAP-2. 661W cells are less easily transfected than 293T cells, so consistent with the results in 293T cells, XIAP expression provided a slight protection of approximately 5% in 661W cells, while expression of c-IAP-1 or c-IAP-2, provided no observable protection. To overcome the low expression of XIAP, a stable line of 661W cells expressing XIAP was generated. Stable expression provided a significant ($P < 0.01$) cell survival of 37.82 ± 0.97% compared to control 661W cells at 25.14 ± 1.52% when exposed to 15μM etoposide. This is a relatively modest level of protection, and is not consistent with a recent study showing that XIAP is protective in both inherited and chemical-induced animal models of retinal degeneration (Petrin *et al.,* 2003; Leonard *et al.,* 2005). With regard to the lack of protection afforded by XIAP in 661W cells exposed to daunorubicin, the chemical agent used initially, differences in the potency of the agent or mechanism of initiating cell death compared to etoposide, may explain this result.

In the current study, XIAP expression from the pcXIAP construct was confirmed at the RNA and protein level by RT-PCR and Western blot analysis. In addition, all three IAP constructs used were the same as those used in the studies by Roy *et al.,* 1997 and Deveraux *et al.,* 1998, demonstrating the anti-apoptotic effect of XIAP, c-IAP-1 and c-IAP-2. However, there may be a number of reasons why XIAP may not have been found to be protective in the current study. Clearly transient transfection of 661W cells is inefficient and may in part explain the low level of protection afforded by XIAP expression. In stable 661W cells expressing XIAP, the level of expression may have varied, as the cell line was not monoclonal in origin. Although XIAP is expressed in the stable cell line (Figure 3.19), the protection afforded to 661W cells exposed to a chemical insult, may have been limited by insufficient levels of XIAP expression. Furthermore, although 661W cells have been used by this and other laboratories previously (Roque *et al.,* 1999; Tuohy *et al.,* 2002; Gomez-Vicente *et al.,* 2005), the 661W cell line is only a representative model of retinal photoreceptors and it cannot be certain how closely a transformed line mirrors *in vivo* cell lineages.

Although the results obtained in this current study with XIAP in 661W cells were not very encouraging, further research may provide support for the use of XIAP as an anti-apoptotic agent and hence it will be interesting to further evaluate the therapeutic efficacy of XIAP in animal models of retinal degenerations, such as the Pro23His and Ser344Ter models carrying rhodopsin mutations, outlined above in the study by Leonard *et al.*, 2005. Furthermore, additional mouse models of RP exist such as the *rds*-307 model carrying a base-pair deletion of the *rds/peripherin* gene (McNally *et al.,* 2002) and the *rd* model with a mutation in the β-subunit of cGMP phosphodiesterase (Bowes *et al.,* 1990). Hence, the anti-apoptotic effects of XIAP could be explored in such animal models to assess how applicable XIAP is as an anti-apoptotic agent for the many causes of RP. As there is increasing evidence to support caspase-independent mechanisms of photoreceptor cell death (Zeiss *et al.,* 2004; Sharma *et al.,* 2004; Doonan *et al.,* 2005), it may be necessary to deliver XIAP with another therapeutic agent. Although it is notable that in a recent study, XIAP was demonstrated to inhibit

caspase and calpain cleavage, thereby significantly inhibiting motor neuron degeneration *in vivo* (Wootz *et al.,* 2006).

Another inhibitor of apoptosis, the p35 baculoviral protein, was evaluated in this laboratory and shown to be very effective at protecting 661W cells against chemical-induced apoptosis, providing a percentage cell rescue of approximately 50% (Tuohy *et al.,* 2002). Considering the results of this study and a number of others demonstrating that p35 protected against photoreceptor loss in *Drosophila* models of retinal degenerations (Davidson *et al.,* 1998; Galy *et al.,* 2005) , there was a clear rationale to further evaluate the therapeutic efficacy of p35 *in vivo*, which forms the basis for the next two chapters of this thesis.

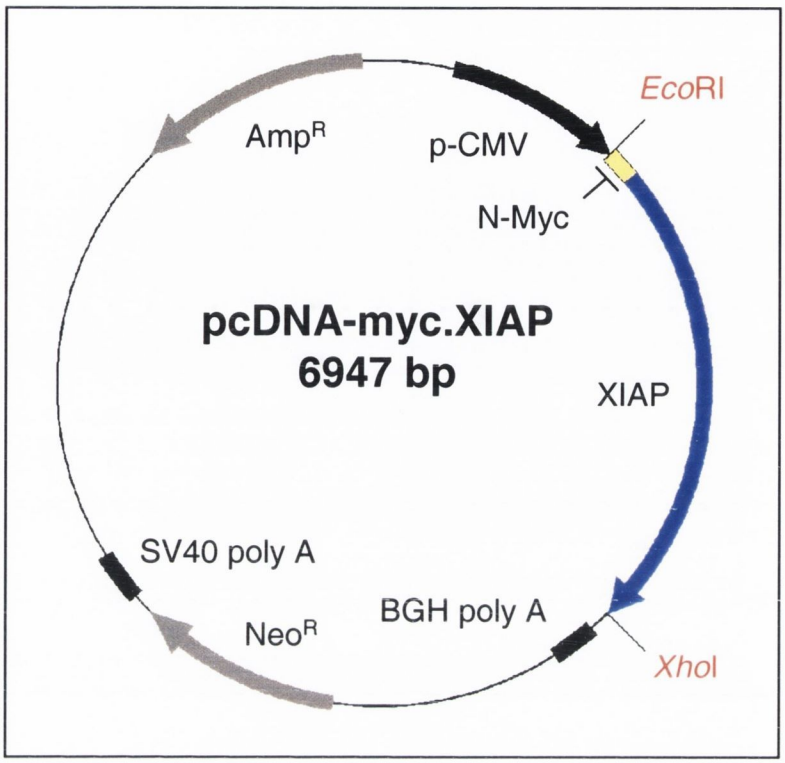

p-CMV: Cytomegalovirus promoter (bases 209-863)

N-Myc: Myc epitope tag (bases 913-939)

XIAP: 1.5 kb of XIAP gene (bases 957-2471)

BGH poly A: Bovine growth hormone polyadenylation signal (bases 2519-2750)

Neo^R: Neomycin resistance gene (bases 3652-4433)

SV40 poly A: SV40 polyadenylation signal (bases 4501-4873)

Amp^R: Ampicillin resistance gene (bases 5951-6811)

Figure 3.1: Plasmid map of pcDNA-myc.XIAP (maps for pcIAP-1 and pcIAP-2 are similar in design). Restriction enzyme sites for *Eco*RI and *Xho*I are shown in red.

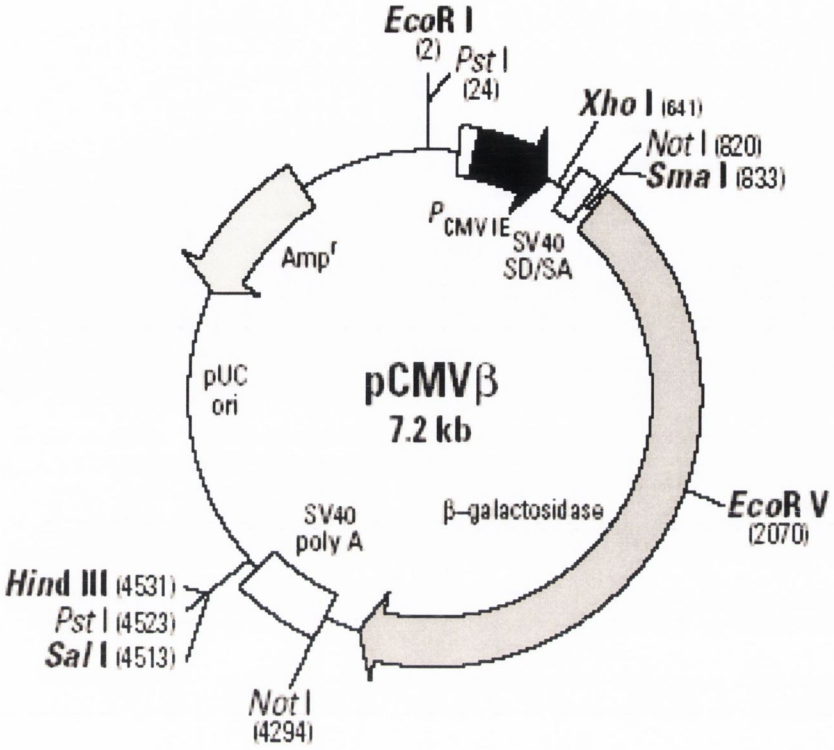

$P_{CMV\ IE}$: Immediate early cytomegalovirus promoter (bases 27-640)

SV40 SD/SA: SV40 splice donor/splice acceptor (bases 672-678)

β-galactosidase: Full length *E.coli* β-gal gene (bases 867-4016)

SV40 poly A: SV40 polyadenylation signal (bases 4426-4445)

Amp^R: Ampicillin resistance gene (bases 5709-6639)

Figure 3.2*: Plasmid map of pCMVβ. pCMVβ is a reporter plasmid that expresses β-galactosidase in mammalian cells. Unique restriction sites are highlighted in bold. *Diagram from http://www.clontech.com (Clontech, Mountain View, CA, USA).

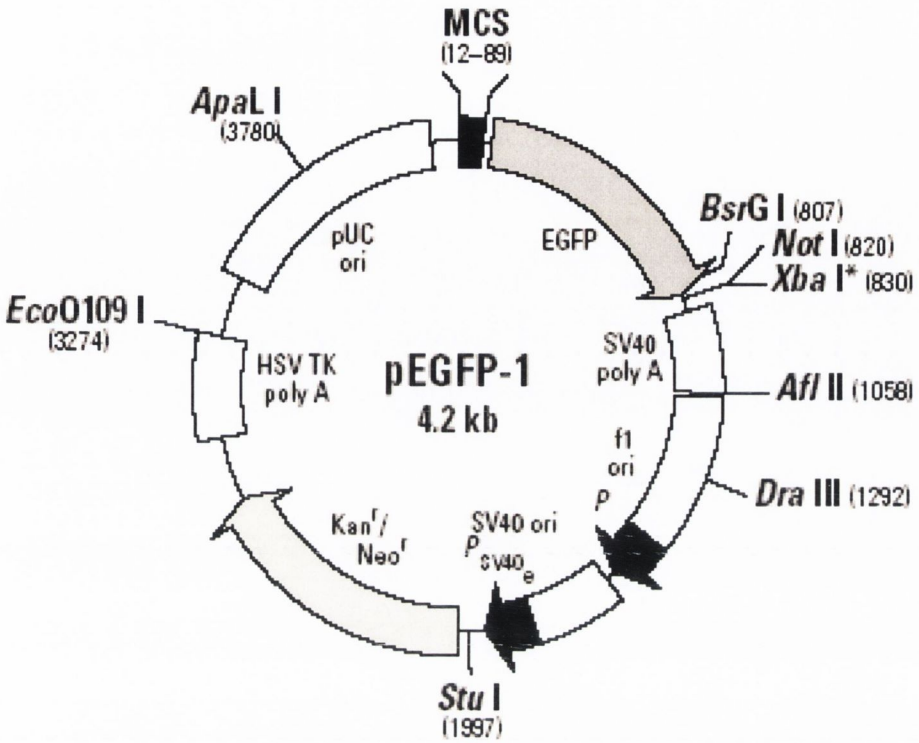

MCS: Multiple cloning site (bases 12-89)

EGFP: Enhanced green fluorescent protein (bases 90-816)

SV 40 poly A: SV 40 early mRNA polyadenylation signal (970-1020)

Kan^R/Neo^R: Kanomycin/neomycin resistance gene (2047-2841)

Figure 3.3*: Plasmid map of pEGFP-1. This plasmid encodes a gene for enhanced green fluorescent protein (EGFP), used as a reporter for gene expression. The promoter of interest is cloned into the multiple cloning site. Unique restriction sites are highlighted in bold. *Diagram from http://www.clontech.com (Mountain View, CA, USA).

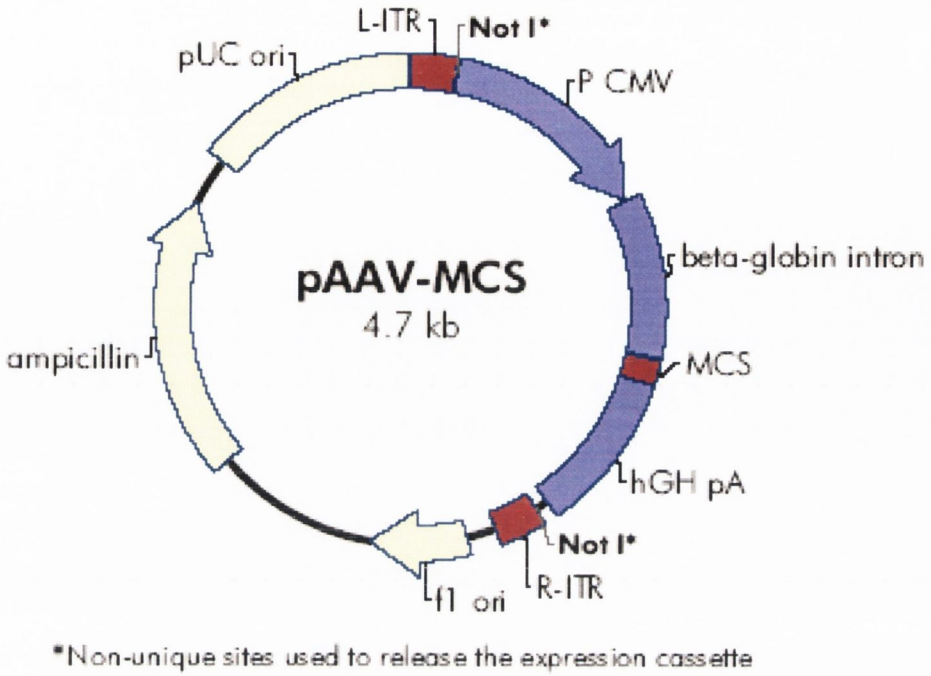

L-ITR: Left inverted terminal repeat (1-141)
P CMV: Cytomegalovirus promoter (150-812)
beta-globin intron: 820-1312
MCS: Multiple cloning site (1319-1394)
hGH pA:Human growth hormone polyadenylation signal (1395-1873)
R-ITR: Right inverted terminal repeat (1913-2053)
ampicillin: Ampicillin resistance gene (2970-3827)

Figure 3.4*: Plasmid map of pAAV-MCS. The gene of interest is cloned into the multiple cloning site, and expression is driven by a CMV promoter. The inverted terminal repeats are necessary to direct AAV viral replication and packaging. Non-unique *Not*I restriction sites are highlighed in bold. *Diagram from http://www.stratagene.com (La Jolla, CA, USA).

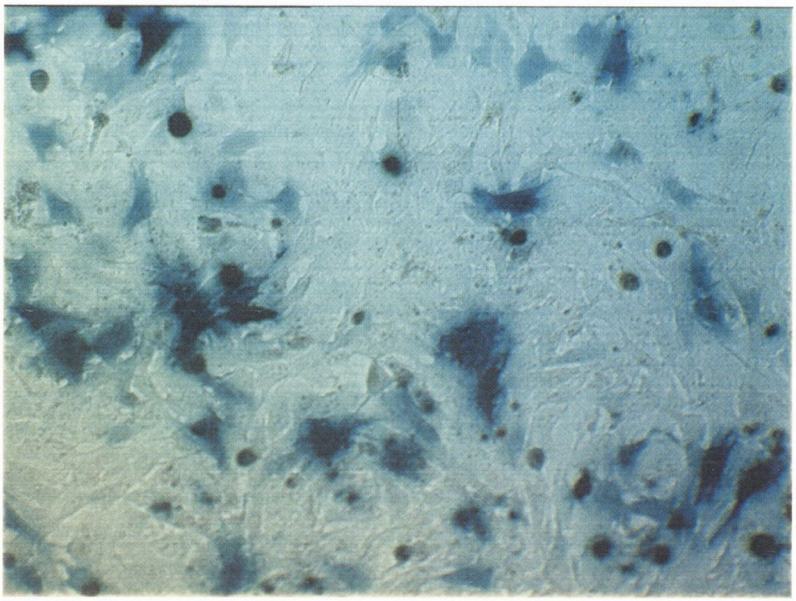

Figure 3.5: 661W cone photoreceptor cells transfected with CMV promoter-driven β–galactosidase. Cells were plated at a density of 1.25 x 10^5 per well of a 12-well plate, transfected with 500ng pCMVβ (Figure 3.2) using Lipofectamine 2000 and assayed for β-gal expression after 48 hours (see 3.2.4). Blue colour indicates expression of the reporter gene in transfected cells (200X magnification).

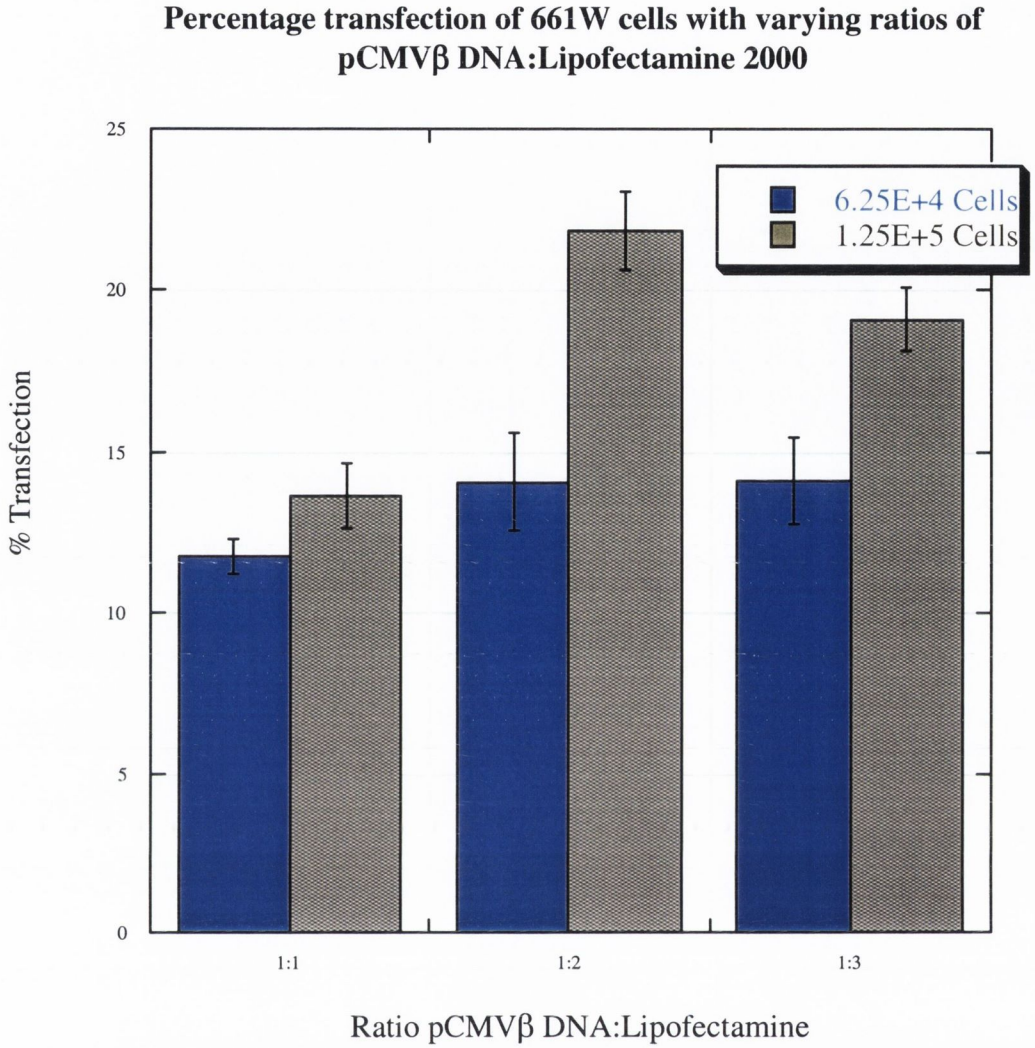

Figure 3.6: Percentage transfection of 661W cells with varying ratios of pCMVβ DNA:Lipofectamine 2000 as measured by staining for β-galactosidase expression. Cells were plated at 6.25 x 10^4 and 1.25 x 10^5 per well of a 12-well plate, transfected with 500ng pCMVβ using a DNA (μg) to Lipofectamine 2000 (μl) ratio of 1:1, 1:2 and 1:3 and assayed for β-gal expression after 48 hours (see 3.2.4). A minimum of 300 cells were scored as blue or white for each well, and the percentage transfection expressed as blue cells/total cells x 100. Bars represent mean ± standard error (S.E.) of duplicate experiments.

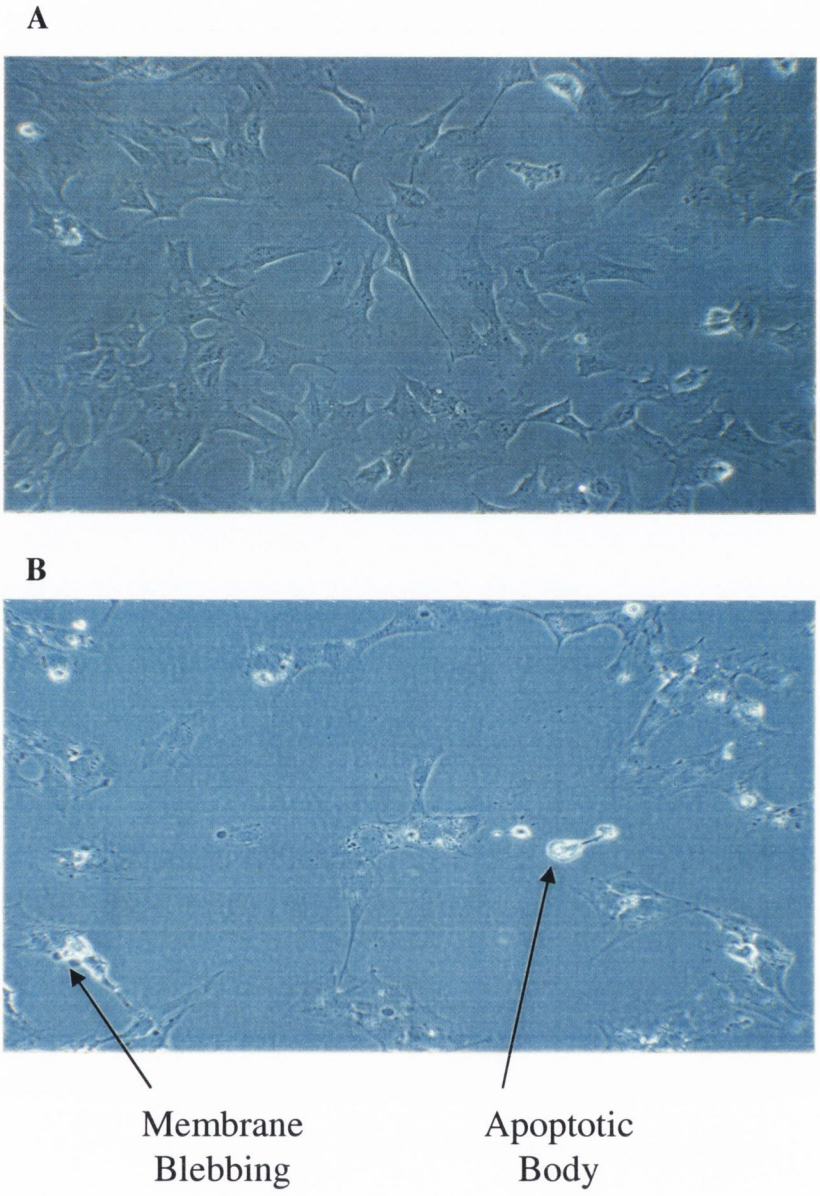

Figure 3.7: 661W cone photoreceptor cells following exposure to UV light. (A) Untreated 661W cells under standard conditions, **(B)** 22 hours following exposure to UV light for 75 seconds (see 3.2.5). Black arrows indicate common features of apoptosis: membrane blebbing and the formation of apoptotic bodies (200X magnification).

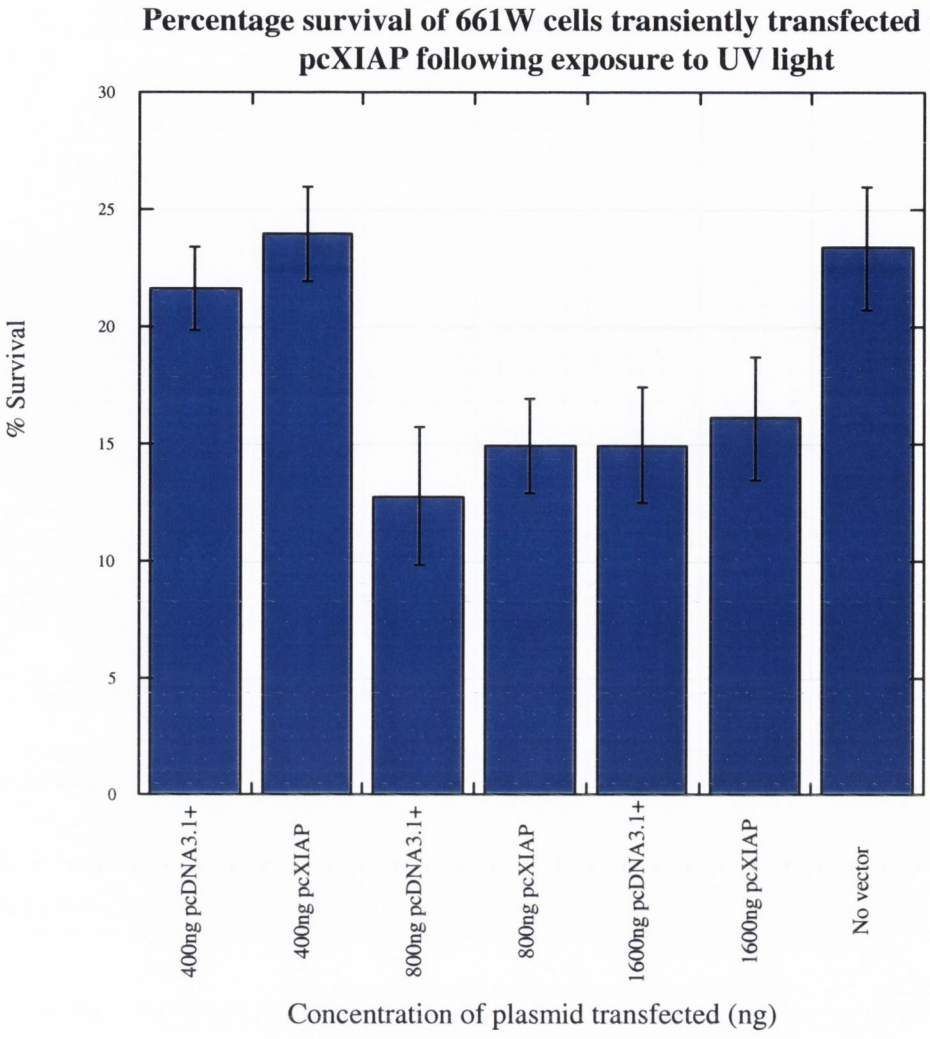

Figure 3.8: Percentage survival of 661W cells transiently transfected with pcXIAP following exposure to UV light. Cells were plated at a density of 2 x 10^5 per well of a 6-well plate and transfected with pcXIAP. After 48 hours cells were exposed to UV light for 75 seconds and scored for apoptotic and viable cells 22 hours later (see 3.2.5). A minimum of 300 cells were scored per well. Bars represent mean ± standard error (S.E) of duplicate experiments. There was no significant difference ($P > 0.05$) in cell survival between cells transfected with pcXIAP, compared to vector alone. The percentage survival of cells transfected with 800ng or 1600ng DNA is lower compared to the control or cells transfected with 400ng DNA, indicating the possibility that the higher concentration of DNA and Lipofectamine was toxic.

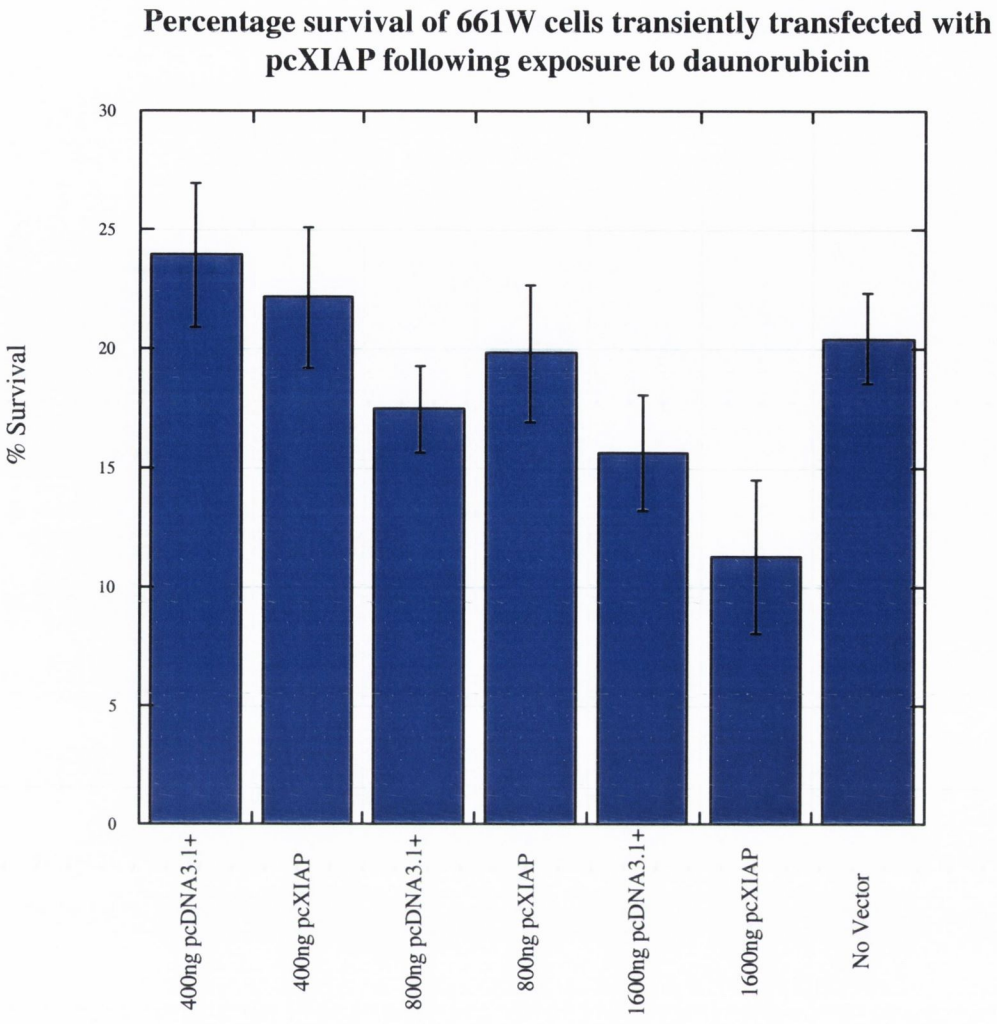

Figure 3.9: Percentage survival of 661W cells transiently transfected with pcXIAP following exposure to 2.5μM daunorubicin. Cells were plated at a density of 2 x 10^5 per well of a 6-well plate and transfected with pcXIAP. After 48 hours cells were exposed to 2.5μM daunorubicin and scored for apoptotic and viable cells 24 hours later (see 3.2.5). A minimum of 300 cells were scored per well. Bars represent mean ± standard error (S.E.) of duplicate experiments. There was no significant difference ($P > 0.05$) in cell survival between cells transfected with pcXIAP, compared to vector alone.

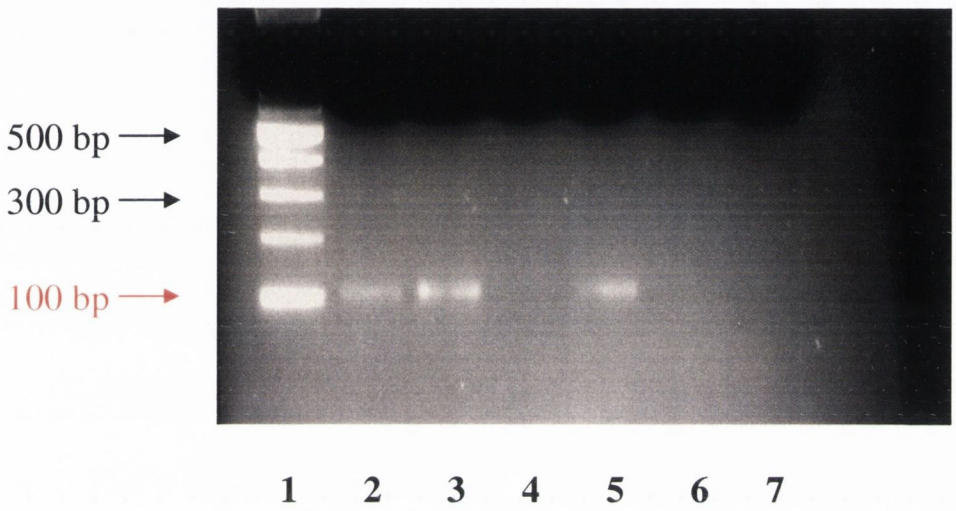

Figure 3.10: RT-PCR analysis on RNA extracted from 661W cells transiently transfected with pcXIAP. Lane 1, 100 bp DNA ladder; Lane 2, amplification of cDNA from 661W cells with primers for XIAP gene (see 3.2.6, 100 bp product); Lane 3, amplification of cDNA from 661W cells with primers for GAPDH gene (see 3.2.6, 100 bp product); Lanes 4-5, amplification of cDNA from untransfected 661W cells with primers for XIAP and GAPDH genes; Lane 6-7, water blanks with primers for XIAP and GAPDH genes. PCR products of 100 bp are indicated in red and DNA size standards in black.

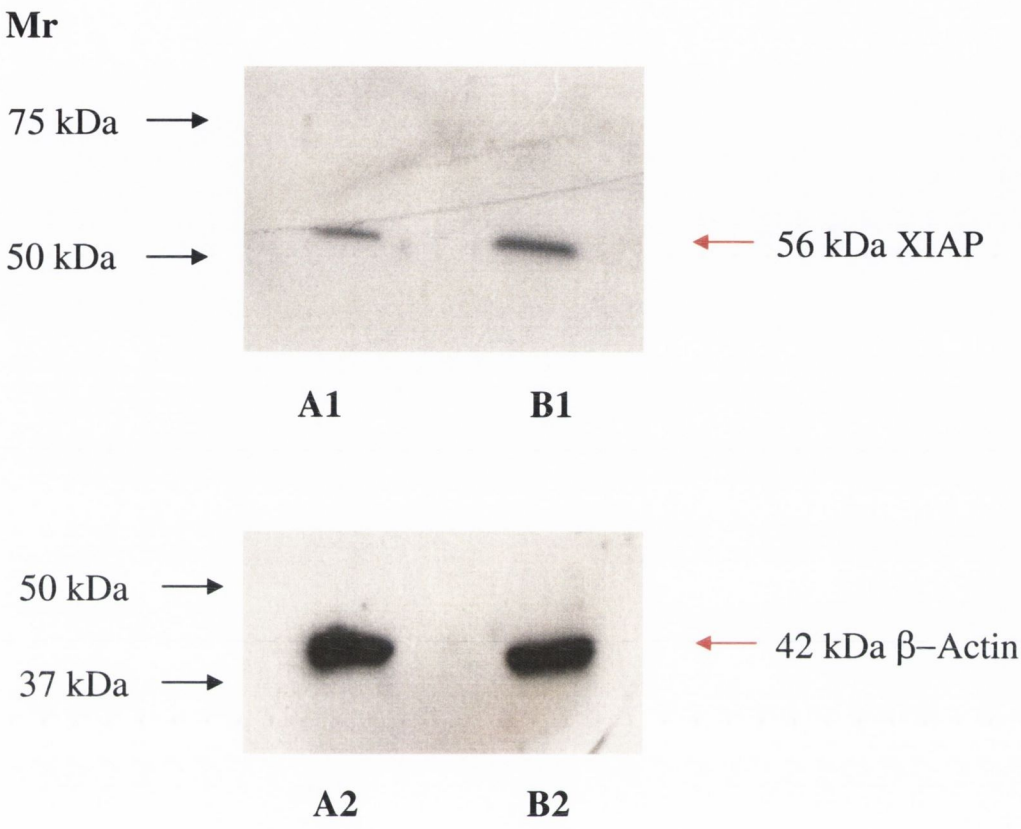

Figure 3.11: Western blot analysis of cell lysate from 661W cells transiently transfected with pcXIAP. Lysates from cells transiently transfected with **(A)** pcDNA3.1+ (2μg), or **(B)** pcXIAP (2μg), were probed using a polyclonal antibody for XIAP **(A1, B1)** and a monoclonal antibody for β–actin **(A2, B2)** (loading control) (see 3.2.7). Molecular weight (Mr) of XIAP and β-actin proteins are shown to the right of the images. The approximate position of protein size standards (Kaleidoscope prestained protein ladder from Bio-Rad Laboratories) are shown to the left of the images.

A

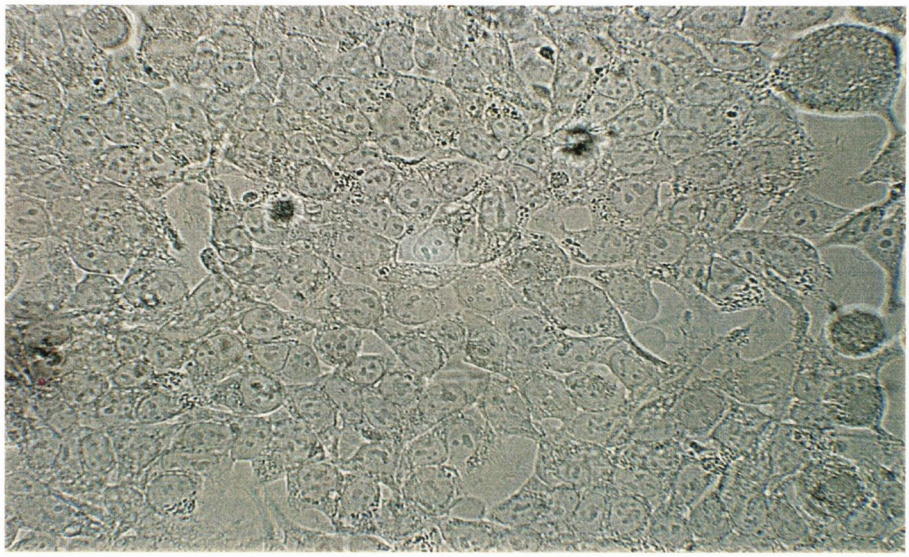

B

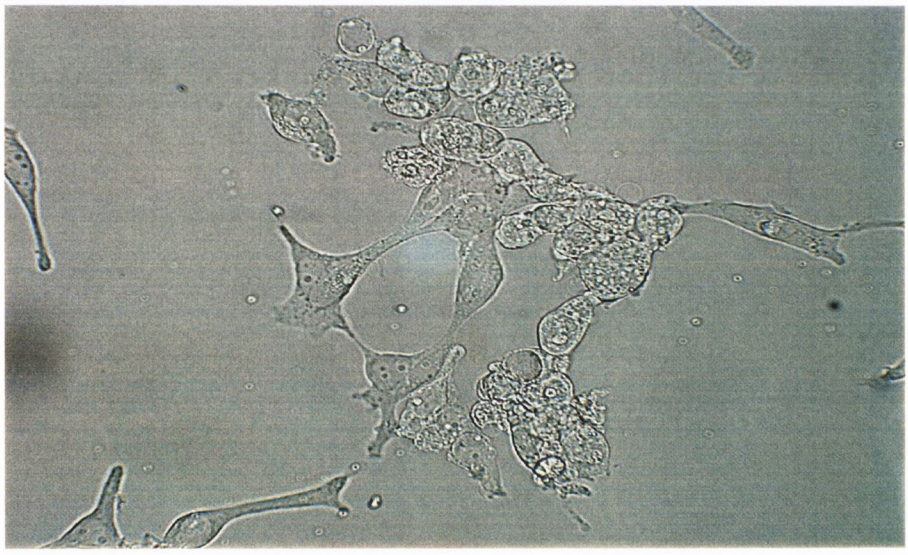

Figure 3.12: 293T cells. **(A)** Untreated 293T cells under standard conditions, **(B)** 293T cells 48 hours following exposure to 30μM etoposide (200X magnification).

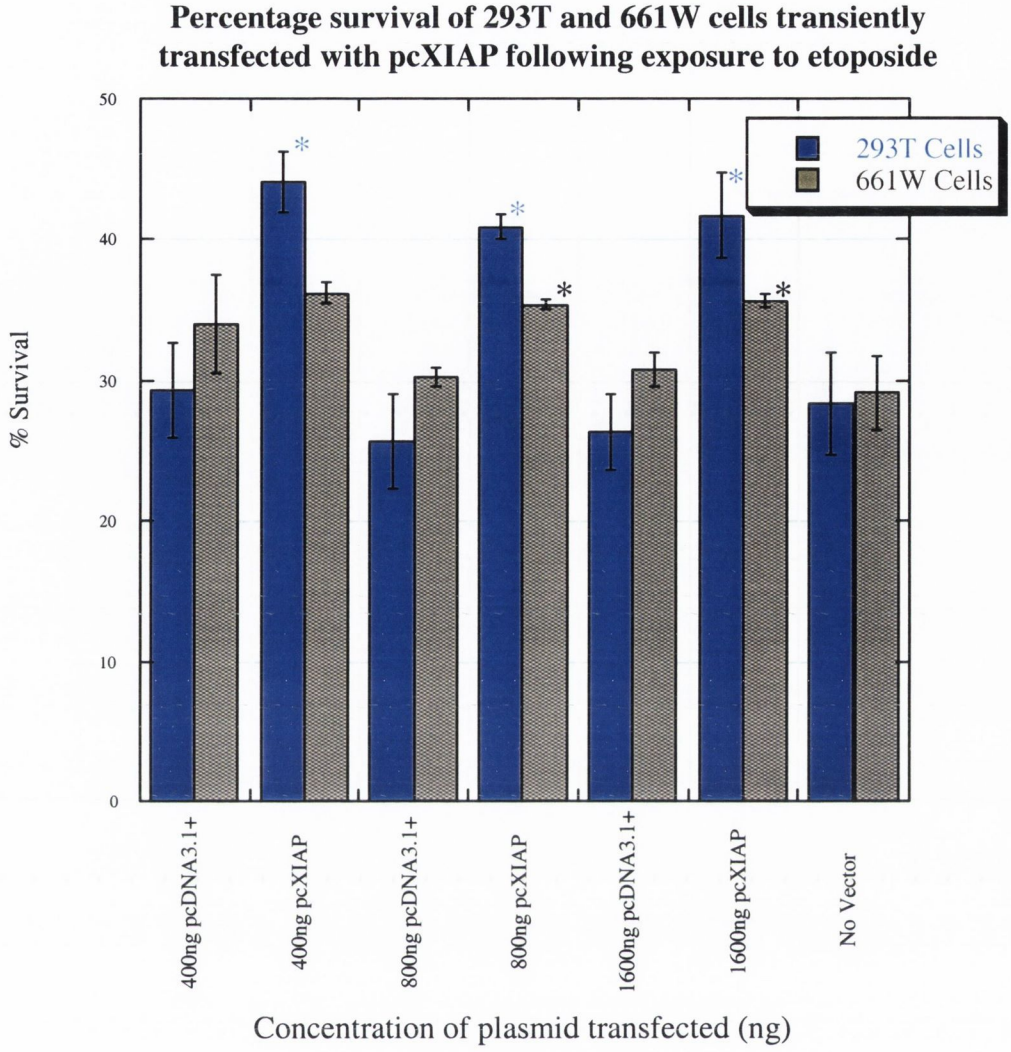

Figure 3.13: Percentage survival of 293T and 661W cells transiently transfected with pcXIAP following exposure to 30μM etoposide. 293T and 661W cells were plated at a density of 5 x 10^5 and 2 x 10^5 respectively, per well of a 6-well plate and transfected with pcXIAP. After 48 hours cells were exposed to 30μM etoposide and scored for apoptotic and viable cells 48 hours later (see 3.2.5). A minimum of 300 cells were scored per well. Bars represent mean ± standard error (S.E.) of triplicate experiments. There was a significant difference ($P < 0.01$*) in cell survival between 293T cells transfected with pcXIAP, compared to vector alone. There was also a significant difference ($P < 0.01$*) in cell survival between 661W cells transfected with the two higher concentrations of pcXIAP, compared to vector alone.

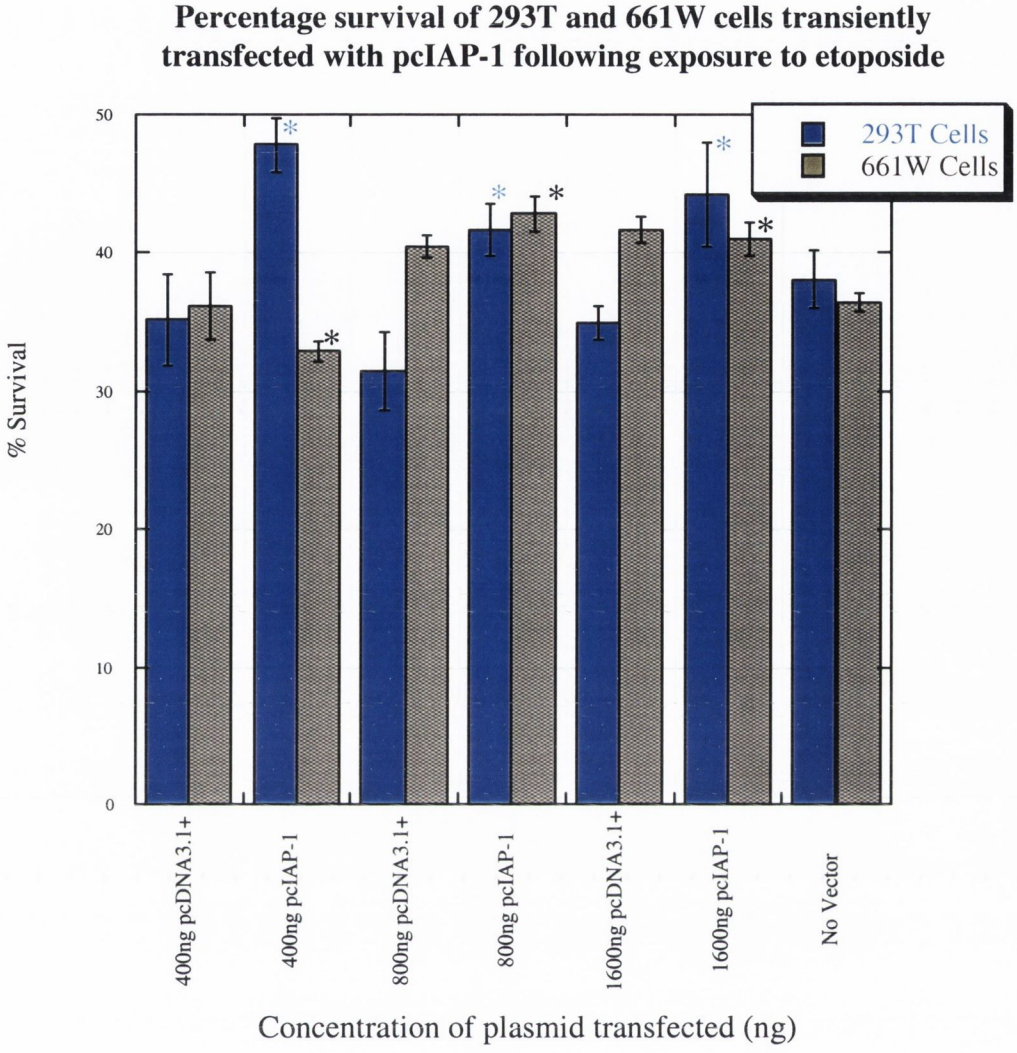

Figure 3.14: Percentage survival of 293T and 661W cells transiently transfected with pcIAP-1 following exposure to 30μM etoposide. 293T and 661W cells were plated at a density of 5 x 10^5 and 2 x 10^5 respectively, of a 6-well plate, and transfected with pcIAP-1. After 48 hours cells exposed to 30μM etoposide and scored for apoptotic and viable cells 48 hours later (see 3.2.5). A minimum of 300 cells were scored per well. Bars represent mean ± standard error (S.E.) of triplicate experiments. There was a significant difference ($P < 0.01$*) in cell survival between 293T cells transfected with pcIAP-1, compared to vector alone. There was no significant difference ($P > 0.05$*) in cell survival between 661W cells transfected with pcIAP-1, compared to vector alone.

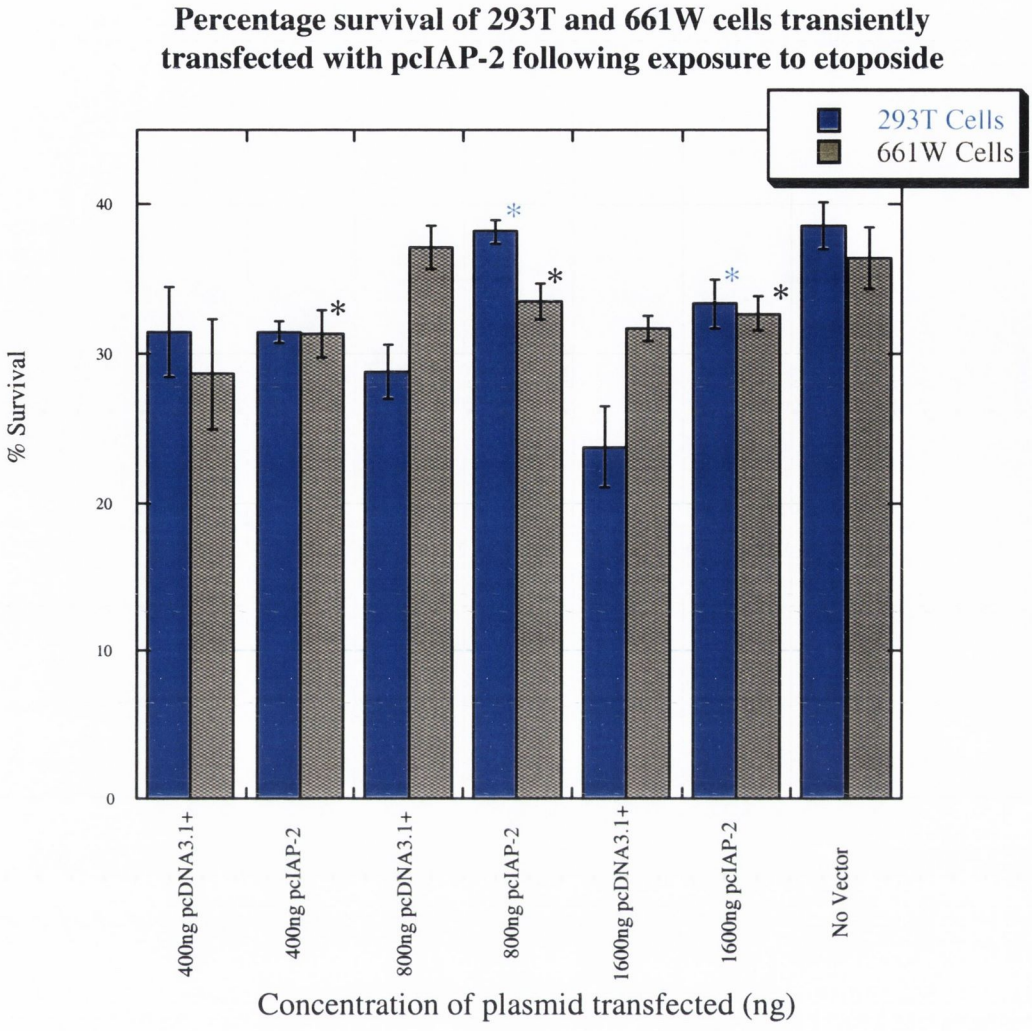

Figure 3.15: Percentage survival of 293T and 661W cells transiently transfected with pcIAP-2 following exposure to 30μM etoposide. 293T and 661W cells were plated at a density of 5 x 10^5 and 2 x 10^5 respectively, of a 6-well plate and transfected with pcIAP-2. After 48 hours cells were exposed to 30μM etoposide and scored for apoptotic and viable cells 48 hours later (see 3.2.5). A minimum of 300 cells were scored per well. Bars represent mean ± S.E. of triplicate experiments. There was a significant difference ($P < 0.01$*) in cell survival between 293T cells transfected with the two higher concentrations of pcIAP-2, compared to vector alone. There was no significant difference ($P > 0.05$*) in cell survival between 661W cells transfected with pcIAP-2, compared to vector alone.

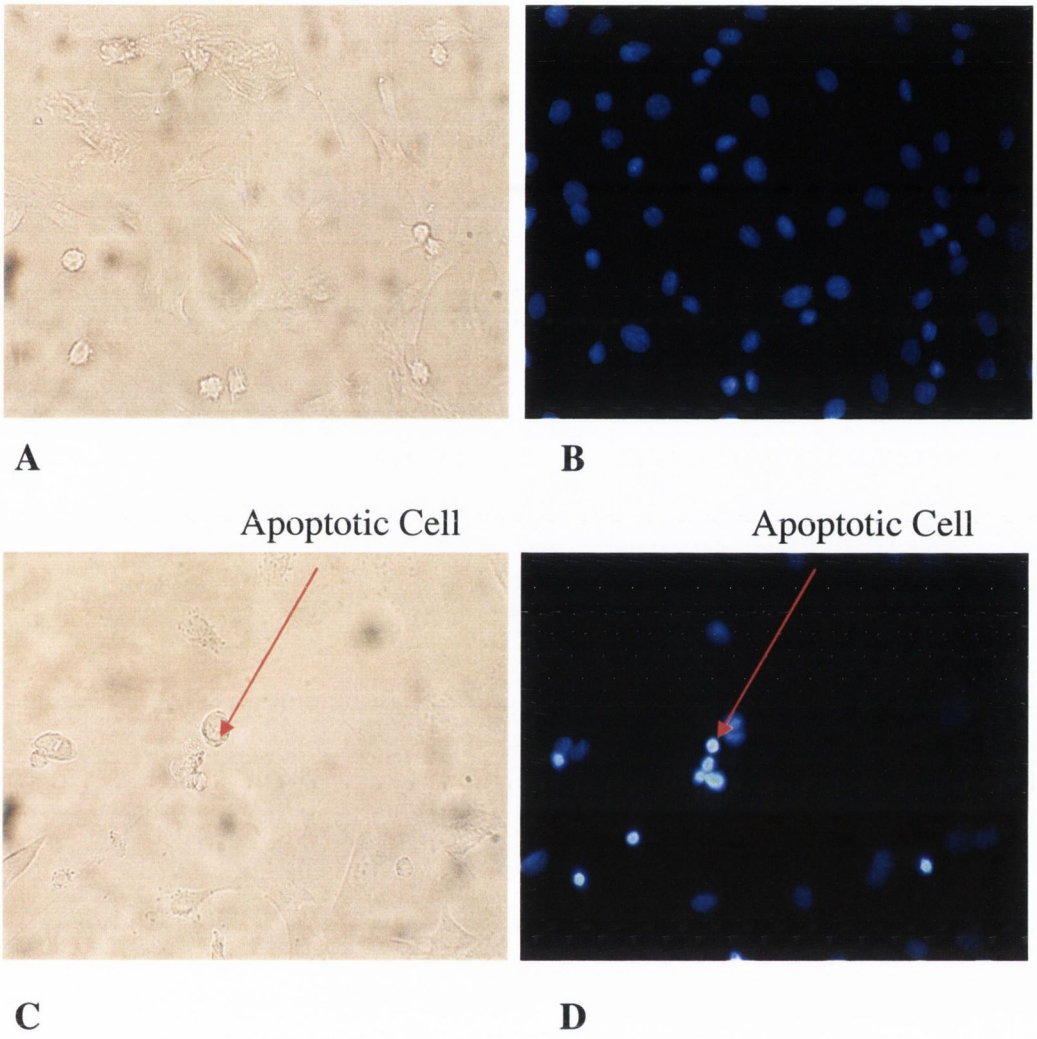

Figure 3.16: 661W cone photoreceptor cells treated with 30μM etoposide and stained with DAPI. Cells were plated at 2 x 10^5 per well of a 6-well plate, exposed to 30μM etoposide for 48 hours, fixed and stained with DAPI (see 3.2.5). **(A)** shows control cells under white light, and **(B)** under UV fluorescent light. **(C)** shows treated cells under white light and **(D)** under fluorescent light (200X magnification).

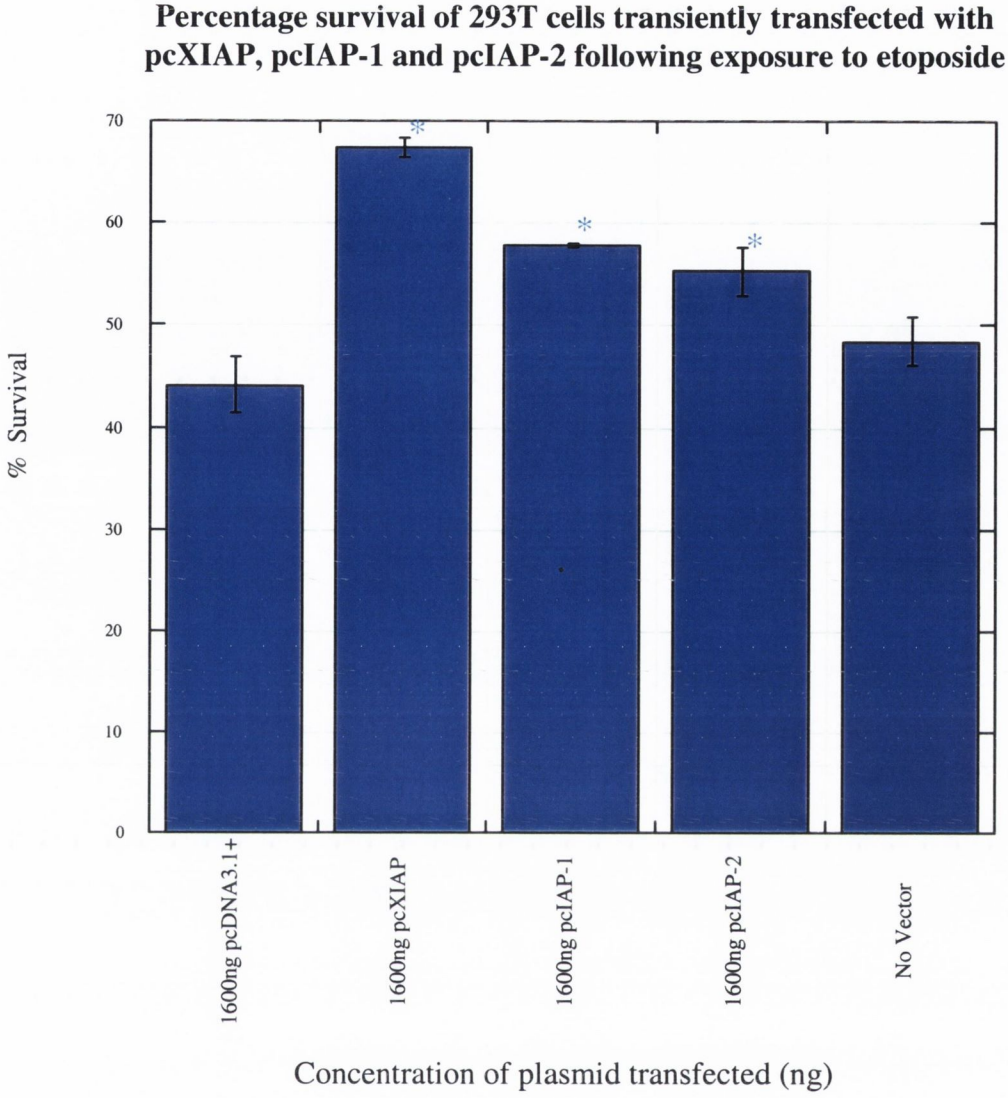

Figure 3.17: Percentage survival of 293T cells transiently transfected with pcXIAP, pcIAP-1 and pcIAP-2 following exposure to 30μM etoposide. Cells were plated at a density of 5 x 10^5 per well of a 6-well plate and transfected with pcXIAP. After 48 hours cells were exposed to 30μM etoposide and scored for apoptotic and viable cells 48 hours later (see 3.2.5). A minimum of 300 cells were scored from 3 fields of view. Bars represent mean ± S.E. of triplicate experiments. There was a significant difference ($P < 0.01$*) in cell survival between 293T cells transfected with pcXIAP, pcIAP-1 and pcIAP-2, compared to vector alone.

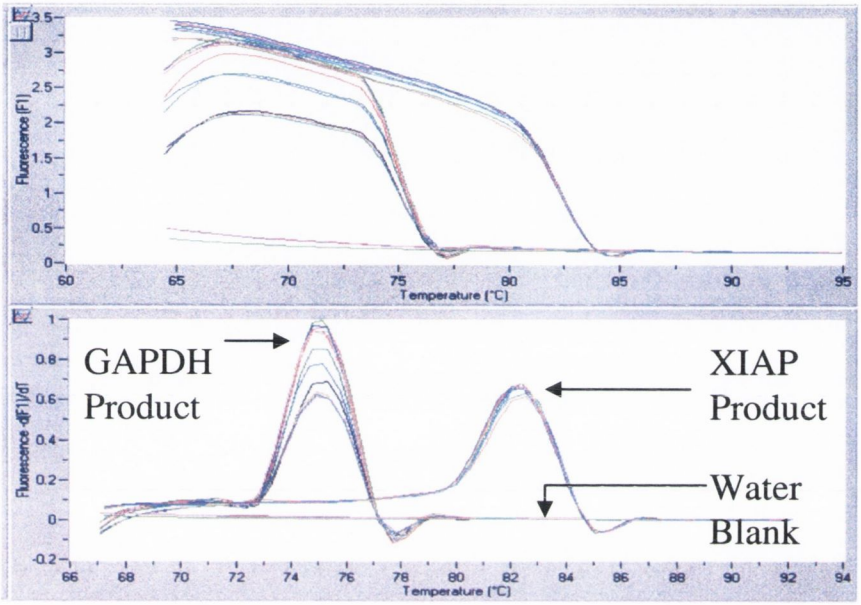

Figure 3.18*: **Melting curve analysis of XIAP and GAPDH PCR products from isolated RNA of 661W cells with stable expression of XIAP.** Black arrows indicate the peaks of specific amplification products: GAPDH, the housekeeping gene and XIAP (see 3.2.8). Note that there are no amplification peaks for the water blanks indicating the absence of contamination in samples (*image is a print-out from the LightCycler {Roche}).

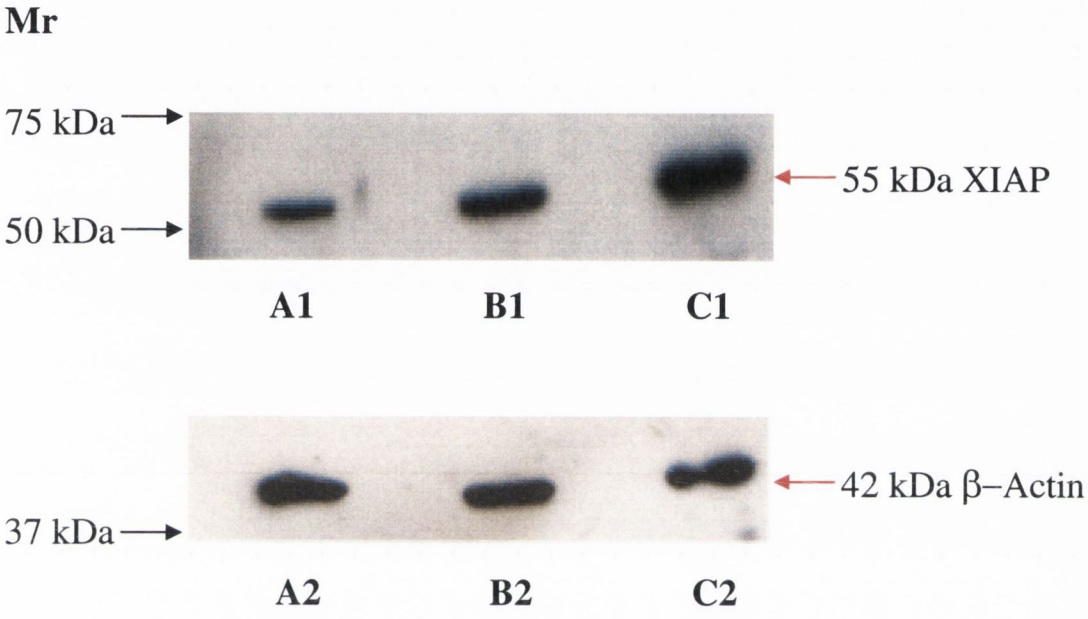

Figure 3.19: Western blot analysis of cell lysate from 661W cells with transient and stable expression of XIAP. Cell lysates from 661W cells transiently transfected with (**A**) 2μg pcDNA3.1+, (**B**) 2μg pcXIAP and (**C**) 661W cells stably expressing XIAP, were analysed by Western blot using a polyclonal antibody for XIAP **(A1, B1, C1)** and a monoclonal antibody for β–actin **(A2, B2, C2)** (loading control) (see 3.2.7). Molecular weight (Mr) of XIAP and β-actin proteins are shown to the right of the images. The approximate position of protein size standards (Kaleidoscope prestained protein ladder from Bio-Rad Laboratories) are shown to the left of the images.

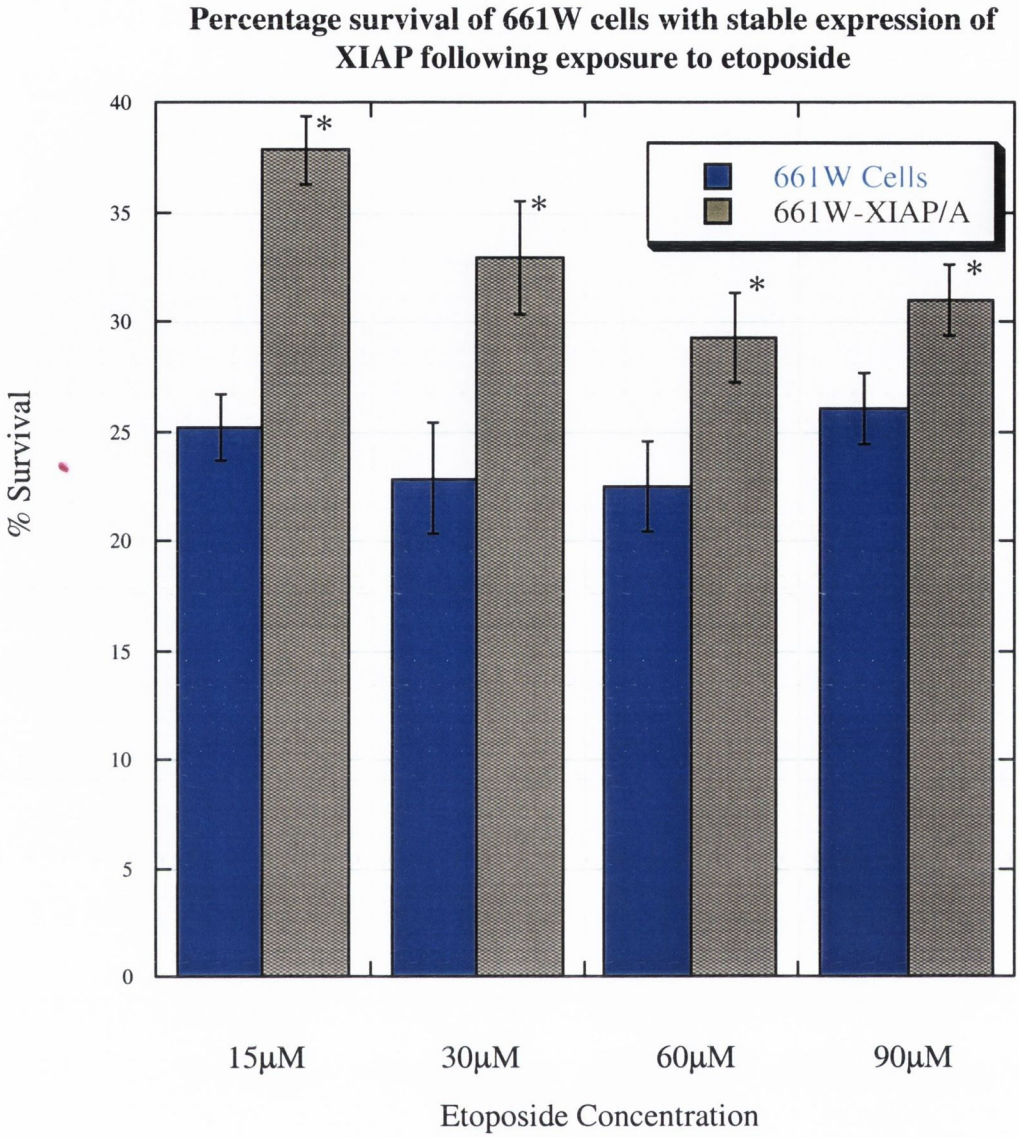

Figure 3.20: Percentage survival of 661W cells stably expressing XIAP following exposure to 15-90μM of etoposide. Cells were plated at a density of 2 x 10^5 per well of a 6-well plate and incubated for 48 hours. Cells were then exposed to 15-90μM etoposide and scored for apoptotic and viable cells 48 hours later (see 3.2.9). A minimum of 300 cells were scored from 3 fields of view. Bars represent mean ± S.E. of triplicate experiments. There is a significant increase in cell survival of 661W cells with stable expression of XIAP, compared to control 661W cells ($P < 0.01$*).

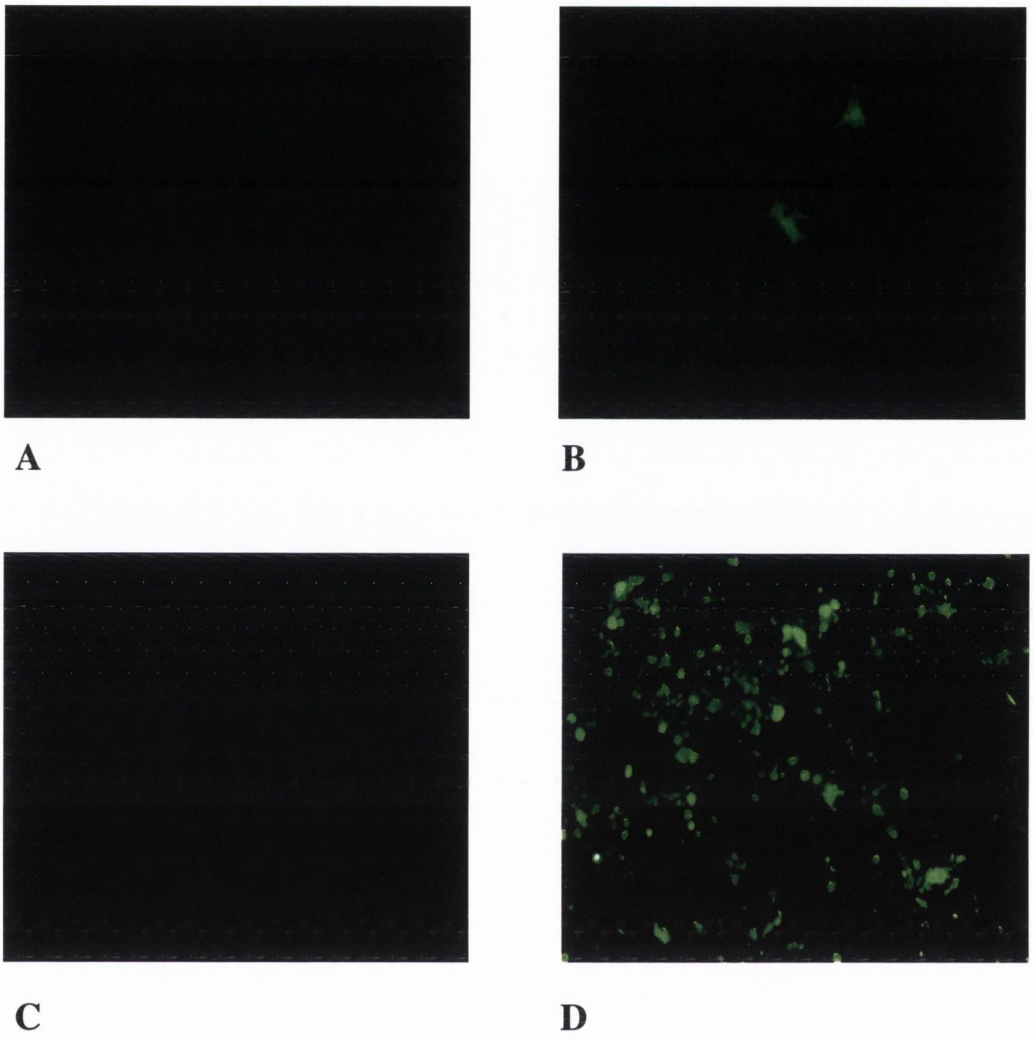

Figure 3.21: 661W cells and 293 cells infected with AAV-EGFP. Cells were plated at 1.5 x 10^4 (661W) and 2.5 x 10^4 (293) per well of a 24-well plate, infected with 10^7 vp and fixed 72 hours later (see 3.2.11). **(A)** and **(B)** show control and infected 661W cells respectively under blue fluorescent light. **(C)** and **(D)** show control and infected 293 cells respectively under fluorescent light (200X magnification).

CHAPTER 4

Generation and *In Cellulo* Evaluation of Photoreceptor-Specific Constructs Expressing iCre Recombinase

4.1 Introduction

Chapter 3 describes a study evaluating three IAPs as potential neuroprotective agents for the retinal degenerative disorder, autosomal dominant retinitis pigmentosa (adRP), a therapeutic approach applicable to other retinal degenerations. Although adRP is genetically heterogeneous, studies have shown that the photoreceptors die by a final common pathway of apoptosis. Thus, inhibition of the apoptotic pathway is one possible approach to overcome the challenge heterogeneity presents to the development of therapeutics for adRP. Although apoptosis has been demonstrated to be responsible for photoreceptor cell loss, the complex pathways leading from the underlying primary mutation to photoreceptor cell death have not been fully elucidated. Increasing our understanding of the complex pathogenesis of adRP should greatly aid future development of effective therapeutic strategies.

Gene targeting technology provides a powerful tool to investigate the function of genes in RP. Gene targeting is defined as the introduction of site-specific modifications into the mouse genome, from single base pair changes to entire chromosomal alterations (Muller 1999). Since the development of the first gene targeted transgenic mouse model in 1987, gene targeting has revolutionised genetics, enabling the generation of numerous models of human disease for studying mechanisms of pathogenesis, and for exploring new therapeutic approaches (Doetschman *et al.,* 1987; Thomas *et al.,* 1987; Muller 1999; van der Weyden *et al.,* 2002). In addition to investigating the role of genes in disease, gene targeting is also used to study diverse aspects of gene function.

Recent technological advances in gene targeting have made it possible to target genes in a tissue or temporal specific manner, hence greatly increasing the resolution of gene targeting (Muller 1999; van der Weyden *et al.,* 2002). Known as conditional gene targeting, this technique has several advantages compared to earlier techniques, which target genes in all tissues of the transgenic animal at each stage of development (Chapter 1: 1.2.11.2). Deleting an essential target gene in all tissues may lead to embryonic or neonatal lethality. Similarly general expression of a transgene may interfere with normal development. One system for conditional gene targeting is the

Cre-*lox*P recombinase system (Porter 1998; Nagy 2000; van der Weyden *et al.,* 2002). Cre recombinase, derived from bacteriophage P1, catalyses recombination at its target *lox*P binding sites (Hamilton *et al.,* 1984). The position, orientation and number of *lox*P sites in the transgene determine the genetic modification catalysed by Cre. For example, when Cre targets two *lox*P sites flanking a target gene in the same orientation, the region is excised from the transgene, deleting the target (Chapter 1: Figure 1.5). The promoter driving expression of Cre controls tissue-specificity, thus the target gene will only be excised in tissues where Cre is present. The most common strategy for the Cre-*loxP* system is to generate two lines of transgenic models, one with tissue-specific expression of Cre and the other expressing the target gene with *loxP* sites. Crossing these lines together generates an F1 generation carrying the target gene modified by Cre in specific tissues. Alternatively, if the necessary lines of Cre recombinase animals are not available, Cre can be delivered to the transgenic model carrying the *lox*P-flanked gene using viral vectors such as AAV and lentiviral vectors (Pfeifer *et al.,* 2001; Kaspar *et al.,* 2002; Ahmed *et al.,* 2004). Another possibility is to deliver Cre as a cell-permeable active enzyme and this was demonstrated in a study using a recombinant Cre fused to a short-peptide from fibroblast growth factor-4 (FGF-4) to enhance cell permeability. Intraperitoneal injection of Cre-FGF-4 into a β-galactosidase reporter mouse, ROSA26R, carrying a β-gal gene flanked by *lox*P sites, resulted in widespread β-gal expression (Chen *et al.,* 2001; Jo *et al.,* 2001). The Cre-*lox*P system has been widely used to generate transgenic mice to investigate the pathogenesis of many human diseases, including Parkinson's disease (Drago *et al.,* 1998), breast cancer (Jonkers *et al.,* 2001) and type 1 diabetes (Apostolou *et al.,* 2003). For a list of Cre expressing lines refer to the database maintained by Professor Andras Nagy (Samuel Lunenfeld Research Institute, Mount Sinai Hospital, Toronto, Canada) (http://www.mshri.on.ca.nagy) or the special issue of the journal Genesis on "Tissue Specific Expression of Cre recombinase in Mice" (Genesis 2000).

Using the Cre-*lox*P system would be of great benefit in studying retinal degenerations such as adRP. For example, it would be of value to establish the effect of deleting pro-apoptotic genes or expressing anti-apoptotic genes specifically in the rod or cone

photoreceptors. For these genes, widespread expression in a transgenic model would more than likely be detrimental to embryonic development. The role of non-photoreceptor-specific genes, involved in normal retinal development or pathogenesis, could be investigated by specifically targeting the photoreceptors, circumventing unwanted phenotypic effects or embryonic lethality that may result from gene targeting in all tissues. As the mechanisms of photoreceptor cell death are not fully understood and involve caspase-dependent and possibly caspase-independent pathways (Chang *et al.,* 1993; Portera-Cailliau *et al.,* 1994; Doonan *et al.,* 2003; Doonan *et al.,* 2005), knocking-out components of these respective pathways may further the understanding of photoreceptor degeneration and reveal novel therapeutic targets. Transgenic lines with photoreceptor-specific expression of Cre, would also represent valuable tools with which to explore the role of genes involved in the pathogenesis of RP. For example, the relative contribution of mutant gene expression in rod and cone photoreceptors to a particular degenerative phenotype, could in principle be explored using conditional knockouts.

At the time of the initiation of this project, there were no transgenic models with photoreceptor specific expression of Cre recombinase available. The aim of this study was to design and generate constructs with rod and cone photoreceptor-specific expression of Cre recombinase and evaluate them using either photoreceptor derived cell lines and *in vitro* cultured retinal explants. Two polymerase II promoters were chosen: the rhodopsin promoter to drive expression of iCre in rod photoreceptors, and the GNAT2 promoter to drive expression of iCre in cone photoreceptors.

More specifically, 1.7 kb of the mouse rhodopsin promoter was selected to drive rod photoreceptor-specific expression of iCre. The size of the mouse rhodopsin promoter previously used for transgenic animal generation has varied from 500 bp to 4.4 kb (Ikawa *et al.,* 2003; Ham *et al.,* 2004; Li *et al.,* 2005). Zack *et al.* investigated the specificity of β-gal expression driven by different bovine rhodopsin promoters in transgenic mouse retinas, and demonstrated the photoreceptor-specific expression of the 2244 bp promoter (Zack *et al.,* 1991). Although shorter rhodopsin promoters have

been shown to direct rod photoreceptor-specific expression (Quiambao *et al.,* 1997; Ham *et al.,* 2004; Pawlyk *et al.,* 2005), to be confident of cell specificity in a transgenic model, 1.7 kb of the rhodopsin promoter was used.

To direct cone photoreceptor expression of iCre, a small 277 bp promoter element of the cone transducin α-subunit gene GNAT2 together with a 214 bp enhancer from the gene of IRBP was used for construct generation. In a study by Morris *et al.*, the activity of different regions of the GNAT2 promoter was investigated in WERI-Rb1 retinoblastoma cells (Morris *et al.,* 1997). A region driving photoreceptor-specific expression of a reporter gene (chloramphenicol acetyltransferase-CAT) was localised to a sequence -151 bp to + 126 bp of the transcription start site. Expression was enhanced using a 214 bp enhancer from the IRBP gene, positioned 3' of the CAT reporter gene. Several subsequent studies have demonstrated that the GNAT2 promoter and IRBP enhancer, drive cone photoreceptor-specific expression in transgenic mouse models (Ying *et al.,* 1998; Ying *et al.,* 2000; Fong *et al.,* 2005).

In addition to selecting promoters with tissue-specific expression for conditional transgenic animals, optimising the level of gene expression *in vivo* is also critical. For the Cre/*lox*P recombination system successful activation or deletion of *lox*P-flanked targeted genes is dependent upon expression levels of Cre recombinase (Cre). Cre was originally derived from the prokaryotic bacteriophage P1 (Sternberg *et al.,* 1981; Hamilton *et al.,* 1984), thus to improve expression in mammalian systems, Shimshek *et al.*, 2002, generated a modified Cre. Several changes were made including, reduction of the number of CpG dinucleotides, introduction of a Kozak sequence and alteration of the stop codon. The improved Cre (iCre) was shown to express at a higher level *in cellulo* than prokaryotic Cre and transgenic mouse models expressing active iCre were also generated (Shimshek *et al.,* 2002). At approximately the same time, another group published similar work, but upon personal communication, they stated the Cre recombinase generated was possibly toxic for transgenic models (Koresawa *et al.,* 2000). For the purpose of this study, Professor Rolf Sprengel kindly provided the novel iCre for construct generation.

Given that a polyadenylation (poly A) signal 3' of a gene is essential for mRNA stability (Bernstein *et al.,* 1989), a poly A signal based on the highly efficient signal of the rabbit β-globin gene was used for construct generation (McLauchlan *et al.,* 1985; Levitt *et al.,* 1989). Studies have demonstrated that using heterologous introns enhances gene expression in transgenic animals (Choi *et al.,* 1991; Palmiter *et al.,* 1991). Hence, in the current study, constructs were engineered to contain two different introns, the human growth hormone (hGH) and chimeric (Chi) introns.

Retinal cell and tissue culture is a useful tool for exploring different aspects of retinal cell biology, including growth, differentiation and death, as well as evaluating retinal specific constructs and therapies for retinal diseases (Seigel 1999). While results obtained using *in vitro* systems may not completely reflect those obtained using *in vivo* models, retinal culture represents an expedient system for studies such as the current one described above. 661W cone photoreceptor cells were used to evaluate the IAPs in Chapter 3, but as these cells do not express rhodopsin, another retinal cell line was selected for evaluating the rhodopsin-driven iCre constructs that were generated during the course of the study. Y79 cells are classified as a human retinoblastoma cell line and were the first such cell line to be described (Reid *et al.,* 1974). Y79 cells were originally thought to be of cone origin, but have since been shown to express rod photoreceptor phosphodiesterase (PDE), in addition to the cone α-subunit of PDE (Di Polo *et al.,* 1995). As Y79 cells also express cone photoreceptor transcripts, they could be used to evaluate the GNAT2-driven iCre constructs also generated.

Primary retinal cell culture represents another possible means of evaluating rhodopsin-driven iCre constructs. However, as cone photoreceptors comprise approximately 3-5% of the total photoreceptor population in the mouse (Curcio *et al.,* 1990; Applebury *et al.,* 2000), primary cultures are not practical for evaluating cone photoreceptor-specific constructs. One type of primary retinal system is retinal explant culture, which involves explanting whole or partial retina from embryonic, neonatal or adult mice and maintaining cultures for up to several weeks (Caffe *et al.,* 1989; Ogilvie *et al.,* 1999; Seigel 1999). Figure 4.1 shows a photograph of a cryosection from a P14 cultured

retinal explant, with developing retinal cell layers clearly distinguishable. One of the principal difficulties with this system is how to effectively deliver DNA to photoreceptors or other retinal cells. One approach is to use viral vectors, based on retroviruses, or adenoviruses (Hatakeyama *et al.,* 2002; Pang *et al.,* 2004), but generation of viral vectors can be time-consuming, and recently a convenient method for delivery has been developed (Matsuda *et al.,* 2004). It involves *in vitro* electroporation of neonatal (P0-P1) explants with plasmid DNA and has also been demonstrated *in vivo*. The current study involved generation and evaluation of retinal specific promoter constructs of iCre and demonstration of the functionality of these constructs. Subsequently it was proposed to use the constructs to generate lines of transgenic mice expressing iCre specifically in photoreceptor cells.

4.2 Materials and Methods

4.2.1 Design of photoreceptor specific constructs

Four constructs with photoreceptor specific expression of improved Cre recombinase (iCre) were designed (Figures 4.2-3). pcDNA3.1- (Invitrogen) was digested with *Nru*I and *Nhe*I to remove 688 bp containing the cytomegalovirus (CMV) promoter, and re-ligated to generate pcDNA3.1-ΔCMV, which had been cloned by Dr. Mary O'Reilly. The methods used here are described in Chapter 2: 2.2.1-17, in more detail. For pRho.hGH.iCre.A (pRho.iCre.A) and pRho.Chi.iCre.B (pRho.iCre.B), 1682 bp of the mouse rhodopsin promoter (-1602 to +80 of the transcription start site, from Dr. O'Reilly) were cloned in via *Nhe*I and *Xho*I vector sites of pcDNA3.1-ΔCMV. The human growth hormone (hGH) intron (270 bp) was amplified from pAAV-LacZ (Stratagene) using the primers hGHF and hGHR with *Xho*I sites and cloned into pcRho.iCre.A (for primer sequences see Appendix: 1.1.1). A chimeric intron (143 bp, composed of the 5'-splice site of the β-globin intron and 3'-splice site from an IgG intron) was amplified from pALTER-MAX (Promega) by PCR using the primers ChiF and ChiR with *Xho*I sites at either end and cloned into pRho.iCre.B (for primer sequences see Appendix: 1.1.1). The gene for improved Cre recombinase, kindly provided by Professor Rolf Sprengel (Max-Planck Institute, Germany), was cloned in via *BamH*I and *Kpn*I sites. A poly A signal based on the highly efficient poly A signal of the rabbit β-globin gene (mrβGpolA; 60 bp) was synthesised by Sigma-Genosys as two single stranded forward and reverse oligonuleotides with *Kpn*I sites at either end (Appendix: 1.1.1) (McLauchlan *et al.,* 1985; Levitt *et al.,* 1989). The forward and reverse strands were annealed by incubating 1 nmol of each oligonucleotide in a 40μl reaction with 25mM NaCl at 94°C for 4 minutes and subsequently incubating at room temperature overnight. The poly A signal was then cloned in via the *Kpn*I site.

For generating the two constructs with cone photoreceptor specific expression of iCre recombinase, pcGNAT2.hGH.iCreA (pcGNAT2.iCre.A) and pcGNAT2.Chi.iCreB (pcGNAT2.iCre.B), the GNAT2 promoter of the cone transducin α-subunit gene with an interphotoreceptor retinol-binding protein (IRBP) enhancer was used.

pCAT.GNAT2 was kindly provided by Professor Shao-Ling Fong (Indiana University, Indianapolis, USA) (Morris *et al.*, 1993; Morris *et al.*, 1997; Ying *et al.*, 1998). A complete sequence of pCAT.GNAT2 was unavailable, so to design primers for amplifying the 277 bp fragment of the GNAT2 promoter and the 214 bp IRBP enhancer, 50 bp regions 5' and 3' of these genes were amplified by PCR from pCAT.GNAT2 and sequenced (see Appendix: 1.1.2 for primer sequences). Primers were then designed to amplify the GNAT2 promoter with *Xba*I sites (Appendix: 1.1.1) and the isolated 277 bp fragment was cloned into the *Xba*I site of pcDNA3.1-ΔCMV. The 214 bp IRBP enhancer was amplified by PCR from the pCAT.GNAT2 vector using primers with *Hind*III sites (Appendix: 1.1.1), and cloned into pcDNA3.1-ΔCMV.GNAT2 via a *Hind*III site. The introns, iCre and poly A tail were cloned in via the same restriction sites as described previously for the rhodopsin promoter-driven constructs of iCre.

At each stage of construct generation, PCR analysis of *E. coli* XL-1B transformants was used to select positive colonies (2.2.9). Minipreps of the selected colonies were then digested with restriction enzymes and sequenced to verify the successful ligation of the insert (2.2.15). Primers used for PCR analysis and sequencing are given in Appendix: 1.1.3.

4.2.2 Design and sequencing of β-galactosidase reporter pCMVβ.Neo, the control construct, pciCre, pCMV.EGFP and pRho.EGFP

To assess the constructs expressing Cre recombinase, a β-galactosidase (β-gal) reporter construct, pCMVβ.Neo based on the paper by Kellendonk *et al.*, 1996, was designed and generated (Figure 4.4). The vector pCMVβ (Clontech) expressing β–gal under the control of a CMV promoter, was digested with *Xho*I, end-filled with a DNA polymerase I enzyme (Klenow, Chapter 2: 2.2.15) and the 5'-phosphorylated ends dephosphorylated with the enzyme Shrimp alkaline phosphatase (SAP, 2.2.17). The p*lox*Pneo-1 vector, kindly provided by Professor Andras Nagy (Samuel Lunenfeld Research Institute, Mount Sinai Hospital, Toronto, Canada) was digested with *Sma*I and *Xho*I. The 1994 bp fragment containing the neomycin gene flanked by *lox*P sites

was isolated by gel extraction (2.2.5), end-filled with Klenow enzyme and cloned into pCMVβ via end-filled *Xho*I sites. Bacterial colonies with plasmid constructs were selected by PCR screening (2.2.9) using FNeo and Rβ–gal primers (for primer sequences see Appendix: 1.1.4). The resulting construct pCMVβ.Neo, contained a β–gal gene, which is not expressed due to the presence of a neomycin gene flanked by *lox*P sites between the CMV promoter and the β–gal gene.

Prior to evaluating the constructs with photoreceptor-specific expression of iCre, the functionality of the pCMVβ.Neo construct was assessed *in cellulo*, using a construct with CMV-driven iCre. Active iCre protein should catalyse recombination between the *lox*P sites, removing the neomycin gene, resulting in β–gal expression. A 1.6 kb fragment with the hGH intron, iCre and poly A tail was isolated from pRho.iCre.A by digestion with *Pme*I and *Sac*I, and end-filled with T4 DNA polymerase (2.2.16). The hGH intron and poly A tail were isolated with the iCre gene to assess their effect on iCre expression. Repeated ligations of the 1.6 kb iCre fragment to pcDNA3.1- digested with *Pme*I, were unsuccessful with frequent rearrangement of the inserted fragment. In an attempt to overcome this, a different strain of *E.coli* (TP611) was used, which carry the vector at a lower copy number but the fragment consistently ligated in the reverse orientation. iCre recombinase was isolated from pRho.iCre.A by digestion with *Bam*HI and *Kpn*I, and ligated into pcDNA3.1- digested with the same restriction enzymes, generating the construct pciCre, with CMV promoter-driven expression of iCre.

pCMV.EGFP was generated by digesting pEGFP-1 from Clontech, (Chapter 3: Figure 3.19) with *Sma*I and ligating in the 688 bp CMV promoter digested with *Nru*I and *Nhe*I and end-filled with Klenow. pRho.EGFP was generated by digesting pEGFP-1 with *Sma*I and ligating in 1682 bp of the mouse rhodopsin promoter digested with *Nhe*I and *Xho*I and end-filled with Klenow (Figure 4.5, cloning of both constructs undertaken by Dr. Naomi Chadderton).

4.2.3 Culturing and passaging of 293T and Y79 retinoblastoma cells

293T cells and Y79 retinoblastoma suspension cells were cultured as described in 2.4.1. For assays 293T cells were seeded at a concentration of 5 x 10^5 per well of a 6-well plate and Y79 cells were seeded at a concentration of 4-8 x 10^5 per well of a 24-well plate.

4.2.4 Evaluation of pCMVβ reporter in 293T cells with pciCre

293T cells were plated in 6-well plates and the following day transfected with pCMVβ, pCMVβ.Neo and pciCre using Lipofectamine 2000 according to the manufacturer's instructions. 48 hours later, 293T cells were fixed and stained for β-gal expression (Chapter 2: 2.4.5). For each well, a total of at least 300 cells were scored for β-gal expression from three fields of view under a 20X objective of a light microscope (CK30, Olympus). The result was expressed as the percentage of blue cells of the total number of cells counted, and graphed as the mean ± S.E. Significant differences ($P < 0.05$) across samples were assessed with an unpaired *t*-test.

4.2.5 Use of RT-PCR to detect photoreceptor-specific transcripts in Y79 retinoblastoma and 661W cells

RNA was isolated from Y79 and 661W cells using TRI reagent as described in Chapter 2: 2.3.3. 1μg of total RNA was used for RT-PCR reactions and these were carried out as described in 2.3.3. RNA was isolated from wild-type C57BL/6J mouse retina as a control for amplification of photoreceptor-specific transcripts (2.3.4). Primers were designed to amplify the following transcripts in Y79 cells: GAPDH, cone transducin α-subunit and rhodopsin, and in 661W cells: GAPDH and cone transducin α-subunit (Table 4.1). Primers were designed to amplify across one intron to distinguish between mRNA amplification and false-positive genomic DNA amplification. Levels of rhodopsin transcript in isolated Y79 RNA were also quantified using real-time RT-PCR, using HPLC-purified primers for rhodopsin and the house-keeping gene β-actin. RNA extracted from COS-7 cells and COS-7.Rhodopsin, a stable line expressing human rhodopsin, were kindly provided by Dr. Sophia Millington-Ward.

Table 4.1: Forward and reverse primers for the amplification of photoreceptor specific transcripts in 661W and Y79 cells

Target*	Forward Primer, 5'- 3'	Reverse Primer, 5'- 3'	Product, bp
H GAPDH	CCTCAAGATCATCAGCA	CATAGTCCTTCCACGATAC	100
H Trans.	TATGCTGAACCAAGCTGTGC	CCTCCTAATGACCTCCACGA	105
H Rho1.	ATGAGCAACTTCGCTTC	GGCAAAGAACGCTGGGATG	459
H Rho2	CTTTCCTGATCTGCTGGGTG	GGCAAAGAACGCTGGGATG	107
H Rho3	AGTGCTCGTGTGGAATC	GGCAAAGAACGCTGGGATG	335
H Actin	AGAGCAAGAGAGGCATCC	TCATTGTAGAAGGTGTGGTGC	102
M Rho.	ATGGTCTTCGGAGGATTCAC	CATGATAGCGTGATTCTCCCC	210
M GAPDH1	CCATGGAGAAGGCTGGGG	CAAAGTTGTCATGGATGACC	196
M GAPDH2	GCAGTGGCAAAGTGGAGATT	GTCTTCTGGGTGGCAGTGAT	490
M Trans.	TATGCAGAGCCAAGCTGTGC	CTTCCTGATGACGTCCACCA	103

* H: Human, M: Mouse

4.2.6 Expression of photoreceptor-specific promoters in Y79 retinoblastoma cells

Y79 cells were plated at concentrations of 4-8 x 10^5 per well of a 24-well plate and transfected the same day with 200ng of the plasmid pCMV.EGFP to optimise transfection conditions using Lipofectamine 2000 according to the manufacturer's instructions. 48 hours later the cells were centrifuged at 3,000 rpm (GS-6 centrifuge) to remove medium and resuspended in 200µl 4% paraformaldehyde for 30 minutes. Following another centrifugation the cells were resuspended in 100µl PBS, 30µl of which was transferred to a polylysine glass slide and a coverslip placed on top. Cells were then examined for EGFP fluorescence using a Zeiss Axioplan-2 Optical Fluorescent Microscope (Carl Zeiss) with filter set 38, excitation maximum 470nm, and analysis^B Imaging Software (Olympus). For each sample, a total of at least 300 cells were scored for EGFP expression from three fields of view under a 20X objective. The result was expressed as the percentage of EGFP expressing cells of the total number of cells counted, and graphed as the mean ± S.E.

For evaluating expression of the rhodopsin promoter in Y79 cells, 6 x 10^5 cells were plated per well of a 24-well plate and transfected the same day with either 200ng: (i) pCMV.EGFP, (ii) pRho.EGFP or (iii) pEGFP-1. Following 48 hours, the cells were fixed using paraformaldehyde, and examined using a Zeiss Axioplan-2 Optical Fluorescent Microscope, as described above.

4.2.7 In vitro *electroporation and culturing of C57BL/6J retinal explants*

C57BL/6J newborn mouse pups were culled at P0-P1 and retinal explants were prepared as described in Chapter 2: 2.7.2. For the first experiment, 8 explants in total were electroporated with the following 100µl solutions of DNA: (i) 50ng/µl pCMVβ.Neo, (ii) 200ng/µl pCMVβ.Neo, (iii) as (i) with 1µg/µl pRho.iCre.A and (iv) as (ii) with 1µg/µl pRho.iCre.A. For the second experiment, 8 explants in total electroporated with: (i) 50ng/µl pCMVβ.Neo and (ii) as (i) with 1µg/µl pRho.iCre.A. Media was changed on the retinal explants every 2-3 days, which were then cultured for 14 days.

4.2.8 β-galactosidase staining of whole retinal explants

Media was removed from retinal explants, and explants were washed twice with PBS, pH 7.2. Fixative was freshly prepared, with 0.5% glutaraldehyde and 2mM $MgCl_2$ in PBS. 1ml of fixative (per insert) was pipetted underneath retinal explants, which were incubated at room temperature for 2 hours, followed by 3 washes with 2mM $MgCl_2$ in PBS to thoroughly remove the fixative. β-gal staining solution was prepared as described in Chapter 2: 2.1.2 (xi) with one addition, 0.1% sodium deoxycholate, and X-gal was freshly added to the required volume of staining solution at a final concentration of 1mg/ml. 1ml of β-gal staining solution with X-gal was added underneath and directly on top of the explants and incubated for 30 minutes at 37°C or until a blue colour had developed.

4.2.9 Sectioning and immunostaining of retinal explants

Retinal explants were fixed in 10% formalin and prepared for cryosectioning as described in Chapter 2: 2.7.4. Sections of 7µm were probed for rhodopsin expression

using the 4D2 anti-rhodopsin antibody (1/10 dilution) kindly provided by Professor Robert Molday, (University of British Columbia, Vancouver, Canada). Sections were also probed for iCre expression using a mouse monoclonal anti-Cre recombinase antibody (1/100 dilution) from Covance Research Products. Sections were blocked using a solution of 3% goat serum and 0.1% Triton X-100 in PBS for 1 hour, followed by incubation with the primary antibody overnight. Following 3-4 washes in PBS for 10 minutes each, sections were incubated with Alexa Fluor 568 goat anti-mouse IgG (1/1000 dilution, Molecular Probes) for 2 hours and nuclear stained with 1mg/ml DAPI for 5 minutes. After 3-4 washes for 10 minutes in PBS, sections were mounted in Aqua-Poly/Mount (Polysciences) and examined using a Zeiss Axioplan-2 Optical Fluorescent Microscope for Alexa Fluor 568 (filter set 14, excitation maximum, 560nm) and DAPI staining (filter set 1, excitation maximum, 365nm).

4.2.10 Infection of C57BL/6J retinal explants with AAV rhodopsin promoter-driven EGFP

C57BL/6J newborn mouse pups were culled at P0-P1 and 4 retinal explants were prepared as described in Chapter 2: 2.7.2 in two independent experiments. The following day, 50µl of AAV-EGFP (generated by Dr. Naomi Chadderton; 5 x 10^8 vp) was pipetted onto 2 retinal explants in each insert, and cultured for 14 days. Media was aspirated from the explants, which were then washed twice with PBS before 1ml of 4% paraformaldehyde was added for 1 hour at room temperature. Following another two washes with PBS, explants were cryoprotected in 30% sucrose solution overnight at 4°C and set in OCT the following day. Sections of 10-15µm were cut on a cryostat at -16°C, placed on polylysine slides and allowed to air dry for several minutes. Sections were set with Aqua-Poly/Mount and examined using a Zeiss Axioplan-2 Optical Fluorescent Microscope (filter set 38) for EGFP expression.

4.3 Results

4.3.1 Generation of constructs with photoreceptor-specific expression of iCre recombinase

Conditional gene expression enables the generation of transgenic animals with tissue-specific expression of genes, to address the function of individual genes and protein products in specific tissues or cell lineages. Given this, it was proposed in the current study to generate a number of constructs necessary for such a system in photoreceptor cells. Hence, four novel constructs were generated with rhodopsin and GNAT-2 promoter-driven expression of iCre recombinase as part of this project, using the cloning methods outlined in 4.2.1 (Figures 4.2-3). The integrity of the constructs was confirmed by sequencing at each stage of construct generation (see Appendix: 1.2.1-4 for construct sequences).

4.3.2 Evaluation of pCMVβ.Neo in 293T cells using pciCre

Given that the tissue-specific iCre constructs developed in the previous section of this chapter would be used to generate transgenic mice, a time consuming and costly process, it was decided that the functionality of these iCre constructs should be evaluated prior to the generation of transgenic mice. To evaluate the activity of the photoreceptor-specific iCre constructs, a β-gal reporter gene construct was designed and generated. pCMVβ was modified by inserting a neomycin gene flanked by *lox*P sites between the promoter and the start site of the β-gal gene (Appendix: 1.3 for construct sequence). Active Cre recombinase excises the neomycin gene by catalysing recombination at the *lox*P sites, allowing expression of the β-gal gene. Thus cells in which the reporter gene has undergone recombination will stain blue when stained for β-gal expression. To assess the functionality of pCMVβ.Neo, increasing quantities of plasmid were transiently transfected into 293T cells alone and with a construct expressing CMV-driven iCre. Activity was expressed as the number of blue cells as a percentage of the total number of cells counted (Table 4.2 below and Figure 4.6).

Table 4.2: Assessment of activity of iCre in 293T cells using pCMVβ.Neo

Test	pCMVβ.Neo (ng)	pCMVβ (ng)	pciCre (ng)	% Blue Cells*
1	0	500	0	58.92 ± 4.19
2	50	0	0	1.33 ± 0.94
3	200	0	0	14.48 ± 1.26
4	400	0	0	25.98 ± 1.03
5	50	0	100	6.83 ± 1.65
6	50	0	500	17.15 ± 3.01
7	50	0	1000	35.67 ± 6.59
8	200	0	100	36.57 ± 4.12
9	200	0	500	50.66 ± 10.68
10	200	0	1000	48.21 ± 6.03
11	400	0	100	53.05 ± 9.42
12	400	0	500	61.09 ± 6.53
13	400	0	1000	63.20 ± 7.16
14	0	0	0	0

*Mean of three independent experiments performed in duplicate, ± S.E.

In the absence of iCre, pCMVβ.Neo was found to be leaky, even at low concentrations of 50ng, with an average percentage expression of 1.33 ± 0.94% increasing to 25.98 ± 1.03% for 400ng pCMVβ.Neo transfected. This leakiness may possibly be due to the strength of the CMV promoter (Foecking *et al.*, 1986). Co-transfection of increasing concentrations of pciCre (100-1000ng) with pCMVβ.Neo resulted in an increase in β-gal expression suggesting successful recombination of the *lox*P sites in pCMVβ.Neo by iCre, thereby activating β-gal expression. Not surprisingly, the highest concentration of pciCre transfected, produced the largest increase in β-gal expression for each concentration of β-gal reporter. For example, co-transfection of 1000ng of pciCre with 50ng of pCMVβ.Neo, resulted in an increase in the level of β-gal expression of

approximately 34% ($P < 0.01$) compared to 50ng of pCMVβ.Neo transfected alone (calculated by subtracting Test 2 from Test 7 in Table 4.2). Increasing the concentration of pCMVβ.Neo (400ng) co-transfected with the same amount of pciCre (1000ng), resulted in an increase in the level of β-gal expression of approximately 37% ($P < 0.01$), compared to 400ng of pCMVβ.Neo transfected alone (calculated by subtracting Test 4 from Test 13 in Table 4.2). Given that there is no significant increase in β-gal expression, as a result of transfecting a higher concentration of pCMVβ.Neo and that the leakiness of pCMVβ.Neo increases with its concentration, using a lower concentration of pCMVβ.Neo may provide a more accurate means of assessing Cre recombinase activity.

4.3.3 Optimisation of the transfection of Y79 retinoblastoma cells using pCMV.EGFP

Y79 retinoblastoma cells were selected to evaluate the tissue specificity and activity of the rhodopsin promoter-driven iCre constructs. Y79 cells have been shown to express rod photoreceptor-specific transcripts, including rod β-phosphodiesterase (PDE) and rhodopsin (Di Polo *et al.,* 1995). Lipofectamine 2000 was optimised for transient transfection of Y79 cells using a construct with CMV-driven expression of EGFP, pCMV.EGFP (Table 4.3 below and Figure 4.7).

Table 4.3: Percentage transfection efficiency of Y79 cells with pCMV.EGFP using Lipofectamine 2000

Cell Number	Ratio DNA(μg):Lipofectamine (μl)	% Transfection Efficiency*
4×10^5	1:3	21.64 ± 4.93
4×10^5	1:4	19.37 ± 3.29
4×10^5	1:5	18.07 ± 0.04
6×10^5	1:3	19.90 ± 0.13
6×10^5	1:4	20.70 ± 0.59
6×10^5	1:5	12.01 ± 0.79
8×10^5	1:3	16.29 ± 1.64
8×10^5	1:4	14.31 ± 0.77
8×10^5	1:5	16.07 ± 01.07

*Mean of two independent experiments with duplicate samples, ± S.E.

The highest transfection efficiency was achieved with 4×10^5 to 6×10^5 cells and a ratio of DNA to Lipofectamine 2000 of 1:3 to 1:4, yielding an average transfection efficiency of approximately 20%. As the transfection efficiency obtained was similar to that of another photoreceptor cell line 661W, evaluated in Chapter 3: 3.3.1, no further transfection agents were tested.

4.3.4 Expression of photoreceptor-specific transcripts in Y79 retinoblastoma cells

Prior to evaluating the iCre constructs in Y79 cells, the expression of rhodopsin and transducin was confirmed using RT-PCR to establish that in principle this cell line could support rhodopsin, or GNAT2 promoter-driven gene expression. As the characteristics of cells can change over time, it was important to confirm the characteristics of the cell line supplied. By RT-PCR analysis, a 105 bp transducin transcript was detected using H Trans primers listed in Table 4.1 (Figure 4.8: Lane 4). Three primer pairs (Table 4.1: H Rho1, 2 and 3) were used to amplify rhodopsin but no rhodopsin transcript was detected. An example of one of these RT-PCR reactions using primer pairs H Rho2, run on a 1% agarose gel is shown in Figure 4.9. Amplification of

a housekeeping gene, GAPDH (Table 4.1: H GAPDH primers) is shown in Lane 2, to assess the quality of the isolated Y79 RNA, however no rhodopsin transcript is present in Lane 3. RNA isolated from a C57BL/6J mouse retina was used as a positive control for the primers and a 210 bp fragment amplified from rhodopsin (Table 4.1: M Rho primers) is present in Lane 5.

As there were papers supporting both the presence of rhodopsin transcript and evaluation of rhodopsin promoter-driven gene expression in Y79 cells, it was possible that the quantity of RNA isolated from Y79 cells was not sufficient for the detection of rhodopsin transcript by RT-PCR. Hence, a highly sensitive quantitative method, real-time RT-PCR was then used to determine whether rhodopsin was being expressed in Y79 cells (Table 4.4 below).

Table 4.4: Relative levels of Rhodopsin RNA in Y79 cells compared to COS-7.Rhodopsin Cells

Cell Line	Rhodopsin RNA Levels Standardised with β-actin (%)*
COS-7.Rhodopsin cells	100.00 ± 4.67
Y79 cells	108.20 ± 9.57

*Mean of three independent experiments with duplicate samples, ± S.E.M. Level of rhodopsin in Y79 cells is expressed as a percentage of the level in Stable COS-7.Rhodopsin cells.

Y79 cells were found to express rhodopsin at a similar level to a line of COS-7 cells with stable expression of rhodopsin, at a relative level of 108.20 ± 9.57%, compared to the level in COS-7.Rhodopsin cells, following standardisation with β-actin as a housekeeping gene. Having established the expression of rhodopsin, in agreement with results from previous studies (Di Polo *et al.,* 1995), Y79 cells were transiently transfected with pRho.EGFP to confirm that the 1.7 kb rhodopsin promoter could drive expression in this cell line. However, no EGFP positive cells were detected, compared

to Y79 cells transfected with pCMV.EGFP (Figure 4.10). In conclusion, the data suggested that Y79 cells were not a suitable cell line to evaluate rhodopsin promoter-driven expression of iCre. As there were no other retinal-derived cell lines readily available, cultured retinal explants were used for evaluation of the rhodopsin promoter-driven iCre recombinase constructs instead.

In contrast to rhodopsin promoter-driven iCre constructs, assessing the tissue specificity and functionality of the constructs with GNAT2 promoter-driven expression is not feasible using retinal explants, due to the low percentage (approximately 3%) of cone cells present in the mouse retina (Curcio *et al.,* 1990). Matsuda *et al.*, also demonstrated that less than 1% of cells from P14 cultured retinal explants, electroporated at P0 with an EGFP reporter, were positive for a cone photoreceptor cell marker (Gt2α) (Matsuda *et al.,* 2004). Although Y79 cells had been shown to express transducin (Figure 4.8), β-gal staining of Y79 cells electroporated with pCMVβ (CMV promoter-driven β-gal) was not reliable, as because of the small size of these suspension cells, determining which cells expressed β-gal was not clear (data not shown). The aim of *in cellulo* evaluation of the GNAT2 constructs was to address two construct elements: tissue specificity of the promoter, and functionality of iCre. Given that the tissue specificity of the GNAT2 promoter had been previously established in transgenic animal models (Ying *et al.,* 1998; Ying *et al.,* 2000; Fong *et al.,* 2005) and the functionality of iCre recombinase could be evaluated using a newly developed system available within the laboratory, based on a method by Matsuda *et al.*, namely electroporation of retinal explants, the further exploration of *in cellulo* systems for evaluation of the GNAT2 constructs was not undertaken. Instead, given the sequence of the constructs was base perfect (Appendix: 1.2.3-4), and that as stated before, tissue-specificity of GNAT2 promoter-driven expression had been established in the literature and iCre functionality was assessed in the current study, it was decided to proceed with transgenic mice generation using the GNAT2 iCre constructs without further evaluation of construct functionality.

4.3.5 Evaluation of pRho.iCre.A in C57BL/6J retinal explants using the reporter plasmid, pCMVβ.Neo

In contrast to GNAT2 iCre constructs, the functionality of the rhodopsin promoter-driven iCre constructs were evaluated in retinal explants. Cultured retinal explants (16) were electroporated at P0 with either pCMVβ.Neo alone or with pcRho.iCre.A. Two concentrations of pCMVβ.Neo were used for electroporation: 50ng/μl or 200ng/μl, as this construct had not been previously evaluated in retinal explants. Following 14 days of culturing, subsequent to electroporation, retinal explants were fixed and stained for β-gal expression. Figure 4.11: I, III show representative photographs of whole mounted retinal explants electroporated with 50ng and 200ng of pCMVβ.Neo respectively. As was observed with transient transfection of 293T cells with this construct (4.3.2), there is some background β-gal expression from the reporter construct. Figures 4.11: II, IV show whole mounted explants electroporated with the same concentrations of pCMVβ.Neo reporter plasmid together with the construct expressing rhodopsin-driven iCre at a concentration of 1μg/μl. There is a significant increase in the amount of β-gal staining in retinal explants co-electroporated with both the β-gal reporter and iCre plasmids, suggesting that active iCre catalysed recombination at the *lox*P sites of the reporter construct, removing the neomycin gene and thereby allowing β-gal expression. The results suggest that functional iCre is being expressed from the pcRho.iCre.A construct.

4.3.6 Immunostaining of C57BL/6J retinal explant sections expressing either pRho.iCre.A and pCMVβ.Neo

The cultured retinal explants described above were sectioned and immunostained for rhodopsin and iCre recombinase proteins. Figure 4.12: A shows a retinal section stained with 4D2 anti-rhodopsin antibody and Alex Fluor 568 secondary antibody. The corresponding DAPI stained section is shown in Figure 4.12: B. The aim of this experiment was to show the photoreceptor-specific expression of iCre in retinal sections from electroporated explants. Co-localisation of immunostaining using rhodopsin and iCre antibodies would have demonstrated the tissue-specificity of the rhodopsin promoter-driven iCre constructs, however no immunostaining for iCre was

observed (Figure 4.12: C). The iCre antibody had been previously evaluated in retinal explants electroporated with CMV-driven iCre at P0, and clear antibody staining was demonstrated (Chapter 5: Figure 5.6). While rhodopsin is highly expressed in rod photoreceptors *in vivo*, in the context of plasmid electroporation into a retinal explant, the level of expression from the rhodopsin promoter is not known. β-gal staining of the whole retinal explants suggests that iCre is being expressed, but possibly not at sufficient level to be detected by immunostaining using the iCre antibody in this assay.

4.3.7 Expression of AAV rhodopsin promoter-driven EGFP in C57BL/6J retinal explants

To verify the tissue specificity of the 1.7 kb rhodopsin construct, an experiment using AAV with rhodopsin promoter-driven expression of EGFP, was undertaken. AAV-EGFP was generated by triple plasmid calcium phosphate transient transfection (undertaken by Dr. Naomi Chadderton), and the viral titre was determined by quantitative real-time PCR to be 1×10^{10} vp/ml. P1 cultured retinal explants were infected with AAV-EGFP (5×10^{8} vp) on two independent occasions and cultured for 14 days. Following cryosectioning, retinal sections were examined for EGFP fluorescence using a Zeiss Axioplan-2 Optical Fluorescent Microscope. A representative image of a cryosectioned retinal section is shown in Figures 4.13:B under 400X magnification. Note strong specific EGFP expression in the rod outer segments (ROS) and outer nuclear layer (ONL), and a notable absence of EGFP expression in the inner nuclear layer (INL) and ganglion cell layer (GCL), suggesting photoreceptor specificity of the 1.7 kb rhodopsin promoter used for the iCre constructs. Clearly the tissue specificity of shorter rhodopsin promoters has been previously demonstrated (Ham *et al.,* 2004; Pawlyk *et al.,* 2005), and the result here is supported by the study by Zack *et al.,* 1991, which showed the photoreceptor-specific expression of the lacZ gene driven by the 2.2 kb bovine rhodopsin promoter in the mouse. Nevertheless, it was important to show that the mouse rhodopsin promoter used in the current study had similar tissue specificity to the bovine promoter, evaluated by Zack *et al.,* 1991 and in light of a study by Woodford *et al.,* 1994, which showed that a 4.4 kb promoter directed β-gal expression to both rod and cone photoreceptors.

4.4 Discussion

The emergence of conditional gene targeting as a tool for generating transgenic animals has facilitated the investigation of the roles of genes and respective protein products in specific tissues and cell lineages. Manipulating genes in a tissue and temporal specific manner generates more accurate animal models of human disease and can overcome potential embryonic lethality associated with ubiquitous expression of the transgene (van der Weyden *et al.,* 2002). For example, global knockouts of a number of the caspases involved in apoptosis including caspase-3, result in a high level of perinatal death (Kuida *et al.,* 1996). Given this, it was proposed to apply conditional gene expression for generating transgenic mouse models to investigate underlying pathologies and possible therapeutic strategies for RP, including adRP. The Cre/*lox*P system is one of the most well characterised conditional gene targeting systems and for this reason was used for the current study.

To generate photoreceptor-specific conditional transgenic models, the first stage is the generation of models with photoreceptor-specific expression of Cre recombinase (Cre). As reviewed in the introduction of this chapter, Cre catalyses recombination at *lox*P recognition sites flanking a transgene, resulting in either activation or silencing of the transgene expression. The current study involved the design and generation of constructs for transgenic mouse models with rod and cone photoreceptor-specific expression of Cre. The rhodopsin promoter was used to drive rod photoreceptor expression of Cre, and the promoter for the α-subunit of cone transducin, GNAT2, was used to drive cone photoreceptor expression of Cre (Figure 4.2-3). To ensure a high level of Cre expression *in vivo*, a Cre gene that had been optimised for mammalian systems was used (iCre) (Shimshek *et al.,* 2002).

Given that generating transgenic animals is a lengthy and costly process, and that at the time of construct design, iCre had been used to establish a transgenic line in just one published study, it was considered important to initially evaluate the constructs *in cellulo* (Shimshek *et al.,* 2002). Y79 human retinoblastoma cells have been shown to express rod and cone photoreceptor-specific transcripts, so they were selected as a

potential cell line for evaluating constructs expressing iCre recombinase (Di Polo *et al.*, 1995). However, transient transfection of a rhodopsin promoter-driven EGFP construct into Y79 cells did not result in any detectable level of EGFP expression (Figure 4.10). This was surprising, as rhodopsin transcript had been previously detected in Y79 cells (Di Polo *et al.*, 1995) and in another study, rhodopsin promoter-driven expression of EGFP had also been demonstrated (May *et al.*, 2003). May, *et al.*, had used a similar sized rhodopsin promoter to the one used in the current study, 1419 bp compared to 1682 bp, so a difference in promoter size was not likely to account for the lack of expression of pRho.EGFP. It was decided to investigate this further, initially using RT-PCR to analyse RNA isolated from Y79 cells. No PCR products were amplified in RT-PCR reactions with cDNA generated from Y79 RNA (Figure 4.9). Y79 RNA was then analysed using by real time RT-PCR on a LightCycler, which detects even very low levels of RNA transcript. The level of rhodopsin RNA was standardised using a housekeeping gene, GADPH, and compared to rhodopsin expression in a Cos-7 cell line with stable expression of human rhodopsin, standardised in the same manner. Expressing the level of rhodopsin as a percentage of the level in Cos-7.Rhodopsin cells, gave similar levels of rhodopsin in both the Y79 and Cos-7.Rhodopsin cells, 108.20 ± 9.57% compared to 100 ± 4.67%. Although Y79 cells are a useful model for some aspects of retinal research, they may not be a suitable system for investigating rhodopsin promoter-driven gene expression. The demonstration by May *et al.*, of EGFP expression in Y79 cells from a 1.4 kb rhodopsin promoter may be explained by the use of fluorescence-activated cell sorter (FACS) analyses of the transfected Y79 cell population in this study, as larger Y79 cell populations could be examined for fluorescence and EGFP expressing Y79 cells separated from those cells not expressing EGFP.

With regard to the GNAT2 constructs, with cone promoter driven expression of iCre, the Y79 cells were considered to be a suitable cell line to evaluate the constructs. Transducin, the protein product of the GNAT2 gene, was detected using RT-PCR to analyse Y79 RNA (Figure 4.8). Expression of iCre from the generated constructs were to be assessed using a β-gal reporter *lox*P plasmid, however, as determining the colour

of Y79 cells expressing β-gal, following a β-gal staining assay, was not clear because of the small size of the Y79 suspension cells, exploration of alternative cell lines for evaluating the GNAT2 promoter-driven constructs was not undertaken.

As a system for electroporation of cultured retinal explants had been established within the laboratory, based on the original method of Matsuda *et al.*, 2004, this was used to evaluate the rhodopsin promoter-driven iCre constructs.To evaluate iCre activity, a β-gal *lox*P reporter (pCMVβ.Neo) was designed and generated. β-gal is not expressed from this construct due to a neomycin gene flanked by *lox*P sites present between the promoter and the gene. Co-expression of iCre should in principle, catalyse recombination between the *lox*P sites, removing the neomycin gene and allowing β-gal expression. Cells in which recombination has taken place, should turn a blue colour following a β-gal staining assay. pCMVβ.Neo was evaluated in 293T cells by co-transfection with CMV promoter-driven iCre. Transfection of the highest concentration of iCre (1000ng) with 50ng pCMVβ.Neo was demonstrated to increase β-gal expression by an average of 35.67 ± 6.59% compared to 1.33 ± 0.94% ($P < 0.01$), when pCMVβ.Neo was transfected alone. As can be seen from this result, the β-gal *lox*P reporter is slightly leaky, but this increases with an increase in reporter plasmid concentration. Transfecting 400ng of pCMVβ.Neo alone, for example, resulted in a level of β-gal expression of 25.98 ± 1.03%.

Having established the activity of the β-gal *lox*P reporter and the iCre enzyme, cultured retinal explants were co-electroporated with the reporter and a rhodopsin-promoter driven iCre construct, pRho.iCre.A. β-gal staining of the retinal explants following 14 days culturing suggested that active iCre had catalysed recombination of the *lox*P sites of the reporter, allowing β-gal expression, demonstrating the functionality of the novel iCre construct (Figure 4.11: II, IV). Given that experiments in retinal explants provided evidence that the rhodopsin promoter-driven iCre constructs were functional, the next stage of the project is the generation of transgenic mouse models using the rhodopsin promoter-driven constructs of iCre. Furthermore, given that the experiments undertaken

with the retinal explants demonstrated the functionality of iCre recombinase and that the tissue-specificity of the GNAT2 promoter has been previously established in the literature (Morris *et al.,* 1997; Ying *et al.,* 1998), no further evaluation of the GNAT2 promoter-driven constructs was undertaken. Hence, the generation of two lines of transgenic animals with rod and cone photoreceptor-specific expression of iCre is currently being initiated.

Meanwhile, subsequent to the initiation of this project, a number of lines of transgenic mouse models with photoreceptor-specific expression of Cre have become available. Li *et al.*, 2005b, recently generated a transgenic mouse line with iCre expression driven by a 4.4 kb rhodopsin promoter. Another group generated two mouse models with rod photoreceptor-specific expression of Cre recombinase, driven by a 5 kb rhodopsin promoter and a 2 kb of the RP1 promoter (Feiner *et al.,* 2003), however subsequently evaluation of the generated transgenic mice established found that Cre expression resulted in severe retinal degeneration (Feiner *et al.,* 2004), possibly due to unwanted DNA recombination (Schmidt *et al.,* 2000; Loonstra *et al.,* 2001). Full morphological and functional assessment of transgenic Cre models is clearly essential to ensure that Cre expression is not toxic. Levels of Cre may depend on several factors, including the precise promoter selected and site of integration (Kaspar *et al.,* 2002).

Three transgenic models with cone photoreceptor-specific expression have been generated (Akimoto *et al.,* 2004; Le *et al.,* 2004). Akimoto *et al.*, used promoters for the blue opsin gene and the red-green opsin gene to direct Cre expression to the S- and M- cone photoreceptors respectively. While Cre expression was shown to be cone specific, there were no results published on functional and morphological assessments of the transgenic lines, which is important in light of the results on the effect of high expression levels of Cre in photoreceptors. In a third model by Le *et al.*, a 6.3 kb promoter of the human red-green pigment (*HRGP*) gene was used to generate a transgenic line with cone specific-expression of Cre. Retinal morphology was shown to be normal in transgenic lines at 6 months and electroretinograms (ERGs) were also comparable to wild-type mice at 6 and 10 months of age.

A collaboration has been established with Dr. Yun-Zheng Le (University of Oaklahoma, OK, USA) to provide the laboratory here with the HRGP-*cre* transgenic mouse line. By mating the HRGP-*cre* transgenic line to mice engineered with *lox*P sites, the resulting F1 generation should in principle, have either cone photoreceptor-specific gene activation or deletion, depending on the position of *lox*P sites. Conditional gene targeting could be applied to investigating the therapeutic potential of disrupting pro-apoptotic genes or expressing anti-apoptotic genes specifically in cone photoreceptors. Choice of target gene is limited by the availability of transgenic models with *lox*P-flanked pro- and anti-apoptotic genes of interest. An example of an available model includes the *lox*P-p35 transgenic mouse, which carries a transgene for the anti-apoptotic protein p35 (Hisahara *et al.,* 2000) , discussed in more detail further on and also in Chapter 5 of this thesis. The subsequent transgenic line with conditional gene modification could then be mated to transgenic models of retinal degeneration to evaluate the therapeutic potential of such cone-specific gene modifications on disease progression. Although RP principally affects the rod photoreceptors, there are a large number of retinal degenerations in which the mutant gene is expressed in both rods and cones or cones alone. Examples include the gene for cone-rod homeobox transcription factor, *Crx*, which is associated with cone-rod dystrophy-2 (adCRD2), Leber congenital amaurosis (LCA) and RP (Freund *et al.,* 1997; Furukawa *et al.,* 1999) and the genes for a GTPase regulator interacting protein *RGRIP*, and aryl hydrocarbon receptor-interacting protein, *AIPL1*, both associated with LCA (Hong *et al.,* 2001; Sohocki *et al.,* 2001). Examples of available mouse models include a *Crx* $^{-/-}$ model (Furukawa *et al.,* 1999), a *RPGRIP* $^{-/-}$ model (Zhao *et al.,* 2003b), and a *AILP1* $^{-/-}$ model (Dyer *et al.,* 2004). For further information on retinal genes associated with retinal degenerations including cone-rod dystrophies or LCA, where mutant retinal genes are expressed either in the cones or in both rods and cones, refer to http://www.sph.uth.tmc.edu/Retnet/. Information on the available mouse models was obtained from the Mouse Genome Informatics website (http://www.informatics.jax.org/), maintained by The Jackson Laboratory (Bar Harbor, ME, USA). Notably, for retinal diseases, where there is involvement of both rods and cones in pathogenesis, conditional targeting technology directing expression of the

mutant gene to either rod or cone photoreceptors, could be used evaluate the relative contribution of the mutant gene in the context of each of these photoreceptor cell types to disease pathology. Likewise the therapeutic benefit of a particular gene product when expressed in either rod or cone photoreceptors could be evaluated using conditional gene targeting (see Chapter 5 for more detail).

Transgenic mice with rod photoreceptor-directed expression of Cre, such as the transgenic lines to be generated as a result of the work undertaken in this study or alternatively the recently derived transgenic lines described above, could be used to modify gene expression in a rod photoreceptor-specific manner. Using animal models of RP, available in the laboratory in Trinity College Dublin, the therapeutic benefit of expressing a gene of interest for example, could be evaluated using conditional gene targeting. There are a number of RP mouse models available including the Pro23His mice, carrying an autosomal dominant proline to histidine mutation at codon 23 of rhodopsin gene (Olsson *et al.,* 1992), the *rds*-307 mice, another adRP model engineered to have a single base pair deletion at codon 307 of the *rds*/peripherin gene (McNally *et al.,* 2002) and the Pro347Ser mouse with an autosomal dominant mutation of rhodopsin (Li *et al.,* 1996).

The potential of transgenic lines with photoreceptor-directed expression of Cre, as tools for evaluating therapies for retinal degenerations, elucidating the mechanisms of cell death and investigating gene function in photoreceptors, is significant. Applying this approach of conditional targeting to further explore anti-apoptotic strategies for RP is the basis of the next chapter of this thesis. p35 is a baculoviral anti-apoptotic protein, which has been demonstrated to inhibit photoreceptor degeneration in several *Drosophila* models of retinal degeneration (Davidson *et al.,* 1998; Alloway *et al.,* 2000; Galy *et al.,* 2005), and chemical-induced apoptosis in a murine cone photoreceptor cell line, 661W (Tuohy *et al.,* 2002). There was a clear rationale to further evaluate the potential protective effect of p35 *in vivo*. However, previous attempts to generate a transgenic model expressing p35 in this laboratory were not successful, possibly due to technical difficulties, as these attempts were undertaken early in the establishment of

the transgenic unit in TCD. It was noted in the literature that Hisahara *et al.*, 2000, had generated a transgenic model of p35 with conditional expression based on the Cre/*lox*P system, hence a collaboration was established with the research team of Professor Masayuki Miura in Japan.

*lox*P-p35 mice carry a transgene with p35 that is not expressed due to the presence of a neomycin gene flanked by *lox*P sites between the promoter and the p35 gene. Expression of Cre recombinase catalyses recombination between the *lox*P sites, removing the neomycin gene and allowing p35 expression. It is proposed to conditionally express p35 in the rod or cone photoreceptors, and subsequently evaluate the effect of p35 expression in transgenic models of retinal degeneration. This should, in principle, be possible using the transgenic animals with rhodopsin promoter-driven and GNAT2 promoter-driven iCre expression generated as a result of the current study. Chapter 5 describes the initial work with the *lox*P-p35 mouse model, to activate p35 expression in cultured retinal explants, subsequent to electroporation of a plasmid expressing iCre recombinase, and further evaluation of the possible protective effect of p35 expression in a chemical-induced model of apoptosis in retinal explants.

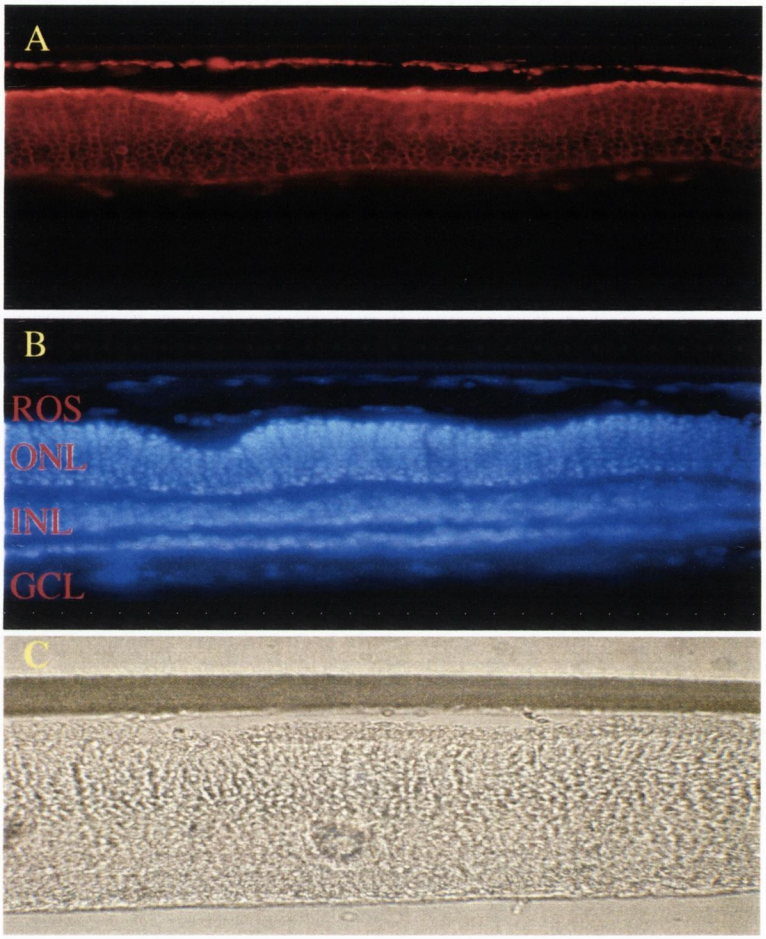

Figure 4.1*: **Cryosection of an immunostained P14 wt C57BL/6J cultured retinal explant.** A P14 cultured retinal explant was cryosectioned and probed for rhodopsin expression (**A**) using the 4D2 anti-rhodopsin antibody and Alexa Fluor 568 secondary antibody. **B** and **C** show the corresponding section stained with DAPI and under white light (400X). The retinal layers are highlighted in red: ROS, rod outer segments, ONL, outer nuclear layer, INL, inner nuclear layer and GCL, ganglion cell layer. *Image kindly provided by Dr. John Neidhardt, University of Zurich, Switzerland, while working in the Ocular Genetics Unit in TCD.

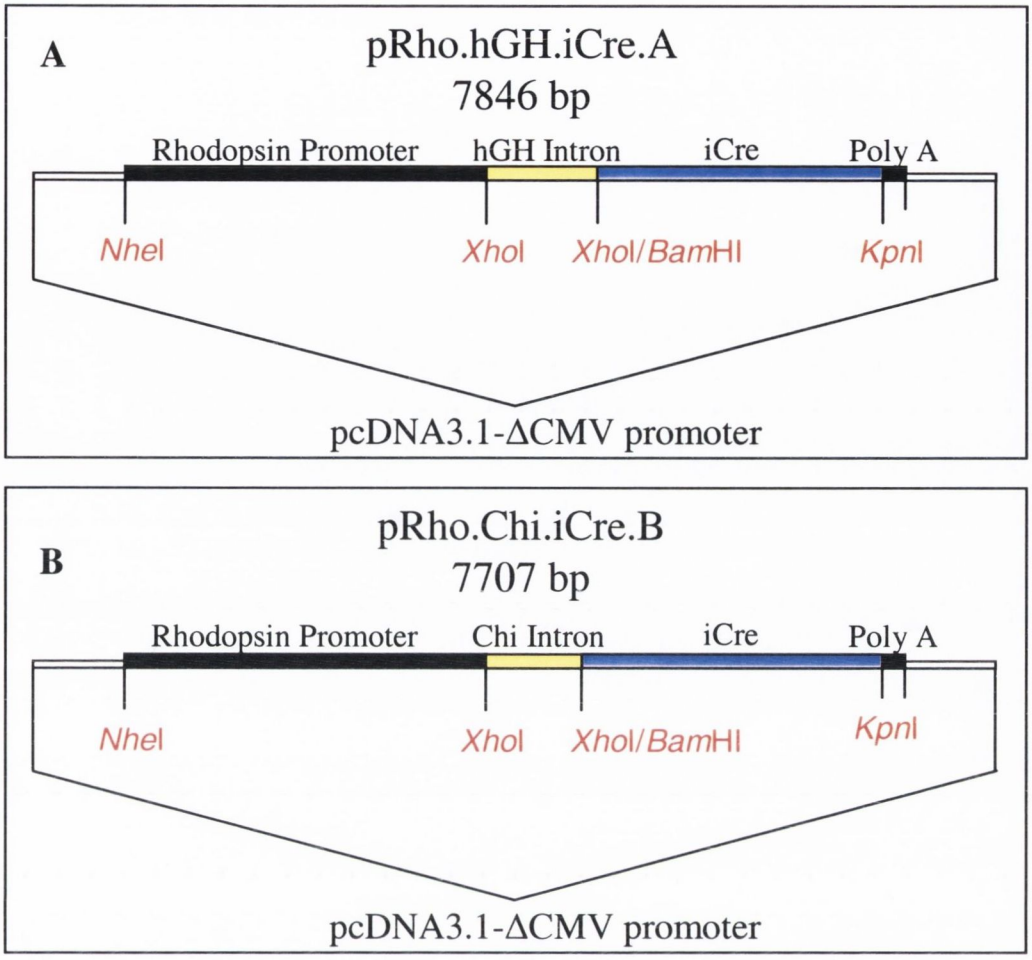

Rhodopsin Promoter: Mouse rhodopsin promoter, 1682 bp

hGH Intron: Human growth hormone intron, 282 bp

Chi Intron: Chimeric intron, 143 bp

iCre: iCre recombinase, 1115 bp

Poly A: Polyadenylation signal, based on rabbit β-globin gene, 60 bp

Figure 4.2: Diagram of the linearised plasmids: (A) pRho.iCre.A, (B) pRho.iCre.B. The constructs are designed to express rhodopsin promoter-driven iCre recombinase (see 4.2.1). Restriction enzyme sites are shown in red. Sequences are given in Appendix 1.2.1-2.

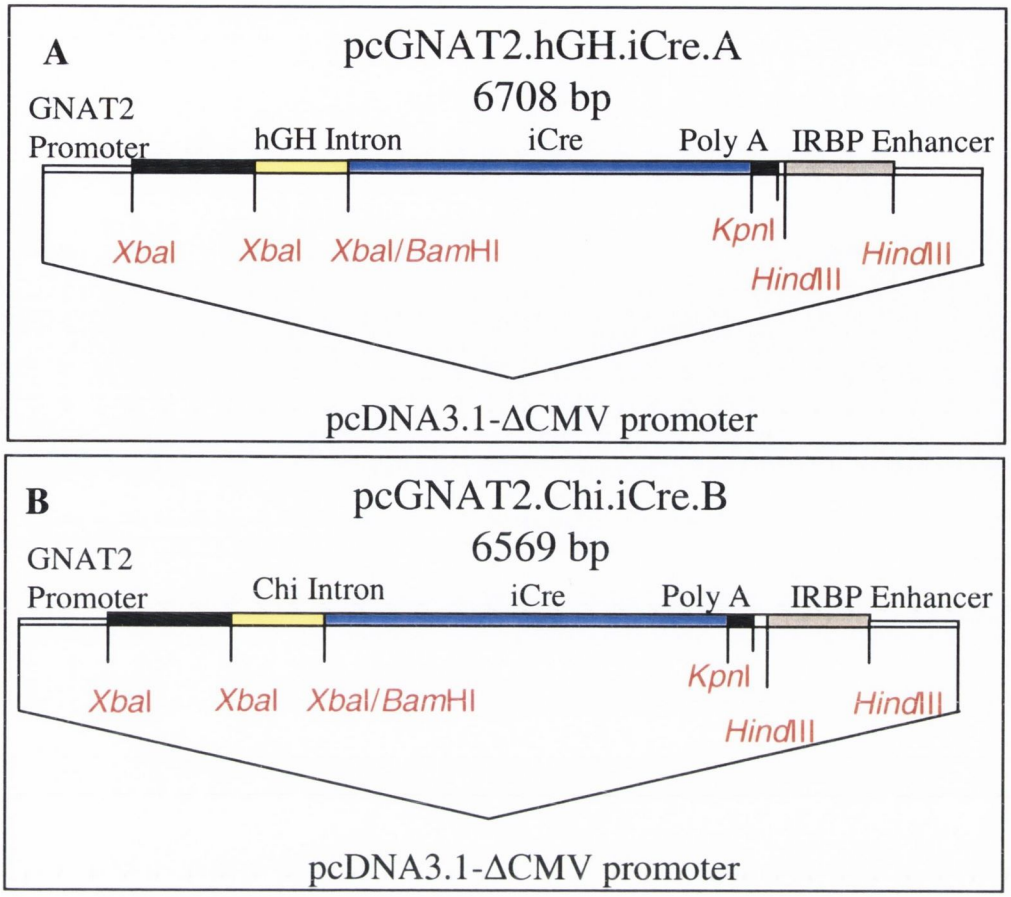

GNAT2 Promoter: Human cone transducin α-subunit promoter, 277 bp

hGH Intron: Human growth hormone intron, 282 bp

Chi Intron: Chimeric intron, 143 bp

iCre: iCre recombinase, 1115 bp

Poly A: Polyadenylation signal, based on rabbit β-globin gene, 60 bp

IRBP Enhancer: Interphotoreceptor binding protein enhancer, 214 bp

Figure 4.3: Diagram of the linearised plasmids: (A) pcGNAT.iCre.A, (B) pcGNAT.iCre.B. The constructs are designed to express GNAT2 promoter-driven iCre recombinase (see 4.2.1). Restriction enzyme sites are shown in red. Sequences are given in Appendix 1.2.3-4.

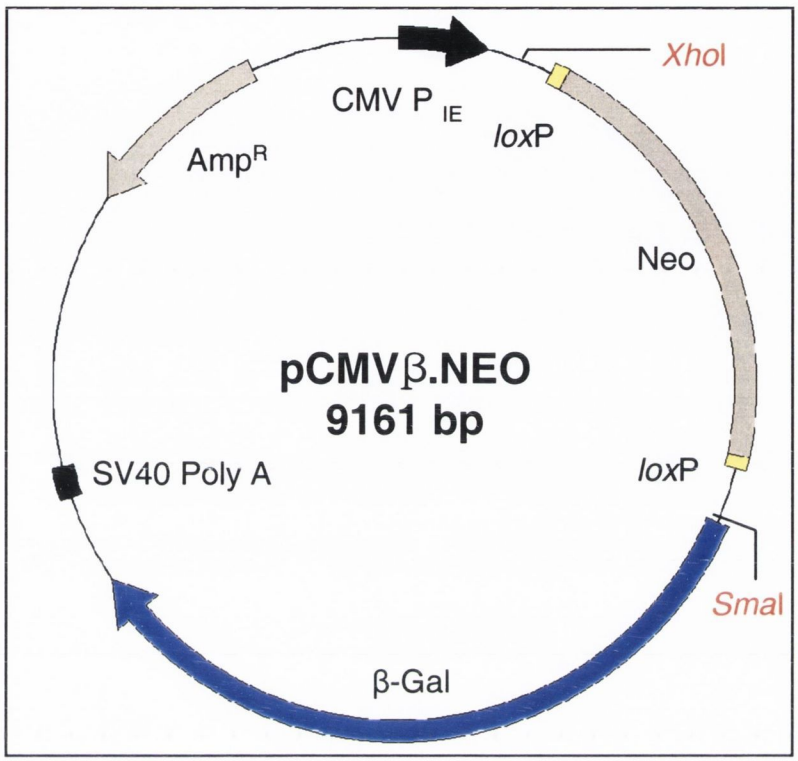

CMV P $_{IE}$: Human cytomegalovirus immediate early promoter (bases 27-341)
***lox*P**: 34 bp recognition sequence for Cre recombinase (bases 693-726, 2592-2625)
Neo: Neomycin gene (bases 727-2591)
β-gal: β-galactosidase gene (bases 2870-6013)
SV40 poly A: SV40 polyadenylation signal (bases 6423-6442)
Amp^R: Ampicillin resistance gene (bases 7706-8556)

Figure 4.4: Plasmid map of pCMVβ.Neo. pCMV β.Neo contains a β-gal gene which is expressed in the presence of Cre recombinase (see 4.2.2). Cre catalyses recombination between the *lox*P sites, removing the neomycin gene and allowing expression of the β-gal gene from the CMV promoter. Restriction enzyme sites are shown in red. Sequence is given in Appendix 1.3.

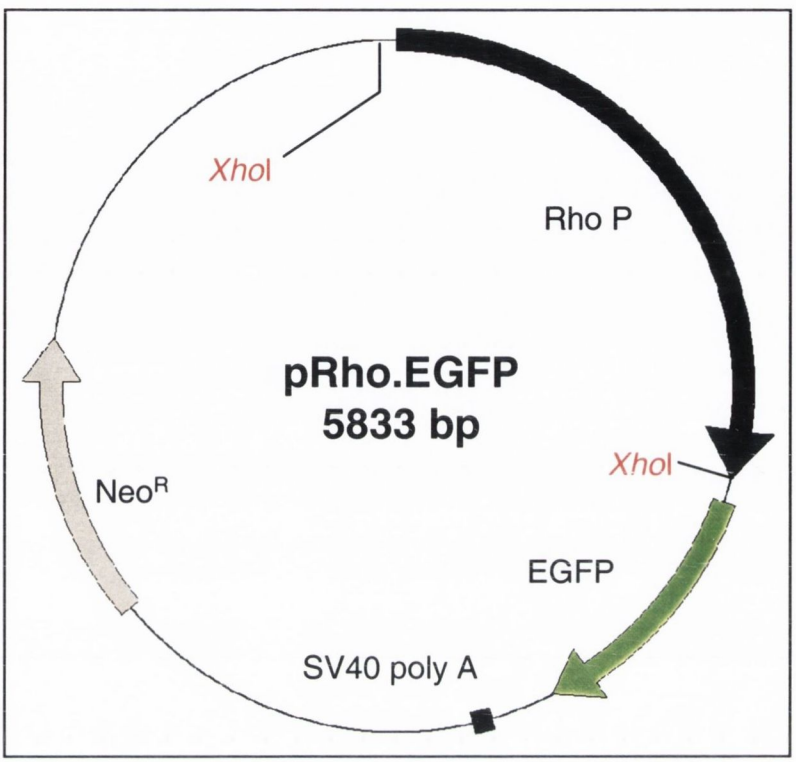

Rho P: Mouse rhodopsin promoter, 1682 bp
EGFP: Enhanced green fluorescent protein gene, 727 bp
SV40 poly A: SV40 polyadenylation signal, 131 bp
Neo^R: Neomycin resistance gene, 795 bp

Figure 4.5: Plasmid map of pRho.EGFP. pRho.EGFP contains an EGFP gene driven by a rhodopsin promoter (map for pCMV.EGFP is similar in design with the CMV promoter inserted at *Xho*I restriction sites) (see 4.2.2). Restriction enzyme sites are shown in red.

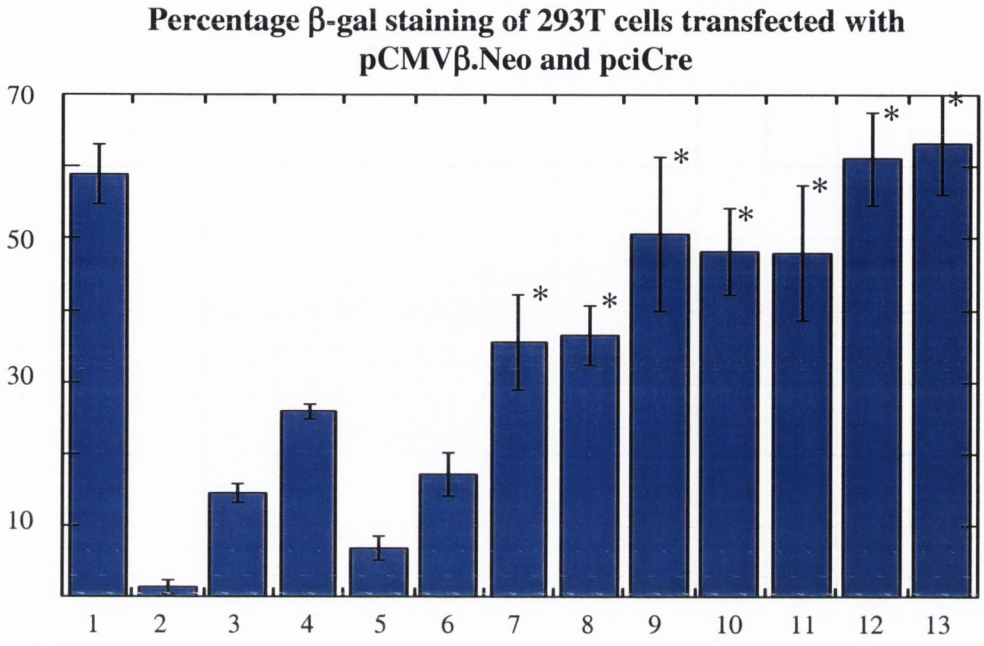

1. 500ng pCMVβ
2. 50ng pCMVβ.Neo
3. 200ng pCMVβ.Neo
4. 400ng pCMVβ.Neo
5. 50ng pCMVβ.Neo + 100ng pciCre
6. 50ng pCMVβ.Neo + 500ng pciCre
7. 50ng pCMVβ.Neo + 1000ng pciCre
8. 200ng pCMVβ.Neo + 100ng pciCre
9. 200ng pCMVβ.Neo + 500ng pciCre
10. 200ng pCMVβ.Neo + 1000ng pciCre
11. 400ng pCMVβ.Neo +100ng pciCre
12. 400ng pCMVβ.Neo + 500ng pciCre
13. 400ng pCMVβ.Neo + 1000ng pciCre

Figure 4.6: β-gal staining of 293T cells transfected with pCMVβ.Neo and pciCre. 293T cells were plated at a concentration of 5 x 10^5 per well of a 6-well plate and transfected the following day with (i) pCMVβ, (ii) pCMVβ.Neo or (iii) pCMVβ.Neo with pciCre. 48 hours subsequent to transfection cells were fixed and stained for β-gal expression (see 4.2.4). Bars represent mean ± standard error (S.E) of triplicate experiments. Co-transfection of pciCre with pCMVβ.Neo results in a significant increase ($P < 0.01$*) in β-gal expression, compared to transfection of the same quantity of pCMVβ.Neo alone, indicating the functionality of the iCre enzyme and the pCMVβ.Neo construct.

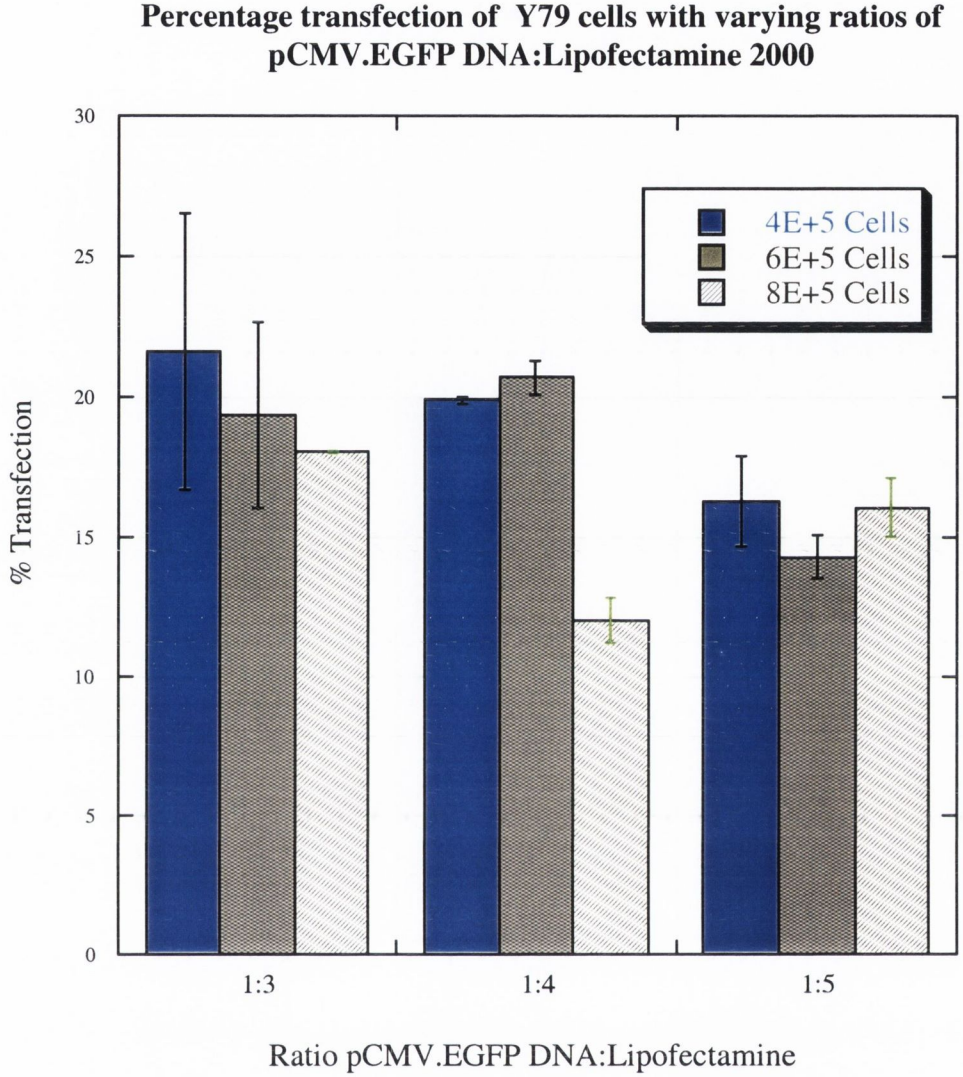

Figure 4.7: Percentage transfection of Y79 cells with varying ratios of DNA: Lipofectamine 2000 as measured by EGFP expression. Y79 cells were plated at a concentrations of 4 x 10^5, 6 x 10^5 and 8 x 10^5 per well of a 24-well plate and transfected the same day with 200ng pCMV.EGFP. 48 hours following transfection, cells were fixed and examined for EGFP fluorescence (see 4.2.6). Bars represent mean ± standard error (S.E) of duplicate experiments.

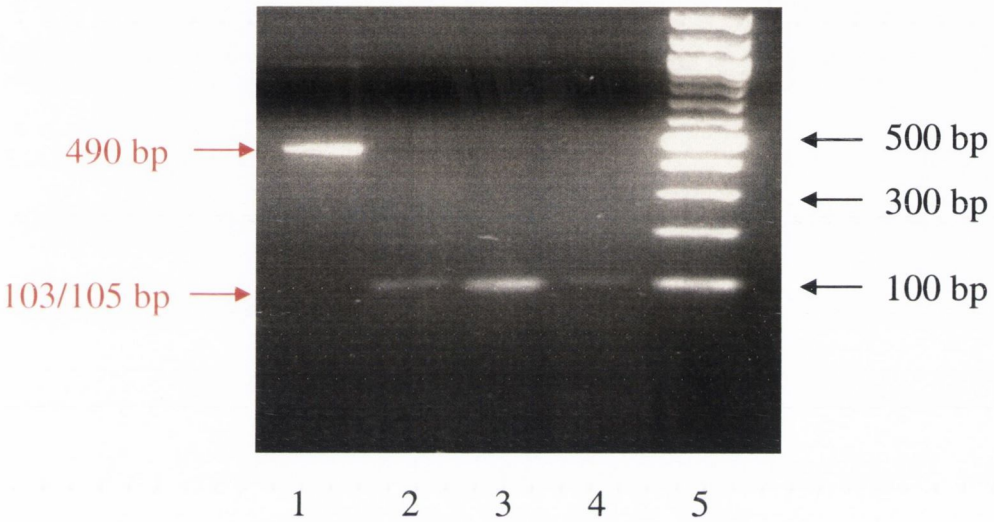

Figure 4.8: RT-PCR analysis on RNA extracted from Y79 cells and a wild-type (wt) mouse retina. Lanes 1-2, amplification of cDNA from wt mouse retina with primers specific for mouse GAPDH (Table 4.1: M GAPDH2 primers, 490 bp) and transducin genes (M Trans primers, 103 bp); Lanes 3-4, amplification of cDNA from human Y79 cells with primers specific for human GAPDH (H GAPDH primers, 100 bp) and transducin genes (H Trans primers, 105 bp); Lane 5, 100 bp ladder (see 4.2.5). PCR products are indicated in red and DNA size standards are indicated in black.

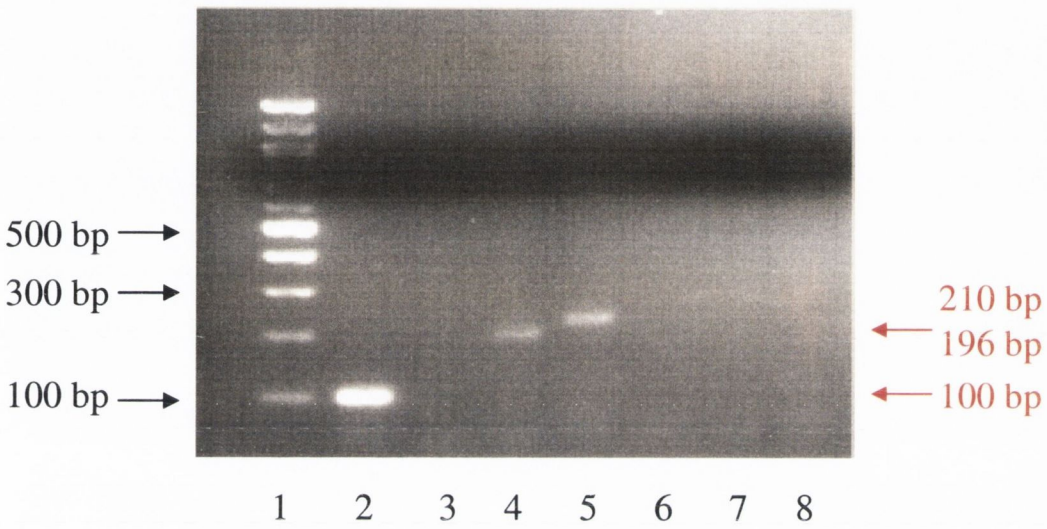

Figure 4.9: RT-PCR analysis on RNA extracted from Y79 retinoblastoma cells and a wild-type (wt) mouse retina. Lane 1, 100 bp DNA ladder; Lanes 2-3, amplification of cDNA from Y79 cells with primers specific for GAPDH (Table 4.1: H GAPDH primers, 100 bp product), and rhodopsin genes (H Rho2, 107 bp product): Lanes 4-5, amplification of cDNA from wt mouse retinas with primers specific for GAPDH (M GAPDH 1 primers, 196 bp product) and rhodopsin genes (M Rho primers, 210 bp product); Lanes 6-8, water blanks with each set of primers (see 4.2.5). PCR products are indicated in red and DNA size standards are indicated in black.

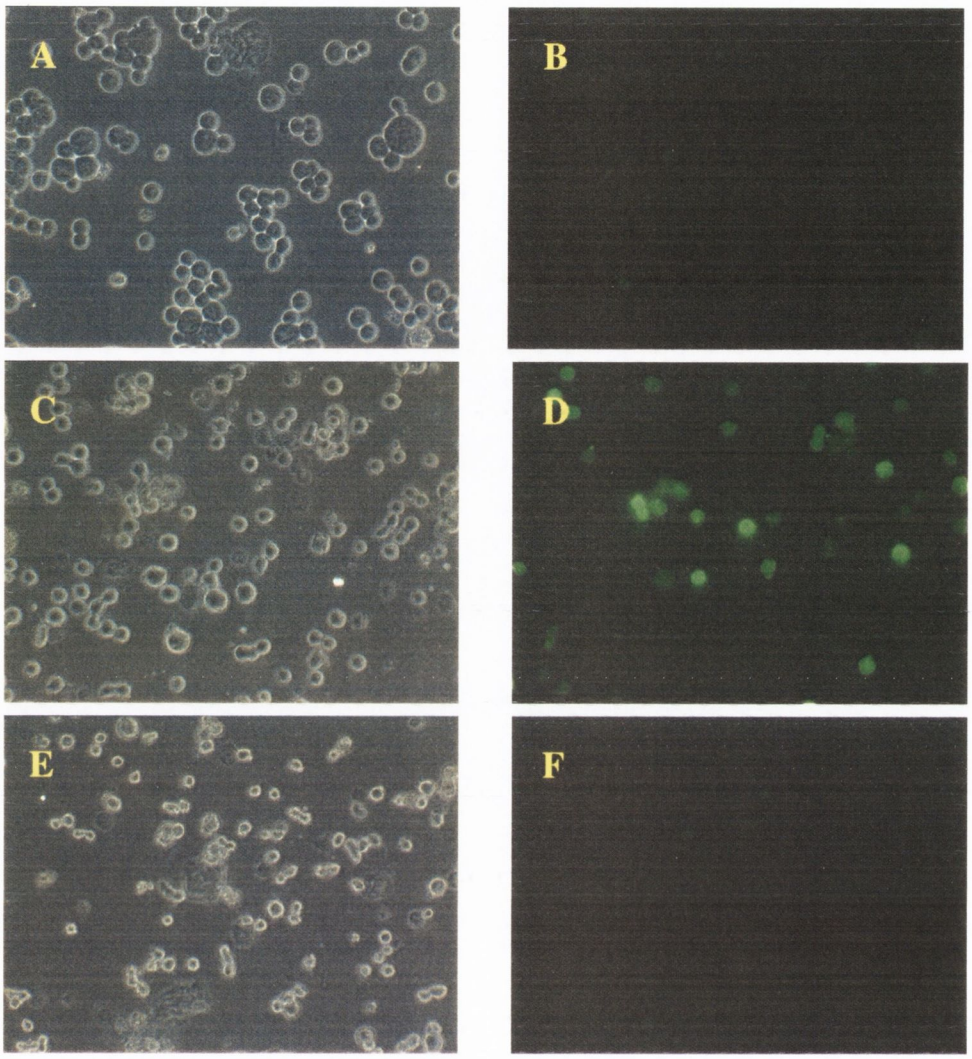

Figure 4.10: Y79 cells transfected with pRho.EGFP. Cells were plated at a concentration of 6 x 10^5 on a 24-well plate, transfected the same day and fixed following 48 hours of culturing (see 4.2.6). (**B**) and (**D**) show cells transfected with control plasmids of pEGFP-1 (no promoter for EGFP expression {Chapter 3: Figure 3.19}) and pCMV.EGFP. (**F**) shows cells transfected with pRho.EGFP (Figure 4.5), under fluorescent light. The corresponding photographs under white light are shown in (**A**), (**C**) and (**E**). These are representative images of triplicate experiments (200X magnification).

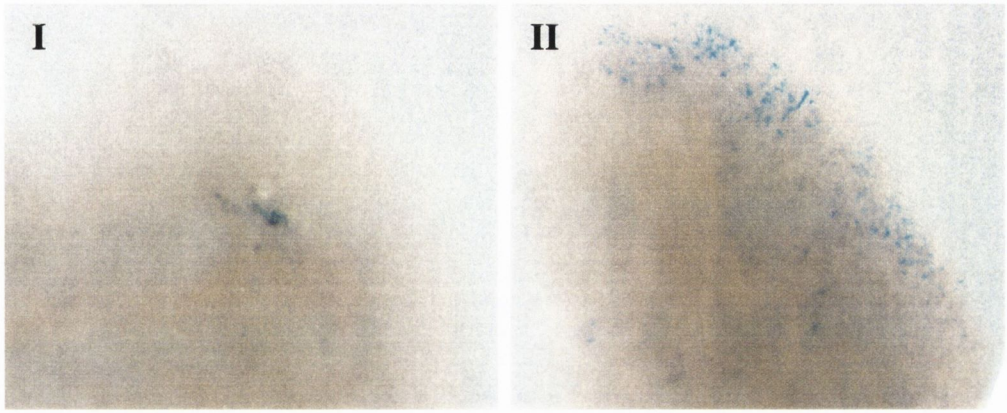

Figure 4.11A: β-gal staining of whole retinal explants expressing pRho.iCre.A and pCMVβ.Neo. At P0, retinal explants were electroporated with 50ng/μl of pCMVβ.Neo (**I**) alone, or (**II**) with 1μg/ul of pRho.iCre.A (see 4.2.7). Following 14 days of culturing, retinal explants were fixed and stained for β-gal expression (see 4.2.8) (50X magnification).

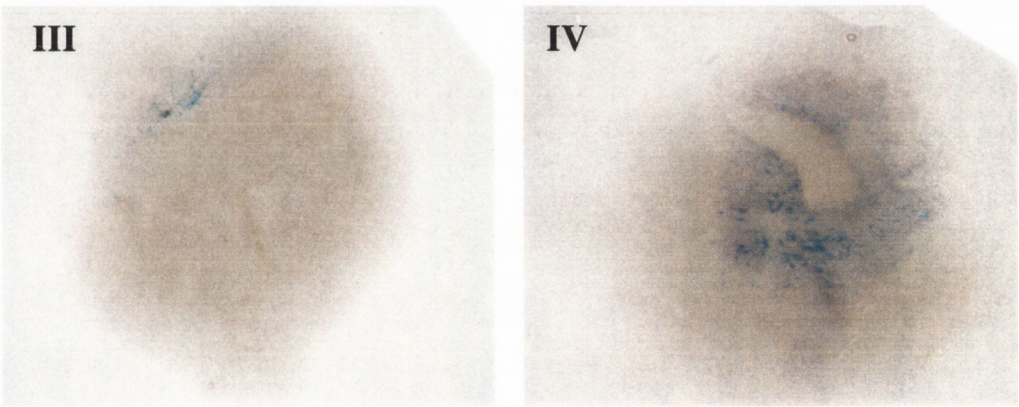

Figure 4.11B: β-gal staining of whole retinal explants expressing pRho.iCre.A and pCMVβ.Neo. At P0, retinal explants were electroporated with 200ng/μl of pCMVβ.Neo (**III**) alone or (**IV**) with 1μg/ul of pRho.iCre.A (see 4.2.7). Following 14 days of culturing, retinal explants were fixed and stained for β-gal expression (see 4.2.8) (25X magnification). Images from both figures are representative of duplicate experiments with 16 retinal explants.

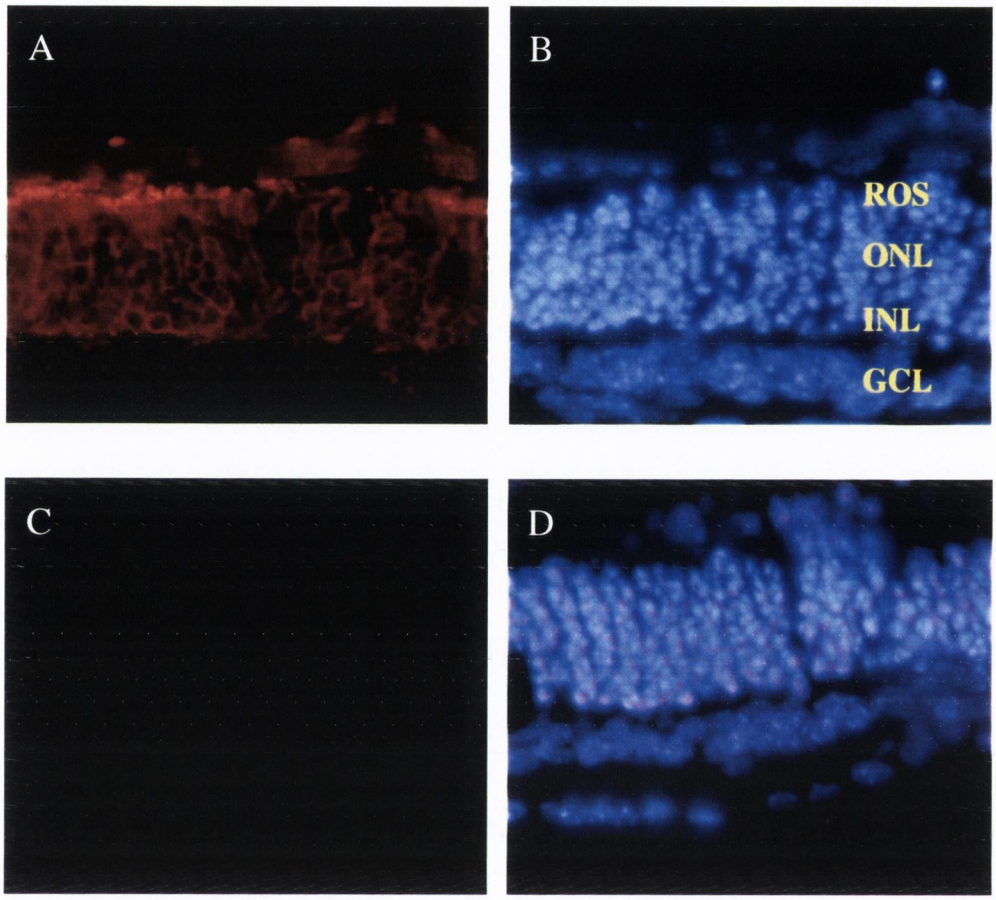

Figure 4.12: Immunostaining of retinal explants expressing pRho.iCre.A and pCMVβ.Neo. Retinal explants from wt C57BL/6J mice were electroporated with 1μg/μl of pRho.iCre.A and 50ng/μl of pCMVβ.Neo at P0 (see 4.2.7). Following 14 days of culturing, explants were fixed, cryosectioned (10μm) and probed for either rhodopsin using 4D2 anti-rhodopsin antibody **(A)**, or iCre using anti-Cre antibody **(C)** with Alex Fluor 568 secondary antibody (see 4.2.9). The corresponding DAPI stained retinal sections are shown in **(B)** and **(D)**. Positive staining for rhodopsin **(A)** but not iCre recombinase was detected. The retinal layers are highlighted in white: ROS, rod outer segments, ONL, outer nuclear layer, INL, inner nuclear layer and GCL, ganglion cell layer.

A

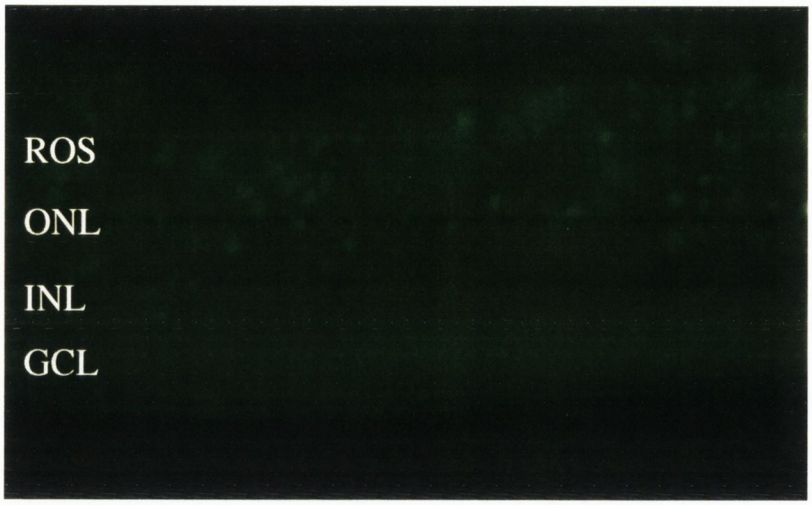

B

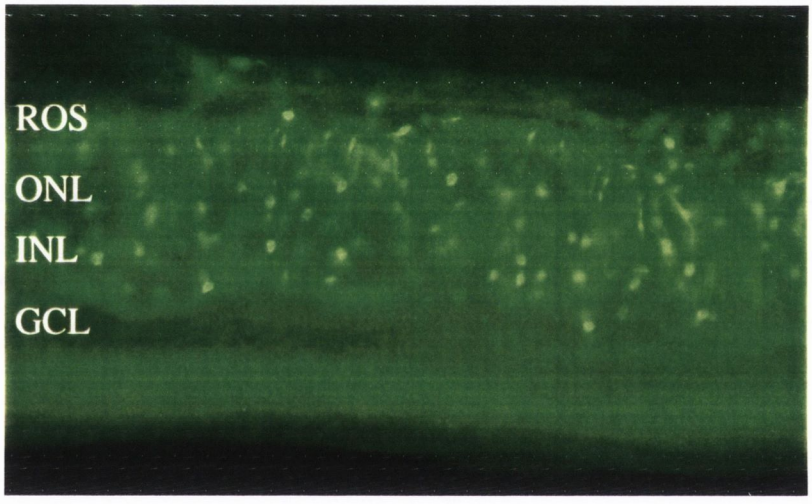

Figure 4.13: Cultured retinal explants expressing AAV rhodopsin promoter-driven EGFP. Retinal explants from wt C57BL/6J mice were either untreated or infected with AAV-EGFP at P1. Following 14 days of culturing, explants were fixed, crysectioned (10μm) and examined for EGFP fluorescence (see 4.2.10). **(B)** shows a representative photograph with photoreceptor-specific expression of EGFP (400X). No EGFP expression is present in the control shown in **(A)**. The retinal layers are highlighted in white: ROS, rod outer segments, ONL, outer nuclear layer, INL, inner nuclear layer and GCL, ganglion cell layer.

CHAPTER 5

Evaluation of the Anti-Apoptotic Protein p35 for Photoreceptor Survival

5.1 Introduction

p35 is a baculoviral caspase inhibitor that has been previously shown in this laboratory to protect against chemical-induced apoptosis in a line of cone photoreceptor cells, 661W, resulting in a percentage cell survival of approximately 75%, compared to 20% of vector alone transfected cells (Tuohy *et al.,* 2002). Given this strong anti-apoptotic activity, there was a clear rationale to further evaluate p35 as a potential therapeutic agent for adRP and other retinal degenerations, as photoreceptors have been shown to die by a common pathway of cell death, apoptosis. Targeting apoptosis as a therapeutic strategy for RP, may halt or slow photoreceptor degeneration, in a manner that is independent of the underlying primary genetic mutation. In addition, p35 has been shown to rescue photoreceptors in *Drosophila* models of retinal degeneration (Davidson *et al.,* 1998; Alloway *et al.,* 2000). Most recently in September 2005, Galy *et al.*, demonstrated that p35 expression in an autosomal dominant RP *Drosophila* model, $Rh1^{P37H}$, analogous to human Rho^{P23H}, protected against photoreceptor cell loss, with a partial rescue of the electroretinogram (ERG) responses. Furthermore, p35 has been evaluated as a therapeutic strategy for a number of other disorders, where apoptosis significantly contributes to disease pathology, including cardiac failure (Laugwitz *et al.,* 2001), seizure-associated neurodegeneration (Viswanath *et al.,* 2000), diabetes (Hollander *et al.,* 2005) and multiple-sclerosis (Hisahara *et al.,* 2000).

To further investigate the potential of p35 as a therapeutic agent for RP, a study was initiated in this laboratory to generate a transgenic model expressing a mouse rhodopsin promoter-driven p35 transgene. However, following injection of pronuclei with the linearised transgene, no founder pups with expression of the p35 transgene were generated (Dr. Gearoid Tuohy, Trinity College Dublin, results unpublished). As the attempts to generate the Rho/p35 transgenic mice were undertaken early in the establishment of the Specific Pathogen Free (SPF) facility in TCD, the absence of founder pups may have been due to technical reasons or possibly due to embryonic lethality, although given the use of the rhodopsin promoter to drive expression of the p35 gene, this would not have been anticipated. To further evaluate p35 *in vivo*, other experimental approaches were explored, including conditional gene expression, which enables the modification of genes in a

tissue or temporal specific manner (Porter 1998; Muller 1999) (Chapter 1: 1.2.11.2). Given that Hisahara *et al.* had generated a transgenic model with conditional expression of p35, a collaboration was established with this group to obtain the *lox*P-p35 transgenic mouse model. p35 expression in this model is silent due to the presence of a neomycin gene flanked by *lox*P sites between the transgene CAG (cytomegalovirus IE enhancer and the chicken β-actin) promoter and the p35 gene (Figure 5.1). Expression of the enzyme Cre recombinase, catalyses recombination at the *lox*P sites removing the neomycin gene, thus activating p35 expression from the CAG promoter.

Thus directing Cre recombinase expression specifically to photoreceptors of the *lox*P-p35 transgenic model, should in principle, activate p35 expression. One approach for achieving tissue-specific recombination is to generate a line of transgenic mice with tissue-specific promoter-driven Cre expression. Subsequent mating of the Cre transgenic line with a second transgenic line carrying the floxed gene, should result in transgene activation only in tissues where Cre is expressed. The previous chapter described the generation and evaluation of a number of constructs with photoreceptor-specific promoter-driven expression of Cre recombinase, for subsequent generation of two transgenic lines with rod and cone photoreceptor-specific expression of Cre. Thus, the potential anti-apoptotic effect of p35 expression in photoreceptors could be evaluated using light- or chemical-induced models of apoptosis (Figure 5.2) (Yuge *et al.,* 1996; Reme *et al.,* 1998; Yoshizawa *et al.,* 2000). Furthermore, inter-crossing transgenic models with photoreceptor specific expression of p35 with models of retinal degeneration available in this laboratory, may allow the evaluation of the possible protective effect of p35 in halting or retarding photoreceptor degeneration (Figure 5.2).

Alternatively Cre recombinase could be delivered to photoreceptors of *lox*P-p35 transgenic models using viral vectors, including adeno-associated viral (AAV) vectors. Following this approach the anti-apoptotic activity of p35 could be evaluated using light- or chemical-induced models of retinal degeneration (Figure 5.3: A). In addition, *lox*P-p35 models could be inter-crossed with models of retinal

degeneration, and following subretinal delivery of Cre using AAV, the anti-apoptotic activity of p35 could be evaluated (Figure 5.3: B).

The projects that have been initiated and developed significantly during the course of my PhD studies, have potentially long life spans, involving the inter-crossing of multiple lines of transgenic mice and the evaluation of potential therapeutic benefit in these mice using a combination of retinal histology and electrophysiology. Hence, the current study describes the evaluation of the *lox*P-35 transgenic model, using electroporation of plasmid expressing Cre recombinase to cultured retinal explants to activate p35 expression. To further assess the possible protective effect of p35, cultured retinal explants were electroporated with a plasmid expressing p35 and apoptotic cell death was assessed following chemical-induction of apoptosis. The generation of AAV constructs expressing p35 and Cre recombinase, and subsequent viral production is also described, with the ultimate aim of using AAV delivery of a p35 gene to evaluate its anti-apoptotic activity in retinal explants and in transgenic models.

5.2 Materials and Methods

5.2.1 lox*P-p35 transgenic mouse model*

The *lox*P-p35 transgenic mouse model was kindly provided by Professor Masayuki Miura (Department of Genetics, University of Tokyo, Japan). Generation of this model has been previously described (Hisahara *et al.*, 2000). The transgene consists of the CAG (cytomegalovirus IE enhancer and chicken β-actin) promoter, the neomycin gene flanked by *lox*P sites (*lox*P-neo-*lox*P), p35 coding sequence and a polyadenylation signal (Figure 5.1). Four male founders were received and housed in the Specific Pathogen Free (SPF) animal facility here in the Department of Genetics, Trinity College Dublin. Founder *lox*P-p35 transgenic mice were mated to C57BL/6J females, and the F1 generation were screened by PCR as described in 5.2.2 below, to identify animals carrying the *lox*P-p35 transgene. Expansion of the colony was continued to build up sufficient stocks before experiments were initiated.

5.2.2 Identification of transgenic lox*P-p35 mice by PCR analysis*

DNA was isolated from tails of *lox*P-p35 mice as described in Chapter 2: 2.7.1, and analysed by PCR to identify animals carrying the *lox*P-p35 transgene. As *lox*P-p35 animals are heterozygous for the p35 transgene, inter-crossing with wt C57BL/6J yields a 1:1 ratio of pups with and without the transgene. PCR reactions were set up and repeated once to verify results. Two sets of primers (shown below) were used to detect the *lox*P-p35 transgene.

Set I:

Fp35-3: 5' TGGATGGATTCCACGATAGC 3'

Rp35-4: 5' TGCACACTGTCCACGTAAGC 3'

Product size: 359 bp

Set II:

FNeo: 5' CTTGCCGAATATCATGGTG 3'

Rp35-B: 5' CATGAGAACGGGTTTTGTCA 3'

Product size: 751 bp

Approximately 1µl or 200ng of DNA isolated from the tail was used for the PCR reactions as described in 2.2.15.

5.2.3 Immunocytochemistry of p35 expression in HeLa cells

HeLa cells were maintained as described in Chapter 2: 2.4.1. For this assay cells were plated at 2.6 x 10^5 per well of a 12-well plate on coverslips, the day before transfection. HeLa cells were transfected with the p35 gene in pcDNA3.1- (kindly provided by Professor Seamus Martin, Trinity College Dublin) using Lipofectamine 2000 according to the manufacturer's instructions. Two days later, cells were washed with PBS, fixed in 4% paraformaldehyde for 5 minutes, and washed with PBS. Cells were then incubated with blocking solution for 1 hour (0.1-3% goat serum or 0.1-3% BSA with 0.1-0.3% Triton X-100), followed by overnight incubation at 4°C with either of the following anti-p35 or -Cre recombinase antibodies: 1) rabbit anti-p35 antibody (1:10-1: 500 dilution), 2) rabbit anti-p35 α–loop antibody (1:250 dilution), 3) mouse anti-p35 antibody (1:100), 4) rabbit polyclonal anti-Cre (1:300-1:2000, Covance Research) or 5) mouse monoclonal anti-Cre (1:100, Covance Research). Cells were washed with PBS three times and then incubated with Alexa Fluor 488, or 568, anti-rabbit or anti-mouse secondary antibody for 2 hours in the dark. Following three washes with PBS, cells were examined using a Zeiss Axioplan-2 Optical Fluorescent Microscope using Zeiss filter sets 14 and 38 with analysis^B Imaging Software (Olympus).

The antibodies were kindly provided by donors as follows:

1) Rabbit anti-p35 antibody: Professor Seamus Martin, Trinity College Dublin
2) Rabbit anti-p35 a-loop antibody: Dr. Masanori Tomioka (Tomioka *et al.*, 2002), RIKEN Brain Science Institute, Saitama, Japan.
3) Mouse anti-p35 antibody: Professor Bruce Hay, (Huh *et al.*, 2004), California Institute of Technology, California, USA.

5.2.4 Electroporation of pciCre into lox*P-p35 retinal explants*

Newborn mouse pups (P0-P2) were culled, and dissected retinas were electroporated (Chapter 2: 2.7.2) with 100µl (1µg/ul) of CMV-driven improved Cre recombinase (iCre), 100µl (1µg/ul) of pcDNA3.1+ or 100µl (1µg/ul) of

pcDNA3.1.p35. Generation of the construct pciCre is described in Chapter 4: 4.2.2. Retinal explants were electroporated in triplicate at least, as mouse pups were subsequently tailed and DNA analysed for presence of the *lox*P-p35 transgene. Electroporated retinas were cultured for 10-14 days at 37°C, 5% CO_2.

5.2.5 Preparation and immunohistochemistry of retinal explant sections

10-14 days following electroporation, retinas from animals positive for the *lox*P-p35 transgene were washed twice with PBS and prepared for either vibratome sectioning or cryosectioning (Chapter 2: 2.7.4). Following sectioning, retinal sections were immunostained as follows:

1) α-loop anti-p35 antibody: Sections were blocked for 1 hour in 0.1% Triton X-100, 1% goat serum and probed with anti-p35 at 1:100 to 1:250 dilutions overnight at 4°C. Following three washes with PBS for 5 minutes, the sections were incubated with Alexa Fluor 568 anti-rabbit secondary antibody (1:1000) for 2 hours at room temperature, stained with 1μg/μl DAPI for 2 minutes and washed in PBS as before. Sections were examined using a Zeiss Axioplan-2 Optical Fluorescent Microscope using Zeiss filter sets 1 and 14 with analysis^B Imaging Software (Olympus).

2) Mouse anti-p35 antibody: Sections were washed with 0.1% Tween-20 in PBS (PBT) for 5 minutes and incubated in permeabilisation buffer (0.3% Triton X-100, 0.3% sodium deoxycholate in PBS) for 30 minutes. Following incubation with 5% BSA for 1 hour, sections were incubated with anti-p35 at dilutions of 1:50 to 1:200 overnight at 4°C. Following three-four washes with PBT, sections were stained with Alexa Fluor 488 anti-mouse secondary antibody (1:1000 in 1% BSA) for 2 hours at room temperature, stained with 1μg/μl DAPI for 2 minutes and washed in PBT as before. Sections were examined as described above with Zeiss filter sets 1 and 38.

3) Mouse anti-Cre antibody: Sections were blocked for 1 hour in 0.05% Tween-20, 0.1% Triton X-100 and 3% goat serum and stained with anti-Cre antibody at a dilution of 1:200 overnight at 4°C. Following three washes with PBS, sections were incubated with Alexa Fluor 488 anti-mouse secondary antibody (1:1000) for 2 hours

at room temperature, stained with DAPI as described above and examined for fluorescence.

5.2.6 Sequencing of the lox*P-p35 transgene*

To confirm the sequence integrity of the two *lox*P sites and the p35 gene, regions of the transgene were amplified by PCR from DNA isolated from *lox*P-p35 animals. Approximately 200ng of tail DNA was used for PCR reactions set up as described in Chapter 2: 2.2.15. The following primers pairs were used:

Table 5.1: Forward and reverse primers for the amplification of regions of the *lox*P-p35 transgene

Target	Forward Primer, 5'- 3'	Reverse Primer, 5'- 3'	Product, bp
*lox*P 5'	GTGCTGGTTGTTGTGCTGTC	CTCGTCCTGCAGTTCATTCA	334
*lox*P 3'	CTTGCCGAATATCATGGTG	CATGAGAACGGGTTTTGTCA	737
p35	TGGATGGATTCCACGATTAGC	TGCACACTGTCCACGTAAGC	354

Following amplification, PCR products were purified using a QIAquick PCR Purification Kit (Qiagen) according to the manufacturer's instructions and sequenced according to 2.2.14 using forward or reverse primers as listed above.

5.2.7 Isolation and real-time RT-PCR analysis of RNA from lox*P-p35 retinal explants electroporated with CMV-driven iCre recombinase*

Newborn mouse pups (P0-P2) were culled, and dissected retinas were electroporated (Chapter 2: 2.7.2) with 100µl (1µg/µl) of CMV-driven improved Cre recombinase (iCre) with 100µl of pCMV.EGFP (0.1µg/µl). Retinal explants were electroporated in triplicate at least, as mouse pups were subsequently tailed and DNA analysed for the *lox*P-p35 transgene. Electroporated retinas were cultured for 8 or 15 days at 37°C, 5% CO_2 and RNA was isolated from the explants according to the method described in 2.7.3. RNA was subsequently analysed by real-time RT-PCR as described in 2.3.5. HPLC-purified primers for the amplification of p35, iCre and the housekeeping gene 18S rRNA are shown below:

Table 5.2: Forward and reverse primers for the amplification of p35, iCre and 18S rRNA fragments

Target	Forward Primer, 5'- 3'	Reverse Primer, 5'- 3'	Product, bp
p35	CGTCGTAGCTTACGTGGACA	CCGAATTTTTGAACGACGAC	95
iCre	AATGCTGTGTCCCTGGTGAT	TGGTCAAAGTCAGTGCGTTC	101
18S r RNA	CAAGAACGAAAGTCGGAGGT	CGGGTCATGGGAATAACG	100

Expression levels of p35 and iCre were standardised against the housekeeping gene 18S rRNA.

5.2.8 Design and construction of pEGFP.p35

A stuffer sequence of 249 bp was PCR amplified from wild-type (wt) mouse genomic DNA using primers for intron I of the rhodopsin gene with *Xho*I and *EcoR*I restriction sites (Appendix: 2.1.1) and cloned into pEGFP-1 (Clontech) via these restriction sites. pStuffer.EGFP-1 was then digested with *Sma*I and the 5'-phosphorylated ends dephosphorylated with SAP (Chapter 2: 2.2.17). The 1210 bp ubiquitin promoter was isolated from pUB6/V5-His (Invitrogen) using *Bgl*II and *Bam*HI, end-filled with Klenow (2.2.16) and ligated with pStuffer-EGFP-1 via the *Sma*I restriction site, generating the vector pUbi.EGFP. Subsequently, pcDNA3.1-with CMV promoter-driven p35 was digested with *Bgl*II, end-filled with Klenow, and the 5'-phosphorylated ends dephosphorylated with SAP. A 2524 bp fragment composed of the stuffer and ubiquitin promoter-driven EGFP, was isolated from pUbi.EGFP using *Bgl*II and *Ssp*I, end-filled with Klenow and ligated with pcDNA3.1.p35 at the end-filled *Bgl*II site (Figure 5.16). The resulting construct contained a ubiquitin promoter-driven EGFP gene, and a CMV promoter-driven p35 gene. pEGFP.p35 was sequenced to verify its integrity using primers listed in Appendix: 2.1.2.

5.2.9 Evaluation of pEGFP.p35 expression in HeLa cells

HeLa cells were maintained as described in Chapter 2: 2.4.1. For this assay cells were plated at 2.6 x 10^5 per well of a 12-well plate on coverslips, the day before transfection. HeLa cells were transfected with pEGFP.p35 using Lipofectamine

2000 according to the manufacturer's instructions. Two days later, cells were washed with PBS, fixed in 4% paraformaldehyde for 5 minutes, and washed with PBS. Cells were examined using a Zeiss Axioplan-2 Optical Fluorescent Microscope using Zeiss filter set 38 with analysis^B Imaging Software (Olympus).

5.2.10 Induction of apoptosis in C57BL/6J cultured retinal explants using A23187 and subsequent evaluation using TUNEL Staining

Newborn C57BL/6J mouse pups (P0-P2) were culled, and dissected retinas were explanted to inserts for 10 days. On day 10, retinal explants were treated with calcimycin, a calcium ionophore, (A23187-Calbiochem {Merck, Darnstadt, Germany}) at a final concentration of 5μM for 24 hours. Explants were then washed with PBS twice for 5 minutes and incubated in fresh retinal explant medium (Chapter 2: 2.1.2 {ix}) for 24 hours to recover. Explants were harvested, and TUNEL stained as described in 2.7.4 and 2.7.6 respectively.

5.2.11 Evaluation of the potential protective effect of pEGFP.p35 expression on C57BL/6J cultured retinal explants exposed to A23187 (calcimycin)

Newborn C57BL/6J mouse pups (P0-P2) were culled, and 20 dissected retinas were electroporated on two independent occasions (Chapter 2: 2.7.2) with 100μl (1μg/μl) of CMV-driven pEGFP.p35 or 100μl of pCMV.EGFP (1μg/μl). On day 9, prior to treatment with A23187 at a final concentration of 5μM for 24 hours, two explants were pre-incubated with 50μM Z-VAD-FMK (Calbiochem), a caspase inhibitor, for 1 hour. The following day, retinal explants were then washed with PBS twice for 5 minutes and incubated in fresh retinal explant medium for 24 hours to recover. Explants were harvested and TUNEL stained as described in 2.7.4 and 2.7.6 respectively. For explant analysis, counts of TUNEL positive and EGFP positive cells were taken from 3 fields of view of three sections, on 3 independent occasions. Results were expressed as the mean ± S.E. Significant differences were assessed using an unpaired *t*-test ($P < 0.05$).

5.2.12 Design and construction of pAAV-iCre.EGFP and pAAV-p35 vector plasmids

pAAV-MCS (Stratagene) was digested with *Bam*HI and end-filled with Klenow. The gene for iCre recombinase was isolated from a previously generated construct,

pRho.Chi.iCre.B (Chapter 4: 4.2.1), using *Hind*III and *Kpn*I, end-filled and ligated with pAAV-MCS. The resulting pAAV-iCre, was digested with *Mlu*I, end-filled and treated with SAP. A 2524 bp fragment composed of the stuffer and ubiquitin promoter-driven EGFP, was isolated from pUbi.EGFP using *Bgl*II and *Ssp*I, end-filled with Klenow and ligated with pAAV-iCre, to generate pAAV-iCre (Figure 5.26). The resulting construct contained a rhodopsin promoter-driven iCre gene and a ubiquitin promoter-driven EGFP gene in a plasmid to be used for the generation of recombinant AAV. To generate pAAV-p35, the 956 bp p35 gene was isolated from pcDNA3.1.p35 (5.2.3) digested with *Xho*I, and ligated with pAAV-MCS digested with *Xho*I. Both plasmid constructs were sequenced to verify their integrity using primers listed in Appendix: 2.1.3. In addition, as the inverted terminal repeats of pAAV-MCS (ITRs) can rearrange, both pAAV constructs were digested with *Pst*I and *Not*I to verify that these sequences were intact. Following digestion, fragments were run on a 3% agarose gel to resolve the 139 and 145 bp ITRs.

5.2.13 Generation and titration of AAV-iCre.EGFP and AAV-p35

Viral stocks of AAV-iCre.EGFP and AAV-p35 were generated using the calcium phosphate transient triple transfection methodology, followed by purification using caesium chloride (Chapter 2: 2.6.1). The genomic viral titre of AAV-iCre.EGFP was then determined using quantitative real-time PCR to amplify a 100 bp sequence of the iCre gene with reference to a standard curve generated from serially diluting a known concentration of a plasmid vector carrying CMV promoter-driven iCre in pcDNA 3.1+ (pciCre) (2.6.2). The same method was used for determining the viral titre for AAV-p35, using primers to amplify a 100 bp sequence of the p35 gene and pcDNA3.1.p35 to generate the standard curve. Primer sequences to amplify the iCre and p35 genes are shown below:

FiCre: 5' AATGCTGTGTCCCTGGTGAT
RiCre: 5' TGGTCAAAGTCAGTGCGTTC

Fp35: 5' CGTCGTAGCTTACGTGGACA 3'
Rp35: 5' CCGAATTTTTTGAACGACGAC 3'

5.2.14 Determination of the infectious titre of AAV-.iCre.EGFP by quantitative real-time PCR

The genomic titre of AAV, refers to the number of genomic copies of AAV, but may not reflect the infectious titre (Zolotukhin *et al.,* 1999). Having established a genomic titre for AAV-iCre.EGFP, the infectious titre was determined using quantitative RT-PCR, as described in Chapter 2: 2.6.3 (Rohr *et al.,* 2005). Briefly 293 cells were infected with 2 x 10^7 vp, incubated for 24 hours and trypsinised. Following treatment with S1 nuclease, to remove single-stranded AAV DNA, which is non-infectious, the remaining double-stranded (ds) viral DNA, was quantified using real-time PCR. A standard curve was generated using a serially diluted plasmid vector, pEGFP, which carries the gene for EGFP. HPLC-purified primers for amplification of the EGFP gene are shown below. By relating the quantitative PCR curves of the ds AAV-iCre.EGFP isolated from 293 cells, to the standard curves generated using the plasmid pEGFP, the infectious titre of AAV-iCre.EGFP was determined.

Forward EGFP: 5' TTCAAGGAGGACGGCAACATCC 3'
Reverse EGFP: 5' CACCTTGATGCCGTTCTTCTGC 3'

5.3 Results

5.3.1 lox*P-p35 transgenic mouse model*

Four male *lox*P-p35 animals were kindly provided by Professor Miura. Importation of these animals was a lengthy process, involving a rigorous health screen according to FELASA (Federation of European Laboratory Animal Science Association) guidelines on site in Japan, as a Specific Pathogen Free (SPF) facility is maintained here in the Department of Genetics, Trinity College Dublin (Senior animal technician: Sylvia Mehigan).

5.3.2 Analysis of mouse tail DNA for the lox*P-p35 transgene*

Tail DNA from potential *lox*P-p35 animals was analysed by PCR using two sets of primers to verify the result. Figure 5.4 shows an example of a set of PCR reactions using primer set I (Fp35-3 and Rp35-4). Amplification of a 359 bp product in lanes 2, 3 and 7 indicate that three mice from this litter of seven are carrying the transgene. The remaining four are negative for the transgene, as evident from the absence of any PCR product in lanes 4, 5, 6 and 8.

5.3.3 Evaluation of anti-p35 antibodies in HeLa cells transiently transfected with CMV-driven p35

Expression of the baculoviral p35 protein in the *lox*P-p35 transgenic model is silent due to a neomycin gene flanked by *lox*P sites between the CAG promoter and the p35 coding sequence in the transgene (Figure 5.1). Active Cre recombinase binds to the *lox*P sites, catalysing the removal of the neomycin gene, thus allowing transcription of the p35 gene. To assess p35 expression in the presence of Cre using either *lox*P-p35 transgenic animals or retinal explants from the *lox*P-p35 model, it was important to source an effective anti-p35 antibody. Professor Seamus Martin kindly provided a polyclonal anti-p35 antibody, which was effective for detection of p35 protein by Western blotting (Dr. Colin Adrian, Trinity College Dublin: personal communication). However, the anti-p35 antibody did not detect p35 expression by immunocytochemistry in HeLa cells transiently transfected with CMV promoter-driven p35 (data not shown). A number of commercial companies generate polyclonal anti-p35 antibody, including BD Biosciences, Biocarta and Promega but

on communication these companies could only recommend the use of the antibody for Western blot analysis.

Dr. Masanori Tomioka generated an α-loop antibody for p35 and kindly provided an aliquot. HeLa cells were transiently transfected with CMV promoter-driven p35 plasmid, cultured for 48 hours and then immunostained for p35 expression (5.2.3). The α-loop antibody detected p35 expression in HeLa cells as shown in Figure 5.5: C. Five different blocking solutions were assessed and 0.1% goat serum with 0.1% Triton X-100 resulted in the strongest specific immunostaining with minimal background. Hence an effective p35 antibody, which could be used for future studies, had been identified.

5.3.4 Evaluation of p35 expression in lox*P-p35 cultured retinal explants electroporated with CMV promoter-driven iCre recombinase*

To assess whether p35 expression could be activated *in vitro* by active iCre recombinase, cultured retinal explants from P0-P1 *lox*P-p35 mouse pups were electroporated with CMV promoter-driven iCre (Table 5.3 below). Preparation and electroporation of retinal explants was undertaken in conjunction with Dr. Marius Ader (Trinity College Dublin) (5.2.4). 8 explants from potential *lox*P-p35 mouse pups (Table 5.3: Litter A) were electroporated with pciCre and subsequent PCR analysis indicated that 2 of these pups were positive for the *lox*P-p35 transgene (Table 5.3). Retinal explants were prepared from a second litter of 9 mice (Table 5.3: Litter B): 8 retinal explants were electroporated with pcDNA3.1+ (negative control), 6 explants with pcDNA3.1.p35 (positive control) and the remaining 6 explants were not electroporated. Subsequent PCR analysis of tail DNA indicated that 3 of the 9 pups were positive for the *lox*P-p35 transgene (Table 5.3). The first *lox*P-p35 positive pup had been electroporated with pcDNA3.1+, the second with pcDNA3.1.p35 and the third had not been electroporated.

Table 5.3: Genotype of cultured retinal explants electroporated with pciCre to assess *in vitro* activation of *lox*P-p35 transgene

Litter	Pup Number	*lox*P-p35 Transgene	Construct Electroporated
A	2	Negative	pciCre
A	2	Positive	pciCre
B	1	Positive	pcDNA3.1+
B	3	Negative	pcDNA3.1+
B	1	Positive	pcDNA3.1.p35
B	2	Negative	pcDNA3.1.p35
B	1	Positive	None
B	2	Negative	None

Following 10-14 days incubation, retinal explants were fixed with 4% paraformaldehyde and 50-100μm sections were cut using a vibratome (5.2.5). Prior to assessing if delivery of iCre had activated the expression of p35 in *lox*P-p35 cultured retinal explants, retinal sections from explants electroporated with CMV promoter-driven p35 were immunostained using the α-loop anti p35 antibody (1:250) as a positive control for p35 expression. However, no positive staining was detected. Immunostaining was repeated using a higher concentration of antibody (1:100) and different blocking solutions. A representative section in Figure 5.6: A shows that no staining for p35 is present.

As no immunostaining for p35 expression was detected in retinal explants electroporated with CMV promoter-driven p35, it was considered that the electroporation might not have been successful. To explore this hypothesis, retinal sections from *lox*P-p35 pups, electroporated with pciCre were probed for iCre recombinase expression. Prior to this, the Cre antibody had been evaluated in HeLa cells transiently transfected with pciCre. Using a reference from Shimshek *et al.*, 2000, a polyclonal anti-Cre antibody was used initially. Unfortunately, no positive staining was detected in HeLa cells (data not shown). On personal communication with Dr. Donald Zack (McGill University, Quebec, Canada), the protocol for immunostaining was modified. Alterations to the protocol included: 1) adding a

permeabilisation step prior to blocking, 2) using different blocking buffers and 3) using increasing concentrations of the antibody (1:2000-1:300). In addition, as a further control, HeLa cells were transiently transfected with a plasmid expressing bacterial Cre recombinase (pML78, kindly provided by Dr. Therese Tuohy, Univeristy of Cincinnati, OH, USA), but on each occasion, immunostaining was negative (data not shown). A monoclonal Cre antibody was then used (Covance), which resulted in immunostaining for Cre transiently expressed in HeLa cells. Figure 5.7: C shows strong, specific staining for Cre recombinase in HeLa cells.

Given the availability of an effective antibody for iCre, retinal explant cryosections from *lox*P-p35 pups were probed for expression of iCre using the monoclonal Cre antibody. Figure 5.8: A shows a representative section from this experiment with strong specific staining for iCre, in the order of approximately 15-20%, demonstrating the successful electroporation of the cultured retinal explant. Given the strong staining for Cre recombinase protein obtained in sections of this retinal explant, a section from the same explant was probed for p35 expression. In the presence of sufficient levels of active Cre recombinase, the *lox*P-flanked neomycin gene should in principle be excised, allowing p35 expression from the CAG promoter of the transgene. However, immunostaining for p35 protein was negative (data not shown). Given that the electroporation was successful as judged by iCre expression, the absence of p35 expression in the explants electroporated with CMV promoter-driven p35 may have been due to the p35 antibody or protocol used. Therefore an alternative method for preparing retinal explants for immunostaining was explored.

Retinal explants from 2 wt C57BL/6J mice were electroporated with pcDNA3.1.p35 at P0 as described before and cultured for 14 days. Fixing in paraformaldehyde can alter the protein epitopes used for antibody binding, so on harvesting at day 14, explants were set directly in OCT with no prior fixing and cryosectioned. In addition, with cryosectioning, thinner sections (7-30μm) can be cut compared to vibratome sectioning (50-100μm) providing sections with greater resolution in terms of tissue structures. The α-loop anti-p35 antibody (1:100) was used to probe

the resulting cryosections but again no p35 expression was detected using this modified methodology (data not shown).

At this time a second batch of α-loop anti-p35 antibody had been received from Dr. Masanori Tomioka. To confirm that the negative results for p35 expression in retinal explants electroporated with pcDNA3.1.p35 were not due to an inactive antibody, α-loop anti-p35 was tested in HeLa cells transiently transfected with pcDNA3.1.p35. Results demonstrated that the second batch of antibody, was much less effective than the first batch received possibly accounting for the negative results observed in the immunostaining of cryosectioned explants electroporated with pcDNA3.1.p35 as the second batch of antibody was used for the experiment (Figure 5.9). Hence, another p35 antibody (anti-mouse) was sourced and an aliquot kindly provided by Professor Bruce Hay. To demonstrate the effectiveness of the newly sourced anti-p35 antibody, HeLa cells transiently transfected with the p35 gene were immunostained for p35 expression. Figure 5.10: C shows positive staining for p35 expression. Retinal cryosections from explants electroporated with pcDNA3.1.p35 were immunostained using the mouse anti-p35 antibody, but no positive staining was detected (data not shown). As the anti-p35 antibody from Professor Hay and the α-loop anti-p35 antibody from Dr. Tomioka, successfully detected p35 protein in HeLa cells transiently transfected with the same p35 construct electroporated into cultured retinal explants, it is possible that the level of p35 expression from delivery by electroporation, was not at a sufficient level to be detected by immunohistochemistry. It is notable that via personal communication, Professor Paul Friesen (Institute for Molecular Virology, University of Wisconsin-Madison, WI, USA) commented that detection of p35 baculoviral protein in mammalian cells can be difficult.

5.3.5 Sequencing of the lox*P-p35 transgene*

Given the absence of expression of p35 and the presence of expression of iCre, in *lox*P-p35 transgenic retinal explants electroporated with CMV promoter-driven iCre, it was important to confirm that the *lox*P sites in the transgenic model were still intact. However, as retinal explants electroporated with the p35 gene, as a positive control (see above) did not show expression of p35, the absence of p35

expression may be a function of the immunohistochemical assay. Nevertheless for completeness, it was valuable to confirm the sequence of the *lox*P sites in the p35 transgene. Primers flanking the sites were used to amplify these regions from DNA isolated from the tails of *lox*P-p35 animals. Notably the sequence of both 34 bp *lox*P sites was shown to be correct. Figure 5.11 shows the reverse sequence of the second *lox*P site, flanked by *Mlu*I and *Xho*I restriction sites. In addition some sequencing of the p35 gene was undertaken to confirm the sequence in the p35 transgene in *lox*P-p35 mice (data not shown).

5.3.6 Analysis of RNA isolated from lox*P-p35 retinal explants electroporated with pciCre using real-time RT-PCR*

As p35 expression could not be detected by immunostaining in retinal explants electroporated with a construct expressing iCre recombinase, the level of p35 mRNA expression was analysed by real-time RT-PCR. Retinal explants from 2 litters of *lox*P-p35 P0 pups were electroporated with either pciCre (18 explants) or pcDNA3.1+ (6 explants) on two independent occasions, and subsequent PCR analysis of isolated tail DNA indicated the genotype (Table 5.4 below). Retinal explants from wt C57BL/6J mice were used as a negative control.

Table 5.4: Genotype of cultured retinal explants electroporated with pciCre to assess *in vitro* activation of *lox*P-p35 transgene by real-time RT-PCR analysis

Litter	Pup Number	*lox*P-p35 Transgene	Construct Electroporated
A	2	Negative	pciCre
A	2	Positive	pciCre
A	1	Negative	pcDNA3.1+
A	2	Positive	pcDNA3.1+
B	3	Negative	pciCre
B	2	Positive	pciCre

RNA was isolated from retinal explants positive for the *lox*P-p35 transgene following 8 or 15 days of culturing, and the level of iCre and p35 expression analysed by real-time RT-PCR (Figures 5.12-13). There was no difference detected

in the level of p35 expression in retinal explants electroporated with pciCre and cultured to either day 8 or day 15 compared to retinal explants electroporated with pcDNA3.1+ (Figure 5.12) suggesting that the level of expression of iCre recombinase present in electroporated retinal explants may not have been sufficient to catalyse recombination at the *lox*P sites on the transgene. Interestingly, there is a base level of p35 expression present in retinal explants from the *lox*P-p35 transgenic mice, suggesting that the CAG promoter may be slightly leaky, as no p35 expression was detected in RNA isolated from wt C57BL/6J retinal explants. In addition, iCre was expressed in the electroporated retinal explants, indicating that the electroporation was successful. A significant difference in the level of iCre expression in retinal explants electroporated with pciCre compared to negative controls was observed (Figure 5.13). However, as an additional control pCMV.EGFP was co-electroporated with the iCre described above for both independent experiments, as an indicator of electroporation efficiency. Figure 5.14: C shows a representative *lox*P-p35 explant electroporated with pCMV.EGFP, with strong diffuse EGFP expression. From an unsectioned retinal explant it is difficult to estimate the percentage of cells expressing EGFP, but Figure 5.14: C indicates that electroporation was successful. This experiment was undertaken to ensure that the lack of p35 expression was not due to inefficient electroporation of pciCre. Given that iCre is expressed in electroporated retinal explants from *lox*P-p35 transgenic animals, evaluated by RNA and protein assays, the lack of p35 expression, as evaluated by immunostaining, may simply be due to insufficient levels of iCre protein present to catalyse recombination at *lox*P sites, and thereby activate p35 expression.

5.3.7 Assessment of the protection of pEGFP.p35 in cultured retinal explants treated with A23187, by TUNEL staining

The *lox*P-p35 transgenic mouse line potentially represents a model in which the effect of p35 expression in photoreceptors can be evaluated. As discussed in the introduction, tissue-specific expression of a transgene can be achieved by mating transgenic models with floxed genes such as the *lox*P-p35 line to a second line of transgenics with iCre driven by a tissue-specific promoter. The previous chapter describes the design and evaluation of constructs with photoreceptor-specific

expression of iCre, for the generation of transgenic lines with rod and cone photoreceptor expression of iCre.

To validate the utility of the *lox*P-p35 transgenic mouse, the experiments in this chapter were undertaken to establish if p35 expression could be activated in retinal explants from *lox*P-p35 mice. This would provide a system to explore the potential anti-apoptotic effect of p35 in retinal explants, and would also assess the functionality of the *lox*P-p35 transgene. However, the results from the experiments described above, indicated that no p35 expression was detected subsequent to the electroporation of pciCre plasmid. The reasons for the absence of p35 expression may be many fold and are discussed later in this chapter. In spite of the results using *lox*P-p35 retinal explants, the availability in the laboratory of a retinal explant system provided another opportunity to explore the potential protective effect of p35 in retinal tissues. The approach adopted for this was to electroporate constructs expressing p35 into retinal explants and subsequently assess the level of chemical-induced apoptosis present in electroporated explants as described below.

A23187 (also known as calcimycin) was selected as the agent to induce cell death (Dr. Maryanne Donovan, University College Cork: personal communication). Originally derived from *Streptomyces chartieusensis*, A23187 forms stable complexes with divalent cations such as calcium, increasing intracellular levels and also inhibits mitochondrial ATPase (Reed *et al.,* 1972). An initial experiment was undertaken to assess apoptosis induced by A23187. This experiment was undertaken in conjunction with the Department of Biochemistry, University College Cork. Figure 5.15: B and D show TUNEL stained untreated and A23187 treated retinal explant sections. There is significantly more TUNEL staining present in the section from the A23187 treated explant, indicating that the chemical agent induced cell death. In addition, the morphology of the treated retinal explant is very disorganised (Figure 5.15: C) compared to the untreated retinal explant (Figure 5.15: A), again as a result of treatment with A23187. Given that there was a significant difference in cell death observed, this system was considered to be appropriate for evaluating the possible protective effect of p35 expression in cultured retinal explants.

The construct with CMV promoter-driven p35 expression was modified to include a ubiquitin promoter-driven EGFP tag (Figure 5.16). Electroporation of retinal explants typically has a relatively low efficiency of approximately 15-20% of cells, so an EGFP tag would allow cell death to be evaluated only in those cells expressing p35. To verify the functionality of the pEGFP.p35 construct, HeLa cells were transiently transfected with pEGFP.p35 and examined for EGFP fluorescence 48 hours later. Figure 5.17: C shows HeLa cells with EGFP fluorescence.

To assess the potential protective effect of p35 expression, a total of 20 retinal explants (2 independent experiments) were electroporated with either pCMV.EGFP, pEGFP.p35 or no vector at P0. At P10, half the explants were treated with an apoptosis-inducing agent A23187 for 24 hours and the remainder left untreated. In addition, two explants electroporated with pCMV.EGFP were incubated with a caspase inhibitor, Z-VAD-FMK, 1 hour prior to addition of A23187 as a positive control for apoptosis inhibition.

P11 retinal explant sections, neither electroporated with a plasmid vector nor treated with A23187, showed no positive TUNEL stained cells (Figure 5.18: A and Figure 5.24: Bar 1). Rosettes are clearly seen in the photograph of the DAPI stained section, which can occur during growth of cultured explants, but individual retinal layers are clear (Figure 5.18: B). Minimising handling of retinas during dissection and transfer to membrane for culturing can also reduce rosette formation (personal communication, Dr. Marius Ader, Trinity College Dublin).

To assess apoptosis, TUNEL positive cells were counted from 3 fields of view of 3 retinal sections on 3 independent occasions, and expressed as a percentage of the total number of cells stained using DAPI. Explant cryosections of electroporated retinas, untreated with A23187, showed a low level of TUNEL staining, indicating that the electroporation procedure itself induces apoptosis. Explants electroporated with pCMV.EGFP and pEGFP.p35 had $1 \pm 0.41\%$ and $0.2 \pm 0.16\%$ respectively of TUNEL positive cells (Figure 5.24: Bars 2 and 3). A representative photograph of a retinal explant section, electroporated with pCMV.EGFP, is shown in Figure 5.19, with a low level of TUNEL staining (A).

P11 retinal explants electroporated with pCMV.EGFP at P0 and treated with A23187 for 24 hours at P10, were assayed for cell death by TUNEL staining, and 26.33 ± 4.62% of cells were TUNEL positive (Figure 5.24: Bar 4). A representative photograph is shown in Figure 5.20, with strong TUNEL staining (A). The corresponding DAPI stained retinal section (C), demonstrates that the retinal morphology is highly disrupted, with no clear retinal layers visible. Treatment for 24 hours with A23187, is clearly a strong apoptosis inducing agent and destructive to the cultured retinal explants.

As a positive control for apoptosis inhibition, retinal explants electroporated with pCMV.EGFP, were pre-treated with Z-VAD-FMK, prior to treatment with A23187 for 24 hours. TUNEL staining of these sections, revealed a level of 13.88 ± 0.63% TUNEL positive cells (Figure 5.24: Bar 5). This represents an approximately 50% reduction in TUNEL positive cells, compared to the explants not pre-treated with Z-VAD-FMK. As Z-VAD-FMK is a caspase inhibitor, inhibition of apoptosis by A23187 in cultured retinal explants, demonstrates that apoptosis is caspase-dependent, at P10/P11, as has been demonstrated in a number of other studies using neonatal retinal explants (Soderpalm *et al.*, 2000; Vallazza-Deschamps *et al.*, 2005). Although apoptosis is partially inhibited using Z-VAD-FMK (Figure 5.21: A), the retinal layers remain disorganized (Figure 5.21: C).

To explore the potential anti-apoptotic effect of p35, retinal explants electroporated with a plasmid construct, (pEGFP.p35), expressing p35 and exposed to A23187 for 24 hours were TUNEL stained and determined to have 20.18 ± 0.89% TUNEL positive cells (Figure 5.23: A, Figure 5.24: Bar 6). This result represents a 6% reduction in TUNEL positive cells, compared to sections analysed from control retinal explants, ($P < 0.05$). As only 15-20% of the cells were electroporated with plasmid, to more accurately assess the possible protective effect of p35, only EGFP expressing cells were examined for TUNEL staining. Analysis involved counting approximately 100-150 cells from 9 retinal sections of explants electroporated with either pCMV.EGFP or pEGFP.p35. Figures 5.22-3 show representative sections from retinal explants electroporated with pCMV.EGFP or pEGFP.p35, illustrating how the counting was undertaken. Of the cells expressing CMV-driven EGFP alone, 34.04 ± 5.54% were TUNEL positive compared to 18.96 ± 5.44% of cells

expressing pEGPF.p35. This represents a reduction in the number of TUNEL positive cells of approximately 50%, suggesting that p35 expression may indeed be protective against caspase-dependent apoptosis in cultured retinal explants, exposed to A23187.

5.3.8 Genomic Titration of AAV-iCre.EGFP, and AAV-p35

Given the results in retinal explants together with previous studies in cell culture (Tuohy *et al.,* 2002), and in *Drosophila* models of retinal degeneration (Davidson *et al.,* 1998; Galy *et al.,* 2005), suggesting that the p35 protein may protect against photoreceptor apoptosis, it would be valuable to establish methodologies to further explore the possible anti-apoptotic properties of p35 in mammalian photoreceptors. Clearly the *lox*P-p35 mouse model referred to in this chapter may provide an animal in which this may be achieved. However, adequate levels of Cre recombinase expression in retinal tissues will be required to utilise this potentially valuable animal model. Hence, efficient methods to deliver Cre recombinase or indeed p35 to retinal tissues must be explored. In this regard, the transgenic mice under development, described in Chapter 4, which should express Cre recombinase specifically in the rod or cone photoreceptors, may provide a solution to the need defined above.

However, an alternative approach was also considered in the current study, that is the viral delivery of either p35 or potentially Cre recombinase. AAV techniques have been established in the laboratory in TCD, as AAV vectors have been demonstrated to be very useful gene delivery vectors for the retina (Rolling 2004; Dinculescu *et al.,* 2005). (Chapter 1: 1.5.3.4). Hence to enable future *in vivo* exploration of the potential anti-apoptotic effects of p35, two AAV vectors were generated: 1) CMV promoter-driven iCre recombinase with a ubiquitin promoter-driven EGFP reporter gene (AAV-EGFP.iCre), and 2) CMV promoter-driven p35 (AAV-p35). To generate AAV, the calcium phosphate transient triple plasmid transfection methodology was followed, based on the original method by Xiao *et al.* 1998. In contrast to AAV-EGFP, described in Chapter 4: 4.2.10, which was purified using ViraKit (Chapter 2: 2.6.1), the AAV generated in this study were purified by caesium chloride density gradient centrifugation. One advantage of this method is

that a greater volume of purified virus is generated (approximately 1ml compared to 100μl).

The genomic titre of each virus was determined using real-time PCR, with titres of 1×10^9 and 9×10^9 vp/ml, for AAV-iCre.EGFP and AAV-p35, respectively (assessed on two independent occasions in triplicate). The genomic titre refers to the number of genomic copies of AAV, but does not necessarily reflect the infectious titre. Hence, to assess the infectious titre of AAV-iCre.EGFP, 293 cells were infected with virus, and the isolated cell lysate was subsequently analysed by real-time PCR. The infectious titre was determined to be 2×10^7 infectious particles/ml (ip/ml), giving an approximate ratio of genomic copy to infectious unit ratio of 47:1, indicating that the AAV generated is highly infectious (Zolotukhin *et al.*, 1999).

Having generated AAV vector stocks for iCre expression (AAV-iCre.EGFP) and p35 expression (AAV-p35), these AAVs will be employed for further experiments to evaluate the potential anti-apoptotic activity of p35. Given that iCre expression from a plasmid (pciCre) may not have been sufficient to activate p35 expression by removing the *lox*P-flanked neomycin gene in cultured *lox*P-p35 retinal explants (5.3.4), it would be valuable to investigate whether adequate levels of iCre expression using AAV delivery to *lox*P-p35 retinal explants would be achieved. Furthermore, AAV delivery of p35 could be used to further investigate the anti-apoptotic activity of p35 against A23187-induced apoptosis in cultured retinal explants described in the current study.

5.4 Discussion

As apoptosis has been shown to be the final common pathway of cell death of photoreceptors in RP, apoptosis inhibition may be of therapeutic benefit, slowing degeneration and possibly providing a window of opportunity to deliver additional therapeutic agents. Apoptosis is mediated by caspases, a family of cysteine aspartyl-specific proteases, which represent a potential site of inhibition (Thornberry *et al.,* 1998; Earnshaw *et al.,* 1999; Nicholson 1999). Although several studies have demonstrated that caspase-3 inhibition in models of retinal degeneration provides limited therapeutic benefit, this may be due to the late activation of caspase-3 in the apoptotic pathway, at which point apoptosis may be irreversible (Yoshizawa *et al.,* 2002; Zeiss *et al.,* 2004). Notably, inhibitors that target more than one caspase and at an earlier point in the apoptotic pathway have shown greater therapeutic potential, including the pan-caspase inhibitors, p35, a baculoviral protein (Tuohy *et al.,* 2002; Galy *et al.,* 2005) and XIAP, a member of the inhibitor of apoptosis (IAP) family of proteins (Petrin *et al.,* 2003; Leonard K.C. 2005), both of which have been explored in relation to photoreceptor apoptosis during the course of studies undertaken as part of this Ph.D.

The p35 baculoviral protein is an example of a pan-caspase inhibitor that targets both initiator (caspase-2, -8, -10) and effector (caspase-3, -6 and -7) caspases (Bump *et al.,* 1995; Xue *et al.,* 1995; Zhou *et al.,* 1998). As reviewed in the introduction, p35 has been shown to rescue photoreceptor degeneration in *Drosophila* models of rhodopsin-linked retinal degeneration (Davidson *et al.,* 1998; Galy *et al.,* 2005), in addition to significantly protecting against chemical-induced apoptosis in a photoreceptor line, 661W (Tuohy *et al.,* 2002). Given these encouraging results, there was a clear rationale to further evaluate p35 expression in a transgenic model. Following unsuccessful attempts in this laboratory to generate a transgenic model with rhodopsin promoter-driven expression of p35, a p35 model (*lox*P-p35) was kindly obtained from Professor Masayuki Muira (Hisahara *et al.,* 2000).

Notably, the *lox*P-p35 mouse model does not express p35 under normal conditions, due to the presence of a neomycin gene flanked by *lox*P sites between the promoter

and the p35 gene. Expression is activated by Cre recombinase (Cre) enzyme, which catalyses recombination at the two *lox*P recognition sites, removing the neomycin gene. This system of conditional gene targeting enables the activation of p35 to be controlled in a tissue-specific manner, by targeted delivery of Cre using for example, viral vectors or mating the *lox*P-p35 model to a second line of transgenics with Cre expression under the control of a tissue-specific promoter (Figures 5.2-3).

The *lox*P-p35 mouse model has been used in several studies to investigate the therapeutic anti-apoptotic potential of p35 expression for a number of degenerative disorders including multiple sclerosis (Araki *et al.,* 2000), myocardial injury (Hisahara *et al.,* 2000) and spinal cord injury (Tamura *et al.,* 2005). Most recently Tamura *et al.,* 2005, investigated the protective effect of p35 using a *lox*P-p35/MBP-cre mouse model, previously generated by inter-crossing a *lox*P-p35 mouse model with a mouse model carrying a transgene for oligodendrocyte-specific expression of Cre (driven by a myelin basic protein promoter; MBP) (Hisahara *et al.,* 2000). Following spinal cord injury, oligodendrocytes from *lox*P-p35/MBP-cre animals were found to be significantly protected from degeneration compared to oligodendrocytes from control MBP-cre animals with no p35 transgene. Furthermore, motor function in *lox*P-p35/MBP-cre animals was shown to recover more rapidly compared to the control animals.

Prior to evaluating the possible anti-apoptotic activity of p35 expression in *lox*P-p35 mice, it was important to establish that p35 expression could be activated by Cre recombinase. In the current study, this was assessed by electroporating cultured retinal explants from *lox*P-p35 mice with CMV promoter-driven iCre. However, unfortunately no immunostaining for p35 protein was detected in retinal sections from P14 cultured explants, on repeated attempts using two different p35 antibodies and modifying experimental protocols (Figure 5.6: A). As iCre protein expression was detected in the same retinal explant sections, indicating a successful electroporation and p35 expression could not be detected in a positive control of a retinal explant electroporated with a p35 plasmid construct, the lack of p35 detection may have been a function of the immunohistochemical assay. Furthermore, the functionality of iCre was shown in a previous study described in Chapter 4: 4.3.2, by co-transfection of a β-gal reporter *lox*P plasmid (pCMVβ.Neo)

with pciCre into 293T cells (Figure 4.6). However, to confirm that the *lox*P sites of the transgene were intact, genomic tail DNA from a *lox*P-p35 animal was sequenced, and the sequences of the *lox*P sites 5' and 3' of the neomycin gene were found to be correct (Figure 5.11).

Both the α-loop anti-p35 and mouse anti-p35 antibodies detected p35 expression in transiently transfected cells (Figure 5.5: C, Figure 5.10: C), but not in a primary system of cultured retinal explants. One hypothesis is that p35 epitopes are masked in mammalian cells due to the conformation of p35 protein folding or interaction with endogenous cellular proteins. It is notable that a study published in 2003, demonstrated that p35 interacts with a subunit of human RNA polymerase II (Takramah *et al.*, 2003). Although several papers have demonstrated p35 expression in neuronal cells and oligodendrocytes from p35 transgenic models, amplification kits were used in each study, indicating the p35 signal is weak (Shibata *et al.*, 2000; Viswanath *et al.*, 2000; Tomioka *et al.*, 2002). Furthermore, several other studies that have undertaken experiments with p35 transgenic models, have used other techniques to detect p35 expression including Western blotting (Izquierdo *et al.*, 1999), RT-PCR and *in situ* hybridization (Araki *et al.*, 2000; Hisahara *et al.*, 2000; Tamura *et al.*, 2005).

An alternative method for assessing p35 expression in cultured retinal explants was explored, namely real-time RT-PCR. Retinal explants from *lox*P-p35 animals were electroporated with iCre constructs at P0, and the level of p35 expression quantified by analysing RNA isolated from retinal explants cultured for either 8 or 15 days. No difference in p35 expression was detected (Figure 5.12), although significant iCre expression was detected in RNA from retinal explants electroporated with iCre constructs, compared to those electroporated with control constructs (Figure 5.13). The result from this experiment suggested that the level of iCre expression from electroporated plasmid constructs in retinal explants may not have been sufficient for recombination of the neomycin gene and subsequent p35 expression.

Prior to continuing work with the *lox*P-p35 animal model using alternative methods of Cre recombinase delivery discussed further on, a study was undertaken to

evaluate the anti-apoptotic activity of p35 in wt cultured retinal explants exposed to a chemical agent, A23187. Following electroporation at P0 with plasmid constructs expressing p35, and control constructs, retinal explants were exposed to 5μM of a calcium ionophore, A23187, for 24 hours. Subsequently retinal explants were cryosectioned and assayed for apoptosis using TUNEL staining. Explants electroporated with p35 were determined to have approximately 20% TUNEL positive cells compared to approximately 26% from retinal explants electroporated with a control construct expressing EGFP, suggesting a modest but significant level of protection against apoptosis mediated by p35 expression ($P < 0.05$) (Figure 5.24).

As on average approximately 15-20% of cells are electroporated, to more accurately assess the level of possible protective effects of p35, only cells expressing EGFP were examined for TUNEL staining. Of the cells expressing EGFP alone, approximately 34% were TUNEL positive compared to approximately 19% of cells expressing pEGFP.p35, a reduction in TUNEL positive staining of approximately 50% (Figure 5.25). While this result is extremely encouraging and supports the further evaluation of p35 using the *lox*P-p35 transgenic model, it will likely require further validation. However, the combination of the result from this study and the earlier studies evaluating p35 in 661W cells and *Drosophila* models of RP, suggest that the further exploration of the anti-apoptotic activity of p35 in mammalian photoreceptors would be valuable. Hence, using viral based delivery methods for p35, were also explored in the current study and are discussed below.

Firstly, the mammalian retina is an ideal target for gene delivery by viral-based vectors, as it is easily accessible, enclosed and immune privileged (Surace *et al.*, 2003; Rolling 2004). Viral vectors based on adeno-associated viruses (AAV) have been demonstrated to be effective and safe gene delivery agents to the retina, due to characteristics including: 1) a lack of pathogenicity, 2) the ability to transduce non-dividing cells, such as photoreceptors, 3) low immunogenicity and 4) the maintenance of long-term gene expression (Carter *et al.*, 2000; Buning *et al.*, 2003). Numerous studies have demonstrated successful AAV retinal delivery of therapeutic genes in animal models of retinal degeneration (Acland *et al.*, 2001; Gorbatyuk *et al.*, 2005; Pawlyk *et al.*, 2005) (see Chapter 1: 1.3.5.1).

Given this, and the results from the current study suggesting that iCre expression from a plasmid construct may not be sufficient to restore p35 activity in *lox*P-p35 explants, two AAV viral vectors expressing iCre (AAV-iCre.EGFP) and p35 (AAV-p35) were generated. Having determined the genomic viral titre and infectious titres of AAV-iCre.EGFP to be 1 x 10^9 vp/ml, and 2 x 10^7 vp/ml respectively, AAV delivery of iCre to cultured retinal explants, may be undertaken to determine whether adequate expression levels of iCre to activate p35 expression, would be achieved. AAV-p35 (9 x 10^9 vp/ml) could be used to further explore the anti-apoptotic potential of p35 expression against chemical-induced apoptosis in retinal explants. Given the difficulties in assessing p35 expression using immunohistochemistry, it may also be worth exploring *in situ* hybridisation as an alternative method.

While the AAV vectors generated in the current study can be utilised in retinal explants, studies have indicated that vectors based on AAV serotype 2, are not optimal for photoreceptor transduction. Numerous different AAV serotypes have been identified in humans and primates (Verma *et al.,* 2005), which vary in cellular tropism and efficiency of expression (Auricchio 2003). As the AAV capsid proteins determine cellular tropism, hybrid AAV vectors have been generated, combining the genome of one serotype and the capsid protein of another (Gao *et al.,* 2002; Rabinowitz *et al.,* 2002). Investigations of the cellular tropism of such hybrid AAV vectors in the retina, have shown that AAV-2/5 (genome of AAV-2, and capsid protein of AAV-5), transduces photoreceptors with a greater efficiency than AAV-2/2, which also transduces retinal pigment epithelial (RPE) cells (Auricchio *et al.,* 2001; Yang *et al.,* 2002). Furthermore, it is also possible to generate higher viral titres of between 10^{10} and 10^{13} vp/ml, which is of critical relevance to the retina, as subretinal delivery is limited to 0.5-2μl in volume.

Given that the technology for generating AAV-2/5 vectors is now available in the laboratory in TCD, it will be likely used to generate AAV-2/5 expressing iCre or p35. For example, delivery of AAV-2/5.iCre to retinas of *lox*P-p35 animals could be undertaken to assess p35 activation *in vivo*. Apoptosis could then be induced using light or chemicals and the potential protective effect of p35 expression assesssed. In

parallel with this, the generation of transgenic animals with photoreceptor-specific expression of iCre (Chapter 4) and use of the *lox*P-p35 transgenic mouse model should in principal, enable the generation of a line of animals with p35 expression specifically in rod or cone photoreceptors. Finally the generation of AAV-2/5.p35 vector will enable the exploration of p35 protection subsequent to sub-retinal delivery, in a range of animal models of retinal degeneration, including light-or chemical-induced retinal damage, or inherited mouse models, such as the Pro23His mouse, carrying an adRP rhodopsin mutation (Olsson *et al.,* 1992).

In addition, results from a number of studies investigating apoptotic pathways of photoreceptor degeneration *in cellulo* and *in vivo*, have indicated that another group of proteases, namely calpains, in addition to the caspases, may be involved in apoptosis (Sanvicens *et al.,* 2004; Sharma *et al.,* 2004). Most recently, Doonan *et al.*, (Doonan *et al.,* 2005) demonstrated that treatment of retinal explants from the *rd* mouse model of retinal degeneration, with a calpain inhibitor, although inhibiting cleavage of a calpain-specific substrate, did not result in any significant protection against photoreceptor degeneration. This result led the authors to suggest that a therapeutic strategy of targeting multiple pathways of apoptosis in photoreceptor degeneration may be more effective for retarding apoptosis. Given this, it may be of interest to explore the possible synergistic effect of delivering p35 with additional therapeutic agents targeting proteases such as the calpains, involved in caspase-independent apoptosis.

While significant steps towards achieving the experiments outlined above have been made in this study, clearly there is still a substantial amount of work to be undertaken. However, the results from the current study support the further evaluation of the p35 protein as an anti-apoptotic agent in degenerating mammalian photoreceptors and continuation of the work, as outlined above, is being planned.

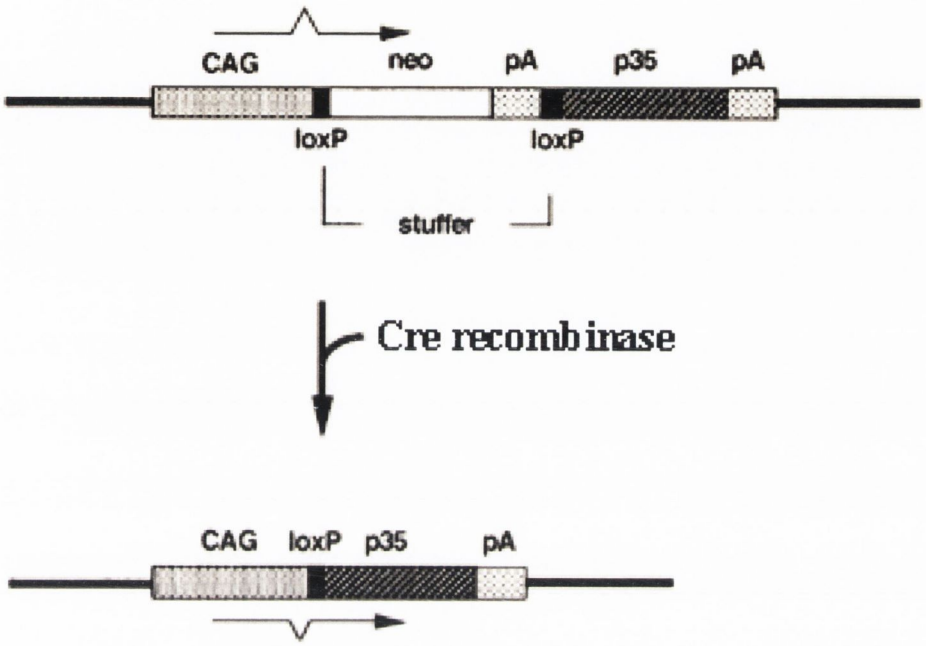

CAG: Cytomegalovirus IE enhancer and chicken β-actin promoter

***lox*P**: Cre recognition site

Neo: Neomycin gene

p35: Coding sequence for baculoviral p35 gene

pA: Polyadenylation signal

Figure 5.1*: Diagram of the *lox*P-p35 transgene: CAG promoter, *lox*P-neo-*lox*P, p35 coding sequence and polyadenylation signal. The arrow indicates the interrupted expression of the p35 gene. Excision of the neo stuffer sequence by Cre recombinase results in expression of the p35 gene. Sequence of the transgene is given in Appendix 2.2. *Diagram modified from Araki *et al.*, 2000.

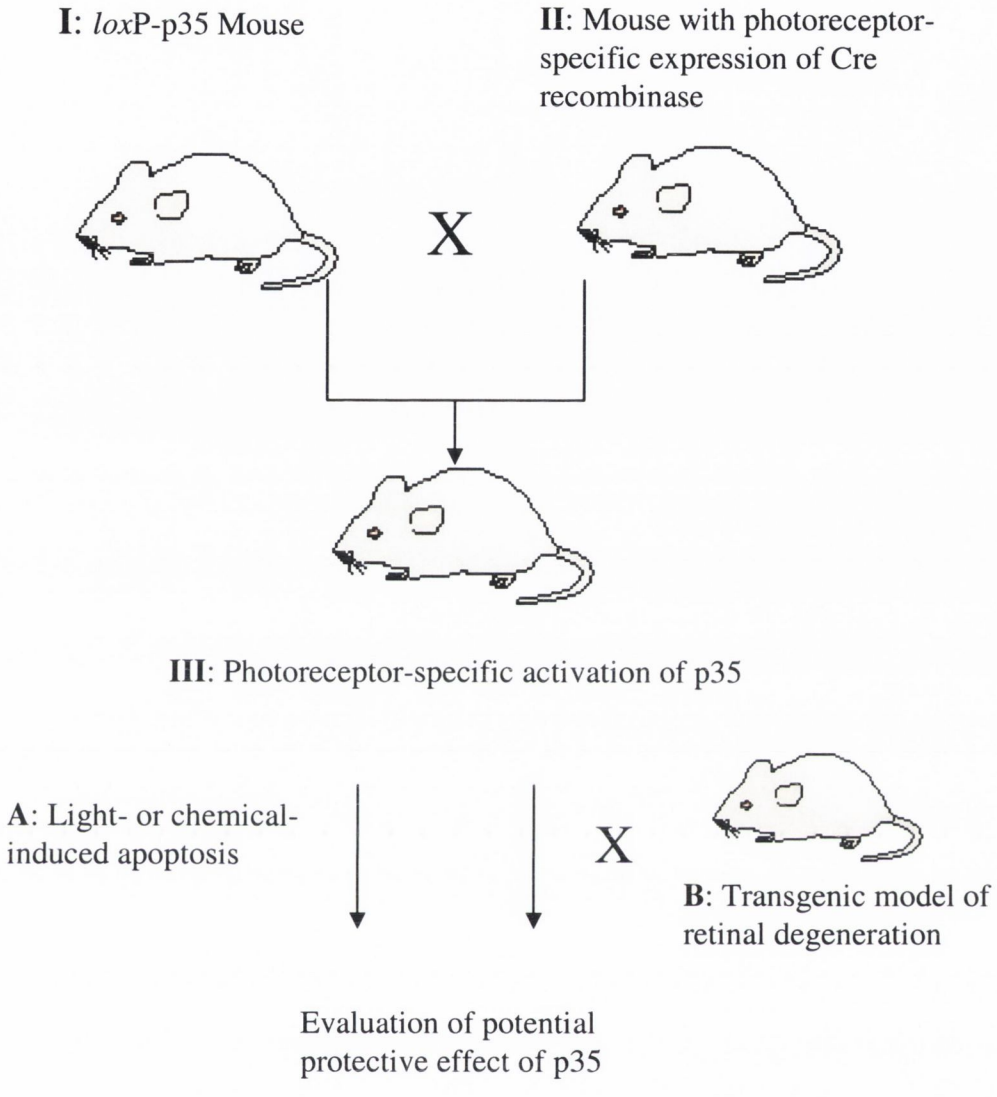

Figure 5.2: Diagram of potential approaches for evaluating the anti-apoptotic activity of p35 *in vivo*. Crossing *lox*P-p35 transgenic mice **(I)** with models with photoreceptor specific expression of Cre recombinase **(II)**, should in principle, generate models with conditional activation of p35 in photoreceptors **(III)**. Two possible approaches could be followed: **(A)** induction of apoptosis using light or chemicals, or **(B)** crossing model **III** with a model of retinal degeneration, to evaluate the potential anti-apoptotic effects of p35 expression.

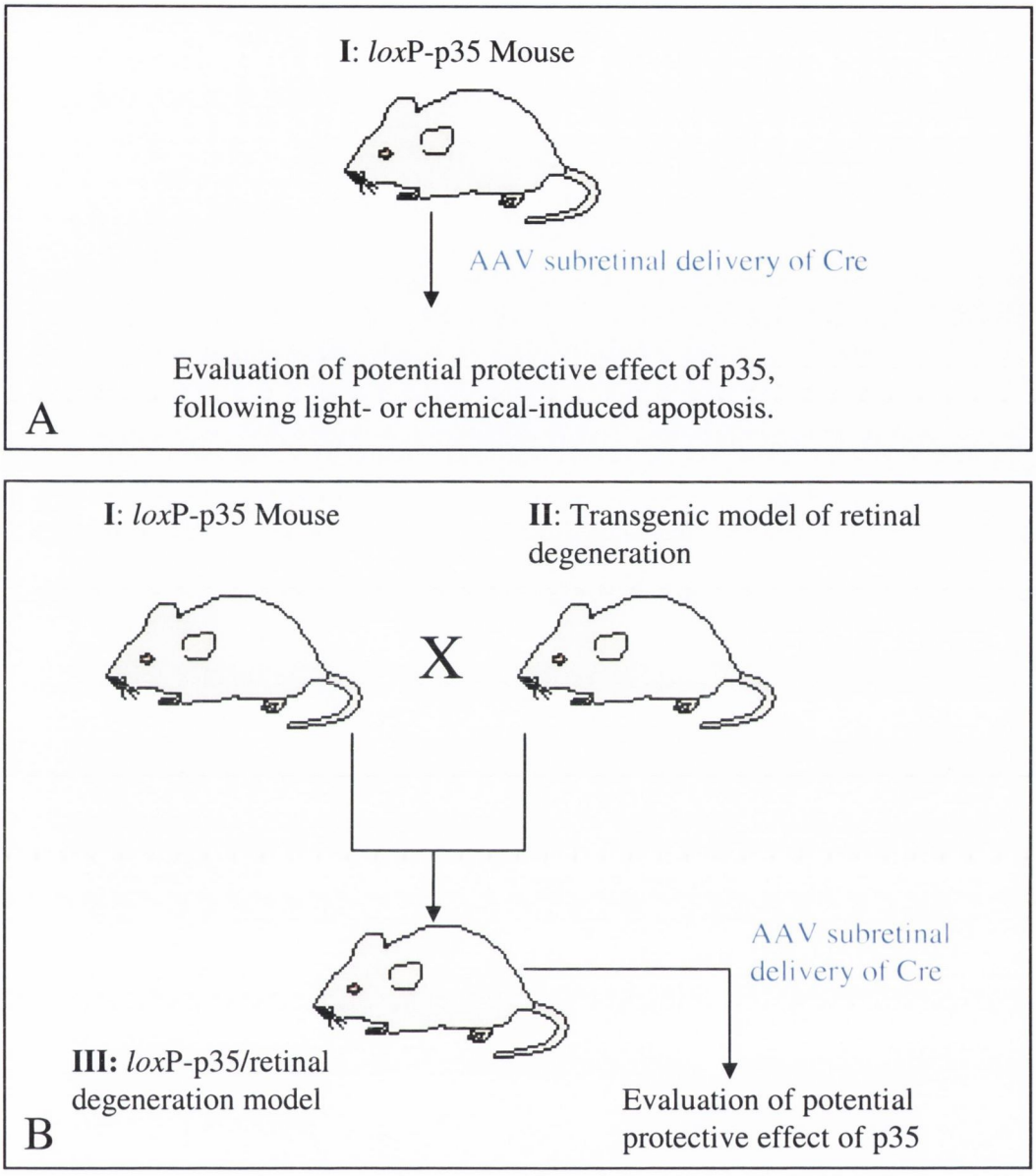

Figure 5.3: Diagram of potential approaches for evaluating the anti-apoptotic activity of p35 *in vivo*. **(A)** p35 expression could be activated in *lox*P-p35 transgenic mice **(I)** by subretinal AAV delivery of Cre. Following induction of apoptosis by light or chemicals, the potential anti-apoptotic activity of p35 could be evaluated. Alternatively **(B)**, *lox*P-p35 models **(I)** could be crossed with models of retinal degeneration **(II)**. p35 expression could then be activated in subsequent transgenic models **(III)** using AAV-Cre, to evaluate the potential protective effect of p35 expression.

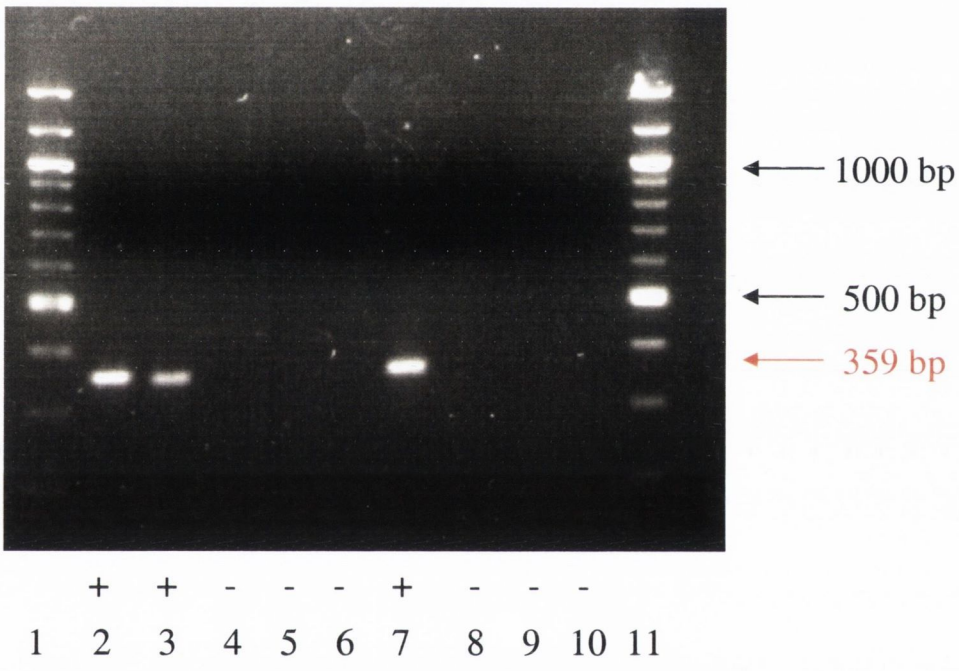

Figure 5.4: PCR analysis of DNA extracted from tails of F1 pups from a mating pair of a C57BL/6J female and *lox*P-p35 male. Fp35-3 and Rp35-4 primers were used for PCR amplifications of the transgene (see 5.2.2). Lane 1, 100 bp DNA ladder; Lanes 2-8, DNA from seven pups with PCR product of 359 bp present in lanes 2, 3 and 7; Lane 9, DNA from a wt C57BL/6J mouse; Lane 10, water blank; Lane 11, 100 bp DNA ladder. The + and – signs indicate the respective presence and absence of the *lox*P-p35 transgene.

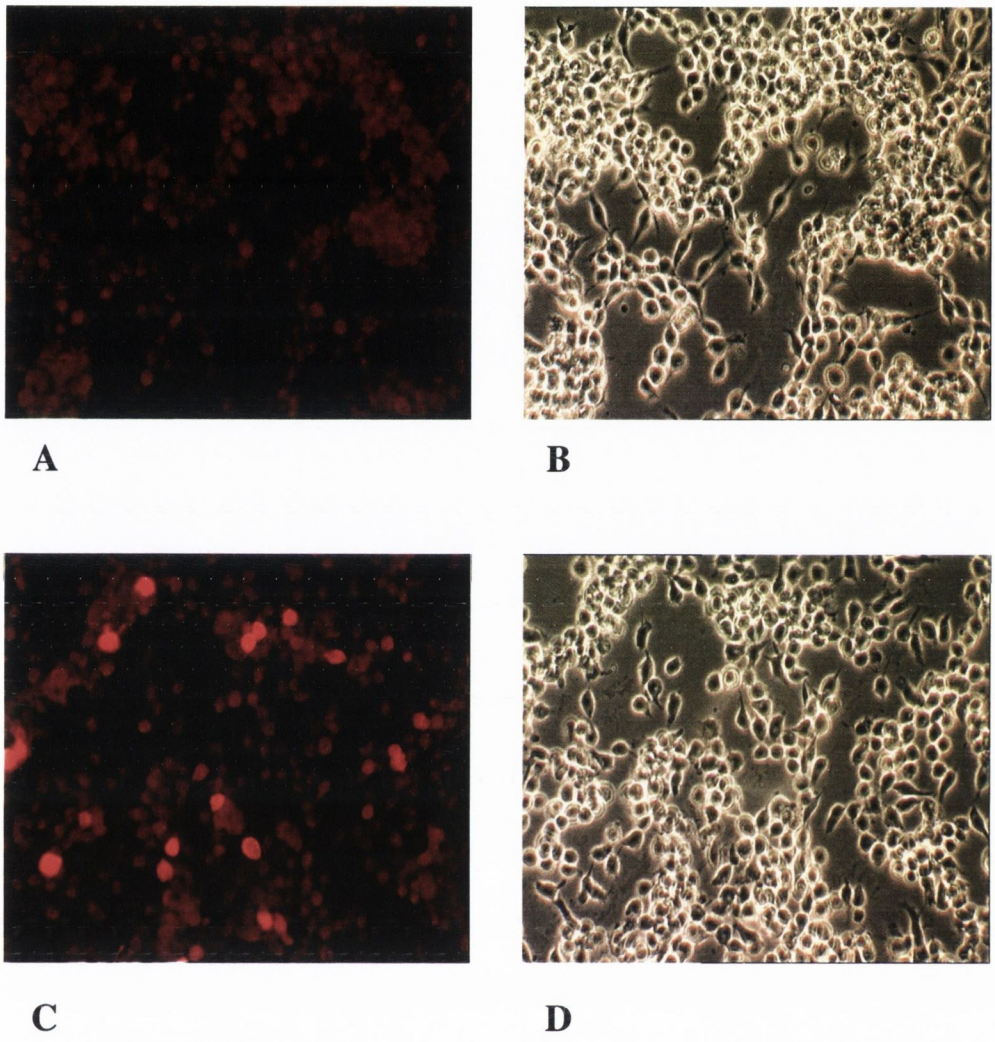

Figure 5.5: Immunostaining of HeLa cells for p35 expression. HeLa cells were transiently transfected and probed for p35 expression with the α-loop anti-p35 antibody (1:250) and Alexa Fluor 568 secondary antibody (1:1000) (see 5.2.3). **(A)** shows HeLa cells transfected with pcDNA3.1+ and **(C)** shows HeLa cells transfected with pcDNA3.1.p35 under fluorescent light. **(B)** and **(D)** show the corresponding images under white light with phase contrast (200X).

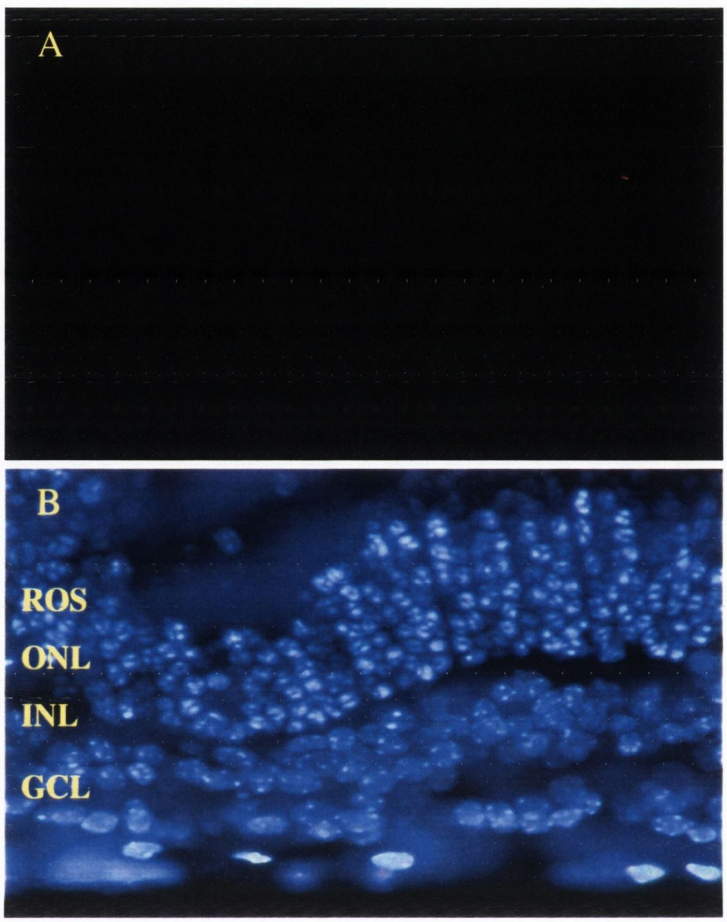

Figure 5.6: Immunostaining of retinal explant vibratome sections for p35 expression. P0 *lox*P-p35 retinal explants, electroporated with pcDNA3.1.p35, were cultured for 14 days, fixed and sectioned (see 5.2.4-5). Sections were probed for p35 expression with the α-loop anti-p35 antibody (1:250) and Alexa Fluor 568 anti-rabbit secondary antibody (1:1000). **(A)** shows the explant section under green fluorescent light for detection of Alexa Fluor 568, with no immunostaining for p35. The same section is shown under UV light with DAPI nuclear staining in **(B)** (400X). The retinal layers are highlighted in yellow: ROS, rod outer segments, ONL, outer nuclear layer, INL, inner nuclear layer and GCL, ganglion cell layer. Clearly the retinal layers are not as uniform compared to retinal sections from wt mice, but it should be noted that retinal explants are cultured in an artificial setting from P0.

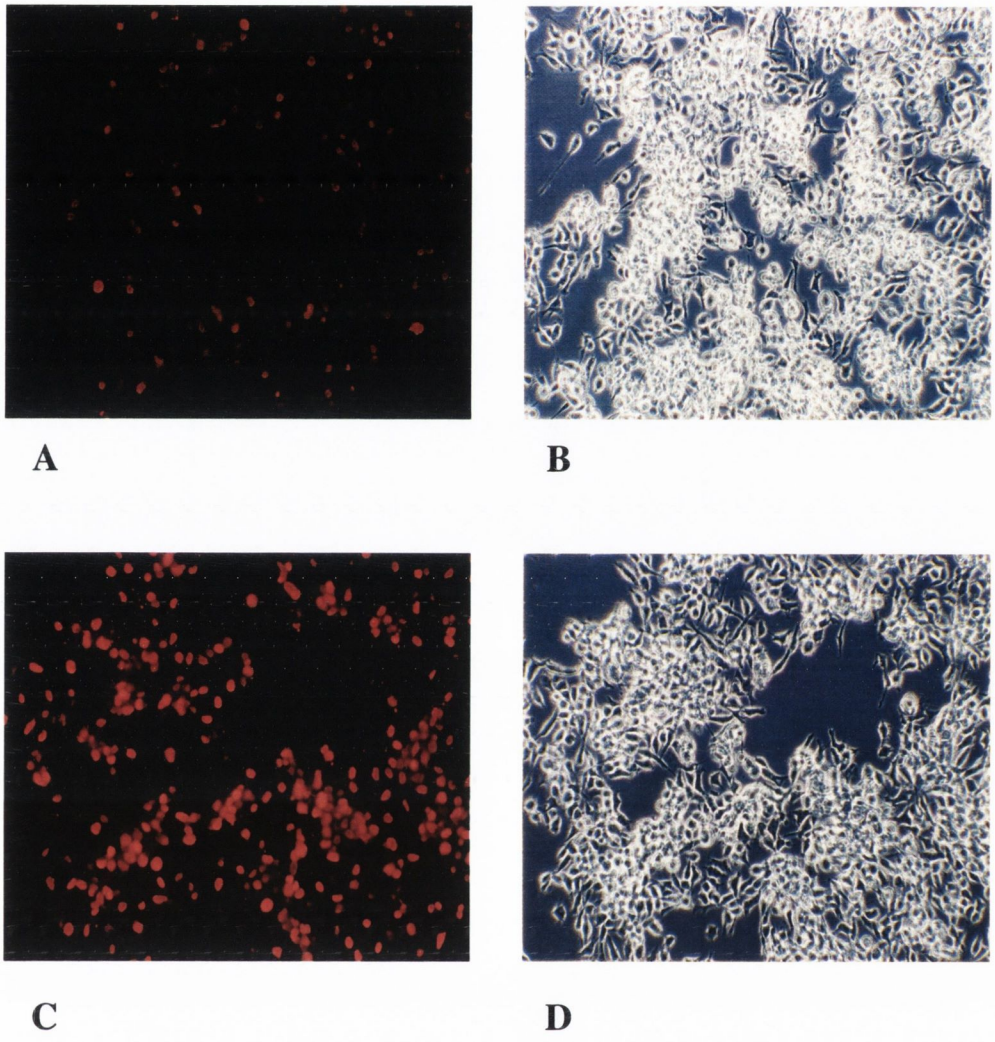

Figure 5.7: Immunostaining of HeLa cells for Cre recombinase expression. HeLa cells were transiently transfected and probed for Cre expression with the anti-Cre antibody (1:500) and Alexa Fluor 568 secondary antibody (1:1000) (see 5.2.3). **(A)** shows HeLa cells transfected with pcDNA3.1+ with background staining and **(C)** shows HeLa cells transfected with pciCre under fluorescent light. **(B)** and **(D)** show the corresponding images under white light with phase contrast (200X).

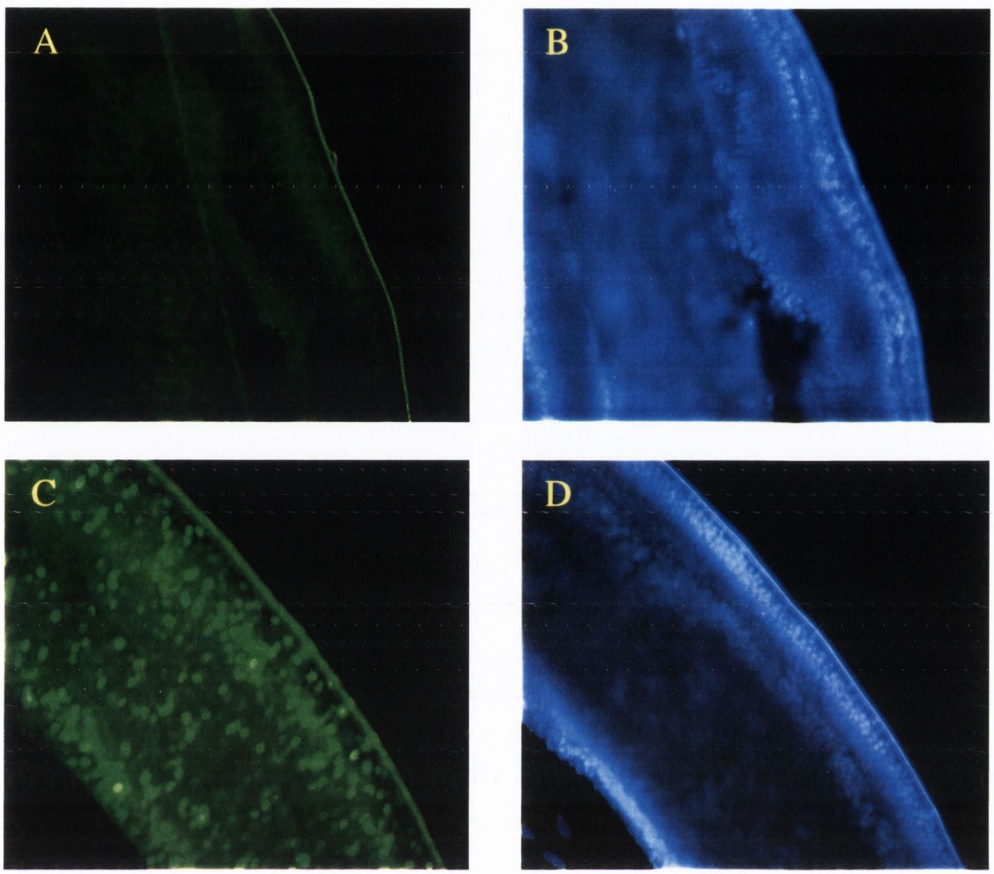

Figure 5.8: Immunostaining of retinal explant vibratome sections for iCre recombinase expression. P0 *lox*P-p35 retinal explants, electroporated with pcDNA3.1+ or pciCre were cultured for 14 days, fixed and sectioned (see 5.2.4-5). Sections were probed for iCre expression with the anti-Cre antibody (1:200) and Alexa Fluor 488 anti-mouse secondary antibody (1:1000). **(A)** and **(C)** show retinal explant sections electroporated with pcDNA3.1+ (200X) and pciCre (400X) respectively, under blue fluorescent light for detection of Alexa Fluor 488. Strong immunostaining for iCre is shown in **(C)**. **(B)** and **(D)** show the corresponding sections under UV light with DAPI nuclear staining.

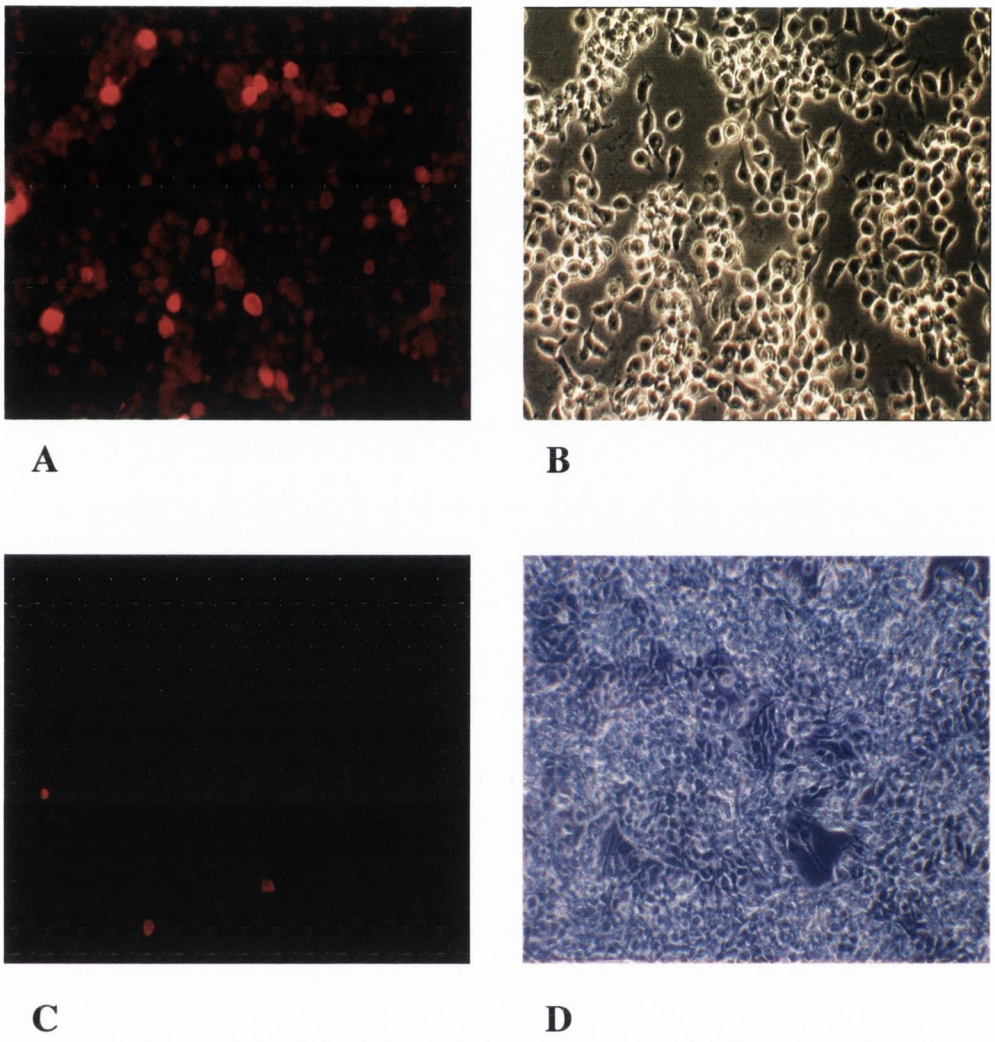

Figure 5.9: Immunostaining of HeLa cells for p35 expression. HeLa cells were transiently transfected and probed for p35 expression with the α-loop anti-p35 antibody (1:250) and Alexa Fluor 568 secondary antibody (1:1000) (see 5.2.3). **(A)** and **(C)** shows HeLa cells transfected with pcDNA3.1.p35, immunostained with Batch 1, and Batch 2, respectively of α-loop anti-p35 antibody, under fluorescent light. **(B)** and **(D)** show the corresponding images under white light with phase contrast (200X).

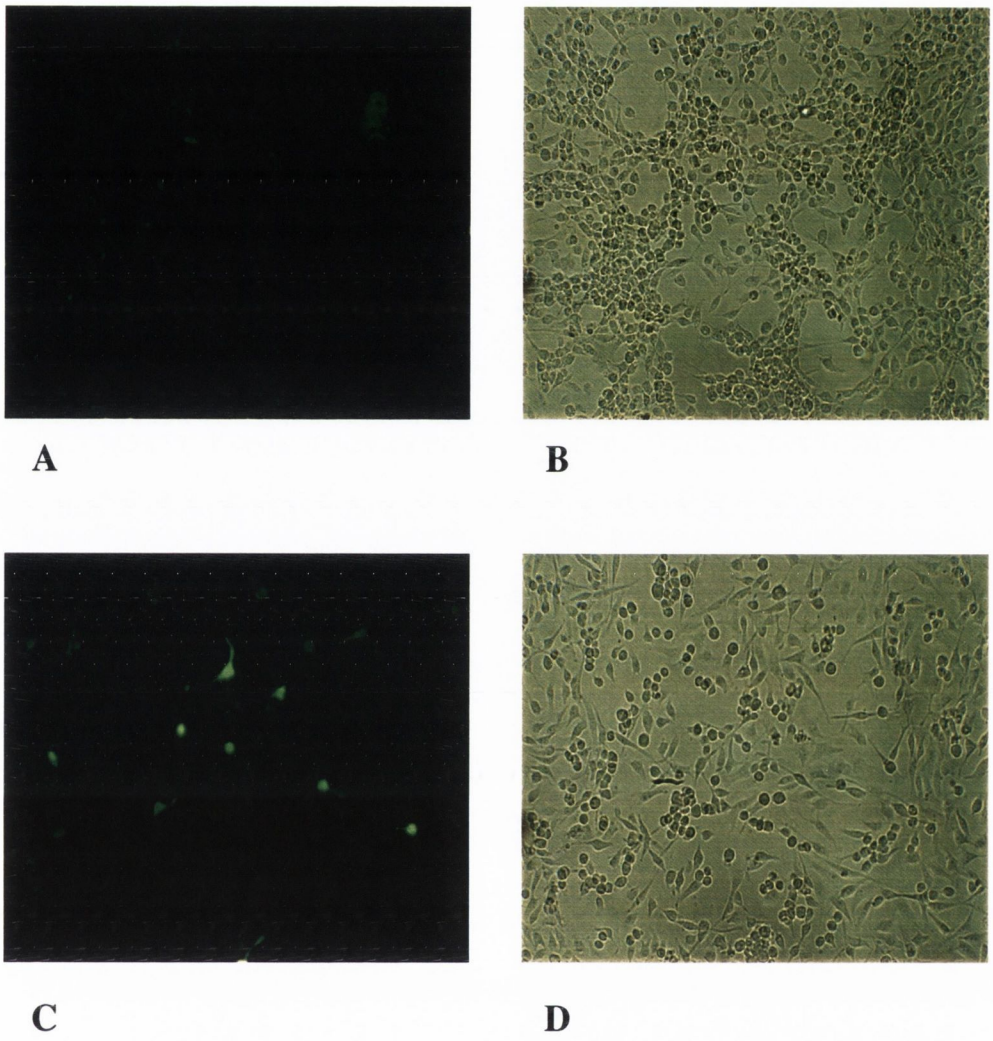

Figure 5.10: Immunostaining of HeLa cells for p35 expression. HeLa cells were transiently transfected and probed for p35 expression with the mouse anti-p35 antibody from Professor Hay (1:100), and Alexa Fluor 488 secondary antibody (1:1000) (see 5.2.3). **(A)** shows HeLa cells transfected with pcDNA3.1+ with background staining and **(C)** shows HeLa cells transfected with pcDNA3.1-.p35 under fluorescent light. **(B)** and **(D)** show the corresponding images under white light with phase contrast (200X).

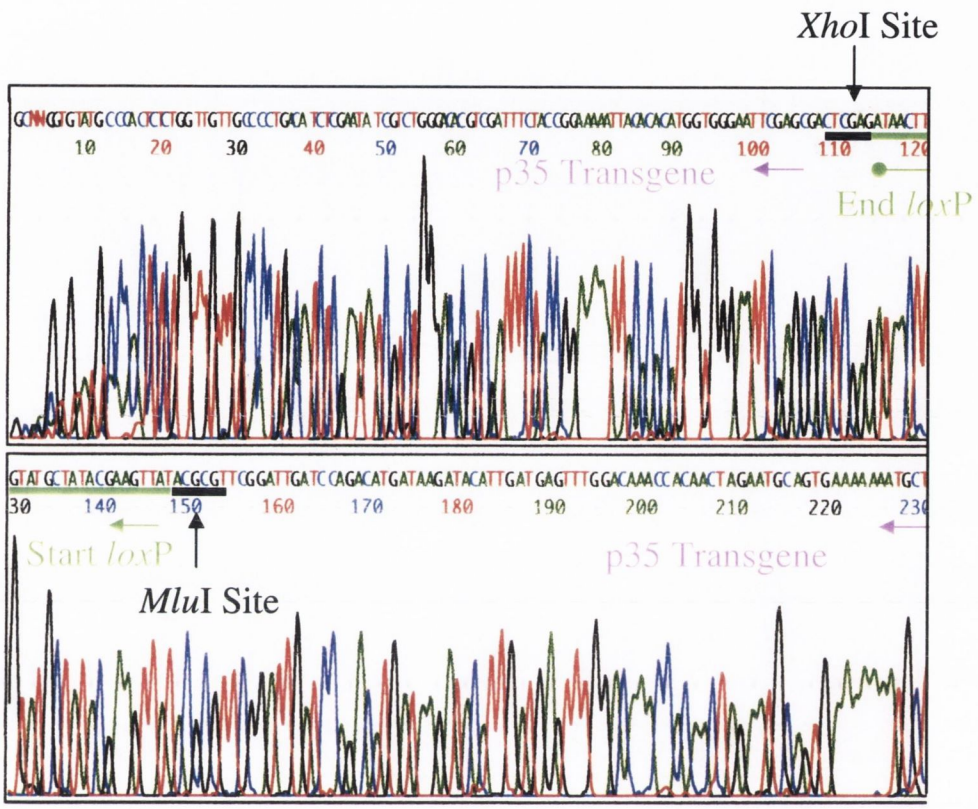

Figure 5.11: Sequence of the second *lox*P site of the *lox*P-p35 transgene: A 750 bp fragment was amplified by PCR from DNA isolated from a *lox*P-p35 transgenic mouse and sequenced using the Rp35B primer (see 5.2.2, 5.2.6). Green underlined sequence indicate the *lox*P sequence in reverse, flanked by *Mlu*I and *Xho*I restriction sites underlined in black. The p35 transgene sequence 5' and 3' of *lox*P site is indicated in purple.

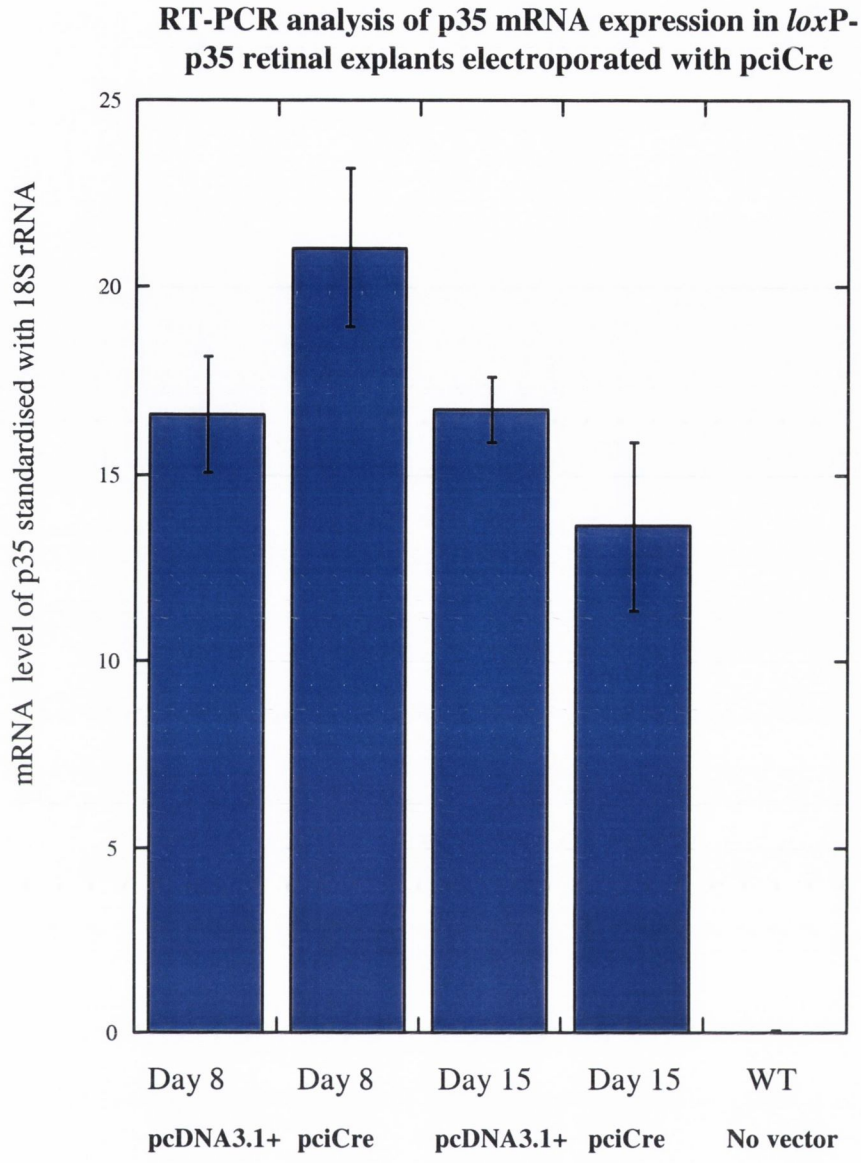

Figure 5.12: RT-PCR analysis of p35 expression in cultured *lox*P-p35 retinal explants. The graph shows the level of p35 expression in retinal explants electroporated with pciCre or pcDNA3.1+ following 8 or 15 days of culturing (see 5.2.7). RNA levels were standardised against the housekeeping gene of 18S rRNA. Bars represent the mean ± S.E. There was no significant increase in the level of p35 expression following electroporation of pciCre ($P > 0.05$). As a negative control, the level of p35 expression was also analysed in retinal explants from wt C57BL/6J mice and as expected was not detected.

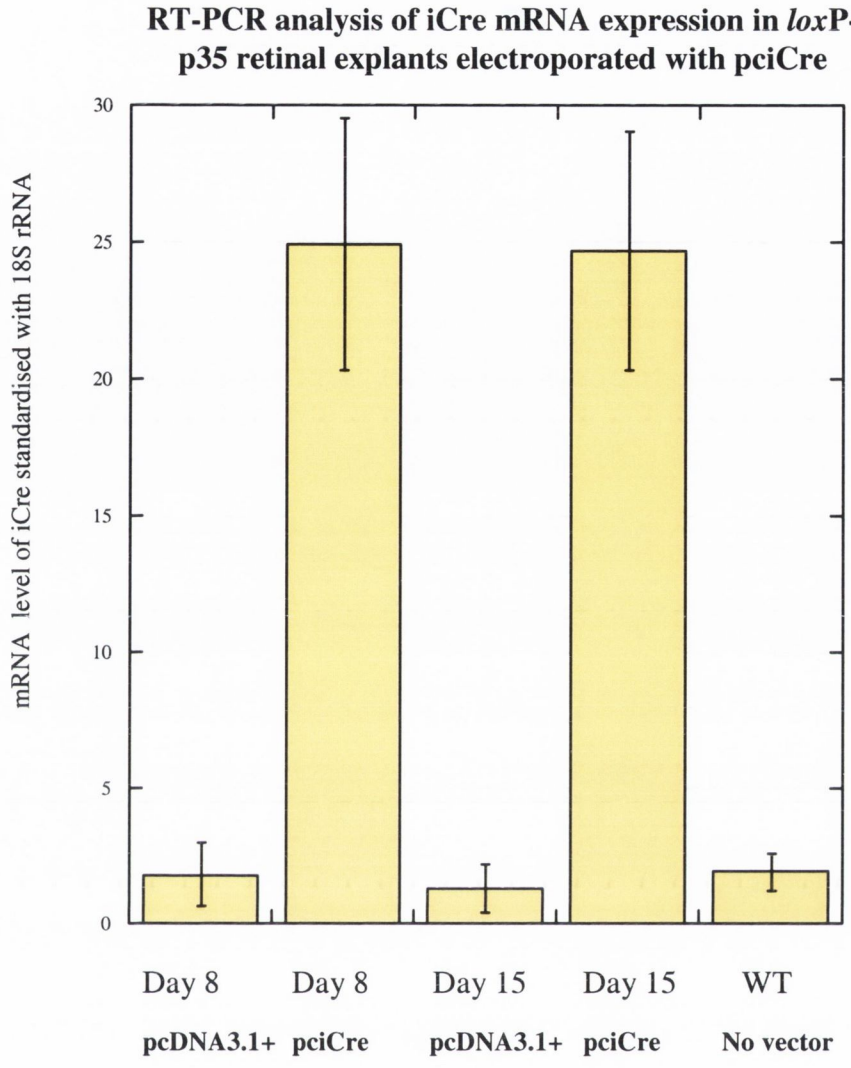

Figure 5.13: RT-PCR analysis of iCre expression in cultured *lox*P-p35 retinal explants. The graph shows the level of iCre expression in retinal explants electroporated with pciCre or pcDNA3.1+ following 8 or 15 days of culturing (see 5.2.7). As a negative control, the level of iCre expression was also analysed in retinal explants from wt C57BL/6J mice. RNA levels were standardised against the housekeeping gene of 18S rRNA. Bars represent the mean ± S.E. Electroporation of pciCre was successful, as indicated by the increase in the level of iCre at both day 8 and 15, compared to retinal explants electroporated with pcDNA3.1+ or wt retinal explants.

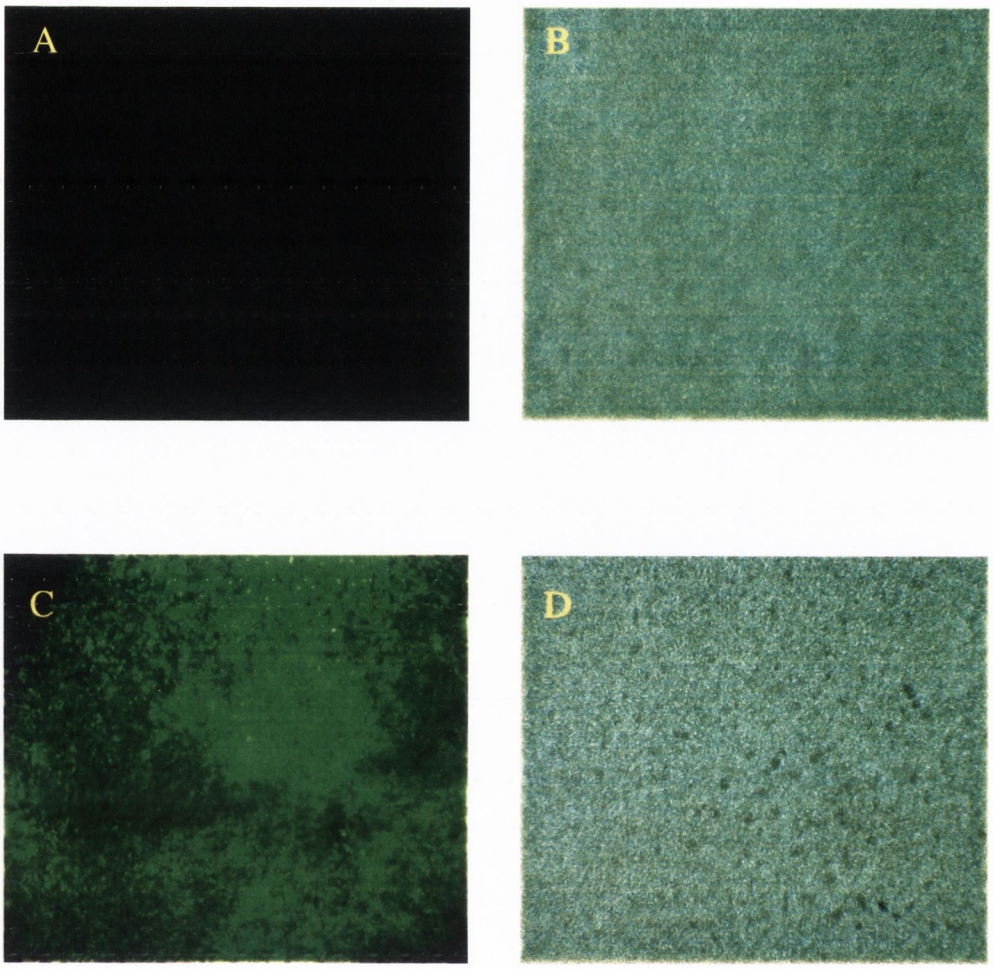

Figure 5.14: *lox*P-p35 retinal explant electroporated with pCMV.EGFP and pciCre. **(A)** and **(C)** show cultured P14 retinal explants, following electroporation with **(A)** pcDNA3.1+ and **(C)** pCMV.EGFP (as an indicator of electroporation efficiency) and pciCre, under fluorescent light (see 5.2.7). The fluorescence in **(C)** indicates that electroporation was successful. **(B)** and **(D)** show the corresponding images under white light (200X).

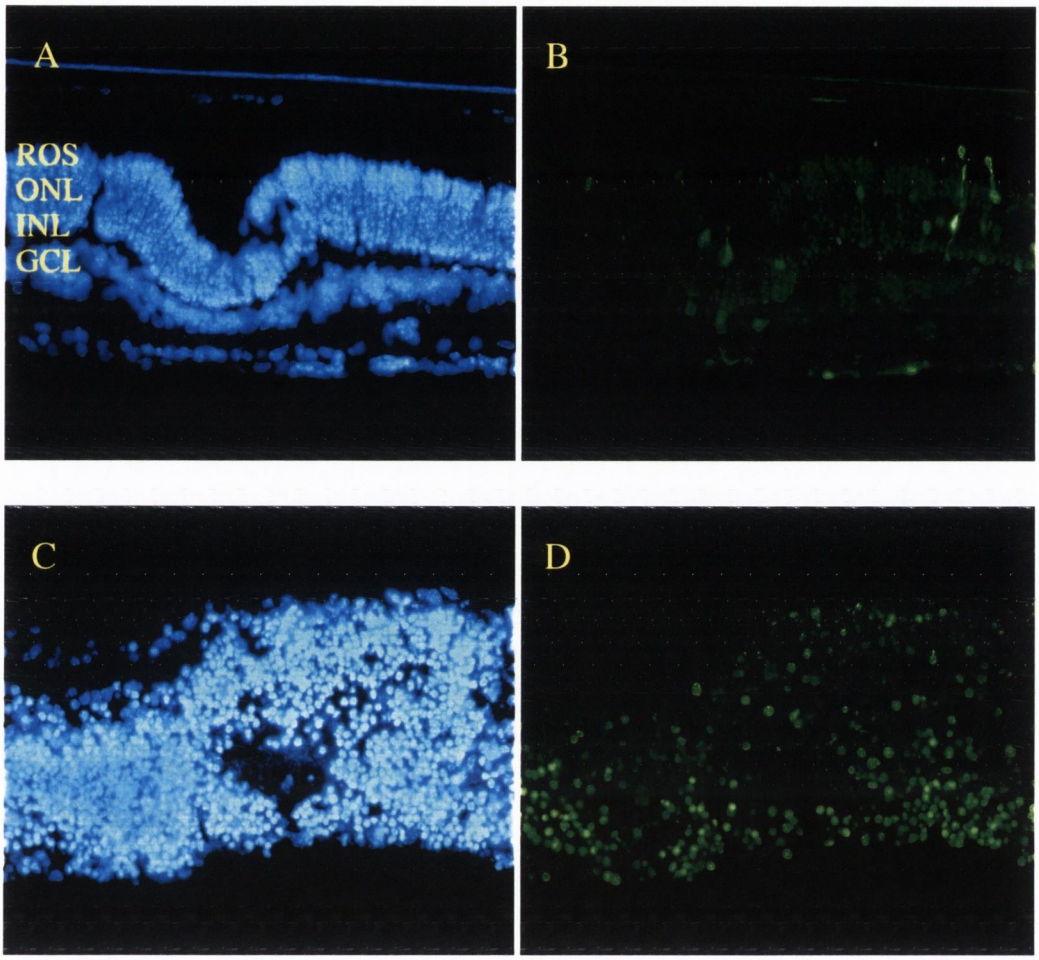

Figure 5.15: Cryosections of cultured wt retinal explants treated with A23187 and TUNEL stained. Retinal explants were treated with 5μM A23187 for 24 hours (P10), sectioned (7μm) and TUNEL stained (see 5.2.10). **(B)** and **(D)** show untreated and treated sections under fluorescent light. The corresponding DAPI stained sections are shown in **(A)** and **(C)** (400X). The retinal layers are marked in yellow: ROS, rod outer segments, ONL, outer nuclear layer, INL, inner nuclear layer and GCL, ganglion cell layer.

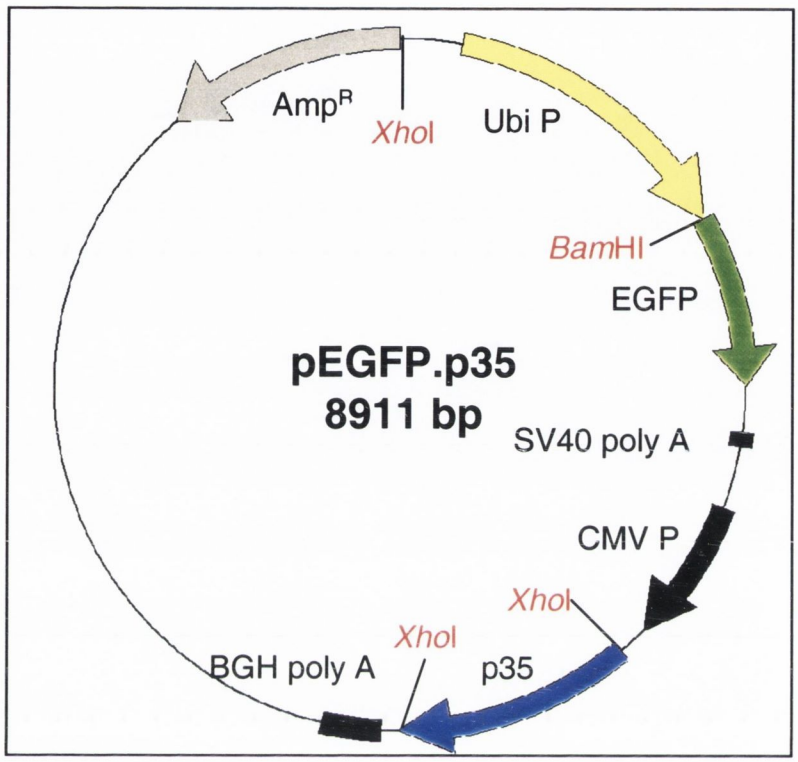

Ubi P: Ubiquitin promoter (bases 300-1509)

EGFP: Enhanced green fluorescent protein (bases 1554-2273)

SV40 poly A: SV40 polyadenylation signal (bases 2427-2477)

CMV P: Cytomegalovirus promoter (bases 2738-3325)

p35: 950 bp of baculoviral p35 gene (bases 3455-4404)

BGH poly A: Bovine growth hormone polyadenylation signal (bases 4512-4736)

Amp^R: Ampicillin resistance gene (bases 7916-8911)

Figure 5.16: Plasmid map of pEGFP.p35. Restriction enzyme sites are shown in red. This construct contains a ubiquitin promoter-driven EGFP gene, and a CMV promoter-driven p35 gene (see 5.2.8). Sequence is given in Appendix 2.3.1.

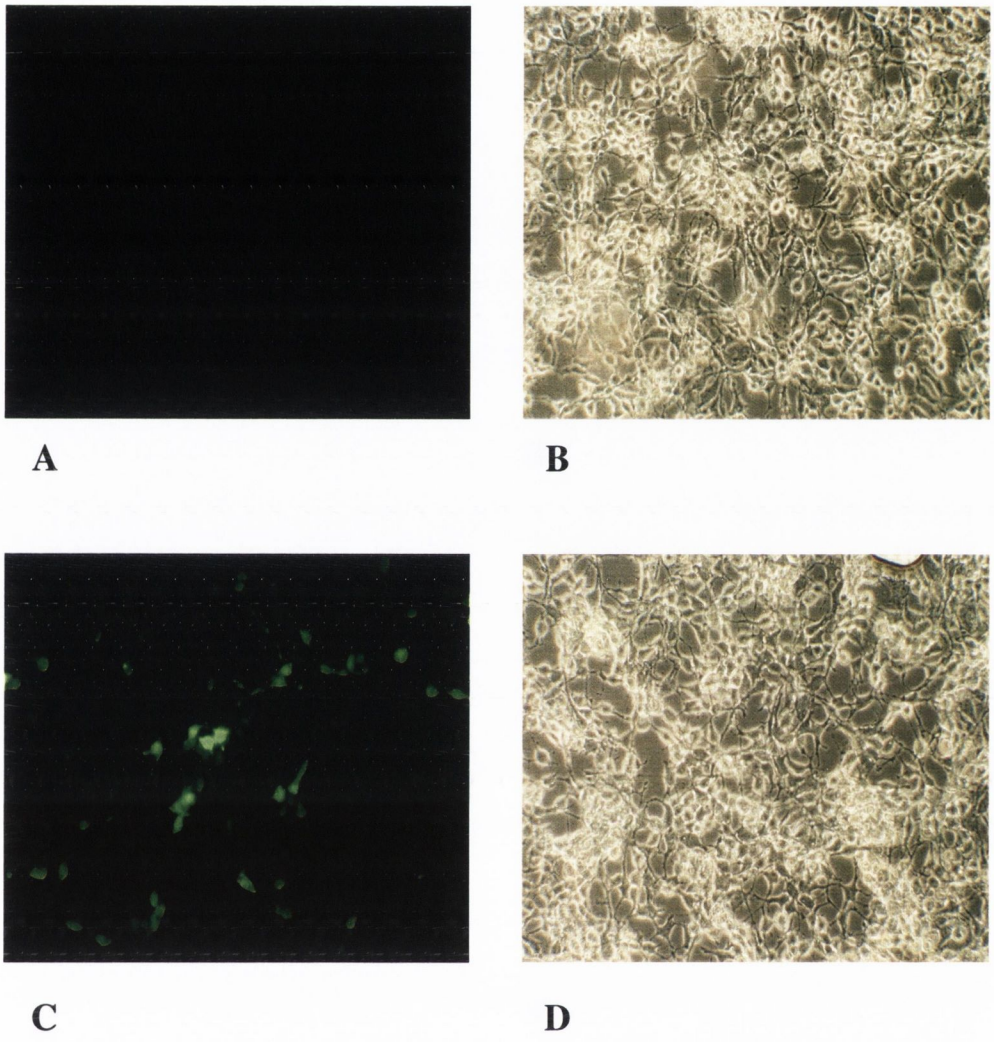

Figure 5.17: HeLa cells transiently expressing pEGFP.p35. HeLa cells were plated at a concentration of 3 x 10^5 per well of a 6-well plate and transfected with pEGFP.p35 or pcDNA3.1+ with Lipofectamine 2000 (see 5.2.9). Following 48 hours cells were fixed and examined using a fluorescent microscope for EGFP expression. **(A)** and **(C)** show HeLa cells transfected with pcDNA3.1+ and pEGFP.p35 respectively under fluorescent light. **(B)** and **(D)** show the corresponding photographs under white light (200X).

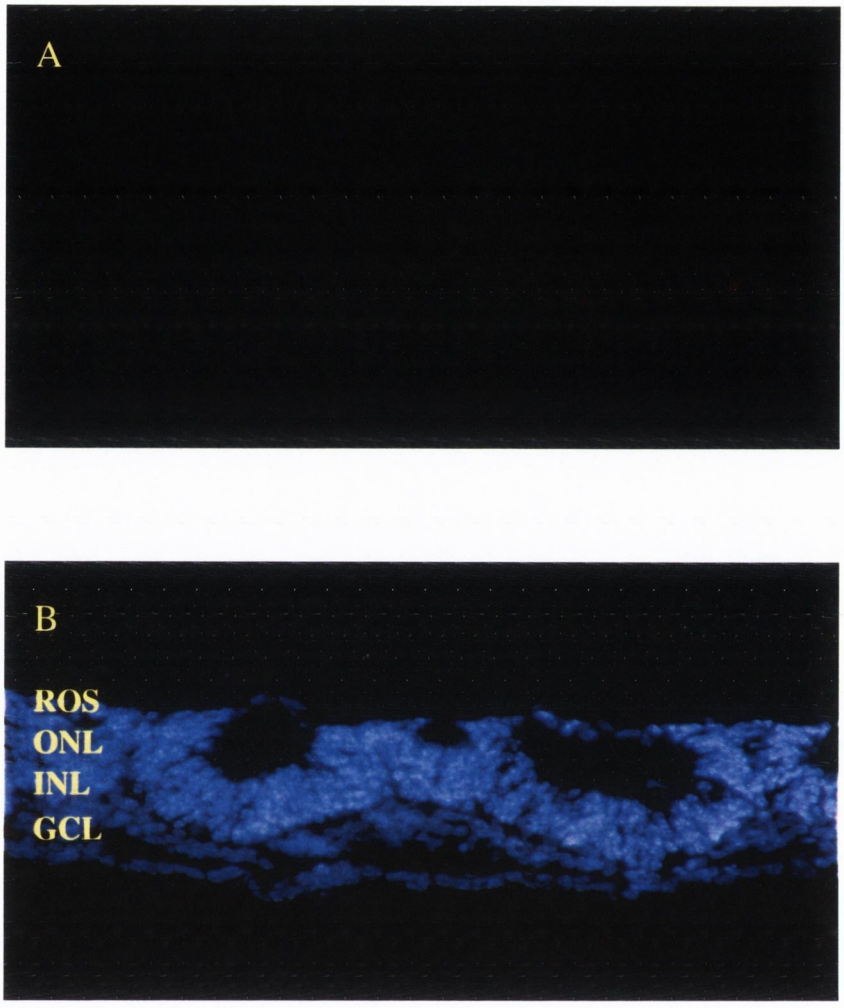

Figure 5.18: Cryosection of a cultured wt retinal explant, TUNEL stained. Representative photograph of a cryosection (7μM) from a P11 cultured retinal explant, assayed for cell death using TUNEL staining (see 5.2.11). **(A)** shows a retinal section under fluorescent light with no TUNEL staining. **(B)** shows the same section, DAPI stained (200X). The retinal layers are marked in yellow: ROS, rod outer segments, ONL, outer nuclear layer, INL, inner nuclear layer and GCL, ganglion cell layer.

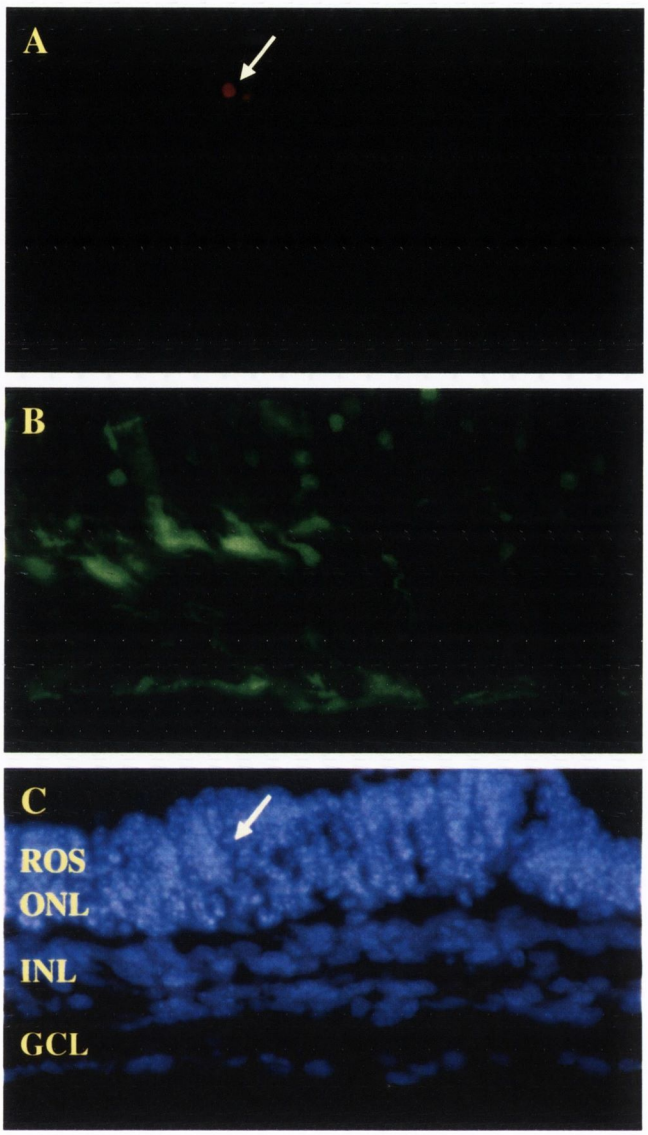

Figure 5.19: Cryosection of a cultured retinal explant, TUNEL stained. Representative photograph of a cryosection (7μM) from a P11 cultured retinal explant, electroporated with pCMV.EGFP, and assayed for cell death using TUNEL staining (see 5.2.11). A retinal section is shown under fluorescent light to examine: **(A)** TUNEL staining (a TUNEL positive cell is indicated by a white arrow), **(B)** EGFP expression, and **(C)** nuclear staining with DAPI. The retinal layers are marked in yellow: ROS, rod outer segments, ONL, outer nuclear layer, INL, inner nuclear layer and GCL, ganglion cell layer.

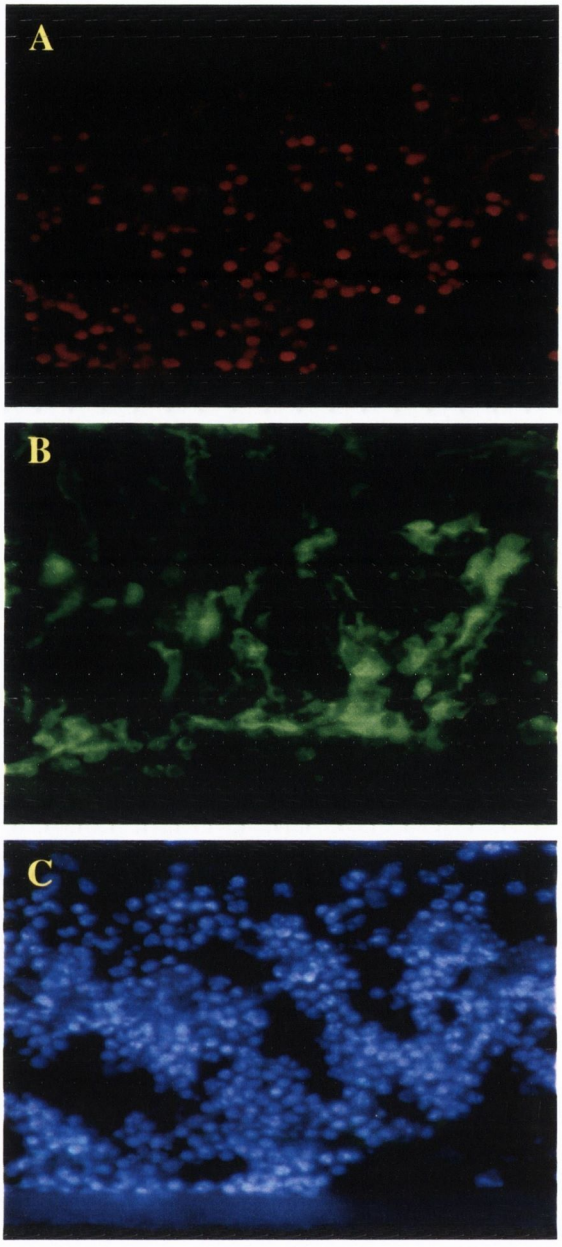

Figure 5.20: Cryosections of cultured retinal explants, TUNEL stained. Representative photographs of cryosections (7μM) from P11 cultured retinal explants, electroporated with pCMV.EGFP, treated with the apoptosis-inducing agent A23187 (5μM) for 24 hours, followed by TUNEL staining for cell death (see 5.2.11). The retinal section is shown under fluorescent light to examine: **(A)** TUNEL staining, **(B)** EGFP expression, and **(C)** nuclear staining with DAPI (400X).

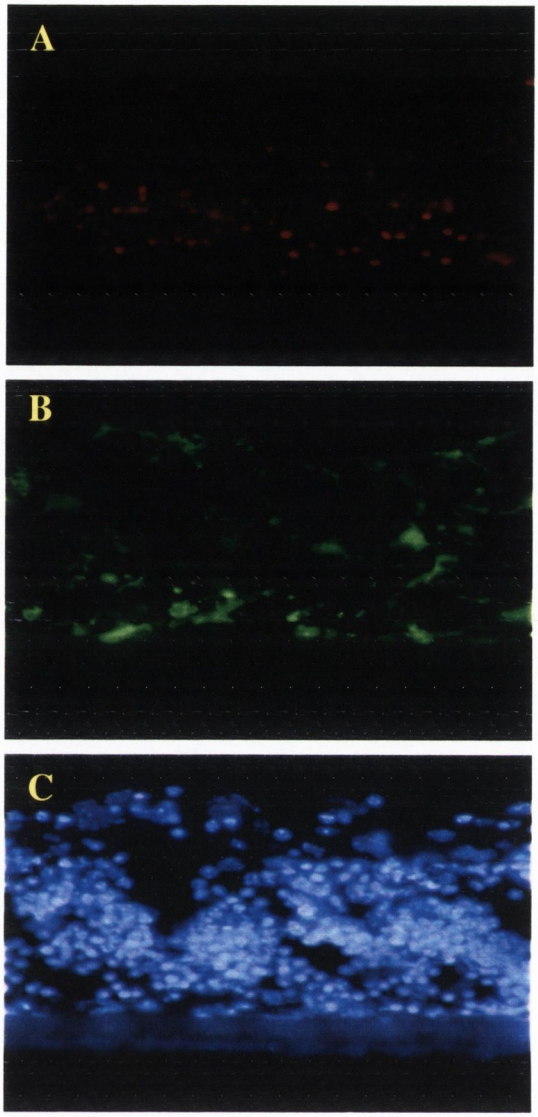

Figure 5.21: Cryosections of cultured retinal explants, TUNEL stained. Representative photographs of cryosections (7μM) from P11 cultured retinal explants electroporated with pCMV.EGFP. Ten days following electroporation, explants were pre-incubated with the pan-caspase inhibitor Z-VAD-FMK (50μM) for 1 hour, treated with the apoptosis-inducing agent A23187 (5μM) for 24 hours, fixed and TUNEL stained (see 5.2.11). The retinal section is shown under fluorescent light to examine: **(A)** TUNEL staining, **(B)** EGFP expression, and **(C)** nuclear staining with DAPI (400X). Note that there is less TUNEL staining compared to retinal explants not pre-incubated with Z-VAD-FMK (Figure 5.20), indicating that apoptosis is caspase-dependent.

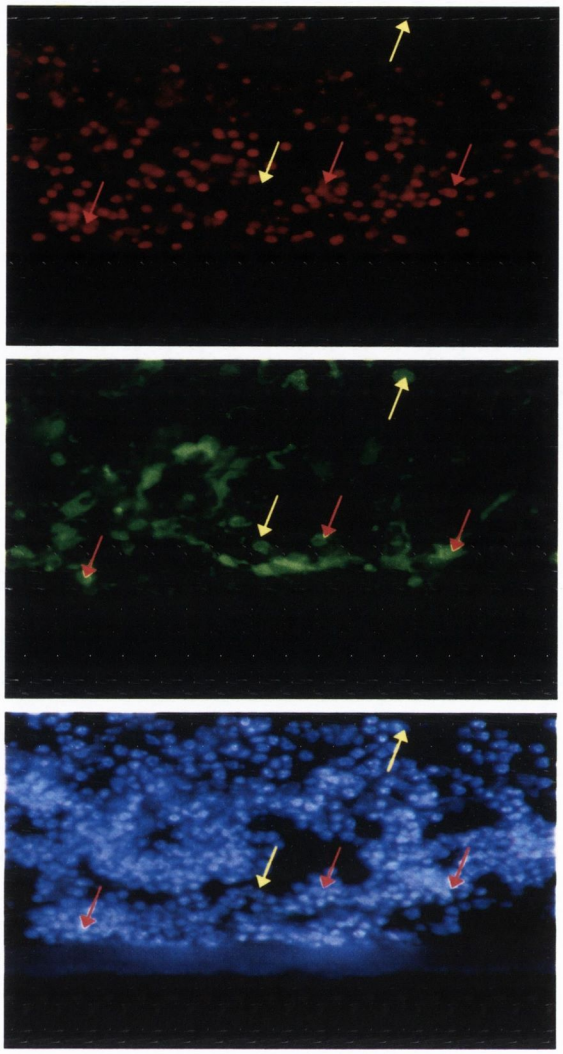

Figure 5.22: Cryosections of cultured retinal explants, TUNEL stained. Representative photographs of cryosections (7μM) from P11 cultured retinal explants, electroporated with pCMV.EGFP, treated with the apoptosis-inducing agent A23187 (5μM) for 24 hours, fixed and TUNEL stained (see 5.2.11). The retinal section is shown under fluorescent light to examine: **(A)** TUNEL staining, **(B)** EGFP expression, and **(C)** nuclear staining with DAPI (400X). EGFP expressing cells are indicated with arrows: red to indicate TUNEL positive cells, and yellow to indicate TUNEL negative cells.

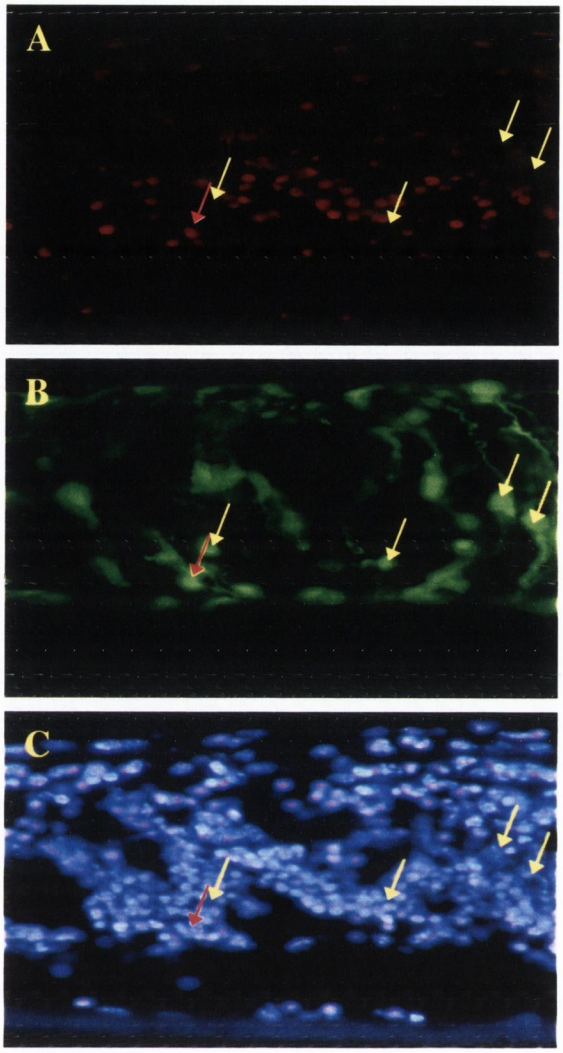

Figure 5.23: Cryosections of cultured retinal explants, TUNEL stained. Representative photographs of cryosections (7μM) from P11 cultured retinal explants, electroporated with pEGFP.p35, treated with the apoptosis-inducing agent A23187 (5μM) for 24 hours, fixed and TUNEL stained (see 5.2.11). The retinal section is shown under fluorescent light to examine: **(A)** TUNEL staining, **(B)** EGFP expression, and **(C)** nuclear staining with DAPI (400X). EGFP expressing cells are indicated with arrows: red to indicate TUNEL positive cells, and yellow to indicate TUNEL negative cells.

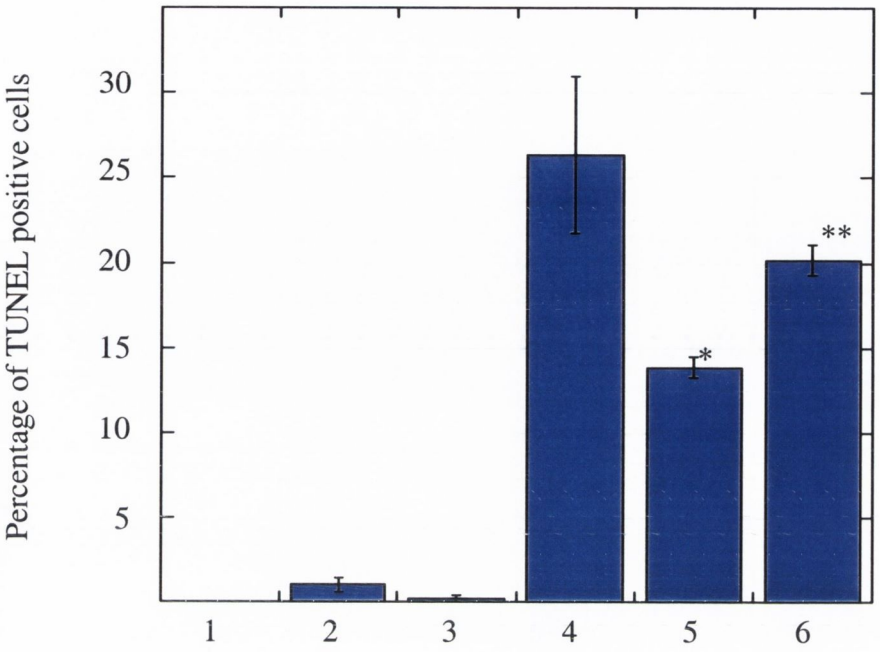

1: No vector

2: pCMV.EGFP

3: pEGFP.p35

4: pCMV.EGFP + A23187

5: pCMV.EGFP + A23187 + Z-VAD-FMK

6: pEGFP.p35 + A23187

Figure 5.24: Graph of percentage TUNEL positive cells from retinal explant cryosections following exposure to an apoptosis-inducing agent, A23187. P0 retinal explants were electroporated with (i) pCMV.EGFP or (ii) pEGFP.p35. Following 10 days culturing, explants were treated with A23187 for 24 hours, fixed, cryosectioned and TUNEL stained (see 5.2.11). There was a significant decrease in TUNEL positive cells in samples pretreated with Z-VAD-FMK (caspase inhibitor), compared to those without ($P < 0.05$*). Samples from retinal explants electroporated with pEGFP.p35 also had a significant decrease in TUNEL positive cells ($P < 0.05$**). Bars represent mean ± standard error (S.E.) of duplicate experiments with a total of 20 retinal explants.

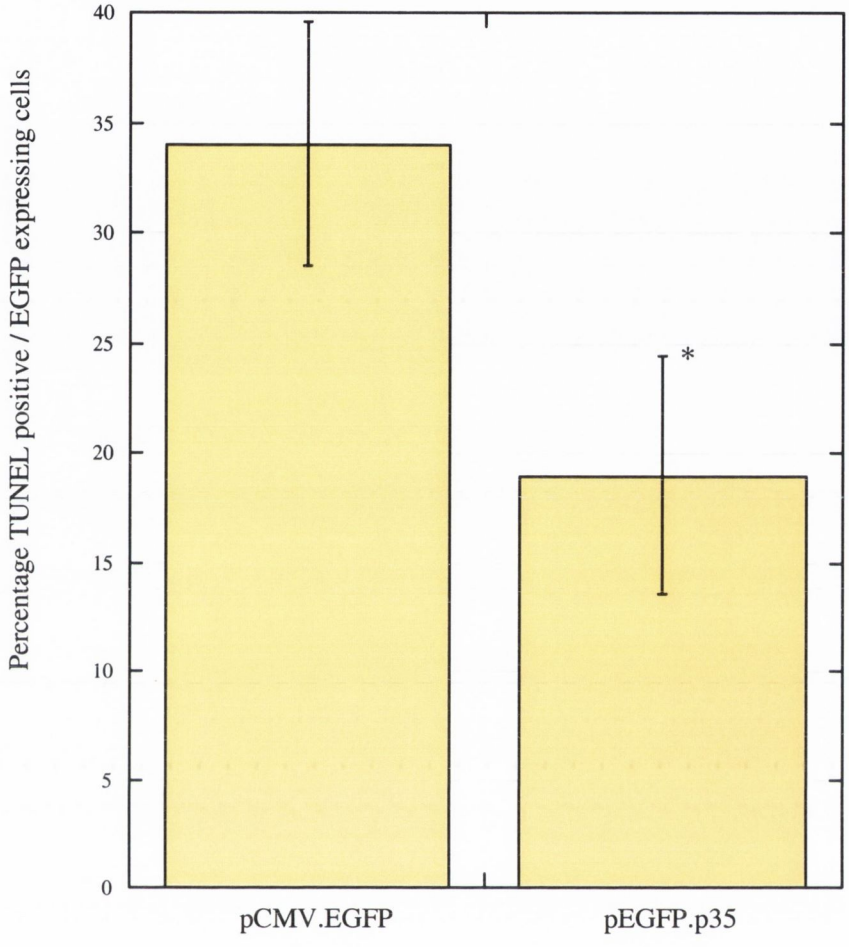

Figure 5.25: Graph of percentage TUNEL positive cells per equivalent EGFP expressing cells from retinal explant cryosections following exposure to an apoptosis-inducing agent, A23187. P0 retinal explants were electroporated with (i) pCMV.EGFP or (ii) pEGFP.p35. Following 10 days culturing, explants were treated with A23187 for 24 hours, fixed, cryosectioned and TUNEL stained. EGFP expressing cells, were examined for TUNEL staining. There was a significant decrease in TUNEL positive cells in samples from retinal explants electroporated with pEGFP.p35 compared to pCMV.EGFP ($P < 0.05$*). Bars represent mean ± standard error (S.E.).

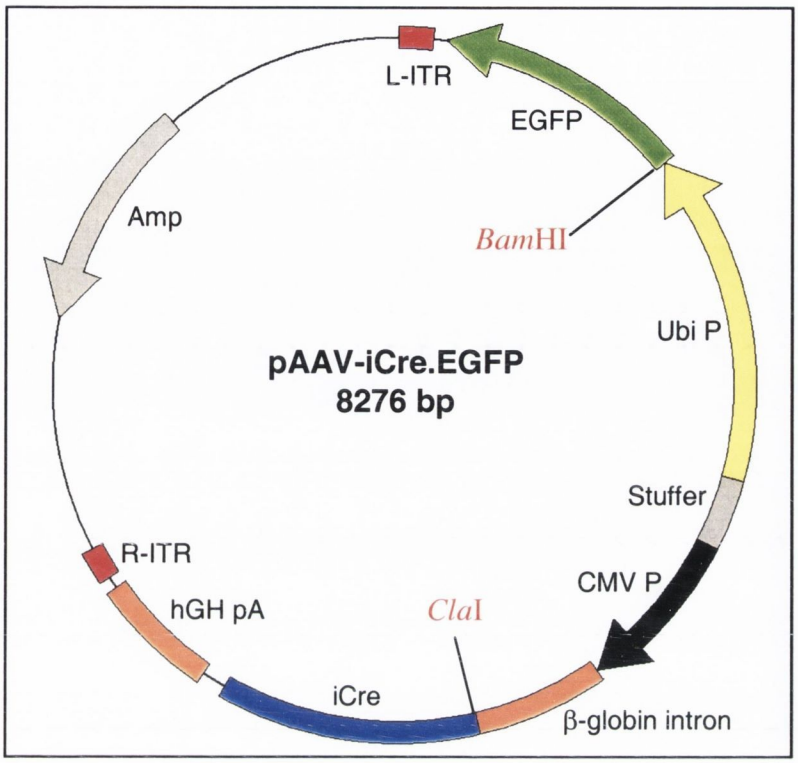

L-ITR: Left inverted terminal repeat (bases 1-141)
EGFP: Enhanced green fluorescent protein (bases 155-1161)
Ubi P: Ubiquitin promoter (bases 1162-2429)
Stuffer: Stuffer sequence (bases 2430-2678)
P CMV: Cytomegalovirus promoter (bases 2687-3349)
β-globin intron: Beta-globin intron (bases 3378-3869)
iCre: improved Cre recombinase (bases 3870-4964)
hGH pA: Human growth hormone polyadenylation signal (bases 4974-5452)
R-ITR: Right inverted terminal repeat (bases 5492-5632)
ampicillin: Ampicillin resistance gene (bases 6545-7402)

Figure 5.26: Plasmid map of pAAV-iCre.EGFP. This construct is for generation of AAV, with a ubiquitin promoter-driven EGFP gene, and a CMV promoter-driven iCre gene (see 5.2.12). Sequence is given in Appendix 2.3.2. Unique restriction enzyme sites are shown in red.

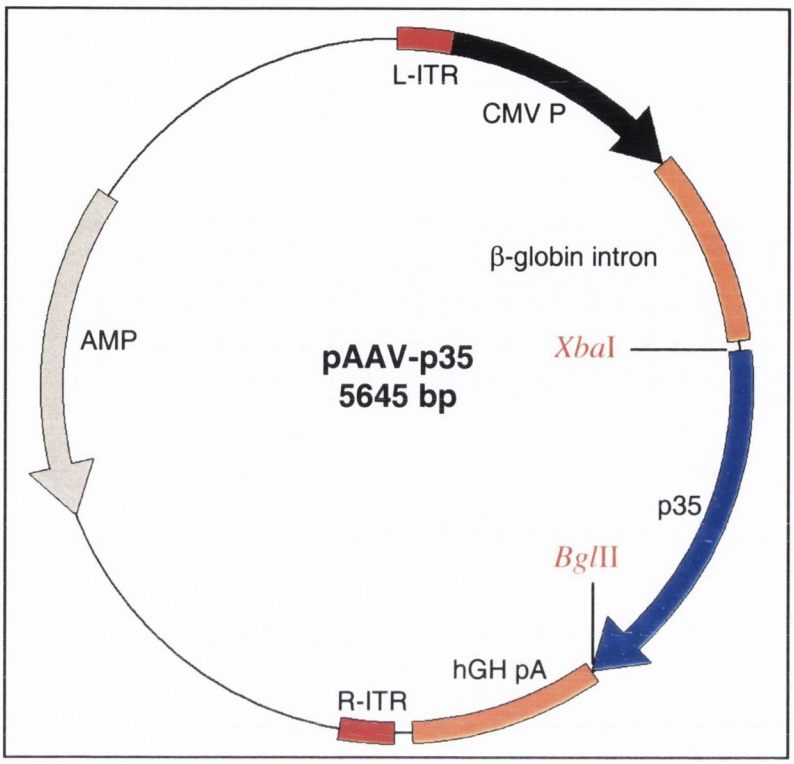

L-ITR: Left inverted terminal repeat (bases 1-141)
P CMV: Cytomegalovirus promoter (bases 150-812)
β-globin intron: Beta-globin intron (bases 820-1312)
p35: 950 bp of the baculoviral p35 gene (bases 1380-2330)
hGH pA: Human growth hormone polyadenylation signal (bases 2331-2869)
R-ITR: Right inverted terminal repeat (bases 2909-3049)
ampicillin: Ampicillin resistance gene (bases 3956-4813)

Figure 5.27: Plasmid map of pAAV-p35. This construct is for generation of AAV-2, with a CMV promoter-driven p35 gene (see 5.2.12). Sequence is given in Appendix 2.3.3. Unique restriction enzyme sites are shown in red.

CHAPTER 6

In Vitro Evaluation of a Ribozyme-Based Mutation-Independent Approach to p53-Related Cancer

6.1 Introduction

The previous three chapters have focused on the evaluation of therapeutic strategies based on targeting a common secondary effect associated with disease pathology of adRP and other retinal degenerations, namely photoreceptor cell death. Another gene therapy-based approach for RP involves targeting the underlying primary mutation, which involves either gene replacement for autosomal recessive RP (arRP), or alternatively some form of gene suppression for autosomal dominant RP (adRP). With regard to gene suppression for adRP, genetic heterogeneity presents a challenge, as tailoring gene therapies to suppress different individual mutations within one gene may not be economically, or indeed in terms of design, feasible. Given this, a number of mutation-independent therapeutic approaches have been developed in the laboratory here, which involve suppression of wt and mutant transcripts, with the introduction of a suppression-resistant replacement gene (Chapter 1: 1.2.10.3). Several *in vitro* and *in vivo* studies have demonstrated the validity of this approach for adRP (Millington-Ward *et al.,* 1997; O'Neill *et al.,* 2000; Kiang *et al.,* 2005; Palfi *et al.,* 2006). Applying mutation-independent gene therapy approaches is not limited to adRP, as approximately 1,500 autosomal dominant Mendelian diseases are known to date (McKusick 1998). Indeed, the research group here has successfully demonstrated the *in cellulo* suppression of a mutated pro-collagen gene *COL1A1* that results in the brittle bone disorder, osteogenesis imperfecta (OI) (Millington-Ward *et al.,* 1999; Millington-Ward *et al.,* 2002). In addition, with the increase in understanding of the genetics underlying multi-factorial diseases such as colorectal tumourigenesis and p53-related cancers, it is evident that causative pathogenic genes may act in a dominant-negative fashion (Harvey *et al.,* 1995; Dihlmann *et al.,* 1999; Sigal *et al.,* 2000; de Vries *et al.,* 2002).

p53 is a tumour suppressor gene mutated in approximately 50% of human cancers and hence is an important therapeutic target for cancer treatment (Hollstein *et al.,* 1991; Hupp *et al.,* 2000; Lane *et al.,* 2002). Given the importance of p53 in tumour development and the increasing evidence to support a dominant-negative function for a large number of p53 missense mutations (Dittmer *et al.,* 1993; Liu *et al.,* 2000; de Vries

et al., 2002; Willis *et al.,* 2004), the p53 gene was considered a suitable target for suppression/replacement gene therapy. As there is a high level of heterogeneity among p53 mutations identified in tumours, with approximately 1,300 different mutations identified to date (Soussi *et al.,* 2001; Soussi *et al.,* 2005), the mutation-independent therapeutic approaches represent a potential strategy to overcome the genetic heterogeneity.

To date, the principle gene therapy-based strategy targeting the p53 gene in p53-related cancers has involved introducing wt p53 using viral vectors including those based on retroviruses and adenoviruses (Roth *et al.,* 1996; Swisher *et al.,* 2003; Holmes *et al.,* 2003). By restoring wt p53 function, results from studies have demonstrated tumour regression in both animal models and clinical trials (Fujiwara *et al.,* 1994a; Roth *et al.,* 1996; Swisher *et al.,* 2003). In addition, p53 mutations may explain the lack of therapeutic efficacy of conventional chemotherapeutic agents and gamma (γ)-radiation for some cancers, as these therapies rely on the activation of p53-dependent stress apoptotic pathways to induce apoptosis of tumour cells. Indeed, several studies have found a strong correlation between p53 mutations and poor clinical response to anti-cancer agents for cancers including breast, lung and colorectal cancer (Borresen-Dale 2003; Campling *et al.,* 2003; Iacopetta 2003). Using a cancer cell line, Lowe *et al.,* 1993, showed that a loss of p53 function resulted in an enhanced cellular resistance to a number of chemotherapeutic agents. Results from studies showing enhanced clinical response to chemotherapeutic agents following wt p53 delivery support this finding (Fujiwara *et al.,* 1994b; Gjerset *et al.,* 1995; Swisher *et al.,* 2003).

However, given the numerous studies supporting the dominant-negative activity of many p53 mutations, including notably the demonstration that the transgenic overexpression of a mutant p53 gene (alanine to valine at codon 135 {A135V}), acclerated tumour development in mouse models with one wt p53 gene ($p53^{+/-}$), compared to nontransgenic $p53^{+/-}$ mice (Harvey *et al.,* 1995), suggest that the efficacy of treatment for p53-related cancers may be limited by not addressing the expression of mutant p53. Approximately 70% of identified p53 mutations are missense, resulting in

full-length mutant proteins that can interfere with wt p53 function (Soussi *et al.,* 2001). In addition, some of these mutant p53 transcripts have been shown to have oncogenic gain-of-function activities, independent of wt p53 (Roemer 1999; Blagosklonny 2000; Sigal *et al.,* 2000; Tsang *et al.,* 2005). Although the mechanisms underlying the actions of mutant p53 remain to be fully elucidated, suppressing p53 mutant genes in conjunction with wt p53 gene replacement represents a valid therapeutic strategy that may be more effective that conventional anticancer therapy or wt p53 replacement alone.

Numerous tools are available to suppress mutant gene expression, including oligodeoxynucleotides, ribozymes, DNAzymes and the most recently developed, short interfering RNA (siRNA) (Santoro *et al.,* 1997; Schubert *et al.,* 2004; Citti *et al.,* 2005; Dykxhoorn *et al.,* 2005). Ribozymes are RNA-based enzymes capable of site-specific cleavage of target mRNAs. Examples include the large self-splicing group I and group II introns and smaller hammerhead, hairpin and hepatitis delta virus (HDV) ribozymes (Doherty *et al.,* 2000; Doudna *et al.,* 2002; Khan *et al.,* 2003; Fedor *et al.,* 2005) (Chapter 1: 1.4.3). For the study described here, the hammerhead ribozyme motif, based on one of the best characterised members of the ribozyme family was chosen as the suppression agent for the p53 gene. The hammerhead ribozyme consists of two antisense arms that are complementary to the target sequence surrounding a single stranded central catalytic core of 13 conserved nucleotides (Haseloff *et al.,* 1988) (Figure 6.3). Hammerhead ribozymes have been developed as therapeutic tools to suppress gene expression for a number of diseases including retinitis pigmentosa (RP) (LaVail *et al.,* 2000; Gorbatyuk *et al.,* 2005), HIV (Li *et al.,* 2005a; Macpherson *et al.,* 2005) and cancer (Sandberg *et al.,* 2000; Usman *et al.,* 2000).

Hammerhead ribozymes cleave at NUX sites (where N is any nucleotide and X is any nucleotide except G) (Shimayama *et al.,* 1995) in the target RNA. Hence, the first part of the current study involved identifying suitable NUX cleavage sites in p53 RNA, and 6 ribozymes were subsequently evaluated using *in vitro* cleavage assays. To validate a mutation-independent based suppression/replacement approach, the cleavage of 2

modified replacement p53 transcripts was assessed. Exploiting the degeneracy of the genetic code, a number of single base pair changes were made to the replacement constructs, destroying the ribozyme cleavage site and in addition reducing binding of ribozyme anti-sense arms to replacement p53 transcripts. As these changes were made to third base wobble positions, the amino-acid coding sequence of the p53 protein should in principle remain unaltered.

6.2 Materials and Methods

6.2.1 p53 mRNA secondary structure and ribozyme design

The sequence for human p53 was retrieved from the GenBank database, accession number NM_000546. The predicted p53 RNA secondary structure was generated using the programs RNAdraw (Matzura *et al.,* 1996) and MFold with its companion program PlotFold (Zuker *et al.,* 1989; Zuker 2003). Both programs use folding algorithms to predict optimal secondary structures of RNA using energy minimisation parameters derived from experimental cleavage of known simple structures (see Chapter 2: 2.3.2 for further details). Using results from both programs, possibly suitable NUX hammerhead ribozyme cleavage sites were identified, where N can be any nucleotide, uracil is conserved and X any nucleotide except guanine. There is a hierarchy of preferred cleavage sites so where possible the most efficiently cleaved sites were chosen (Zoumadakis *et al.,* 1995). In addition the cleavage sites had to be located in large, accessible open loops, within the p53 mRNA, which the ribozymes could easily bind to and cleave.

6.2.2 Ribozyme constructs

Hammerhead ribozyme constructs (Rz 359, Rz 639, Rz 850, Rz 1398, Rz 1561 and Rz 1613) were designed according to the criteria outlined above in 6.2.1. DNA templates were cloned into the *Hind*III and *Xba*I sites of the cloning vector pcDNA3.1+ (Invitrogen).

Table 6.1 Position and NUX cleavage sites of each of the ribozymes

Ribozyme	Position	NUX Site
359	359-361	GUC
639	639-641	CUC
850	850-852	AUU
1398	1398-1400	CUC
1561	1561-1563	AUU
1613	1613-1615	GUU

The DNA templates from which the ribozymes were transcribed, were synthesised by Sigma-Genosys as two single-stranded forward and reverse oligonucleotides. The forward and reverse strands were annealed by incubating 1nmol of each oligonucleotide in a 40µl reaction with a final concentration of 25mM NaCl at 94°C for 4 minutes, followed by an overnight incubation at room temperature. All ribozyme designs (shown below) were hammerhead ribozymes with a conserved catalytic core as determined by Haseloff *et al.*, 1988. Antisense sequences flanking the ribozyme catalytic cores are highlighted in bold print:

Ribozyme 359: **UUGCUUGG**CUGAUGAGUCCGUGAGGACGAA**ACGGCAA**

Ribozyme 639: **UCUUGUU**CUGAUGAGUCCGUGAGGACGAA**AGGGCAGG**

Ribozyme 850: **ACACGCA**CUGAUGAGUCCGUGAGGACGAA**AUUUCCUU**

Ribozyme 1398: **UGAACAU**CUGAUGAGUCCGUGAGGACGAA**AGUUUUUU**

Ribozyme 1561: **CAAAGCA**CUGAUGAGUCCGUGAGGACGA**AAUGGAAGU**

Ribozyme 1613: **UCCCCAC**CUGAUGAGUCCGUGAGGACGA**ACAAAACA**

6.2.3 Cloning, transformation and purification of plasmids

DNA templates of hammerhead ribozymes were cloned into the *Hind*III and *Xba*I sites of pcDNA3.1+ in 15µl ligation reactions as described in Chapter 2: 2.2.6. Competent XL-1B cells were prepared and transformed with 5µl of the ligation reactions (2.2.7-8). The cells were then plated onto selective solid LB plates and colonies containing inserts were identified using PCR analysis (2.2.9). 10mls LB selective medium was inoculated with selected clones and grown overnight at 37°C for plasmid purification (mini-prep) the next day (2.2.10). Prior to sequencing positive clones, the presence of the insert was confirmed by digesting the plasmid with a number of restriction enzymes. High quality, clean plasmid DNA for RNA expression was then isolated using a Qiagen HiSpeed Plasmid Maxi Kit in accordance with the manufacturer's instructions, or by caesium chloride density gradient centrifugation (2.2.12).

6.2.4 Automated DNA sequencing

Positive clones were sequenced on an ABI Prism 310 Genetic Analyser (PerkinElmer) using standard protocols (Chapter 2: 2.2.14).

6.2.5 Ribozyme target constructs

6.2.5.1 Human p53 cDNA

The full-length human p53 cDNA including part of the 5'-and 3'-UTR, was kindly provided by Dr. Xu Lu of the Ludwig Institute for Cancer Research, UK. The p53 element of the construct (1.8 kb) was excised from the pC53-SN3 plasmid (Baker *et al.*, 1990) with *Bam*HI and cloned into the *Bam*HI site of pcDNA3.1+ under the control of the T7 promoter, resulting in pCMV.p53. A second construct was made by digestion of pCMV.p53 with *Nhe*I and *Bsu*36I, removing 0.8 kb of the 5' end of the p53 gene. This was named pCMV.p53subclone (pCMV.p53sc). Appropriate RNA targets for several ribozymes were transcribed from this subclone, as the maximum transcript length that can be readily expressed *in vitro* is approximately 1kb.

6.2.5.2 Replacement p53 constructs, p53Re359 and p53Re639

Two human p53 replacement constructs with an altered p53 sequence were generated using the QuikChange Site Directed Mutagenesis Kit (Stratagene) according to the manufacturer's protocols. Mutagenesis primers used for each construct are indicated below. Substituted nucleotides are underlined and in bold-type:

(1) Forward Primer p53Re359:
5'-TGTCCCCCTT**A**CCG**AG**CCA**G**GCAATGGATGATTTGATGCTG-3'

(2) Reverse Primer p53Re359:
5'-AATCCATTGC**C**TGG**CT**CGG**T**AAGGGGGACAGAACGTTGT-3'

(3) Forward Primer p53Re639:
5'-ACGTACTCCCC**A**GCCCT**G**AA**T**AAGATGTTTTGCCAACTG-3'

(4) Reverse Primer p53Re639:
5'-GCAAAACATCTT**A**TT**C**AGGGC**T**GGGGAGTACGTGCAAGTCAC-3'

The changes made to each construct were designed to destroy the ribozyme cleavage site or alter the binding sites for the ribozyme arms. Nucleotide changes, indicated in the table below, were made at wobble positions and so should not give rise to amino acid substitutions.

Table 6.2 Nucleotide changes made to the p53 replacement constructs

Replacement	Altered Cleavage Site	Altered Binding Site
p53Re359	360, 361: UCC Ser-AGC Ser	356: UUG Leu-UUA Leu 365: CAA Gln- CAG Gln
p53Re639	639: CUC Leu-CUG Leu	633: CCU Pro-CCA Pro 642: AAC Asn-AAU Asn

6.2.6 In vitro *transcription and radioactive labeling of RNA*

The pCMV.p53, pCMV.p53sc and ribozyme constructs were prepared either using the Qiagen Plasmid Maxi Kit (Chapter 2: 2.2.11) or the caesium chloride method for plasmid maxipreps (2.2.12). Following digestion with the appropriate restriction enzymes as listed in Table 6.3, plasmids were purified using four phenol/chloroform washes and precipitated (2.2.1). RNA was transcribed from constructs *in vitro* using Ribomax transcription kits (Promega) in accordance with the manufacturer's guidelines (2.3.6).

Table 6.3 Restriction endonuclease sites used for linearisation of p53 target and replacement constructs, and sizes of predicted RNA cleavage products yielded after incubation with ribozymes

Construct	Restriction Enzyme	Transcript Length	Cleavage Product Length
p53 + Rz359	*Bsu*361	907	558, 349
p53Re359 + Rz359	*Bsu*361	907	907
p53 + Rz639	*Bsu*361	907	629, 278
p53Re639 + Rz639	*Bsu*361	907	907
p53 + Rz850	*Ssp*I	1218	840, 378
p53 + Rz1398	*Bam*HI	1081	551, 530
p53 + Rz1561	*Bam*HI	1081	714, 367
p53 + Rz1613	*Bam*HI	1081	766, 315
All Rzs	*Xba*I	125	

6.2.7 Isolation and purification of RNA

Target RNA and ribozymes were electrophoresed on 4% polyacrylamide gels and RNA bands of appropriate sizes were excised and purified using phenol/chloroform (Chapter 2: 2.3.7- 8). The radioactivity of 1µl of each RNA transcript was quantified using a

scintillation counter (Beckman LS-6500) and molar ratios of target p53 to ribozyme were determined.

6.2.8 Calculating molar ratios of target: ribozyme for cleavage reactions

To evaluate ribozyme efficiency the ratio of ribozyme to target in the cleavage reactions was varied in cleavage reactions from 0.6:1 to 320:1. The following formula was used to calculate how many counts per minute (cpm), determined on a scintillation counter, of ribozyme and target were required for a 1:1 ratio.

A x F x D / C x E = B = 1:1

A = cpm of target

B = cpm of ribozyme required for a 1:1 ratio

C= ratio of radioactively labelled rUTP to non-ratioactive rUTP used in target transcription reaction

D= ratio of radioactively labelled rUTP to non-ratioactive rUTP used in ribozyme transcription reaction

E = length of target RNA

F= length of ribozyme

Using the B value and cpm of each ribozyme, the volume of ribozyme required to achieve a 1:1 ratio of target RNA: ribozyme in cleavage reactions was calculated.

6.2.9 Ribozyme: target cleavage reactions

Cleavage reactions were carried out in 10-20µl reaction volumes with 50mM Tris-HCl (pH 8.0) and 10mM $MgCl_2$, at 37°C. Sample aliquots of 2µl were removed at various timepoints (up to 2-3 hours) and quenched in 5µl of RNA loading buffer (Chapter 2: 2.1.2{vii}). Samples were electrophoresed on 4% polyacrylamide gels and analysed by autoradiography (2.3.9). Gels were dried under vacuum and exposed to a phosphor screen, which was used to quantify the level of cleavage using a Typhoon 8600 Imager (Amersham Biosciences) with ImageQuant software (Molecular Dynamics). Rectangles

were drawn around each band to be quantified (as shown in Figure 6.13) and assigned a pixel value by ImageQuant based on the optical density of the gel. The values for the uncleaved target and cleavage products were added at each time point and the cleavage products were expressed as a percentage of the total value.

6.2.10 Molecular weight markers for RNA

pBR322 digested with *Msp*I was end-labeled with dCTP [α P^{32}] using Klenow enzyme (Chapter 2: 2.3.10). DNA and RNA migrate through polyacrylamide gels at slightly different speeds (estimated to be up to a 10% difference) so the DNA ladder is an approximate marker for sizing target and cleavage products.

6.2.11 Transient transfection of 293T cells with construct expressing Rz 1561

One day prior to transfection 1.25 x 10^5 293T cells, were seeded per well of a 24-well plate. The next day cells were transfected in duplicate with either 0.5μg or 1μg of vector DNA using Lipofectamine 2000 according to the manufacturer's instructions. The following vectors were used: pcDNA3.1+ with Rz 1561, or a non-targeting Rz (Rz 40, targeting rhodopsin, kindly provided by Dr. Brian O'Neill). After a 36-48 hour incubation period, during which the medium was changed, total cellular RNA was isolated from transfected cells using TRI reagent (Chapter 2: 2.3.3).

6.2.12 Quantitation of p53 RNA expression using real-time RT PCR

p53 RNA suppression levels in total RNA samples from transfected 293T cells were quantified using a QuantiTect SYBR Green PCR Kit (Qiagen), on a LightCycler (Roche). Levels of p53 PCR product, in different RNA samples were standardised with a housekeeping gene, glyceraldehyde-6-phosphate dehydrogenase (GAPDH). For each independent experiment, pooled samples were analysed in duplicate, on two occasions. Real-time RT-PCR reactions contained 10μl SYBR Green Master Mix, 10pmol of forward and reverse primer in a 2μl volume (see below), 0.14μl QuantiTect RT Mix, 2.86μl RNase-free water and 5μl RNA. The following program was used: 1) reverse transcription for 20 minutes at 50°C, 2) activation of HotStarTaq for 15 minutes at 94°C, 3) denaturation for 15 seconds at 95°C, annealing for 20 seconds at 57°C and

extension for 7 seconds at 72°C, repeated for 35 cycles. Primers were HPLC-purified and designed to amplify 100 bp products:

(1) GAPDH F: 5' CAGCCTCAAGATCATCAGCA-3'

(2) GAPDH R: 5' CATGAGTCCTTCCACGATAC-3'

(3) p53 F: 5' GCGCACAGAGGAAGAGAATC-3'

(4) p53 R: 5' AGAGGAGCTGGTGTTGTTGG-3'

6.3 Results

6.3.1 Predicting the secondary structure of p53 mRNA

Two programs, RNAdraw and Mfold/PlotFold, were used to predict the secondary structure of p53 RNA and predictions were used to identify possible suitable cleavage sites for hammerhead ribozymes (Figures 6.1, 6.2). NUX sites present in predicted open loops within the p53 mRNA were deemed to be suitable ribozyme target sites. Zoumadakis *et al.* demonstrated a hierarchy of preferred cleavage sites for ribozymes (Zoumadakis *et al.,* 1995). Preferred cleavage sites were selected for the current study. 18 potential sites were identified in the 5' untranslated region (UTR), coding region and 3'-UTR of p53 RNA. Of these, 6 were chosen as potential targets. Choosing target sites was limited by the availability of full-length p53 cDNA with 5'- and 3'-UTRs. Initially, Professor Thierry Soussi (Marie Curie Institute, Paris) kindly provided the plasmid, pcDNA-Hp53wt, but this clone contained only a partial p53 cDNA, and many of the ribozyme target sites were not present. Dr. Xu Lu provided pCMV-SN3, which contained part of the p53 5'- and 3'-UTRs. In addition, since only parts of the p53 transcript were transcribed for the *in vitro* work (Ribomax transcription kit can transcribe only up to approximately 1 kb), secondary RNA structures of these shorter transcripts were predicted using the RNAdraw program to confirm that the predicted open loop structures in the full length mRNA were still present in the predicted structure for the partial mRNA.

6.3.2 Evaluating methods for p53 mRNA target and ribozyme preparation

Initially Qiagen Plasmid Maxi Kits were used to prepare plasmid DNA. However, subsequent to *in vitro* transcription, p53 target mRNA degraded in the presence of magnesium, indicating that there were RNases present in the sample. As can be seen from Figure 6.10, p53 target mRNA and Rz 359 incubated without magnesium for 30 minutes are present in Lane 1, but in the presence of magnesium the target is almost completely degraded (Lane 2, Lane 4). To resolve the problem of degradation, fresh solutions of magnesium and Tris-HCl were prepared, commercial solutions were then ordered in and plasmid DNA expressing p53 and ribozyme constructs were purified with extra phenol/chloroform washes. However, the target RNA continued to be

degraded, so alternative methods of evaluating ribozymes *in vitro* were explored. One group in the University of Delaware published a paper on a non-radioactive method for the evaluation of ribozyme activity (Liu *et al.*, 2002). The method involved resolving the target mRNA, ribozyme and cleavage products on a high-percentage agarose gel. The radioactive method of evaluating ribozyme cleavage has several disadvantages including the short half-life of the radioactive label (14 days) and the possibility of contamination. As there were fewer steps in this alternative protocol, there was a reduced risk of contamination. However, target RNA degradation was observed once again. Additionally the resolution of the cleavage products using this methodology was found to be poor, compared to the radioactive method (data not shown).

Caesium chloride (CsCl) density gradient purification is another method of purifying plasmid DNA, involving more work than commercially available kits. Moreover this method holds several advantages including the production of very clean DNA and large yields (approximately 2-5mg per 1000ml growth medium). Plasmid DNA was prepared using CsCl density gradient purification followed by the radioactive method (6.2.6-9) to evaluate ribozyme cleavage and notably no degradation of RNA was observed. Plasmid DNA prepared using commercial kits is suitable for most techniques. However, it would seem that for *in vitro* RNA cleavage reactions, DNA cleaned on a CsCl density gradient is preferable.

6.3.3 Assessment of Rz 359 cleavage efficiency at different time points

Subsequent to *in vitro* transcription of the ribozyme 359 (Rz 359) and p53 target RNA, *in vitro* cleavage reactions were set up using a ribozyme to target ratio of 64:1. 2.5µl aliquots of cleavage reactions were removed at various time-points (0, 30, 60, 90, 120, 150 and 180 minutes), quenched, and products resolved on a 4% polyacrylamide gel. Following drying, the gel was analysed by autoradiography. Figure 6.11 shows an image of the autoradiograph from this time point cleavage reaction. Cleavage products of 558 and 349 bases, visible from 60 minutes (Lane 6) are highlighted with blue arrows. The faint banding at 180 minutes is probably due to slight degradation of the RNA. As the ladder in this autoradiograph is poor, the products were sized more

accurately on a second gel (Figure 6.12). Levels of cleavage were quantified by exposing the dried gel to a phosphor screen, and the exposed screen analysed using a Typhoon Imager with ImageQuant software. The percentage ribozyme cleavage obtained was calculated to be approximately (~) 15%. Rz 359 was also incubated with transcripts from the replacement p53 gene, p53Re359, for 180 minutes and notably no ribozyme cleavage was observed (Figure 6.11, Lane 11; Figure 6.12, Lane 5). No cleavage of the p53 transcript by Rz 359 was observed in the absence of $MgCl_2$ (Figure 6.11, Lane 3).

6.3.4 Assessment of Rz 639 cleavage efficiency at different time points

Rz 639 was incubated for up to 240 minutes with p53 transcript using a ribozyme to target ratio of 31 to 1 (Figure 6.13). Cleavage products of 629 and 278 bases were visible from 30 minutes (Lane 4). Again no ribozyme cleavage of the p53 transcript was observed in the absence of $MgCl_2$ (Lane 2). The level of p53 transcript cleavage was quantified using a phosphorimager as described previously in 6.3.2. Table 6.4 (below) demonstrates how the percentage cleavage at each time point was calculated. The pixel value for the Rz 639 cleavage products (Column 3), as calculated by ImageQuant, was expressed as a percentage of the total pixel value for the cleavage products and uncleaved p53 target (Column 2). The majority of cleavage of the p53 target RNA occurred within the first 90 minutes (~41%), reaching a maximum level of cleavage of approximately 50% by 150 minutes (Table 6.4, Figure 6.13).

Table 6.4: Quantitation of the cleavage of p53 target RNA by Rz 639

Time (min)	Total (px)*	Cleavage Products (px)	% Cleavage
30	1046637	207898	19.86
90	1160471	473070	40.76
120	1462498	619321	42.35
150	858415	438226	51.05
180	1920184	89427	46.57
210	1890331	89712	47.46
240	3642692	1925349	52.85

*Gross pixel (px) value for target and cleavage products at each time point.

6.3.5 Assessment of Rz 639 cleavage efficiency using different ratios of ribozyme to target

As Rz 639 was shown to be moderately efficient at cleaving the p53 target RNA, further experiments were undertaken using this ribozyme to examine the effect of varying the ratio of ribozyme to target. Rz 639 was incubated with p53 target RNA at ratios of 0.6:1, 6:1, 32:1 and 128:1 (Figures 6.14-15) for times of 1, 5, 15, 30 and 120 minutes. In addition, Rz 639 was incubated with p53 target at a molar ratio of 320:1 for 5 and 120 minutes and samples analysed as described in 6.2.9 (Figure 6.15). Figure 6.14B also shows an additional autoradiograph to Figure 6.14A of the resolved target and cleavage products from Rz 639 incubated with p53 at a ratio of 0.6:1 for time frames of 0-180 minutes. In addition, no ribozyme cleavage was observed when transcripts from the replacement p53 construct were incubated with Rz 639 for 180 minutes in the presence of 20mM $MgCl_2$ (Figure 6.14B, Lane 1). The level of p53 transcript cleavage was quantified using a phosphorimager and the results were plotted as two graphs (Figure 6.16-17). Figure 6.16 shows the percentage cleavage of p53 target RNA versus time observed using various ratios of ribozyme to target RNA. Most p53 RNA cleavage occurs within the first 30 minutes of the reaction. Additionally, higher levels of cleavage are observed at higher ratios of ribozyme to target RNA (128:1) than lower ratios (6:1) (~70% and ~30% respectively). Figure 6.17 shows the

percentage cleavage of p53 versus the ratio of ribozyme to target after a 120 minute incubation with Rz 639. There is a sharp increase in the percentage of cleaved target RNA as the ratio increases from 0.6:1 to 128:1. However, no further increase in cleaved target RNA is observed at a ratio of Rz 639 to target of 320:1, suggesting that Rz 639 saturation has been reached by a ratio of 128:1. The maximum percentage of the p53 target cleaved at this ratio is ~80%. This only increases minimally to ~83% as the ratio increases by 2.5 fold to 320.

6.3.6 Assessment of Rz 850 cleavage efficiency at different time points

Rz 850 was incubated with p53 transcript at a ribozyme to p53 target RNA ratio of 94:1 and sample aliquots were removed at different time points over a 180 minute period and analysed as described in 6.2.9. Figure 6.18A shows the 840 base ribozyme cleavage product. The second ribozyme cleavage product of 378 bases was only visible after a longer exposure time (Figure 6.18B). Using a phosphorimager to quantify the level of cleavage, the percentage cleavage at 180 minutes was calculated to be ~13%. Rz 850 is clearly inefficient in this *in vitro* assay. Hence no further experiments were undertaken with this ribozyme.

6.3.7 Assessment of Rz 1398 efficiency at different time points

Rz 1398 was incubated with transcripts from the pCMV.p53subclone (pCMV.p53sc) at a ribozyme to p53 target RNA ratio of 60:1. Sample aliquots were removed at various time points (1, 5, 15 and 60 minutes), quenched, and cleavage levels were assessed as described in 6.2.9. The ribozyme cleavage products of 551 and 530 bases were visible from 1 minute in Figure 6.19. The target RNA and cleavage products were quantified using a phosphorimager and the percentage cleavage at 60 minutes was estimated to be ~60%. To further characterise Rz 1398, the ribozyme was incubated with p53sc transcript at a molar excess of 200 and sample aliquots were removed at various time points (0, 30, 60 and 120 minutes), quenched, and cleavage levels were assessed as described (Figure 6.20). The percentage cleavage of the target at this point was estimated to be ~66%. The quantified p53 target RNA and ribozyme cleavage products from these autoradiographs are shown as graphs in Figures 6.21, 6.22.

6.3.8 Assessment of Rz 1561 cleavage efficiency at different time points

Rz 1561 was incubated with p53sc transcripts at a ribozyme to target RNA ratio of 26:1 and sample aliquots were removed at various time points (5, 15 and 90 minutes), quenched, and cleavage levels were assessed as described. Cleavage products of 714 and 367 bases were visible from 5 minutes. Quantification of the cleavage bands showed that ~90% of the transcript was cleaved by the final time point (Figure 6.23).

6.3.9 Assessment of Rz 1561 cleavage efficiency using different ratios of ribozyme to target

Since Rz 1561 demonstrated a high level of cleavage efficiency further experiments were undertaken with this ribozyme. Rz 1561 was incubated with the p53 target RNA at a ratio of 0.6:1, 6:1, 29:1 and 115:1, and resolved on 4% polyacrylamide gels (Figure 6.24-25). p53 target RNA and ribozyme cleavage products were quantified using a phosphorimager and results graphed (Figure 6.26). Figure 6.26 shows the level of cleavage of p53 target (%) versus time. By 30 minutes, between 40% and 70% of the p53 target RNA had been cleaved, depending on the molar excess of ribozyme used in the cleavage reaction. However, there was no significant difference in the final percentage of RNA cleavage at 120 minutes, except for the ratio of ribozyme to target of 0.6:1 (Figure 6.27) suggesting that the ribozyme may have reached saturation at a molar excess of approximately 6.

6.3.10 Assessment of cleavage efficiency of Rz 1613 at different time points

Rz 1613 was incubated with p53sc target RNA at a ribozyme to target ratio of 6 to 1. Sample aliquots were removed at various time points (5, 15, 30 and 120 minutes), quenched, and cleavage levels were assessed as described in 6.2.9. Ribozyme cleavage products of 766 and 315 bases were visible from 5 minutes (Figure 6.28). Quantification of cleavage bands showed that at the final time point, ~59% of the p53 transcript had been cleaved. To further characterise Rz 1613 another reaction undertaken with a molar excess of ribozyme to target p53 RNA of 94:1 (Figure 6.29). After 120 minutes, ~75% of the p53 target RNA had been cleaved (Figure 6.29), suggesting that Rz 1613 is a relatively efficient ribozyme. However, although a high

percentage of p53 target RNA was cleaved by Rz 1613, a greater molar ratio of Rz 1613 to target (50:1) was required to achieve high cleavage levels than by Rz 1561 (10:1). Hence, in the current study evaluation of Rz 1561 was continued *in cellulo*.

6.3.11 Quantitation of p53 RNA in 293T cells transfected with a construct expressing Rz 1561

In vitro data suggested that Rz 1561 may be a more efficient ribozyme than the other 5 ribozymes assessed *in vitro*. Therefore, Rz 1561 was further evaluated in 293T cells known to express p53 endogenously, by transiently transfecting cells with a plasmid carrying the DNA template for Rz 1561. Total RNA was isolated 48 hours post-transfection and analysed by real-time RT PCR. p53 expression levels were standardised with several housekeeping genes. GADPH was considered the most appropriate housekeeping gene with which to standardise p53 expression since p53 and GAPDH were expressed at comparable levels (data not shown). Transient transfection of Rz 1561 in 293T cells on two independent occasions did not result in p53 downregulation (Figure 6.31). There was no significant difference ($P > 0.05$) between the level of p53 expression in 293T cells transfected with either 0.5μg or 1.0μg of Rz 1561 compared to cells transfected with a non-targeting ribozyme (Rz40, 6.2.11), with a mean expression of 103.50+/- 18.42% for 0.5μg Rz 1561 and 102.42 +/- 19.65% for 1.0μg Rz 1561.

6.3.12 Evaluation of computer-folding programs based on in vitro results

For this study, the MFold/PlotFold and RNAdraw computer-folding programs were used to predict optimal secondary structures for p53 to identify potential NUX ribozyme cleavage sites in open accessible loops. The *in vitro* cleavage results for the 6 ribozymes were used to assess the reliability of these predicted open loop structures. Rz 1561 was demonstrated to be the most efficient ribozyme, as would have been predicted from examining the large size and accessible location of the open loop in computer-folded structures (Table 6.5). Consistent with this result, Rz 359 and Rz 850, which targeted the smallest predicted open loops of between 4 and 8 bases, were found to be the least efficient ribozymes *in vitro*. In addition, these loops were present in the

lowest number of suboptimal structures out of total of 9 generated by Mfold/Plotfold, indicating that the predicted folding of these regions may be less reliable. As the factors that influence RNA folding are not fully understood, the predicted structure with the lowest free energy, i.e. 'optimal', may not be correct so suboptimal structures with free energies close to the optimal structure can also be generated. Open loops that are present in most of the optimal and suboptimal structures may be predicted more reliably.

Table 6.5: Predicted sizes and locations of open loops in p53 RNA targeted for ribozyme cleavage

Target Site	MFold/PlotFold			RNAdraw	
	Loop Size (bases)	Loop at end of hairpin	Number of suboptimal structures with loop present (out of 9 total)	Loop Size (bases)	Loop at end of hairpin
359-361	8	Yes	5	8	Yes
639-641	18	No	8	18	No
850-852	4-8	No	6	9	No
1398-1400	12	No	8	17	Yes
1561-1563	13-14	Yes	8	13	Yes
1613-1615	8-9	No	8	9	No

Considering the size of the open loops targeted by Rz 639, Rz 1398 and Rz 1613, the predicted order of efficiency would be Rzs 639>1398>1613 but based on *in vitro* cleavage results, this order has been shown to be Rzs 1613>639>1398. This is likely to be due to a number of other factors influencing RNA folding, such as tertiary structure, which computer-folding programs do not take into consideration. However, all 6 ribozymes cleaved their p53 target sites and the cleavage efficiencies of the most and least efficient ribozymes were consistent with the secondary structures generated by MFold/PlotFold and RNAdraw.

6.4 Discussion

p53 is a tumour suppressor gene mutated in approximately 50% of human cancers, thus making it an important therapeutic target for anti-cancer strategies (Hollstein *et al.*, 1991). Gene based therapy for disease can involve either targeting the primary mutation or a secondary effect associated with disease pathology. The experiments described in the previous three chapters were focused on exploring methods of inhibiting apoptosis, which is the common pathway by which photoreceptors degenerate in retinal degenerations such as RP. Modulating a common secondary effect, such as apoptosis, provides a therapeutic strategy independent of the underlying genetic mutation, thus overcoming the challenge of genetic heterogeneity, which is a feature of diseases including RP and p53-related cancers. As a result of the mutational heterogeneity, present in disorders such as rhodopsin-linked RP or p53-related cancers, targeting the primary mutations is extremely challenging, and most probably not economically or indeed technically possible in many cases. In this regard, the mutation-independent strategies devised in the laboratory here (Chapter 1: 1.2.10.3), offer a means of circumventing this mutational variability. Targeting the primary mutation typically involves suppression of the mutant gene transcript using a suppression agent targeting a specific mutation. The current study describes a mutation-independent based suppression/replacement strategy for p53-related cancers. The essence of the approach is suppression of both the wild-type (wt) and mutant alleles of the p53 gene, in conjunction with the provision of a modified replacement gene transcript, resistant to suppression.

Hammerhead ribozymes, catalytic RNA molecules that can cleave RNA in a highly sequence-specific manner, were used as the suppression tool for the study described here. Hammerhead ribozymes have been evaluated as therapeutic agents for a wide range of genetic diseases and viral infections, where down-regulation of specific RNA transcripts may be of therapeutic benefit (Chapter 1: 1.4.3.3). With regard to p53, results from studies have demonstrated that targeting mutant p53 *in cellulo* using RNAi based suppression or Group I ribozyme mediated transcript repair resulted in a restoration of wt p53 function (Watanabe *et al.*, 2000; Martinez *et al.*, 2002).

Furthermore, there is increasing evidence to support oncogenic gain-of-function activities for some p53 mutations (Roemer 1999; Blagosklonny 2000; van Oijen *et al.,* 2000). Hence suppression of these mutant transcripts may be of potential therapeutic benefit.

The current study involved the evaluation of 6 hammerhead ribozymes targeting p53 RNA at NUX cleavage sites located in predicted open loops structures in the transcript, which were identified using computer modeling of secondary RNA structure. Experimental methods are available for selecting potential cleavage sites, including accessibility mapping using RNase H (Birikh *et al.,* 1997), however, these methods are typically more time-consuming and expensive compared to computer modeling. To increase the probability of selecting accessible cleavage sites in this study, two computer modeling programs were used, Mfold/PlotFold and RNAdraw (Matzura *et al.,* 1996; Zuker 2003). Only NUX target sites that were present in open loops in secondary structures generated by both programs were selected.

Subsequent to *in vitro* transcription of ribozyme and p53 RNA, ribozyme cleavage efficiency was evaluated using an *in vitro* assay with the ribozyme and p53 target RNA labeled with rUTP [α–P^{32}]. A nonradioactive method involving resolution of the ribozyme cleavage bands on high-resolution agarose gels was explored, but was found to be less sensitive and require large quantities of transcribed ribozyme and p53 target (data not shown). All 6 ribozymes cleaved p53 target RNA with varying success, with Rz 359 and 850 being the least efficient. Rz 359 targets a NUX (GUC) site at position 359-361 of mRNA sequence of p53 (NM_000546). With a ribozyme to target ratio of 64:1, approximately 15% of p53 target was cleaved after 3 hours incubation (Figure 6.11). Although GUC has been demonstrated to be a preferred codon for ribozyme cleavage (Zoumadakis *et al.,* 1995), in this study, possibly due to inaccessibility of the cleavage site, codon 359-361 was not efficiently cleaved by Rz 359. Rz 850 targeting an AUU codon (position 850-852) was also shown to be inefficient, cleaving approximately 13% of p53 target (ratio 91:1 of ribozyme to target RNA), after 3 hours

incubation possibly due to insufficient levels of ribozyme or inaccessibility of the cleavage site (Figure 6.18).

Rz 1398 was considerably more efficient cleaving ~ 60% of target p53 (ratio 60:1) after 1 hour (Figure 6.19, 6.21). Increasing the ratio of Rz 1398 to target (200:1) did not substantially increase the percentage target cleavage, ~66% compared to ~60% previously (Figure 6.20, 6.22). Rz 639 and Rz 1613 were similarly efficient at cleaving target p53. After a 2 hour incubation Rz 639 (ratio 128:1) cleaved ~80% of the p53 target (Figure 6.16), while Rz 1613 (ratio 94:1) cleaved ~75% (Figure 6.30). The most effective ribozyme, as estimated using this *in vitro* assay was Rz 1561, which targets an AUU codon (position 1561-1563). Although AUU is not believed to be the most preferred cleavage site for hammerhead ribozymes (Zoumadakis *et al.,* 1995), the site is positioned in a large open loop structure predicted by RnaDraw (Figure 6.1) and Mfold/Plotfold computer modeling of the p53 RNA target. Rz 1561 cleaved approximately 82% of the p53 target RNA (ratio 6:1) after 2 hours (Figure 6.25, 6.26). Increasing the molar ratio of Rz 1561 to 115, resulted in a target cleavage of approximately 90% (Figure 6.24B, 6.26).

In addition to identifying Rz 1561 as a potential therapeutic ribozyme for mutant p53, a mutation-independent based approach to gene suppression was also validated for Rzs 359 and 639, which in principle could be applied to Rz 1561 or any other ribozyme targeting p53. Two replacement p53 genes were generated with altered NUX sites, to protect expressed transcripts from ribozyme cleavage. Although a single base change has been deemed sufficient for the ribozyme to discriminate between endogenous transcripts and replacement transcripts (Millington-Ward *et al.,* 1997), two additional changes were introduced into the replacement p53 gene, in the region of the sequence used by the antisense arms of the ribozyme for binding. These nucleotide sequence changes exploited the degeneracy of the genetic code; by altering bases at wobble positions and so the amino acid sequence of the protein should in principle, remain unchanged. Transcripts from both p53 replacement constructs, p53Re359 and

p53Re639, were shown to remain intact in ribozyme cleavage assays with Rz 359 and Rz 639 respectively (Figure 6.11, Lane 11: Figure 6.14:B, Lane 2).

As Rz 1561 was found to be effective at cleaving the target p53 RNA *in vitro*, this ribozyme was further evaluated in 293T cells that express endogenous p53 (Maeda *et al.*, 2002). Total RNA was analysed by real-time RT PCR to determine the relative levels of p53 in 293T cells transfected with a plasmid vector with CMV promoter-driven Rz 1561 compared to levels in 293T cells transfected with a plasmid carrying a non-targeting ribozyme (Rz 40, targeting rhodopsin). No significant suppression of p53 was shown ($P > 0.05$), with a relative level of p53 in 293T cells transfected with Rz 1561 of 103.50 ± 18.42% for 0.5μg Rz 1561 transfected and 102.42 ± 19.65% for 1.0μg Rz 1561 (Figure 6.31).

This lack of *in cellulo* activity of Rz 1561 may be due a number of reasons. Firstly, the level of Rz 1561 may not have been sufficiently high to downregulate p53 expression in cell culture. Rz 1561 expression was driven by a polymerase II promoter, and it has been suggested that these promoters may be more suitable for expressing long RNAs (Shiota *et al.*, 2004). Using a polymerase III promoter, such as U1, U6 or H1 promoters, all of which express short RNAs *in vivo*, may be more effective for expressing Rz 1561. In addition, transfection of the plasmid vector was transient, whereas suppression of target transcripts by ribozymes *in cellulo* has been demonstrated in several studies using generate stable cell lines expressing the ribozyme or using viral vectors as delivery agents (Kashani-Sabet *et al.*, 1994; Cai *et al.*, 1995; Millington-Ward *et al.*, 2002; Tekur *et al.*, 2002). However, as 293T cells in the current study were shown to be efficiently transfected at a rate of approximately 70% using a β-gal reporter construct (data not shown), generating a stable cell line expressing Rz 1561 would not be expected to result in an increased level of p53 suppression. With regard to viral vector delivery, it is notable that Dr. Sophia Millington-Ward (Trinity College Dublin) found that transient expression of a ribozyme from a plasmid targeting the transcript of *COL1A1*, a gene frequently mutated in a degenerative bone disorder, osteogenesis imperfecta (OI), did not suppress COLIA1 expression (unpublished

results). In contrast retroviral vector delivery of the same hammerhead ribozyme, suppressed COLIA1 at the mRNA and protein level in bone stem cells by approximately 40% (Millington-Ward *et al.,* 2002).

As Rz 1561 was expressed from a plasmid construct, it was not chemically modified to increase intracellular stability, which may also account for the lack of observed suppression of p53 in 293T cells, as endogenous nucleases may degrade the expressed ribozyme too rapidly for it to mediate suppression. Although studies have demonstrated suppression with unmodified ribozymes *in cellulo* (Lee *et al.,* 1999; Tekur *et al.,* 2002), the level and activity of endogenous nucleases may vary between cell lines, possibly accounting for lack of p53 target suppression by Rz 1561 in 293T cells.

However, prior to further evaluation of alternative expression systems for Rz 1561, kinetic studies to determine parameters such as V_{max}, the maximum velocity of the cleavage reaction when the ribozyme is saturated, and K_m (Michaelis Constant), the ribozyme concentration at which the cleavage velocity is half maximal would be valuable (Voet 1990). Further studies evaluating additional ribozymes targeting 12 more NUX cleavage sites identified in the current study, may also identify more efficient ribozymes that cleave p53 RNA. In addition, further evaluation of Rz 1613, which was also demonstrated to be efficient in the current study (Figures 6.28-30), would be worthwhile. Following *in vitro* evaluation, ribozymes targeting p53, possibly delivered by retroviral or adenoviral vectors could be assessed in cell lines expressing dominant-negative mutants of p53, such as CCL 227 (Arg237His), CCL 11731 (Arg175His), available from American Type Culture Collection (ATCC), Manassas VA, USA (http://www.atcc.org) (Dittmer *et al.,* 1993). Furthermore there are a number of transgenic mouse models available that express dominant-negative mutants of p53 including, Trp53 A135V (alanine to valine at codon 135) (Harvey *et al.,* 1995) and Trp53R172H (arginine to histidine at codon 172) (Li *et al.,* 1998a), both available from The Jackson Laboratory, Bar Harbor, MD, USA.

The current study describes the assessment of 6 hammerhead ribozymes targeting p53 *in vitro*. One potentially efficient ribozyme, Rz 1561, which requires further *in vitro* and *in vivo* evaluation, has been identified. In addition, the feasibility of a mutation-independent approach to targeting mutant p53 transcripts was also validated. Replacement p53 transcripts for Rzs 359 and 639 were generated with a number of base changes to alter the ribozyme cleavage site and the region where the antisense arms of the ribozyme bind. As these changes were made to third base wobble positions, the amino-acid sequence of the p53 protein should be unaltered. The replacement p53 transcripts were shown to be protected from cleavage by Rz 359 (Figure 6.11) and Rz 639 (Figure 6.14B). Clearly for future evaluation of Rz 1561, a replacement construct would be generated, although given the results of the current study demonstrating that suppression-resistant p53 transcripts can be generated, and the previous studies of the laboratory in TCD (Millington-Ward *et al.*, 1997; Kiang *et al.*, 2005; Palfi *et al.*, 2006), it would be expected that similar protection of a replacement p53 RNA transcript for Rz 1561 may be observed. A mutation-independent approach could be applied to other suppression tools including RNAi and several studies have demonstrated p53 suppression using RNAi to target specific mutations (Martinez *et al.*, 2002; Shen *et al.*, 2003). Exploiting the degeneracy of the genetic code, as described in the current study, targeting polymorphisms or untranslated regions (UTR) of RNA, reviewed in Chapter 1: 1.2.10.3, would enable p53 suppression in a mutation-independent manner. Suppression of mutant p53 with co-delivery of a suppression resistant replacement gene, may be of great potential therapeutic value for p53-related cancers. Given that delivery of wt-p53 enhances tumour cells' sensitivity to conventional chemotherapeutic agents (Fujiwara *et al.*, 1994b; Gallardo *et al.*, 1996), suppression/replacement gene therapy would possibly be used in conjunction with conventional chemotherapeutic agents. Furthermore, results from studies have demonstrated that delivering additional tumour suppressors, such as *p16INK4*, or pro-apoptotic genes such as *Apaf-1* and *caspase-9*, in addition to p53 enhance apoptosis of tumour cells (Sandig *et al.*, 1997; Shinoura *et al.*, 2003).

As the pathways underlying tumourogenesis continue to be unraveled, more effective therapeutic strategies for p53-related cancers are being developed. The dominant-negative effect of many of the p53 missense mutations and the increasing evidence to support oncogenic gain-of-function activities of the mutant p53, suggest that suppression/replacement based gene therapy may potentially form part of the therapeutic strategy for patients suffering from p53-related cancers in the future.

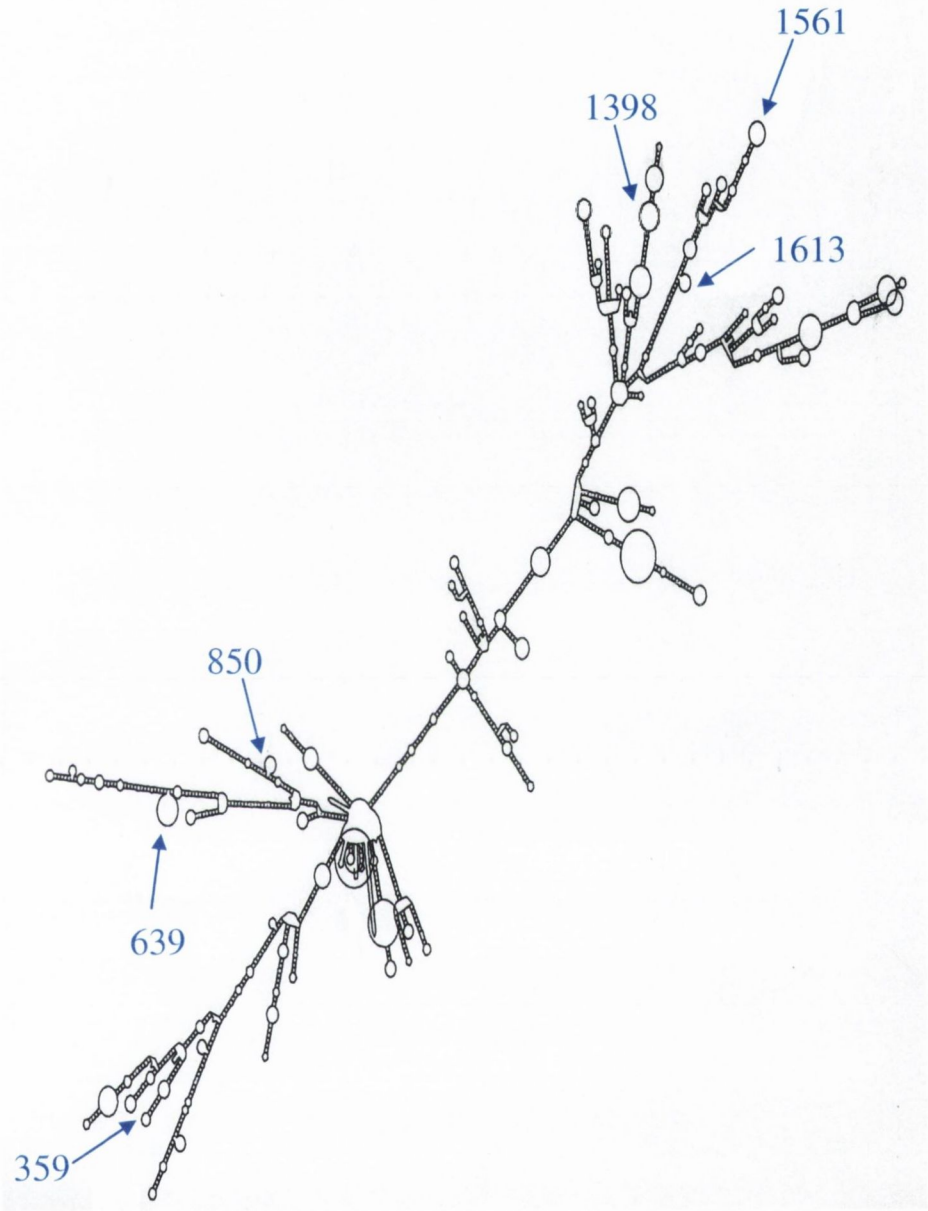

Figure 6.1: Secondary structure of p53 RNA (1-2629 bp) as predicted by the computer program RNAdraw. Potential ribozyme cleavage target sites are marked in blue (see 6.2.1).

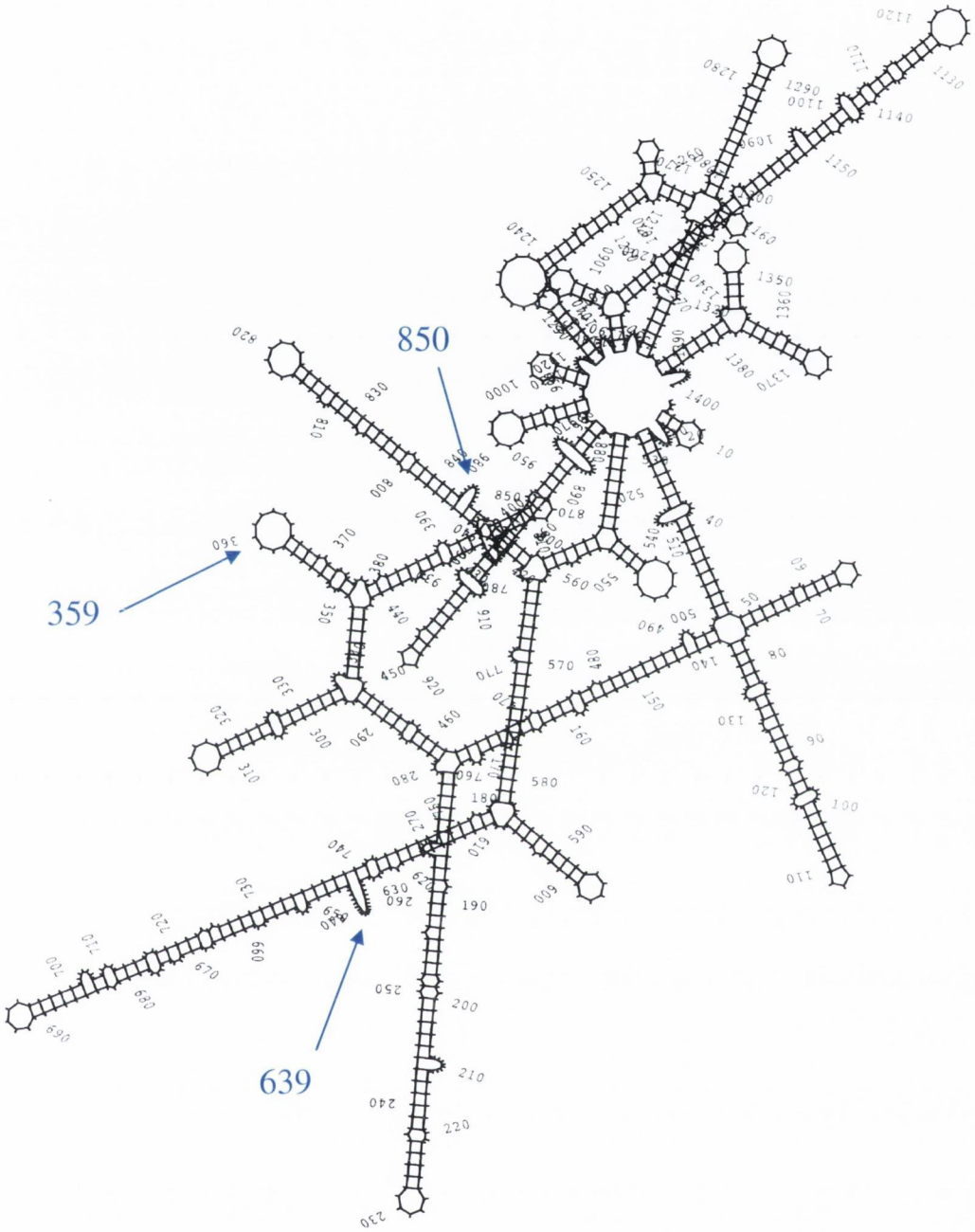

Figure 6.2: Secondary structure of p53 RNA (1-1400 bp) as predicted by the program Mfold and its companion program PlotFold. Potential ribozyme cleavage target sites are marked in blue (see 6.2.1).

Ribozyme 359

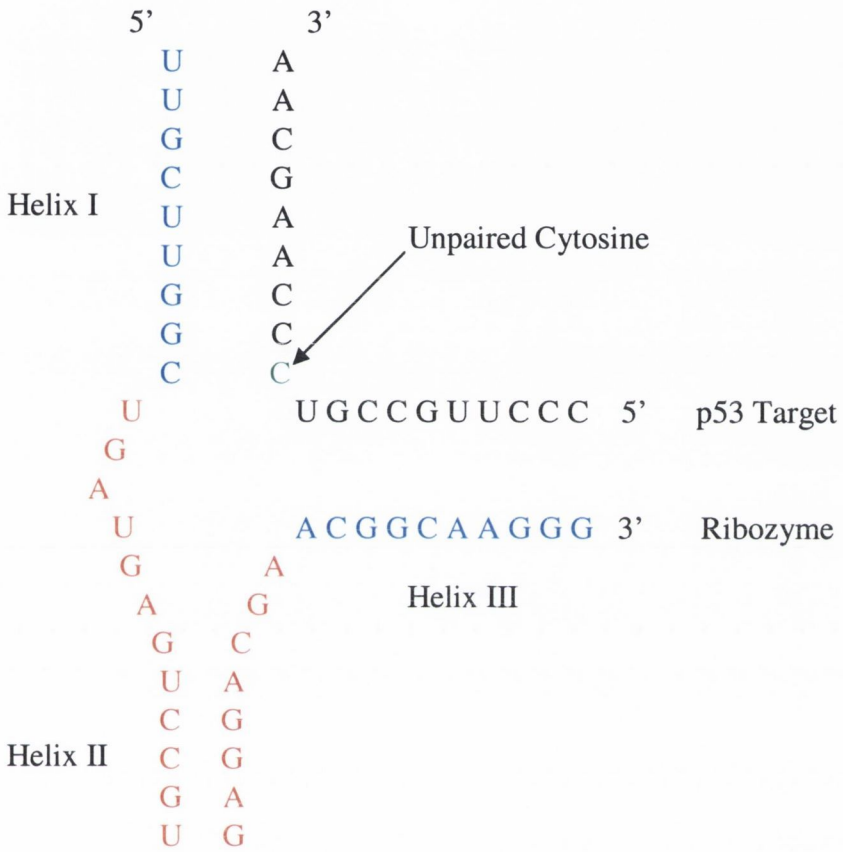

Figure 6.3: Sequence of hammerhead ribozyme 359. p53 RNA target is in black and the unpaired cytosine of the GUC cleavage codon is in green. The antisense arms of Rz 359 are in blue, forming helices I and III with the target RNA, and the conserved region is in red, which forms helix II (see 6.2.2).

Ribozyme 639

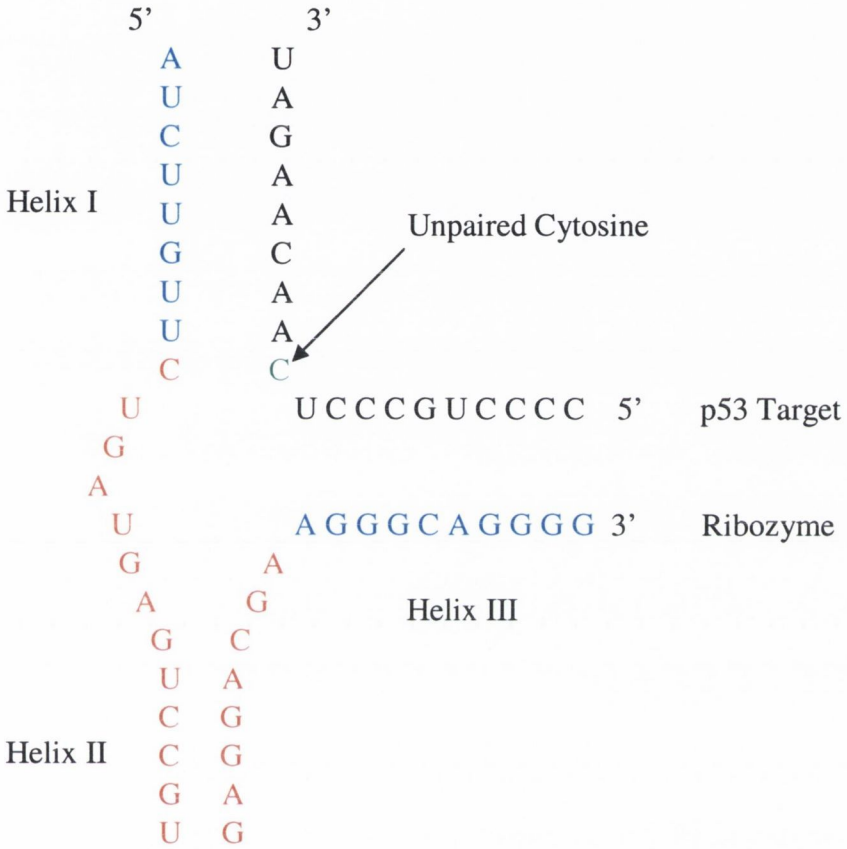

Figure 6.4: Sequence of hammerhead ribozyme 639. p53 RNA target is in black and the unpaired cytosine of the CUC cleavage codon is in green. The antisense arms of Rz 639 are in blue, forming helices I and III with the target RNA, and the conserved region is in red, which forms helix II (see 6.2.2).

Ribozyme 850

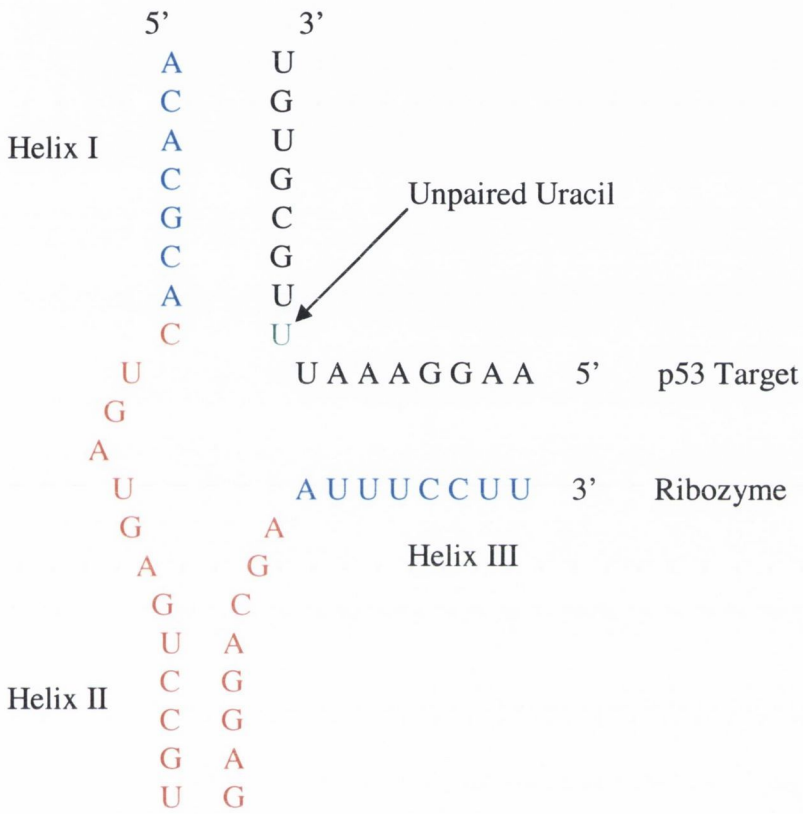

Figure 6.5: Sequence of hammerhead ribozyme 850. p53 RNA target is in black and the unpaired cytosine of the AUU cleavage codon is in green. The antisense arms of Rz 850 are in blue, forming helices I and III with the target RNA, and the conserved region is in red, which forms helix II (see 6.2.2).

Riboyzme 1398

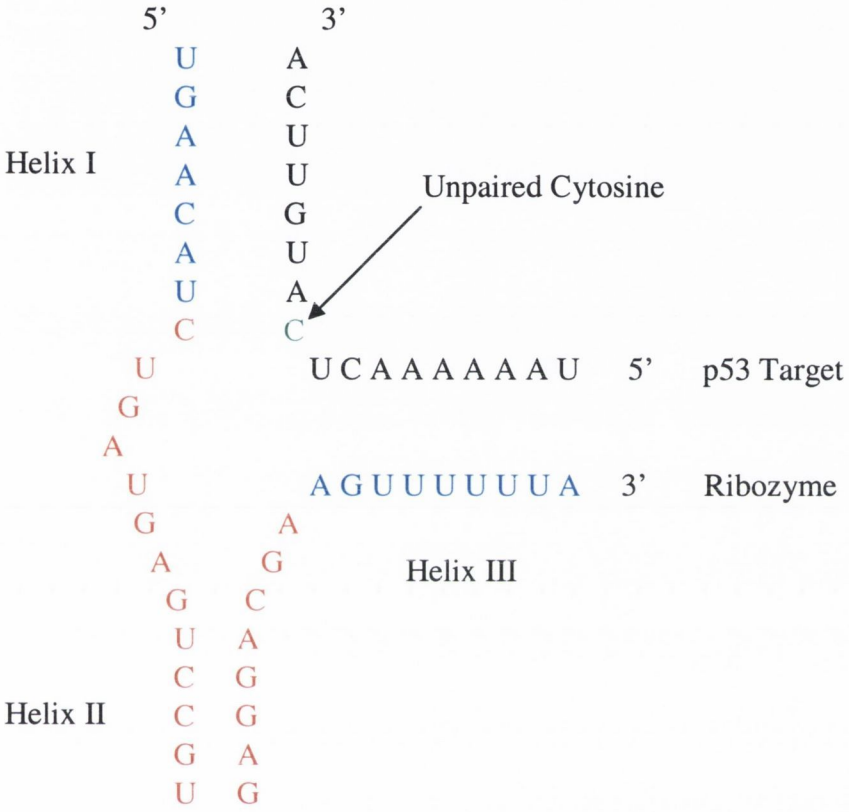

Figure 6.6: Sequence of hammerhead ribozyme 1398. p53 RNA target is in black and the unpaired cytosine of the CUC cleavage codon is in green. The antisense arms of Rz 1398 are in blue, forming helices I and III with the target RNA, and the conserved region is in red, which forms helix II (see 6.2.2).

Ribozyme 1561

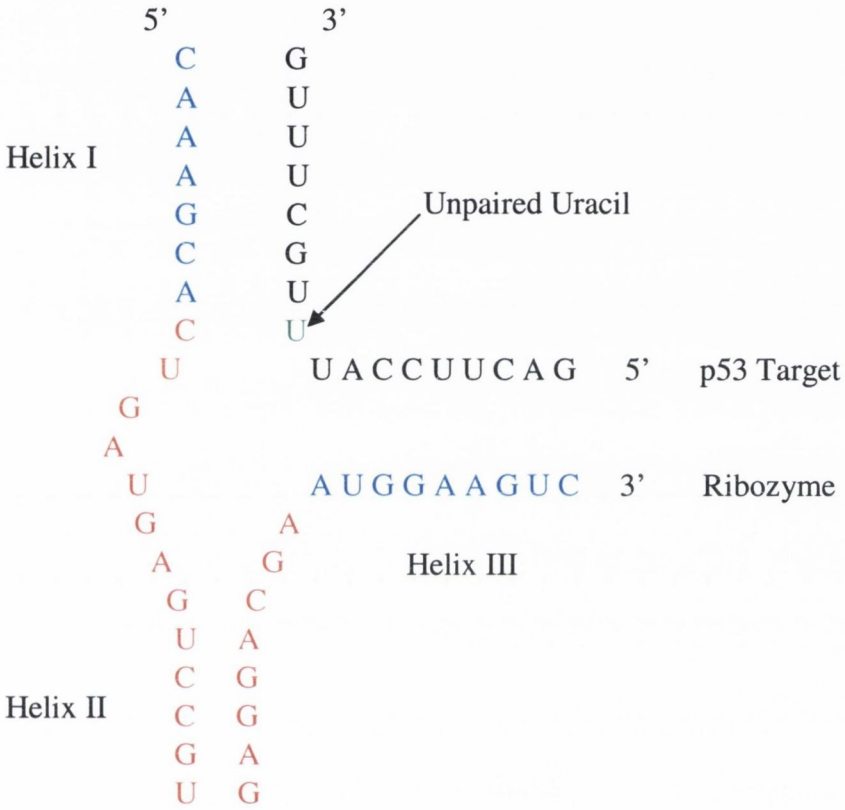

Figure 6.7: Sequence of hammerhead ribozyme 1561. p53 RNA target is in black and the unpaired uracil of the AUU cleavage codon is in green. The antisense arms of Rz 1561 are in blue, forming helices I and III with the target RNA, and the conserved region is in red, which forms helix II (see 6.2.2).

Ribozyme 1613

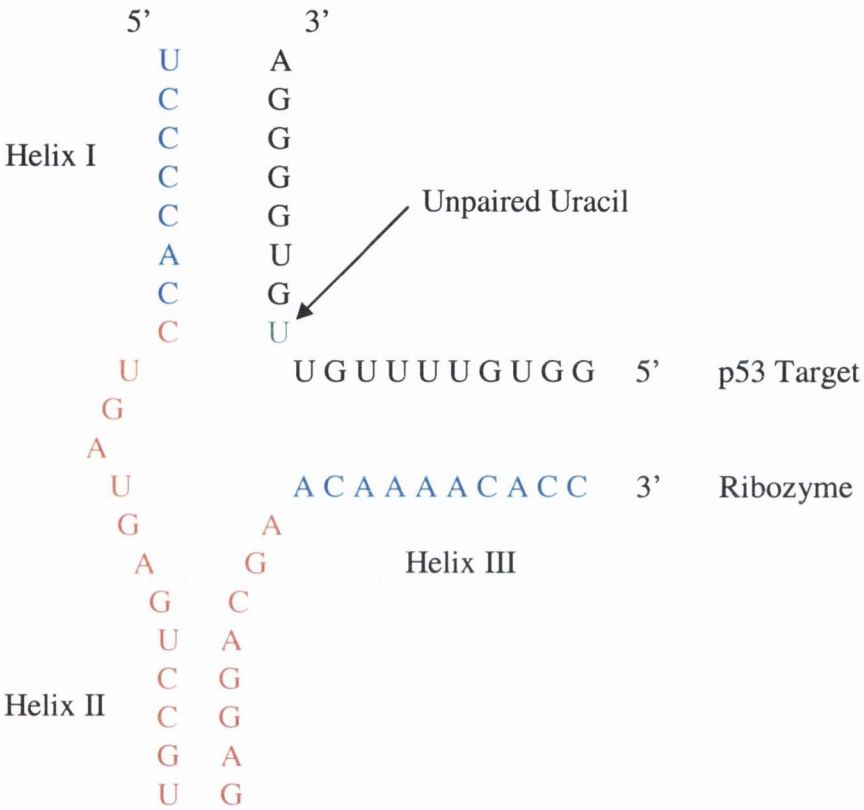

Figure 6.8: Sequence of hammerhead ribozyme 1613. p53 RNA target is in black and the unpaired cytosine of the GUU cleavage codon is in green. The antisense arms of Rz 1613 are in blue, forming helices I and III with the target RNA, and the conserved region is in red, which forms helix II (see 6.2.2).

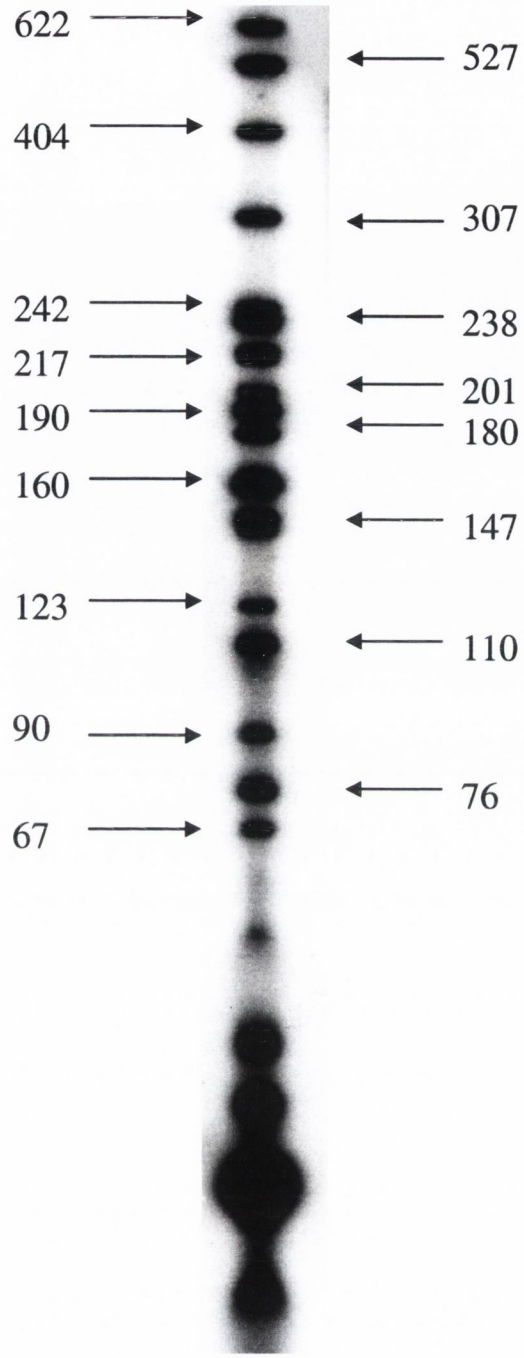

Figure 6.9: ***Msp*I cut pBr322 labeled with the radionucleotide dCTP [α–P^{32}].** This was used as a DNA ladder to approximate the size of uncut and cleavage products of *in vitro* expressed RNA (see 6.2.10).

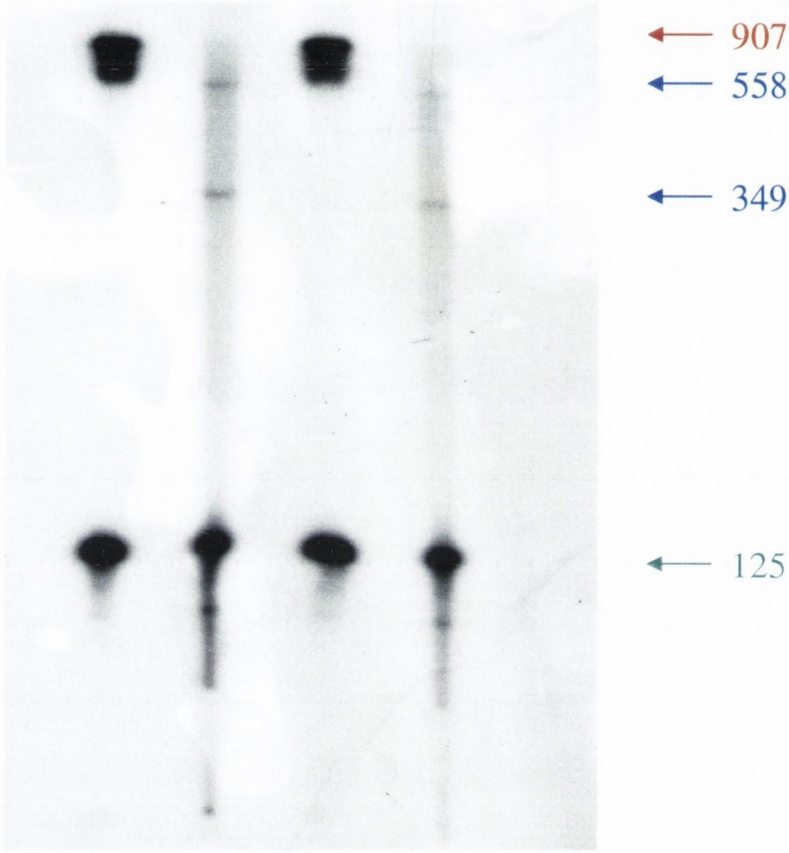

Figure 6.10: Time point cleavage reaction of p53 RNA by Rz 359. Lanes 1 and 3, p53 RNA at 0mM $MgCl_2$ for 1 hr at 37°C; Lane 2, Rz 359 with p53 RNA at 20mM $MgCl_2$ for 1 hr at 37°C (Ratio 100:1); Lane 4, as Lane 2 with commercial 20mM $MgCl_2$ (see 6.2.6-6.2.9). The red arrow indicates full-length p53 RNA of 907 bases and blue arrows indicate the cleavage products of 558 and 349 bases. Rz 359 is indicated by a green arrow at 125 bases.

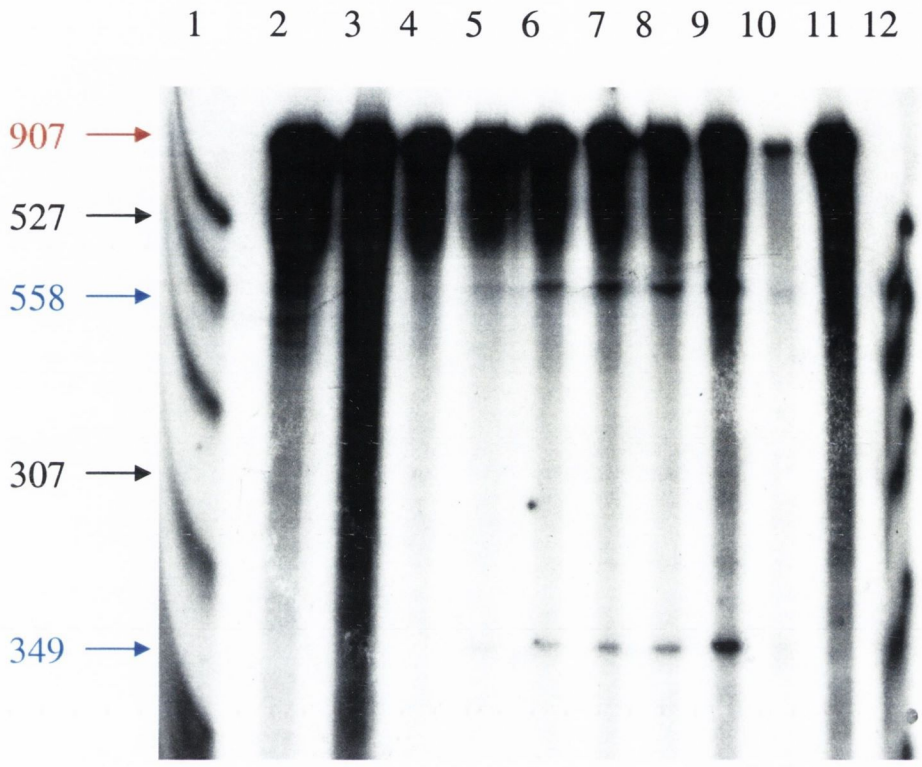

Figure 6.11: Time point cleavage reaction of p53 RNA and p53Re359 by Rz 359. Lane 1, DNA ladder; Lane 2, Rz 359 with p53 RNA at 0mM $MgCl_2$ for 180 mins at 37°C; Lane 3, p53 RNA at 0mM $MgCl_2$ for 180 mins at 37°C; Lanes 4-10, Rz 359 with p53 RNA at 20mM $MgCl_2$ at 0, 30, 60, 90, 120, 150, and 180 mins at 37°C (Ratio 64:1); Lane 11, Rz 359 with p53Re359 RNA at 20mM $MgCl_2$ for 180 mins (see 6.2.6-6.2.9). DNA size standards are indicated in black. The red arrow indicates full-length p53 RNA of 907 bases and blue arrows indicate the cleavage products of 558 and 349 bases.

Figure 6.12: Time point cleavage reaction of p53 RNA and p53Re359 by Rz 359. Lane 1, p53 RNA at 0mM $MgCl_2$ for 180 mins at 37°C; Lanes 2-4, Rz 359 with p53 RNA at 20mM $MgCl_2$ at 0, 60 and 120 mins at 37°C (Ratio 64:1); Lane 5, Rz 359 with p53Re359 RNA at 20mM $MgCl_2$ for 180 mins; Lane 6, DNA ladder (see 6.2.6-6.2.9). DNA size standards are indicated in black on the right side of the image. The red arrow indicates full-length p53 RNA of 907 bp and blue arrows indicate the cleavage products of 558 and 349 bp.

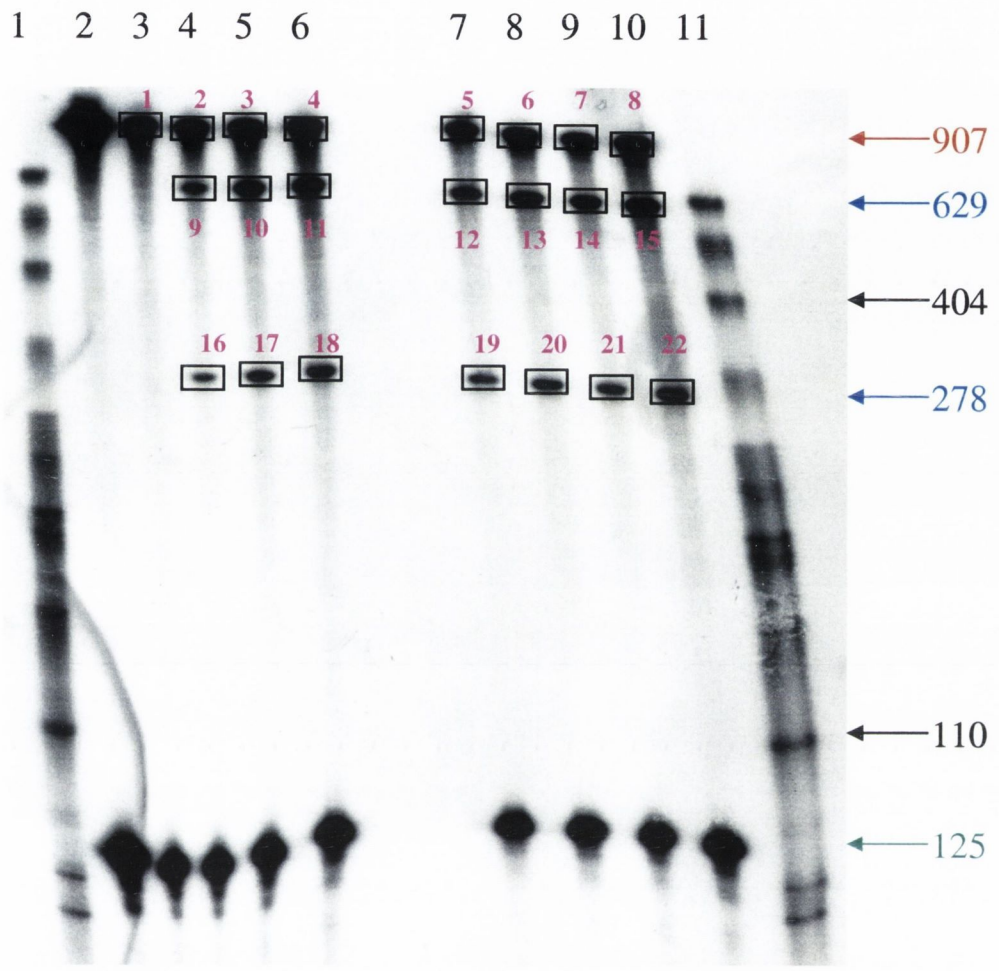

Figure 6.13: Time point cleavage reaction of p53 RNA by Rz 639. Lane 1, DNA ladder; Lane 2, Rz 639 with p53 RNA at 0mM $MgCl_2$ for 180 mins at 37°C; Lanes 3-10 (Ratio 31:1), Rz 639 with p53 RNA at 20mM $MgCl_2$ at 1, 30, 90, 120, 157, 180, 210 and 240 mins at 37°C; Lane 11, DNA ladder (see 6.2.6-6.2.9). DNA size standards are indicated in black on the right side of the image. The red arrow indicates full-length p53 mRNA of 907 bases and blue arrows indicate the cleavage products of 629 and 278 bases. Rz 639 is indicated by a green arrow at 125 bases. Rectangular boxes, numbered in purple illustrate the bands to be quantified using ImageQuant Software (Molecular Dynamics).

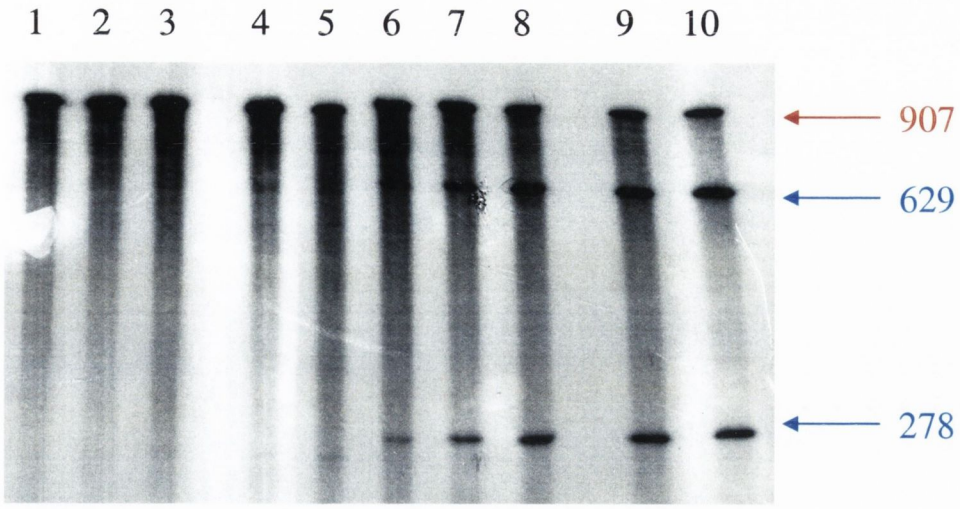

Figure 6.14A: Time point cleavage reaction of p53 RNA by Rz 639. Lanes 1-5, Rz 639 with p53 RNA at 20mM $MgCl_2$ at 1, 5, 15, 30 and 120 mins at 37°C (Ratio 0.6:1); Lanes 6-11, Rz 639 with p53 RNA at 20mM $MgCl_2$ at 1, 5, 15, 30, 120 mins at 37°C (Ratio 32:1). The red arrow indicates full-length p53 RNA of 907 bases and blue arrows indicate the cleavage products of 629 and 278 bases.

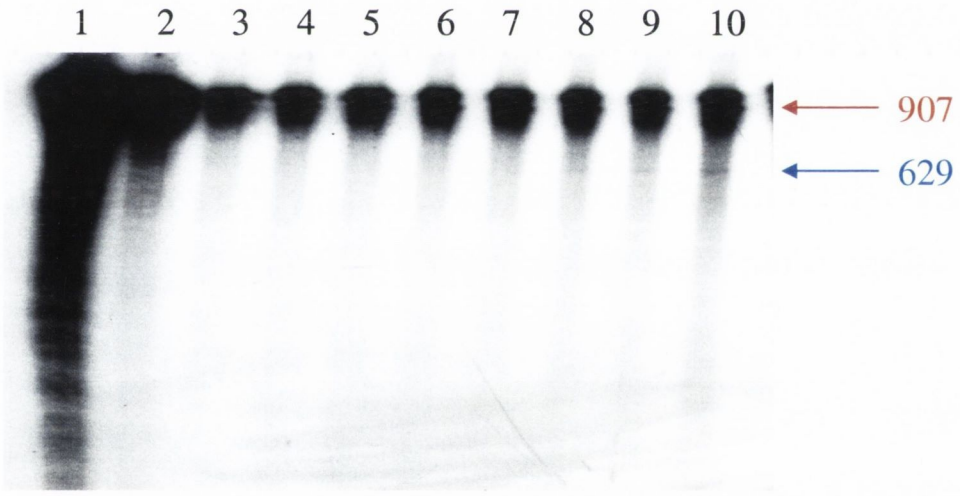

Figure 6.14B: Time point cleavage reaction of p53 RNA by Rz 639. Lanes 1, Rz 639 with p53 RNA at 0mM $MgCl_2$ at 120 mins at 37°C; Lane 2, Rz 639 with p53Re639 at 20mM $MgCl_2$ at 180 mins at 37°C (Ratio 32:1); Lanes 3-10, Rz 639 with p53 RNA at 20mM $MgCl_2$ at 0, 5, 7, 10, 20, 30, 90, 180 mins at 37°C (Ratio 0.6:1) (see 6.2.6-6.2.9). The red arrow indicates full-length p53 RNA of 907 bases and blue arrows indicate the cleavage product of 629 bases. The second cleavage produce of 278 bases is not visible, due to low level of cleavage.

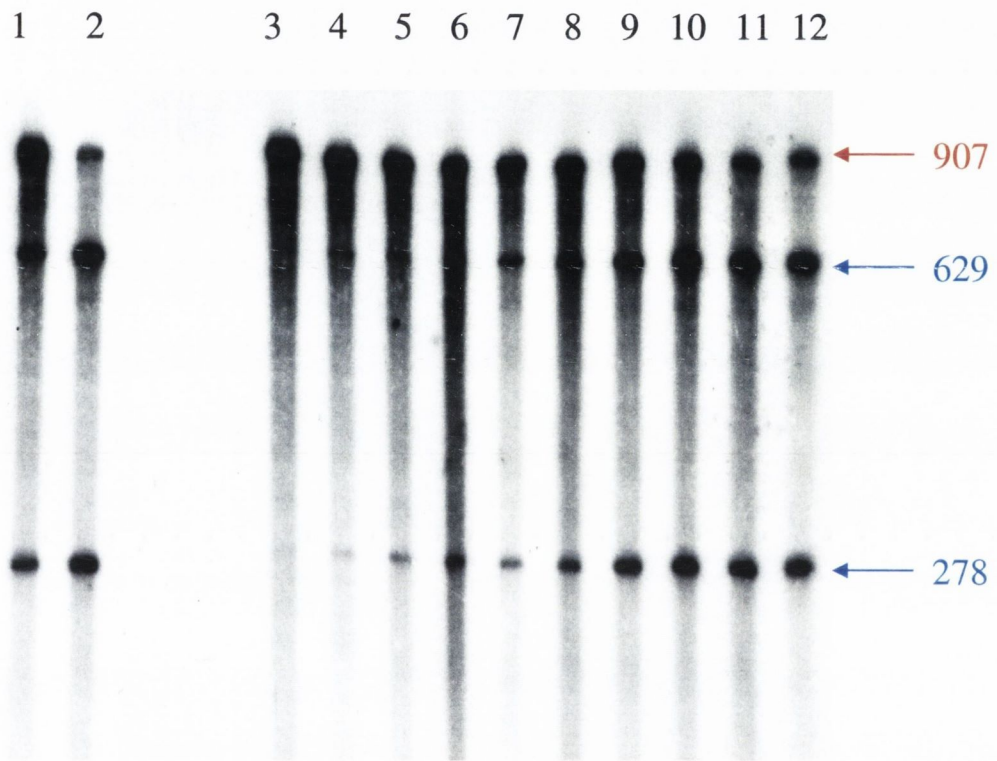

Figure 6.15: Time point cleavage reaction of p53 RNA by Rz 639. Lanes 1-2, Rz 639 with p53 RNA at 20mM $MgCl_2$ at 1 and 120 mins at 37°C (Ratio 320:1); Lanes 3-7, Rz 639 with p53 mRNA at 20mM $MgCl_2$ at 1, 5, 15, 30 and 120 mins at 37°C (Ratio 6:1); Lanes 8-12, Rz 639 with p53 RNA at 20mM $MgCl_2$ at 1, 5, 15, 30 and 120 mins at 37°C (Ratio 128:1) (see 6.2.6-6.2.9). The red arrow indicates full-length p53 RNA of 907 bases and blue arrows indicate the cleavage products of 629 and 278 bases.

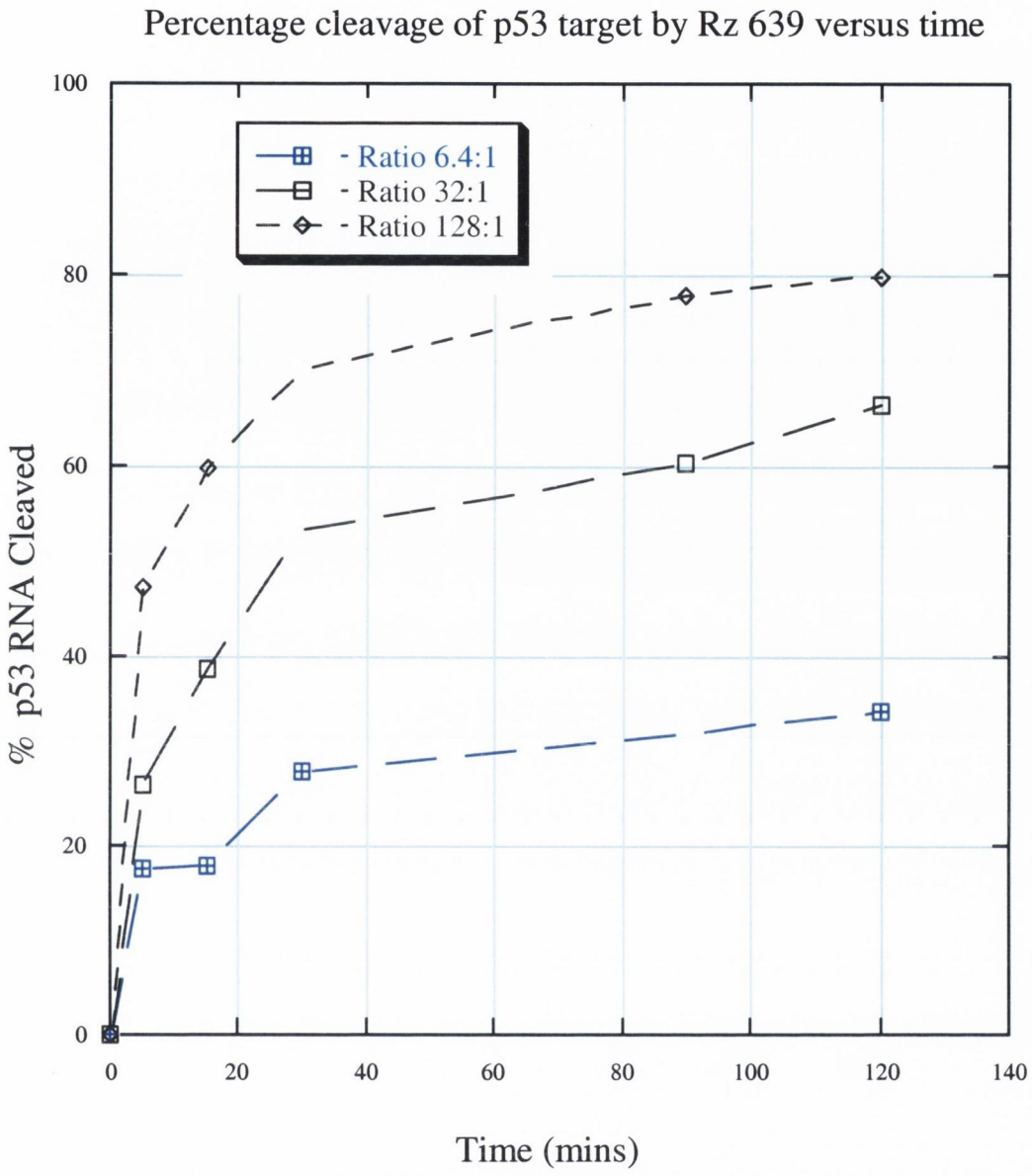

Figure 6.16 : Graph of percentage cleavage of p53 target RNA with varying ratios of Rz 639 versus time. Varying excess molar ratios (6:1, 32:1, 128:1) of Rz 639 and transcribed p53 target were incubated in cleavage reactions and aliquots taken at various time points for resolution on a 4% acrylamide gel. Percentage cleavage was analysed by exposing the dried gel to phosphor screens, and quantifying the bands using a Typhoon Imager with ImageQuant software (see 6.2.6-6.2.9).

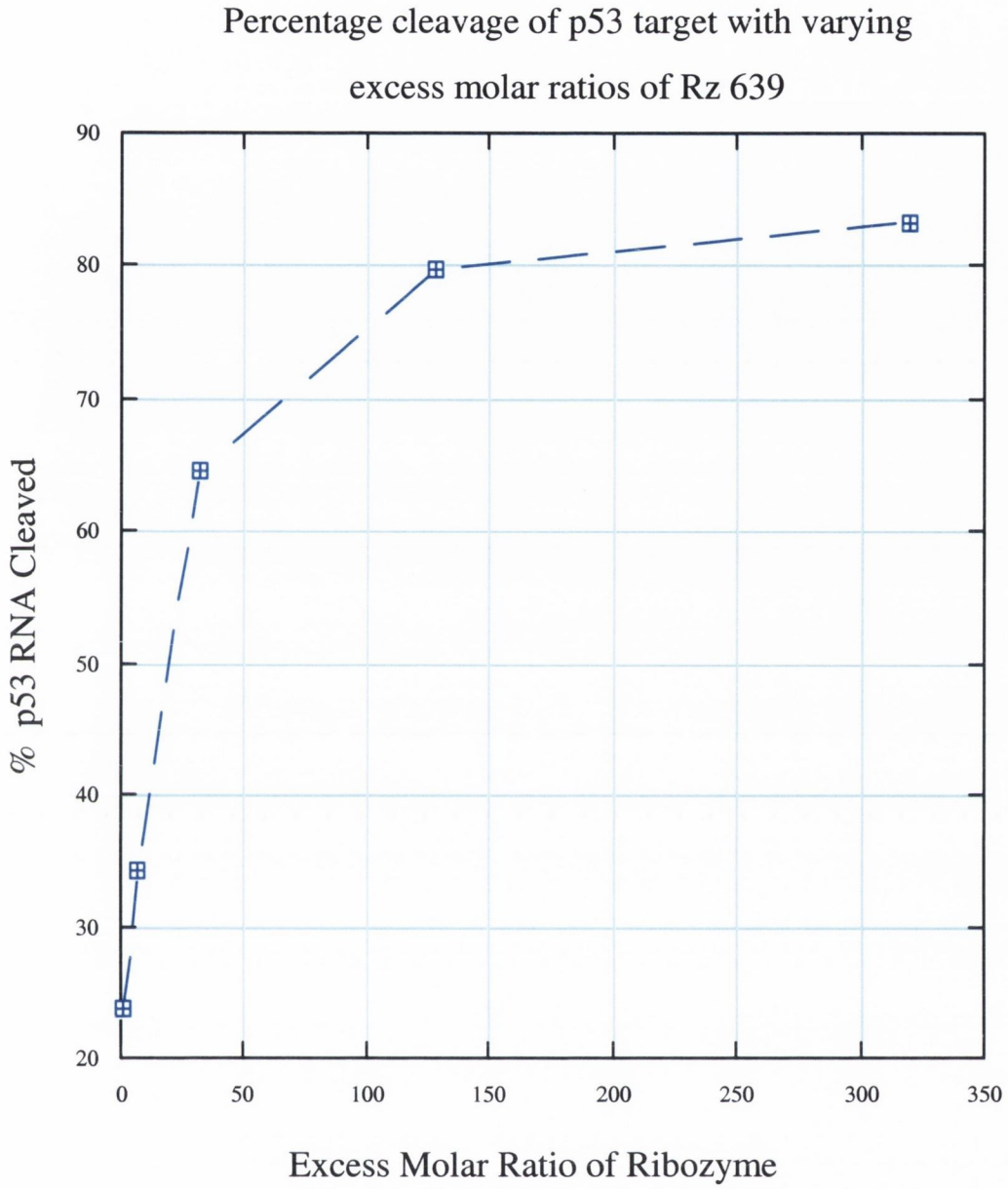

Figure 6.17: Graph of percentage cleavage of p53 RNA with varying ratios of Rz 639 after 120 mins incubation. Varying excess molar ratios (0.6:1, 6:1, 32:1, 128:1, 320:1) of Rz 639 and transcribed p53 target were incubated in cleavage reactions and aliquots taken at various time points for resolution on a 4% acrylamide gel. Percentage cleavage at 120 minutes was analysed by exposing the dried gel to phosphor screens, and quantifying the bands using a Typhoon Imager with ImageQuant software (see 6.2.6-6.2.9).

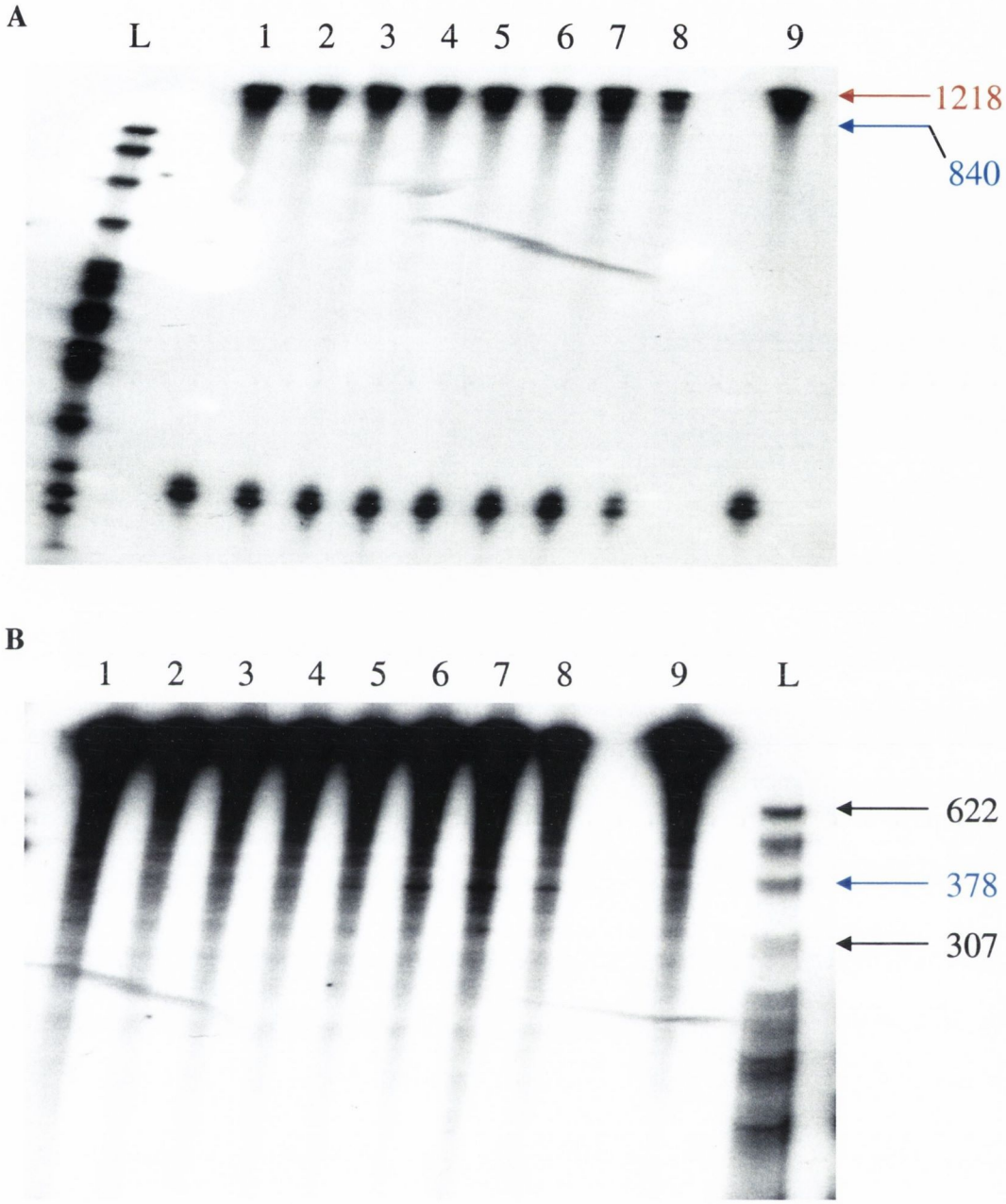

Figure 6.18A: Time point cleavage reaction of p53 RNA by Rz 850. Lanes 1-8, Rz 850 with p53 RNA at 20mM $MgCl_2$ at 1, 5, 7.5, 10, 20, 60, 120, and 180 mins at 37°C (Ratio 94:1); Lane 9, Rz 850 with p53 RNA at 0mM $MgCl_2$ at 180 mins at 37°C; Lane L, DNA ladder (see 6.2.6-6.2.9). The red arrow indicates the full-length p53 RNA of 1218 bases and the blue arrows indicate the cleavage products at 840 and 378 bases. **B:** As above but the audioradiograph was developed after 7 more days of exposure.

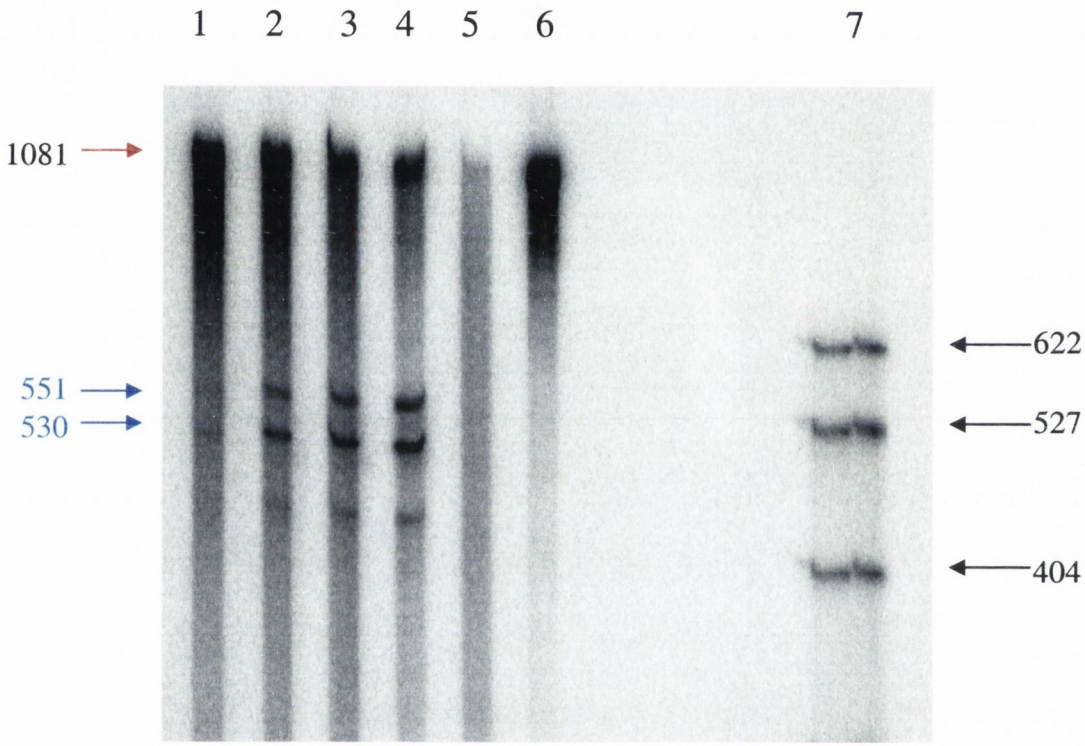

Figure 6.19: Time point cleavage reaction of p53scRNA by Rz 1398. Lanes 1-4, Rz 1398 with p53sc RNA at 20mM $MgCl_2$ at 1, 5, 15 and 60 minutes at 37°C; Lane 5, p53sc RNA at 20mM $MgCl_2$ at 120 mins at 37°C (Ratio 60:1); Lane 6, Rz 1398 with p53sc RNA at 0mM $MgCl_2$ at 120 mins at 37°C; Lane 7, DNA ladder (see 6.2.6-6.2.9). The red arrow indicates full-length p53sc RNA of 1081 bases and blue arrows indicate the cleavage products of 551 and 530 bases. DNA size standards are indicated in black to the right of the image.

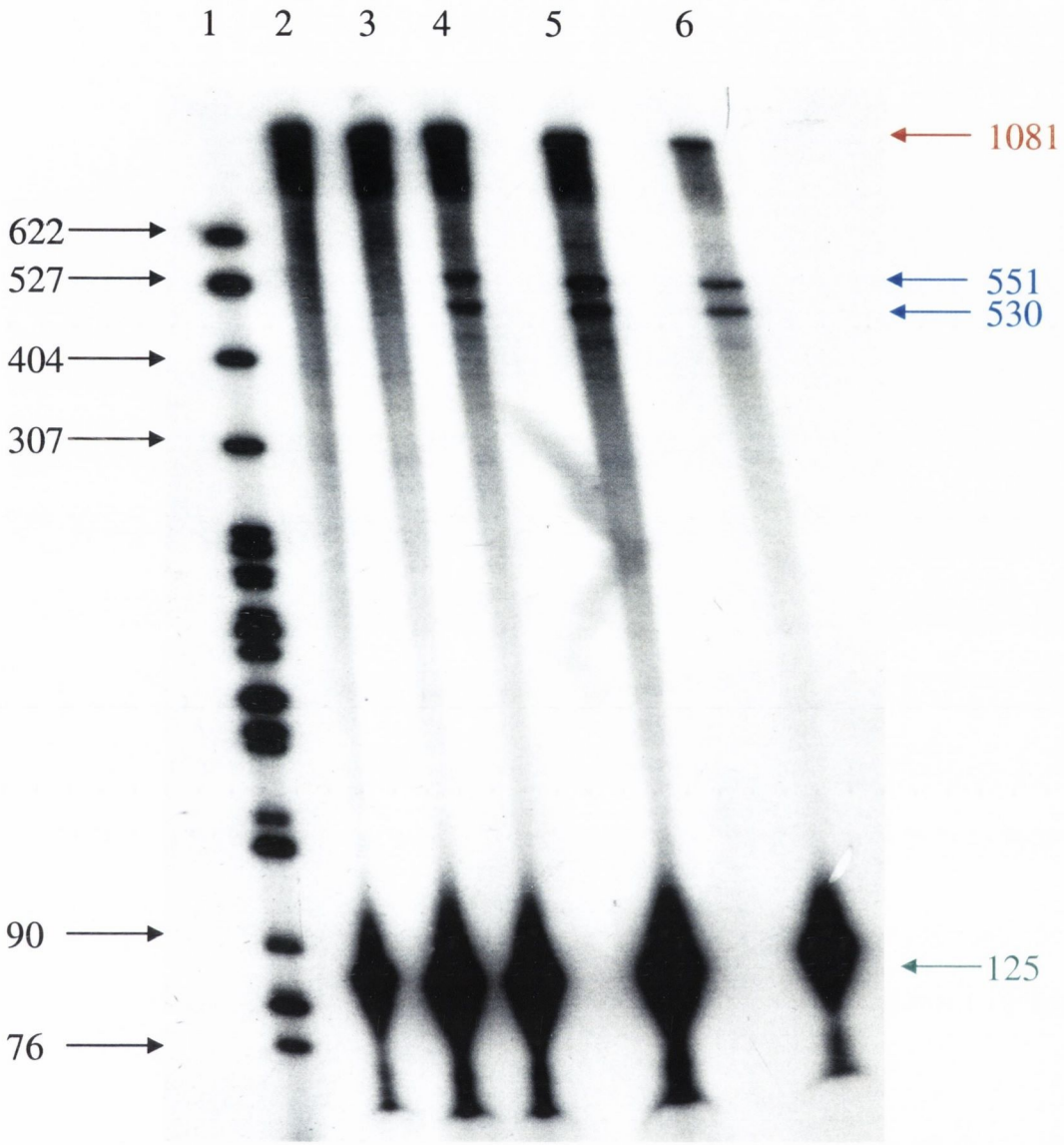

Figure 6.20: Time point cleavage reaction of p53scRNA by Rz 1398. Lane 1, DNA ladder; Lane 2, Rz 1398 with p53sc RNA at 0mM $MgCl_2$ for 2 hrs at 37°C; Lanes 3-6, Rz 1398 with p53sc RNA at 20mM $MgCl_2$ at 0, 30, 60, 120 mins. (Ratio 200:1) (see 6.2.6-6.2.9). Numbers on left hand side of the gel beside the DNA ladder indicate approximate size markers. Red arrow indicates full-length p53sc mRNA of 1081 bases and blue arrows indicate the cleavage products of 551 and 530 bases. Rz 1398 is indicated by a green arrow at 125 bases.

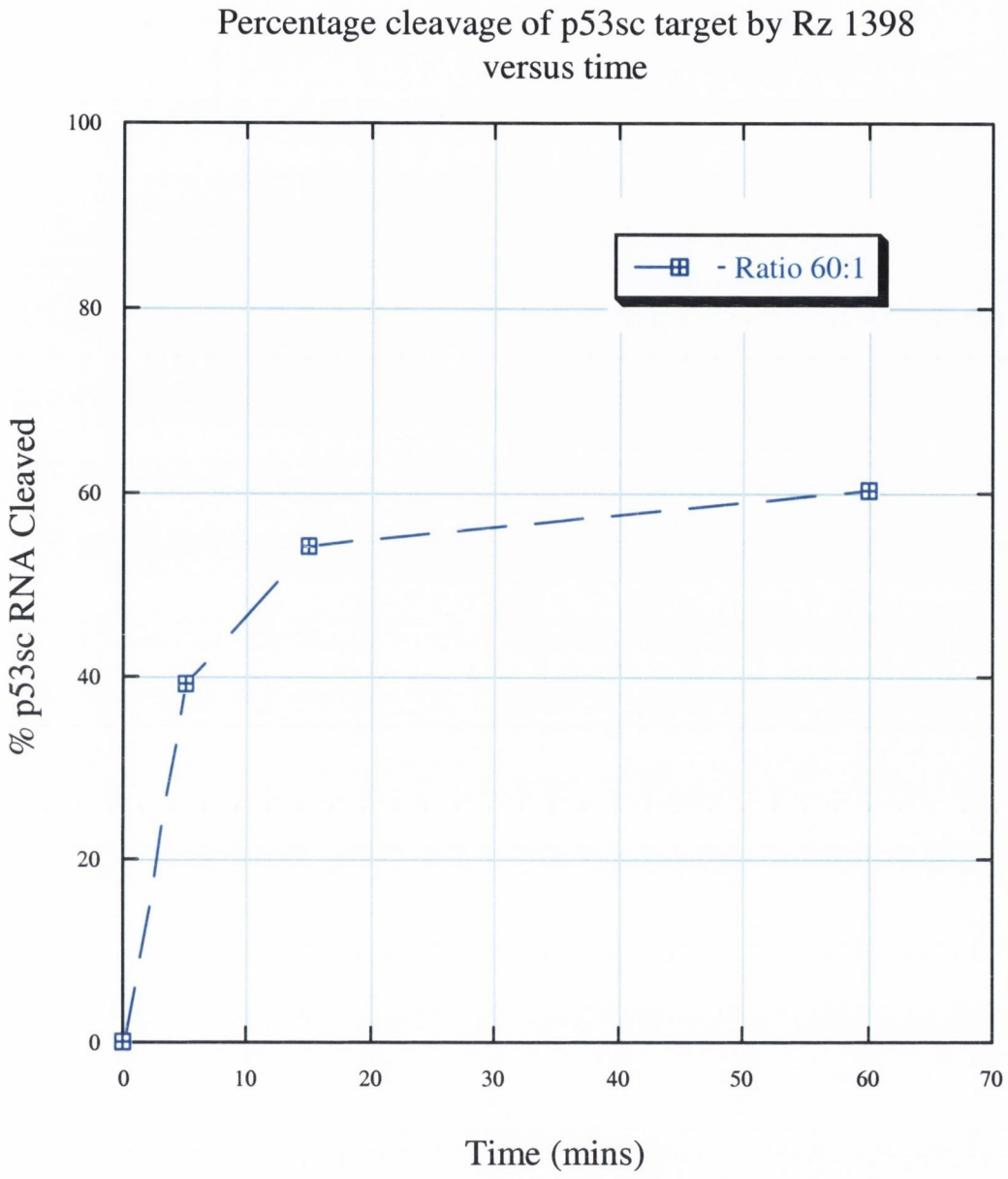

Figure 6.21: Graph of percentage cleavage of p53sc RNA with 60 fold excess of Rz 1398 versus time. Rz 1398 and transcribed p53 target (60:1) were incubated in cleavage reactions and aliquots taken at various time points for resolution on a 4% acrylamide gel. Percentage cleavage was analysed by exposing the dried gel to phosphor screens, and quantifying the bands using a Typhoon Imager with ImageQuant software (see 6.2.6-6.2.9).

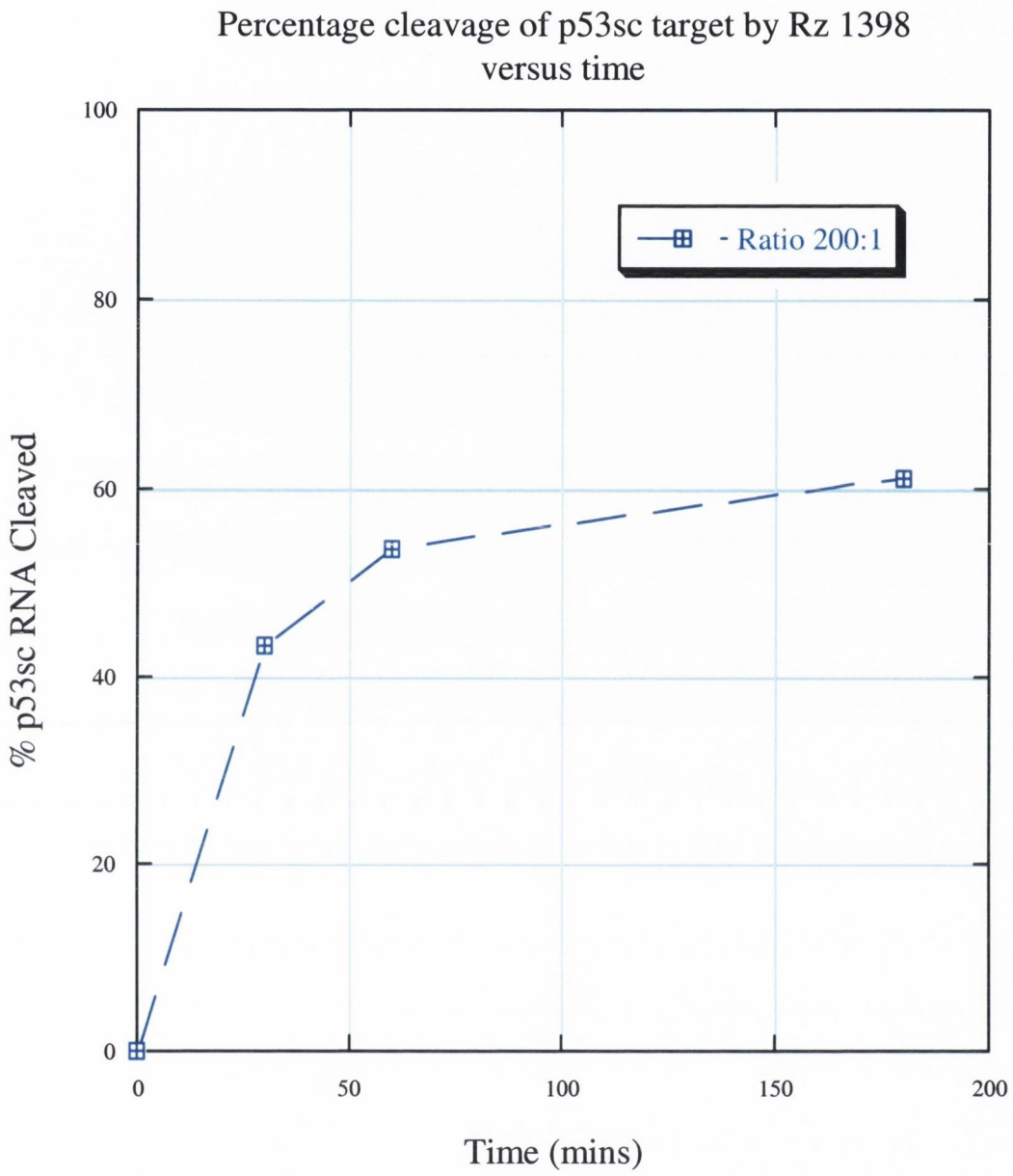

Figure 6.22: Graph of percentage cleavage of p53sc RNA with 200 fold excess of Rz 1398 versus time. Rz 1398 and transcribed p53 target (200:1) were incubated in cleavage reactions and aliquots taken at various time points for resolution on a 4% acrylamide gel. Percentage cleavage was analysed by exposing the dried gel to phosphor screens, and quantifying the bands using a Typhoon Imager with ImageQuant software (see 6.2.6-6.2.9).

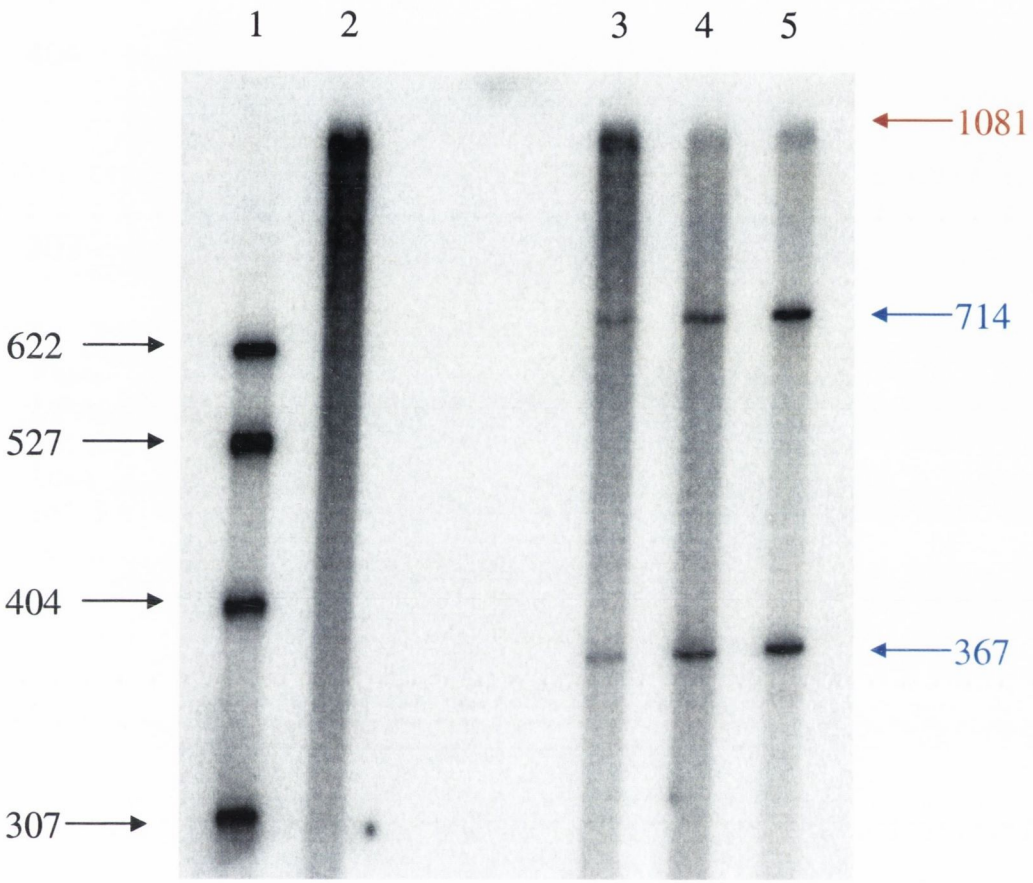

Figure 6.23: Time point cleavage reaction of p53scRNA by Rz 1561. Lane 1, DNA Ladder; Lanes 2-5, Rz 1561 with p53sc RNA at 20mM $MgCl_2$ at 0, 5, 15, 90 minutes at 37°C (Ratio 26:1) (see 6.2.6-6.2.9). The red arrow indicates the full-length p53 RNA of 1081 bases and blue arrows indicate the cleavage products of 714 and 367 bases. DNA size standards are indicated in black to the left of the image.

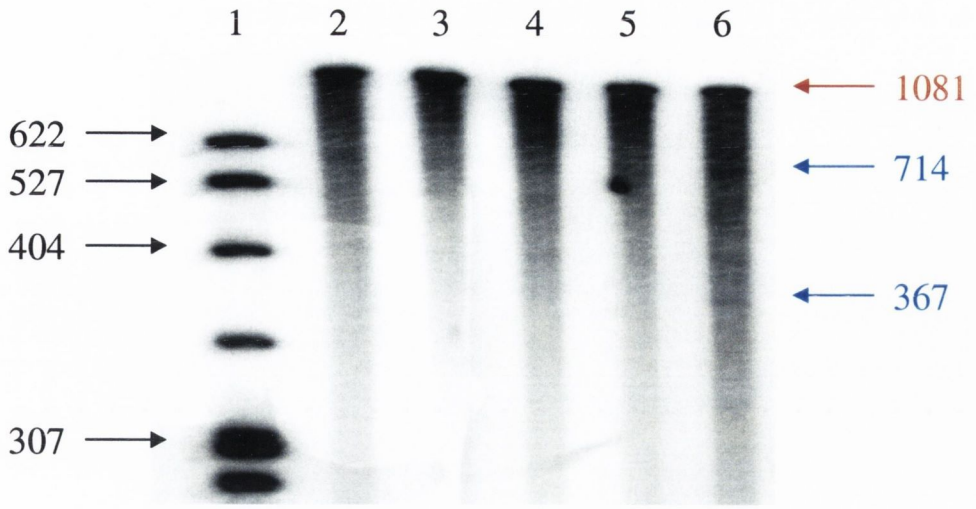

Figure 6.24A: Time point cleavage reaction of p53scRNA by Rz 1561. Lane 1, DNA ladder; Lanes 2-6, Rz 1561 with p53sc RNA at 20mM $MgCl_2$ at 1, 5, 15, 30 and 120 mins at 37°C (Ratio 0.6:1). Numbers on left hand side of the gel beside the DNA ladder indicate approximate size markers. Red arrow indicates full-length p53 mRNA of 1081 bases and blue arrows indicate the cleavage products of 714 and 367 bases. DNA size standards are indicated in black.

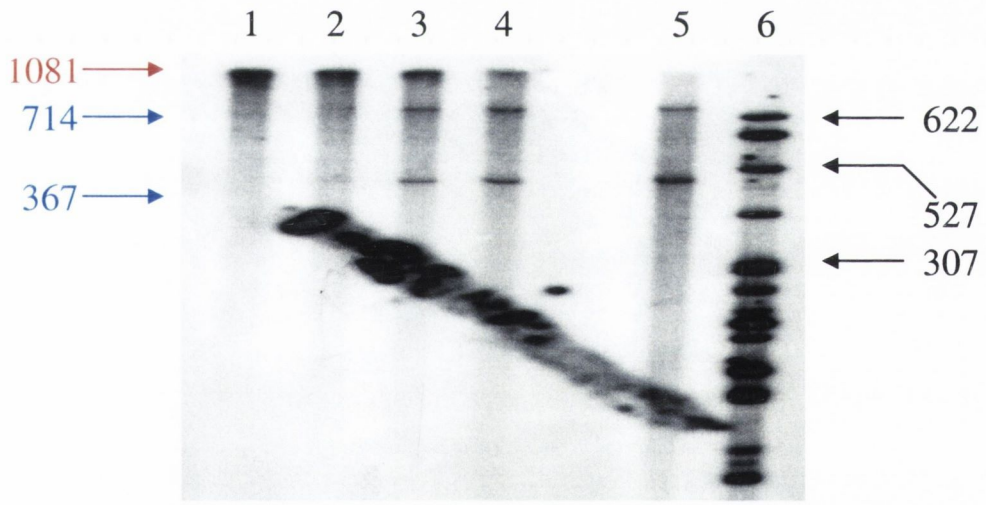

Figure 6.24B: Time point cleavage reaction of p53scRNA by Rz 1561. Lanes 1-5, Rz 1561 with p53sc RNA at 20mM $MgCl_2$ at 1, 5, 15, 30 and 120 mins at 37°C (Ratio 115:1) (see 6.2.6-6.2.9). Numbers on right hand side of the gel beside the DNA ladder indicate approximate size markers. The red arrow indicates full-length p53 mRNA of 1081 bases and blue arrows indicate the cleavage products of 714 and 367 bases. DNA size standards are indicated in black.

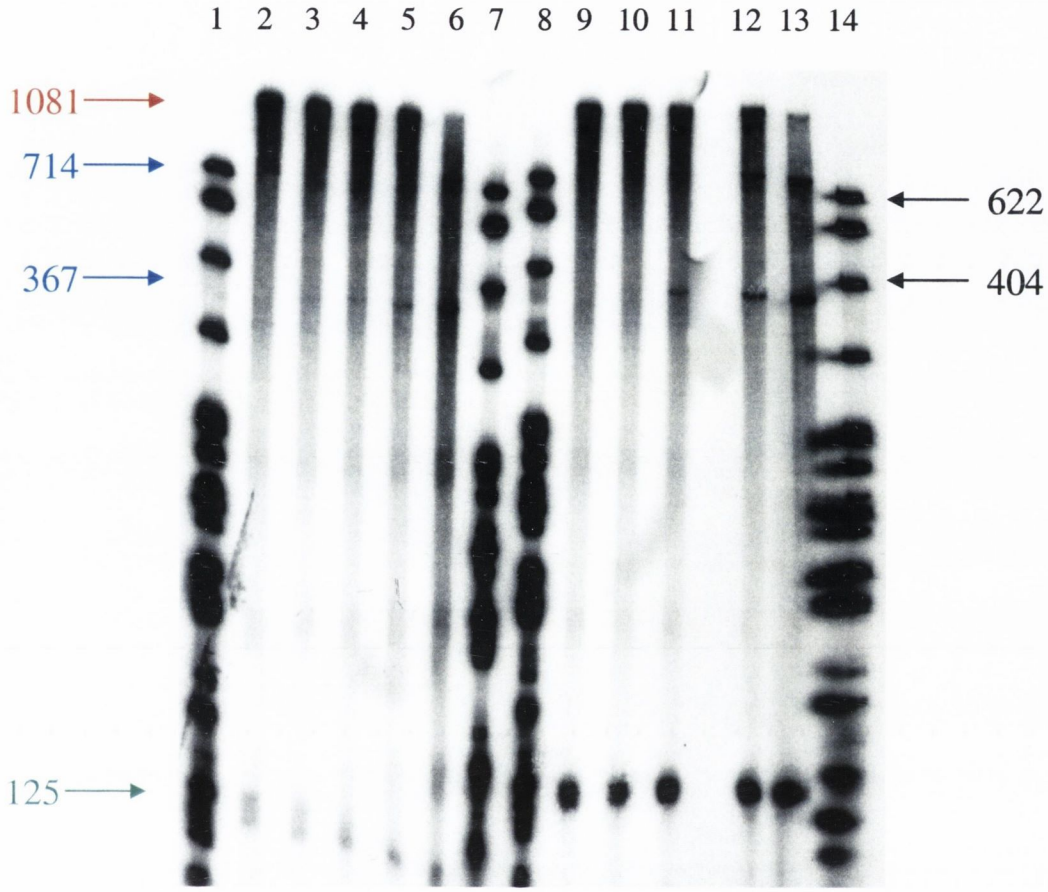

Figure 6.25: Time point cleavage reaction of p53scRNA by Rz 1561. Lane 1, DNA ladder; Lanes 2-6, Rz 1561 with p53sc RNA at 20mM $MgCl_2$ at 1, 5, 15, 30 and 120 mins at 37°C (Ratio 6:1); Lanes 7-8, DNA ladder; Lanes 9-13, Rz 1561 with p53sc mRNA at 20mM $MgCl_2$ at 1, 5, 15, 30 and 120 mins at 37°C (Ratio 29:1); Lane 14, DNA Ladder (see 6.2.6-6.2.9). Red arrow indicated the full-length p53sc RNA of 1081 bases and blue arrows indicate the cleavage products of 714 and 367 bases. DNA size standards are indicated in black. Rz 1561 is indicated by a green arrow at 125 bases.

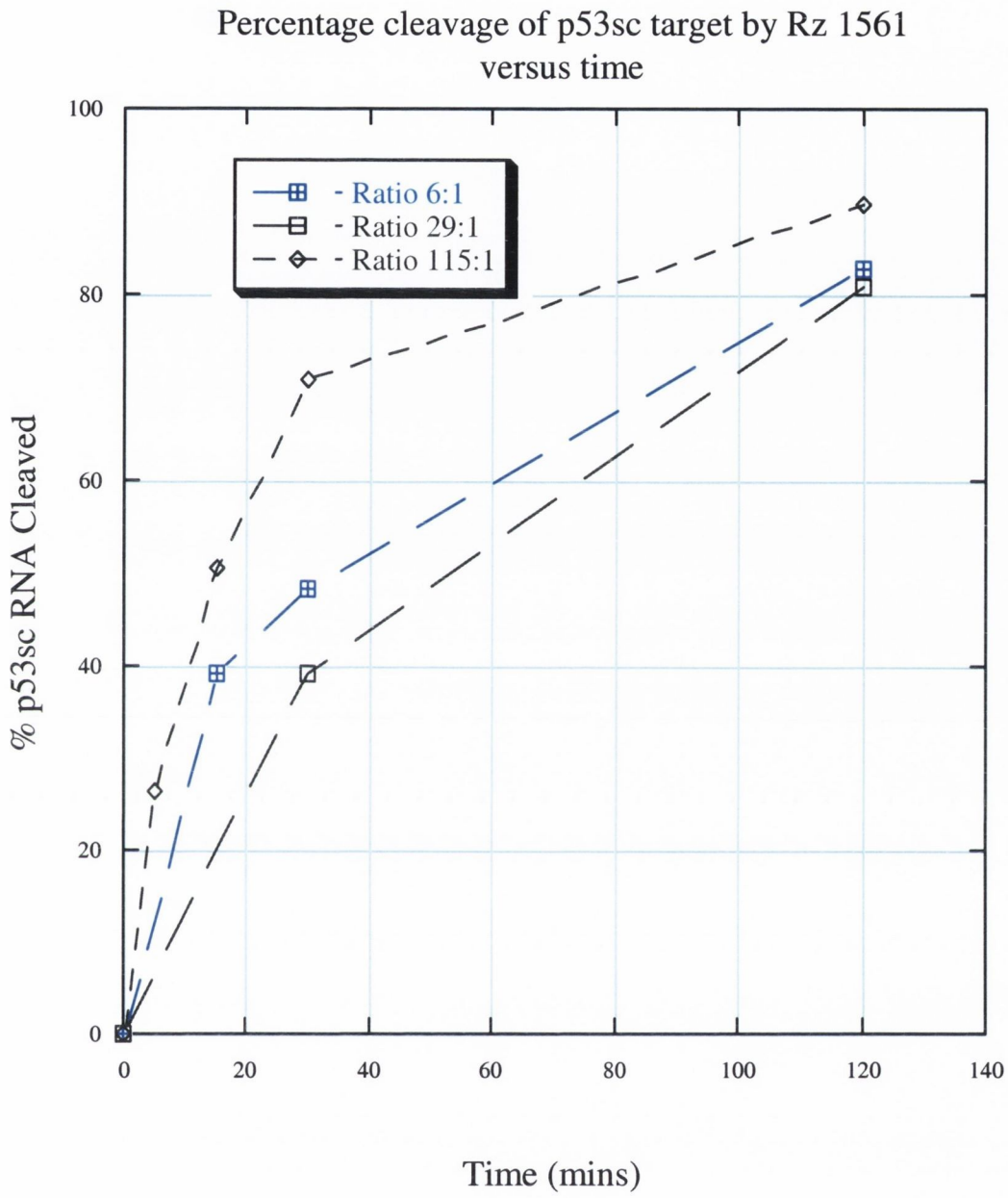

Figure 6.26: Graph of percentage cleavage of p53sc RNA with varying ratios of Rz 1561 versus time. Varying excess molar ratios (6:1, 29:1, 115:1) of Rz 1561 and transcribed p53sc target were incubated in cleavage reactions and aliquots taken at various time points for resolution on a 4% acrylamide gel. Percentage cleavage was analysed by exposing the dried gel to phosphor screens, and quantifying the bands using a Typhoon Imager with ImageQuant software (see 6.2.6-6.2.9).

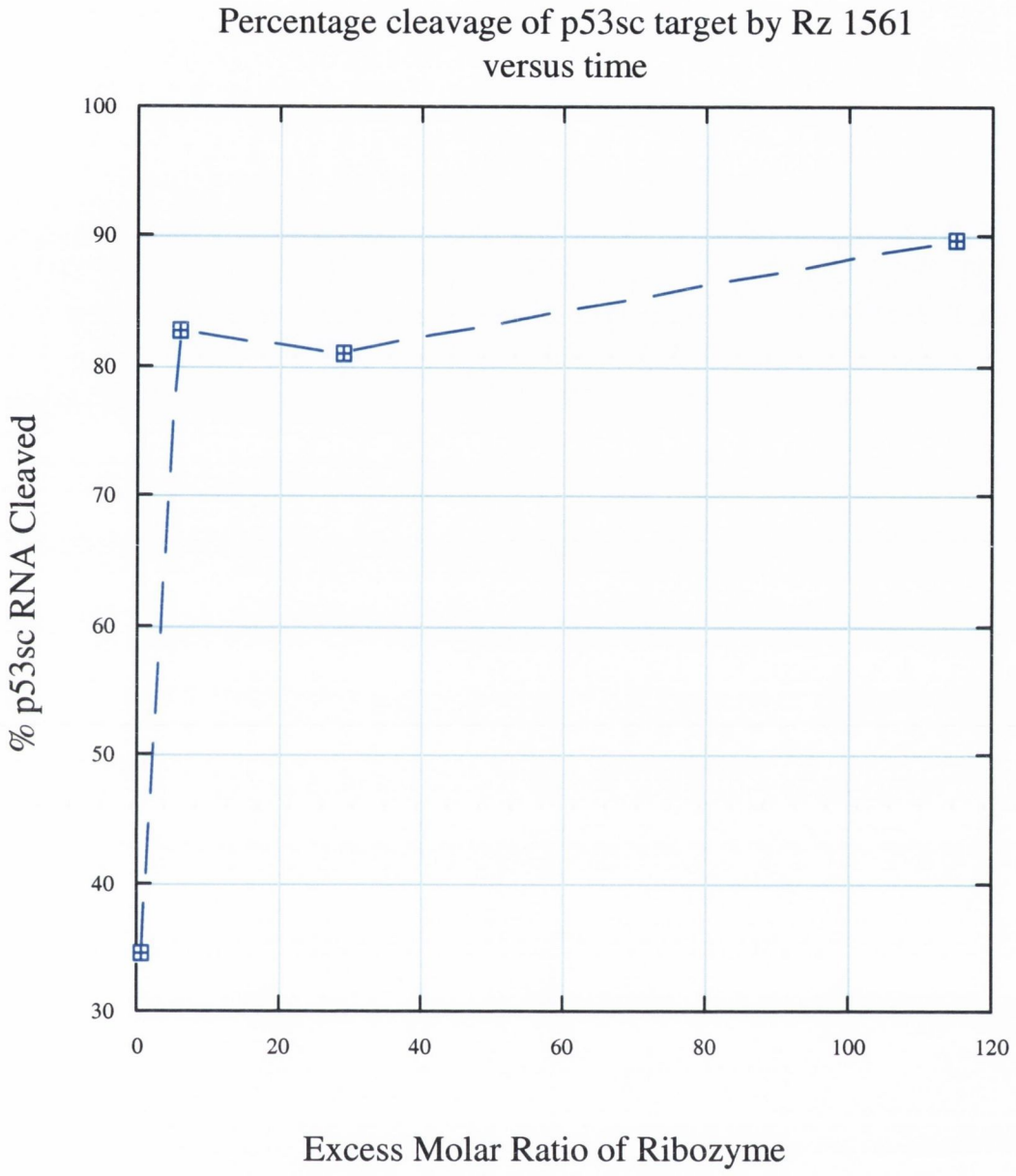

Figure 6.27: Graph of percentage cleavage of p53sc RNA with varying ratios of Rz 1561 after 120 mins incubation. Varying excess molar ratios (6:1, 29:1, 115:1) of Rz 1561 and transcribed p53sc target were incubated in cleavage reactions and aliquots taken at various time points for resolution on a 4% acrylamide gel. Percentage cleavage at 120 minutes was analysed by exposing the dried gel to phosphor screens, and quantifying the bands using a Typhoon Imager with ImageQuant software (see 6.2.6-6.2.9).

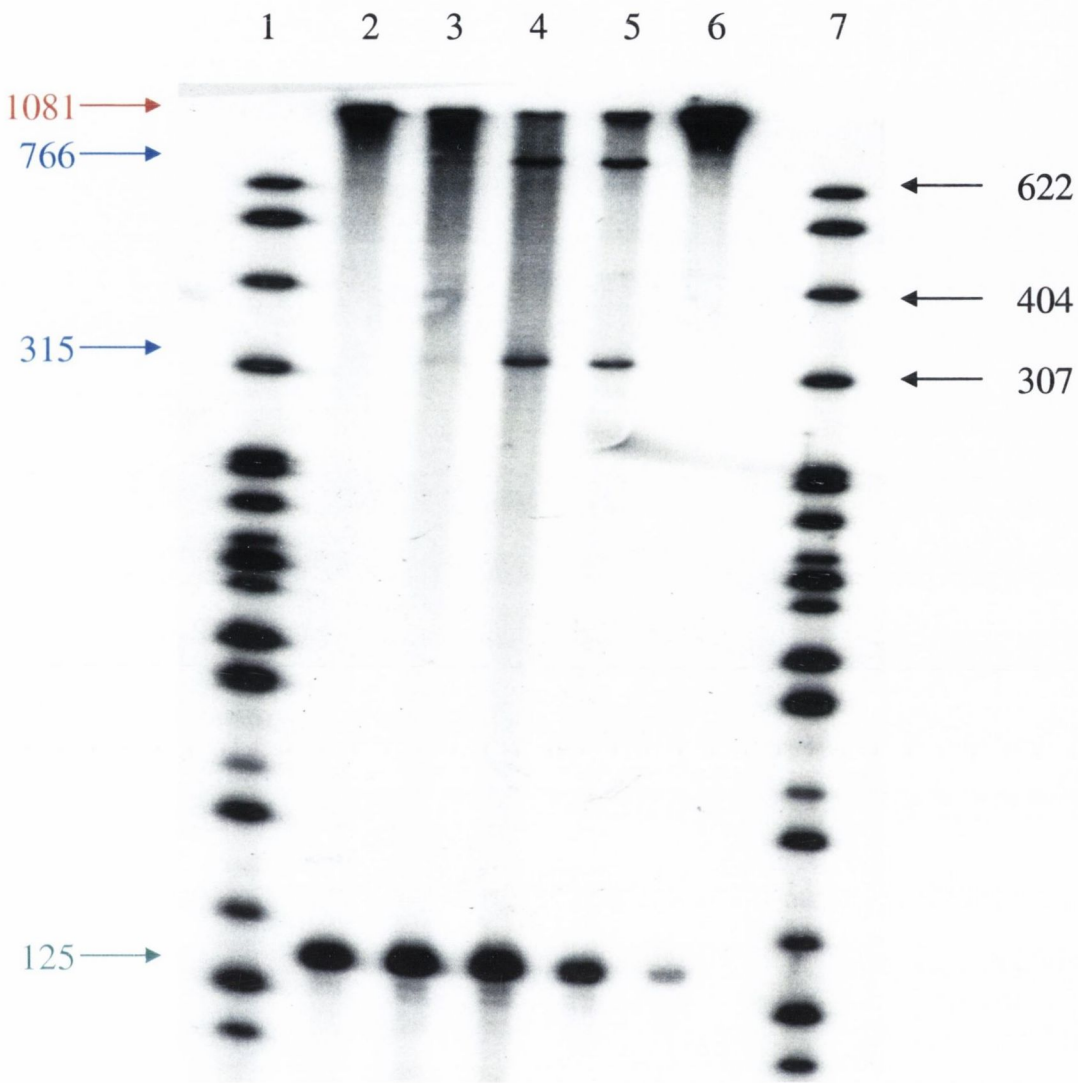

Figure 6.28: Time point cleavage reaction of p53scRNA by Rz 1613. Lane 1, DNA ladder; Lanes 2-5, Rz 1613 with p53sc RNA at 20mM $MgCl_2$ 1, 5, 90 and 120 mins at 37°C (Ratio 6:1); Lane 6, Rz 1613 with p53 RNA at 120 mins with 0mM $MgCl_2$; Lane 7, DNA ladder (see 6.2.6-6.2.9). The red arrow indicates the full-length p53sc RNA of 1081 bases and blue arrows indicate the cleavage products of 766 and 315 bases. Rz 1613 is indicated by a green arrow at 125 bases. DNA size standards are indicated in black.

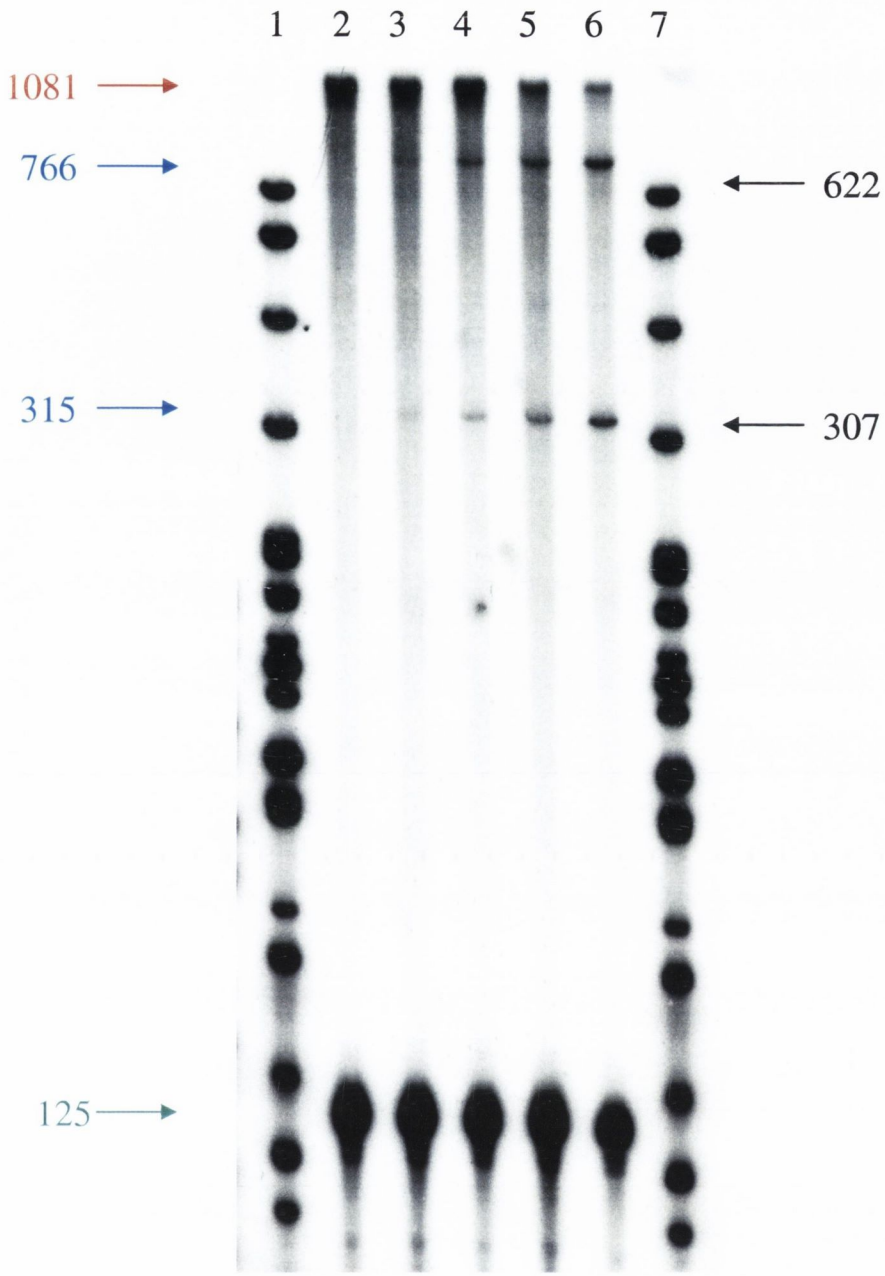

Figure 6.29: Time point cleavage reaction of p53scRNA by Rz 1613. Lane 1, DNA ladder; Lanes 2-5, Rz 1613 with p53sc RNA at 20mM $MgCl_2$ 1, 5, 90 and 120 mins at 37°C (Ratio 94:1); Lane 6, DNA ladder (see 6.2.6-6.2.9). The red arrow indicates the full-length p53sc RNA of 1081 bases and blue arrows indicate the cleavage products of 766 and 315 bases. Rz 1613 is indicated by a green arrow at 125 bases. DNA size standards are indicated in black.

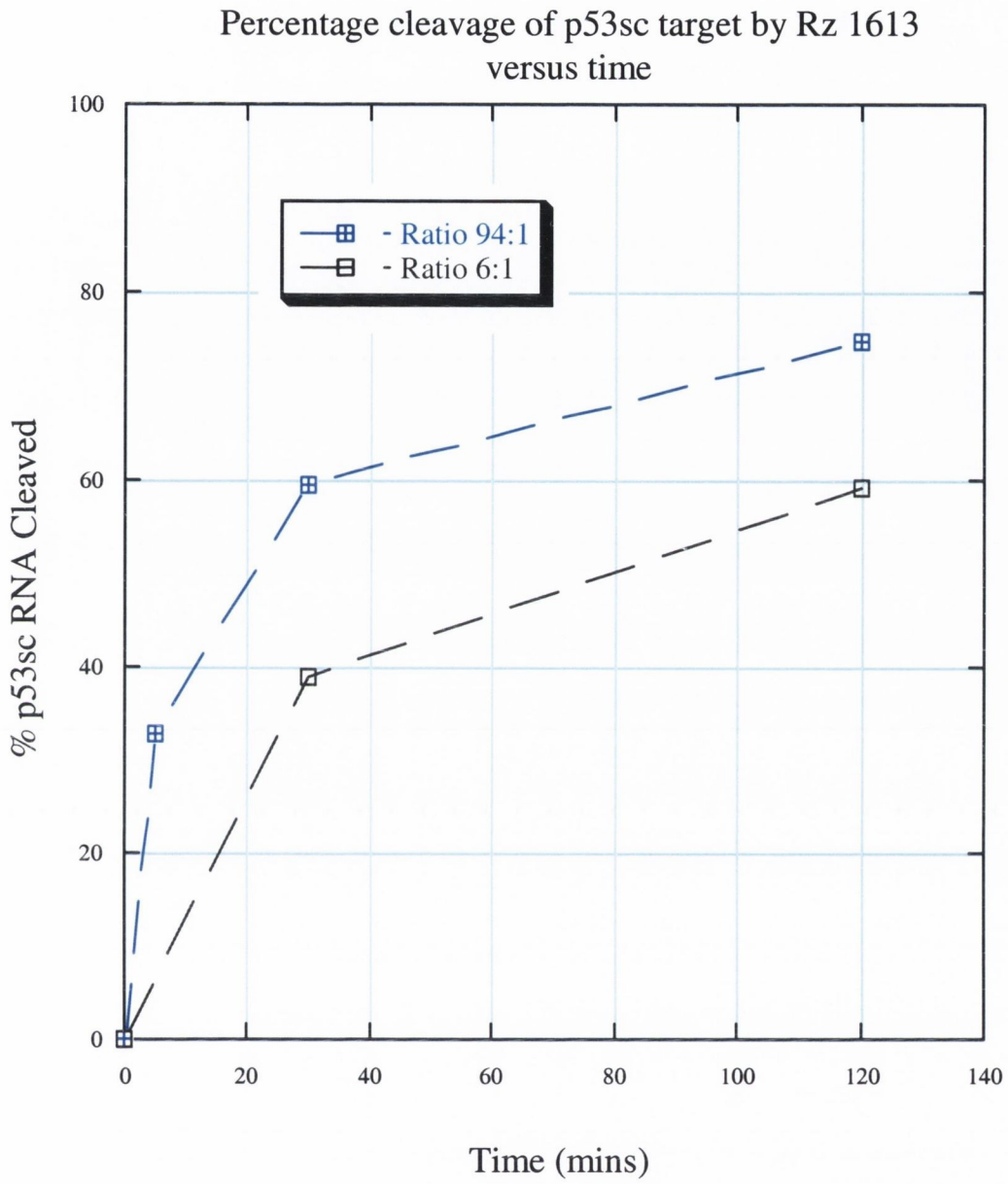

Figure 6.30: Graph of percentage cleavage of p53sc RNA with varying ratios of Rz 1613 versus time. Varying excess molar ratios (6:1, 94:1) of Rz 1613 and transcribed p53sc target were incubated in cleavage reactions and aliquots taken at various time points for resolution on a 4% acrylamide gel. Percentage cleavage at 120 minutes was analysed by exposing the dried gel to phosphor screens, and quantifying the bands using a Typhoon Imager with ImageQuant software (see 6.2.6-6.2.9).

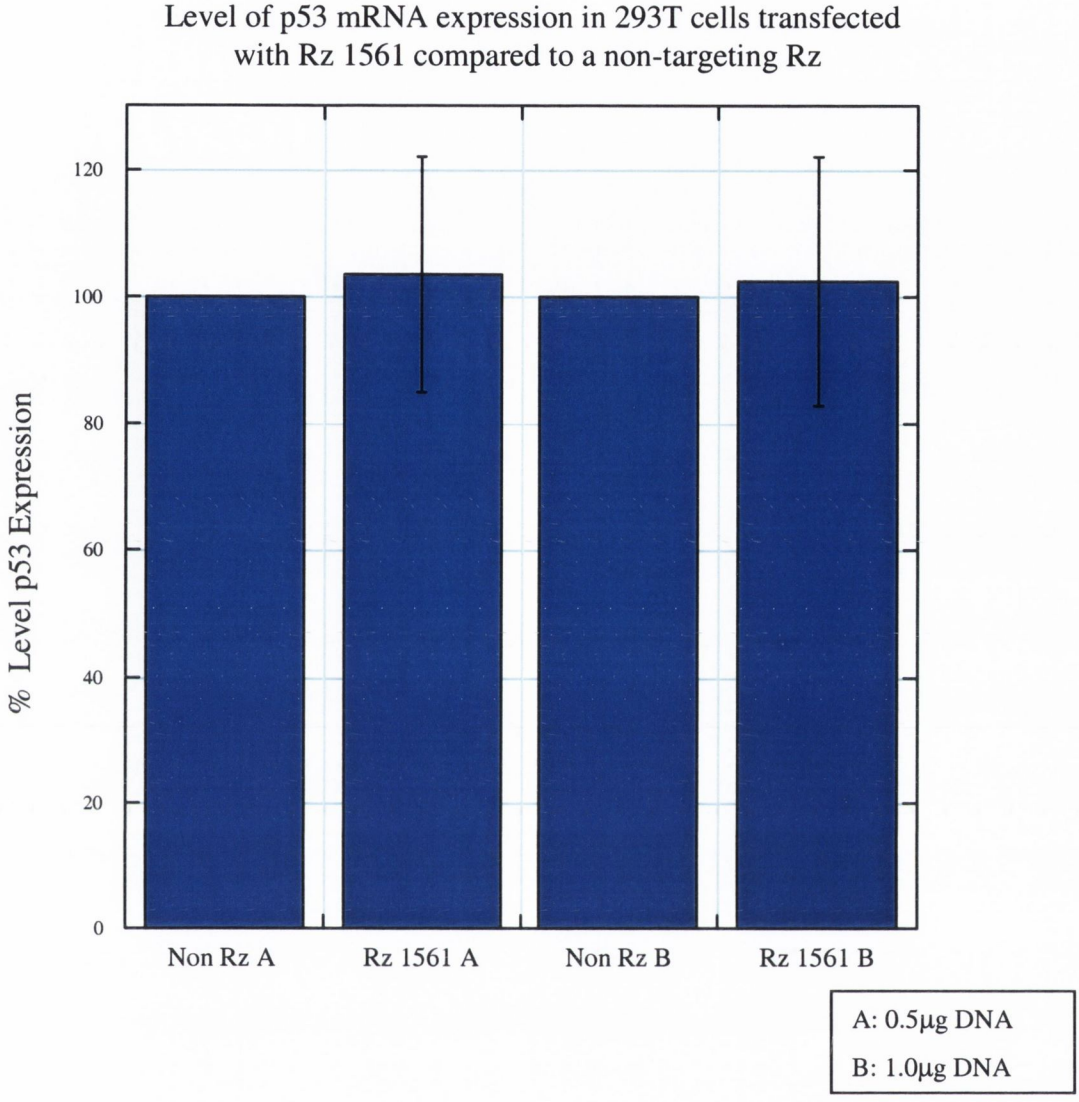

Figure 6.31: Graph of percentage level of p53 expression in 293T cells transfected with Rz 1561 compared with a non-targeting Rz. 293T cells were plated at a concentration of 1.25 x 10^5 per well of a 24-well plate with 0.5μg or 1μg of plasmid DNA with: 1) Rz 1561 or 2) Rz 40, non targeting (see 6.2.11). After 48 hours, the total RNA was isolated from each well, the level of p53 expression analysed by quantitative RT-PCR, and expresssion standardised to β-actin expression (see 6.2.12). Bars represent mean ± standard error (S.E) of duplicate experiments, each analysed by RT-PCR on two independent occasions. There was no significant difference in the level of p53 expression between 293T cells transfected with Rz 1561, compared to transfection with Rz 9, a non-targeting ribozyme ($P > 0.05$).

CHAPTER 7

General Discussion

Autosomal-dominant disorders exhibit a phenotype when one allele is mutated; examples include Huntington's disease, osteogenesis imperfecta and epidermolysis bullosa. Dominance of the mutant allele may result from a dominant-negative effect, as the mutant protein interferes with the function of the wild-type (wt) protein. Furthermore, the mutant allele may have additional functions that contribute to disease pathology, known as gain-of-function effects. Dominant-negative mutations may also contribute to the pathology of multi-factorial diseases such as p53-related cancer and Alzheimer's disease (Farrar *et al.*, 2002).

Developing gene therapies for dominant disorders caused by dominant-negative and/or gain-of-function mutations presents a particular challenge, as delivery of the wild-type gene alone may not be sufficient and hence suppression of the mutant gene may be necessary. An alternative or possibly complementary approach to targeting the primary mutation is to modulate a secondary effect associated with disease pathology. For this thesis a number of therapeutic strategies based on targeting the primary genetic mutation or modulating a secondary effect, were explored for two diseases where dominant-negative mutations contribute to disease pathology; autosomal-dominant retinitis pigmentosa (adRP) and p53-related cancer.

adRP is a degenerative disease of the retina, for which there is limited treatment available. Currently the only clinically validated intervention is Vitamin A supplementation, which has been shown to marginally slow the degeneration of cone photoreceptors (Berson *et al.*, 1993). Although a genetically heterogeneous disease, photoreceptors have been shown to degenerate by a common mechanism of cell death, apoptosis. Thus, inhibiting apoptosis may provide therapeutic benefit by slowing or halting photoreceptor degeneration, preserving vision for longer. As this approach is independent of the primary mutation, it may potentially overcome the challenge of genetic heterogeneity exhibited by adRP and other retinal degenerations. How diverse mutations associated with adRP initiate cell death pathways leading to a similar phenotype, is an important focus of retinal degenerative research, as by understanding the mechanisms involved, more effective therapies may be developed.

One potential group of therapeutic targets are caspases, a group of cysteine aspartyl-specific proteases that can mediate apoptosis (Thornberry *et al.,* 1998; Nicholson 1999). Studies have demonstrated that caspases are activated in various animal models of retinal degeneration, including the *rd* mouse (Kim *et al.,* 2002; Sharma *et al.,* 2004); hence caspase inhibition has been explored as a potential therapeutic strategy to slow photoreceptor cell loss in retinal degenerations. Caspases can be inhibited using either endogenous inhibitors or pharmacological compounds (Philchenkov *et al.,* 2004; Lavrik *et al.,* 2005).

For the study undertaken in Chapter 3, three endogenous inhibitors which are members of the inhibitor of apoptosis protein (IAP) family (XIAP, c-IAP-1 and c-IAP-2) were explored as potential therapeutic agents against chemical-induced apoptosis in 661W cells, a transformed line of mouse cone photoreceptor cells (Agarwal *et al.,* 1998). XIAP is the best characterised member of the IAPs and has been evaluated as a therapeutic anti-apoptotic agent for a number of disorders including forebrain ischaemia (Xu *et al.,* 1999), diabetes (Emammaullee *et al.,* 2005) and amyotrophic lateral sclerosis (Wootz *et al.,* 2006). c-IAP-1 and c-IAP-2 have been shown to inhibit caspases with similar specificity to XIAP, although less potently (Roy *et al.,* 1997; Deveraux *et al.,* 1998).

To evaluate the IAPs, apoptosis was induced using UV light and two chemotherapeutic agents, daunorubicin and etoposide. Transient expression of a plasmid construct expressing XIAP (pcXIAP) was not found to be protective in 661W cells exposed either to UV light or daunorubicin. UV light exposure and daunorubicin had previously been used by Tuohy *et al.* to induce apoptosis in 661W cells and evaluate the protective effect of natural and pharmacological caspase inhibitors (Tuohy 2001; *et al.,* 2002). Given the complexity of cell death pathways, reflected by the array of regulatory proteins and proteases identified to date (Leist *et al.,* 2001; Shi 2002; Kroemer *et al.,* 2005), slight variations in caspase specificity or potency of inhibition might explain the lack of protection afforded by XIAP expression against UV light and daunorubicin induced-apoptosis in 661W cells observed in this study.

However, a previous study had shown that c-IAP-1 and c-IAP-2 expression protected against chemical-induced apoptosis in a line of human embryonic kidney cells, 293T (Roy *et al.,* 1997). Thus, to exclude errors associated with experimental technique or other parameter as the reason for the lack of protection afforded by XIAP, 293T cells were used as a control cell line and treated in parallel with 661W cells. In the current study, transient expression of XIAP provided a significant percentage cell rescue of approximately 23% in 293T cells treated with etoposide confirming that functional XIAP was being expressed (Figure 3.17). Expression of the two other IAPs, c-IAP-1 and c-IAP-2 provided lower, but significant cell rescue of approximately 14% and 11% respectively (Figure 3.17). Transient expression of XIAP afforded a slight but significant rescue of 5% in 661W cells exposed to the same concentration of etoposide as 293T cells (Figure 3.13). Consistent with the trend observed in 293T cells where c-IAP-1 and c-IAP-2 protected significantly less than XIAP against etoposide-induced apoptosis, a similar trend emerged for 661W cells, with no significant protection afforded by c-IAP-1 or c-IAP-2 (Figures 3.14-15).

Given that c-IAP-1 and c-IAP-2 do not appear to protect against apoptosis, no further experiments were undertaken to assess them as potential therapeutic agents for retinal degenerations. When the study described in Chapter 3 was undertaken, c-IAP-1 and c-IAP-2 were selected for evaluation, as they had been shown to inhibit caspases-3 and -7 and potentially other unidentified cellular targets (Roy *et al.,* 1997). However, a more recent study has shown that c-IAP-1 and c-IAP-2 are very weak inhibitors of caspases as they lack key interacting proteins, compared to XIAP, for potent inhibition, supporting the results described here (Eckelman *et al.,* 2005). It has been suggested that the earlier results were an artifact of using glutathione-S-transferase (GST), which have been shown to confer caspase inhibitory properties on GST-tagged proteins (Scott *et al.,* 2005).

As the transfection efficiency of 661W cells was clearly a limiting factor in assessing the protective effect of XIAP, a stable cell line was generated and XIAP expression was found to modestly inhibit (approximately 13%) etoposide-induced apoptosis (Figure

3.20). XIAP has since been demonstrated to protect against apoptosis in a chemical-induced model of retinal degeneration (Petrin *et al.,* 2003). Furthermore, XIAP was also shown to provide significant protection of photoreceptors in two inherited rat models of degeneration, Pro23His and Ser344Ter, carrying autosomal dominant mutations of the rhodopsin gene (Leonard *et al.,* 2005).

Further evaluation of XIAP as a potential therapeutic agent using additional mouse models of retinal degeneration, such as the *rds-307* model with a single base-pair deletion at codon 307 of the *rds* gene, would be worthwhile (McNally *et al.,* 2002). There is increasing evidence to support caspase-independent mechanisms of cell death in photoreceptor cell loss (Sharma *et al.,* 2004; Doonan *et al.,* 2005). A recent paper demonstrated that XIAP overexpression in a mouse model of motor neuron degeneration resulted in inhibition of both caspase-12 and calpain cleavage (Wootz *et al.,* 2006).

Another natural caspase inhibitor, p35, has also been shown to be effective at protecting 661W cells against chemical-induced apoptosis, providing a percentage cell rescue of approximately 50% (Tuohy *et al.,* 2002). p35 was originally identified in a baculovirus (Clem *et al.,* 1991) and has been shown to target both initiator and effector caspases (Bump *et al.,* 1995; Zhou *et al.,* 1998). In addition, p35 expression has also been shown to protect against retinal degeneration in *Drosophila* models of RP (Davidson *et al.,* 1998; Galy *et al.,* 2005). Therefore, there was a clear rationale to evaluate the protective effect of p35 *in vivo* which is the basis for the work described in Chapters 4 and 5 of this thesis.

As attempts to generate a transgenic animal model expressing p35 had not been successful, a conditional *lox*P-p35 mouse model, provided by Professor Miura, was obtained (Hisahara *et al.,* 2000). In this mouse model p35 expression is silent due to the presence of a neomycin gene flanked by *lox*P sites between the transgene promoter and p35 gene (Figure 5.1). Expression of Cre recombinase (Cre), catalyses recombination at the *lox*P sites removing the neomycin gene, thus activating p35 expression. One

approach to activating p35 expression in photoreceptors, is to cross the *lox*P-p35 model with a model expressing Cre from a photoreceptor-specific promoter (Figure 5.2). At the time of the project initiation, no models with photoreceptor-specific expression of Cre were available, so the aim of the study described in Chapter 4 was to design, generate and evaluate constructs with rod and cone photoreceptor-specific expression of Cre.

Four constructs were generated with either rhodopsin or GNAT2 promoter-driven Cre expression for rod and cone photoreceptor-specific expression respectively. A Cre gene that had been genetically engineered to optimise expression in mammalian tissue was used for the constructs, improved Cre (iCre) (Shimshek *et al.,* 2002). Functionality of this iCre was demonstrated *in cellulo* using a β-gal reporter *lox*P plasmid (Figure 4.6). To demonstrate that Cre expression from these novel constructs was tissue-specific, a human retinoblastoma cell line, Y79, was used. However, although Y79 cells had been shown to express rod and cone-photoreceptor-specific transcripts, they were ultimately found to be an unsuitable system for investigating photoreceptor promoter-driven gene expression (Figure 4.10).

Given this result, in combination with the difficulties encountered with the other retinoblastoma cell line, 661W, used for the studies described in Chapter 3, the relevance of using these and similar cell lines for retinal research should be considered. Although transformed cells have a number of advantages compared to culturing primary retinal tissue, results generated from them may not reflect the scenario in a photoreceptor *in vivo*, particularly considering the complex structure of retinal tissue. The main reason for using these cell lines is the difficulties encountered with using primary retinal tissue, but more recently, a new technique became available, namely electroporation of primary retinal explants (Matsuda *et al.,* 2004). This technique involves *in vitro* electroporation of neonatal (P0-P1) retinal explants with plasmid DNA, followed by culturing for up to 30 days. By two weeks, *in vitro* differentiation of the retinal layers is complete, reflecting the time-course of *in vivo* retinal development (Figure 4.1).

Using this technique, a rhodopsin promoter-driven construct (pRho.hGH.iCre.A) was evaluated by co-electroporation with a β-gal reporter *lox*P plasmid in wild-type retinal explants. β-gal staining of the retinal explants after 14 days culturing, indicated that active iCre had catalysed recombination of the *lox*P sites of the reporter, allowing β-gal expression, demonstrating the functionality of the iCre construct (Figure 4.11). Evaluation of the GNAT2-driven constructs could not be undertaken in cultured explants, as cone photoreceptors comprise only 3-5% of the total photoreceptor population in the mouse. Given that tissue-specificity of the GNAT2 promoter had been previously established and iCre functionality was assessed *in cellulo* and using cultured retinal explants in this study, no further evaluation of the GNAT2 promoter-driven constructs was undertaken.

Using the constructs (pRho.hGH.iCre.A, pcGNAT2.hGH.iCre.A) generated for this thesis, transgenic mouse lines with rod and cone photoreceptor-specific expression of iCre are being generated. Recently, a number of transgenic mouse models with photoreceptor-specific expression of Cre have become available (Le *et al.*, 2004; Akimoto *et al.*, 2004). A collaboration has been established with Dr. Yun Zheng Le to provide the *HRGP-cre* line, with cone photoreceptor-specific expression of Cre (Le *et al.*, 2004). In addition, two transgenic mouse models with rhodopsin promoter-driven Cre expression have been described (Le *et al.*, 2006), which are now available for academic research.

These existing transgenic models could be compared to the models being generated with the constructs described in Chapter 4. Since no two Cre expressing mouse models are identical, with variation in both the level and specificity of Cre expression, it is very beneficial to have several transgenic mouse Cre-lines available. Initially those transgenic mouse models with photoreceptor-specific Cre expression will be crossed with the *lox*P-p35 mouse model, described in Chapter 5, to generate lines with rod or cone-specific p35 expression. By inducing apoptosis using light or chemicals the potential protective effect of p35 against photoreceptor degeneration could be evaluated using retinal histology and electroretinography.

The application of these transgenic mouse Cre-lines is not limited to exploring the potential therapeutic benefit of p35 expression. In principle, the effect of expressing any other anti-apoptotic gene or disrupting any pro-apoptotic gene specifically in photoreceptors could be investigated using these mouse Cre-lines. Given the increasing evidence to support caspase independent mechanisms of cell death, it would be of interest to knock out calpains or cathepsin D, other proteases implicated in photoreceptor cell death (Doonan *et al.*, 2005). Transgenic mouse Cre-lines could also be used to dissect gene function for which systemic deletion may be embryonically lethal. In one study this approach was used to establish the role of the *KIF3A* gene, which codes for a kinesin II subunit involved in protein transport, as systemic deletion of this gene results in embryonic lethality (Marszalek *et al.*, 2000). Knocking out *KIF3A* only in photoreceptors resulted in abnormal opsin and arrestin transport leading to photoreceptor degeneration, thus establishing the function of *KIF3A* in photoreceptors.

Transgenic mouse models with photoreceptor promoter-driven Cre expression had not been generated at the time of this study, so given the availability of retinal explant electroporation, this technique was used to evaluate to potential protective effect of p35 in primary retinal tissue. Retinal explants electroporated with a plasmid expressing p35/EGFP were exposed to an apoptosis inducing agent, A23187, and cell death was assessed using TUNEL staining. Compared to controls, p35 expression was found to provide a marginal but significant level of protection against chemical-induced apoptosis in retinal explants (Figure 5.24). Furthermore, on analysing only EGFP expressing cells, those that had been electroporated, a reduction of approximately 50% in the level of TUNEL staining was shown in those explants expressing p35/EGFP compared to control explants expressing EGFP alone (Figure 5.25). This demonstrates for the first time p35-mediated protection against chemical-induced apoptosis in primary mammalian tissue.

To achieve higher levels of p35 expression and verify the result described here, AAV-mediated delivery of p35 to retinal explants treated with A23187 will be undertaken.

For this study, AAV based on serotype 2 was used to generate AAV-p35, however photoreceptors have been shown to be more efficiently transduced with a hybrid AAV-2/5 (genome of AAV-2 and capsid protein of AAV-5) (Auricchio *et al.*, 2001). Given that the technology to generate AAV-2/5 has now been developed in the laboratory, an AAV-2/5-p35 has recently been produced. This high-titre AAV-2/5 will be of particular importance for *in vivo* evaluation of p35 as only small volumes can be subretinally injected into a mouse eye to obtain sufficient expression levels for a therapeutic dose.

Using AAV-2/5-p35, the potential therapeutic effect of p35 may be explored *in vivo* using transgenic mice with inherited retinal degenerations, such as Pro23His, and Pro347Ser, carrying rhodopsin mutations. An important aspect of this future project will be optimising the level of p35 expression delivered by AAV-2/5 *in vivo*, by altering various components of the AAV vectors used. Rhodopsin promoters of various sizes may be evaluated for p35 expression and the addition of enhancer elements such as the CMV enhancer (Wang *et al.*, 2005) or the woodchuck post-transcriptional regulatory element (WPRE) (Johansen *et al.*, 2003) may also be assessed.

In parallel with this work the *lox*P-p35 mouse model described in Chapter 5 may be used to evaluate the potential protective effect of p35. Attempts to activate p35 expression in retinal explants by the electroporation of plasmid expressing iCre were unsuccessful, when assessed at the mRNA and protein levels. However, as the integrity of the p35 transgene was confirmed and the functionality of iCre had been demonstrated *in cellulo* (Figure 4.11), lack of p35 expression was probably due to inadequate levels of iCre. To achieve higher levels of iCre expression, an AAV-iCre.EGFP based on serotype 2 was generated by Dr. Naomi Chadderton, AAV-2/5-iCre.EGFP. This AAV-2/5 will be used to deliver Cre to the retina of the *lox*P-p35 mouse by subretinal injection, providing another route for exploring the potential protective effect of p35.

In summary, modulating apoptosis, a secondary effect of the primary genetic defect, provides a mutation- and gene-independent approach for treating adRP and other

similar retinal degenerations. The results described in Chapter 5, demonstrating that p35 protects against apoptosis in primary mammalian retinal tissue, indicate that p35 expression within the retina is a potentially useful therapeutic for protecting against photoreceptor cell loss. Using the conditional *lox*P-p35 mouse, AAV-mediated delivery with optimised serotypes for photoreceptor expression and the transgenic models of retinal degeneration available, will enable a detailed, comprehensive evaluation of p35 as a neuroprotective agent.

An alternative therapeutic approach for diseases caused either entirely or in part by dominant-negative mutations is to correct the primary genetic defect, using for example a strategy known as mutation-independent suppression/replacement. This method involves suppressing both the mutant and wild-type allele at a nucleotide site independent of the disease mutation, while introducing a replacement gene that is protected from suppression but still encoding the wild-type protein.

p53 is a tumour suppressor protein frequently mutated in human cancer and many studies have demonstrated that many missense p53 mutations act in dominant-negative manner with possible gain-of-function activites. As over 1,300 different p53 mutations have been identified to date the mutation-independent strategies developed in the laboratory here offer a means of overcoming this mutational heterogeneity. Chapter 6 describes an *in vitro* study using a mutation-independent approach to evaluate hammerhead ribozyme-mediated suppression of the p53 gene.

Computer-folding programs, Mfold/PlotFold and RNAdraw were used to model the secondary structure of p53 mRNA and identify NUX ribozyme cleavage sites in predicted open loops. Using this information, six ribozymes targeting p53, radioactively labelled with rUTP [α-P^{32}] were evaluated using *in vitro* cleavage assays. All six ribozymes were found to cleave the p53 target with varying degrees of efficiency and two particularly efficient ribozymes were identified, Rz 1561 and Rz 1613. Targeting an AUU codon, Rz 1561 cleaved approximately 80-90% of the target p53 following an incubation of two hours (Figure 6.26). Rz 1613, targeting a GUU site

further downstream of Rz 1561 cleaved approximately 75% of the p53 target, although a higher molar excess of ribozyme was required compared to Rz 1561, indicating that Rz 1613 is less efficient (Figure 6.30).

To demonstrate the principle of the mutation-independent approach for targeting the p53 gene, two replacement p53 transcripts with altered NUX cleavage sites for Rz 359 and Rz 639 were generated. These nucleotide changes exploited the degeneracy of the genetic code; by altering bases at wobble positions, the amino acid sequence of the protein should remain unchanged. Both p53 replacement constructs were shown to be protected from cleavage in ribozyme cleavage assays with Rz 359 and Rz 639 (Figure 6.11: Figure 6.14). In principle, replacement p53 transcripts could be generated for future studies using Rz 1561 or any other efficient ribozyme.

Initial *in cellulo* assessment expressing Rz 1561 in 293T cells with endogenous expression of p53, did not result in a significant suppression of p53. However, further studies to enhance ribozyme expression using a more suitable polymerase III promoter, such as U1 or H1, which express short RNAs *in vivo*, may be more effective. Given that AAV technology is now available in the laboratory, AAV-mediated expression of ribozymes may also achieve higher levels of expression. A recently published paper demonstrated that a ribozyme expressed from AAV targeting α-synuclein implicated in neurodegeneration, significantly downregulated α-synuclein expression in a chemical-induced rat model of Parkinson's disease (Hayashito-Kinoh *et al.*, 2006). Transgenic animal models that express dominant-negative mutants of p53 are available and could be used to evaluate the *in vivo* suppression of p53 using ribozymes or possibly siRNA.

In conclusion this Ph.D. thesis involved the evaluation of two therapeutic strategies for treating diseases for which dominant-negative mutations contribute to disease pathology. The first involves correction of the primary genetic defect, as demonstrated by the study describing the suppression of the p53 transcript, a gene frequently mutated in human cancer using a ribozyme-based mutation-independent approach. The second involves modulating a secondary effect associated with disease pathology, such as

photoreceptor degeneration via a common cell death pathway in adRP and other retinopathies. Several projects were undertaken using this approach, one of which involved investigating natural protein apoptosis inhibitors, IAPs and p35, in either transformed photoreceptor cells or primary retinal explants. Another was establishing the functionality of a conditional transgenic animal with p35 expression and generating constructs for transgenic mouse lines with photoreceptor-specific expression of Cre. These transgenic Cre lines, together with the AAV vectors expressing p35 and Cre generated as part of this thesis, should prove to be valuable tools for dissecting retinal gene function and evaluating the potential therapeutic potential of p35, which has been demonstrated here to significantly inhibit chemical-induced apoptosis in primary retinal mammalian tissue.

References

Acland, G. M., G. D. Aguirre, J. Bennett, T. S. Aleman, A. V. Cideciyan, J. Bennicelli, N. S. Dejneka, S. E. Pearce-Kelling, A. M. Maguire, K. Palczewski, W. W. Hauswirth and S. G. Jacobson (2005). "Long-Term Restoration of Rod and Cone Vision by Single Dose rAAV-Mediated Gene Transfer to the Retina in a Canine Model of Childhood Blindness." Mol Ther.

Acland, G. M., G. D. Aguirre, J. Ray, Q. Zhang, T. S. Aleman, A. V. Cideciyan, S. E. Pearce-Kelling, V. Anand, Y. Zeng, A. M. Maguire, S. G. Jacobson, W. W. Hauswirth and J. Bennett (2001). "Gene therapy restores vision in a canine model of childhood blindness." Nat Genet **28**(1): 92-5.

Agarwal, N., Crawford, M.J., Krishnamoorthy, R., Sheedlo, H.J., Roque, R.S., Organisciak, D.T., Al-Ubaidi, M. (1998). "Characterization of a SV-40 antigen transformed 661W mouse photoreceptor cell line." Invest Ophthalmol Vis Sci **39**(4): 4874-B625.

Ahmad, I. (2001). "Stem cells: new opportunities to treat eye diseases." Invest Ophthalmol Vis Sci **42**(12): 2743-8.

Ahmed, B. Y., S. Chakravarthy, R. Eggers, W. T. Hermens, J. Y. Zhang, S. P. Niclou, C. Levelt, F. Sablitzky, P. N. Anderson, A. R. Lieberman and J. Verhaagen (2004). "Efficient delivery of Cre-recombinase to neurons in vivo and stable transduction of neurons using adeno-associated and lentiviral vectors." BMC Neurosci **5**: 4.

Aigner, A., D. Fischer, T. Merdan, C. Brus, T. Kissel and F. Czubayko (2002). "Delivery of unmodified bioactive ribozymes by an RNA-stabilizing polyethylenimine (LMW-PEI) efficiently down-regulates gene expression." Gene Ther **9**(24): 1700-7.

Akimoto, M., E. Filippova, P. J. Gage, X. Zhu, C. M. Craft and A. Swaroop (2004). "Transgenic mice expressing Cre-recombinase specifically in M- or S-cone photoreceptors." Invest Ophthalmol Vis Sci **45**(1): 42-7.

Ali, R. R., G. M. Sarra, C. Stephens, M. D. Alwis, J. W. Bainbridge, P. M. Munro, S. Fauser, M. B. Reichel, C. Kinnon, D. M. Hunt, S. S. Bhattacharya and A. J. Thrasher (2000). "Restoration of photoreceptor ultrastructure and function in retinal degeneration slow mice by gene therapy." Nat Genet **25**(3): 306-10.

Allikmets, R. (2004). "Leber congenital amaurosis: a genetic paradigm." Ophthalmic Genet **25**(2): 67-79.

Alloway, P. G., L. Howard and P. J. Dolph (2000). "The formation of stable rhodopsin-arrestin complexes induces apoptosis and photoreceptor cell degeneration." Neuron **28**(1): 129-38.

Angeletti, B., J. Loster, A. Auricchio, F. Gekeler, K. Shinoda, A. Ballabio, J. Graw and V. Marigo (2003). "An in vivo doxycycline-controlled expression system for functional studies of the retina." Invest Ophthalmol Vis Sci **44**(2): 755-60.

Anson, D. S. (2004). "The use of retroviral vectors for gene therapy-what are the risks? A review of retroviral pathogenesis and its relevance to retroviral vector-mediated gene delivery." Genet Vaccines Ther **2**(1): 9.

Apostolou, I., Z. Hao, K. Rajewsky and H. von Boehmer (2003). "Effective destruction of Fas-deficient insulin-producing beta cells in type 1 diabetes." J Exp Med **198**(7): 1103-6.

Applebury, M. L., M. P. Antoch, L. C. Baxter, L. L. Chun, J. D. Falk, F. Farhangfar, K. Kage, M. G. Krzystolik, L. A. Lyass and J. T. Robbins (2000). "The murine cone photoreceptor: a single cone type expresses both S and M opsins with retinal spatial patterning." Neuron **27**(3): 513-23.

Araki, T., M. Shibata, R. Takano, S. Hisahara, S. Imamura, Y. Fukuuchi, T. Saruta, H. Okano and M. Miura (2000). "Conditional expression of anti-apoptotic protein p35 by Cre-mediated DNA recombination in cardiomyocytes from loxP-p35-transgenic mice." Cell Death Differ **7**(5): 485-92.

Arruda, V. R., H. H. Stedman, T. C. Nichols, M. E. Haskins, M. Nicholson, R. W. Herzog, L. B. Couto and K. A. High (2005). "Regional intravascular delivery of AAV-2-F.IX to skeletal muscle achieves long-term correction of hemophilia B in a large animal model." Blood **105**(9): 3458-64.

Arundine, M. and M. Tymianski (2003). "Molecular mechanisms of calcium-dependent neurodegeneration in excitotoxicity." Cell Calcium **34**(4-5): 325-37.

Athanasopoulos, T., I. R. Graham, H. Foster and G. Dickson (2004). "Recombinant adeno-associated viral (rAAV) vectors as therapeutic tools for Duchenne muscular dystrophy (DMD)." Gene Ther **11 Suppl 1**: S109-21.

Auricchio, A. (2003). "Pseudotyped AAV vectors for constitutive and regulated gene expression in the eye." Vision Res **43**(8): 913-8.

Auricchio, A., G. Kobinger, V. Anand, M. Hildinger, E. O'Connor, A. M. Maguire, J. M. Wilson and J. Bennett (2001). "Exchange of surface proteins impacts on viral vector cellular specificity and transduction characteristics: the retina as a model." Hum Mol Genet **10**(26): 3075-81.

Badros, A. Z., O. Goloubeva, A. P. Rapoport, B. Ratterree, N. Gahres, B. Meisenberg, N. Takebe, M. Heyman, J. Zwiebel, H. Streicher, C. D. Gocke, D. Tomic, J. A. Flaws, B. Zhang and R. G. Fenton (2005). "Phase II study of G3139, a Bcl-2 antisense oligonucleotide, in combination with dexamethasone and thalidomide in relapsed multiple myeloma patients." J Clin Oncol **23**(18): 4089-99.

Bainbridge, J. W., C. Stephens, K. Parsley, C. Demaison, A. Halfyard, A. J. Thrasher and R. R. Ali (2001). "In vivo gene transfer to the mouse eye using an HIV-based lentiviral vector; efficient long-term transduction of corneal endothelium and retinal pigment epithelium." Gene Ther **8**(21): 1665-8.

Baker, S. J., *et al.* (1990). "Suppression of human colorectal carcinoma cell growth by wild-type p53." Science **249**(4971): 912-5.

Balint, E. E. and K. H. Vousden (2001). "Activation and activities of the p53 tumour suppressor protein." Br J Cancer **85**(12): 1813-23.

Barzon, L., R. Bonaguro, I. Castagliuolo, M. Chilosi, E. Franchin, C. Del Vecchio, I. Giaretta, M. Boscaro and G. Palu (2003). "Gene therapy of thyroid cancer via retrovirally-driven combined expression of human interleukin-2 and herpes simplex virus thymidine kinase." Eur J Endocrinol **148**(1): 73-80.

Bassi, G. S., A. I. Murchie, F. Walter, R. M. Clegg and D. M. Lilley (1997). "Ion-induced folding of the hammerhead ribozyme: a fluorescence resonance energy transfer study." Embo J **16**(24): 7481-9.

Beidler, D. R., M. Tewari, P. D. Friesen, G. Poirier and V. M. Dixit (1995). "The baculovirus p35 protein inhibits Fas- and tumor necrosis factor-induced apoptosis." J Biol Chem **270**(28): 16526-8.

Beigelman, L., J. A. McSwiggen, K. G. Draper, C. Gonzalez, K. Jensen, A. M. Karpeisky, A. S. Modak, J. Matulic-Adamic, A. B. DiRenzo, P. Haeberli and et al. (1995). "Chemical modification of hammerhead ribozymes. Catalytic activity and nuclease resistance." J Biol Chem **270**(43): 25702-8.

Bennett, J., T. Tanabe, D. Sun, Y. Zeng, H. Kjeldbye, P. Gouras and A. M. Maguire (1996). "Photoreceptor cell rescue in retinal degeneration (rd) mice by in vivo gene therapy." Nat Med **2**(6): 649-54.

Bernstein, E., A. A. Caudy, S. M. Hammond and G. J. Hannon (2001). "Role for a bidentate ribonuclease in the initiation step of RNA interference." Nature **409**(6818): 363-6.

Bernstein, P. and J. Ross (1989). "Poly(A), poly(A) binding protein and the regulation of mRNA stability." Trends Biochem Sci **14**(9): 373-7.

Berson, E. L., B. Rosner, M. A. Sandberg, K. C. Hayes, B. W. Nicholson, C. Weigel-DiFranco and W. Willett (1993). "A randomized trial of vitamin A and vitamin E supplementation for retinitis pigmentosa." Arch Ophthalmol **111**(6): 761-72.

Bertrand, E., D. Castanotto, C. Zhou, C. Carbonnelle, N. S. Lee, P. Good, S. Chatterjee, T. Grange, R. Pictet, D. Kohn, D. Engelke and J. J. Rossi (1997). "The expression cassette determines the functional activity of ribozymes in mammalian cells by controlling their intracellular localization." Rna **3**(1): 75-88.

Birikh, K. R., Y. A. Berlin, H. Soreq and F. Eckstein (1997). "Probing accessible sites for ribozymes on human acetylcholinesterase RNA." Rna **3**(4): 429-37.

Birnbaum, M. J., R. J. Clem and L. K. Miller (1994). "An apoptosis-inhibiting gene from a nuclear polyhedrosis virus encoding a polypeptide with Cys/His sequence motifs." J Virol **68**(4): 2521-8.

Blagosklonny, M. V. (2000). "p53 from complexity to simplicity: mutant p53 stabilization, gain-of-function, and dominant-negative effect." Faseb J **14**(13): 1901-7.

Blomgren, K., C. Zhu, X. Wang, J. O. Karlsson, A. L. Leverin, B. A. Bahr, C. Mallard and H. Hagberg (2001). "Synergistic activation of caspase-3 by m-calpain after neonatal hypoxia-ischemia: a mechanism of "pathological apoptosis"?" J Biol Chem **276**(13): 10191-8.

Bode, C. and U. Wolfrum (2003). "Caspase-3 inhibitor reduces apototic photoreceptor cell death during inherited retinal degeneration in tubby mice." Mol Vis **9**: 144-50.

Bok, D., D. Yasumura, M. T. Matthes, A. Ruiz, J. L. Duncan, A. V. Chappelow, S. Zolutukhin, W. Hauswirth and M. M. LaVail (2002). "Effects of adeno-associated virus-vectored ciliary neurotrophic factor on retinal structure and function in mice with a P216L rds/peripherin mutation." Exp Eye Res **74**(6): 719-35.

Borresen-Dale, A. L. (2003). "TP53 and breast cancer." Hum Mutat **21**(3): 292-300.

Bowes, C., T. Li, M. Danciger, L. C. Baxter, M. L. Applebury and D. B. Farber (1990). "Retinal degeneration in the rd mouse is caused by a defect in the beta subunit of rod cGMP-phosphodiesterase." Nature **347**(6294): 677-80.

Bowne, S. J., L. S. Sullivan, S. H. Blanton, C. L. Cepko, S. Blackshaw, D. G. Birch, D. Hughbanks-Wheaton, J. R. Heckenlively and S. P. Daiger (2002). "Mutations in the inosine monophosphate dehydrogenase 1 gene (IMPDH1) cause the RP10 form of autosomal dominant retinitis pigmentosa." Hum Mol Genet **11**(5): 559-68.

Brachmann, R. K. (2004). "p53 mutants: the achilles' heel of human cancers?" Cell Cycle **3**(8): 1030-4.

Bridge, A. J., S. Pebernard, A. Ducraux, A. L. Nicoulaz and R. Iggo (2003). "Induction of an interferon response by RNAi vectors in mammalian cells." Nat Genet **34**(3): 263-4.

Briscoe, A. D., C. Gaur and S. Kumar (2004). "The spectrum of human rhodopsin disease mutations through the lens of interspecific variation." Gene **332**: 107-18.

Brummelkamp, T. R., R. Bernards and R. Agami (2002). "A system for stable expression of short interfering RNAs in mammalian cells." Science **296**(5567): 550-3.

Bueler, H. (1999). "Adeno-associated viral vectors for gene transfer and gene therapy." Biol Chem **380**(6): 613-22.

Bump, N. J., M. Hackett, M. Hugunin, S. Seshagiri, K. Brady, P. Chen, C. Ferenz, S. Franklin, T. Ghayur, P. Li and et al. (1995). "Inhibition of ICE family proteases by baculovirus antiapoptotic protein p35." Science **269**(5232): 1885-8.

Buning, H., S. A. Nicklin, L. Perabo, M. Hallek and A. H. Baker (2003). "AAV-based gene transfer." Curr Opin Mol Ther **5**(4): 367-75.

Buning, H., S. A. Nicklin, L. Perabo, M. Hallek and A. H. Baker (2003). "AAV-based gene transfer." Curr Opin Mol Ther **5**(4): 367-75.

Caffe, A. R., H. Visser, H. G. Jansen and S. Sanyal (1989). "Histotypic differentiation of neonatal mouse retina in organ culture." Curr Eye Res **8**(10): 1083-92.

Cai, D. W., *et al.* (1995). "Suppression of lung cancer cell growth by ribozyme-mediated modification of p53 pre-mRNA." Cancer Gene Ther **2**(3): 199-205.

Campling, B. G. and W. S. El-Deiry (2003). "Clinical implication of p53 mutation in lung cancer." Mol Biotechnol **24**(2): 141-56.

Caplen, N. J., S. Parrish, F. Imani, A. Fire and R. A. Morgan (2001). "Specific inhibition of gene expression by small double-stranded RNAs in invertebrate and vertebrate systems." Proc Natl Acad Sci U S A **98**(17): 9742-7.

Carter, P. J. and R. J. Samulski (2000). "Adeno-associated viral vectors as gene delivery vehicles." Int J Mol Med **6**(1): 17-27.

Cashman, S. M., S. L. Sadowski, D. J. Morris, J. Frederick and R. Kumar-Singh (2002). "Intercellular trafficking of adenovirus-delivered HSV VP22 from the retinal pigment epithelium to the photoreceptors--implications for gene therapy." Mol Ther **6**(6): 813-23.

Chader, G. J. (2002). "Animal models in research on retinal degenerations: past progress and future hope." Vision Res **42**(4): 393-9.

Chakarova, C. F., M. M. Hims, H. Bolz, L. Abu-Safieh, R. J. Patel, M. G. Papaioannou, C. F. Inglehearn, T. J. Keen, C. Willis, A. T. Moore, T. Rosenberg, A. R. Webster, A. C. Bird, A. Gal, D. Hunt, E. N. Vithana and S. S. Bhattacharya (2002). "Mutations in HPRP3, a third member of pre-mRNA splicing factor genes, implicated in autosomal dominant retinitis pigmentosa." Hum Mol Genet **11**(1): 87-92.

Chanan-Khan, A., R. Niesvizky and R. Hohl (2004). "Randomized multicenter Phase 3 trial of high-dose dexamethasone (dex) with or without Obilmersen sodium (G3139; Bcl-2 antisense; Genasense) for patients with advanced multiple myeloma (MM)." Blood **104: abstract #1477**.

Chang, G. Q., Y. Hao and F. Wong (1993). "Apoptosis: final common pathway of photoreceptor death in rd, rds, and rhodopsin mutant mice." Neuron **11**(4): 595-605.

Chang, M. A., J. W. Horner, B. R. Conklin, R. A. DePinho, D. Bok and D. J. Zack (2000). "Tetracycline-inducible system for photoreceptor-specific gene expression." Invest Ophthalmol Vis Sci **41**(13): 4281-7.

Chen, C. M. and R. R. Behringer (2001). "CREating breakthroughs." Nat Biotechnol **19**(10): 921-2.

Cheng, J., J. Luo, X. Zhang, J. Hu, H. Hui, C. Wang and A. Stern (2000). "Inhibition of cell proliferation in HCC-9204 hepatoma cells by a c-myc specific ribozyme." Cancer Gene Ther **7**(3): 407-12.

Chiu, Y. L. and T. M. Rana (2003). "siRNA function in RNAi: a chemical modification analysis." Rna **9**(9): 1034-48.

Choi, K. S., T. H. Lee and M. H. Jung (2003). "Ribozyme-mediated cleavage of the human survivin mRNA and inhibition of antiapoptotic function of survivin in MCF-7 cells." Cancer Gene Ther **10**(2): 87-95.

Choi, T., M. Huang, C. Gorman and R. Jaenisch (1991). "A generic intron increases gene expression in transgenic mice." Mol Cell Biol **11**(6): 3070-4.

Chuang, J. Z., C. Vega, W. Jun and C. H. Sung (2004). "Structural and functional impairment of endocytic pathways by retinitis pigmentosa mutant rhodopsin-arrestin complexes." J Clin Invest **114**(1): 131-40.

Citti, L. and G. Rainaldi (2005). "Synthetic hammerhead ribozymes as therapeutic tools to control disease genes." Curr Gene Ther **5**(1): 11-24.

Clem, R. J. and L. K. Miller (1994). "Control of programmed cell death by the baculovirus genes p35 and iap." Mol Cell Biol **14**(8): 5212-22.

Clem, R. J., M. Fechheimer and L. K. Miller (1991). "Prevention of apoptosis by a baculovirus gene during infection of insect cells." Science **254**(5036): 1388-90.

Consiglio, A., A. Quattrini, S. Martino, J. C. Bensadoun, D. Dolcetta, A. Trojani, G. Benaglia, S. Marchesini, V. Cestari, A. Oliverio, C. Bordignon and L. Naldini (2001). "In vivo gene therapy of metachromatic leukodystrophy by lentiviral vectors: correction of neuropathology and protection against learning impairments in affected mice." Nat Med **7**(3): 310-6.

Crook, N. E., R. J. Clem and L. K. Miller (1993). "An apoptosis-inhibiting baculovirus gene with a zinc finger-like motif." J Virol **67**(4): 2168-74.

Crooke, R. M., M. J. Graham, K. M. Lemonidis, C. P. Whipple, S. Koo and R. J. Perera (2005). "An apolipoprotein B antisense oligonucleotide lowers LDL cholesterol in hyperlipidemic mice without causing hepatic steatosis." J Lipid Res **46**(5): 872-84.

Crooke, S. T. (1998). "Vitravene--another piece in the mosaic." Antisense Nucleic Acid Drug Dev **8**(4): vii-viii.

Crystal, R. G., N. G. McElvaney, M. A. Rosenfeld, C. S. Chu, A. Mastrangeli, J. G. Hay, S. L. Brody, H. A. Jaffe, N. T. Eissa and C. Danel (1994). "Administration of an adenovirus containing the human CFTR cDNA to the respiratory tract of individuals with cystic fibrosis." Nat Genet **8**(1): 42-51.

Cullinan, A. E. and C. R. Brandt (2004). "Cytokine induced apoptosis in human retinoblastoma cells." Mol Vis **10**: 315-22.

Curcio, C. A., K. R. Sloan, R. E. Kalina and A. E. Hendrickson (1990). "Human photoreceptor topography." J Comp Neurol **292**(4): 497-523.

Danial, N. N. and S. J. Korsmeyer (2004). "Cell death: critical control points." Cell **116**(2): 205-19.

Datta, R., H. Kojima, D. Banach, N. J. Bump, R. V. Talanian, E. S. Alnemri, R. R. Weichselbaum, W. W. Wong and D. W. Kufe (1997). "Activation of a CrmA-insensitive, p35-sensitive pathway in ionizing radiation-induced apoptosis." J Biol Chem **272**(3): 1965-9.

Dave, R. S. and R. J. Pomerantz (2004). "Antiviral effects of human immunodeficiency virus type 1-specific small interfering RNAs against targets conserved in select neurotropic viral strains." J Virol **78**(24): 13687-96.

Davidson, F. F. and H. Steller (1998). "Blocking apoptosis prevents blindness in Drosophila retinal degeneration mutants." Nature **391**(6667): 587-91.

de Vries, A., *et al.* (2002). "Targeted point mutations of p53 lead to dominant-negative inhibition of wild-type p53 function." Proc Natl Acad Sci U S A **99**(5): 2948-53.

Delenda, C. (2004). "Lentiviral vectors: optimization of packaging, transduction and gene expression." J Gene Med **6 Suppl 1**: S125-38.

Deveraux, Q. L., N. Roy, H. R. Stennicke, T. Van Arsdale, Q. Zhou, S. M. Srinivasula, E. S. Alnemri, G. S. Salvesen and J. C. Reed (1998). "IAPs block apoptotic events induced by caspase-8 and cytochrome c by direct inhibition of distinct caspases." Embo J **17**(8): 2215-23.

Deveraux, Q. L., R. Takahashi, G. S. Salvesen and J. C. Reed (1997). "X-linked IAP is a direct inhibitor of cell-death proteases." Nature **388**(6639): 300-4.

Di Como, C. J., C. Gaiddon and C. Prives (1999). "p73 function is inhibited by tumor-derived p53 mutants in mammalian cells." Mol Cell Biol **19**(2): 1438-49.

Di Polo, A. and D. B. Farber (1995). "Rod photoreceptor-specific gene expression in human retinoblastoma cells." Proc Natl Acad Sci U S A **92**(9): 4016-20.

Dihlmann, S., *et al.* (1999). "Dominant negative effect of the APC1309 mutation: a possible explanation for genotype-phenotype correlations in familial adenomatous polyposis." Cancer Res **59**(8): 1857-60.

Dinculescu, A., L. Glushakova, S. H. Min and W. W. Hauswirth (2005). "Adeno-associated virus-vectored gene therapy for retinal disease." Hum Gene Ther **16**(6): 649-63.

Dittmer, D., S. Pati, G. Zambetti, S. Chu, A. K. Teresky, M. Moore, C. Finlay and A. J. Levine (1993). "Gain of function mutations in p53." Nat Genet **4**(1): 42-6.

Doetschman, T., R. G. Gregg, N. Maeda, M. L. Hooper, D. W. Melton, S. Thompson and O. Smithies (1987). "Targetted correction of a mutant HPRT gene in mouse embryonic stem cells." Nature **330**(6148): 576-8.

Doherty, E. A. and J. A. Doudna (2000). "Ribozyme structures and mechanisms." Annu Rev Biochem **69**: 597-615.

Donovan, M. and T. G. Cotter (2002). "Caspase-independent photoreceptor apoptosis in vivo and differential expression of apoptotic protease activating factor-1 and caspase-3 during retinal development." Cell Death Differ **9**(11): 1220-31.

Doonan, F., M. Donovan and T. G. Cotter (2003). "Caspase-independent photoreceptor apoptosis in mouse models of retinal degeneration." J Neurosci **23**(13): 5723-31.

Doonan, F., M. Donovan and T. G. Cotter (2005). "Activation of Multiple Pathways during Photoreceptor Apoptosis in the rd Mouse." Invest Ophthalmol Vis Sci **46**(10): 3530-8.

Doudna, J. A. and T. R. Cech (2002). "The chemical repertoire of natural ribozymes." Nature **418**(6894): 222-8.

Drago, J., P. Padungchaichot, J. Y. Wong, A. J. Lawrence, J. F. McManus, S. H. Sumarsono, A. L. Natoli, M. Lakso, N. Wreford, H. Westphal, I. Kola and D. I. Finkelstein (1998). "Targeted expression of a toxin gene to D1 dopamine receptor neurons by cre-mediated site-specific recombination." J Neurosci **18**(23): 9845-57.

Dryja, T. P., J. T. Finn, Y. W. Peng, T. L. McGee, E. L. Berson and K. W. Yau (1995). "Mutations in the gene encoding the alpha subunit of the rod cGMP-gated channel in autosomal recessive retinitis pigmentosa." Proc Natl Acad Sci U S A **92**(22): 10177-81.

Duckett, C. S., F. Li, Y. Wang, K. J. Tomaselli, C. B. Thompson and R. C. Armstrong (1998). "Human IAP-like protein regulates programmed cell death downstream of Bcl-xL and cytochrome c." Mol Cell Biol **18**(1): 608-15.

Dummer, R., J. C. Hassel, F. Fellenberg, S. Eichmuller, T. Maier, P. Slos, B. Acres, P. Bleuzen, V. Bataille, P. Squiban, G. Burg and M. Urosevic (2004). "Adenovirus-mediated intralesional interferon-gamma gene transfer induces tumor regressions in cutaneous lymphomas." Blood **104**(6): 1631-8.

Dyer, M. A., S. L. Donovan, J. Zhang, J. Gray, A. Ortiz, R. Tenney, J. Kong, R. Allikmets and M. M. Sohocki (2004). "Retinal degeneration in Aipl1-deficient mice: a new genetic model of Leber congenital amaurosis." Brain Res Mol Brain Res **132**(2): 208-20.

Dykxhoorn, D. M. and J. Lieberman (2005). "The silent revolution: RNA interference as basic biology, research tool, and therapeutic." Annu Rev Med **56**: 401-23.

Dykxhoorn, D. M., C. D. Novina and P. A. Sharp (2003). "Killing the messenger: short RNAs that silence gene expression." Nat Rev Mol Cell Biol **4**(6): 457-67.

Earnshaw, D. J. and M. J. Gait (1997). "Progress toward the structure and therapeutic use of the hairpin ribozyme." Antisense Nucleic Acid Drug Dev **7**(4): 403-11.

Earnshaw, W. C., L. M. Martins and S. H. Kaufmann (1999). "Mammalian caspases: structure, activation, substrates, and functions during apoptosis." Annu Rev Biochem **68**: 383-424.

El-Aneed, A. (2004). "An overview of current delivery systems in cancer gene therapy." J Control Release **94**(1): 1-14.

Elbashir, S. M., W. Lendeckel and T. Tuschl (2001). "RNA interference is mediated by 21- and 22-nucleotide RNAs." Genes Dev **15**(2): 188-200.

el-Deiry, W. S., T. Tokino, V. E. Velculescu, D. B. Levy, R. Parsons, J. M. Trent, D. Lin, W. E. Mercer, K. W. Kinzler and B. Vogelstein (1993). "WAF1, a potential mediator of p53 tumor suppression." Cell **75**(4): 817-25.

El-Zawahry, A., P. Lu, S. J. White and C. Voelkel-Johnson (2005). "In vitro efficacy of AdTRAIL gene therapy of bladder cancer is enhanced by trichostatin A-mediated restoration of CAR expression and downregulation of cFLIP and Bcl-X(L)." Cancer Gene Ther.

Emamaullee, J. A., R. V. Rajotte, P. Liston, R. G. Korneluk, J. R. Lakey, A. M. Shapiro and J. F. Elliott (2005). "XIAP overexpression in human islets prevents early posttransplant apoptosis and reduces the islet mass needed to treat diabetes." Diabetes **54**(9): 2541-8.

Farrar, G. J., P. F. Kenna and P. Humphries (2002). "On the genetics of retinitis pigmentosa and on mutation-independent approaches to therapeutic intervention." Embo J **21**(5): 857-64.

Farrar, G. J., P. McWilliam, D. G. Bradley, P. Kenna, M. Lawler, E. M. Sharp, M. M. Humphries, H. Eiberg, P. M. Conneally, J. A. Trofatter and et al. (1990). "Autosomal dominant retinitis pigmentosa: linkage to rhodopsin and evidence for genetic heterogeneity." Genomics **8**(1): 35-40.

Farrar, G. J., S. A. Jordan, P. Kenna, M. M. Humphries, R. Kumar-Singh, P. McWilliam, V. Allamand, E. Sharp and P. Humphries (1991). "Autosomal dominant retinitis pigmentosa: localization of a disease gene (RP6) to the short arm of chromosome 6." Genomics **11**(4): 870-4.

Fedor, M. J. and J. R. Williamson (2005). "The catalytic diversity of RNAs." Nat Rev Mol Cell Biol **6**(5): 399-412.

Feiner, L., Navaratnarajah, M., Pierce, E.A. (2003). Photoreceptor Expression of Cre-Recombinase. Assocation for Research in Vision and Ophalmology, Fort Launderdale, FL, USA.

Feiner, L., Navaratnarajah, M., Pierce, E.A. (2004). Expression of Cre Recombinase in Photoreceptors Leads to Retinal Degeneration. Association for Research in Vision and Opthalmology, Fort Launderdale, FL, USA.

Finger, C., Y. Sun, L. Sanz, L. Alvarez-Vallina, C. J. Buchholz and K. Cichutek (2005). "Replicating retroviral vectors mediating continuous production and secretion of therapeutic gene products from cancer cells." Cancer Gene Ther **12**(5): 464-74.

Fire, A., S. Xu, M. K. Montgomery, S. A. Kostas, S. E. Driver and C. C. Mello (1998). "Potent and specific genetic interference by double-stranded RNA in Caenorhabditis elegans." Nature **391**(6669): 806-11.

Flores, E. R., K. Y. Tsai, D. Crowley, S. Sengupta, A. Yang, F. McKeon and T. Jacks (2002). "p63 and p73 are required for p53-dependent apoptosis in response to DNA damage." Nature **416**(6880): 560-4.

Flotte, T. R. and B. L. Laube (2001). "Gene therapy in cystic fibrosis." Chest **120**(3 Suppl): 124S-131S.

Foecking, M. K. and H. Hofstetter (1986). "Powerful and versatile enhancer-promoter unit for mammalian expression vectors." Gene **45**(1): 101-5.

Follenzi, A., M. Battaglia, A. Lombardo, A. Annoni, M. G. Roncarolo and L. Naldini (2004). "Targeting lentiviral vector expression to hepatocytes limits transgene-specific immune response and establishes long-term expression of human antihemophilic factor IX in mice." Blood **103**(10): 3700-9.

Fong, S. L., M. H. Criswell, T. Belecky-Adams, W. B. Fong, J. N. McClintick, W. W. Kao and H. J. Edenberg (2005). "Characterization of a transgenic mouse line lacking photoreceptor development within the ventral retina." Exp Eye Res.

Fox, D. A., A. T. Poblenz and L. He (1999). "Calcium overload triggers rod photoreceptor apoptotic cell death in chemical-induced and inherited retinal degenerations." Ann N Y Acad Sci **893**: 282-5.

Frasson, M., S. Picaud, T. Leveillard, M. Simonutti, S. Mohand-Said, H. Dreyfus, D. Hicks and J. Sabel (1999). "Glial cell line-derived neurotrophic factor induces histologic and functional protection of rod photoreceptors in the rd/rd mouse." Invest Ophthalmol Vis Sci **40**(11): 2724-34.

Frederick, C. A., L. D. Williams, G. Ughetto, G. A. van der Marel, J. H. van Boom, A. Rich and A. H. Wang (1990). "Structural comparison of anticancer drug-DNA complexes: adriamycin and daunomycin." Biochemistry **29**(10): 2538-49.

Freier, S. M., R. Kierzek, J. A. Jaeger, N. Sugimoto, M. H. Caruthers, T. Neilson and D. H. Turner (1986). "Improved free-energy parameters for predictions of RNA duplex stability." Proc Natl Acad Sci U S A **83**(24): 9373-7.

Freund, C. L., C. Y. Gregory-Evans, T. Furukawa, M. Papaioannou, J. Looser, L. Ploder, J. Bellingham, D. Ng, J. A. Herbrick, A. Duncan, S. W. Scherer, L. C. Tsui, A. Loutradis-Anagnostou, S. G. Jacobson, C. L. Cepko, S. S. Bhattacharya and R. R. McInnes (1997). "Cone-rod dystrophy due to mutations in a novel photoreceptor-specific homeobox gene (CRX) essential for maintenance of the photoreceptor." Cell **91**(4): 543-53.

Fritz, J. J., M. Gorbatyuk, A. S. Lewin and W. W. Hauswirth (2004). "Design and validation of therapeutic hammerhead ribozymes for autosomal dominant diseases." Methods Mol Biol **252**: 221-36.

Fujiwara, T., D. W. Cai, R. N. Georges, T. Mukhopadhyay, E. A. Grimm and J. A. Roth (1994a). "Therapeutic effect of a retroviral wild-type p53 expression vector in an orthotopic lung cancer model." J Natl Cancer Inst **86**(19): 1458-62.

Fujiwara, T., E. A. Grimm, T. Mukhopadhyay, W. W. Zhang, L. B. Owen-Schaub and J. A. Roth (1994b). "Induction of chemosensitivity in human lung cancer cells in vivo by adenovirus-mediated transfer of the wild-type p53 gene." Cancer Res **54**(9): 2287-91.

Furukawa, T., E. M. Morrow, T. Li, F. C. Davis and C. L. Cepko (1999). "Retinopathy and attenuated circadian entrainment in Crx-deficient mice." Nat Genet **23**(4): 466-70.

Gafni, J. and L. M. Ellerby (2002). "Calpain activation in Huntington's disease." J Neurosci **22**(12): 4842-9.

Gallardo, D., *et al.* (1996). "Adenovirus-based transfer of wild-type p53 gene increases ovarian tumor radiosensitivity." Cancer Res **56**(21): 4891-3.

Galy, A., M. J. Roux, J. A. Sahel, T. Leveillard and A. Giangrande (2005). "Rhodopsin maturation defects induce photoreceptor death by apoptosis: a fly model for RhodopsinPro23His human retinitis pigmentosa." Hum Mol Genet **14**(17): 2547-57.

Gao, G. P., M. R. Alvira, L. Wang, R. Calcedo, J. Johnston and J. M. Wilson (2002). "Novel adeno-associated viruses from rhesus monkeys as vectors for human gene therapy." Proc Natl Acad Sci U S A **99**(18): 11854-9.

Gautschi, O., S. Tschopp, R. A. Olie, S. H. Leech, A. P. Simoes-Wust, A. Ziegler, B. Baumann, B. Odermatt, J. Hall, R. A. Stahel and U. Zangemeister-Wittke (2001). "Activity of a novel bcl-2/bcl-xL-bispecific antisense oligonucleotide against tumors of diverse histologic origins." J Natl Cancer Inst **93**(6): 463-71.

Ge, Q., L. Filip, A. Bai, T. Nguyen, H. N. Eisen and J. Chen (2004). "Inhibition of influenza virus production in virus-infected mice by RNA interference." Proc Natl Acad Sci U S A **101**(23): 8676-81.

Genesis (2000). "Tissue Specific Expression of Cre recombinase in Mice." Genesis **26**(2).

Gewirtz, D. A. (1999). "A critical evaluation of the mechanisms of action proposed for the antitumor effects of the anthracycline antibiotics adriamycin and daunorubicin." Biochem Pharmacol **57**(7): 727-41.

Ghobrial, I. M., T. E. Witzig and A. A. Adjei (2005). "Targeting apoptosis pathways in cancer therapy." CA Cancer J Clin **55**(3): 178-94.

Giladi, H., M. Ketzinel-Gilad, L. Rivkin, Y. Felig, O. Nussbaum and E. Galun (2003). "Small interfering RNA inhibits hepatitis B virus replication in mice." Mol Ther **8**(5): 769-76.

Gjerset, R. A., *et al.* (1995). "Use of wild-type p53 to achieve complete treatment sensitization of tumor cells expressing endogenous mutant p53." Mol Carcinog **14**(4): 275-85.

Goll, D. E., V. F. Thompson, H. Li, W. Wei and J. Cong (2003). "The calpain system." Physiol Rev **83**(3): 731-801.

Gomez-Vicente, V., M. Donovan and T. G. Cotter (2005). "Multiple death pathways in retina-derived 661W cells following growth factor deprivation: crosstalk between caspases and calpains." Cell Death Differ.

Good, P. D., A. J. Krikos, S. X. Li, E. Bertrand, N. S. Lee, L. Giver, A. Ellington, J. A. Zaia, J. J. Rossi and D. R. Engelke (1997). "Expression of small, therapeutic RNAs in human cell nuclei." Gene Ther **4**(1): 45-54.

Goodchild, J. (1992). "Enhancement of ribozyme catalytic activity by a contiguous oligodeoxynucleotide (facilitator) and by 2'-O-methylation." Nucleic Acids Res **20**(17): 4607-12.

Gorbatyuk, M. S., J. J. Pang, J. Thomas, Jr., W. W. Hauswirth and A. S. Lewin (2005). "Knockdown of wild-type mouse rhodopsin using an AAV vectored ribozyme as part of an RNA replacement approach." Mol Vis **11**: 648-56.

Green, D. R. and G. Kroemer (2004). "The pathophysiology of mitochondrial cell death." Science **305**(5684): 626-9.

Gu, J. L., H. Pei, L. Thomas, J. L. Nadler, J. J. Rossi, L. Lanting and R. Natarajan (2001). "Ribozyme-mediated inhibition of rat leukocyte-type 12-lipoxygenase prevents intimal hyperplasia in balloon-injured rat carotid arteries." Circulation **103**(10): 1446-52.

Hacein-Bey-Abina, S., C. Von Kalle, M. Schmidt, M. P. McCormack, N. Wulffraat, P. Leboulch, A. Lim, C. S. Osborne, R. Pawliuk, E. Morillon, R. Sorensen, A. Forster, P. Fraser, J. I. Cohen, G. de Saint Basile, I. Alexander, U. Wintergerst, T. Frebourg, A. Aurias, D. Stoppa-Lyonnet, S. Romana, I. Radford-Weiss, F. Gross, F. Valensi, E. Delabesse, E. Macintyre, F. Sigaux, J. Soulier, L. E. Leiva, M. Wissler, C. Prinz, T. H. Rabbitts, F. Le Deist, A. Fischer and M. Cavazzana-Calvo (2003). "LMO2-associated clonal T cell proliferation in two patients after gene therapy for SCID-X1." Science **302**(5644): 415-9.

Hacker, U. T., L. Wingenfeld, D. M. Kofler, N. K. Schuhmann, S. Lutz, T. Herold, S. B. King, F. M. Gerner, L. Perabo, J. Rabinowitz, D. M. McCarty, R. J. Samulski, M. Hallek and H. Buning (2005). "Adeno-associated virus serotypes 1 to 5 mediated tumor cell directed gene transfer and improvement of transduction efficiency." J Gene Med **7**(11): 1429-1438.

Hafezi, F., J. P. Steinbach, A. Marti, K. Munz, Z. Q. Wang, E. F. Wagner, A. Aguzzi and C. E. Reme (1997). "The absence of c-fos prevents light-induced apoptotic cell death of photoreceptors in retinal degeneration in vivo." Nat Med **3**(3): 346-9.

Hafezi, F., J. P. Steinbach, A. Marti, K. Munz, Z. Q. Wang, E. F. Wagner, A. Aguzzi and C. E. Reme (1997). "The absence of c-fos prevents light-induced apoptotic cell death of photoreceptors in retinal degeneration in vivo." Nat Med **3**(3): 346-9.

Hafezi, F., M. Abegg, C. Grimm, A. Wenzel, K. Munz, J. Sturmer, D. B. Farber and C. E. Reme (1998). "Retinal degeneration in the rd mouse in the absence of c-fos." Invest Ophthalmol Vis Sci **39**(12): 2239-44.

Hall, J. (2004). "Opinion: Unravelling the general properties of siRNAs: strength in numbers and lessons from the past." Nat Rev Genet **5**(7): 552-7.

Ham, D. I., S. J. Kim, J. Chen, B. P. Vistica, R. N. Fariss, R. S. Lee, E. F. Wawrousek, H. Takase, C. R. Yu, C. E. Egwuagu, C. C. Chan and I. Gery (2004). "Central immunotolerance in transgenic mice expressing a foreign antigen under control of the rhodopsin promoter." Invest Ophthalmol Vis Sci **45**(3): 857-62.

Hamar, P., E. Song, G. Kokeny, A. Chen, N. Ouyang and J. Lieberman (2004). "Small interfering RNA targeting Fas protects mice against renal ischemia-reperfusion injury." Proc Natl Acad Sci U S A **101**(41): 14883-8.

Hamilton, D. L. and K. Abremski (1984). "Site-specific recombination by the bacteriophage P1 lox-Cre system. Cre-mediated synapsis of two lox sites." J Mol Biol **178**(2): 481-6.

Hammond, S. M., A. A. Caudy and G. J. Hannon (2001). "Post-transcriptional gene silencing by double-stranded RNA." Nat Rev Genet **2**(2): 110-9.

Hanahan, D. and R. A. Weinberg (2000). "The hallmarks of cancer." Cell **100**(1): 57-70.

Hao, W., A. Wenzel, M. S. Obin, C. K. Chen, E. Brill, N. V. Krasnoperova, P. Eversole-Cire, Y. Kleyner, A. Taylor, M. I. Simon, C. Grimm, C. E. Reme and J. Lem (2002). "Evidence for two apoptotic pathways in light-induced retinal degeneration." Nat Genet **32**(2): 254-60.

Harper, J. W., G. R. Adami, N. Wei, K. Keyomarsi and S. J. Elledge (1993). "The p21 Cdk-interacting protein Cip1 is a potent inhibitor of G1 cyclin-dependent kinases." Cell **75**(4): 805-16.

Harvey, M., H. Vogel, D. Morris, A. Bradley, A. Bernstein and L. A. Donehower (1995). "A mutant p53 transgene accelerates tumour development in heterozygous but not nullizygous p53-deficient mice." Nat Genet **9**(3): 305-11.

Haseloff, J. and W. L. Gerlach (1988). "Simple RNA enzymes with new and highly specific endoribonuclease activities." Nature **334**(6183): 585-91.

Hasenjager, A., B. Gillissen, A. Muller, G. Normand, P. G. Hemmati, M. Schuler, B. Dorken and P. T. Daniel (2004). "Smac induces cytochrome c release and apoptosis independently from Bax/Bcl-x(L) in a strictly caspase-3-dependent manner in human carcinoma cells." Oncogene **23**(26): 4523-35.

Hatakeyama, J. and R. Kageyama (2002). "Retrovirus-mediated gene transfer to retinal explants." Methods **28**(4): 387-95.

Hayashita-Kinoh, H., M. Yamada, T. Yokota, Y. Mizuno and H. Mochizuki (2006). "Down-regulation of alpha-synuclein expression can rescue dopaminergic cells from cell death in the substantia nigra of Parkinson's disease rat model." Biochem Biophys Res Commun **341**(4): 1088-95.

Heidenreich, O., F. Benseler, A. Fahrenholz and F. Eckstein (1994). "High activity and stability of hammerhead ribozymes containing 2'-modified pyrimidine nucleosides and phosphorothioates." J Biol Chem **269**(3): 2131-8.

Hendry, P. and M. McCall (1996). "Unexpected anisotropy in substrate cleavage rates by asymmetric hammerhead ribozymes." Nucleic Acids Res **24**(14): 2679-84.

Hertel, K. J., D. Herschlag and O. C. Uhlenbeck (1994). "A kinetic and thermodynamic framework for the hammerhead ribozyme reaction." Biochemistry **33**(11): 3374-85.

Hertel, K. J., D. Herschlag and O. C. Uhlenbeck (1996). "Specificity of hammerhead ribozyme cleavage." Embo J **15**(14): 3751-7.

Higuchi, M., D. O'Brien, P. Kumaravelu, N. Lenny, E. J. Yeoh and J. R. Downing (2002). "Expression of a conditional AML1-ETO oncogene bypasses embryonic lethality and establishes a murine model of human t(8;21) acute myeloid leukemia." Cancer Cell **1**(1): 63-74.

Hillgenberg, M., J. R. Schlehofer, M. von Knebel Doeberitz and P. Klein-Bauernschmitt (1999). "Enhanced sensitivity of small cell lung cancer cell lines to cisplatin and etoposide after infection with adeno-associated virus type 2." Eur J Cancer **35**(1): 106-10.

Hisahara, S., T. Araki, F. Sugiyama, K. Yagami, M. Suzuki, K. Abe, K. Yamamura, J. Miyazaki, T. Momoi, T. Saruta, C. C. Bernard, H. Okano and M. Miura (2000). "Targeted expression of baculovirus p35 caspase inhibitor in oligodendrocytes protects mice against autoimmune-mediated demyelination." Embo J **19**(3): 341-8.

Hobson, A. H., M. Donovan, M. M. Humphries, G. Tuohy, N. McNally, R. Carmody, T. Cotter, G. J. Farrar, P. F. Kenna and P. Humphries (2000). "Apoptotic photoreceptor death in the rhodopsin knockout mouse in the presence and absence of c-fos." Exp Eye Res **71**(3): 247-54.

Hofacker, I. L., W. Fontana, P. F. Stadler, L. S. Bonheoffer, M. Tacker and P. Schuster (1994). "Fast folding and comparison of RNA secondary structures." Chemical Monthly **125**: 167-188.

Hollander, K., M. Bar-Chen and S. Efrat (2005). "Baculovirus p35 increases pancreatic beta-cell resistance to apoptosis." Biochem Biophys Res Commun **332**(2): 550-6.
Hollstein, M., D. Sidransky, B. Vogelstein and C. C. Harris (1991). "p53 mutations in human cancers." Science **253**(5015): 49-53.
Holmes, M., E. Rosenberg and K. Valerie (2003). "Adenovirus expressing p53." Methods Mol Biol **234**: 1-16.
Hong, D. H., G. Yue, M. Adamian and T. Li (2001). "Retinitis pigmentosa GTPase regulator (RPGRr)-interacting protein is stably associated with the photoreceptor ciliary axoneme and anchors RPGR to the connecting cilium." J Biol Chem **276**(15): 12091-9.
Horowitz, J. (1999). "Adenovirus-mediated p53 gene therapy: overview of preclinical studies and potential clinical applications." Curr Opin Mol Ther **1**(4): 500-9.
Hsiao, M., V. Tse, J. Carmel, Y. Tsai, P. L. Felgner, M. Haas and G. D. Silverberg (1997). "Intracavitary liposome-mediated p53 gene transfer into glioblastoma with endogenous wild-type p53 in vivo results in tumor suppression and long-term survival." Biochem Biophys Res Commun **233**(2): 359-64.
Huang, S. H., S. J. Pittler, X. Huang, L. Oliveira, E. L. Berson and T. P. Dryja (1995). "Autosomal recessive retinitis pigmentosa caused by mutations in the alpha subunit of rod cGMP phosphodiesterase." Nat Genet **11**(4): 468-71.
Hudson, A. J., N. Normand, J. Ackroyd and S. Akhtar (1999). "Cellular delivery of hammerhead ribozymes conjugated to a transferrin receptor antibody." Int J Pharm **182**(1): 49-58.
Huettner, C. S., S. Koschmieder, H. Iwasaki, J. Iwasaki-Arai, H. S. Radomska, K. Akashi and D. G. Tenen (2003). "Inducible expression of BCR/ABL using human CD34 regulatory elements results in a megakaryocytic myeloproliferative syndrome." Blood **102**(9): 3363-70.
Huh, J. R., M. Guo and B. A. Hay (2004). "Compensatory proliferation induced by cell death in the Drosophila wing disc requires activity of the apical cell death caspase Dronc in a nonapoptotic role." Curr Biol **14**(14): 1262-6.
Humphries, M. M., D. Rancourt, G. J. Farrar, P. Kenna, M. Hazel, R. A. Bush, P. A. Sieving, D. M. Sheils, N. McNally, P. Creighton, A. Erven, A. Boros, K. Gulya, M. R. Capecchi and P. Humphries (1997). "Retinopathy induced in mice by targeted disruption of the rhodopsin gene." Nat Genet **15**(2): 216-9.
Hupp, T. R., D. P. Lane and K. L. Ball (2000). "Strategies for manipulating the p53 pathway in the treatment of human cancer." Biochem J **352 Pt 1**: 1-17.
Hurwitz, H., L. Fehrenbacher, W. Novotny, T. Cartwright, J. Hainsworth, W. Heim, J. Berlin, A. Baron, S. Griffing, E. Holmgren, N. Ferrara, G. Fyfe, B. Rogers, R. Ross and F. Kabbinavar (2004). "Bevacizumab plus irinotecan, fluorouracil, and leucovorin for metastatic colorectal cancer." N Engl J Med **350**(23): 2335-42.
Iacopetta, B. (2003). "TP53 mutation in colorectal cancer." Hum Mutat **21**(3): 271-6.
Ikawa, M., N. Tanaka, W. W. Kao and I. M. Verma (2003). "Generation of transgenic mice using lentiviral vectors: a novel preclinical assessment of lentiviral vectors for gene therapy." Mol Ther **8**(4): 666-73.
Illing, M. E., R. S. Rajan, N. F. Bence and R. R. Kopito (2002). "A rhodopsin mutant linked to autosomal dominant retinitis pigmentosa is prone to aggregate and interacts with the ubiquitin proteasome system." J Biol Chem **277**(37): 34150-60.

Irie, A., K. Matsumoto, B. Anderegg, H. Kuruma, M. Kashani-Sabet, K. J. Scanlon, T. Uchida and S. Baba (2005). "Growth inhibition efficacy of an adenovirus expressing dual therapeutic genes, wild-type p53, and anti-erbB2 ribozyme, against human bladder cancer cells." Cancer Gene Ther.

Izquierdo, M., A. Grandien, L. M. Criado, S. Robles, E. Leonardo, J. P. Albar, G. G. de Buitrago and A. C. Martinez (1999). "Blocked negative selection of developing T cells in mice expressing the baculovirus p35 caspase inhibitor." Embo J **18**(1): 156-66.

Jackson, A. L., S. R. Bartz, J. Schelter, S. V. Kobayashi, J. Burchard, M. Mao, B. Li, G. Cavet and P. S. Linsley (2003). "Expression profiling reveals off-target gene regulation by RNAi." Nat Biotechnol **21**(6): 635-7.

Jacobson, M. D., M. Weil and M. C. Raff (1997). "Programmed cell death in animal development." Cell **88**(3): 347-54.

Jansen, B. and U. Zangemeister-Wittke (2002). "Antisense therapy for cancer--the time of truth." Lancet Oncol **3**(11): 672-83.

Jansen, B., V. Wacheck, E. Heere-Ress, H. Schlagbauer-Wadl, C. Hoeller, T. Lucas, M. Hoermann, U. Hollenstein, K. Wolff and H. Pehamberger (2000). "Chemosensitisation of malignant melanoma by BCL2 antisense therapy." Lancet **356**(9243): 1728-33.

Jo, D., A. Nashabi, C. Doxsee, Q. Lin, D. Unutmaz, J. Chen and H. E. Ruley (2001). "Epigenetic regulation of gene structure and function with a cell-permeable Cre recombinase." Nat Biotechnol **19**(10): 929-33.

Johansen, J., J. Tornoe, A. Moller and T. E. Johansen (2003). "Increased in vitro and in vivo transgene expression levels mediated through cis-acting elements." J Gene Med **5**(12): 1080-9.

Jomary, C., M. J. Neal and S. E. Jones (2001). "Characterization of cell death pathways in murine retinal neurodegeneration implicates cytochrome c release, caspase activation, and bid cleavage." Mol Cell Neurosci **18**(4): 335-46.

Jonkers, J., R. Meuwissen, H. van der Gulden, H. Peterse, M. van der Valk and A. Berns (2001). "Synergistic tumor suppressor activity of BRCA2 and p53 in a conditional mouse model for breast cancer." Nat Genet **29**(4): 418-25.

Jorgensen, R. A., P. D. Cluster, J. English, Q. Que and C. A. Napoli (1996). "Chalcone synthase cosuppression phenotypes in petunia flowers: comparison of sense vs. antisense constructs and single-copy vs. complex T-DNA sequences." Plant Mol Biol **31**(5): 957-73.

Kafri, T., U. Blomer, D. A. Peterson, F. H. Gage and I. M. Verma (1997). "Sustained expression of genes delivered directly into liver and muscle by lentiviral vectors." Nat Genet **17**(3): 314-7.

Kajiwara, K., L. B. Hahn, S. Mukai, G. H. Travis, E. L. Berson and T. P. Dryja (1991). "Mutations in the human retinal degeneration slow gene in autosomal dominant retinitis pigmentosa." Nature **354**(6353): 480-3.

Kalloniatis, M. and E. L. Fletcher (2004). "Retinitis pigmentosa: understanding the clinical presentation, mechanisms and treatment options." Clin Exp Optom **87**(2): 65-80.

Kashani-Sabet, M., *et al.* (1994). "Suppression of the neoplastic phenotype in vivo by an anti-ras ribozyme." Cancer Res **54**(4): 900-2.

Kaspar, B. K., B. Vissel, T. Bengoechea, S. Crone, L. Randolph-Moore, R. Muller, E. P. Brandon, D. Schaffer, I. M. Verma, K. F. Lee, S. F. Heinemann and F. H. Gage (2002). "Adeno-associated virus effectively mediates conditional gene modification in the brain." Proc Natl Acad Sci U S A **99**(4): 2320-5.

Kato, Y., M. Tsunemi, M. Miyagishi, H. Kawasaki and K. Taira (2004). "Functional gene discovery using hybrid ribozyme libraries." Methods Mol Biol **252**: 245-56.

Kato, Y., T. Kuwabara, M. Warashina, H. Toda and K. Taira (2001). "Relationships between the activities in vitro and in vivo of various kinds of ribozyme and their intracellular localization in mammalian cells." J Biol Chem **276**(18): 15378-85.

Kaushal, S., K. D. Ridge and H. G. Khorana (1994). "Structure and function in rhodopsin: the role of asparagine-linked glycosylation." Proc Natl Acad Sci U S A **91**(9): 4024-8.

Kellendonk, C., F. Tronche, A. P. Monaghan, P. O. Angrand, F. Stewart and G. Schutz (1996). "Regulation of Cre recombinase activity by the synthetic steroid RU 486." Nucleic Acids Res **24**(8): 1404-11.

Kennan, A., A. Aherne and P. Humphries (2005). "Light in retinitis pigmentosa." Trends Genet **21**(2): 103-10.

Kennan, A., A. Aherne, A. Palfi, M. Humphries, A. McKee, A. Stitt, D. A. Simpson, K. Demtroder, T. Orntoft, C. Ayuso, P. F. Kenna, G. J. Farrar and P. Humphries (2002). "Identification of an IMPDH1 mutation in autosomal dominant retinitis pigmentosa (RP10) revealed following comparative microarray analysis of transcripts derived from retinas of wild-type and Rho(-/-) mice." Hum Mol Genet **11**(5): 547-57.

Kern, S. E., J. A. Pietenpol, S. Thiagalingam, A. Seymour, K. W. Kinzler and B. Vogelstein (1992). "Oncogenic forms of p53 inhibit p53-regulated gene expression." Science **256**(5058): 827-30.

Kern, S. E., J. A. Pietenpol, S. Thiagalingam, A. Seymour, K. W. Kinzler and B. Vogelstein (1992). "Oncogenic forms of p53 inhibit p53-regulated gene expression." Science **256**(5058): 827-30.

Kerr, J. F., A. H. Wyllie and A. R. Currie (1972). "Apoptosis: a basic biological phenomenon with wide-ranging implications in tissue kinetics." Br J Cancer **26**(4): 239-57.

Khan, A. U. and S. K. Lal (2003). "Ribozymes: a modern tool in medicine." J Biomed Sci **10**(5): 457-67.

Khani, S. C., L. Nielsen and T. M. Vogt (1998). "Biochemical evidence for pathogenicity of rhodopsin kinase mutations correlated with the oguchi form of congenital stationary night blindness." Proc Natl Acad Sci U S A **95**(6): 2824-7.

Kiang, A. S., A. Palfi, M. Ader, P. F. Kenna, S. Millington-Ward, G. Clark, A. Kennan, M. O'Reilly, L. C. Tam, A. Aherne, N. McNally, P. Humphries and G. J. Farrar (2005). "Toward a gene therapy for dominant disease: validation of an RNA interference-based mutation-independent approach." Mol Ther **12**(3): 555-61.

Kijima, H., H. Yamazaki, M. Nakamura, K. J. Scanlon, R. Y. Osamura and Y. Ueyama (2004). "Ribozyme against mutant K-ras mRNA suppresses tumor growth of pancreatic cancer." Int J Oncol **24**(3): 559-64.

Kim, D. H., J. A. Kim, J. S. Choi and C. K. Joo (2002). "Activation of caspase-3 during degeneration of the outer nuclear layer in the rd mouse retina." Ophthalmic Res **34**(3): 150-7.

Kim, R., M. Emi, K. Tanabe and T. Toge (2004). "Preclinical evaluation of antisense bcl-2 as a chemosensitizer for patients with gastric carcinoma." Cancer **101**(10): 2177-86.

Kluck, R. M., E. Bossy-Wetzel, D. R. Green and D. D. Newmeyer (1997). "The release of cytochrome c from mitochondria: a primary site for Bcl-2 regulation of apoptosis." Science **275**(5303): 1132-6.

Kobayashi, H., S. G. Eckhardt, J. A. Lockridge, M. L. Rothenberg, A. B. Sandler, C. L. O'Bryant, W. Cooper, S. N. Holden, R. D. Aitchison, N. Usman, M. Wolin and M. L. Basche (2005). "Safety and pharmacokinetic study of RPI.4610 (ANGIOZYME), an anti-VEGFR-1 ribozyme, in combination with carboplatin and paclitaxel in patients with advanced solid tumors." Cancer Chemother Pharmacol **56**(4): 329-36.

Koenekoop, R. K. (2004). "An overview of Leber congenital amaurosis: a model to understand human retinal development." Surv Ophthalmol **49**(4): 379-98.

Kordower, J. H., M. E. Emborg, J. Bloch, S. Y. Ma, Y. Chu, L. Leventhal, J. McBride, E. Y. Chen, S. Palfi, B. Z. Roitberg, W. D. Brown, J. E. Holden, R. Pyzalski, M. D. Taylor, P. Carvey, Z. Ling, D. Trono, P. Hantraye, N. Deglon and P. Aebischer (2000). "Neurodegeneration prevented by lentiviral vector delivery of GDNF in primate models of Parkinson's disease." Science **290**(5492): 767-73.

Koresawa, Y., S. Miyagawa, M. Ikawa, K. Matsunami, M. Yamada, M. Okabe and R. Shirakura (2000). "A new Cre recombinase gene based on optimal codon usage in mammals: a powerful material for organ-specific gene targeting." Transplant Proc **32**(7): 2516-7.

Kroemer, G. and S. J. Martin (2005). "Caspase-independent cell death." Nat Med **11**(7): 725-30.

Kruger, K., P. J. Grabowski, A. J. Zaug, J. Sands, D. E. Gottschling and T. R. Cech (1982). "Self-splicing RNA: autoexcision and autocyclization of the ribosomal RNA intervening sequence of Tetrahymena." Cell **31**(1): 147-57.

Kruger, M., C. Beger, P. J. Welch, J. R. Barber and F. Wong-Staal (2001). "C-SPACE (cleavage-specific amplification of cDNA ends): a novel method of ribozyme-mediated gene identification." Nucleic Acids Res **29**(19): E94.

Kugler, S., G. Straten, F. Kreppel, S. Isenmann, P. Liston and M. Bahr (2000). "The X-linked inhibitor of apoptosis (XIAP) prevents cell death in axotomized CNS neurons in vivo." Cell Death Differ **7**(9): 815-24.

Kuida, K., T. S. Zheng, S. Na, C. Kuan, D. Yang, H. Karasuyama, P. Rakic and R. A. Flavell (1996). "Decreased apoptosis in the brain and premature lethality in CPP32-deficient mice." Nature **384**(6607): 368-72.

Kumar, R., S. K. Singh, A. A. Koshkin, V. K. Rajwanshi, M. Meldgaard and J. Wengel (1998). "The first analogues of LNA (locked nucleic acids): phosphorothioate-LNA and 2'-thio-LNA." Bioorg Med Chem Lett **8**(16): 2219-22.

Lane, D. P. (1992). "Cancer. p53, guardian of the genome." Nature **358**(6381): 15-6.

Lane, D. P. and S. Lain (2002). "Therapeutic exploitation of the p53 pathway." Trends Mol Med **8**(4 Suppl): S38-42.

Laugwitz, K. L., A. Moretti, H. J. Weig, A. Gillitzer, K. Pinkernell, T. Ott, I. Pragst, C. Stadele, M. Seyfarth, A. Schomig and M. Ungerer (2001). "Blocking caspase-activated apoptosis improves contractility in failing myocardium." Hum Gene Ther **12**(17): 2051-63.

LaVail, M. M., D. Yasumura, M. T. Matthes, K. A. Drenser, J. G. Flannery, A. S. Lewin and W. W. Hauswirth (2000). "Ribozyme rescue of photoreceptor cells in P23H transgenic rats: long-term survival and late-stage therapy." Proc Natl Acad Sci U S A **97**(21): 11488-93.

Lavrik, I. N., A. Golks and P. H. Krammer (2005). "Caspases: pharmacological manipulation of cell death." J Clin Invest **115**(10): 2665-72.

Lawrence, J. M., D. J. Keegan, E. M. Muir, P. J. Coffey, J. H. Rogers, M. J. Wilby, J. W. Fawcett and R. D. Lund (2004). "Transplantation of Schwann cell line clones secreting GDNF or BDNF into the retinas of dystrophic Royal College of Surgeons rats." Invest Ophthalmol Vis Sci **45**(1): 267-74.

Le, Y. Z., J. D. Ash, M. R. Al-Ubaidi, Y. Chen, J. X. Ma and R. E. Anderson (2004). "Targeted expression of Cre recombinase to cone photoreceptors in transgenic mice." Mol Vis **10**: 1011-8.

Le, Y. Z., L. Zheng, W. Zheng, J. D. Ash, M. P. Agbaga, M. Zhu and R. E. Anderson (2006). "Mouse opsin promoter-directed Cre recombinase expression in transgenic mice." Molecular Vision **12**: 389-398.

Lee, K. F., *et al.* (1999). "Generation and characterization of hammerhead ribozymes targeting rodent metallothionein-I and -II ribonucleic acid." Toxicol Appl Pharmacol **161**(3): 294-301.

Lee, P. A., L. M. Blatt, K. S. Blanchard, K. S. Bouhana, P. A. Pavco, L. Bellon and J. A. Sandberg (2000). "Pharmacokinetics and tissue distribution of a ribozyme directed against hepatitis C virus RNA following subcutaneous or intravenous administration in mice." Hepatology **32**(3): 640-6.

Leist, M. and M. Jaattela (2001). "Four deaths and a funeral: from caspases to alternative mechanisms." Nat Rev Mol Cell Biol **2**(8): 589-98.

Leonard K.C., P. D., Coupland S.G., Baker A.N., Leonard B.C., Korneluk R.G., Tsifidis C. (2005). XIAP Gene Therapy Protects Photoreceptors in Animal Models of Retinitis Pigmentosa (RP). ARVO, Fort Lauderdale, Florida, USA, Investigative Opthalmology and Visual Science.

Leung, R. K. and P. A. Whittaker (2005). "RNA interference: from gene silencing to gene-specific therapeutics." Pharmacol Ther **107**(2): 222-39.

Leveillard, T., S. Mohand-Said, O. Lorentz, D. Hicks, A. C. Fintz, E. Clerin, M. Simonutti, V. Forster, N. Cavusoglu, F. Chalmel, P. Dolle, O. Poch, G. Lambrou and J. A. Sahel (2004). "Identification and characterization of rod-derived cone viability factor." Nat Genet **36**(7): 755-9.

Levine, A. J. (1997). "p53, the cellular gatekeeper for growth and division." Cell **88**(3): 323-31.

Levitt, N., D. Briggs, A. Gil and N. J. Proudfoot (1989). "Definition of an efficient synthetic poly(A) site." Genes Dev **3**(7): 1019-25.

Lewin, A. S., K. A. Drenser, W. W. Hauswirth, S. Nishikawa, D. Yasumura, J. G. Flannery and M. M. LaVail (1998). "Ribozyme rescue of photoreceptor cells in a transgenic rat model of autosomal dominant retinitis pigmentosa." Nat Med **4**(8): 967-71.

Li, B., K. L. Murphy, R. Laucirica, F. Kittrell, D. Medina and J. M. Rosen (1998a). "A transgenic mouse model for mammary carcinogenesis." Oncogene **16**(8): 997-1007.

Li, M. J., J. Kim, S. Li, J. Zaia, J. K. Yee, J. Anderson, R. Akkina and J. J. Rossi (2005a). "Long-Term Inhibition of HIV-1 Infection in Primary Hematopoietic Cells by Lentiviral Vector Delivery of a Triple Combination of Anti-HIV shRNA, Anti-CCR5 Ribozyme, and a Nucleolar-Localizing TAR Decoy." Mol Ther.

Li, S., D. Chen, Y. Sauve, J. McCandless, Y. J. Chen and C. K. Chen (2005b). "Rhodopsin-iCre transgenic mouse line for Cre-mediated rod-specific gene targeting." Genesis **41**(2): 73-80.

Li, S., J. E. Rosenberg, A. A. Donjacour, I. L. Botchkina, Y. K. Hom, G. R. Cunha and E. H. Blackburn (2004). "Rapid inhibition of cancer cell growth induced by lentiviral delivery and expression of mutant-template telomerase RNA and anti-telomerase short-interfering RNA." Cancer Res **64**(14): 4833-40.

Li, T., M. A. Sandberg, B. S. Pawlyk, B. Rosner, K. C. Hayes, T. P. Dryja and E. L. Berson (1998b). "Effect of vitamin A supplementation on rhodopsin mutants threonine-17 --> methionine and proline-347 --> serine in transgenic mice and in cell cultures." Proc Natl Acad Sci U S A **95**(20): 11933-8.

Li, T., M. Adamian, D. J. Roof, E. L. Berson, T. P. Dryja, B. J. Roessler and B. L. Davidson (1994). "In vivo transfer of a reporter gene to the retina mediated by an adenoviral vector." Invest Ophthalmol Vis Sci **35**(5): 2543-9.

Li, T., W. K. Snyder, J. E. Olsson and T. P. Dryja (1996). "Transgenic mice carrying the dominant rhodopsin mutation P347S: evidence for defective vectorial transport of rhodopsin to the outer segments." Proc Natl Acad Sci U S A **93**(24): 14176-81.

Li, Z. Y., F. Wong, J. H. Chang, D. E. Possin, Y. Hao, R. M. Petters and A. H. Milam (1998c). "Rhodopsin transgenic pigs as a model for human retinitis pigmentosa." Invest Ophthalmol Vis Sci **39**(5): 808-19.

Liang, F. Q., T. S. Aleman, N. S. Dejneka, L. Dudus, K. J. Fisher, A. M. Maguire, S. G. Jacobson and J. Bennett (2001). "Long-term protection of retinal structure but not function using RAAV.CNTF in animal models of retinitis pigmentosa." Mol Ther **4**(5): 461-72.

Lieber, A. and M. Strauss (1995). "Selection of efficient cleavage sites in target RNAs by using a ribozyme expression library." Mol Cell Biol **15**(1): 540-51.

Lisman, J. and G. Fain (1995). "Support for the equivalent light hypothesis for RP." Nat Med **1**(12): 1254-5.

Liu, C., Y. Li, M. Peng, A. M. Laties and R. Wen (1999). "Activation of caspase-3 in the retina of transgenic rats with the rhodopsin mutation s334ter during photoreceptor degeneration." J Neurosci **19**(12): 4778-85.

Liu, G., T. J. McDonnell, R. Montes de Oca Luna, M. Kapoor, B. Mims, A. K. El-Naggar and G. Lozano (2000). "High metastatic potential in mice inheriting a targeted p53 missense mutation." Proc Natl Acad Sci U S A **97**(8): 4174-9.

Liu, R., B. Rohe, D. D. Carson and M. C. Farach-Carson (2002). "A rapid and simple nonradioactive method for in vitro testing of ribozyme activity." Antisense Nucleic Acid Drug Dev **12**(4): 283-8.

Liu, X. D., S. M. Ma, Y. Liu, S. Z. Liu and A. Sehon (2004). "Short hairpin RNA and retroviral vector-mediated silencing of p53 in mammalian cells." Biochem Biophys Res Commun **324**(4): 1173-8.

Liu, X. D., S. M. Ma, Y. Liu, S. Z. Liu and A. Sehon (2004). "Short hairpin RNA and retroviral vector-mediated silencing of p53 in mammalian cells." Biochem Biophys Res Commun **324**(4): 1173-8.

Logunov, D. Y., G. V. Ilyinskaya, L. V. Cherenova, L. V. Verhovskaya, M. M. Shmarov, P. M. Chumakov, B. P. Kopnin and B. S. Naroditsky (2004). "Restoration of p53 tumor-suppressor activity in human tumor cells in vitro and in their xenografts in vivo by recombinant avian adenovirus CELO-p53." Gene Ther **11**(1): 79-84.

Loonstra, A., M. Vooijs, H. B. Beverloo, B. A. Allak, E. van Drunen, R. Kanaar, A. Berns and J. Jonkers (2001). "Growth inhibition and DNA damage induced by Cre recombinase in mammalian cells." Proc Natl Acad Sci U S A **98**(16): 9209-14.

Lowe, S. W., H. E. Ruley, T. Jacks and D. E. Housman (1993). "p53-dependent apoptosis modulates the cytotoxicity of anticancer agents." Cell **74**(6): 957-67.

Lu, X. (2005). "p53: a heavily dictated dictator of life and death." Curr Opin Genet Dev **15**(1): 27-33.

Lu, X., G. Lozano and L. A. Donehower (2003). "Activities of wildtype and mutant p53 in suppression of homologous recombination as measured by a retroviral vector system." Mutat Res **522**(1-2): 69-83.

Lund, R. D., S. J. Ono, D. J. Keegan and J. M. Lawrence (2003). "Retinal transplantation: progress and problems in clinical application." J Leukoc Biol **74**(2): 151-60.

Lundstrom, K. (2003). "Latest development in viral vectors for gene therapy." Trends Biotechnol **21**(3): 117-22.

Macejak, D. G., K. L. Jensen, P. A. Pavco, K. M. Phipps, B. A. Heinz, J. M. Colacino and L. M. Blatt (2001). "Enhanced antiviral effect in cell culture of type 1 interferon and ribozymes targeting HCV RNA." J Viral Hepat **8**(6): 400-5.

Macpherson, J. L., M. P. Boyd, A. J. Arndt, A. V. Todd, G. C. Fanning, J. A. Ely, F. Elliott, A. Knop, M. Raponi, J. Murray, W. Gerlach, L. Q. Sun, R. Penny, G. P. Symonds, A. Carr and D. A. Cooper (2005). "Long-term survival and concomitant gene expression of ribozyme-transduced CD4+ T-lymphocytes in HIV-infected patients." J Gene Med **7**(5): 552-64.

Maddison, L. A., B. W. Sutherland, R. J. Barrios and N. M. Greenberg (2004). "Conditional deletion of Rb causes early stage prostate cancer." Cancer Res **64**(17): 6018-25.

Maeda, Y., S. D. Seidel, G. Wei, X. Liu and F. M. Sladek (2002). "Repression of hepatocyte nuclear factor 4alpha tumor suppressor p53: involvement of the ligand-binding domain and histone deacetylase activity." Mol Endocrinol **16**(2): 402-10.

Marlhens, F., C. Bareil, J. M. Griffoin, E. Zrenner, P. Amalric, C. Eliaou, S. Y. Liu, E. Harris, T. M. Redmond, B. Arnaud, M. Claustres and C. P. Hamel (1997). "Mutations in RPE65 cause Leber's congenital amaurosis." Nat Genet **17**(2): 139-41.

Marszalek, J. R., X. Liu, E. A. Roberts, D. Chui, J. D. Marth, D. S. Williams and L. S. Goldstein (2000). "Genetic evidence for selective transport of opsin and arrestin by kinesin-II in mammalian photoreceptors." Cell **102**(2): 175-87.

Martinez, L. A., I. Naguibneva, H. Lehrmann, A. Vervisch, T. Tchenio, G. Lozano and A. Harel-Bellan (2002). "Synthetic small inhibiting RNAs: efficient tools to inactivate oncogenic mutations and restore p53 pathways." Proc Natl Acad Sci U S A **99**(23): 14849-54.

Martinez-Mir, A., E. Paloma, R. Allikmets, C. Ayuso, T. del Rio, M. Dean, L. Vilageliu, R. Gonzalez-Duarte and S. Balcells (1998). "Retinitis pigmentosa caused by a homozygous mutation in the Stargardt disease gene ABCR." Nat Genet **18**(1): 11-2.

Martinou, I., P. A. Fernandez, M. Missotten, E. White, B. Allet, R. Sadoul and J. C. Martinou (1995). "Viral proteins E1B19K and p35 protect sympathetic neurons from cell death induced by NGF deprivation." J Cell Biol **128**(1-2): 201-8.

Mathews, D. H., J. Sabina, M. Zuker and D. H. Turner (1999). "Expanded sequence dependence of thermodynamic parameters improves prediction of RNA secondary structure." J Mol Biol **288**(5): 911-40.

Matsuda, T. and C. L. Cepko (2004). "Electroporation and RNA interference in the rodent retina in vivo and in vitro." Proc Natl Acad Sci U S A **101**(1): 16-22.

Matzura, O. and A. Wennborg (1996). "RNAdraw: an integrated program for RNA secondary structure calculation and analysis under 32-bit Microsoft Windows." Comput Appl Biosci **12**(3): 247-9.

Maw, M. A., B. Kennedy, A. Knight, R. Bridges, K. E. Roth, E. J. Mani, J. K. Mukkadan, D. Nancarrow, J. W. Crabb and M. J. Denton (1997). "Mutation of the gene encoding cellular retinaldehyde-binding protein in autosomal recessive retinitis pigmentosa." Nat Genet **17**(2): 198-200.

May, L. A., C. M. Lai and P. E. Rakoczy (2003). "In vitro comparison studies of truncated rhodopsin promoter fragments from various species in human cell lines." Clin Experiment Ophthalmol **31**(5): 445-50.

McCaffrey, A. P., K. Ohashi, L. Meuse, S. Shen, A. M. Lancaster, P. J. Lukavsky, P. Sarnow and M. A. Kay (2002). "Determinants of hepatitis C translational initiation in vitro, in cultured cells and mice." Mol Ther **5**(6): 676-84.

McGee Sanftner, L. H., H. Abel, W. W. Hauswirth and J. G. Flannery (2001). "Glial cell line derived neurotrophic factor delays photoreceptor degeneration in a transgenic rat model of retinitis pigmentosa." Mol Ther **4**(6): 622-9.

McKie, A. B., J. C. McHale, T. J. Keen, E. E. Tarttelin, R. Goliath, J. J. van Lith-Verhoeven, J. Greenberg, R. S. Ramesar, C. B. Hoyng, F. P. Cremers, D. A. Mackey, S. S. Bhattacharya, A. C. Bird, A. F. Markham and C. F. Inglehearn (2001). "Mutations in the pre-mRNA splicing factor gene PRPC8 in autosomal dominant retinitis pigmentosa (RP13)." Hum Mol Genet **10**(15): 1555-62.

McKinnon, S. J., D. M. Lehman, N. G. Tahzib, N. L. Ransom, H. A. Reitsamer, P. Liston, E. LaCasse, Q. Li, R. G. Korneluk and W. W. Hauswirth (2002). "Baculoviral IAP repeat-containing-4 protects optic nerve axons in a rat glaucoma model." Mol Ther **5**(6): 780-7.

McKusick, V. A. (1998). Mendelian Inheritance In Man, John Hopkins University Press.

McLauchlan, J., D. Gaffney, J. L. Whitton and J. B. Clements (1985). "The consensus sequence YGTGTTYY located downstream from the AATAAA signal is required for efficient formation of mRNA 3' termini." Nucleic Acids Res **13**(4): 1347-68.

McNally, N., P. F. Kenna, D. Rancourt, T. Ahmed, A. Stitt, W. H. Colledge, D. G. Lloyd, A. Palfi, B. O'Neill, M. M. Humphries, P. Humphries and G. J. Farrar (2002). "Murine model of autosomal dominant retinitis pigmentosa generated by targeted deletion at codon 307 of the rds-peripherin gene." Hum Mol Genet **11**(9): 1005-16.

McWilliam, P., G. J. Farrar, P. Kenna, D. G. Bradley, M. M. Humphries, E. M. Sharp, D. J. McConnell, M. Lawler, D. Sheils, C. Ryan and et al. (1989). "Autosomal dominant retinitis pigmentosa (ADRP): localization of an ADRP gene to the long arm of chromosome 3." Genomics **5**(3): 619-22.

Michienzi, A., S. Li, J. A. Zaia and J. J. Rossi (2002). "A nucleolar TAR decoy inhibitor of HIV-1 replication." Proc Natl Acad Sci U S A **99**(22): 14047-52.

Miller, T. J., R. J. Schneider, J. A. Miller, B. P. Martin, M. R. Al-Ubaidi, N. Agarwal, L. A. Dethloff and M. A. Philbert (2005). "Photoreceptor cell apoptosis induced by the 2-nitroimidazole radiosensitizer, CI-1010, is mediated by p53-linked activation of caspase-3." Neurotoxicology.

Millington-Ward, S., B. O'Neill, A. S. Kiang, P. Humphries, P. F. Kenna and G. J. Farrar (1999). "A mutation-independent therapeutic strategem for osteogenesis imperfecta." Antisense Nucleic Acid Drug Dev **9**(6): 537-42.

Millington-Ward, S., B. O'Neill, G. Tuohy, N. Al-Jandal, A. S. Kiang, P. F. Kenna, A. Palfi, P. Hayden, F. Mansergh, A. Kennan, P. Humphries and G. J. Farrar (1997). "Strategems in vitro for gene therapies directed to dominant mutations." Hum Mol Genet **6**(9): 1415-26.

Millington-Ward, S., C. Allers, G. Tuohy, P. Conget, D. Allen, H. P. McMahon, P. F. Kenna, P. Humphries and G. J. Farrar (2002). "Validation in mesenchymal progenitor cells of a mutation-independent ex vivo approach to gene therapy for osteogenesis imperfecta." Hum Mol Genet **11**(19): 2201-6.

Mitchell, R. S., B. F. Beitzel, A. R. Schroder, P. Shinn, H. Chen, C. C. Berry, J. R. Ecker and F. D. Bushman (2004). "Retroviral DNA integration: ASLV, HIV, and MLV show distinct target site preferences." PLoS Biol **2**(8): E234.

Mittal, V. (2004). "Improving the efficiency of RNA interference in mammals." Nat Rev Genet **5**(5): 355-65.

Miyoshi, H., M. Takahashi, F. H. Gage and I. M. Verma (1997). "Stable and efficient gene transfer into the retina using an HIV-based lentiviral vector." Proc Natl Acad Sci U S A **94**(19): 10319-23.

Moiseyev, G., Y. Chen, Y. Takahashi, B. X. Wu and J. X. Ma (2005). "RPE65 is the isomerohydrolase in the retinoid visual cycle." Proc Natl Acad Sci U S A **102**(35): 12413-8.

Molday, R. S. (1998). "Photoreceptor membrane proteins, phototransduction, and retinal degenerative diseases. The Friedenwald Lecture." Invest Ophthalmol Vis Sci **39**(13): 2491-513.

Monneret, C. (2001). "Recent developments in the field of antitumour anthracyclines." Eur J Med Chem **36**(6): 483-93.

Morris, T. A. and S. L. Fong (1993). "Characterization of the gene encoding human cone transducin alpha-subunit (GNAT2)." Genomics **17**(2): 442-8.

Morris, T. A., W. B. Fong, M. J. Ward, H. Hu and S. L. Fong (1997). "Localization of upstream silencer elements involved in the expression of cone transducin alpha-subunit (GNAT2)." Invest Ophthalmol Vis Sci **38**(1): 196-206.

Moss, R. B., D. Rodman, L. T. Spencer, M. L. Aitken, P. L. Zeitlin, D. Waltz, C. Milla, A. S. Brody, J. P. Clancy, B. Ramsey, N. Hamblett and A. E. Heald (2004). "Repeated adeno-associated virus serotype 2 aerosol-mediated cystic fibrosis transmembrane regulator gene transfer to the lungs of patients with cystic fibrosis: a multicenter, double-blind, placebo-controlled trial." Chest **125**(2): 509-21.

Muller, U. (1999). "Ten years of gene targeting: targeted mouse mutants, from vector design to phenotype analysis." Mech Dev **82**(1-2): 3-21.

Muul, L. M., L. M. Tuschong, S. L. Soenen, G. J. Jagadeesh, W. J. Ramsey, Z. Long, C. S. Carter, E. K. Garabedian, M. Alleyne, M. Brown, W. Bernstein, S. H. Schurman, T. A. Fleisher, S. F. Leitman, C. E. Dunbar, R. M. Blaese and F. Candotti (2003). "Persistence and expression of the adenosine deaminase gene for 12 years and immune reaction to gene transfer components: long-term results of the first clinical gene therapy trial." Blood **101**(7): 2563-9.

Myers, K. J., S. Murthy, A. Flanigan, D. R. Witchell, M. Butler, S. Murray, A. Siwkowski, D. Goodfellow, K. Madsen and B. Baker (2003). "Antisense oligonucleotide blockade of tumor necrosis factor-alpha in two murine models of colitis." J Pharmacol Exp Ther **304**(1): 411-24.

Nagy, A. (2000). "Cre recombinase: the universal reagent for genome tailoring." Genesis **26**(2): 99-109.

Nakagawa, T. and J. Yuan (2000). "Cross-talk between two cysteine protease families. Activation of caspase-12 by calpain in apoptosis." J Cell Biol **150**(4): 887-94.

Nambu, H., N. Umeda, S. Kachi, Y. Oshima, H. Akiyama, R. Nambu and P. A. Campochiaro (2005). "Angiopoietin 1 prevents retinal detachment in an aggressive model of proliferative retinopathy, but has no effect on established neovascularization." J Cell Physiol **204**(1): 227-35.

Narfstrom, K., M. L. Katz, R. Bragadottir, M. Seeliger, A. Boulanger, T. M. Redmond, L. Caro, C. M. Lai and P. E. Rakoczy (2003). "Functional and structural recovery of the retina after gene therapy in the RPE65 null mutation dog." Invest Ophthalmol Vis Sci **44**(4): 1663-72.

Nemunaitis, J., S. G. Swisher, T. Timmons, D. Connors, M. Mack, L. Doerksen, D. Weill, J. Wait, D. D. Lawrence, B. L. Kemp, F. Fossella, B. S. Glisson, W. K. Hong, F. R. Khuri, J. M. Kurie, J. J. Lee, J. S. Lee, D. M. Nguyen, J. C. Nesbitt, R. Perez-Soler, K. M. Pisters, J. B. Putnam, W. R. Richli, D. M. Shin, G. L. Walsh, J. Merritt and J. Roth (2000). "Adenovirus-mediated p53 gene transfer in sequence with cisplatin to tumors of patients with non-small-cell lung cancer." J Clin Oncol **18**(3): 609-22.

Newell, F. W. (1996). Opthalmology: Principles and Concepts. Missouri, USA, Mosby.
Nicholson, D. W. (1999). "Caspase structure, proteolytic substrates, and function during apoptotic cell death." Cell Death Differ **6**(11): 1028-42.
Nielsen, L. L. and D. C. Maneval (1998). "P53 tumor suppressor gene therapy for cancer." Cancer Gene Ther **5**(1): 52-63.
Nissen, P., J. Hansen, N. Ban, P. B. Moore and T. A. Steitz (2000). "The structural basis of ribosome activity in peptide bond synthesis." Science **289**(5481): 920-30.
Nosrati, M., S. Li, S. Bagheri, D. Ginzinger, E. H. Blackburn, R. J. Debs and M. Kashani-Sabet (2004). "Antitumor activity of systemically delivered ribozymes targeting murine telomerase RNA." Clin Cancer Res **10**(15): 4983-90.
Nykanen, A., B. Haley and P. D. Zamore (2001). "ATP requirements and small interfering RNA structure in the RNA interference pathway." Cell **107**(3): 309-21.
Oda, E., R. Ohki, H. Murasawa, J. Nemoto, T. Shibue, T. Yamashita, T. Tokino, T. Taniguchi and N. Tanaka (2000). "Noxa, a BH3-only member of the Bcl-2 family and candidate mediator of p53-induced apoptosis." Science **288**(5468): 1053-8.
Ogilvie, J. M., J. D. Speck, J. M. Lett and T. T. Fleming (1999). "A reliable method for organ culture of neonatal mouse retina with long-term survival." J Neurosci Methods **87**(1): 57-65.
Ohiro, Y., A. Usheva, S. Kobayashi, S. L. Duffy, R. Nantz, D. Gius and N. Horikoshi (2003). "Inhibition of stress-inducible kinase pathways by tumorigenic mutant p53." Mol Cell Biol **23**(1): 322-34.
Olsson, J. E., J. W. Gordon, B. S. Pawlyk, D. Roof, A. Hayes, R. S. Molday, S. Mukai, G. S. Cowley, E. L. Berson and T. P. Dryja (1992). "Transgenic mice with a rhodopsin mutation (Pro23His): a mouse model of autosomal dominant retinitis pigmentosa." Neuron **9**(5): 815-30.
O'Neill, B., S. Millington-Ward, M. O'Reilly, G. Tuohy, A. S. Kiang, P. F. Kenna, P. Humphries and G. J. Farrar (2000). "Ribozyme-based therapeutic approaches for autosomal dominant retinitis pigmentosa." Invest Ophthalmol Vis Sci **41**(10): 2863-9.
Oren, M. (2003). "Decision making by p53: life, death and cancer." Cell Death Differ **10**(4): 431-42.
Paddison, P. J., A. A. Caudy, E. Bernstein, G. J. Hannon and D. S. Conklin (2002). "Short hairpin RNAs (shRNAs) induce sequence-specific silencing in mammalian cells." Genes Dev **16**(8): 948-58.
Pagliaro, L. C., A. Keyhani, D. Williams, D. Woods, B. Liu, P. Perrotte, J. W. Slaton, J. A. Merritt, H. B. Grossman and C. P. Dinney (2003). "Repeated intravesical instillations of an adenoviral vector in patients with locally advanced bladder cancer: a phase I study of p53 gene therapy." J Clin Oncol **21**(12): 2247-53.
Palfi, A., M. Ader, A. S. Kiang, S. Millington-Ward, G. Clark, M. O'Reilly, H. P. McMahon, P. F. Kenna, P. Humphries and G. J. Farrar (2006). "RNAi-based suppression and replacement of rds-peripherin in retinal organotypic culture." Hum Mutat **27**(3): 260-8.
Palfner, K., M. Kneba, W. Hiddemann and J. Bertram (1995). "Short technical reports. Quantification of ribozyme-mediated RNA cleavage using silver-stained polyacrylamide gels." Biotechniques **19**(6): 926-9.

Palmiter, R. D., E. P. Sandgren, M. R. Avarbock, D. D. Allen and R. L. Brinster (1991). "Heterologous introns can enhance expression of transgenes in mice." Proc Natl Acad Sci U S A **88**(2): 478-82.

Paquet-Durand, F., S. Azadi, S. M. Hauck, M. Ueffing, T. van Veen and P. Ekstrom (2006). "Calpain is activated in degenerating photoreceptors in the rd1 mouse." Journal of Neurochemistry **96**(3): 802-14.

Pang, J., M. Cheng, D. Stevenson, M. D. Trousdale, C. K. Dorey and J. C. Blanks (2004). "Adenoviral-mediated gene transfer to retinal explants during development and degeneration." Exp Eye Res **79**(2): 189-201.

Patil, S. D., D. G. Rhodes and D. J. Burgess (2005). "DNA-based therapeutics and DNA delivery systems: a comprehensive review." Aaps J **7**(1): E61-77.

Pavco, P. A., K. S. Bouhana, A. M. Gallegos, A. Agrawal, K. S. Blanchard, S. L. Grimm, K. L. Jensen, L. E. Andrews, F. E. Wincott, P. A. Pitot, R. J. Tressler, C. Cushman, M. A. Reynolds and T. J. Parry (2000). "Antitumor and antimetastatic activity of ribozymes targeting the messenger RNA of vascular endothelial growth factor receptors." Clin Cancer Res **6**(5): 2094-103.

Pawlyk, B. S., A. J. Smith, P. K. Buch, M. Adamian, D. H. Hong, M. A. Sandberg, R. R. Ali and T. Li (2005). "Gene replacement therapy rescues photoreceptor degeneration in a murine model of Leber congenital amaurosis lacking RPGRIP." Invest Ophthalmol Vis Sci **46**(9): 3039-45.

Pearson, S., H. Jia and K. Kandachi (2004). "China approves first gene therapy." Nat Biotechnol **22**(1): 3-4.

Pennati, M., M. Binda, G. Colella, M. Zoppe, M. Folini, S. Vignati, A. Valentini, L. Citti, M. De Cesare, G. Pratesi, M. Giacca, M. G. Daidone and N. Zaffaroni (2004). "Ribozyme-mediated inhibition of survivin expression increases spontaneous and drug-induced apoptosis and decreases the tumorigenic potential of human prostate cancer cells." Oncogene **23**(2): 386-94.

Perrelet, D., A. Ferri, P. Liston, P. Muzzin, R. G. Korneluk and A. C. Kato (2002). "IAPs are essential for GDNF-mediated neuroprotective effects in injured motor neurons in vivo." Nat Cell Biol **4**(2): 175-9.

Petrin, D., A. Baker, S. G. Coupland, P. Liston, M. Narang, K. Damji, B. Leonard, V. A. Chiodo, A. Timmers, W. Hauswirth, R. G. Korneluk and C. Tsilfidis (2003). "Structural and functional protection of photoreceptors from MNU-induced retinal degeneration by the X-linked inhibitor of apoptosis." Invest Ophthalmol Vis Sci **44**(6): 2757-63.

Petters, R. M., C. A. Alexander, K. D. Wells, E. B. Collins, J. R. Sommer, M. R. Blanton, G. Rojas, Y. Hao, W. L. Flowers, E. Banin, A. V. Cideciyan, S. G. Jacobson and F. Wong (1997). "Genetically engineered large animal model for studying cone photoreceptor survival and degeneration in retinitis pigmentosa." Nat Biotechnol **15**(10): 965-70.

Pfeifer, A., E. P. Brandon, N. Kootstra, F. H. Gage and I. M. Verma (2001). "Delivery of the Cre recombinase by a self-deleting lentiviral vector: efficient gene targeting in vivo." Proc Natl Acad Sci U S A **98**(20): 11450-5.

Phelan, J. K. and D. Bok (2000). "A brief review of retinitis pigmentosa and the identified retinitis pigmentosa genes." Mol Vis **6**: 116-24.

Philchenkov, A. (2004). "Caspases: potential targets for regulating cell death." J Cell Mol Med **8**(4): 432-44.

Pieken, W. A., D. B. Olsen, F. Benseler, H. Aurup and F. Eckstein (1991). "Kinetic characterization of ribonuclease-resistant 2'-modified hammerhead ribozymes." Science **253**(5017): 314-7.

Ponjavic, V., M. Abrahamson, S. Andreasson, B. Ehinger and G. Fex (1997). "Autosomal dominant retinitis pigmentosa with a rhodopsin mutation (Arg-135-Trp). Disease phenotype in a Swedish family." Acta Ophthalmol Scand **75**(2): 218-23.

Porta, H. and P. M. Lizardi (1995). "An allosteric hammerhead ribozyme." Biotechnology (N Y) **13**(2): 161-4.

Porter, A. (1998). "Controlling your losses: conditional gene silencing in mammals." Trends Genet **14**(2): 73-9.

Portera-Cailliau, C., C. H. Sung, J. Nathans and R. Adler (1994). "Apoptotic photoreceptor cell death in mouse models of retinitis pigmentosa." Proc Natl Acad Sci U S A **91**(3): 974-8.

Puerta-Fernandez, E., C. Romero-Lopez, A. Barroso-delJesus and A. Berzal-Herranz (2003). "Ribozymes: recent advances in the development of RNA tools." FEMS Microbiol Rev **27**(1): 75-97.

Putney, S. D., J. Brown, C. Cucco, R. Lee, T. Skorski, C. Leonetti, T. Geiser, B. Calabretta, G. Zupi and G. Zon (1999). "Enhanced anti-tumor effects with microencapsulated c-myc antisense oligonucleotide." Antisense Nucleic Acid Drug Dev **9**(5): 451-8.

Pyle, A. M. (1996). "Role of metal ions in ribozymes." Met Ions Biol Syst **32**: 479-520.

Quiambao, A. B., N. S. Peachey, N. J. Mangini, P. Rohlich, J. G. Hollyfield and M. R. al-Ubaidi (1997). "A 221-bp fragment of the mouse opsin promoter directs expression specifically to the rod photoreceptors of transgenic mice." Vis Neurosci **14**(4): 617-25.

Rabinowitz, J. E., F. Rolling, C. Li, H. Conrath, W. Xiao, X. Xiao and R. J. Samulski (2002). "Cross-packaging of a single adeno-associated virus (AAV) type 2 vector genome into multiple AAV serotypes enables transduction with broad specificity." J Virol **76**(2): 791-801.

Rami, A. (2003). "Ischemic neuronal death in the rat hippocampus: the calpain-calpastatin-caspase hypothesis." Neurobiol Dis **13**(2): 75-88.

Rao, R. V., E. Hermel, S. Castro-Obregon, G. del Rio, L. M. Ellerby, H. M. Ellerby and D. E. Bredesen (2001). "Coupling endoplasmic reticulum stress to the cell death program. Mechanism of caspase activation." J Biol Chem **276**(36): 33869-74.

Raper, S. E., M. Yudkoff, N. Chirmule, G. P. Gao, F. Nunes, Z. J. Haskal, E. E. Furth, K. J. Propert, M. B. Robinson, S. Magosin, H. Simoes, L. Speicher, J. Hughes, J. Tazelaar, N. A. Wivel, J. M. Wilson and M. L. Batshaw (2002). "A pilot study of in vivo liver-directed gene transfer with an adenoviral vector in partial ornithine transcarbamylase deficiency." Hum Gene Ther **13**(1): 163-75.

Rattner, A., H. Sun and J. Nathans (1999). "Molecular genetics of human retinal disease." Annu Rev Genet **33**: 89-131.

Rebello, G., R. Ramesar, A. Vorster, L. Roberts, L. Ehrenreich, E. Oppon, D. Gama, S. Bardien, J. Greenberg, G. Bonapace, A. Waheed, G. N. Shah and W. S. Sly (2004). "Apoptosis-inducing signal sequence mutation in carbonic anhydrase IV identified in patients with the RP17 form of retinitis pigmentosa." Proc Natl Acad Sci U S A **101**(17): 6617-22.

Reed, P. W. and H. A. Lardy (1972). "A23187: a divalent cation ionophore." J Biol Chem **247**(21): 6970-7.

Reid, T. W., D. M. Albert, A. S. Rabson, P. Russell, J. Craft, E. W. Chu, T. S. Tralka and J. L. Wilcox (1974). "Characteristics of an established cell line of retinoblastoma." J Natl Cancer Inst **53**(2): 347-60.

Reme, C. E., C. Grimm, F. Hafezi, A. Marti and A. Wenzel (1998). "Apoptotic cell death in retinal degenerations." Prog Retin Eye Res **17**(4): 443-64.

Robbins, P. D. and S. C. Ghivizzani (1998). "Viral vectors for gene therapy." Pharmacol Ther **80**(1): 35-47.

Robertson, J. D., V. Gogvadze, B. Zhivotovsky and S. Orrenius (2000). "Distinct pathways for stimulation of cytochrome c release by etoposide." J Biol Chem **275**(42): 32438-43.

Roemer, K. (1999). "Mutant p53: gain-of-function oncoproteins and wild-type p53 inactivators." Biol Chem **380**(7-8): 879-87.

Rohr, U. P., F. Heyd, J. Neukirchen, M. A. Wulf, I. Queitsch, G. Kroener-Lux, U. Steidl, R. Fenk, R. Haas and R. Kronenwett (2005). "Quantitative real-time PCR for titration of infectious recombinant AAV-2 particles." J Virol Methods **127**(1): 40-5.

Rohr, U. P., M. A. Wulf, S. Stahn, U. Steidl, R. Haas and R. Kronenwett (2002). "Fast and reliable titration of recombinant adeno-associated virus type-2 using quantitative real-time PCR." J Virol Methods **106**(1): 81-8.

Rolling, F. (2004). "Recombinant AAV-mediated gene transfer to the retina: gene therapy perspectives." Gene Ther **11 Suppl 1**: S26-32.

Roque, R. S., A. A. Rosales, L. Jingjing, N. Agarwal and M. R. Al-Ubaidi (1999). "Retina-derived microglial cells induce photoreceptor cell death in vitro." Brain Res **836**(1-2): 110-9.

Roth, J. A., *et al.* (1996). "Retrovirus-mediated wild-type p53 gene transfer to tumors of patients with lung cancer." Nat Med **2**(9): 985-91.

Roy, N., Q. L. Deveraux, R. Takahashi, G. S. Salvesen and J. C. Reed (1997). "The c-IAP-1 and c-IAP-2 proteins are direct inhibitors of specific caspases." Embo J **16**(23): 6914-25.

Ruffner, D. E., G. D. Stormo and O. C. Uhlenbeck (1990). "Sequence requirements of the hammerhead RNA self-cleavage reaction." Biochemistry **29**(47): 10695-702.

Rutkowski, D. T. and R. J. Kaufman (2004). "A trip to the ER: coping with stress." Trends Cell Biol **14**(1): 20-8.

Saido, T. C., H. Sorimachi and K. Suzuki (1994). "Calpain: new perspectives in molecular diversity and physiological-pathological involvement." Faseb J **8**(11): 814-22.

Salvesen, G. S. and C. S. Duckett (2002). "IAP proteins: blocking the road to death's door." Nat Rev Mol Cell Biol **3**(6): 401-10.

Sandberg, J. A., V. P. Parker, K. S. Blanchard, D. Sweedler, J. A. Powell, A. Kachensky, L. Bellon, N. Usman, T. Rossing, E. Borden and L. M. Blatt (2000). "Pharmacokinetics and tolerability of an antiangiogenic ribozyme (ANGIOZYME) in healthy volunteers." J Clin Pharmacol **40**(12 Pt 2): 1462-9.

Sandig, V., K. Brand, S. Herwig, J. Lukas, J. Bartek and M. Strauss (1997). "Adenovirally transferred p16INK4/CDKN2 and p53 genes cooperate to induce apoptotic tumor cell death." Nat Med **3**(3): 313-9.

Santoro, S. W. and G. F. Joyce (1997). "A general purpose RNA-cleaving DNA enzyme." Proc Natl Acad Sci U S A **94**(9): 4262-6.

Sanvicens, N., V. Gomez-Vicente, I. Masip, A. Messeguer and T. G. Cotter (2004). "Oxidative stress-induced apoptosis in retinal photoreceptor cells is mediated by calpains and caspases and blocked by the oxygen radical scavenger CR-6." J Biol Chem **279**(38): 39268-78.

Sarra, G. M., C. Stephens, M. de Alwis, J. W. Bainbridge, A. J. Smith, A. J. Thrasher and R. R. Ali (2001). "Gene replacement therapy in the retinal degeneration slow (rds) mouse: the effect on retinal degeneration following partial transduction of the retina." Hum Mol Genet **10**(21): 2353-61.

Sattler, R. and M. Tymianski (2000). "Molecular mechanisms of calcium-dependent excitotoxicity." J Mol Med **78**(1): 3-13.

Sauerwald, T. M., M. J. Betenbaugh and G. A. Oyler (2002). "Inhibiting apoptosis in mammalian cell culture using the caspase inhibitor XIAP and deletion mutants." Biotechnol Bioeng **77**(6): 704-16.

Scacheri, P. C., O. Rozenblatt-Rosen, N. J. Caplen, T. G. Wolfsberg, L. Umayam, J. C. Lee, C. M. Hughes, K. S. Shanmugam, A. Bhattacharjee, M. Meyerson and F. S. Collins (2004). "Short interfering RNAs can induce unexpected and divergent changes in the levels of untargeted proteins in mammalian cells." Proc Natl Acad Sci U S A **101**(7): 1892-7.

Scanlon, K. J. (2004). "Anti-genes: siRNA, ribozymes and antisense." Curr Pharm Biotechnol **5**(5): 415-20.

Schlichtenbrede, F. C., A. J. Smith, J. W. Bainbridge, A. J. Thrasher, T. E. Salt and R. R. Ali (2004). "Improvement of neuronal visual responses in the superior colliculus in Prph2(Rd2/Rd2) mice following gene therapy." Mol Cell Neurosci **25**(1): 103-10.

Schlichtenbrede, F. C., A. MacNeil, J. W. Bainbridge, M. Tschernutter, A. J. Thrasher, A. J. Smith and R. R. Ali (2003). "Intraocular gene delivery of ciliary neurotrophic factor results in significant loss of retinal function in normal mice and in the Prph2Rd2/Rd2 model of retinal degeneration." Gene Ther **10**(6): 523-7.

Schmidt, E. E., D. S. Taylor, J. R. Prigge, S. Barnett and M. R. Capecchi (2000). "Illegitimate Cre-dependent chromosome rearrangements in transgenic mouse spermatids." Proc Natl Acad Sci U S A **97**(25): 13702-7.

Schubert, S. and J. Kurreck (2004). "Ribozyme- and deoxyribozyme-strategies for medical applications." Curr Drug Targets **5**(8): 667-81.

Scott, F. L., J. B. Denault, S. J. Riedl, H. Shin, M. Renatus and G. S. Salvesen (2005). "XIAP inhibits caspase-3 and -7 using two binding sites: evolutionarily conserved mechanism of IAPs." Embo J **24**(3): 645-55.

Seigel, G. M. (1999). "The golden age of retinal cell culture." Mol Vis **5**: 4.

Selsek, O. a. B., J (2004). Delivery Agents for Oligonucleotides. Ribozymes and siRNA Protocols. M. Sioud. Totowa, New Jersey, Humana Press.

Selzer, E., H. Schlagbauer-Wadl, I. Okamoto, H. Pehamberger, R. Potter and B. Jansen (1998). "Expression of Bcl-2 family members in human melanocytes, in melanoma metastases and in melanoma cell lines." Melanoma Res **8**(3): 197-203.

Shao, M. X., T. Nakanaga and J. A. Nadel (2004). "Cigarette smoke induces MUC5AC mucin overproduction via tumor necrosis factor-alpha-converting enzyme in human airway epithelial (NCI-H292) cells." Am J Physiol Lung Cell Mol Physiol **287**(2): L420-7.

Sharma, A. K. and B. Rohrer (2004). "Calcium-induced calpain mediates apoptosis via caspase-3 in a mouse photoreceptor cell line." J Biol Chem **279**(34): 35564-72.

Sharp, J. G., M. R. Bishop, B. Copple, T. C. Greiner, P. L. Iversen, J. D. Jackson, S. S. Joshi, E. J. Benner, S. L. Mann, A. K. Rao and J. M. Vose (2001). "Oligonucleotide enhanced cytotoxicity of Idarubicin for lymphoma cells." Leuk Lymphoma **42**(3): 417-27.

Shaw, L. C., A. Skold, F. Wong, R. Petters, W. W. Hauswirth and A. S. Lewin (2001). "An allele-specific hammerhead ribozyme gene therapy for a porcine model of autosomal dominant retinitis pigmentosa." Mol Vis **7**: 6-13.

Shen, C., A. K. Buck, X. Liu, M. Winkler and S. N. Reske (2003). "Gene silencing by adenovirus-delivered siRNA." FEBS Lett **539**(1-3): 111-4.

Shi, N., Y. Zhang, C. Zhu, R. J. Boado and W. M. Pardridge (2001). "Brain-specific expression of an exogenous gene after i.v. administration." Proc Natl Acad Sci U S A **98**(22): 12754-9.

Shi, Y. (2002). "Mechanisms of caspase activation and inhibition during apoptosis." Mol Cell **9**(3): 459-70.

Shibata, M., S. Hisahara, H. Hara, T. Yamawaki, Y. Fukuuchi, J. Yuan, H. Okano and M. Miura (2000). "Caspases determine the vulnerability of oligodendrocytes in the ischemic brain." J Clin Invest **106**(5): 643-53.

Shimayama, T., S. Nishikawa and K. Taira (1995). "Generality of the NUX rule: kinetic analysis of the results of systematic mutations in the trinucleotide at the cleavage site of hammerhead ribozymes." Biochemistry **34**(11): 3649-54.

Shimshek, D. R., J. Kim, M. R. Hubner, D. J. Spergel, F. Buchholz, E. Casanova, A. F. Stewart, P. H. Seeburg and R. Sprengel (2002). "Codon-improved Cre recombinase (iCre) expression in the mouse." Genesis **32**(1): 19-26.

Shin, K. S., B. A. Sullenger and S. W. Lee (2004). "Ribozyme-mediated induction of apoptosis in human cancer cells by targeted repair of mutant p53 RNA." Mol Ther **10**(2): 365-72.

Shinoura, N. and H. Hamada (2003). "Gene therapy using an adenovirus vector for apoptosis-related genes is a highly effective therapeutic modality for killing glioma cells." Curr Gene Ther **3**(2): 147-53.

Shiota, M., M. Sano, M. Miyagishi and K. Taira (2004). "Ribozymes: applications to functional analysis and gene discovery." J Biochem (Tokyo) **136**(2): 133-47.

Sigal, A. and V. Rotter (2000). "Oncogenic mutations of the p53 tumor suppressor: the demons of the guardian of the genome." Cancer Res **60**(24): 6788-93.

Silke, J., C. J. Hawkins, P. G. Ekert, J. Chew, C. L. Day, M. Pakusch, A. M. Verhagen and D. L. Vaux (2002). "The anti-apoptotic activity of XIAP is retained upon mutation of both the caspase 3- and caspase 9-interacting sites." J Cell Biol **157**(1): 115-24.

Silke, J., P. G. Ekert, C. L. Day, C. J. Hawkins, M. Baca, J. Chew, M. Pakusch, A. M. Verhagen and D. L. Vaux (2001). "Direct inhibition of caspase 3 is dispensable for the anti-apoptotic activity of XIAP." Embo J **20**(12): 3114-23.

Sionov, R. V. and Y. Haupt (1999). "The cellular response to p53: the decision between life and death." Oncogene **18**(45): 6145-57.

Sledz, C. A., M. Holko, M. J. de Veer, R. H. Silverman and B. R. Williams (2003). "Activation of the interferon system by short-interfering RNAs." Nat Cell Biol **5**(9): 834-9.

Slevin, M. L. (1991). "The clinical pharmacology of etoposide." Cancer **67**(1 Suppl): 319-29.

Slos, P., M. De Meyer, P. Leroy, C. Rousseau and B. Acres (2001). "Immunotherapy of established tumors in mice by intratumoral injection of an adenovirus vector harboring the human IL-2 cDNA: induction of CD8(+) T-cell immunity and NK activity." Cancer Gene Ther **8**(5): 321-32.

Smeyne, R. J., M. Vendrell, M. Hayward, S. J. Baker, G. G. Miao, K. Schilling, L. M. Robertson, T. Curran and J. I. Morgan (1993). "Continuous c-fos expression precedes programmed cell death in vivo." Nature **363**(6425): 166-9.

Smith, A. J., F. C. Schlichtenbrede, M. Tschernutter, J. W. Bainbridge, A. J. Thrasher and R. R. Ali (2003). "AAV-Mediated gene transfer slows photoreceptor loss in the RCS rat model of retinitis pigmentosa." Mol Ther **8**(2): 188-95.

Soda, Y., K. Tani, Y. Bai, M. Saiki, M. Chen, K. Izawa, S. Kobayashi, S. Takahashi, K. Uchimaru, T. Kuwabara, M. Warashina, T. Tanabe, H. Miyoshi, K. Sugita, S. Nakazawa, A. Tojo, K. Taira and S. Asano (2004). "A novel maxizyme vector targeting a bcr-abl fusion gene induced specific cell death in Philadelphia chromosome-positive acute lymphoblastic leukemia." Blood **104**(2): 356-63.

Soderpalm, A. K., D. A. Fox, J. O. Karlsson and T. van Veen (2000). "Retinoic acid produces rod photoreceptor selective apoptosis in developing mammalian retina." Invest Ophthalmol Vis Sci **41**(3): 937-47.

Sohocki, M. M., L. S. Sullivan, D. L. Tirpak and S. P. Daiger (2001). "Comparative analysis of aryl-hydrocarbon receptor interacting protein-like 1 (Aipl1), a gene associated with inherited retinal disease in humans." Mamm Genome **12**(7): 566-8.

Song, E., S. K. Lee, J. Wang, N. Ince, N. Ouyang, J. Min, J. Chen, P. Shankar and J. Lieberman (2003). "RNA interference targeting Fas protects mice from fulminant hepatitis." Nat Med **9**(3): 347-51.

Soussi, T. and C. Beroud (2001). "Assessing TP53 status in human tumours to evaluate clinical outcome." Nat Rev Cancer **1**(3): 233-40.

Soussi, T., S. Kato, P. P. Levy and C. Ishioka (2005). "Reassessment of the TP53 mutation database in human disease by data mining with a library of TP53 missense mutations." Hum Mutat **25**(1): 6-17.

Sproat, B. S., P. Rider and B. Beijer (1986). "Highly efficient oligodeoxyribonucleotide synthesis using fully base protected phosphodiester building blocks carrying 2-(1-methylimidazol-2-yl) phenyl protection of the phosphate." Nucleic Acids Res **14**(4): 1811-24.

St George, J. A. (2003). "Gene therapy progress and prospects: adenoviral vectors." Gene Ther **10**(14): 1135-41.

Sternberg, N. and D. Hamilton (1981). "Bacteriophage P1 site-specific recombination. I. Recombination between loxP sites." J Mol Biol **150**(4): 467-86.

Sun, L. Q., D. Warrilow, L. Wang, C. Witherington, J. Macpherson and G. Symonds (1994). "Ribozyme-mediated suppression of Moloney murine leukemia virus and human immunodeficiency virus type I replication in permissive cell lines." Proc Natl Acad Sci U S A **91**(21): 9715-9.

Sun, L. Q., J. Pyati, J. Smythe, L. Wang, J. Macpherson, W. Gerlach and G. Symonds (1995). "Resistance to human immunodeficiency virus type 1 infection conferred by transduction of human peripheral blood lymphocytes with ribozyme, antisense, or polymeric trans-activation response element constructs." Proc Natl Acad Sci U S A **92**(16): 7272-6.

Sung, C. H., B. G. Schneider, N. Agarwal, D. S. Papermaster and J. Nathans (1991). "Functional heterogeneity of mutant rhodopsins responsible for autosomal dominant retinitis pigmentosa." Proc Natl Acad Sci U S A **88**(19): 8840-4.

Sung, C. H., C. Makino, D. Baylor and J. Nathans (1994). "A rhodopsin gene mutation responsible for autosomal dominant retinitis pigmentosa results in a protein that is defective in localization to the photoreceptor outer segment." J Neurosci **14**(10): 5818-33.

Surace, E. M. and A. Auricchio (2003). "Adeno-associated viral vectors for retinal gene transfer." Prog Retin Eye Res **22**(6): 705-19.

Swisher, S. G., J. A. Roth, J. Nemunaitis, D. D. Lawrence, B. L. Kemp, C. H. Carrasco, D. G. Connors, A. K. El-Naggar, F. Fossella, B. S. Glisson, W. K. Hong, F. R. Khuri, J. M. Kurie, J. J. Lee, J. S. Lee, M. Mack, J. A. Merritt, D. M. Nguyen, J. C. Nesbitt, R. Perez-Soler, K. M. Pisters, J. B. Putnam, Jr., W. R. Richli, M. Savin, D. S. Schrump, D. M. Shin, A. Shulkin, G. L. Walsh, J. Wait, D. Weill and M. K. Waugh (1999). "Adenovirus-mediated p53 gene transfer in advanced non-small-cell lung cancer." J Natl Cancer Inst **91**(9): 763-71.

Swisher, S. G., J. A. Roth, R. Komaki, J. Gu, J. J. Lee, M. Hicks, J. Y. Ro, W. K. Hong, J. A. Merritt, K. Ahrar, N. E. Atkinson, A. M. Correa, M. Dolormente, L. Dreiling, A. K. El-Naggar, F. Fossella, R. Francisco, B. Glisson, S. Grammer, R. Herbst, A. Huaringa, B. Kemp, F. R. Khuri, J. M. Kurie, Z. Liao, T. J. McDonnell, R. Morice, F. Morello, R. Munden, V. Papadimitrakopoulou, K. M. Pisters, J. B. Putnam, Jr., A. J. Sarabia, T. Shelton, C. Stevens, D. M. Shin, W. R. Smythe, A. A. Vaporciyan, G. L. Walsh and M. Yin (2003). "Induction of p53-regulated genes and tumor regression in lung cancer patients after intratumoral delivery of adenoviral p53 (INGN 201) and radiation therapy." Clin Cancer Res **9**(1): 93-101.

Symons, R. H. (1992). "Small catalytic RNAs." Annu Rev Biochem **61**: 641-71.

Takahashi, M., H. Miyoshi, I. M. Verma and F. H. Gage (1999). "Rescue from photoreceptor degeneration in the rd mouse by human immunodeficiency virus vector-mediated gene transfer." J Virol **73**(9): 7812-6.

Takeuchi, N., H. Ito, K. Namiki and A. Kamei (2001). "Effect of calpain on hereditary cataractous rat, ICR/f." Biol Pharm Bull **24**(11): 1246-51.

Takramah, D., B. M. Seiffert, S. Schaller, M. Vigneron and G. Hacker (2003). "Baculovirus P35 interacts with a subunit of human RNA polymerase II and can enhance promoter activity in human cells." J Gen Virol **84**(Pt 11): 3011-9.

Tamura, M., M. Nakamura, Y. Ogawa, Y. Toyama, M. Miura and H. Okano (2005). "Targeted expression of anti-apoptotic protein p35 in oligodendrocytes reduces delayed demyelination and functional impairment after spinal cord injury." Glia.

Tan, E., X. Q. Ding, A. Saadi, N. Agarwal, M. I. Naash and M. R. Al-Ubaidi (2004). "Expression of cone-photoreceptor-specific antigens in a cell line derived from retinal tumors in transgenic mice." Invest Ophthalmol Vis Sci **45**(3): 764-8.

Tanabe, T., T. Kuwabara, M. Warashina, K. Tani, K. Taira and S. Asano (2000). "Oncogene inactivation in a mouse model." Nature **406**(6795): 473-4.

Tanaka, Y., S. Igarashi, M. Nakamura, J. Gafni, C. Torcassi, G. Schilling, D. Crippen, J. D. Wood, A. Sawa, N. A. Jenkins, N. G. Copeland, D. R. Borchelt, C. A. Ross and L. M. Ellerby (2005). "Progressive phenotype and nuclear accumulation of an amino-terminal cleavage fragment in a transgenic mouse model with inducible expression of full-length mutant huntingtin." Neurobiol Dis.

Tao, W., R. Wen, M. B. Goddard, S. D. Sherman, P. J. O'Rourke, P. F. Stabila, W. J. Bell, B. J. Dean, K. A. Kauper, V. A. Budz, W. G. Tsiaras, G. M. Acland, S. Pearce-Kelling, A. M. Laties and G. D. Aguirre (2002). "Encapsulated cell-based delivery of CNTF reduces photoreceptor degeneration in animal models of retinitis pigmentosa." Invest Ophthalmol Vis Sci **43**(10): 3292-8.

Tekur, S. and S. M. Ho (2002). "Ribozyme-mediated downregulation of human metallothionein II(a) induces apoptosis in human prostate and ovarian cancer cell lines." Mol Carcinog **33**(1): 44-55.

Thomas, K. R. and M. R. Capecchi (1987). "Site-directed mutagenesis by gene targeting in mouse embryo-derived stem cells." Cell **51**(3): 503-12.

Thornberry, N. A. and Y. Lazebnik (1998). "Caspases: enemies within." Science **281**(5381): 1312-6.

Thornborrow, E. C., S. Patel, A. E. Mastropietro, E. M. Schwartzfarb and J. J. Manfredi (2002). "A conserved intronic response element mediates direct p53-dependent transcriptional activation of both the human and murine bax genes." Oncogene **21**(7): 990-9.

Tomioka, M., K. Shirotani, N. Iwata, H. J. Lee, F. Yang, G. M. Cole, Y. Seyama and T. C. Saido (2002). "In vivo role of caspases in excitotoxic neuronal death: generation and analysis of transgenic mice expressing baculoviral caspase inhibitor, p35, in postnatal neurons." Brain Res Mol Brain Res **108**(1-2): 18-32.

Trapp, T., L. Korhonen, M. Besselmann, R. Martinez, E. A. Mercer and D. Lindholm (2003). "Transgenic mice overexpressing XIAP in neurons show better outcome after transient cerebral ischemia." Mol Cell Neurosci **23**(2): 302-13.

Tsang, W. P., F. Y. Ho, K. P. Fung, S. K. Kong and T. T. Kwok (2005). "p53-R175H mutant gains new function in regulation of doxorubicin-induced apoptosis." Int J Cancer **114**(3): 331-6.

Tschernutter, M., F. C. Schlichtenbrede, S. Howe, K. S. Balaggan, P. M. Munro, J. W. Bainbridge, A. J. Thrasher, A. J. Smith and R. R. Ali (2005). "Long-term preservation of retinal function in the RCS rat model of retinitis pigmentosa following lentivirus-mediated gene therapy." Gene Ther **12**(8): 694-701.

Tuohy, G. (2001). Therapeutic Approaches To Halting Photoreceptor Cell Death In The Retina. Department of Genetics. Dublin, Trinity College Dublin**:** 215.

Tuohy, G., S. Millington-Ward, P. F. Kenna, P. Humphries and G. J. Farrar (2002). "Sensitivity of photoreceptor-derived cell line (661W) to baculoviral p35, Z-VAD.FMK, and Fas-associated death domain." Invest Ophthalmol Vis Sci **43**(11): 3583-9.

Turturro, F., H. L. Heineke, T. F. Drevyanko, C. J. Link, Jr. and P. Seth (2000). "Adenovirus-p53-mediated gene therapy of anaplastic large cell lymphoma with t(2;5) in a nude mouse model." Gene Ther **7**(11): 930-3.

Tweddle, D. A., A. J. Malcolm, N. Bown, A. D. Pearson and J. Lunec (2001). "Evidence for the development of p53 mutations after cytotoxic therapy in a neuroblastoma cell line." Cancer Res **61**(1): 8-13.

Uhlenbeck, O. C. (1987). "A small catalytic oligoribonucleotide." Nature **328**(6131): 596-600.

Uhlenbeck, O. C., A. Pardi and J. Feigon (1997). "RNA structure comes of age." Cell **90**(5): 833-40.

Urban-Klein, B., S. Werth, S. Abuharbeid, F. Czubayko and A. Aigner (2005). "RNAi-mediated gene-targeting through systemic application of polyethylenimine (PEI)-complexed siRNA in vivo." Gene Ther **12**(5): 461-6.

Usman, N. and L. M. Blatt (2000). "Nuclease-resistant synthetic ribozymes: developing a new class of therapeutics." J Clin Invest **106**(10): 1197-202.

Vallazza-Deschamps, G., D. Cia, J. Gong, A. Jellali, A. Duboc, V. Forster, J. A. Sahel, L. H. Tessier and S. Picaud (2005). "Excessive activation of cyclic nucleotide-gated channels contributes to neuronal degeneration of photoreceptors." Eur J Neurosci **22**(5): 1013-22.

van der Weyden, L., D. J. Adams and A. Bradley (2002). "Tools for targeted manipulation of the mouse genome." Physiol Genomics **11**(3): 133-64.

van Oijen, M. G. and P. J. Slootweg (2000). "Gain-of-function mutations in the tumor suppressor gene p53." Clin Cancer Res **6**(6): 2138-45.

Vaux, D. L. and R. A. Flavell (2000). "Apoptosis genes and autoimmunity." Curr Opin Immunol **12**(6): 719-24.

Verma, I. M. and M. D. Weitzman (2005). "Gene therapy: twenty-first century medicine." Annu Rev Biochem **74**: 711-38.

Viswanath, V., Z. Wu, C. Fonck, Q. Wei, R. Boonplueang and J. K. Andersen (2000). "Transgenic mice neuronally expressing baculoviral p35 are resistant to diverse types of induced apoptosis, including seizure-associated neurodegeneration." Proc Natl Acad Sci U S A **97**(5): 2270-5.

Vithana, E. N., L. Abu-Safieh, M. J. Allen, A. Carey, M. Papaioannou, C. Chakarova, M. Al-Maghtheh, N. D. Ebenezer, C. Willis, A. T. Moore, A. C. Bird, D. M. Hunt and S. S. Bhattacharya (2001). "A human homolog of yeast pre-mRNA splicing gene, PRP31, underlies autosomal dominant retinitis pigmentosa on chromosome 19q13.4 (RP11)." Mol Cell **8**(2): 375-81.

Voet, J. G., Voet, D. (1990). Rate of Enzymatic Reactions. Biochemistry. J. Stiefel, Wiley, New York, NY, USA.

Vogelstein, B., D. Lane and A. J. Levine (2000). "Surfing the p53 network." Nature **408**(6810): 307-10.

Vollrath, D., W. Feng, J. L. Duncan, D. Yasumura, P. M. D'Cruz, A. Chappelow, M. T. Matthes, M. A. Kay and M. M. LaVail (2001). "Correction of the retinal dystrophy phenotype of the RCS rat by viral gene transfer of Mertk." Proc Natl Acad Sci U S A **98**(22): 12584-9.

Volpers, C. and S. Kochanek (2004). "Adenoviral vectors for gene transfer and therapy." J Gene Med **6 Suppl 1**: S164-71.

Vousden, K. H. and X. Lu (2002). "Live or let die: the cell's response to p53." Nat Rev Cancer **2**(8): 594-604.

Wagner, T. E., P. C. Hoppe, J. D. Jollick, D. R. Scholl, R. L. Hodinka and J. B. Gault (1981). "Microinjection of a rabbit beta-globin gene into zygotes and its subsequent expression in adult mice and their offspring." Proc Natl Acad Sci U S A **78**(10): 6376-80.

Walter, A. E., D. H. Turner, J. Kim, M. H. Lyttle, P. Muller, D. H. Mathews and M. Zuker (1994). "Coaxial stacking of helixes enhances binding of oligoribonucleotides and improves predictions of RNA folding." Proc Natl Acad Sci U S A **91**(20): 9218-22.

Walz, C., J. R. Schlehofer, M. Flentje, V. Rudat and H. zur Hausen (1992). "Adeno-associated virus sensitizes HeLa cell tumors to gamma rays." J Virol **66**(9): 5651-7.

Wang, C. H., L. J. Tsai, Y. P. Tsao, J. T. Hsieh, W. W. Chien, C. L. Liao, H. W. Wang, H. S. Liu and S. L. Chen (2002). "Recombinant adenovirus encoding H-ras ribozyme induces apoptosis in laryngeal cancer cells through caspase- and mitochondria-dependent pathways." Biochem Biophys Res Commun **298**(5): 805-14.

Wang, C. Y., H. Y. Guo, T. M. Lim, Y. K. Ng, H. P. Neo, P. Y. Hwang, W. C. Yee and S. Wang (2005). "Improved neuronal transgene expression from an AAV-2 vector with a hybrid CMV enhancer/PDGF-beta promoter." J Gene Med **7**(7): 945-55.

Wang, H., L. Nan, D. Yu, S. Agrawal and R. Zhang (2001). "Antisense anti-MDM2 oligonucleotides as a novel therapeutic approach to human breast cancer: in vitro and in vivo activities and mechanisms." Clin Cancer Res **7**(11): 3613-24.

Wang, L., C. Witherington, A. King, W. L. Gerlach, A. Carr, R. Penny, D. Cooper, G. Symonds and L. Q. Sun (1998). "Preclinical characterization of an anti-tat ribozyme for therapeutic application." Hum Gene Ther **9**(9): 1283-91.

Watanabe, T. and B. A. Sullenger (2000). "Induction of wild-type p53 activity in human cancer cells by ribozymes that repair mutant p53 transcripts." Proc Natl Acad Sci U S A **97**(15): 8490-4.

Weleber, R. G., and Gregory-Evans, K. (2001). Retinitis pigmentosa and allied disorders. Retina. S. J. Ryan. St. Louis, MO, Mosby: 362-470.

Weng, D. E. and N. Usman (2001). "Angiozyme: a novel angiogenesis inhibitor." Curr Oncol Rep **3**(2): 141-6.

Wenzel, A., C. E. Reme, T. P. Williams, F. Hafezi and C. Grimm (2001). "The Rpe65 Leu450Met variation increases retinal resistance against light-induced degeneration by slowing rhodopsin regeneration." J Neurosci **21**(1): 53-8.

Wesselborg, S., I. H. Engels, E. Rossmann, M. Los and K. Schulze-Osthoff (1999). "Anticancer drugs induce caspase-8/FLICE activation and apoptosis in the absence of CD95 receptor/ligand interaction." Blood **93**(9): 3053-63.

Willis, A., *et al.* (2004). "Mutant p53 exerts a dominant negative effect by preventing wild-type p53 from binding to the promoter of its target genes." Oncogene **23**(13): 2330-8.

Wilson, J. A., S. Jayasena, A. Khvorova, S. Sabatinos, I. G. Rodrigue-Gervais, S. Arya, F. Sarangi, M. Harris-Brandts, S. Beaulieu and C. D. Richardson (2003). "RNA interference blocks gene expression and RNA synthesis from hepatitis C replicons propagated in human liver cells." Proc Natl Acad Sci U S A **100**(5): 2783-8.

Wolf, J. K., D. C. Bodurka, J. B. Gano, M. Deavers, L. Ramondetta, P. T. Ramirez, C. Levenback and D. M. Gershenson (2004). "A phase I study of Adp53 (INGN 201; ADVEXIN) for patients with platinum- and paclitaxel-resistant epithelial ovarian cancer." Gynecol Oncol **94**(2): 442-8.

Woodford, B. J., J. Chen and M. I. Simon (1994). "Expression of rhodopsin promoter transgene product in both rods and cones." Exp Eye Res **58**(5): 631-5.

Wootz, H., I. Hansson, L. Korhonen and D. Lindholm (2006). "XIAP decreases caspase-12 cleavage and calpain activity in spinal cord of ALS transgenic mice." Exp Cell Res.

Wu, X., Y. Li, B. Crise and S. M. Burgess (2003). "Transcription start regions in the human genome are favored targets for MLV integration." Science **300**(5626): 1749-51.

Xiao, X., J. Li and R. J. Samulski (1998). "Production of high-titer recombinant adeno-associated virus vectors in the absence of helper adenovirus." J Virol **72**(3): 2224-32.

Xu, D., Y. Bureau, D. C. McIntyre, D. W. Nicholson, P. Liston, Y. Zhu, W. G. Fong, S. J. Crocker, R. G. Korneluk and G. S. Robertson (1999). "Attenuation of ischemia-induced cellular and behavioral deficits by X chromosome-linked inhibitor of apoptosis protein overexpression in the rat hippocampus." J Neurosci **19**(12): 5026-33.

Xue, D. and H. R. Horvitz (1995). "Inhibition of the Caenorhabditis elegans cell-death protease CED-3 by a CED-3 cleavage site in baculovirus p35 protein." Nature **377**(6546): 248-51.

Yamamoto, S., K. C. Sippel, E. L. Berson and T. P. Dryja (1997). "Defects in the rhodopsin kinase gene in the Oguchi form of stationary night blindness." Nat Genet **15**(2): 175-8.

Yamanaka, K., P. Rocchi, H. Miyake, L. Fazli, B. Vessella, U. Zangemeister-Wittke and M. E. Gleave (2005). "A novel antisense oligonucleotide inhibiting several antiapoptotic Bcl-2 family members induces apoptosis and enhances chemosensitivity in androgen-independent human prostate cancer PC3 cells." Mol Cancer Ther **4**(11): 1689-98.

Yan, N. and Y. Shi (2005). "Mechanisms of apoptosis through structural biology." Annu Rev Cell Dev Biol **21**: 35-56.

Yang, G. S., M. Schmidt, Z. Yan, J. D. Lindbloom, T. C. Harding, B. A. Donahue, J. F. Engelhardt, R. Kotin and B. L. Davidson (2002). "Virus-mediated transduction of murine retina with adeno-associated virus: effects of viral capsid and genome size." J Virol **76**(15): 7651-60.

Ying, S., H. T. Jansen, M. N. Lehman, S. L. Fong and W. W. Kao (2000). "Retinal degeneration in cone photoreceptor cell-ablated transgenic mice." Mol Vis **6**: 101-8.

Ying, S., S. L. Fong, W. B. Fong, C. W. Kao, R. L. Converse and W. W. Kao (1998). "A CAT reporter construct containing 277bp GNAT2 promoter and 214bp IRBP enhancer is specifically expressed by cone photoreceptor cells in transgenic mice." Curr Eye Res **17**(8): 777-82.

Yoshizawa, K., J. Yang, H. Senzaki, Y. Uemura, Y. Kiyozuka, N. Shikata, Y. Oishi, H. Miki and A. Tsubura (2000). "Caspase-3 inhibitor rescues N -methyl- N -nitrosourea-induced retinal degeneration in Sprague-Dawley rats." Exp Eye Res **71**(6): 629-35.

Yoshizawa, K., K. Kiuchi, H. Nambu, J. Yang, H. Senzaki, Y. Kiyozuka, N. Shikata and A. Tsubura (2002). "Caspase-3 inhibitor transiently delays inherited retinal degeneration in C3H mice carrying the rd gene." Graefes Arch Clin Exp Ophthalmol **240**(3): 214-9.

Yu, D. Y. and S. J. Cringle (2001). "Oxygen distribution and consumption within the retina in vascularised and avascular retinas and in animal models of retinal disease." Prog Retin Eye Res **20**(2): 175-208.

Yuge, K., H. Nambu, H. Senzaki, I. Nakao, H. Miki, M. Uyama and A. Tsubura (1996). "N-methyl-N-nitrosourea-induced photoreceptor apoptosis in the mouse retina." In Vivo **10**(5): 483-8.

Zack, D. J., J. Bennett, Y. Wang, C. Davenport, B. Klaunberg, J. Gearhart and J. Nathans (1991). "Unusual topography of bovine rhodopsin promoter-lacZ fusion gene expression in transgenic mouse retinas." Neuron **6**(2): 187-99.

Zaffaroni, N., M. Pennati and M. G. Daidone (2005). "Survivin as a target for new anticancer interventions." J Cell Mol Med **9**(2): 360-72.

Zamecnik, P. C. and M. L. Stephenson (1978). "Inhibition of Rous sarcoma virus replication and cell transformation by a specific oligodeoxynucleotide." Proc Natl Acad Sci U S A **75**(1): 280-4.

Zangemeister-Wittke, U., S. H. Leech, R. A. Olie, A. P. Simoes-Wust, O. Gautschi, G. H. Luedke, F. Natt, R. Haner, P. Martin, J. Hall, C. M. Nalin and R. A. Stahel (2000). "A novel bispecific antisense oligonucleotide inhibiting both bcl-2 and bcl-xL expression efficiently induces apoptosis in tumor cells." Clin Cancer Res **6**(6): 2547-55.

Zeiss, C. J., J. Neal and E. A. Johnson (2004). "Caspase-3 in postnatal retinal development and degeneration." Invest Ophthalmol Vis Sci **45**(3): 964-70.

Zhang, Y. A., J. Nemunaitis and A. W. Tong (2000). "Generation of a ribozyme-adenoviral vector against K-ras mutant human lung cancer cells." Mol Biotechnol **15**(1): 39-49.

Zhang, Y., F. Schlachetzki, J. Y. Li, R. J. Boado and W. M. Pardridge (2003). "Organ-specific gene expression in the rhesus monkey eye following intravenous non-viral gene transfer." Mol Vis **9**: 465-72.

Zhang, Y., Y. F. Zhang, J. Bryant, A. Charles, R. J. Boado and W. M. Pardridge (2004a). "Intravenous RNA interference gene therapy targeting the human epidermal growth factor receptor prolongs survival in intracranial brain cancer." Clin Cancer Res **10**(11): 3667-77.

Zhang, Z., H. Wang, G. Prasad, M. Li, D. Yu, J. A. Bonner, S. Agrawal and R. Zhang (2004b). "Radiosensitization by antisense anti-MDM2 mixed-backbone oligonucleotide in in vitro and in vivo human cancer models." Clin Cancer Res **10**(4): 1263-73.

Zhao, L. J., H. Jian and H. Zhu (2003a). "Specific gene inhibition by adenovirus-mediated expression of small interfering RNA." Gene **316**: 137-41.

Zhao, R., K. Gish, M. Murphy, Y. Yin, D. Notterman, W. H. Hoffman, E. Tom, D. H. Mack and A. J. Levine (2000). "Analysis of p53-regulated gene expression patterns using oligonucleotide arrays." Genes Dev **14**(8): 981-93.

Zhao, Y., D. H. Hong, B. Pawlyk, G. Yue, M. Adamian, M. Grynberg, A. Godzik and T. Li (2003b). "The retinitis pigmentosa GTPase regulator (RPGR)- interacting protein: subserving RPGR function and participating in disk morphogenesis." Proc Natl Acad Sci U S A **100**(7): 3965-70.

Zhou, Q., J. F. Krebs, S. J. Snipas, A. Price, E. S. Alnemri, K. J. Tomaselli and G. S. Salvesen (1998). "Interaction of the baculovirus anti-apoptotic protein p35 with caspases. Specificity, kinetics, and characterization of the caspase/p35 complex." Biochemistry **37**(30): 10757-65.

Zolotukhin, S., B. J. Byrne, E. Mason, I. Zolotukhin, M. Potter, K. Chesnut, C. Summerford, R. J. Samulski and N. Muzyczka (1999). "Recombinant adeno-associated virus purification using novel methods improves infectious titer and yield." Gene Ther **6**(6): 973-85.

Zolotukhin, S., B. J. Byrne, E. Mason, I. Zolotukhin, M. Potter, K. Chesnut, C. Summerford, R. J. Samulski and N. Muzyczka (1999). "Recombinant adeno-associated virus purification using novel methods improves infectious titer and yield." Gene Ther **6**(6): 973-85.

Zoumadakis, M. and M. Tabler (1995). "Comparative analysis of cleavage rates after systematic permutation of the NUX consensus target motif for hammerhead ribozymes." Nucleic Acids Res **23**(7): 1192-6.

Zuker, M. (1989). "On finding all suboptimal foldings of an RNA molecule." Science **244**(4900): 48-52.

Zuker, M. (2003). "Mfold web server for nucleic acid folding and hybridization prediction." Nucleic Acids Res **31**(13): 3406-15.

Appendix

A1.1 Primer sequences

A1.1.1 Primers for generation of photoreceptor-specific Cre recombinase constructs

Primers for amplification of hGH and Chi introns from pAAV-LacZ and pALTER-Max are shown below with restriction sites for *Xho*I underlined:

hGHF: 5' CCGCTCGAG ACCGGTTCGAACAGGTAAG 3'

hGHR: 5' CCGCTCGAGCTTCGAACCTGGGGAGAAAC 3'

ChiF: 5' CCGCTCGAGGGCAGGTAAGTATCAAGGTTA 3'

ChiR: 5' CCGCTCGAGGACACCTGTGGAGAGAAAGG 3'

Primers for amplification of GNAT2 promoter (with *Xba*I sites) and IRBP enhancer (with *Hind*III sites) from pCAT.GNAT2 are shown below with restriction sites underlined:

GNAT2 F: 5' CTAGTCTAGAGCTTGCATCCTATCCTTC 3'

GNAT2 R: 5' CTAGTCTAGATAGCGGATTGAGTATCCC 3'

IRBP F: 5' CCCAAGCTTATCCGGCCCAGGCTTCCCAGC 3'

IRBP R: 5' CCCAAGCTTATCCGGCCAAAGAGGTCAATTAG 3'

Primers for the generation of the poly A signal based on mrβGpolA, synthesised with *Kpn*I sites:

F5' CGGGGTACCAATAAAGGAAATTTATTTTCATTGCAATAGTGTGTTGGTTT TTTGTGTGGGTACCCCG 3'

R 5' CGGGGTACCCACACAAAAAACCAACACACTATTGCAATGAAAATAAAT TTCCTTTATTGGTACCCCG 3'

A1.1.2 Primers for sequencing pCAT.GNAT2

FpCAT: 5'ATGCTTCCGGCTCGTATGTTG 3'

RpCAT: 5' CAACGGTGGTATATCCAG 3

RpCAT2 5' GTGCTGCAAGGCGATTAAG 3"

A1.1.3 Primers for sequencing photoreceptor-specific Cre recombinase constructs

FGNAT2: 5' TGCTCTCTCACCTGCCATCG 3'

FRho1: 5' CCCCTCTGCAAGCCAATTA 3'

FRho2 5' AAGCAGCCTTGGTCTC 3'

FiCre: 5' ACCAATGTGAACATAGTGATG 3'

RiCre: 5' ACAGTCAGCAGGTTGGAGAC 3'

RIRBP: 5' TTGCATATCCTTAGCCCTGC 3'

RpcDNA: 5' CCAGGGTCAAGGAAGGCACG 3'

A1.1.4 Primers for bacterial PCR analysis of positive transformants with pCMVβ.Neo

FNeo 5' ACTTCGTATAATGTATGC 3'

Rβ-gal 5' TACAGCAAATGAAACTGGTTG 3'

A1.2 Sequences of photoreceptor-specific constructs expressing iCre recombinase

A1.2.1 Sequence of pRho.iCre.hGH.A

```
   1 GACGGATCGG GAGATCTCCC GATCCCCTAT GGTGCACTCT
  41 CAGTACAATC TGCTCTGATG CCGCATAGTT AAGCCAGTAT
  81 CTGCTCCCTG CTTGTGTGTT GGAGGTCGCT GAGTAGTGCG
 121 CGAGCAAAAT TTAAGCTACA ACAAGGCAAG GCTTGACCGA
 161 CAATTGCATG AAGAATCTGC TTAGGGTTAG GCGTTTTGCG
 201 CTGCTTCGCT AGCTGGGGAT GGGGGCAGGG TAGATCTGGG
 241 GCTGACCACC AGGGTCAGAA TCAGAACCTC CATCTTGACC
 281 TCATTAACGC TGGTCTTAAT CACCAAGCCA AGCTCCTTAA
 321 ACTGCTAGTG GCCAACTCCC AGGCCCTGAC ACACATACCT
 361 GCCCTGTGTT CCCAAACAAG ACACCTGCAT GGAAGGAAGG
 401 GGGTTGCTTT TCTAAGCAAA CATCTAGGAA TCCCGGGTGC
 441 AGTGTGAGGA GACTAGGCGA GGGAGTACTT TAAGGGCCTC
 481 CAAGGCTCAG AGAGGAATAC TTCTTCCCTG GTTAGCCTCG
 521 TGCCTAGGTC CAGGGTCTTT GTCCGTCCTG GATACCTATG
 561 TGGCAAGGGG CATAGCATTT ACCCCACCAT CAGCTCTTAG
 601 CTCAACCTTA TCTTCTGGGA AAGGCTGCGA GTGTAAACGC
 641 ACAGCAGAGA CTTTTCTTTT GTCCCTGTCT ACCCCTGTAA
 681 CTGCTACTCA GAAGCATCTT TCTCACAGGG CACTGGCTTC
 721 TTGCATCCAG TGTTTTTTTG TCTCCCTCGG CCCCCAGAAT
 761 AAATTCTTCT TCTGGGACTC AGTGGATGTT TCACACACGT
 801 ATCGGCCTGA CAGTCATCCT GGAGCATCTA CACAGGGGCC
 841 ATCACAGCTG CATGTCAGAG ATGCTGGCCT CACATCCTCA
 881 GACACCAGGC CTAGTGCTGG TCTTCCTCAG ACTGGCATCC
 921 CCAGCAGGCC AGTAGGATCA TCTTTTAGCC TACAGAGTTC
 961 TGAAGCCTCA GAGCCCCAGG TCCCTGGTCA TCTTCTCTGC
1001 CCCTGAGATT TACCAAGTTG TATGCCTTCT AGGTAAGGCA
1041 AAACTTCTTA CGCCCCTCCT GCTGGCCTCC AGGCCACACT
1081 GCTCACCTGA ATAACCTGGC AGCCTGCTCC CTCATGCAGG
1121 GACCACGTCT GCTGCACCCA GCAGCCATCC CGTCTCCATA
1161 GCCCATGGTA TCCCTCCCTG GACAGGAATG TGTCTCCTCC
1201 CTGGCTGAGT CTTGCTCAAG CTAGAAGCAC TCCGAACAGG
1241 GTTATGGGGC CGCTCTCATC TCCCAAGTGG CTGGCTTATG
1281 AATGTTTAAT GTACATGTGA GTGAACAAAT TCCAATTGAA
1321 CGCAACAAAT AGTTATCGAG CCGCTGAGCC GGGGGGTGGG
1361 GGGGTGTGAG ACTGGAGGCG ATGGACGGAG CTGACGGCAC
1401 ACACAGCTCA GATCTGTCAA GTGAGCCATT GTCAGGGCTT
1441 GGGGACTGGA TAAGTCAGGG GGTCTCCTGG GAAGAGATGG
1481 GATAGGTGAG TTCAGGAGGA GACATTGTCA ACTGGAGCCA
1521 TTGTGGAGAA GTGAATTTAG GGCCCAAGGG TTCCAGTCGC
1561 AGCCTGAGGC CACCAGACTG ACATGGGGAG GAATTCCCAG
1601 AGGACTCTGG GGCAGACAAG ATGAGACACC CTTTCCTTTC
1641 TTTACCTAAG GGCCTCCACC CGATGTCACC TTGGCCCCTC
1681 TGCAAGCCAA TTAGGCCCCG GTGGCAGCAG TGGGATTAGC
1721 GTTAGTATGA TATCTCGCGG ATGCTGAATC AGCCTCTGGC
```

1761 TTAGGGAGAG AAGGTCACTT TATAAGGGTC TGGGGGGGGT
1801 CAGTGCCTGG AGTTGCGCTG TGGGAGCCGT CAGTGGCTGA
1841 GCTCGCCAAG CAGCCTTGGT CTCTGTCTAC GAAGAGCCCG
1881 TGGGGCAGCT CGAGACCGGT TCGAACAGGT AAGCGCCCCT
1921 AAAATCCCTT TGGGCACAAT GTGTCCTGAG GGGAGAGGCA
1961 GCGACCTGTA GATGGGACGG GGGCACTAAC CCTCAGGTTT
2001 GGGGCTTCTG AATGTGAGTA TCGCCATGTA AGCCCAGTAT
2041 TTGGCCAATC TCAGAAAGCT CCTGGTCCCT GGAGGGATGG
2081 AGAGAGAAAA ACAAACAGCT CCTGGAGCAG GGAGAGTGCT
2121 GGCCTCTTGC TCTCCGGCTC CCTCTGTTGC CCTCTGGTTT
2161 CTCCCCAGGT TCGAAGCTCG AGCGGCCGCC ACTGTGCTGG
2201 ATATCTGCAG AATTCCACCA CACTGGACTA GTGGATCCCC
2241 CGGGCTGCAG GAATTCGATA TCAAGCTTGT CCACCATGGT
2281 GCCCAAGAAG AAGAGGAAAG TCTCCAACCT GCTGACTGTG
2321 CACCAAAACC TGCCTGCCCT CCCTGTGGAT GCCACCTCTG
2361 ATGAAGTCAG GAAGAACCTG ATGGACATGT TCAGGGACAG
2401 GCAGGCCTTC TCTGAACACA CCTGGAAGAT GCTCCTGTCT
2441 GTGTGCAGAT CCTGGGCTGC CTGGTGCAAG CTGAACAACA
2481 GGAAATGGTT CCCTGCTGAA CCTGAGGATG TGAGGGACTA
2521 CCTCCTGTAC CTGCAAGCCA GAGGCCTGGC TGTGAAGACC
2561 ATCCAACAGC ACCTGGGCCA GCTCAACATG CTGCACAGGA
2601 GATCTGGCCT GCCTCGCCCT TCTGACTCCA ATGCTGTGTC
2641 CCTGGTGATG AGGAGAATCA GAAAGGAGAA TGTGGATGCT
2681 GGGGAGAGAG CCAAGCAGGC CCTGGCCTTT GAACGCACTG
2721 ACTTTGACCA AGTCAGATCC CTGATGGAGA ACTCTGACAG
2761 ATGCCAGGAC ATCAGGAACC TGGCCTTCCT GGGCATTGCC
2801 TACAACACCC TGCTGCGCAT TGCCGAAATT GCCAGAATCA
2841 GAGTGAAGGA CATCTCCCGC ACCGATGGTG GGAGAATGCT
2881 GATCCACATT GGCAGGACCA AGACCCTGGT GTCCACAGCT
2921 GGTGTGGAGA AGGCCCTGTC CCTGGGGGTT ACCAAGCTGG
2961 TGGAGAGATG GATCTCTGTG TCTGGTGTGG CTGATGACCC
3001 CAACAACTAC CTGTTCTGCC GGGTCAGAAA GAATGGTGTG
3041 GCTGCCCCTT CTGCCACCTC CCAACTGTCC ACCCGGGCCC
3081 TGGAAGGGAT CTTTGAGGCC ACCCACCGCC TGATCTATGG
3121 TGCCAAGGAT GACTCTGGGC AGAGATACCT GGCCTGGTCT
3161 GGCCACTCTG CCAGAGTGGG TGCTGCCAGG GACATGGCCA
3201 GGGCTGGTGT GTCCATCCCT GAAATCATGC AGGCTGGTGG
3241 CTGGACCAAT GTGAACATAG TGATGAACTA CATCAGAAAC
3281 CTGGACTCTG AGACTGGGGC CATGGTGAGG CTGCTCGAGG
3321 ATGGGGACTG AAACTGAGTC GAGGGGGGGC CCGGTACCAA
3361 TAAAGGAAAT TTATTTTCAT TGCAATAGTG TGTTGGTTTT
3401 TTGTGTGGGT ACCAAGCTTA AGTTTAAACC GCTGATCAGC
3441 CTCGACTGTG CCTTCTAGTT GCCAGCCATC TGTTGTTTGC
3481 CCCTCCCCCG TGCCTTCCTT GACCCTGGAA GGTGCCACTC
3521 CCACTGTCCT TTCCTAATAA AATGAGGAAA TTGCATCGCA
3561 TTGTCTGAGT AGGTGTCATT CTATTCTGGG GGGTGGGGTG
3601 GGGCAGGACA GCAAGGGGGA GGATTGGGAA GACAATAGCA

3641 GGCATGCTGG GGATGCGGTG GGCTCTATGG CTTCTGAGGC
3681 GGAAAGAACC AGCTGGGGCT CTAGGGGGTA TCCCCACGCG
3721 CCCTGTAGCG GCGCATTAAG CGCGGCGGGT GTGGTGGTTA
3761 CGCGCAGCGT GACCGCTACA CTTGCCAGCG CCCTAGCGCC
3801 CGCTCCTTTC GCTTTCTTCC CTTCCTTTCT CGCCACGTTC
3841 GCCGGCTTTC CCCGTCAAGC TCTAAATCGG GGGCTCCCTT
3881 TAGGGTTCCG ATTTAGTGCT TTACGGCACC TCGACCCCAA
3921 AAAACTTGAT TAGGGTGATG GTTCACGTAG TGGGCCATCG
3961 CCCTGATAGA CGGTTTTTCG CCCTTTGACG TTGGAGTCCA
4001 CGTTCTTTAA TAGTGGACTC TTGTTCCAAA CTGGAACAAC
4041 ACTCAACCCT ATCTCGGTCT ATTCTTTTGA TTTATAAGGG
4081 ATTTTGCCGA TTTCGGCCTA TTGGTTAAAA AATGAGCTGA
4121 TTTAACAAAA ATTTAACGCG AATTAATTCT GTGGAATGTG
4161 TGTCAGTTAG GGTGTGGAAA GTCCCCAGGC TCCCCAGCAG
4201 GCAGAAGTAT GCAAAGCATG CATCTCAATT AGTCAGCAAC
4241 CAGGTGTGGA AAGTCCCCAG GCTCCCCAGC AGGCAGAAGT
4281 ATGCAAAGCA TGCATCTCAA TTAGTCAGCA ACCATAGTCC
4321 CGCCCCTAAC TCCGCCCATC CCGCCCCTAA CTCCGCCCAG
4361 TTCCGCCCAT TCTCCGCCCC ATGGCTGACT AATTTTTTTT
4401 ATTTATGCAG AGGCCGAGGC CGCCTCTGCC TCTGAGCTAT
4441 TCCAGAAGTA GTGAGGAGGC TTTTTTGGAG GCCTAGGCTT
4481 TTGCAAAAAG CTCCCGGGAG CTTGTATATC CATTTTCGGA
4521 TCTGATCAAG AGACAGGATG AGGATCGTTT CGCATGATTG
4561 AACAAGATGG ATTGCACGCA GGTTCTCCGG CCGCTTGGGT
4601 GGAGAGGCTA TTCGGCTATG ACTGGGCACA ACAGACAATC
4641 GGCTGCTCTG ATGCCGCCGT GTTCCGGCTG TCAGCGCAGG
4681 GGCGCCCGGT TCTTTTTGTC AAGACCGACC TGTCCGGTGC
4721 CCTGAATGAA CTGCAGGACG AGGCAGCGCG GCTATCGTGG
4761 CTGGCCACGA CGGGCGTTCC TTGCGCAGCT GTGCTCGACG
4801 TTGTCACTGA AGCGGGAAGG GACTGGCTGC TATTGGGCGA
4841 AGTGCCGGGG CAGGATCTCC TGTCATCTCA CCTTGCTCCT
4881 GCCGAGAAAG TATCCATCAT GGCTGATGCA ATGCGGCGGC
4921 TGCATACGCT TGATCCGGCT ACCTGCCCAT TCGACCACCA
4961 AGCGAAACAT CGCATCGAGC GAGCACGTAC TCGGATGGAA
5001 GCCGGTCTTG TCGATCAGGA TGATCTGGAC GAAGAGCATC
5041 AGGGGCTCGC GCCAGCCGAA CTGTTCGCCA GGCTCAAGGC
5081 GCGCATGCCC GACGGCGAGG ATCTCGTCGT GACCCATGGC
5121 GATGCCTGCT TGCCGAATAT CATGGTGGAA AATGGCCGCT
5161 TTTCTGGATT CATCGACTGT GGCCGGCTGG GTGTGGCGGA
5201 CCGCTATCAG GACATAGCGT TGGCTACCCG TGATATTGCT
5241 GAAGAGCTTG GCGGCGAATG GGCTGACCGC TTCCTCGTGC
5281 TTTACGGTAT CGCCGCTCCC GATTCGCAGC GCATCGCCTT
5321 CTATCGCCTT CTTGACGAGT TCTTCTGAGC GGGACTCTGG
5361 GGTTCGAAAT GACCGACCAA GCGACGCCCA ACCTGCCATC
5401 ACGAGATTTC GATTCCACCG CCGCCTTCTA TGAAAGGTTG
5441 GGCTTCGGAA TCGTTTTCCG GGACGCCGGC TGGATGATCC
5481 TCCAGCGCGG GGATCTCATG CTGGAGTTCT TCGCCCACCC

5521 CAACTTGTTT ATTGCAGCTT ATAATGGTTA CAAATAAAGC
5561 AATAGCATCA CAAATTTCAC AAATAAAGCA TTTTTTTCAC
5601 TGCATTCTAG TTGTGGTTTG TCCAAACTCA TCAATGTATC
5641 TTATCATGTC TGTATACCGT CGACCTCTAG CTAGAGCTTG
5681 GCGTAATCAT GGTCATAGCT GTTTCCTGTG TGAAATTGTT
5721 ATCCGCTCAC AATTCCACAC AACATACGAG CCGGAAGCAT
5761 AAAGTGTAAA GCCTGGGGTG CCTAATGAGT GAGCTAACTC
5801 ACATTAATTG CGTTGCGCTC ACTGCCCGCT TTCCAGTCGG
5841 GAAACCTGTC GTGCCAGCTG CATTAATGAA TCGGCCAACG
5881 CGCGGGGAGA GGCGGTTTGC GTATTGGGCG CTCTTCCGCT
5921 TCCTCGCTCA CTGACTCGCT GCGCTCGGTC GTTCGGCTGC
5961 GGCGAGCGGT ATCAGCTCAC TCAAAGGCGG TAATACGGTT
6001 ATCCACAGAA TCAGGGGATA ACGCAGGAAA GAACATGTGA
6041 GCAAAAGGCC AGCAAAAGGC CAGGAACCGT AAAAAGGCCG
6081 CGTTGCTGGC GTTTTTCCAT AGGCTCCGCC CCCCTGACGA
6121 GCATCACAAA AATCGACGCT CAAGTCAGAG GTGGCGAAAC
6161 CCGACAGGAC TATAAAGATA CCAGGCGTTT CCCCCTGGAA
6201 GCTCCCTCGT GCGCTCTCCT GTTCCGACCC TGCCGCTTAC
6241 CGGATACCTG TCCGCCTTTC TCCCTTCGGG AAGCGTGGCG
6281 CTTTCTCATA GCTCACGCTG TAGGTATCTC AGTTCGGTGT
6321 AGGTCGTTCG CTCCAAGCTG GGCTGTGTGC ACGAACCCCC
6361 CGTTCAGCCC GACCGCTGCG CCTTATCCGG TAACTATCGT
6401 CTTGAGTCCA ACCCGGTAAG ACACGACTTA TCGCCACTGG
6441 CAGCAGCCAC TGGTAACAGG ATTAGCAGAG CGAGGTATGT
6481 AGGCGGTGCT ACAGAGTTCT TGAAGTGGTG GCCTAACTAC
6521 GGCTACACTA GAAGAACAGT ATTTGGTATC TGCGCTCTGC
6561 TGAAGCCAGT TACCTTCGGA AAAAGAGTTG GTAGCTCTTG
6601 ATCCGGCAAA CAAACCACCG CTGGTAGCGG TTTTTTTGTT
6641 TGCAAGCAGC AGATTACGCG CAGAAAAAAA GGATCTCAAG
6681 AAGATCCTTT GATCTTTTCT ACGGGGTCTG ACGCTCAGTG
6721 GAACGAAAAC TCACGTTAAG GGATTTTGGT CATGAGATTA
6761 TCAAAAAGGA TCTTCACCTA GATCCTTTTA AATTAAAAAT
6801 GAAGTTTTAA ATCAATCTAA AGTATATATG AGTAAACTTG
6841 GTCTGACAGT TACCAATGCT TAATCAGTGA GGCACCTATC
6881 TCAGCGATCT GTCTATTTCG TTCATCCATA GTTGCCTGAC
6921 TCCCCGTCGT GTAGATAACT ACGATACGGG AGGGCTTACC
6961 ATCTGGCCCC AGTGCTGCAA TGATACCGCG AGACCCACGC
7001 TCACCGGCTC CAGATTTATC AGCAATAAAC CAGCCAGCCG
7041 GAAGGGCCGA GCGCAGAAGT GGTCCTGCAA CTTTATCCGC
7081 CTCCATCCAG TCTATTAATT GTTGCCGGGA AGCTAGAGTA
7121 AGTAGTTCGC CAGTTAATAG TTTGCGCAAC GTTGTTGCCA
7161 TTGCTACAGG CATCGTGGTG TCACGCTCGT CGTTTGGTAT
7201 GGCTTCATTC AGCTCCGGTT CCCAACGATC AAGGCGAGTT
7241 ACATGATCCC CCATGTTGTG CAAAAAAGCG GTTAGCTCCT
7281 TCGGTCCTCC GATCGTTGTC AGAAGTAAGT TGGCCGCAGT
7321 GTTATCACTC ATGGTTATGG CAGCACTGCA TAATTCTCTT
7361 ACTGTCATGC CATCCGTAAG ATGCTTTTCT GTGACTGGTG

```
7401 AGTACTCAAC CAAGTCATTC TGAGAATAGT GTATGCGGCG
7441 ACCGAGTTGC TCTTGCCCGG CGTCAATACG GGATAATACC
7481 GCGCCACATA GCAGAACTTT AAAAGTGCTC ATCATTGGAA
7521 AACGTTCTTC GGGGCGAAAA CTCTCAAGGA TCTTACCGCT
7561 GTTGAGATCC AGTTCGATGT AACCCACTCG TGCACCCAAC
7601 TGATCTTCAG CATCTTTTAC TTTCACCAGC GTTTCTGGGT
7641 GAGCAAAAAC AGGAAGGCAA AATGCCGCAA AAAAGGGAAT
7681 AAGGGCGACA CGGAAATGTT GAATACTCAT ACTCTTCCTT
7721 TTTCAATATT ATTGAAGCAT TTATCAGGGT TATTGTCTCA
7761 TGAGCGGATA CATATTTGAA TGTATTTAGA AAAATAAACA
7801 AATAGGGGTT CCGCGCACAT TTCCCCGAAA AGTGCCACCT
7841 GACGTC
```

A1.2.2 Sequence of pRho.iCre.Chi.B

```
   1 GACGGATCGG GAGATCTCCC GATCCCCTAT GGTGCACTCT
  41 CAGTACAATC TGCTCTGATG CCGCATAGTT AAGCCAGTAT
  81 CTGCTCCCTG CTTGTGTGTT GGAGGTCGCT GAGTAGTGCG
 121 CGAGCAAAAT TTAAGCTACA ACAAGGCAAG GCTTGACCGA
 161 CAATTGCATG AAGAATCTGC TTAGGGTTAG GCGTTTTGCG
 201 CTGCTTCGCT AGCTGGGGAT GGGGGCAGGG TAGATCTGGG
 241 GCTGACCACC AGGGTCAGAA TCAGAACCTC CATCTTGACC
 281 TCATTAACGC TGGTCTTAAT CACCAAGCCA AGCTCCTTAA
 321 ACTGCTAGTG GCCAACTCCC AGGCCCTGAC ACACATACCT
 361 GCCCTGTGTT CCCAAACAAG ACACCTGCAT GGAAGGAAGG
 401 GGGTTGCTTT TCTAAGCAAA CATCTAGGAA TCCCGGGTGC
 441 AGTGTGAGGA GACTAGGCGA GGGAGTACTT TAAGGGCCTC
 481 CAAGGCTCAG AGAGGAATAC TTCTTCCCTG GTTAGCCTCG
 521 TGCCTAGGTC CAGGGTCTTT GTCCGTCCTG GATACCTATG
 561 TGGCAAGGGG CATAGCATTT ACCCCACCAT CAGCTCTTAG
 601 CTCAACCTTA TCTTCTGGGA AAGGCTGCGA GTGTAAACGC
 641 ACAGCAGAGA CTTTTCTTTT GTCCCTGTCT ACCCCTGTAA
 681 CTGCTACTCA GAAGCATCTT TCTCACAGGG CACTGGCTTC
 721 TTGCATCCAG TGTTTTTTTG TCTCCCTCGG CCCCCAGAAT
 761 AAATTCTTCT TCTGGGACTC AGTGGATGTT TCACACACGT
 801 ATCGGCCTGA CAGTCATCCT GGAGCATCTA CACAGGGGCC
 841 ATCACAGCTG CATGTCAGAG ATGCTGGCCT CACATCCTCA
 881 GACACCAGGC CTAGTGCTGG TCTTCCTCAG ACTGGCATCC
 921 CCAGCAGGCC AGTAGGATCA TCTTTTAGCC TACAGAGTTC
 961 TGAAGCCTCA GAGCCCCAGG TCCCTGGTCA TCTTCTCTGC
1001 CCCTGAGATT TACCAAGTTG TATGCCTTCT AGGTAAGGCA
1041 AAACTTCTTA CGCCCCTCCT GCTGGCCTCC AGGCCACACT
1081 GCTCACCTGA ATAACCTGGC AGCCTGCTCC CTCATGCAGG
1121 GACCACGTCT GCTGCACCCA GCAGCCATCC CGTCTCCATA
1161 GCCCATGGTA TCCCTCCCTG GACAGGAATG TGTCTCCTCC
1201 CTGGCTGAGT CTTGCTCAAG CTAGAAGCAC TCCGAACAGG
1241 GTTATGGGGC CGCTCTCATC TCCCAAGTGG CTGGCTTATG
1281 AATGTTTAAT GTACATGTGA GTGAACAAAT TCCAATTGAA
1321 CGCAACAAAT AGTTATCGAG CCGCTGAGCC GGGGGGTGGG
1361 GGGGTGTGAG ACTGGAGGCG ATGGACGGAG CTGACGGCAC
1401 ACACAGCTCA GATCTGTCAA GTGAGCCATT GTCAGGGCTT
1441 GGGGACTGGA TAAGTCAGGG GGTCTCCTGG GAAGAGATGG
1481 GATAGGTGAG TTCAGGAGGA GACATTGTCA ACTGGAGCCA
1521 TTGTGGAGAA GTGAATTTAG GGCCCAAGGG TTCCAGTCGC
1561 AGCCTGAGGC CACCAGACTG ACATGGGGAG GAATTCCCAG
1601 AGGACTCTGG GGCAGACAAG ATGAGACACC CTTTCCTTTC
1641 TTTACCTAAG GGCCTCCACC CGATGTCACC TTGGCCCCTC
1681 TGCAAGCCAA TTAGGCCCCG GTGGCAGCAG TGGGATTAGC
1721 GTTAGTATGA TATCTCGCGG ATGCTGAATC AGCCTCTGGC
1761 TTAGGGAGAG AAGGTCACTT TATAAGGGTC TGGGGGGGGT
```

1801 CAGTGCCTGG AGTTGCGCTG TGGGAGCCGT CAGTGGCTGA
1841 GCTCGCCAAG CAGCCTTGGT CTCTGTCTAC GAAGAGCCCG
1881 TGGGGCAGCT CGAGGGCAGG TAAGTATCAA GGTTACAAGA
1921 CAGGTTTAAG GAGACCAATA GAAACTGGGC TTGTCGAGAC
1961 AGAGAAGACT CTTGCGTTTC TGATAGGCAC CTATTGGTCT
2001 TACTGACATC CACTTTGCCT TTCTCTCCAC AGGTGTCCTC
2041 GAGCGGCCGC CACTGTGCTG GATATCTGCA GAATTCCACC
2081 ACACTGGACT AGTGGATCCC CCGGGCTGCA GGAATTCGAT
2121 ATCAAGCTTG TCCACCATGG TGCCCAAGAA GAAGAGGAAA
2161 GTCTCCAACC TGCTGACTGT GCACCAAAAC CTGCCTGCCC
2201 TCCCTGTGGA TGCCACCTCT GATGAAGTCA GGAAGAACCT
2241 GATGGACATG TTCAGGGACA GGCAGGCCTT CTCTGAACAC
2281 ACCTGGAAGA TGCTCCTGTC TGTGTGCAGA TCCTGGGCTG
2321 CCTGGTGCAA GCTGAACAAC AGGAAATGGT TCCCTGCTGA
2361 ACCTGAGGAT GTGAGGGACT ACCTCCTGTA CCTGCAAGCC
2401 AGAGGCCTGG CTGTGAAGAC CATCCAACAG CACCTGGGCC
2441 AGCTCAACAT GCTGCACAGG AGATCTGGCC TGCCTCGCCC
2481 TTCTGACTCC AATGCTGTGT CCCTGGTGAT GAGGAGAATC
2521 AGAAAGGAGA ATGTGGATGC TGGGGAGAGA GCCAAGCAGG
2561 CCCTGGCCTT TGAACGCACT GACTTTGACC AAGTCAGATC
2601 CCTGATGGAG AACTCTGACA GATGCCAGGA CATCAGGAAC
2641 CTGGCCTTCC TGGGCATTGC CTACAACACC CTGCTGCGCA
2681 TTGCCGAAAT TGCCAGAATC AGAGTGAAGG ACATCTCCCG
2721 CACCGATGGT GGGAGAATGC TGATCCACAT TGGCAGGACC
2761 AAGACCCTGG TGTCCACAGC TGGTGTGGAG AAGGCCCTGT
2801 CCCTGGGGGT TACCAAGCTG GTGGAGAGAT GGATCTCTGT
2841 GTCTGGTGTG GCTGATGACC CCAACAACTA CCTGTTCTGC
2881 CGGGTCAGAA AGAATGGTGT GGCTGCCCCT TCTGCCACCT
2921 CCCAACTGTC CACCCGGGCC CTGGAAGGGA TCTTTGAGGC
2961 CACCCACCGC CTGATCTATG GTGCCAAGGA TGACTCTGGG
3001 CAGAGATACC TGGCCTGGTC TGGCCACTCT GCCAGAGTGG
3041 GTGCTGCCAG GGACATGGCC AGGGCTGGTG TGTCCATCCC
3081 TGAAATCATG CAGGCTGGTG GCTGGACCAA TGTGAACATA
3121 GTGATGAACT ACATCAGAAA CCTGGACTCT GAGACTGGGG
3161 CCATGGTGAG GCTGCTCGAG GATGGGGACT GAAACTGAGT
3201 CGAGGGGGGG CCCGGTACCA ATAAAGGAAA TTTATTTTCA
3241 TTGCAATAGT GTGTTGGTTT TTTGTGTGGG TACCAAGCTT
3281 AAGTTTAAAC CGCTGATCAG CCTCGACTGT GCCTTCTAGT
3321 TGCCAGCCAT CTGTTGTTTG CCCCTCCCCC GTGCCTTCCT
3361 TGACCCTGGA AGGTGCCACT CCCACTGTCC TTTCCTAATA
3401 AAATGAGGAA ATTGCATCGC ATTGTCTGAG TAGGTGTCAT
3441 TCTATTCTGG GGGGTGGGGT GGGGCAGGAC AGCAAGGGGG
3481 AGGATTGGGA AGACAATAGC AGGCATGCTG GGGATGCGGT
3521 GGGCTCTATG GCTTCTGAGG CGGAAAGAAC CAGCTGGGGC
3561 TCTAGGGGGT ATCCCCACGC GCCCTGTAGC GGCGCATTAA
3601 GCGCGGCGGG TGTGGTGGTT ACGCGCAGCG TGACCGCTAC
3641 ACTTGCCAGC GCCCTAGCGC CCGCTCCTTT CGCTTTCTTC

3681 CCTTCCTTTC TCGCCACGTT CGCCGGCTTT CCCCGTCAAG
3721 CTCTAAATCG GGGGCTCCCT TTAGGGTTCC GATTTAGTGC
3761 TTTACGGCAC CTCGACCCCA AAAAACTTGA TTAGGGTGAT
3801 GGTTCACGTA GTGGGCCATC GCCCTGATAG ACGGTTTTTC
3841 GCCCTTTGAC GTTGGAGTCC ACGTTCTTTA ATAGTGGACT
3881 CTTGTTCCAA ACTGGAACAA CACTCAACCC TATCTCGGTC
3921 TATTCTTTTG ATTTATAAGG GATTTTGCCG ATTTCGGCCT
3961 ATTGGTTAAA AAATGAGCTG ATTTAACAAA AATTTAACGC
4001 GAATTAATTC TGTGGAATGT GTGTCAGTTA GGGTGTGGAA
4041 AGTCCCCAGG CTCCCCAGCA GGCAGAAGTA TGCAAAGCAT
4081 GCATCTCAAT TAGTCAGCAA CCAGGTGTGG AAAGTCCCCA
4121 GGCTCCCCAG CAGGCAGAAG TATGCAAAGC ATGCATCTCA
4161 ATTAGTCAGC AACCATAGTC CCGCCCCTAA CTCCGCCCAT
4201 CCCGCCCCTA ACTCCGCCCA GTTCCGCCCA TTCTCCGCCC
4241 CATGGCTGAC TAATTTTTTT TATTTATGCA GAGGCCGAGG
4281 CCGCCTCTGC CTCTGAGCTA TTCCAGAAGT AGTGAGGAGG
4321 CTTTTTTGGA GGCCTAGGCT TTTGCAAAAA GCTCCCGGGA
4361 GCTTGTATAT CCATTTTCGG ATCTGATCAA GAGACAGGAT
4401 GAGGATCGTT TCGCATGATT GAACAAGATG GATTGCACGC
4441 AGGTTCTCCG GCCGCTTGGG TGGAGAGGCT ATTCGGCTAT
4481 GACTGGGCAC AACAGACAAT CGGCTGCTCT GATGCCGCCG
4521 TGTTCCGGCT GTCAGCGCAG GGGCGCCCGG TTCTTTTTGT
4561 CAAGACCGAC CTGTCCGGTG CCCTGAATGA ACTGCAGGAC
4601 GAGGCAGCGC GGCTATCGTG GCTGGCCACG ACGGGCGTTC
4641 CTTGCGCAGC TGTGCTCGAC GTTGTCACTG AAGCGGGAAG
4681 GGACTGGCTG CTATTGGGCG AAGTGCCGGG GCAGGATCTC
4721 CTGTCATCTC ACCTTGCTCC TGCCGAGAAA GTATCCATCA
4761 TGGCTGATGC AATGCGGCGG CTGCATACGC TTGATCCGGC
4801 TACCTGCCCA TTCGACCACC AAGCGAAACA TCGCATCGAG
4841 CGAGCACGTA CTCGGATGGA AGCCGGTCTT GTCGATCAGG
4881 ATGATCTGGA CGAAGAGCAT CAGGGGCTCG CGCCAGCCGA
4921 ACTGTTCGCC AGGCTCAAGG CGCGCATGCC CGACGGCGAG
4961 GATCTCGTCG TGACCCATGG CGATGCCTGC TTGCCGAATA
5001 TCATGGTGGA AAATGGCCGC TTTTCTGGAT TCATCGACTG
5041 TGGCCGGCTG GGTGTGGCGG ACCGCTATCA GGACATAGCG
5081 TTGGCTACCC GTGATATTGC TGAAGAGCTT GGCGGCGAAT
5121 GGGCTGACCG CTTCCTCGTG CTTTACGGTA TCGCCGCTCC
5161 CGATTCGCAG CGCATCGCCT TCTATCGCCT TCTTGACGAG
5201 TTCTTCTGAG CGGGACTCTG GGGTTCGAAA TGACCGACCA
5241 AGCGACGCCC AACCTGCCAT CACGAGATTT CGATTCCACC
5281 GCCGCCTTCT ATGAAAGGTT GGGCTTCGGA ATCGTTTTCC
5321 GGGACGCCGG CTGGATGATC CTCCAGCGCG GGGATCTCAT
5361 GCTGGAGTTC TTCGCCCACC CCAACTTGTT TATTGCAGCT
5401 TATAATGGTT ACAAATAAAG CAATAGCATC ACAAATTTCA
5441 CAAATAAAGC ATTTTTTTCA CTGCATTCTA GTTGTGGTTT
5481 GTCCAAACTC ATCAATGTAT CTTATCATGT CTGTATACCG
5521 TCGACCTCTA GCTAGAGCTT GGCGTAATCA TGGTCATAGC

5561 TGTTTCCTGT GTGAAATTGT TATCCGCTCA CAATTCCACA
5601 CAACATACGA GCCGGAAGCA TAAAGTGTAA AGCCTGGGGT
5641 GCCTAATGAG TGAGCTAACT CACATTAATT GCGTTGCGCT
5681 CACTGCCCGC TTTCCAGTCG GGAAACCTGT CGTGCCAGCT
5721 GCATTAATGA ATCGGCCAAC GCGCGGGGAG AGGCGGTTTG
5761 CGTATTGGGC GCTCTTCCGC TTCCTCGCTC ACTGACTCGC
5801 TGCGCTCGGT CGTTCGGCTG CGGCGAGCGG TATCAGCTCA
5841 CTCAAAGGCG GTAATACGGT TATCCACAGA ATCAGGGGAT
5881 AACGCAGGAA AGAACATGTG AGCAAAAGGC CAGCAAAAGG
5921 CCAGGAACCG TAAAAAGGCC GCGTTGCTGG CGTTTTTCCA
5961 TAGGCTCCGC CCCCCTGACG AGCATCACAA AAATCGACGC
6001 TCAAGTCAGA GGTGGCGAAA CCCGACAGGA CTATAAAGAT
6041 ACCAGGCGTT TCCCCCTGGA AGCTCCCTCG TGCGCTCTCC
6081 TGTTCCGACC CTGCCGCTTA CCGGATACCT GTCCGCCTTT
6121 CTCCCTTCGG GAAGCGTGGC GCTTTCTCAT AGCTCACGCT
6161 GTAGGTATCT CAGTTCGGTG TAGGTCGTTC GCTCCAAGCT
6201 GGGCTGTGTG CACGAACCCC CCGTTCAGCC CGACCGCTGC
6241 GCCTTATCCG GTAACTATCG TCTTGAGTCC AACCCGGTAA
6281 GACACGACTT ATCGCCACTG GCAGCAGCCA CTGGTAACAG
6321 GATTAGCAGA GCGAGGTATG TAGGCGGTGC TACAGAGTTC
6361 TTGAAGTGGT GGCCTAACTA CGGCTACACT AGAAGAACAG
6401 TATTTGGTAT CTGCGCTCTG CTGAAGCCAG TTACCTTCGG
6441 AAAAAGAGTT GGTAGCTCTT GATCCGGCAA ACAAACCACC
6481 GCTGGTAGCG GTTTTTTTGT TTGCAAGCAG CAGATTACGC
6521 GCAGAAAAAA AGGATCTCAA GAAGATCCTT TGATCTTTTC
6561 TACGGGGTCT GACGCTCAGT GGAACGAAAA CTCACGTTAA
6601 GGGATTTTGG TCATGAGATT ATCAAAAAGG ATCTTCACCT
6641 AGATCCTTTT AAATTAAAAA TGAAGTTTTA AATCAATCTA
6681 AAGTATATAT GAGTAAACTT GGTCTGACAG TTACCAATGC
6721 TTAATCAGTG AGGCACCTAT CTCAGCGATC TGTCTATTTC
6761 GTTCATCCAT AGTTGCCTGA CTCCCCGTCG TGTAGATAAC
6801 TACGATACGG GAGGGCTTAC CATCTGGCCC CAGTGCTGCA
6841 ATGATACCGC GAGACCCACG CTCACCGGCT CCAGATTTAT
6881 CAGCAATAAA CCAGCCAGCC GGAAGGGCCG AGCGCAGAAG
6921 TGGTCCTGCA ACTTTATCCG CCTCCATCCA GTCTATTAAT
6961 TGTTGCCGGG AAGCTAGAGT AAGTAGTTCG CCAGTTAATA
7001 GTTTGCGCAA CGTTGTTGCC ATTGCTACAG GCATCGTGGT
7041 GTCACGCTCG TCGTTTGGTA TGGCTTCATT CAGCTCCGGT
7081 TCCCAACGAT CAAGGCGAGT TACATGATCC CCCATGTTGT
7121 GCAAAAAAGC GGTTAGCTCC TTCGGTCCTC CGATCGTTGT
7161 CAGAAGTAAG TTGGCCGCAG TGTTATCACT CATGGTTATG
7201 GCAGCACTGC ATAATTCTCT TACTGTCATG CCATCCGTAA
7241 GATGCTTTTC TGTGACTGGT GAGTACTCAA CCAAGTCATT
7281 CTGAGAATAG TGTATGCGGC GACCGAGTTG CTCTTGCCCG
7321 GCGTCAATAC GGGATAATAC CGCGCCACAT AGCAGAACTT
7361 TAAAAGTGCT CATCATTGGA AAACGTTCTT CGGGGCGAAA
7401 ACTCTCAAGG ATCTTACCGC TGTTGAGATC CAGTTCGATG

```
7441 TAACCCACTC GTGCACCCAA CTGATCTTCA GCATCTTTTA
7481 CTTTCACCAG CGTTTCTGGG TGAGCAAAAA CAGGAAGGCA
7521 AAATGCCGCA AAAAAGGGAA TAAGGGCGAC ACGGAAATGT
7561 TGAATACTCA TACTCTTCCT TTTTCAATAT TATTGAAGCA
7601 TTTATCAGGG TTATTGTCTC ATGAGCGGAT ACATATTTGA
7641 ATGTATTTAG AAAAATAAAC AAATAGGGGT TCCGCGCACA
7681 TTTCCCCGAA AAGTGCCACC TGACGTC
```

A1.2.3 Sequence of pGNAT2.iCre.hGH.A

```
   1 GACGGATCGG GAGATCTCCC GATCCCCTAT GGTGCACTCT
  41 CAGTACAATC TGCTCTGATG CCGCATAGTT AAGCCAGTAT
  81 CTGCTCCCTG CTTGTGTGTT GGAGGTCGCT GAGTAGTGCG
 121 CGAGCAAAAT TTAAGCTACA ACAAGGCAAG GCTTGACCGA
 161 CAATTGCATG AAGAATCTGC TTAGGGTTAG GCGTTTTGCG
 201 CTGCTTCGCT AGCGTTTAAA CGGGCCCTCT AGAGCTTGCA
 241 TCCTATCCTT CCGTCAGAAC CCAGCAGATC ATTTCCCTAG
 281 TTATAGAAAC ATTTGAGTCT TTACCCCTTG CCATATTGAC
 321 AAAGCTCTTA ATTGGCTTGA CCTATCACAT TGCTAGATAT
 361 AAAGGCTACA ATCCCTAGAC TAAGAAGTAG GTCTCCAGTT
 401 GAAGTAGGGA GTCTCAGTCA ATGTAGGCAG AGTACAAGAC
 441 CCTACAGCCT GCTCTCTCAC CTGCCATCGT ACAGACCAGC
 481 TTTTAGGGGA GCCAAGTTGG GATACTCAAT CCGCTATCTA
 521 GACTCGAGAC CGGTTCGAAC AGGTAAGCGC CCCTAAAATC
 561 CCTTTGGGCA CAATGTGTCC TGAGGGGAGA GGCAGCGACC
 601 TGTAGATGGG ACGGGGGCAC TAACCCTCAG GTTTGGGGCT
 641 TCTGAATGTG AGTATCGCCA TGTAAGCCCA GTATTTGGCC
 681 AATCTCAGAA AGCTCCTGGT CCCTGGAGGG ATGGAGAGAG
 721 AAAAACAAAC AGCTCCTGGA GCAGGGAGAG TGCTGGCCTC
 761 TTGCTCTCCG GCTCCCTCTG TTGCCCTCTG GTTTCTCCCC
 801 AGGTTCGAAG CTCGAGCGGC CGCCACTGTG CTGGATATCT
 841 GCAGAATTCC ACCACACTGG ACTAGTGGAT CCCCCGGGCT
 881 GCAGGAATTC GATATCAAGC TTGTCCACCA TGGTGCCCAA
 921 GAAGAAGAGG AAAGTCTCCA ACCTGCTGAC TGTGCACCAA
 961 AACCTGCCTG CCCTCCCTGT GGATGCCACC TCTGATGAAG
1001 TCAGGAAGAA CCTGATGGAC ATGTTCAGGG ACAGGCAGGC
1041 CTTCTCTGAA CACACCTGGA AGATGCTCCT GTCTGTGTGC
1081 AGATCCTGGG CTGCCTGGTG CAAGCTGAAC AACAGGAAAT
1121 GGTTCCCTGC TGAACCTGAG GATGTGAGGG ACTACCTCCT
1161 GTACCTGCAA GCCAGAGGCC TGGCTGTGAA GACCATCCAA
1201 CAGCACCTGG GCCAGCTCAA CATGCTGCAC AGGAGATCTG
1241 GCCTGCCTCG CCCTTCTGAC TCCAATGCTG TGTCCCTGGT
1281 GATGAGGAGA ATCAGAAAGG AGAATGTGGA TGCTGGGGAG
1321 AGAGCCAAGC AGGCCCTGGC CTTTGAACGC ACTGACTTTG
1361 ACCAAGTCAG ATCCCTGATG GAGAACTCTG ACAGATGCCA
1401 GGACATCAGG AACCTGGCCT TCCTGGGCAT TGCCTACAAC
1441 ACCCTGCTGC GCATTGCCGA AATTGCCAGA ATCAGAGTGA
1481 AGGACATCTC CCGCACCGAT GGTGGGAGAA TGCTGATCCA
1521 CATTGGCAGG ACCAAGACCC TGGTGTCCAC AGCTGGTGTG
1561 GAGAAGGCCC TGTCCCTGGG GGTTACCAAG CTGGTGGAGA
1601 GATGGATCTC TGTGTCTGGT GTGGCTGATG ACCCCAACAA
1641 CTACCTGTTC TGCCGGGTCA GAAAGAATGG TGTGGCTGCC
1681 CCTTCTGCCA CCTCCCAACT GTCCACCCGG GCCCTGGAAG
1721 GGATCTTTGA GGCCACCCAC CGCCTGATCT ATGGTGCCAA
1761 GGATGACTCT GGGCAGAGAT ACCTGGCCTG GTCTGGCCAC
```

1801 TCTGCCAGAG TGGGTGCTGC CAGGGACATG GCCAGGGCTG
1841 GTGTGTCCAT CCCTGAAATC ATGCAGGCTG GTGGCTGGAC
1881 CAATGTGAAC ATAGTGATGA ACTACATCAG AAACCTGGAC
1921 TCTGAGACTG GGGCCATGGT GAGGCTGCTC GAGGATGGGG
1961 ACTGAAACTG AGTCGAGGGG GGGCCCGGTA CCAATAAAGG
2001 AAATTTATTT TCATTGCAAT AGTGTGTTGG TTTTTTGTGT
2041 GGGTACCAAG CTTATCCGGC CCAGGCTTCC CAGCAGGGCT
2081 AAGGATATGC AAGGAGTGCA TTCATCCGGA GGTGTTGGCA
2121 GCATCCCAGC CCCACCCCAT TCTCATCGTA AATCAGGCTC
2161 ACTTCCATTG GCTGCATACG GTGGAGTGAT GTGACCATAT
2201 GTCACTTGAG CATTACACAA ATCCTAATGA GCTAAAAATA
2241 TGTTTGTTTT AGCTAATTGA CCTCTTTGGC CGGATAAGCT
2281 TAAGTTTAAA CCGCTGATCA GCCTCGACTG TGCCTTCTAG
2321 TTGCCAGCCA TCTGTTGTTT GCCCCTCCCC CGTGCCTTCC
2361 TTGACCCTGG AAGGTGCCAC TCCCACTGTC CTTTCCTAAT
2401 AAAATGAGGA AATTGCATCG CATTGTCTGA GTAGGTGTCA
2441 TTCTATTCTG GGGGGTGGGG TGGGGCAGGA CAGCAAGGGG
2481 GAGGATTGGG AAGACAATAG CAGGCATGCT GGGGATGCGG
2521 TGGGCTCTAT GGCTTCTGAG GCGGAAAGAA CCAGCTGGGG
2561 CTCTAGGGGG TATCCCCACG CGCCCTGTAG CGGCGCATTA
2601 AGCGCGGCGG GTGTGGTGGT TACGCGCAGC GTGACCGCTA
2641 CACTTGCCAG CGCCCTAGCG CCCGCTCCTT TCGCTTTCTT
2681 CCCTTCCTTT CTCGCCACGT TCGCCGGCTT TCCCCGTCAA
2721 GCTCTAAATC GGGGGCTCCC TTTAGGGTTC CGATTTAGTG
2761 CTTTACGGCA CCTCGACCCC AAAAAACTTG ATTAGGGTGA
2801 TGGTTCACGT AGTGGGCCAT CGCCCTGATA GACGGTTTTT
2841 CGCCCTTTGA CGTTGGAGTC CACGTTCTTT AATAGTGGAC
2881 TCTTGTTCCA AACTGGAACA ACACTCAACC CTATCTCGGT
2921 CTATTCTTTT GATTTATAAG GGATTTTGCC GATTTCGGCC
2961 TATTGGTTAA AAAATGAGCT GATTTAACAA AAATTTAACG
3001 CGAATTAATT CTGTGGAATG TGTGTCAGTT AGGGTGTGGA
3041 AAGTCCCCAG GCTCCCCAGC AGGCAGAAGT ATGCAAAGCA
3081 TGCATCTCAA TTAGTCAGCA ACCAGGTGTG GAAAGTCCCC
3121 AGGCTCCCCA GCAGGCAGAA GTATGCAAAG CATGCATCTC
3161 AATTAGTCAG CAACCATAGT CCCGCCCCTA ACTCCGCCCA
3201 TCCCGCCCCT AACTCCGCCC AGTTCCGCCC ATTCTCCGCC
3241 CCATGGCTGA CTAATTTTTT TTATTTATGC AGAGGCCGAG
3281 GCCGCCTCTG CCTCTGAGCT ATTCCAGAAG TAGTGAGGAG
3321 GCTTTTTTGG AGGCCTAGGC TTTTGCAAAA AGCTCCCGGG
3361 AGCTTGTATA TCCATTTTCG GATCTGATCA AGAGACAGGA
3401 TGAGGATCGT TTCGCATGAT TGAACAAGAT GGATTGCACG
3441 CAGGTTCTCC GGCCGCTTGG GTGGAGAGGC TATTCGGCTA
3481 TGACTGGGCA CAACAGACAA TCGGCTGCTC TGATGCCGCC
3521 GTGTTCCGGC TGTCAGCGCA GGGGCGCCCG GTTCTTTTTG
3561 TCAAGACCGA CCTGTCCGGT GCCCTGAATG AACTGCAGGA
3601 CGAGGCAGCG CGGCTATCGT GGCTGGCCAC GACGGGCGTT
3641 CCTTGCGCAG CTGTGCTCGA CGTTGTCACT GAAGCGGGAA

3681 GGGACTGGCT GCTATTGGGC GAAGTGCCGG GGCAGGATCT
3721 CCTGTCATCT CACCTTGCTC CTGCCGAGAA AGTATCCATC
3761 ATGGCTGATG CAATGCGGCG GCTGCATACG CTTGATCCGG
3801 CTACCTGCCC ATTCGACCAC CAAGCGAAAC ATCGCATCGA
3841 GCGAGCACGT ACTCGGATGG AAGCCGGTCT TGTCGATCAG
3881 GATGATCTGG ACGAAGAGCA TCAGGGGCTC GCGCCAGCCG
3921 AACTGTTCGC CAGGCTCAAG GCGCGCATGC CCGACGGCGA
3961 GGATCTCGTC GTGACCCATG GCGATGCCTG CTTGCCGAAT
4001 ATCATGGTGG AAAATGGCCG CTTTTCTGGA TTCATCGACT
4041 GTGGCCGGCT GGGTGTGGCG GACCGCTATC AGGACATAGC
4081 GTTGGCTACC CGTGATATTG CTGAAGAGCT TGGCGGCGAA
4121 TGGGCTGACC GCTTCCTCGT GCTTTACGGT ATCGCCGCTC
4161 CCGATTCGCA GCGCATCGCC TTCTATCGCC TTCTTGACGA
4201 GTTCTTCTGA GCGGGACTCT GGGGTTCGAA ATGACCGACC
4241 AAGCGACGCC CAACCTGCCA TCACGAGATT TCGATTCCAC
4281 CGCCGCCTTC TATGAAAGGT TGGGCTTCGG AATCGTTTTC
4321 CGGGACGCCG GCTGGATGAT CCTCCAGCGC GGGGATCTCA
4361 TGCTGGAGTT CTTCGCCCAC CCCAACTTGT TTATTGCAGC
4401 TTATAATGGT TACAAATAAA GCAATAGCAT CACAAATTTC
4441 ACAAATAAAG CATTTTTTTC ACTGCATTCT AGTTGTGGTT
4481 TGTCCAAACT CATCAATGTA TCTTATCATG TCTGTATACC
4521 GTCGACCTCT AGCTAGAGCT TGGCGTAATC ATGGTCATAG
4561 CTGTTTCCTG TGTGAAATTG TTATCCGCTC ACAATTCCAC
4601 ACAACATACG AGCCGGAAGC ATAAAGTGTA AAGCCTGGGG
4641 TGCCTAATGA GTGAGCTAAC TCACATTAAT TGCGTTGCGC
4681 TCACTGCCCG CTTTCCAGTC GGGAAACCTG TCGTGCCAGC
4721 TGCATTAATG AATCGGCCAA CGCGCGGGGA GAGGCGGTTT
4761 GCGTATTGGG CGCTCTTCCG CTTCCTCGCT CACTGACTCG
4801 CTGCGCTCGG TCGTTCGGCT GCGGCGAGCG GTATCAGCTC
4841 ACTCAAAGGC GGTAATACGG TTATCCACAG AATCAGGGGA
4881 TAACGCAGGA AAGAACATGT GAGCAAAAGG CCAGCAAAAG
4921 GCCAGGAACC GTAAAAAGGC CGCGTTGCTG GCGTTTTTCC
4961 ATAGGCTCCG CCCCCCTGAC GAGCATCACA AAAATCGACG
5001 CTCAAGTCAG AGGTGGCGAA ACCCGACAGG ACTATAAAGA
5041 TACCAGGCGT TTCCCCCTGG AAGCTCCCTC GTGCGCTCTC
5081 CTGTTCCGAC CCTGCCGCTT ACCGGATACC TGTCCGCCTT
5121 TCTCCCTTCG GGAAGCGTGG CGCTTTCTCA TAGCTCACGC
5161 TGTAGGTATC TCAGTTCGGT GTAGGTCGTT CGCTCCAAGC
5201 TGGGCTGTGT GCACGAACCC CCCGTTCAGC CCGACCGCTG
5241 CGCCTTATCC GGTAACTATC GTCTTGAGTC CAACCCGGTA
5281 AGACACGACT TATCGCCACT GGCAGCAGCC ACTGGTAACA
5321 GGATTAGCAG AGCGAGGTAT GTAGGCGGTG CTACAGAGTT
5361 CTTGAAGTGG TGGCCTAACT ACGGCTACAC TAGAAGAACA
5401 GTATTTGGTA TCTGCGCTCT GCTGAAGCCA GTTACCTTCG
5441 GAAAAAGAGT TGGTAGCTCT TGATCCGGCA AACAAACCAC
5481 CGCTGGTAGC GGTTTTTTTG TTTGCAAGCA GCAGATTACG
5521 CGCAGAAAAA AAGGATCTCA AGAAGATCCT TTGATCTTTT

```
5561 CTACGGGGTC TGACGCTCAG TGGAACGAAA ACTCACGTTA
5601 AGGGATTTTG GTCATGAGAT TATCAAAAAG GATCTTCACC
5641 TAGATCCTTT TAAATTAAAA ATGAAGTTTT AAATCAATCT
5681 AAAGTATATA TGAGTAAACT TGGTCTGACA GTTACCAATG
5721 CTTAATCAGT GAGGCACCTA TCTCAGCGAT CTGTCTATTT
5761 CGTTCATCCA TAGTTGCCTG ACTCCCCGTC GTGTAGATAA
5801 CTACGATACG GGAGGGCTTA CCATCTGGCC CCAGTGCTGC
5841 AATGATACCG CGAGACCCAC GCTCACCGGC TCCAGATTTA
5881 TCAGCAATAA ACCAGCCAGC CGGAAGGGCC GAGCGCAGAA
5921 GTGGTCCTGC AACTTTATCC GCCTCCATCC AGTCTATTAA
5961 TTGTTGCCGG GAAGCTAGAG TAAGTAGTTC GCCAGTTAAT
6001 AGTTTGCGCA ACGTTGTTGC CATTGCTACA GGCATCGTGG
6041 TGTCACGCTC GTCGTTTGGT ATGGCTTCAT TCAGCTCCGG
6081 TTCCCAACGA TCAAGGCGAG TTACATGATC CCCCATGTTG
6121 TGCAAAAAAG CGGTTAGCTC CTTCGGTCCT CCGATCGTTG
6161 TCAGAAGTAA GTTGGCCGCA GTGTTATCAC TCATGGTTAT
6201 GGCAGCACTG CATAATTCTC TTACTGTCAT GCCATCCGTA
6241 AGATGCTTTT CTGTGACTGG TGAGTACTCA ACCAAGTCAT
6281 TCTGAGAATA GTGTATGCGG CGACCGAGTT GCTCTTGCCC
6321 GGCGTCAATA CGGGATAATA CCGCGCCACA TAGCAGAACT
6361 TTAAAAGTGC TCATCATTGG AAAACGTTCT TCGGGGCGAA
6401 AACTCTCAAG GATCTTACCG CTGTTGAGAT CCAGTTCGAT
6441 GTAACCCACT CGTGCACCCA ACTGATCTTC AGCATCTTTT
6481 ACTTTCACCA GCGTTTCTGG GTGAGCAAAA ACAGGAAGGC
6521 AAAATGCCGC AAAAAAGGGA ATAAGGGCGA CACGGAAATG
6561 TTGAATACTC ATACTCTTCC TTTTTCAATA TTATTGAAGC
6601 ATTTATCAGG GTTATTGTCT CATGAGCGGA TACATATTTG
6641 AATGTATTTA GAAAAATAAA CAAATAGGGG TTCCGCGCAC
6681 ATTTCCCCGA AAAGTGCCAC CTGACGTC
```

A1.2.4 Sequence of pGNAT2.iCre.Chi.B

```
   1 GACGGATCGG GAGATCTCCC GATCCCCTAT GGTGCACTCT
  41 CAGTACAATC TGCTCTGATG CCGCATAGTT AAGCCAGTAT
  81 CTGCTCCCTG CTTGTGTGTT GGAGGTCGCT GAGTAGTGCG
 121 CGAGCAAAAT TTAAGCTACA ACAAGGCAAG GCTTGACCGA
 161 CAATTGCATG AAGAATCTGC TTAGGGTTAG GCGTTTTGCG
 201 CTGCTTCGCT AGCGTTTAAA CGGGCCCTCT AGAGCTTGCA
 241 TCCTATCCTT CCGTCAGAAC CCAGCAGATC ATTTCCCTAG
 281 TTATAGAAAC ATTTGAGTCT TTACCCCTTG CCATATTGAC
 321 AAAGCTCTTA ATTGGCTTGA CCTATCACAT TGCTAGATAT
 361 AAAGGCTACA ATCCCTAGAC TAAGAAGTAG GTCTCCAGTT
 401 GAAGTAGGGA GTCTCAGTCA ATGTAGGCAG AGTACAAGAC
 441 CCTACAGCCT GCTCTCTCAC CTGCCATCGT ACAGACCAGC
 481 TTTTAGGGGA GCCAAGTTGG GATACTCAAT CCGCTATCTA
 521 GACTCGAGGG CAGGTAAGTA TCAAGGTTAC AAGACAGGTT
 561 TAAGGAGACC AATAGAAACT GGGCTTGTCG AGACAGAGAA
 601 GACTCTTGCG TTTCTGATAG GCACCTATTG GTCTTACTGA
 641 CATCCACTTT GCCTTTCTCT CCACAGGTGT CCTCGAGCGG
 681 CCGCCACTGT GCTGGATATC TGCAGAATTC CACCACACTG
 721 GACTAGTGGA TCCCCCGGGC TGCAGGAATT CGATATCAAG
 761 CTTGTCCACC ATGGTGCCCA AGAAGAAGAG GAAAGTCTCC
 801 AACCTGCTGA CTGTGCACCA AAACCTGCCT GCCCTCCCTG
 841 TGGATGCCAC CTCTGATGAA GTCAGGAAGA ACCTGATGGA
 881 CATGTTCAGG GACAGGCAGG CCTTCTCTGA ACACACCTGG
 921 AAGATGCTCC TGTCTGTGTG CAGATCCTGG GCTGCCTGGT
 961 GCAAGCTGAA CAACAGGAAA TGGTTCCCTG CTGAACCTGA
1001 GGATGTGAGG GACTACCTCC TGTACCTGCA AGCCAGAGGC
1041 CTGGCTGTGA AGACCATCCA ACAGCACCTG GGCCAGCTCA
1081 ACATGCTGCA CAGGAGATCT GGCCTGCCTC GCCCTTCTGA
1121 CTCCAATGCT GTGTCCCTGG TGATGAGGAG AATCAGAAAG
1161 GAGAATGTGG ATGCTGGGGA GAGAGCCAAG CAGGCCCTGG
1201 CCTTTGAACG CACTGACTTT GACCAAGTCA GATCCCTGAT
1241 GGAGAACTCT GACAGATGCC AGGACATCAG GAACCTGGCC
1281 TTCCTGGGCA TTGCCTACAA CACCCTGCTG CGCATTGCCG
1321 AAATTGCCAG AATCAGAGTG AAGGACATCT CCCGCACCGA
1361 TGGTGGGAGA ATGCTGATCC ACATTGGCAG GACCAAGACC
1401 CTGGTGTCCA CAGCTGGTGT GGAGAAGGCC CTGTCCCTGG
1441 GGGTTACCAA GCTGGTGGAG AGATGGATCT CTGTGTCTGG
1481 TGTGGCTGAT GACCCCAACA ACTACCTGTT CTGCCGGGTC
1521 AGAAAGAATG GTGTGGCTGC CCCTTCTGCC ACCTCCCAAC
1561 TGTCCACCCG GGCCCTGGAA GGGATCTTTG AGGCCACCCA
1601 CCGCCTGATC TATGGTGCCA AGGATGACTC TGGGCAGAGA
1641 TACCTGGCCT GGTCTGGCCA CTCTGCCAGA GTGGGTGCTG
1681 CCAGGGACAT GGCCAGGGCT GGTGTGTCCA TCCCTGAAAT
1721 CATGCAGGCT GGTGGCTGGA CCAATGTGAA CATAGTGATG
1761 AACTACATCA GAAACCTGGA CTCTGAGACT GGGGCCATGG
```

```
1801 TGAGGCTGCT CGAGGATGGG GACTGAAACT GAGTCGAGGG
1841 GGGGCCCGGT ACCAATAAAG GAAATTTATT TTCATTGCAA
1881 TAGTGTGTTG GTTTTTTGTG TGGGTACCAA GCTTATCCGG
1921 CCCAGGCTTC CCAGCAGGGC TAAGGATATG CAAGGAGTGC
1961 ATTCATCCGG AGGTGTTGGC AGCATCCCAG CCCCACCCCA
2001 TTCTCATCGT AAATCAGGCT CACTTCCATT GGCTGCATAC
2041 GGTGGAGTGA TGTGACCATA TGTCACTTGA GCATTACACA
2081 AATCCTAATG AGCTAAAAAT ATGTTTGTTT TAGCTAATTG
2121 ACCTCTTTGG CCGGATAAGC TTAAGTTTAA ACCGCTGATC
2161 AGCCTCGACT GTGCCTTCTA GTTGCCAGCC ATCTGTTGTT
2201 TGCCCCTCCC CCGTGCCTTC CTTGACCCTG GAAGGTGCCA
2241 CTCCCACTGT CCTTTCCTAA TAAAATGAGG AAATTGCATC
2281 GCATTGTCTG AGTAGGTGTC ATTCTATTCT GGGGGGTGGG
2321 GTGGGGCAGG ACAGCAAGGG GGAGGATTGG GAAGACAATA
2361 GCAGGCATGC TGGGGATGCG GTGGGCTCTA TGGCTTCTGA
2401 GGCGGAAAGA ACCAGCTGGG GCTCTAGGGG GTATCCCCAC
2441 GCGCCCTGTA GCGGCGCATT AAGCGCGGCG GGTGTGGTGG
2481 TTACGCGCAG CGTGACCGCT ACACTTGCCA GCGCCCTAGC
2521 GCCCGCTCCT TTCGCTTTCT TCCCTTCCTT TCTCGCCACG
2561 TTCGCCGGCT TTCCCCGTCA AGCTCTAAAT CGGGGGCTCC
2601 CTTTAGGGTT CCGATTTAGT GCTTTACGGC ACCTCGACCC
2641 CAAAAAACTT GATTAGGGTG ATGGTTCACG TAGTGGGCCA
2681 TCGCCCTGAT AGACGGTTTT TCGCCCTTTG ACGTTGGAGT
2721 CCACGTTCTT TAATAGTGGA CTCTTGTTCC AAACTGGAAC
2761 AACACTCAAC CCTATCTCGG TCTATTCTTT TGATTTATAA
2801 GGGATTTTGC CGATTTCGGC CTATTGGTTA AAAAATGAGC
2841 TGATTTAACA AAAATTTAAC GCGAATTAAT TCTGTGGAAT
2881 GTGTGTCAGT TAGGGTGTGG AAAGTCCCCA GGCTCCCCAG
2921 CAGGCAGAAG TATGCAAAGC ATGCATCTCA ATTAGTCAGC
2961 AACCAGGTGT GGAAAGTCCC CAGGCTCCCC AGCAGGCAGA
3001 AGTATGCAAA GCATGCATCT CAATTAGTCA GCAACCATAG
3041 TCCCGCCCCT AACTCCGCCC ATCCCGCCCC TAACTCCGCC
3081 CAGTTCCGCC CATTCTCCGC CCCATGGCTG ACTAATTTTT
3121 TTTATTTATG CAGAGGCCGA GGCCGCCTCT GCCTCTGAGC
3161 TATTCCAGAA GTAGTGAGGA GGCTTTTTTG GAGGCCTAGG
3201 CTTTTGCAAA AAGCTCCCGG GAGCTTGTAT ATCCATTTTC
3241 GGATCTGATC AAGAGACAGG ATGAGGATCG TTTCGCATGA
3281 TTGAACAAGA TGGATTGCAC GCAGGTTCTC CGGCCGCTTG
3321 GGTGGAGAGG CTATTCGGCT ATGACTGGGC ACAACAGACA
3361 ATCGGCTGCT CTGATGCCGC CGTGTTCCGG CTGTCAGCGC
3401 AGGGGCGCCC GGTTCTTTTT GTCAAGACCG ACCTGTCCGG
3441 TGCCCTGAAT GAACTGCAGG ACGAGGCAGC GCGGCTATCG
3481 TGGCTGGCCA CGACGGGCGT TCCTTGCGCA GCTGTGCTCG
3521 ACGTTGTCAC TGAAGCGGGA AGGGACTGGC TGCTATTGGG
3561 CGAAGTGCCG GGGCAGGATC TCCTGTCATC TCACCTTGCT
3601 CCTGCCGAGA AAGTATCCAT CATGGCTGAT GCAATGCGGC
3641 GGCTGCATAC GCTTGATCCG GCTACCTGCC CATTCGACCA
```

3681 CCAAGCGAAA CATCGCATCG AGCGAGCACG TACTCGGATG
3721 GAAGCCGGTC TTGTCGATCA GGATGATCTG GACGAAGAGC
3761 ATCAGGGGCT CGCGCCAGCC GAACTGTTCG CCAGGCTCAA
3801 GGCGCGCATG CCCGACGGCG AGGATCTCGT CGTGACCCAT
3841 GGCGATGCCT GCTTGCCGAA TATCATGGTG GAAAATGGCC
3881 GCTTTTCTGG ATTCATCGAC TGTGGCCGGC TGGGTGTGGC
3921 GGACCGCTAT CAGGACATAG CGTTGGCTAC CCGTGATATT
3961 GCTGAAGAGC TTGGCGGCGA ATGGGCTGAC CGCTTCCTCG
4001 TGCTTTACGG TATCGCCGCT CCCGATTCGC AGCGCATCGC
4041 CTTCTATCGC CTTCTTGACG AGTTCTTCTG AGCGGGACTC
4081 TGGGGTTCGA AATGACCGAC CAAGCGACGC CCAACCTGCC
4121 ATCACGAGAT TTCGATTCCA CCGCCGCCTT CTATGAAAGG
4161 TTGGGCTTCG GAATCGTTTT CCGGGACGCC GGCTGGATGA
4201 TCCTCCAGCG CGGGGATCTC ATGCTGGAGT TCTTCGCCCA
4241 CCCCAACTTG TTTATTGCAG CTTATAATGG TTACAAATAA
4281 AGCAATAGCA TCACAAATTT CACAAATAAA GCATTTTTTT
4321 CACTGCATTC TAGTTGTGGT TTGTCCAAAC TCATCAATGT
4361 ATCTTATCAT GTCTGTATAC CGTCGACCTC TAGCTAGAGC
4401 TTGGCGTAAT CATGGTCATA GCTGTTTCCT GTGTGAAATT
4441 GTTATCCGCT CACAATTCCA CACAACATAC GAGCCGGAAG
4481 CATAAAGTGT AAAGCCTGGG GTGCCTAATG AGTGAGCTAA
4521 CTCACATTAA TTGCGTTGCG CTCACTGCCC GCTTTCCAGT
4561 CGGGAAACCT GTCGTGCCAG CTGCATTAAT GAATCGGCCA
4601 ACGCGCGGGG AGAGGCGGTT TGCGTATTGG GCGCTCTTCC
4641 GCTTCCTCGC TCACTGACTC GCTGCGCTCG GTCGTTCGGC
4681 TGCGGCGAGC GGTATCAGCT CACTCAAAGG CGGTAATACG
4721 GTTATCCACA GAATCAGGGG ATAACGCAGG AAAGAACATG
4761 TGAGCAAAAG GCCAGCAAAA GGCCAGGAAC CGTAAAAAGG
4801 CCGCGTTGCT GGCGTTTTTC CATAGGCTCC GCCCCCCTGA
4841 CGAGCATCAC AAAAATCGAC GCTCAAGTCA GAGGTGGCGA
4881 AACCCGACAG GACTATAAAG ATACCAGGCG TTTCCCCCTG
4921 GAAGCTCCCT CGTGCGCTCT CCTGTTCCGA CCCTGCCGCT
4961 TACCGGATAC CTGTCCGCCT TTCTCCCTTC GGGAAGCGTG
5001 GCGCTTTCTC ATAGCTCACG CTGTAGGTAT CTCAGTTCGG
5041 TGTAGGTCGT TCGCTCCAAG CTGGGCTGTG TGCACGAACC
5081 CCCCGTTCAG CCCGACCGCT GCGCCTTATC CGGTAACTAT
5121 CGTCTTGAGT CCAACCCGGT AAGACACGAC TTATCGCCAC
5161 TGGCAGCAGC CACTGGTAAC AGGATTAGCA GAGCGAGGTA
5201 TGTAGGCGGT GCTACAGAGT TCTTGAAGTG GTGGCCTAAC
5241 TACGGCTACA CTAGAAGAAC AGTATTTGGT ATCTGCGCTC
5281 TGCTGAAGCC AGTTACCTTC GGAAAAAGAG TTGGTAGCTC
5321 TTGATCCGGC AAACAAACCA CCGCTGGTAG CGGTTTTTTT
5361 GTTTGCAAGC AGCAGATTAC GCGCAGAAAA AAAGGATCTC
5401 AAGAAGATCC TTTGATCTTT TCTACGGGGT CTGACGCTCA
5441 GTGGAACGAA AACTCACGTT AAGGGATTTT GGTCATGAGA
5481 TTATCAAAAA GGATCTTCAC CTAGATCCTT TTAAATTAAA
5521 AATGAAGTTT TAAATCAATC TAAAGTATAT ATGAGTAAAC

```
5561 TTGGTCTGAC AGTTACCAAT GCTTAATCAG TGAGGCACCT
5601 ATCTCAGCGA TCTGTCTATT TCGTTCATCC ATAGTTGCCT
5641 GACTCCCCGT CGTGTAGATA ACTACGATAC GGGAGGGCTT
5681 ACCATCTGGC CCCAGTGCTG CAATGATACC GCGAGACCCA
5721 CGCTCACCGG CTCCAGATTT ATCAGCAATA AACCAGCCAG
5761 CCGGAAGGGC CGAGCGCAGA AGTGGTCCTG CAACTTTATC
5801 CGCCTCCATC CAGTCTATTA ATTGTTGCCG GGAAGCTAGA
5841 GTAAGTAGTT CGCCAGTTAA TAGTTTGCGC AACGTTGTTG
5881 CCATTGCTAC AGGCATCGTG GTGTCACGCT CGTCGTTTGG
5921 TATGGCTTCA TTCAGCTCCG GTTCCCAACG ATCAAGGCGA
5961 GTTACATGAT CCCCCATGTT GTGCAAAAAA GCGGTTAGCT
6001 CCTTCGGTCC TCCGATCGTT GTCAGAAGTA AGTTGGCCGC
6041 AGTGTTATCA CTCATGGTTA TGGCAGCACT GCATAATTCT
6081 CTTACTGTCA TGCCATCCGT AAGATGCTTT TCTGTGACTG
6121 GTGAGTACTC AACCAAGTCA TTCTGAGAAT AGTGTATGCG
6161 GCGACCGAGT TGCTCTTGCC CGGCGTCAAT ACGGGATAAT
6201 ACCGCGCCAC ATAGCAGAAC TTTAAAAGTG CTCATCATTG
6241 GAAAACGTTC TTCGGGGCGA AAACTCTCAA GGATCTTACC
6281 GCTGTTGAGA TCCAGTTCGA TGTAACCCAC TCGTGCACCC
6321 AACTGATCTT CAGCATCTTT TACTTTCACC AGCGTTTCTG
6361 GGTGAGCAAA AACAGGAAGG CAAAATGCCG CAAAAAAGGG
6401 AATAAGGGCG ACACGGAAAT GTTGAATACT CATACTCTTC
6441 CTTTTTCAAT ATTATTGAAG CATTTATCAG GGTTATTGTC
6481 TCATGAGCGG ATACATATTT GAATGTATTT AGAAAAATAA
6521 ACAAATAGGG GTTCCGCGCA CATTTCCCCG AAAAGTGCCA
6561 CCTGACGTC
```

A1.3 Sequence of β-galactosidase reporter (pCMVβ.Neo) with a lox*P-flanked neomycin gene*

```
   1 GAATTCGAGC TTGCATGCCT GCAGGTCGTT ACATAACTTA
  41 CGGTAAATGG CCCGCCTGGC TGACCGCCCA ACGACCCCCG
  81 CCCATTGACG TCAATAATGA CGTATGTTCC CATAGTAACG
 121 CCAATAGGGA CTTTCCATTG ACGTCAATGG GTGGAGTATT
 161 TACGGTAAAC TGCCCACTTG GCAGTACATC AAGTGTATCA
 201 TATGCCAAGT ACGCCCCCTA TTGACGTCAA TGACGGTAAA
 241 TGGCCCGCCT GGCATTATGC CCAGTACATG ACCTTATGGG
 281 ACTTTCCTAC TTGGCAGTAC ATCTACGTAT TAGTCATCGC
 321 TATTACCATG GTGATGCGGT TTTGGCAGTA CATCAATGGG
 361 CGTGGATAGC GGTTTGACTC ACGGGGATTT CCAAGTCTCC
 401 ACCCCATTGA CGTCAATGGG AGTTTGTTTT GGCACCAAAA
 441 TCAACGGGAC TTTCCAAAAT GTCGTAACAA CTCCGCCCCA
 481 TTGACGCAAA TGGGCGGTAG GCGTGTACGG TGGGAGGTCT
 521 ATATAAGCAG AGCTCGTTTA GTGAACCGTC AGATCGCCTG
 561 GAGACGCCAT CCACGCTGTT TTGACCTCCA TAGAAGACAC
 601 CGGGACCGAT CCAGCCTCCG GACTCTAGAG GATCCGGTAC
 641 TCGAGGGCTG CAGGAATTCG ATATCAAGCT TATCGATACC
 681 GTCGAGGAAT TCATAACTTC GTATAATGTA TGCTATACGA
 721 AGTTATGTCG ACGGTATCGA TAAGCTTGAT ATCGAATTTC
 761 GAGGGCCCCT GCAGGTCAAT TCTACCGGGT AGGGGAGGCG
 801 CTTTTCCCAA GGCAGTCTGG AGCATGCGCT TTAGCAGCCC
 841 CGCTGGCACT TGGCGCTACA CAAGTGGCCT CTGGCCTCGC
 881 ACACATTCCA CATCCACCGG TAGCGCCAAC CGGCTCCGTT
 921 CTTTGGTGGC CCCTTCGCGC CACCTTCTAC TCCTCCCCTA
 961 GTCAGGAAGT TCCCCCCCGC CCCGCAGCTC GCGTCGTGCA
1001 GGACGTGACA AATGGAAGTA GCACGTCTCA CTAGTCTCGT
1041 GCAGATGGAC AGCACCGCTG AGCAATGGAA GCGGGTAGGC
1081 CTTTGGGGCA GCGGCCAATA GCAGCTTTCT CCTTCGCTTT
1121 CTGGGCTCAG AGGCTGGGAA GGGGTGGGTC CGGGGGCGGG
1161 CTCAGGGGCG GGCTCAGGGG CGGGGCGGGC GCGAAGGTCC
1201 TCCCGAGGCC CGGCATTCTC GCACGCTTCA AAAGCGACGT
1241 CTGCCGCGCT GTTCTCCTCT TCCTCATCTC CGGGCCTTTC
1281 GACCTGCAGC CAATATGGGA TCGGCCATTG AACAAGATGG
1321 ATTGCACGCA GGTTCTCCGG CCGCTTGGGT GGAGAGGCTA
1361 TTCGGCTATG ACTGGGCACA ACAGACAATC GGCTGCTCTG
1401 ATGCCGCCGT GTTCCGGCTG TCAGCGCAGG GGCGCCCGGT
1441 TCTTTTTGTC AAGACCGACC TGTCCGGTGC CCTGAATGAA
1481 CTGCAGGACG AGGCAGCGCG GCTATCGTGG CTGGCCACGA
1521 CGGGCGTTCC TTGCGCAGCT GTGCTCGACG TTGTCACTGA
1561 AGCGGGAAGG GACTGGCTGC TATTGGGCGA AGTGCCGGGG
1601 CAGGATCTCC TGTCATCTCA CCTTGCTCCT GCCGAGAAAG
1641 TATCCATCAT GGCTGATGCA ATGCGGCGGC TGCATACGCT
1681 TGATCCGGCT ACCTGCCCAT TCGACCACCA AGCGAAACAT
1721 CGCATCGAGC GAGCACGTAC TCGGATGGAA GCCGGTCTTG
```

1761 TCGATCAGGA TGATCTGGAC GAAGAGCATC AGGGGCTCGC
1801 GCCAGCCGAA CTGTTCGCCA GGCTCAAGGC GCGCATGCCC
1841 GACGGCGATG ATCTCGTCGT GACCCATGGC GATGCCTGCT
1881 TGCCGAATAT CATGGTGGAA AATGGCCGCT TTTCTGGATT
1921 CATCGACTGT GGCCGGCTGG GTGTGGCGGA CCGCTATCAG
1961 GACATAGCGT TGGCTACCCG TGATATTGCT GAAGAGCTTG
2001 GCGGCGAATG GGCTGACCGC TTCCTCGTGC TTTACGGTAT
2041 CGCCGCTCCC GATTCGCAGC GCATCGCCTT CTATCGCCTT
2081 CTTGACGAGT TCTTCTGAGG GGATCGATCC GTCCTGTAAG
2121 TCTGCAGAAA TTGATGATCT ATTAAACAAT AAAGATGTCC
2161 ACTAAAATGG AAGTTTTTCC TGTCATACTT TGTTAAGAAG
2201 GGTGAGAACA GAGTACCTAC ATTTTGAATG GAAGGATTGG
2241 AGCTACGGGG GTGGGGGTGG GGTGGGATTA GATAAATGCC
2281 TGCTCTTTAC TGAAGGCTCT TTACTATTGC TTTATGATAA
2321 TGTTTCATAG TTGGATATCA TAATTTAAAC AAGCAAAACC
2361 AAATTAAGGG CCAGCTCATT CCTCCCACTC ATGATCTATA
2401 GATCTATAGA TCTCTCGTGG GATCATTGTT TTTCTCTTGA
2441 TTCCCACTTT GTGGTTCTAA GTACTGTGGT TTCCAAATGT
2481 GTCAGTTTCA TAGCCTGAAG AACGAGATCA GCAGCCTCTG
2521 TTCCACATAC ACTTCATTCT CAGTATTGTT TTGCCAAGTT
2561 CTAATTCCAT CAGAAGCTGA CTCTAGAGCT TATAACTTCG
2601 TATAATGTAT GCATTACGAA GTTATTAGGT CCCTCGATCG
2641 AGGAACTGAA AAACCAGAAA GTTAACTGGT AAGTTTAGTC
2681 TTTTTGTCTT TTATTTCAGG TCCCGGATCC GGTGGTGGTG
2721 CAAATCAAAG AACTGCTCCT CAGTGGATGT TGCCTTTACT
2761 TCTAGGCCTG TACGGAAGTG TTACTTCTGC TCTAAAAGCT
2801 GCGGAATTGT ACCCGCGGCC GCAATTCCCG GGGATCGAAA
2841 GAGCCTGCTA AAGCAAAAAA GAAGTCACCA TGTCGTTTAC
2881 TTTGACCAAC AAGAACGTGA TTTTCGTTGC CGGTCTGGGA
2921 GGCATTGGTC TGGACACCAG CAAGGAGCTG CTCAAGCGCG
2961 ATCCCGTCGT TTTACAACGT CGTGACTGGG AAAACCCTGG
3001 CGTTACCCAA CTTAATCGCC TTGCAGCACA TCCCCCTTTC
3041 GCCAGCTGGC GTAATAGCGA AGAGGCCCGC ACCGATCGCC
3081 CTTCCCAACA GTTGCGCAGC CTGAATGGCG AATGGCGCTT
3121 TGCCTGGTTT CCGGCACCAG AAGCGGTGCC GGAAAGCTGG
3161 CTGGAGTGCG ATCTTCCTGA GGCCGATACT GTCGTCGTCC
3201 CCTCAAACTG GCAGATGCAC GGTTACGATG CGCCCATCTA
3241 CACCAACGTA ACCTATCCCA TTACGGTCAA TCCGCCGTTT
3281 GTTCCCACGG AGAATCCGAC GGGTTGTTAC TCGCTCACAT
3321 TTAATGTTGA TGAAAGCTGG CTACAGGAAG GCCAGACGCG
3361 AATTATTTTT GATGGCGTTA ACTCGGCGTT TCATCTGTGG
3401 TGCAACGGGC GCTGGGTCGG TTACGGCCAG GACAGTCGTT
3441 TGCCGTCTGA ATTTGACCTG AGCGCATTTT TACGCGCCGG
3481 AGAAAACCGC CTCGCGGTGA TGGTGCTGCG TTGGAGTGAC
3521 GGCAGTTATC TGGAAGATCA GGATATGTGG CGGATGAGCG
3561 GCATTTTCCG TGACGTCTCG TTGCTGCATA AACCGACTAC
3601 ACAAATCAGC GATTTCCATG TTGCCACTCG CTTTAATGAT

3641 GATTTCAGCC GCGCTGTACT GGAGGCTGAA GTTCAGATGT
3681 GCGGCGAGTT GCGTGACTAC CTACGGGTAA CAGTTTCTTT
3721 ATGGCAGGGT GAAACGCAGG TCGCCAGCGG CACCGCGCCT
3761 TTCGGCGGTG AAATTATCGA TGAGCGTGGT GGTTATGCCG
3801 ATCGCGTCAC ACTACGTCTG AACGTCGAAA ACCCGAAACT
3841 GTGGAGCGCC GAAATCCCGA ATCTCTATCG TGCGGTGGTT
3881 GAACTGCACA CCGCCGACGG CACGCTGATT GAAGCAGAAG
3921 CCTGCGATGT CGGTTTCCGC GAGGTGCGGA TTGAAAATGG
3961 TCTGCTGCTG CTGAACGGCA AGCCGTTGCT GATTCGAGGC
4001 GTTAACCGTC ACGAGCATCA TCCTCTGCAT GGTCAGGTCA
4041 TGGATGAGCA GACGATGGTG CAGGATATCC TGCTGATGAA
4081 GCAGAACAAC TTTAACGCCG TGCGCTGTTC GCATTATCCG
4121 AACCATCCGC TGTGGTACAC GCTGTGCGAC CGCTACGGCC
4161 TGTATGTGGT GGATGAAGCC AATATTGAAA CCCACGGCAT
4201 GGTGCCAATG AATCGTCTGA CCGATGATCC GCGCTGGCTA
4241 CCGGCGATGA GCGAACGCGT AACGCGAATG GTGCAGCGCG
4281 ATCGTAATCA CCCGAGTGTG ATCATCTGGT CGCTGGGGAA
4321 TGAATCAGGC CACGGCGCTA ATCACGACGC GCTGTATCGC
4361 TGGATCAAAT CTGTCGATCC TTCCCGCCCG GTGCAGTATG
4401 AAGGCGGCGG AGCCGACACC ACGGCCACCG ATATTATTTG
4441 CCCGATGTAC GCGCGCGTGG ATGAAGACCA GCCCTTCCCG
4481 GCTGTGCCGA AATGGTCCAT CAAAAAATGG CTTTCGCTAC
4521 CTGGAGAGAC GCGCCCGCTG ATCCTTTGCG AATACGCCCA
4561 CGCGATGGGT AACAGTCTTG GCGGTTTCGC TAAATACTGG
4601 CAGGCGTTTC GTCAGTATCC CCGTTTACAG GGCGGCTTCG
4641 TCTGGGACTG GGTGGATCAG TCGCTGATTA AATATGATGA
4681 AAACGGCAAC CCGTGGTCGG CTTACGGCGG TGATTTTGGC
4721 GATACGCCGA ACGATCGCCA GTTCTGTATG AACGGTCTGG
4761 TCTTTGCCGA CCGCACGCCG CATCCAGCGC TGACGGAAGC
4801 AAAACACCAG CAGCAGTTTT TCCAGTTCCG TTTATCCGGG
4841 CAAACCATCG AAGTGACCAG CGAATACCTG TTCCGTCATA
4881 GCGATAACGA GCTCCTGCAC TGGATGGTGG CGCTGGATGG
4921 TAAGCCGCTG GCAAGCGGTG AAGTGCCTCT GGATGTCGCT
4961 CCACAAGGTA AACAGTTGAT TGAACTGCCT GAACTACCGC
5001 AGCCGGAGAG CGCCGGGCAA CTCTGGCTCA CAGTACGCGT
5041 AGTGCAACCG AACGCGACCG CATGGTCAGA AGCCGGGCAC
5081 ATCAGCGCCT GGCAGCAGTG GCGTCTGGCG GAAAACCTCA
5121 GTGTGACGCT CCCCGCCGCG TCCCACGCCA TCCCGCATCT
5161 GACCACCAGC GAAATGGATT TTTGCATCGA GCTGGGTAAT
5201 AAGCGTTGGC AATTTAACCG CCAGTCAGGC TTTCTTTCAC
5241 AGATGTGGAT TGGCGATAAA AAACAACTGC TGACGCCGCT
5281 GCGCGATCAG TTCACCCGTG CACCGCTGGA TAACGACATT
5321 GGCGTAAGTG AAGCGACCCG CATTGACCCT AACGCCTGGG
5361 TCGAACGCTG GAAGGCGGCG GGCCATTACC AGGCCGAAGC
5401 AGCGTTGTTG CAGTGCACGG CAGATACACT TGCTGATGCG
5441 GTGCTGATTA CGACCGCTCA CGCGTGGCAG CATCAGGGGA
5481 AAACCTTATT TATCAGCCGG AAAACCTACC GGATTGATGG

5521 TAGTGGTCAA ATGGCGATTA CCGTTGATGT TGAAGTGGCG
5561 AGCGATACAC CGCATCCGGC GCGGATTGGC CTGAACTGCC
5601 AGCTGGCGCA GGTAGCAGAG CGGGTAAACT GGCTCGGATT
5641 AGGGCCGCAA GAAAACTATC CCGACCGCCT TACTGCCGCC
5681 TGTTTTGACC GCTGGGATCT GCCATTGTCA GACATGTATA
5721 CCCCGTACGT CTTCCCGAGC GAAAACGGTC TGCGCTGCGG
5761 GACGCGCGAA TTGAATTATG GCCCACACCA GTGGCGCGGC
5801 GACTTCCAGT TCAACATCAG CCGCTACAGT CAACAGCAAC
5841 TGATGGAAAC CAGCCATCGC CATCTGCTGC ACGCGGAAGA
5881 AGGCACATGG CTGAATATCG ACGGTTTCCA TATGGGGATT
5921 GGTGGCGACG ACTCCTGGAG CCCGTCAGTA TCGGCGGAAT
5961 TACAGCTGAG CGCCGGTCGC TACCATTACC AGTTGGTCTG
6001 GTGTCAAAAA TAATAATAAC CGGGCAGGCC ATGTCTGCCC
6041 GTATTTCGCG TAAGGAAATC CATTATGTAC TATTTAAAAA
6081 ACACAAACTT TTGGATGTTC GGTTTATTCT TTTTCTTTTA
6121 CTTTTTTATC ATGGGAGCCT ACTTCCCGTT TTTCCCGATT
6161 TGGCTACATG ACATCAACCA TATCAGCAAA AGTGATACGG
6201 GTATTATTTT TGCCGCTATT TCTCTGTTCT CGCTATTATT
6241 CCAACCGCTG TTTGGTCTGC TTTCTGACAA ACTCGGCCTC
6281 GACTCTAGGC GGCCGCGGGG ATCCAGACAT GATAAGATAC
6321 ATTGATGAGT TTGGACAAAC CACAACTAGA ATGCAGTGAA
6361 AAAAATGCTT TATTTGTGAA ATTTGTGATG CTATTGCTTT
6401 ATTTGTAACC ATTATAAGCT GCAATAAACA AGTTAACAAC
6441 AACAATTGCA TTCATTTTAT GTTTCAGGTT CAGGGGGAGG
6481 TGTGGGAGGT TTTTTCGGAT CCTCTAGAGT CGACCTGCAG
6521 GCATGCAAGC TTGGCGTAAT CATGGTCATA GCTGTTTCCT
6561 GTGTGAAATT GTTATCCGCT CACAATTCCA CACAACATAC
6601 GAGCCGGAAG CATAAAGTGT AAAGCCTGGG GTGCCTAATG
6641 AGTGAGCTAA CTCACATTAA TTGCGTTGCG CTCACTGCCC
6681 GCTTTCCAGT CGGGAAACCT GTCGTGCCAG CTGCATTAAT
6721 GAATCGGCCA ACGCGCGGGG AGAGGCGGTT TGCGTATTGG
6761 GCGCTCTTCC GCTTCCTCGC TCACTGACTC GCTGCGCTCG
6801 GTCGTTCGGC TGCGGCGAGC GGTATCAGCT CACTCAAAGG
6841 CGGTAATACG GTTATCCACA GAATCAGGGG ATAACGCAGG
6881 AAAGAACATG TGAGCAAAAG GCCAGCAAAA GGCCAGGAAC
6921 CGTAAAAAGG CCGCGTTGCT GGCGTTTTTC CATAGGCTCC
6961 GCCCCCCTGA CGAGCATCAC AAAAATCGAC GCTCAAGTCA
7001 GAGGTGGCGA AACCCGACAG GACTATAAAG ATACCAGGCG
7041 TTTCCCCCTG GAAGCTCCCT CGTGCGCTCT CCTGTTCCGA
7081 CCCTGCCGCT TACCGGATAC CTGTCCGCCT TTCTCCCTTC
7121 GGGAAGCGTG GCGCTTTCTC ATAGCTCACG CTGTAGGTAT
7161 CTCAGTTCGG TGTAGGTCGT TCGCTCCAAG CTGGGCTGTG
7201 TGCACGAACC CCCCGTTCAG CCCGACCGCT GCGCCTTATC
7241 CGGTAACTAT CGTCTTGAGT CCAACCCGGT AAGACACGAC
7281 TTATCGCCAC TGGCAGCAGC CACTGGTAAC AGGATTAGCA
7321 GAGCGAGGTA TGTAGGCGGT GCTACAGAGT TCTTGAAGTG
7361 GTGGCCTAAC TACGGCTACA CTAGAAGGAC AGTATTTGGT

7401 ATCTGCGCTC TGCTGAAGCC AGTTACCTTC GGAAAAAGAG
7441 TTGGTAGCTC TTGATCCGGC AAACAAACCA CCGCTGGTAG
7481 CGGTGGTTTT TTTGTTTGCA AGCAGCAGAT TACGCGCAGA
7521 AAAAAAGGAT CTCAAGAAGA TCCTTTGATC TTTTCTACGG
7561 GGTCTGACGC TCAGTGGAAC GAAAACTCAC GTTAAGGGAT
7601 TTTGGTCATG AGATTATCAA AAAGGATCTT CACCTAGATC
7641 CTTTTAAATT AAAAATGAAG TTTTAAATCA ATCTAAAGTA
7681 TATATGAGTA AACTTGGTCT GACAGTTACC AATGCTTAAT
7721 CAGTGAGGCA CCTATCTCAG CGATCTGTCT ATTTCGTTCA
7761 TCCATAGTTG CCTGACTCCC CGTCGTGTAG ATAACTACGA
7801 TACGGGAGGG CTTACCATCT GGCCCCAGTG CTGCAATGAT
7841 ACCGCGAGAC CCACGCTCAC CGGCTCCAGA TTTATCAGCA
7881 ATAAACCAGC CAGCCGGAAG GGCCGAGCGC AGAAGTGGTC
7921 CTGCAACTTT ATCCGCCTCC ATCCAGTCTA TTAATTGTTG
7961 CCGGGAAGCT AGAGTAAGTA GTTCGCCAGT TAATAGTTTG
8001 CGCAACGTTG TTGCCATTGC TACAGGCATC GTGGTGTCAC
8041 GCTCGTCGTT TGGTATGGCT TCATTCAGCT CCGGTTCCCA
8081 ACGATCAAGG CGAGTTACAT GATCCCCCAT GTTGTGCAAA
8121 AAAGCGGTTA GCTCCTTCGG TCCTCCGATC GTTGTCAGAA
8161 GTAAGTTGGC CGCAGTGTTA TCACTCATGG TTATGGCAGC
8201 ACTGCATAAT TCTCTTACTG TCATGCCATC CGTAAGATGC
8241 TTTTCTGTGA CTGGTGAGTA CTCAACCAAG TCATTCTGAG
8281 AATAGTGTAT GCGGCGACCG AGTTGCTCTT GCCCGGCGTC
8321 AATACGGGAT AATACCGCGC CACATAGCAG AACTTTAAAA
8361 GTGCTCATCA TTGGAAAACG TTCTTCGGGG CGAAAACTCT
8401 CAAGGATCTT ACCGCTGTTG AGATCCAGTT CGATGTAACC
8441 CACTCGTGCA CCCAACTGAT CTTCAGCATC TTTTACTTTC
8481 ACCAGCGTTT CTGGGTGAGC AAAAACAGGA AGGCAAAATG
8521 CCGCAAAAAA GGGAATAAGG GCGACACGGA AATGTTGAAT
8561 ACTCATACTC TTCCTTTTTC AATATTATTG AAGCATTTAT
8601 CAGGGTTATT GTCTCATGAG CGGATACATA TTTGAATGTA
8641 TTTAGAAAAA TAAACAAATA GGGGTTCCGC GCACATTTCC
8681 CCGAAAAGTG CCACCTGACG TCTAAGAAAC CATTATTATC
8721 ATGACATTAA CCTATAAAAA TAGGCGTATC ACGAGGCCCT
8761 TTCGTCTCGC GCGTTTCGGT GATGACGGTG AAAACCTCTG
8801 ACACATGCAG CTCCCGGAGA CGGTCACAGC TTGTCTGTAA
8841 GCGGATGCCG GGAGCAGACA AGCCCGTCAG GGCGCGTCAG
8881 CGGGTGTTGG CGGGTGTCGG GGCTGGCTTA ACTATGCGGC
8921 ATCAGAGCAG ATTGTACTGA GAGTGCACCA TATGCGGTGT
8961 GAAATACCGC ACAGATGCGT AAGGAGAAAA TACCGCATCA
9001 GGCGCCATTC GCCATTCAGG CTGCGCAACT GTTGGGAAGG
9041 GCGATCGGTG CGGGCCTCTT CGCTATTACG CCAGCTGGCG
9081 AAAGGGGGAT GTGCTGCAAG GCGATTAAGT TGGGTAACGC
9121 CAGGGTTTTC CCAGTCACGA CGTTGTAAAA CGACGGCCAG
9161 T

A2.1 Primer sequences

A2.1.1 Primers for amplification of stuffer sequence

Primers for amplification of stuffer sequence from an intron of the wt mouse genome. Restriction sites for *Xho*I and *Eco*RI are underlined below:

StuF: 5' AAACTCGAGAAAACTGAGGCAGGGAGC 3'
StuR: 5' GAATTCTGTGACCACAGAAGGTAAC 3'

A2.1.2 Primers for sequencing pEGFP.p35

F EGFP: 5' AAAACGCCAGCAACGCGGCCTT 3'
R EGFP: 5' CCGTTTACGTCGCCGTCCAGC 3'

A2.1.3 Primers for sequencing pAAV-iCre.EGFP and pAAV-p35

F β-globin: 5'ATTCTGAGTCCAAGCTAGGC 3'
R hGH: 5' TAGAAGGACACCTAGTCAGA 3
ORI F: 5' TTTGTGATGCTCGTCAGG 3'
10R: 5' AAGAAAGCGAAAGGAGCG 3'

A2.2 Sequence of lox*P-p35 plasmid construct for transgene generation*

```
   1 GTCGACATTG ATTATTGACT AGTTATTAAT AGTAATCAAT
  41 TACGGGGTCA TTAGTTCATA GCCCATATAT GGAGTTCCGC
  81 GTTACATAAC TTACGGTAAA TGGCCCGCCT GGCTGACCGC
 121 CCAACGACCC CCGCCCATTG ACGTCAATAA TGACGTATGT
 161 TCCCATAGTA ACGCCAATAG GGACTTTCCA TTGACGTCAA
 201 TGGGTGGACT ATTTACGGTA AACTGCCCAC TTGGCAGTAC
 241 ATCAAGTGTA TCATATGCCA AGTACGCCCC CTATTGACGT
 281 CAATGACGGT AAATGGCCCG CCTGGCATTA TGCCCAGTAC
 321 ATGACCTTAT GGGACTTTCC TACTTGGCAG TACATCTACG
 361 TATTAGTCAT CGCTATTACC ATGGGTCGAG GTGAGCCCCA
 401 CGTTCTGCTT CACTCTCCCC ATCTCCCCCC CCTCCCCACC
 441 CCCAATTTTG TATTTATTTA TTTTTTAATT ATTTTGTGCA
 481 GCGATGGGGG CGGGGGGGGG GGGGGCGCGC GCCAGGCGGG
 521 GCGGGGCGGG GCGAGGGGCG GGGCGGGGCG AGGCGGAGAG
 561 GTGCGGCGGC AGCCAATCAG AGCGGCGCGC TCCGAAAGTT
 601 TCCTTTTATG GCGAGGCGGC GGCGGCGGCG GCCCTATAAA
 641 AAGCGAAGCG CGCGGCGGGC GGGAGTCGCT GCGTTGCCTT
 681 CGCCCCGTGC CCCGCTCCGC GCCGCCTCGC GCCGCCCGCC
 721 CCGGCTCTGA CTGACCGCGT TACTCCCACA GGTGAGCGGG
 761 CGGGACGGCC CTTCTCCTCC GGGCTGTAAT TAGCGCTTGG
 801 TTTAATGACG GCTCGTTTCT TTTCTGTGGC TGCGTGAAAG
 841 CCTTAAAGGG CTCCGGGAGG GCCCTTTGTG CGGGGGGGAG
 881 CGGCTCGGGG GGTGCGTGCG TGTGTGTGTG CGTGGGGAGC
 921 GCCGCGTGCG GCCCGCGCTG CCCGGCGGCT GTGAGCGCTG
 961 CGGGCGCGGC GCGGGGCTTT GTGCGCTCCG CGTGTGCGCG
1001 AGGGGAGCGC GGCCGGGGGC GGTGCCCCGC GGTGCGGGGG
1041 GGCTGCGAGG GGAACAAAGG CTGCGTGCGG GGTGTGTGCG
1081 TGGGGGGGTG AGCAGGGGGT GTGGGCGCGG CGGTCGGGCT
1121 GTAACCCCCC CCTGCACCCC CCTCCCCGAG TTGCTGAGCA
1161 CGGCCCGGCT TCGGGTGCGG GGCTCCGTGC GGGGCGTGGC
1201 GCGGGGCTCG CCGTGCCGGG CGGGGGGTGG CGGCAGGTGG
1241 GGGTGCCGGG CGGGGCGGGG CCGCCTCGGG CCGGGGAGGG
1281 CTCGGGGGAG GGGCGCGGCG GCCCCGGAGC GCCGGCGGCT
1321 GTCGAGGCGC GGCGAGCCGC AGCCATTGCC TTTTATGGTA
1361 ATCGTGCGAG AGGGCGCAGG GACTTCCTTT GTCCCAAATC
1401 TGGCGGAGCC GAAATCTGGG AGGCGCCGCC GCACCCCCTC
1441 TAGCGGGCGC GGGCGAAGCG GTGCGGCGCC GGCAGGAAGG
1481 AAATGGGCGG GGAGGGCCTT CGTGCGTCGC CGCGCCGCCG
1521 TCCCCTTCTC CATCTCCAGC CTCGGGGCTG CCGCAGGGGG
1561 ACGGCTGCCT TCGGGGGGGA CGGGGCAGGG CGGGGTTCGG
1601 CTTCTGGCGT GTGACCGGCG GCTCTAGAGC CTCTGCTAAC
1641 CATGTTCATG CCTTCTTCTT TTTCCTACAG CTCCTGGGCA
1681 ACGTGCTGGT TGTTGTGCTG TCTCATCATT TTGGCAAAGA
1721 ATTGATTAAT TCGAGCGAAC GCGTATAACT TCGTATAGCA
1761 TACATTATAC GAAGTTATCT CGAGTCGGAT TTGATCTGAT
1801 CAAGAGACAG GATGAGGATC GTTTCGCATG ATTGAACAAG
1841 ATGGATTGCA CGCAGGTTCT CCGGCCGCTT GGGTGGAGAG
1881 GCTATTCGGC TATGACTGGG CACAACAGAC AATCGGCTGC
1921 TCTGATGCCG CCGTGTTCCG GCTGTCAGCG CAGGGGCGCC
1961 CGGTTCTTTT TGTCAAGACC GACCTGTCCG GTGCCCTGAA
2001 TGAACTGCAG GACGAGGCAG CGCGGCTATC GTGGCTGGCC
2041 ACGACGGGCG TTCCTTGCGC AGCTGTGCTC GACGTTGTCA
```

2081 CTGAAGCGGG AAGGGACTGG CTGCTATTGG GCGAAGTGCC
2121 GGGGCAGGAT CTCCTGTCAT CTCACCTTGC TCCTGCCGAG
2161 AAAGTATCCA TCATGGCTGA TGCAATGCGG CGGCTGCATA
2201 CGCTTGATCC GGCTACCTGC CCATTCGACC ACCAAGCGAA
2241 ACATCGCATC GAGCGAGCAC GTACTCGGAT GGAAGCCGGT
2281 CTTGTCGATC AGGATGATCT GGACGAAGAG CATCAGGGGC
2321 TCGCGCCAGC CGAACTGTTC GCCAGGCTCA AGGCGCGCAT
2361 GCCCGACGGC GAGGATCTCG TCGTGACCCA TGGCGATGCC
2401 TGCTTGCCGA ATATCATGGT GGAAAATGGC CGCTTTTCTG
2441 GATTCATCGA CTGTGGCCGG CTGGGTGTGG CGGACCGCTA
2481 TCAGGACATA GCGTTGGCTA CCCGTGATAT TGCTGAAGAG
2521 CTTGGCGGCG AATGGGCTGA CCGCTTCCTC GTGCTTTACG
2561 GTATCGCCGC TCCCGATTCG CAGCGCATCG CCTTCTATCG
2601 CCTTCTTGAC GAGTTCTTCT GAGCGGGACT CTGGGGTTCG
2641 AAATGACCGA CCAAGCGACG CCCAACCTGC CATCACGAGA
2681 TTTCGATTCC ACCGCCGCCT TCTATGAAAG GTTGGGCTTC
2721 GGAATCGTTT TCCGGGACGC CGGCTGGATG ATCCTCCAGC
2761 GCGGGGATCT CATGCTGGAG TTCTTCGCCC ACCCCATCGA
2801 TAACTTGTTT ATTGCAGCTT ATAATGGTTA CAAATAAAGC
2841 AATAGCATCA CAAATTTCAC AAATAAAGCA TTTTTTTCAC
2881 TGCATTCTAG TTGTGGTTTG TCCAAACTCA TCAATGTATC
2921 TTATCATGTC TGGATCAAAT CCGAACGCGT ATAACTTCGT
2961 ATAGCATACA TTATACGAAG TTATCTCGAG TCGCTCGGTA
3001 CGATTTAATT CTAGCAAAAT GTGTGTAATT TTTCCGGTAG
3041 AAATCGACGT GTCCCAGACG ATTATTCGAG ATTGTCAGGT
3081 GGACAAACAA ACCAGAGAGT TGGTGTACAT TAACAAGATT
3121 ATGAACACGC AATTGACAAA ACCCGTTCTC ATGATGTTTA
3161 ACATTTCGGG TCCTATACGA AGCGTTACGC GCAAGAACAA
3201 CAATTTGCGC GACAGAATAA AATCAAAAGT CGATGAACAA
3241 TTTGATCAAC TAGAACGCGA TTACAGCGAT CAAATGGATG
3281 GATTCCACGA TAGCATCAAG TATTTTAAAG ATGAACACTA
3321 TTCGGTAAGT TGCCAAAATG GCAGCGTGTT GAAAAGCAAG
3361 TTTGCTAAAA TTTTAAAGAG TCATGATTAT ACCGATAAAA
3401 AGTCTATTGA AGCTTACGAG AAATACTGTT TGCCCAAATT
3441 GGTCGACGAA CGCAACGACT ACTACGTGGC GGTATGCGTG
3481 TTGAAGCCGG GATTTGAGAA CGGCAGCAAC CAAGTGCTAT
3521 CTTTCGAGTA CAACCCGATT GGTAACAAAG TTATTGTGCC
3561 GTTTGCTCAC GAAATTAACG ACACGGGACT TTACGAGTAC
3601 GACGTCGTAG CTTACGTGGA CAGTGTGCAG TTTGATGGCG
3641 AACAATTTGA AGAGTTTGTG CAGAGTTTAA TATTGCCGTC
3681 GTCGTTCAAA AATTCGGAAA AGGTTTTATA TTACAACGAA
3721 GCGTCGAAAA ACAAAAGCAT GATCTACAAG GCTTTAGAGT
3761 TTACTACAGA ATCGAGCTGG GGCAAATCCG AAAAGTATAA
3801 TTGGAAAATT TTTTGTAACG GTTTTATTTA TGATAAAAAA
3841 TCAAAAGTGT TGTATGTTAA ATTGCACAAT GTAACTAGTG
3881 CACTCAACAA AAATGTAATA TTAAACACAA TTAAATAAAT
3921 GTTAAAATTT ATTGCCTAAT ATTATTTTGT CATTGCTTGT
3961 CATTTATCTA GAAATCAATT CACTCCTCAG GTGCAGGCTG
4001 CCTATCAGAA GGTGGTGGCT GGTGTGGCCA ATGCCCTGGC
4041 TCACAAATAC CACTGAGATC TTTTTCCCTC TGCCAAAAAT
4081 TATGGGGACA TCATGAAGCC CCTTGAGCAT CTGACTTCTG
4121 GCTAATAAAG GAAATTTATT TTCATTGCAA TAGTGTGTTG
4161 GAATTTTTTG TGTCTCTCAC TCGGAAGGAC ATATGGGAGG
4201 GCAAATCATT TAAAACATCA GAATGAGTAT TTGGTTTAGA

```
4241 GTTTGGCAAC ATATGCCATA TGCTGGCTGC CATGAACAAA
4281 GGTGGCTATA AAGAGGTCAT CAGTATATGA AACAGCCCCC
4321 TGCTGTCCAT TCCTTATTCC ATAGAAAAGC CTTGACTTGA
4361 GGTTAGATTT TTTTTATATT TTGTTTTGTG TTATTTTTTT
4401 CTTTAACATC CCTAAAATTT TCCTTACATG TTTTACTAGC
4441 CAGATTTTTC CTCCTCTCCT GACTACTCCC AGTCATAGCT
4481 GTCCCTCTTC TCTTATGAAG ATCCCTCGAC CTGCAGCCCA
4521 AGCTTGGCGT AATCATGGTC ATAGCTGTTT CCTGTGTGAA
4561 ATTGTTATCC GCTCACAATT CCACACAACA TACGAGCCGG
4601 AAGCATAAAG TGTAAAGCCT GGGGTGCCTA ATGAGTGAGC
4641 TAACTCACAT TAATTGCGTT GCGCTCACTG CCCGCTTTCC
4681 AGTCGGGAAA CCTGTCGTGC CAGCGGATCC GCATCTCAAT
4721 TAGTCAGCAA CCATAGTCCC GCCCCTAACT CCGCCCATCC
4761 CGCCCCTAAC TCCGCCCAGT TCCGCCCATT CTCCGCCCCA
4801 TGGCTGACTA ATTTTTTTTA TTTATGCAGA GGCCGAGGCC
4841 GCCTCGGCCT CTGAGCTATT CCAGAAGTAG TGAGGAGGCT
4881 TTTTTGGAGG CCTAGGCTTT TGCAAAAAGC TAACTTGTTT
4921 ATTGCAGCTT ATAATGGTTA CAAATAAAGC AATAGCATCA
4961 CAAATTTCAC AAATAAAGCA TTTTTTTCAC TGCATTCTAG
5001 TTGTGGTTTG TCCAAACTCA TCAATGTATC TTATCATGTC
5041 TGGATCCGCT GCATTAATGA ATCGGCCAAC GCGCGGGGAG
5081 AGGCGGTTTG CGTATTGGGC GCTCTTCCGC TTCCTCGCTC
5121 ACTGACTCGC TGCGCTCGGT CGTTCGGCTG CGGCGAGCGG
5161 TATCAGCTCA CTCAAAGGCG GTAATACGGT TATCCACAGA
5201 ATCAGGGGAT AACGCAGGAA AGAACATGTG AGCAAAAGGC
5241 CAGCAAAAGG CCAGGAACCG TAAAAAGGCC GCGTTGCTGG
5281 CGTTTTTCCA TAGGCTCCGC CCCCCTGACG AGCATCACAA
5321 AAATCGACGC TCAAGTCAGA GGTGGCGAAA CCCGACAGGA
5361 CTATAAAGAT ACCAGGCGTT TCCCCCTGGA AGCTCCCTCG
5401 TGCGCTCTCC TGTTCCGACC CTGCCGCTTA CCGGATACCT
5441 GTCCGCCTTT CTCCCTTCGG GAAGCGTGGC GCTTTCTCAA
5481 TGCTCACGCT GTAGGTATCT CAGTTCGGTG TAGGTCGTTC
5521 GCTCCAAGCT GGGCTGTGTG CACGAACCCC CCGTTCAGCC
5561 CGACCGCTGC GCCTTATCCG GTAACTATCG TCTTGAGTCC
5601 AACCCGGTAA GACACGACTT ATCGCCACTG GCAGCAGCCA
5641 CTGGTAACAG GATTAGCAGA GCGAGGTATG TAGGCGGTGC
5681 TACAGAGTTC TTGAAGTGGT GGCCTAACTA CGGCTACACT
5721 AGAAGGACAG TATTTGGTAT CTGCGCTCTG CTGAAGCCAG
5761 TTACCTTCGG AAAAAGAGTT GGTAGCTCTT GATCCGGCAA
5801 ACAAACCACC GCTGGTAGCG GTGGTTTTTT TGTTTGCAAG
5841 CAGCAGATTA CGCGCAGAAA AAAAGGATCT CAAGAAGATC
5881 CTTTGATCTT TTCTACGGGG TCTGACGCTC AGTGGAACGA
5921 AAACTCACGT TAAGGGATTT TGGTCATGAG ATTATCAAAA
5961 AGGATCTTCA CCTAGATCCT TTTAAATTAA AAATGAAGTT
6001 TTAAATCAAT CTAAAGTATA TATGAGTAAA CTTGGTCTGA
6041 CAGTTACCAA TGCTTAATCA GTGAGGCACC TATCTCAGCG
6081 ATCTGTCTAT TTCGTTCATC CATAGTTGCC TGACTCCCCG
6121 TCGTGTAGAT AACTACGATA CGGGAGGGCT TACCATCTGG
6161 CCCCAGTGCT GCAATGATAC CGCGAGACCC ACGCTCACCG
6201 GCTCCAGATT TATCAGCAAT AAACCAGCCA GCCGGAAGGG
6241 CCGAGCGCAG AAGTGGTCCT GCAACTTTAT CCGCCTCCAT
6281 CCAGTCTATT AATTGTTGCC GGGAAGCTAG AGTAAGTAGT
6321 TCGCCAGTTA ATAGTTTGCG CAACGTTGTT GCCATTGCTA
6361 CAGGCATCGT GGTGTCACGC TCGTCGTTTG GTATGGCTTC
```

```
6401 ATTCAGCTCC GGTTCCCAAC GATCAAGGCG AGTTACATGA
6441 TCCCCCATGT TGTGCAAAAA AGCGGTTAGC TCCTTCGGTC
6481 CTCCGATCGT TGTCAGAAGT AAGTTGGCCG CAGTGTTATC
6521 ACTCATGGTT ATGGCAGCAC TGCATAATTC TCTTACTGTC
6561 ATGCCATCCG TAAGATGCTT TTCTGTGACT GGTGAGTACT
6601 CAACCAAGTC ATTCTGAGAA TAGTGTATGC GGCGACCGAG
6641 TTGCTCTTGC CCGGCGTCAA TACGGGATAA TACCGCGCCA
6681 CATAGCAGAA CTTTAAAAGT GCTCATCATT GGAAAACGTT
6721 CTTCGGGGCG AAAACTCTCA AGGATCTTAC CGCTGTTGAG
6761 ATCCAGTTCG ATGTAACCCA CTCGTGCACC CAACTGATCT
6801 TCAGCATCTT TTACTTTCAC CAGCGTTTCT GGGTGAGCAA
6841 AAACAGGAAG GCAAAATGCC GCAAAAAAGG GAATAAGGGC
6881 GACACGGAAA TGTTGAATAC TCATACTCTT CCTTTTTCAA
6921 TATTATTGAA GCATTTATCA GGGTTATTGT CTCATGAGCG
6961 GATACATATT TGAATGTATT TAGAAAAATA AACAAATAGG
7001 GGTTCCGCGC ACATTTCCCC GAAAAGTGCC ACCTG
```

A2.3 Sequence of generated constructs

A2.3.1 pEGFP.p35

```
   1 GACGGATCGG GAGATCGATC TCGAGAAAAC TGAGGCAGGG
  41 AGCAGGCAAA AATCACATCT AGAGATATGG GAGAGCCAGG
  81 ACCAGAGCCA GGGTCTCCGG GCTGGGACCT AGAGATGTTT
 121 CCAGTGGATA CAGGAGGAAA CAGAAGTGGG TGTAGCAAAG
 161 CCCAAAGCCA GGGTGATGGG TGGGTCGAGC TTGCTTATCT
 201 CCCCGTGTCC AGGGTACTGC CTTGGTAGCA CTGTTGGGCA
 241 TCTCTGTTAC CTTCTGTGGT CACAGAATTC TGCAGTCGAC
 281 GGTACCGCGG GCCCGATCTG GCCTCCGCGC CGGGTTTTGG
 321 CGCCTCCCGC GGGCGCCCCC CTCCTCACGG CGAGCGCTGC
 361 CACGTCAGAC GAAGGGCGCA GGAGCGTCCT GATCCTTCCG
 401 CCCGGACGCT CAGGACAGCG GCCCGCTGCT CATAAGACTC
 441 GGCCTTAGAA CCCCAGTATC AGCAGAAGGA CATTTTAGGA
 481 CGGGACTTGG GTGACTCTAG GGCACTGGTT TTCTTTCCAG
 521 AGAGCGGAAC AGGCGAGGAA AAGTAGTCCC TTCTCGGCGA
 561 TTCTGCGGAG GGATCTCCGT GGGGCGGTGA ACGCCGATGA
 601 TTATATAAGG ACGCGCCGGG TGTGGCACAG CTAGTTCCGT
 641 CGCAGCCGGG ATTTGGGTCG CGGTTCTTGT TTGTGGATCG
 681 CTGTGATCGT CACTTGGTGA GTAGCGGGCT GCTGGGCTGG
 721 CCGGGGCTTT CGTGGCCGCC GGGCCGCTCG GTGGGACGGA
 761 AGCGTGTGGA GAGACCGCCA AGGGCTGTAG TCTGGGTCCG
 801 CGAGCAAGGT TGCCCTGAAC TGGGGGTTGG GGGGAGCGCA
 841 GCAAAATGGC GGCTGTTCCC GAGTCTTGAA TGGAAGACGC
 881 TTGTGAGGCG GGCTGTGAGG TCGTTGAAAC AAGGTGGGGG
 921 GCATGGTGGG CGGCAAGAAC CCAAGGTCTT GAGGCCTTCG
 961 CTAATGCGGG AAAGCTCTTA TTCGGGTGAG ATGGGCTGGG
1001 GCACCATCTG GGGACCCTGA CGTGAAGTTT GTCACTGACT
1041 GGAGAACTCG GTTTGTCGTC TGTTGCGGGG GCGGCAGTTA
1081 TGCGGTGCCG TTGGGCAGTG CACCCGTACC TTTGGGAGCG
1121 CGCGCCCTCG TCGTGTCGTG ACGTCACCCG TTCTGTTGGC
1161 TTATAATGCA GGGTGGGGCC ACCTGCCGGT AGGTGTGCGG
1201 TAGGCTTTTC TCCGTCGCAG GACGCAGGGT TCGGGCCTAG
1241 GGTAGGCTCT CCTGAATCGA CAGGCGCCGG ACCTCTGGTG
1281 AGGGGAGGGA TAAGTGAGGC GTCAGTTTCT TTGGTCGGTT
1321 TTATGTACCT ATCTTCTTAA GTAGCTGAAG CTCCGGTTTT
1361 GAACTATGCG CTCGGGGTTG GCGAGTGTGT TTTGTGAAGT
1401 TTTTTAGGCA CCTTTTGAAA TGTAATCATT TGGGTCAATA
1441 TGTAATTTTC AGTGTTAGAC TAGTAAATTG TCCGCTAAAT
1481 TCTGGCCGTT TTTGGCTTTT TTGTTAGACG AAGCTTGGTA
1521 CCGAGCTCGG ATCGGGATCC ACCGGTCGCC ACCATGGTGA
1561 GCAAGGGCGA GGAGCTGTTC ACCGGGGTGG TGCCCATCCT
1601 GGTCGAGCTG GACGGCGACG TAAACGGCCA CAAGTTCAGC
1641 GTGTCCGGCG AGGGCGAGGG CGATGCCACC TACGGCAAGC
1681 TGACCCTGAA GTTCATCTGC ACCACCGGCA AGCTGCCCGT
1721 GCCCTGGCCC ACCCTCGTGA CCACCCTGAC CTACGGCGTG
1761 CAGTGCTTCA GCCGCTACCC CGACCACATG AAGCAGCACG
1801 ACTTCTTCAA GTCCGCCATG CCCGAAGGCT ACGTCCAGGA
1841 GCGCACCATC TTCTTCAAGG ACGACGGCAA CTACAAGACC
1881 CGCGCCGAGG TGAAGTTCGA GGGCGACACC CTGGTGAACC
1921 GCATCGAGCT GAAGGGCATC GACTTCAAGG AGGACGGCAA
1961 CATCCTGGGG CACAAGCTGG AGTACAACTA CAACAGCCAC
```

```
2001 AACGTCTATA TCATGGCCGA CAAGCAGAAG AACGGCATCA
2041 AGGTGAACTT CAAGATCCGC CACAACATCG AGGACGGCAG
2081 CGTGCAGCTC GCCGACCACT ACCAGCAGAA CACCCCCATC
2121 GGCGACGGCC CCGTGCTGCT GCCCGACAAC CACTACCTGA
2161 GCACCCAGTC CGCCCTGAGC AAAGACCCCA ACGAGAAGCG
2201 CGATCACATG GTCCTGCTGG AGTTCGTGAC CGCCGCCGGG
2241 ATCACTCTCG GCATGGACGA GCTGTACAAG TAAAGCGGCC
2281 GCGACTCTAG ATCATAATCA GCCATACCAC ATTTGTAGAG
2321 GTTTTACTTG CTTTAAAAAA CCTCCCACAC CTCCCCCTGA
2361 ACCTGAAACA TAAAATGAAT GCAATTGTTG TTGTTAACTT
2401 GTTTATTGCA GCTTATAATG GTTACAAATA AAGCAATAGC
2441 ATCACAAATT TCACAAATAA AGCATTTTTT TCACTGCATT
2481 CTAGTTGTGG TTTGTCCAAA CTCATCAATG TATCTTAAGG
2521 CGTAAATTGT AAGCGTTAAT GATCTCCCGA TCCCCTATGG
2561 TGCACTCTCA GTACAATCTG CTCTGATGCC GCATAGTTAA
2601 GCCAGTATCT GCTCCCTGCT TGTGTGTTGG AGGTCGCTGA
2641 GTAGTGCGCG AGCAAAATTT AAGCTACAAC AAGGCAAGGC
2681 TTGACCGACA ATTGCATGAA GAATCTGCTT AGGGTTAGGC
2721 GTTTTGCGCT GCTTCGCGAT GTACGGGCCA GATATACGCG
2761 TTGACATTGA TTATTGACTA GTTATTAATA GTAATCAATT
2801 ACGGGGTCAT TAGTTCATAG CCCATATATG GAGTTCCGCG
2841 TTACATAACT TACGGTAAAT GGCCCGCCTG GCTGACCGCC
2881 CAACGACCCC CGCCCATTGA CGTCAATAAT GACGTATGTT
2921 CCCATAGTAA CGCCAATAGG GACTTTCCAT TGACGTCAAT
2961 GGGTGGAGTA TTTACGGTAA ACTGCCCACT TGGCAGTACA
3001 TCAAGTGTAT CATATGCCAA GTACGCCCCC TATTGACGTC
3041 AATGACGGTA AATGGCCCGC CTGGCATTAT GCCCAGTACA
3081 TGACCTTATG GGACTTTCCT ACTTGGCAGT ACATCTACGT
3121 ATTAGTCATC GCTATTACCA TGGTGATGCG GTTTTGGCAG
3161 TACATCAATG GGCGTGGATA GCGGTTTGAC TCACGGGGAT
3201 TTCCAAGTCT CCACCCCATT GACGTCAATG GGAGTTTGTT
3241 TTGGCACCAA AATCAACGGG ACTTTCCAAA ATGTCGTAAC
3281 AACTCCGCCC CATTGACGCA AATGGGCGGT AGGCGTGTAC
3321 GGTGGGAGGT CTATATAAGC AGAGCTCTCT GGCTAACTAG
3361 AGAACCCACT GCTTACTGGC TTATCGAAAT TAATACGACT
3401 CACTATAGGG AGACCCAAGC TGGCTAGCGT TTAAACGGGC
3441 CCTCTAGACT CGAGAATGTG TGTAATTTTT CCGGTAGAAA
3481 TCGACGTGTC CCAGACGATT ATTCGAGATT GTCAGGTGGA
3521 CAAACAAACC AGAGAGTTGG TGTACATTAA CAAGATTATG
3561 AACACGCAAT TGACAAAACC CGTTCTCATG ATGTTTAACA
3601 TTTCGGGTCC TATACGAAGC GTTACGCGCA AGAACAACAA
3641 TTTGCGCGAC AGAATAAAAT CAAAAGTCGA TGAACAATTT
3681 GATCAACTAG AACGCGATTA CAGCGATCAA ATGGATGGAT
3721 TCCACGATAG CATCAAGTAT TTTAAAGATG AACACTATTC
3761 GGTAAGTTGC CAAAATGGCA GCGTGTTGAA AAGCAAGTTT
3801 GCTAAAATTT TAAAGAGTCA TGATTATACC GATAAAAAGT
3841 CTATTGAAGC TTACGAGAAA TACTGTTTGC CCAAATTGGT
3881 CGACGAACGC AACGACTACT ACGTGGCGGT ATGCGTGTTG
3921 AAGCCGGGAT TTGAGAACGG CAGCAACCAA GTGCTATCTT
3961 TCGAGTACAA CCCGATTGGT AACAAAGTTA TTGTGCCGTT
4001 TGCTCACGAA ATTAACGACA CGGGACTTTA CGAGTACGAC
4041 GTCGTAGCTT ACGTGGACAG TGTGCAGTTT GATGGCGAAC
4081 AATTTGAAGA GTTTGTGCAG AGTTTAATAT TGCCGTCGTC
4121 GTTCAAAAAT TCGGAAAAGG TTTTATATTA CAACGAAGCG
```

4161 TCGAAAAACA AAAGCATGAT CTACAAGGCT TTAGAGTTTA
4201 CTACAGAATC GAGCTGGGGC AAATCCGAAA AGTATAATTG
4241 GAAAATTTTT TGTAACGGTT TTATTTATGA TAAAAAATCA
4281 AAAGTGTTGT ATGTTAAATT GCACAATGTA ACTAGTGCAC
4321 TCAACAAAAA TGTAATATTA AACACAATTA AATAAATGTT
4361 AAAATTTATT GCCTAATATT ATTTTGTCAT TGCTTGTCAT
4401 TTATCTCGAG CGGCCGCCAC TGTGCTGGAT ATCTGCAGAA
4441 TTCCACCACA CTGGACTAGT GGATCCGAGC TCGGTACCAA
4481 GCTTAAGTTT AAACCGCTGA TCAGCCTCGA CTGTGCCTTC
4521 TAGTTGCCAG CCATCTGTTG TTTGCCCCTC CCCCGTGCCT
4561 TCCTTGACCC TGGAAGGTGC CACTCCCACT GTCCTTTCCT
4601 AATAAAATGA GGAAATTGCA TCGCATTGTC TGAGTAGGTG
4641 TCATTCTATT CTGGGGGGTG GGGTGGGGCA GGACAGCAAG
4681 GGGGAGGATT GGGAAGACAA TAGCAGGCAT GCTGGGGATG
4721 CGGTGGGCTC TATGGCTTCT GAGGCGGAAA GAACCAGCTG
4761 GGGCTCTAGG GGGTATCCCC ACGCGCCCTG TAGCGGCGCA
4801 TTAAGCGCGG CGGGTGTGGT GGTTACGCGC AGCGTGACCG
4841 CTACACTTGC CAGCGCCCTA GCGCCCGCTC CTTTCGCTTT
4881 CTTCCCTTCC TTTCTCGCCA CGTTCGCCGG CTTTCCCCGT
4921 CAAGCTCTAA ATCGGGGGCT CCCTTTAGGG TTCCGATTTA
4961 GTGCTTTACG GCACCTCGAC CCCAAAAAAC TTGATTAGGG
5001 TGATGGTTCA CGTAGTGGGC CATCGCCCTG ATAGACGGTT
5041 TTTCGCCCTT TGACGTTGGA GTCCACGTTC TTTAATAGTG
5081 GACTCTTGTT CCAAACTGGA ACAACACTCA ACCCTATCTC
5121 GGTCTATTCT TTTGATTTAT AAGGGATTTT GCCGATTTCG
5161 GCCTATTGGT TAAAAAATGA GCTGATTTAA CAAAAATTTA
5201 ACGCGAATTA ATTCTGTGGA ATGTGTGTCA GTTAGGGTGT
5241 GGAAAGTCCC CAGGCTCCCC AGCAGGCAGA AGTATGCAAA
5281 GCATGCATCT CAATTAGTCA GCAACCAGGT GTGGAAAGTC
5321 CCCAGGCTCC CCAGCAGGCA GAAGTATGCA AAGCATGCAT
5361 CTCAATTAGT CAGCAACCAT AGTCCCGCCC CTAACTCCGC
5401 CCATCCCGCC CCTAACTCCG CCCAGTTCCG CCCATTCTCC
5441 GCCCCATGGC TGACTAATTT TTTTTATTTA TGCAGAGGCC
5481 GAGGCCGCCT CTGCCTCTGA GCTATTCCAG AAGTAGTGAG
5521 GAGGCTTTTT TGGAGGCCTA GGCTTTTGCA AAAAGCTCCC
5561 GGGAGCTTGT ATATCCATTT TCGGATCTGA TCAAGAGACA
5601 GGATGAGGAT CGTTTCGCAT GATTGAACAA GATGGATTGC
5641 ACGCAGGTTC TCCGGCCGCT TGGGTGGAGA GGCTATTCGG
5681 CTATGACTGG GCACAACAGA CAATCGGCTG CTCTGATGCC
5721 GCCGTGTTCC GGCTGTCAGC GCAGGGGCGC CCGGTTCTTT
5761 TTGTCAAGAC CGACCTGTCC GGTGCCCTGA ATGAACTGCA
5801 GGACGAGGCA GCGCGGCTAT CGTGGCTGGC CACGACGGGC
5841 GTTCCTTGCG CAGCTGTGCT CGACGTTGTC ACTGAAGCGG
5881 GAAGGGACTG GCTGCTATTG GGCGAAGTGC CGGGGCAGGA
5921 TCTCCTGTCA TCTCACCTTG CTCCTGCCGA GAAAGTATCC
5961 ATCATGGCTG ATGCAATGCG GCGGCTGCAT ACGCTTGATC
6001 CGGCTACCTG CCCATTCGAC CACCAAGCGA AACATCGCAT
6041 CGAGCGAGCA CGTACTCGGA TGGAAGCCGG TCTTGTCGAT
6081 CAGGATGATC TGGACGAAGA GCATCAGGGG CTCGCGCCAG
6121 CCGAACTGTT CGCCAGGCTC AAGGCGCGCA TGCCCGACGG
6161 CGAGGATCTC GTCGTGACCC ATGGCGATGC CTGCTTGCCG
6201 AATATCATGG TGGAAAATGG CCGCTTTTCT GGATTCATCG
6241 ACTGTGGCCG GCTGGGTGTG GCGGACCGCT ATCAGGACAT
6281 AGCGTTGGCT ACCCGTGATA TTGCTGAAGA GCTTGGCGGC

6321 GAATGGGCTG ACCGCTTCCT CGTGCTTTAC GGTATCGCCG
6361 CTCCCGATTC GCAGCGCATC GCCTTCTATC GCCTTCTTGA
6401 CGAGTTCTTC TGAGCGGGAC TCTGGGGTTC GAAATGACCG
6441 ACCAAGCGAC GCCCAACCTG CCATCACGAG ATTTCGATTC
6481 CACCGCCGCC TTCTATGAAA GGTTGGGCTT CGGAATCGTT
6521 TTCCGGGACG CCGGCTGGAT GATCCTCCAG CGCGGGGATC
6561 TCATGCTGGA GTTCTTCGCC CACCCCAACT TGTTTATTGC
6601 AGCTTATAAT GGTTACAAAT AAAGCAATAG CATCACAAAT
6641 TTCACAAATA AAGCATTTTT TTCACTGCAT TCTAGTTGTG
6681 GTTTGTCCAA ACTCATCAAT GTATCTTATC ATGTCTGTAT
6721 ACCGTCGACC TCTAGCTAGA GCTTGGCGTA ATCATGGTCA
6761 TAGCTGTTTC CTGTGTGAAA TTGTTATCCG CTCACAATTC
6801 CACACAACAT ACGAGCCGGA AGCATAAAGT GTAAAGCCTG
6841 GGGTGCCTAA TGAGTGAGCT AACTCACATT AATTGCGTTG
6881 CGCTCACTGC CCGCTTTCCA GTCGGGAAAC CTGTCGTGCC
6921 AGCTGCATTA ATGAATCGGC CAACGCGCGG GGAGAGGCGG
6961 TTTGCGTATT GGGCGCTCTT CCGCTTCCTC GCTCACTGAC
7001 TCGCTGCGCT CGGTCGTTCG GCTGCGGCGA GCGGTATCAG
7041 CTCACTCAAA GGCGGTAATA CGGTTATCCA CAGAATCAGG
7081 GGATAACGCA GGAAAGAACA TGTGAGCAAA AGGCCAGCAA
7121 AAGGCCAGGA ACCGTAAAAA GGCCGCGTTG CTGGCGTTTT
7161 TCCATAGGCT CCGCCCCCCT GACGAGCATC ACAAAAATCG
7201 ACGCTCAAGT CAGAGGTGGC GAAACCCGAC AGGACTATAA
7241 AGATACCAGG CGTTTCCCCC TGGAAGCTCC CTCGTGCGCT
7281 CTCCTGTTCC GACCCTGCCG CTTACCGGAT ACCTGTCCGC
7321 CTTTCTCCCT TCGGGAAGCG TGGCGCTTTC TCATAGCTCA
7361 CGCTGTAGGT ATCTCAGTTC GGTGTAGGTC GTTCGCTCCA
7401 AGCTGGGCTG TGTGCACGAA CCCCCCGTTC AGCCCGACCG
7441 CTGCGCCTTA TCCGGTAACT ATCGTCTTGA GTCCAACCCG
7481 GTAAGACACG ACTTATCGCC ACTGGCAGCA GCCACTGGTA
7521 ACAGGATTAG CAGAGCGAGG TATGTAGGCG GTGCTACAGA
7561 GTTCTTGAAG TGGTGGCCTA ACTACGGCTA CACTAGAAGA
7601 ACAGTATTTG GTATCTGCGC TCTGCTGAAG CCAGTTACCT
7641 TCGGAAAAAG AGTTGGTAGC TCTTGATCCG GCAAACAAAC
7681 CACCGCTGGT AGCGGTTTTT TTGTTTGCAA GCAGCAGATT
7721 ACGCGCAGAA AAAAAGGATC TCAAGAAGAT CCTTTGATCT
7761 TTTCTACGGG GTCTGACGCT CAGTGGAACG AAAACTCACG
7801 TTAAGGGATT TTGGTCATGA GATTATCAAA AAGGATCTTC
7841 ACCTAGATCC TTTTAAATTA AAAATGAAGT TTTAAATCAA
7881 TCTAAAGTAT ATATGAGTAA ACTTGGTCTG ACAGTTACCA
7921 ATGCTTAATC AGTGAGGCAC CTATCTCAGC GATCTGTCTA
7961 TTTCGTTCAT CCATAGTTGC CTGACTCCCC GTCGTGTAGA
8001 TAACTACGAT ACGGGAGGGC TTACCATCTG GCCCCAGTGC
8041 TGCAATGATA CCGCGAGACC CACGCTCACC GGCTCCAGAT
8081 TTATCAGCAA TAAACCAGCC AGCCGGAAGG GCCGAGCGCA
8121 GAAGTGGTCC TGCAACTTTA TCCGCCTCCA TCCAGTCTAT
8161 TAATTGTTGC CGGGAAGCTA GAGTAAGTAG TTCGCCAGTT
8201 AATAGTTTGC GCAACGTTGT TGCCATTGCT ACAGGCATCG
8241 TGGTGTCACG CTCGTCGTTT GGTATGGCTT CATTCAGCTC
8281 CGGTTCCCAA CGATCAAGGC GAGTTACATG ATCCCCCATG
8321 TTGTGCAAAA AAGCGGTTAG CTCCTTCGGT CCTCCGATCG
8361 TTGTCAGAAG TAAGTTGGCC GCAGTGTTAT CACTCATGGT
8401 TATGGCAGCA CTGCATAATT CTCTTACTGT CATGCCATCC
8441 GTAAGATGCT TTTCTGTGAC TGGTGAGTAC TCAACCAAGT

```
8481 CATTCTGAGA ATAGTGTATG CGGCGACCGA GTTGCTCTTG
8521 CCCGGCGTCA ATACGGGATA ATACCGCGCC ACATAGCAGA
8561 ACTTTAAAAG TGCTCATCAT TGGAAAACGT TCTTCGGGGC
8601 GAAAACTCTC AAGGATCTTA CCGCTGTTGA GATCCAGTTC
8641 GATGTAACCC ACTCGTGCAC CCAACTGATC TTCAGCATCT
8681 TTTACTTTCA CCAGCGTTTC TGGGTGAGCA AAAACAGGAA
8721 GGCAAAATGC CGCAAAAAAG GGAATAAGGG CGACACGGAA
8761 ATGTTGAATA CTCATACTCT TCCTTTTTCA ATATTATTGA
8801 AGCATTTATC AGGGTTATTG TCTCATGAGC GGATACATAT
8841 TTGAATGTAT TTAGAAAAAT AAACAAATAG GGGTTCCGCG
8881 CACATTTCCC CGAAAAGTGC CACCTGACGT C
```

A2.3.2 pAAV-iCre.EGFP

```
   1 CCTGCAGGCA GCTGCGCGCT CGCTCGCTCA CTGAGGCCGC
  41 CCGGGCAAAG CCCGGGCGTC GGGCGACCTT TGGTCGCCCG
  81 GCCTCAGTGA GCGAGCGAGC GCGCAGAGAG GGAGTGGCCA
 121 ACTCCATCAC TAGGGGTTCC TGCGGCCGCA CGCGATTAAC
 161 GCTTACAATT TACGCCTTAA GATACATTGA TGAGTTTGGA
 201 CAAACCACAA CTAGAATGCA GTGAAAAAAA TGCTTTATTT
 241 GTGAAATTTG TGATGCTATT GCTTTATTTG TAACCATTAT
 281 AAGCTGCAAT AAACAAGTTA ACAACAACAA TTGCATTCAT
 321 TTTATGTTTC AGGTTCAGGG GGAGGTGTGG GAGGTTTTTT
 361 AAAGCAAGTA AAACCTCTAC AAATGTGGTA TGGCTGATTA
 401 TGATCTAGAG TCGCGGCCGC TTTACTTGTA CAGCTCGTCC
 441 ATGCCGAGAG TGATCCCGGC GGCGGTCACG AACTCCAGCA
 481 GGACCATGTG ATCGCGCTTC TCGTTGGGGT CTTTGCTCAG
 521 GGCGGACTGG GTGCTCAGGT AGTGGTTGTC GGGCAGCAGC
 561 ACGGGGCCGT CGCCGATGGG GGTGTTCTGC TGGTAGTGGT
 601 CGGCGAGCTG CACGCTGCCG TCCTCGATGT TGTGGCGGAT
 641 CTTGAAGTTC ACCTTGATGC CGTTCTTCTG CTTGTCGGCC
 681 ATGATATAGA CGTTGTGGCT GTTGTAGTTG TACTCCAGCT
 721 TGTGCCCCAG GATGTTGCCG TCCTCCTTGA AGTCGATGCC
 761 CTTCAGCTCG ATGCGGTTCA CCAGGGTGTC GCCCTCGAAC
 801 TTCACCTCGG CGCGGGTCTT GTAGTTGCCG TCGTCCTTGA
 841 AGAAGATGGT GCGCTCCTGG ACGTAGCCTT CGGGCATGGC
 881 GGACTTGAAG AAGTCGTGCT GCTTCATGTG GTCGGGGTAG
 921 CGGCTGAAGC ACTGCACGCC GTAGGTCAGG GTGGTCACGA
 961 GGGTGGGCCA GGGCACGGGC AGCTTGCCGG TGGTGCAGAT
1001 GAACTTCAGG GTCAGCTTGC CGTAGGTGGC ATCGCCCTCG
1041 CCCTCGCCGG ACACGCTGAA CTTGTGGCCG TTTACGTCGC
1081 CGTCCAGCTC GACCAGGATG GGCACCACCC CGGTGAACAG
1121 CTCCTCGCCC TTGCTCACCA TGGTGGCGAC CGGTGGATCC
1161 CGATCCGAGC TCGGTACCAA GCTTCGTCTA ACAAAAAAGC
1201 CAAAAACGGC CAGAATTTAG CGGACAATTT ACTAGTCTAA
1241 CACTGAAAAT TACATATTGA CCCAAATGAT TACATTTCAA
1281 AAGGTGCCTA AAAAACTTCA CAAAACACAC TCGCCAACCC
1321 CGAGCGCATA GTTCAAAACC GGAGCTTCAG CTACTTAAGA
1361 AGATAGGTAC ATAAAACCGA CCAAAGAAAC TGACGCCTCA
1401 CTTATCCCTC CCCTCACCAG AGGTCCGGCG CCTGTCGATT
1441 CAGGAGAGCC TACCCTAGGC CCGAACCCTG CGTCCTGCGA
1481 CGGAGAAAAG CCTACCGCAC ACCTACCGGC AGGTGGCCCC
1521 ACCCTGCATT ATAAGCCAAC AGAACGGGTG ACGTCACGAC
1561 ACGACGAGGG CGCGCGCTCC CAAAGGTACG GGTGCACTGC
1601 CCAACGGCAC CGCATAACTG CCGCCCCCGC AACAGACGAC
1641 AAACCGAGTT CTCCAGTCAG TGACAAACTT CACGTCAGGG
1681 TCCCCAGATG GTGCCCCAGC CCATCTCACC CGAATAAGAG
1721 CTTTCCCGCA TTAGCGAAGG CCTCAAGACC TTGGGTTCTT
1761 GCCGCCCACC ATGCCCCCCA CCTTGTTTCA ACGACCTCAC
1801 AGCCCGCCTC ACAAGCGTCT TCCATTCAAG ACTCGGGAAC
1841 AGCCGCCATT TTGCTGCGCT CCCCCCAACC CCCAGTTCAG
1881 GGCAACCTTG CTCGCGGACC CAGACTACAG CCCTTGGCGG
1921 TCTCTCCACA CGCTTCCGTC CCACCGAGCG GCCCGGCGGC
1961 CACGAAAGCC CCGGCCAGCC CAGCAGCCCG CTACTCACCA
2001 AGTGACGATC ACAGCGATCC ACAAACAAGA ACCGCGACCC
```

```
2041 AAATCCCGGC TGCGACGGAA CTAGCTGTGC CACACCCGGC
2081 GCGTCCTTAT ATAATCATCG GCGTTCACCG CCCCACGGAG
2121 ATCCCTCCGC AGAATCGCCG AGAAGGGACT ACTTTTCCTC
2161 GCCTGTTCCG CTCTCTGGAA AGAAAACCAG TGCCCTAGAG
2201 TCACCCAAGT CCCGTCCTAA AATGTCCTTC TGCTGATACT
2241 GGGGTTCTAA GGCCGAGTCT TATGAGCAGC GGGCCGCTGT
2281 CCTGAGCGTC CGGGCGGAAG GATCAGGACG CTCCTGCGCC
2321 CTTCGTCTGA CGTGGCAGCG CTCGCCGTGA GGAGGGGGGC
2361 GCCCGCGGGA GGCGCCAAAA CCCGGCGCGG AGGCCAGATC
2401 GGGCCCGCGG TACCGTCGAC TGCAGAATTC TGTGACCACA
2441 GAAGGTAACA GAGATGCCCA ACAGTGCTAC CAAGGCAGTA
2481 CCCTGGACAC GGGGAGATAA GCAAGCTCGA CCCACCCATC
2521 ACCCTGGCTT TGGGCTTTGC TACACCCACT TCTGTTTCCT
2561 CCTGTATCCA CTGGAAACAT CTCTAGGTCC CAGCCCGGAG
2601 ACCCTGGCTC TGGTCCTGGC TCTCCCATAT CTCTAGATGT
2641 GATTTTTGCC TGCTCCCTGC CTCAGTTTTC TCGAGATCCG
2681 CGTGGAGCTA GTTATTAATA GTAATCAATT ACGGGGTCAT
2721 TAGTTCATAG CCCATATATG GAGTTCCGCG TTACATAACT
2761 TACGGTAAAT GGCCCGCCTG GCTGACCGCC CAACGACCCC
2801 CGCCCATTGA CGTCAATAAT GACGTATGTT CCCATAGTAA
2841 CGTCAATAGG GACTTTCCAT TGACGTCAAT GGGTGGAGTA
2881 TTTACGGTAA ACTGCCCACT TGGCAGTACA TCAAGTGTAT
2921 CATATGCCAA GTACGCCCCC TATTGACGTC AATGACGGTA
2961 AATGGCCCGC CTGGCATTAT GCCCAGTACA TGACCTTATG
3001 GGACTTTCCT ACTTGGCAGT ACATCTACGT ATTAGTCATC
3041 GCTATTACCA TGGTGATGCG GTTTTGGCAG TACATCAATG
3081 GGCGTGGATA GCGGTTTGAC TCACGGGGAT TTCCAAGTCT
3121 CCACCCCATT GACGTCAATG GGAGTTTGTT TTGCACCAAA
3161 ATCAACGGGA CTTTCCAAAA TGTCGTAACA ACTCCGCCCC
3201 ATTGACGCAA ATGGGCGGTA GGCGTGTACG GTGGGAGGTC
3241 TATATAAGCA GAGCTCGTTT AGTGAACCGT CAGATCGCCT
3281 GGAGACGCCA TCCACGCTGT TTTGACCTCC ATAGAAGACA
3321 CCGGGACCGA TCCAGCCTCC GCGGATTCGA ATCCCGGCCG
3361 GGAACGGTGC ATTGGAACGC GGATTCCCCG TGCCAAGAGT
3401 GACGTAAGTA CCGCCTATAG AGTCTATAGG CCCACAAAAA
3441 ATGCTTTCTT CTTTTAATAT ACTTTTTTGT TTATCTTATT
3481 TCTAATACTT TCCCTAATCT CTTTCTTTCA GGGCAATAAT
3521 GATACAATGT ATCATGCCTC TTTGCACCAT TCTAAAGAAT
3561 AACAGTGATA ATTTCTGGGT TAAGGCAATA GCAATATTTC
3601 TGCATATAAA TATTTCTGCA TATAAATTGT AACTGATGTA
3641 AGAGGTTTCA TATTGCTAAT AGCAGCTACA ATCCAGCTAC
3681 CATTCTGCTT TTATTTTATG GTTGGGATAA GGCTGGATTA
3721 TTCTGAGTCC AAGCTAGGCC CTTTTGCTAA TCATGTTCAT
3761 ACCTCTTATC TTCCTCCCAC AGCTCCTGGG CAACGTGCTG
3801 GTCTGTGTGC TGGCCCATCA CTTTGGCAAA GAATTGGGAT
3841 TCGAACATCG ATTGAATTCC CCGGGGATCA GCTTGTCCAC
3881 CATGGTGCCC AAGAAGAAGA GGAAAGTCTC CAACCTGCTG
3921 ACTGTGCACC AAAACCTGCC TGCCCTCCCT GTGGATGCCA
3961 CCTCTGATGA AGTCAGGAAG AACCTGATGG ACATGTTCAG
4001 GGACAGGCAG GCCTTCTCTG AACACACCTG GAAGATGCTC
4041 CTGTCTGTGT GCAGATCCTG GGCTGCCTGG TGCAAGCTGA
4081 ACAACAGGAA ATGGTTCCCT GCTGAACCTG AGGATGTGAG
4121 GGACTACCTC CTGTACCTGC AAGCCAGAGG CCTGGCTGTG
4161 AAGACCATCC AACAGCACCT GGGCCAGCTC AACATGCTGC
```

4201 ACAGGAGATC TGGCCTGCCT CGCCCTTCTG ACTCCAATGC
4241 TGTGTCCCTG GTGATGAGGA GAATCAGAAA GGAGAATGTG
4281 GATGCTGGGG AGAGAGCCAA GCAGGCCCTG GCCTTTGAAC
4321 GCACTGACTT TGACCAAGTC AGATCCCTGA TGGAGAACTC
4361 TGACAGATGC CAGGACATCA GGAACCTGGC CTTCCTGGGC
4401 ATTGCCTACA ACACCCTGCT GCGCATTGCC GAAATTGCCA
4441 GAATCAGAGT GAAGGACATC TCCCGCACCG ATGGTGGGAG
4481 AATGCTGATC CACATTGGCA GGACCAAGAC CCTGGTGTCC
4521 ACAGCTGGTG TGGAGAAGGC CCTGTCCCTG GGGGTTACCA
4561 AGCTGGTGGA GAGATGGATC TCTGTGTCTG GTGTGGCTGA
4601 TGACCCCAAC AACTACCTGT TCTGCCGGGT CAGAAAGAAT
4641 GGTGTGGCTG CCCCTTCTGC CACCTCCCAA CTGTCCACCC
4681 GGGCCCTGGA AGGGATCTTT GAGGCCACCC ACCGCCTGAT
4721 CTATGGTGCC AAGGATGACT CTGGGCAGAG ATACCTGGCC
4761 TGGTCTGGCC ACTCTGCCAG AGTGGGTGCT GCCAGGGACA
4801 TGGCCAGGGC TGGTGTGTCC ATCCCTGAAA TCATGCAGGC
4841 TGGTGGCTGG ACCAATGTGA ACATAGTGAT GAACTACATC
4881 AGAAACCTGG ACTCTGAGAC TGGGGCCATG GTGAGGCTGC
4921 TCGAGGATGG GGACTGAAAC TGAGTCGAGG GGGGGCCCGG
4961 TACgatccTC TAGAGTCGAC CTGCAGAAGC TTGCCtcgag
5001 cagcgctgcT CGAGAGATCT ACGGGTGGCA TCCCTGTGAC
5041 CCCTCCCCAG TGCCTCTCCT GGCCCTGGAA GTTGCCACTC
5081 CAGTGCCCAC CAGCCTTGTC CTAATAAAAT TAAGTTGCAT
5121 CATTTTGTCT GACTAGGTGT CCTTCTATAA TATTATGGGG
5161 TGGAGGGGGG TGGTATGGAG CAAGGGGCAA GTTGGGAAGA
5201 CAACCTGTAG GGCCTGCGGG GTCTATTGGG AACCAAGCTG
5241 GAGTGCAGTG GCACAATCTT GGCTCACTGC AATCTCCGCC
5281 TCCTGGGTTC AAGCGATTCT CCTGCCTCAG CCTCCCGAGT
5321 TGTTGGGATT CCAGGCATGC ATGACCAGGC TCAGCTAATT
5361 TTTGTTTTTT TGGTAGAGAC GGGGTTTCAC CATATTGGCC
5401 AGGCTGGTCT CCAACTCCTA ATCTCAGGTG ATCTACCCAC
5441 CTTGGCCTCC CAAATTGCTG GGATTACAGG CGTGAACCAC
5481 TGCTCCCTTC CCTGTCCTTC TGATTTTGTA GGTAACCACG
5521 TGCGGACCGA GCGGCCGCAG GAACCCCTAG TGATGGAGTT
5561 GGCCACTCCC TCTCTGCGCG CTCGCTCGCT CACTGAGGCC
5601 GGGCGACCAA AGGTCGCCCG ACGCCCGGGC TTTGCCCGGG
5641 CGGCCTCAGT GAGCGAGCGA GCGCGCAGCT GCCTGCAGGG
5681 GCGCCTGATG CGGTATTTTC TCCTTACGCA TCTGTGCGGT
5721 ATTTCACACC GCATACGTCA AAGCAACCAT AGTACGCGCC
5761 CTGTAGCGGC GCATTAAGCG CGGCGGGTGT GGTGGTTACG
5801 CGCAGCGTGA CCGCTACACT TGCCAGCGCC CTAGCGCCCG
5841 CTCCTTTCGC TTTCTTCCCT TCCTTTCTCG CCACGTTCGC
5881 CGGCTTTCCC CGTCAAGCTC TAAATCGGGG GCTCCCTTTA
5921 GGGTTCCGAT TTAGTGCTTT ACGGCACCTC GACCCCAAAA
5961 AACTTGATTT GGGTGATGGT TCACGTAGTG GGCCATCGCC
6001 CTGATAGACG GTTTTTCGCC CTTTGACGTT GGAGTCCACG
6041 TTCTTTAATA GTGGACTCTT GTTCCAAACT GGAACAACAC
6081 TCAACCCTAT CTCGGGCTAT TCTTTTGATT TATAAGGGAT
6121 TTTGCCGATT TCGGCCTATT GGTTAAAAAA TGAGCTGATT
6161 TAACAAAAAT TTAACGCGAA TTTTAACAAA ATATTAACGT
6201 TTACAATTTT ATGGTGCACT CTCAGTACAA TCTGCTCTGA
6241 TGCCGCATAG TTAAGCCAGC CCCGACACCC GCCAACACCC
6281 GCTGACGCGC CCTGACGGGC TTGTCTGCTC CCGGCATCCG
6321 CTTACAGACA AGCTGTGACC GTCTCCGGGA GCTGCATGTG

6361 TCAGAGGTTT TCACCGTCAT CACCGAAACG CGCGAGACGA
6401 AAGGGCCTCG TGATACGCCT ATTTTTATAG GTTAATGTCA
6441 TGATAATAAT GGTTTCTTAG ACGTCAGGTG GCACTTTTCG
6481 GGGAAATGTG CGCGGAACCC CTATTTGTTT ATTTTTCTAA
6521 ATACATTCAA ATATGTATCC GCTCATGAGA CAATAACCCT
6561 GATAAATGCT TCAATAATAT TGAAAAAGGA AGAGTATGAG
6601 TATTCAACAT TTCCGTGTCG CCCTTATTCC CTTTTTTGCG
6641 GCATTTTGCC TTCCTGTTTT TGCTCACCCA GAAACGCTGG
6681 TGAAAGTAAA AGATGCTGAA GATCAGTTGG GTGCACGAGT
6721 GGGTTACATC GAACTGGATC TCAACAGCGG TAAGATCCTT
6761 GAGAGTTTTC GCCCCGAAGA ACGTTTTCCA ATGATGAGCA
6801 CTTTTAAAGT TCTGCTATGT GGCGCGGTAT TATCCCGTAT
6841 TGACGCCGGG CAAGAGCAAC TCGGTCGCCG CATACACTAT
6881 TCTCAGAATG ACTTGGTTGA GTACTCACCA GTCACAGAAA
6921 AGCATCTTAC GGATGGCATG ACAGTAAGAG AATTATGCAG
6961 TGCTGCCATA ACCATGAGTG ATAACACTGC GGCCAACTTA
7001 CTTCTGACAA CGATCGGAGG ACCGAAGGAG CTAACCGCTT
7041 TTTTGCACAA CATGGGGGAT CATGTAACTC GCCTTGATCG
7081 TTGGGAACCG GAGCTGAATG AAGCCATACC AAACGACGAG
7121 CGTGACACCA CGATGCCTGT AGCAATGGCA ACAACGTTGC
7161 GCAAACTATT AACTGGCGAA CTACTTACTC TAGCTTCCCG
7201 GCAACAATTA ATAGACTGGA TGGAGGCGGA TAAAGTTGCA
7241 GGACCACTTC TGCGCTCGGC CCTTCCGGCT GGCTGGTTTA
7281 TTGCTGATAA ATCTGGAGCC GGTGAGCGTG GGTCTCGCGG
7321 TATCATTGCA GCACTGGGGC CAGATGGTAA GCCCTCCCGT
7361 ATCGTAGTTA TCTACACGAC GGGGAGTCAG GCAACTATGG
7401 ATGAACGAAA TAGACAGATC GCTGAGATAG GTGCCTCACT
7441 GATTAAGCAT TGGTAACTGT CAGACCAAGT TTACTCATAT
7481 ATACTTTAGA TTGATTTAAA ACTTCATTTT TAATTTAAAA
7521 GGATCTAGGT GAAGATCCTT TTTGATAATC TCATGACCAA
7561 AATCCCTTAA CGTGAGTTTT CGTTCCACTG AGCGTCAGAC
7601 CCCGTAGAAA AGATCAAAGG ATCTTCTTGA GATCCTTTTT
7641 TTCTGCGCGT AATCTGCTGC TTGCAAACAA AAAAACCACC
7681 GCTACCAGCG GTGGTTTGTT TGCCGGATCA AGAGCTACCA
7721 ACTCTTTTTC CGAAGGTAAC TGGCTTCAGC AGAGCGCAGA
7761 TACCAAATAC TGTCCTTCTA GTGTAGCCGT AGTTAGGCCA
7801 CCACTTCAAG AACTCTGTAG CACCGCCTAC ATACCTCGCT
7841 CTGCTAATCC TGTTACCAGT GGCTGCTGCC AGTGGCGATA
7881 AGTCGTGTCT TACCGGGTTG GACTCAAGAC GATAGTTACC
7921 GGATAAGGCG CAGCGGTCGG GCTGAACGGG GGGTTCGTGC
7961 ACACAGCCCA GCTTGGAGCG AACGACCTAC ACCGAACTGA
8001 GATACCTACA GCGTGAGCTA TGAGAAAGCG CCACGCTTCC
8041 CGAAGGGAGA AAGGCGGACA GGTATCCGGT AAGCGGCAGG
8081 GTCGGAACAG GAGAGCGCAC GAGGGAGCTT CCAGGGGGAA
8121 ACGCCTGGTA TCTTTATAGT CCTGTCGGGT TTCGCCACCT
8161 CTGACTTGAG CGTCGATTTT TGTGATGCTC GTCAGGGGGG
8201 CGGAGCCTAT GGAAAAACGC CAGCAACGCG GCCTTTTTAC
8241 GGTTCCTGGC CTTTTGCTGG CCTTTTGCTC ACATGT

A2.3.3 pAAV-p35

```
   1 CCTGCAGGCA GCTGCGCGCT CGCTCGCTCA CTGAGGCCGC
  41 CCGGGCAAAG CCCGGGCGTC GGGCGACCTT TGGTCGCCCG
  81 GCCTCAGTGA GCGAGCGAGC GCGCAGAGAG GGAGTGGCCA
 121 ACTCCATCAC TAGGGGTTCC TGCGGCCGCA CGCGTGGAGC
 161 TAGTTATTAA TAGTAATCAA TTACGGGGTC ATTAGTTCAT
 201 AGCCCATATA TGGAGTTCCG CGTTACATAA CTTACGGTAA
 241 ATGGCCCGCC TGGCTGACCG CCCAACGACC CCCGCCCATT
 281 GACGTCAATA ATGACGTATG TTCCCATAGT AACGTCAATA
 321 GGGACTTTCC ATTGACGTCA ATGGGTGGAG TATTTACGGT
 361 AAACTGCCCA CTTGGCAGTA CATCAAGTGT ATCATATGCC
 401 AAGTACGCCC CCTATTGACG TCAATGACGG TAAATGGCCC
 441 GCCTGGCATT ATGCCCAGTA CATGACCTTA TGGGACTTTC
 481 CTACTTGGCA GTACATCTAC GTATTAGTCA TCGCTATTAC
 521 CATGGTGATG CGGTTTTGGC AGTACATCAA TGGGCGTGGA
 561 TAGCGGTTTG ACTCACGGGG ATTTCCAAGT CTCCACCCCA
 601 TTGACGTCAA TGGGAGTTTG TTTTGCACCA AAATCAACGG
 641 GACTTTCCAA AATGTCGTAA CAACTCCGCC CCATTGACGC
 681 AAATGGGCGG TAGGCGTGTA CGGTGGGAGG TCTATATAAG
 721 CAGAGCTCGT TTAGTGAACC GTCAGATCGC CTGGAGACGC
 761 CATCCACGCT GTTTTGACCT CCATAGAAGA CACCGGGACC
 801 GATCCAGCCT CCGCGGATTC GAATCCCGGC CGGGAACGGT
 841 GCATTGGAAC GCGGATTCCC CGTGCCAAGA GTGACGTAAG
 881 TACCGCCTAT AGAGTCTATA GGCCCACAAA AAATGCTTTC
 921 TTCTTTTAAT ATACTTTTTT GTTTATCTTA TTTCTAATAC
 961 TTTCCCTAAT CTCTTTCTTT CAGGGCAATA ATGATACAAT
1001 GTATCATGCC TCTTTGCACC ATTCTAAAGA ATAACAGTGA
1041 TAATTTCTGG GTTAAGGCAA TAGCAATATT TCTGCATATA
1081 AATATTTCTG CATATAAATT GTAACTGATG TAAGAGGTTT
1121 CATATTGCTA ATAGCAGCTA CAATCCAGCT ACCATTCTGC
1161 TTTTATTTTA TGGTTGGGAT AAGGCTGGAT TATTCTGAGT
1201 CCAAGCTAGG CCCTTTTGCT AATCATGTTC ATACCTCTTA
1241 TCTTCCTCCC ACAGCTCCTG GGCAACGTGC TGGTCTGTGT
1281 GCTGGCCCAT CACTTTGGCA AAGAATTGGG ATTCGAACAT
1321 CGATTGAATT CCCCGGGGAT CCTCTAGAGT CGACCTGCAG
1361 AAGCTTGCCT CGAGAATGTG TGTAATTTTT CCGGTAGAAA
1401 TCGACGTGTC CCAGACGATT ATTCGAGATT GTCAGGTGGA
1441 CAAACAAACC AGAGAGTTGG TGTACATTAA CAAGATTATG
1481 AACACGCAAT TGACAAAACC CGTTCTCATG ATGTTTAACA
1521 TTTCGGGTCC TATACGAAGC GTTACGCGCA AGAACAACAA
1561 TTTGCGCGAC AGAATAAAAT CAAAAGTCGA TGAACAATTT
1601 GATCAACTAG AACGCGATTA CAGCGATCAA ATGGATGGAT
1641 TCCACGATAG CATCAAGTAT TTTAAAGATG AACACTATTC
1681 GGTAAGTTGC CAAAATGGCA GCGTGTTGAA AAGCAAGTTT
1721 GCTAAAATTT TAAAGAGTCA TGATTATACC GATAAAAAGT
1761 CTATTGAAGC TTACGAGAAA TACTGTTTGC CCAAATTGGT
```

1801 CGACGAACGC AACGACTACT ACGTGGCGGT ATGCGTGTTG
1841 AAGCCGGGAT TTGAGAACGG CAGCAACCAA GTGCTATCTT
1881 TCGAGTACAA CCCGATTGGT AACAAAGTTA TTGTGCCGTT
1921 TGCTCACGAA ATTAACGACA CGGGACTTTA CGAGTACGAC
1961 GTCGTAGCTT ACGTGGACAG TGTGCAGTTT GATGGCGAAC
2001 AATTTGAAGA GTTTGTGCAG AGTTTAATAT TGCCGTCGTC
2041 GTTCAAAAAT TCGGAAAAGG TTTTATATTA CAACGAAGCG
2081 TCGAAAAACA AAAGCATGAT CTACAAGGCT TTAGAGTTTA
2121 CTACAGAATC GAGCTGGGGC AAATCCGAAA AGTATAATTG
2161 GAAAATTTTT TGTAACGGTT TTATTTATGA TAAAAAATCA
2201 AAAGTGTTGT ATGTTAAATT GCACAATGTA ACTAGTGCAC
2241 TCAACAAAAA TGTAATATTA AACACAATTA AATAAATGTT
2281 AAAATTTATT GCCTAATATT ATTTTGTCAT TGCTTGTCAT
2321 TTATCTCGAG AGATCTACGG GTGGCATCCC TGTGACCCCT
2361 CCCCAGTGCC TCTCCTGGCC CTGGAAGTTG CCACTCCAGT
2401 GCCCACCAGC CTTGTCCTAA TAAAATTAAG TTGCATCATT
2441 TTGTCTGACT AGGTGTCCTT CTATAATATT ATGGGGTGGA
2481 GGGGGGTGGT ATGGAGCAAG GGGCAAGTTG GGAAGACAAC
2521 CTGTAGGGCC TGCGGGGTCT ATTGGGAACC AAGCTGGAGT
2561 GCAGTGGCAC AATCTTGGCT CACTGCAATC TCCGCCTCCT
2601 GGGTTCAAGC GATTCTCCTG CCTCAGCCTC CCGAGTTGTT
2641 GGGATTCCAG GCATGCATGA CCAGGCTCAG CTAATTTTTG
2681 TTTTTTTGGT AGAGACGGGG TTTCACCATA TTGGCCAGGC
2721 TGGTCTCCAA CTCCTAATCT CAGGTGATCT ACCCACCTTG
2761 GCCTCCCAAA TTGCTGGGAT TACAGGCGTG AACCACTGCT
2801 CCCTTCCCTG TCCTTCTGAT TTTGTAGGTA ACCACGTGCG
2841 GACCGAGCGG CCGCAGGAAC CCCTAGTGAT GGAGTTGGCC
2881 ACTCCCTCTC TGCGCGCTCG CTCGCTCACT GAGGCCGGGC
2921 GACCAAAGGT CGCCCGACGC CCGGGCTTTG CCCGGGCGGC
2961 CTCAGTGAGC GAGCGAGCGC GCAGCTGCCT GCAGGGGCGC
3001 CTGATGCGGT ATTTTCTCCT TACGCATCTG TGCGGTATTT
3041 CACACCGCAT ACGTCAAAGC AACCATAGTA CGCGCCCTGT
3081 AGCGGCGCAT TAAGCGCGGC GGGTGTGGTG GTTACGCGCA
3121 GCGTGACCGC TACACTTGCC AGCGCCCTAG CGCCCGCTCC
3161 TTTCGCTTTC TTCCCTTCCT TTCTCGCCAC GTTCGCCGGC
3201 TTTCCCCGTC AAGCTCTAAA TCGGGGGCTC CCTTTAGGGT
3241 TCCGATTTAG TGCTTTACGG CACCTCGACC CCAAAAAACT
3281 TGATTTGGGT GATGGTTCAC GTAGTGGGCC ATCGCCCTGA
3321 TAGACGGTTT TTCGCCCTTT GACGTTGGAG TCCACGTTCT
3361 TTAATAGTGG ACTCTTGTTC CAAACTGGAA CAACACTCAA
3401 CCCTATCTCG GGCTATTCTT TTGATTTATA AGGGATTTTG
3441 CCGATTTCGG CCTATTGGTT AAAAAATGAG CTGATTTAAC
3481 AAAAATTTAA CGCGAATTTT AACAAAATAT TAACGTTTAC
3521 AATTTTATGG TGCACTCTCA GTACAATCTG CTCTGATGCC
3561 GCATAGTTAA GCCAGCCCCG ACACCCGCCA ACACCCGCTG
3601 ACGCGCCCTG ACGGGCTTGT CTGCTCCCGG CATCCGCTTA
3641 CAGACAAGCT GTGACCGTCT CCGGGAGCTG CATGTGTCAG

```
3681 AGGTTTTCAC CGTCATCACC GAAACGCGCG AGACGAAAGG
3721 GCCTCGTGAT ACGCCTATTT TTATAGGTTA ATGTCATGAT
3761 AATAATGGTT TCTTAGACGT CAGGTGGCAC TTTTCGGGGA
3801 AATGTGCGCG GAACCCCTAT TTGTTTATTT TTCTAAATAC
3841 ATTCAAATAT GTATCCGCTC ATGAGACAAT AACCCTGATA
3881 AATGCTTCAA TAATATTGAA AAAGGAAGAG TATGAGTATT
3921 CAACATTTCC GTGTCGCCCT TATTCCCTTT TTTGCGGCAT
3961 TTTGCCTTCC TGTTTTTGCT CACCCAGAAA CGCTGGTGAA
4001 AGTAAAAGAT GCTGAAGATC AGTTGGGTGC ACGAGTGGGT
4041 TACATCGAAC TGGATCTCAA CAGCGGTAAG ATCCTTGAGA
4081 GTTTTCGCCC CGAAGAACGT TTTCCAATGA TGAGCACTTT
4121 TAAAGTTCTG CTATGTGGCG CGGTATTATC CCGTATTGAC
4161 GCCGGGCAAG AGCAACTCGG TCGCCGCATA CACTATTCTC
4201 AGAATGACTT GGTTGAGTAC TCACCAGTCA CAGAAAAGCA
4241 TCTTACGGAT GGCATGACAG TAAGAGAATT ATGCAGTGCT
4281 GCCATAACCA TGAGTGATAA CACTGCGGCC AACTTACTTC
4321 TGACAACGAT CGGAGGACCG AAGGAGCTAA CCGCTTTTTT
4361 GCACAACATG GGGGATCATG TAACTCGCCT TGATCGTTGG
4401 GAACCGGAGC TGAATGAAGC CATACCAAAC GACGAGCGTG
4441 ACACCACGAT GCCTGTAGCA ATGGCAACAA CGTTGCGCAA
4481 ACTATTAACT GGCGAACTAC TTACTCTAGC TTCCCGGCAA
4521 CAATTAATAG ACTGGATGGA GGCGGATAAA GTTGCAGGAC
4561 CACTTCTGCG CTCGGCCCTT CCGGCTGGCT GGTTTATTGC
4601 TGATAAATCT GGAGCCGGTG AGCGTGGGTC TCGCGGTATC
4641 ATTGCAGCAC TGGGGCCAGA TGGTAAGCCC TCCCGTATCG
4681 TAGTTATCTA CACGACGGGG AGTCAGGCAA CTATGGATGA
4721 ACGAAATAGA CAGATCGCTG AGATAGGTGC CTCACTGATT
4761 AAGCATTGGT AACTGTCAGA CCAAGTTTAC TCATATATAC
4801 TTTAGATTGA TTTAAAACTT CATTTTTAAT TTAAAAGGAT
4841 CTAGGTGAAG ATCCTTTTTG ATAATCTCAT GACCAAAATC
4881 CCTTAACGTG AGTTTTCGTT CCACTGAGCG TCAGACCCCG
4921 TAGAAAAGAT CAAAGGATCT TCTTGAGATC CTTTTTTTCT
4961 GCGCGTAATC TGCTGCTTGC AAACAAAAAA ACCACCGCTA
5001 CCAGCGGTGG TTTGTTTGCC GGATCAAGAG CTACCAACTC
5041 TTTTTCCGAA GGTAACTGGC TTCAGCAGAG CGCAGATACC
5081 AAATACTGTC CTTCTAGTGT AGCCGTAGTT AGGCCACCAC
5121 TTCAAGAACT CTGTAGCACC GCCTACATAC CTCGCTCTGC
5161 TAATCCTGTT ACCAGTGGCT GCTGCCAGTG GCGATAAGTC
5201 GTGTCTTACC GGGTTGGACT CAAGACGATA GTTACCGGAT
5241 AAGGCGCAGC GGTCGGGCTG AACGGGGGGT TCGTGCACAC
5281 AGCCCAGCTT GGAGCGAACG ACCTACACCG AACTGAGATA
5321 CCTACAGCGT GAGCTATGAG AAAGCGCCAC GCTTCCCGAA
5361 GGGAGAAAGG CGGACAGGTA TCCGGTAAGC GGCAGGGTCG
5401 GAACAGGAGA GCGCACGAGG GAGCTTCCAG GGGGAAACGC
5441 CTGGTATCTT TATAGTCCTG TCGGGTTTCG CCACCTCTGA
5481 CTTGAGCGTC GATTTTTGTG ATGCTCGTCA GGGGGGCGGA
5521 GCCTATGGAA AAACGCCAGC AACGCGGCCT TTTTACGGTT
```

5561 CCTGGCCTTT TGCTGGCCTT TTGCTCACAT GT